



**HAL**  
open science

# An analysis on second generation intact stability criteria

Arman Ariffin

► **To cite this version:**

Arman Ariffin. An analysis on second generation intact stability criteria. Fluid mechanics [physics.class-ph]. Université de Bretagne occidentale - Brest, 2017. English. NNT : 2017BRES0043 . tel-01610056

**HAL Id: tel-01610056**

**<https://theses.hal.science/tel-01610056v1>**

Submitted on 4 Oct 2017

**HAL** is a multi-disciplinary open access archive for the deposit and dissemination of scientific research documents, whether they are published or not. The documents may come from teaching and research institutions in France or abroad, or from public or private research centers.

L'archive ouverte pluridisciplinaire **HAL**, est destinée au dépôt et à la diffusion de documents scientifiques de niveau recherche, publiés ou non, émanant des établissements d'enseignement et de recherche français ou étrangers, des laboratoires publics ou privés.



université de bretagne  
occidentale

UNIVERSITE  
BRETAGNE  
LOIRE

THÈSE / UNIVERSITÉ DE BRETAGNE OCCIDENTALE

*sous le sceau de l'Université Bretagne Loire*  
pour obtenir le titre de

DOCTEUR DE L'UNIVERSITÉ DE BRETAGNE OCCIDENTALE

*Mention : Génie Mécanique - mécanique des fluides et énergétique*

École Doctorale des Sciences de la Mer

présentée par

**Arman ARIFFIN**

Préparée au Institut de Recherche  
Dupuy de Lôme CNRS FRE 3744,  
ENSTA Bretagne

**Thèse soutenue le 9 juin 2017**

devant le jury composé de :

**Xavier CARTON**

Professeur - UBO / *Président de Jury*

**Volker BERTRAM**

Professeur - DNV-GL, Hambourg (Allemagne) / *Rapporteur*

**Luis PEREZ ROJAS**

Professeur - ETSIN Madrid (Espagne) / *Rapporteur*

**Mohammed Abdelkader DJEBLI**

Maîtres de conférences - Université des Sciences et de la Technologie d'Oran,  
(Algérie) / *Rapporteur*

**Jean-Yves BILLARD**

Professeur - École Navale / *Examineur*

**Jean-Marc LAURENS**

Enseignant Chercheur - HDR, ENSTA Bretagne / *Directeur de thèse*

**Shuhaimi MANSOR**

Professeur - UTM (Malaisie) / *Co-Directeur de thèse*

**Jean-Francois LEGUEN**

DGA Techniques Hydrodynamiques / *invité*

**Alain ROCHAIS**

DCNS / *invité*

# Etude des Critères de Seconde Génération de la Stabilité du Navire à l'Etat Intact

## An Analysis on Second Generation Intact Stability Criteria





## Acknowledgements

I would never have been able to finish my dissertation without the guidance of my supervisors, help from friends, and support from my family and wife.

I would like to express my deepest gratitude to my supervisor, Dr. Jean-Marc Laurens from the École Nationale Supérieure de Techniques Avancées (ENSTA) Bretagne, Brest, France and Dr Shuhaimi Mansor from Universiti Teknologi Malaysia, Johor Bahru, Malaysia for their excellent guidance, care, patience, and providing me with an excellent atmosphere for doing research. I would like to thank Dr. Maxime Feraille, Attache for Higher Education and Science, Embassy of France in Malaysia, DCNS, Government of Malaysia and Royal Malaysian Navy Headquarters who enabled this research and financially supported my research for three years in France. I am especially grateful to everyone who helped, supported, encouraged me and made this project possible: En Abd Basid Abd Rahman, En Anuar Murad, PM Ainulotfi Abdul Latif, Alain Rochais, Antoine Denardou, Cecile Augor-Thebault, PM Ir Hayati Abdullah, Hamza Benyahia, Imane Hadja Beloufa, Jeroen Wackers, Capt Kannan Perumal, Mahrez Ait Mohammed, Effi Helmy Ariffin, Dr Shabudin Mat, Stéphane Dardel, Stéphane Toulliou, Prof Wan Khairuddin Wan Ali, En Wan Zaidi Wan Omar, William Havet, the staff of the Aerolab UTM, the staff of ENSTA Bretagne and everyone who directly or indirectly helped me. I would also like to thank my parents, Ariffin Mahmud and Yatima Hamid. They always supported and encouraged me with their best wishes.

Finally, I would like to thank my wife, Abida Abidin and my children; Amanina Syuhada, Ahmad Abbasy, Auni Madihah and Ahmad Ariq. They were always there cheering me up and stood by me through the good times and bad.

# Abstract

The second generation intact stability criteria (SGISC) are currently under finalisation by the International Maritime Organisation. These criteria should be based on the physics of the specific phenomena leading to stability failures. The justification of SGICS can be completed in the form of a multi-tiered approach, whereby a ship would be checked for vulnerability in the first tiers and, if found vulnerable, then the ship would be evaluated using the second level vulnerability criteria. If still found vulnerable, then the ship would be evaluated using state-of-the-art direct assessment methods. The first level is meant to be very simple and conservative. Its main purpose is to distinguish ships (and the loading conditions) that clearly are not vulnerable to a given stability failure mode, from those that, in principle, may be. Because further analysis of the vessels that are not vulnerable would be redundant, the cost of performing such further analysis should be avoided. Due to the level-one criteria being simple and conservative, some occasional “false positives” may be expected. Again, to reduce the time and cost of stability assessment, a second level of vulnerability criteria has been introduced. The second level is meant to be less conservative than the first, based on simplified physics and involving calculations with reduced computational efforts and straightforward applications following suitable guidelines. Direct assessment procedures for stability failure are intended to employ the most advanced state-of-the-art technology available either by numerical analysis or experimental work for quantitative validation. Considering the current state-of-the-art of computational ship hydrodynamics for these problems, general direct stability assessment options appear to be limited to model tests and fast time-domain simulations. In this thesis, an analysis with the hydrostatic solver, experimental approach for dead ship condition and RANS simulation are presented. In conclusion, it was possible to implement the stability criteria of the intact second-generation vessel in the GHS © code of stability, a code commonly used by industrialists in the field. Five vessels were considered to verify this implementation. An experimental wind tunnel method and a simplified CFD calculation method were proposed. In both cases, the results show that the maximum roll angle reached by the two vessels studied is lower than that given by the regulatory calculation. The experimental method is certainly closer to reality and the CFD calculation remains conservative without being as binding as the regulation.

## List of Symbols

Symbol	Name	SI - unit
<b>Latin characters</b>		
$A$	Projected lateral area	$m^2$
$A_K$	Total underwater projected area	$m^2$
$A_W$	Waterplane area at design draught	$m^2$
$B$	Ship Breadth	$m$
$C$	Wave speed	$ms^{-1}$
$CoG$	Centre of gravity	
$C_D$	Coefficient of drag	
$C_M$	Coefficient of midship	
$C_Y$	Coefficient for y-axis	
$F_n$	Froude Number	
$g$	Acceleration due to gravity	$ms^{-2}$
$GM$	Metacentric height	$m$
$GZ$	Righting arm	$m$
$GZ_{MAX}$	Maximum righting arm	$m$
$h$	Wave height	$m$
$I_H$	Moment inertia at horizontal axis	$m^4$
$I_L$	Moment inertia at vertical axis	$m^4$
$k$	Factor of the underwater surface with bilge keel or bar keel	
$k_x$	Radius of gyration about the longitudinal axis	$m$
$k_L$	Factor taking into account simultaneous action roll, yaw and pitch motions	
$L$	Length of the ship	$m$
$LCG$	Longitudinal centre of gravity	$m$
$l_{W1}$	Wind heeling with steady wind	$m$
$l_{W2}$	Wind heeling with steady wind and gust	$m$
$M$	Heeling moment	$Nm$
$maxVCG$	Maximum VCG	$m$
$N$	Bertin's roll damping coefficient	
$OG$	Vertical distance between G and water line	$m$
$P$	Pressure	$Pa$
$r$	Effective wave slope factor	
$s$	Wave steepness	$m$

$T$	Ship draught	m
$TCG$	Transverse centre of gravity	m
$V$	Wind velocity	$\text{ms}^{-1}$ or knots
$VCG$	Vertical centre of gravity	m
$V_s$	Vessel speed	$\text{ms}^{-1}$ or knots
$WHA$	Wind heeling arm	m
$Z$	Vertical distance from centre of wind force to half draught	m

***Greek characters***

$\Delta$	Displacement	tonnes
$\lambda$	Wave length	m
$\phi_0$	Angle of equilibrium	radians
$\phi_1$	Angle of roll to windward due to wave action	radians
$\phi_2$	Roll back angle	radians
$\phi_{2^*}$	Roll back angle (calculated from $\phi_0$ )	radians
$\phi_w$	Wave slope	radians

## List of Abbreviations

<b>Symbol</b>	<b>Name</b>
2008 IS Code	International Code of Intact Stability 2008
2D	2-dimensional
3D	3-dimensional
AGR	Automatic Grid Refinement
CFD	Computational Fluid Dynamics
DDS	Design Data Sheet
DOF	Degree of freedom
DTMB	David Taylor Model Basin
ECN	École Centrale de Nantes
EMN	Equipe Modélisation Numérique
ENSTA	École Nationale Supérieure de Techniques Avancées
FSA	Formal Safety Assessment
GHS	General Hydrostatics
IIHR	Iowa Institute of Hydraulic Research, US
ILLC	International Load Lines Convention
IMO	International Maritime Organisation
INSEAN	Istituto Nazionale per Studi ed Esperienze di Architettura Navale, Italy
ISO	International Standards Organisation
ISSW	International Ship Stability Workshop
ITTC	International Towing Tank Conference
MSC	Maritime Safety Committee
NA	Not available
NIST	National Institute of Standards and Technology
NR	Naval Rules
NRIFE	National Research Institute of Fisheries Engineering
NURBS	Non-Uniform Rational Basis Spline
PBC	Performance Based Criteria
RANSE	Reynolds Average Navier-Stoke Equations
SDC	Ship Design and Construction
SGISC	Second Generation Intact Stability Criteria
SLF	Stability and Load Lines and on Fishing Vessel Safety
SOLAS	Safety of Life at Sea
STAB	International Conference on Stability of Ship Ocean Vehicles
UK	United Kingdom

UN	United Nations
US	Unites States of America
UTM	Univeriti Teknologi Malaysia
USSR	Union of Soviet Socialist Republics
VOF	Volume of fluid
WGIS	Working group
WWII	World War II



## List of Figures

Figure 1.1 Scenario of dead ship condition. Extracted from (IMO 2016)	5
Figure 1.2 Thesis organisation	7
Figure 2.1 GZ curve for the weather criterion. Extracted from (IMO 2009)	15
Figure 2.2 US Navy Stability Criteria. Extracted from (Deybach 1997)	17
Figure 2.3 The IMO weather criterion. Extracted from (Spyrou 2011)	19
Figure 2.4 The Naval rules weather criterion. Extracted from (Spyrou 2011)	20
Figure 2.5 Flow chart for the implementation of second generation intact stability criteria. Extracted from (IMO 2011)	25
Figure 2.6 Stability corresponding to water plane changes during the water trough and the wave crest. Extracted from (Belenky, Bassler, and Spyrou 2011)	26
Figure 2.7 Development of parametric resonance. Extracted from (IMO 2015)	27
Figure 2.8 Force acting on a ship in following waves. Extracted from (IMO 2016)	28
Figure 2.9 Scenario of stability failure in dead ship conditions. Extracted from (Belenky, Bassler, and Spyrou 2011)	29
Figure 2.10 Scenario of stability failure related to excessive accelerations. Extracted from (IMO 2015)	29
Figure 2.11 Test configuration at Vienna Model Basin. Extracted from (Bertaglia et al. 2003)	38
Figure 2.12 Wind blower used for the experiment at NRIFE. Extracted from (Umeda et al. 2014)	38
Figure 2.13 An overview of test setup; Top view (Left) Lateral view (Right). Extracted from (Umeda et al. 2014)	39
Figure 2.14 Schematic diagram (left) and actual realisation (right) of the experimental arrangement used for roll decay tests. Extracted from (Bulian, Francescutto, and Fucile 2010)	39
Figure 2.15 Flow chart for the weather criterion	42
Figure 2.16 Rules 1 for the weather criterion	42
Figure 2.17 Rules 2 for the weather criterion	42
Figure 2.18 Input values for determining wind heeling arm	43
Figure 2.19 Input values for determining $\phi_1$	43
Figure 2.20 Arrangement for test in wind tunnel. Extracted from (IMO MSC.1/Circ.1200 2006)	44
Figure 2.21 Arrangement for drifting test. Extracted from (IMO MSC.1/Circ.1200 2006)	45
Figure 2.22 Arrangement for roll test in beam waves. Extracted from (IMO MSC.1/Circ.1200 2006)	45
Figure 2.23 Sources of roll damping	49

Figure 2.24 Conceptual scheme of the assumed simplified physical modelling for the short-term assessment. Extracted from (IMO 2016)	51
Figure 3.1 Process flow of GHS for the 2008 IS Code	53
Figure 3.2 The ASL shape	54
Figure 3.3 The 5415 shape	55
Figure 3.4 The PV shape	55
Figure 3.5 The 120m containership shape	55
Figure 3.6 The KL shape	56
Figure 3.7 GZ curve for the ASL shape	57
Figure 3.8 GZ curve for the 5415 shape	57
Figure 3.9 GZ curve for the PV shape	57
Figure 3.10 GZ curve for the 120m containership shape	58
Figure 3.11 GZ curve for the KL shape	58
Figure 3.12 Limits in righting arm curve	59
Figure 3.13 Interface for 2008 IS Code righting arm curve evaluation	60
Figure 3.14 Results of righting arm properties for ASL shape	60
Figure 3.15 Results of righting arm properties for 5415 shape	61
Figure 3.16 Results of righting arm properties for PV shape	61
Figure 3.17 Results of righting arm properties for 120m containership shape	62
Figure 3.18 Results of righting arm properties for KL shape	62
Figure 3.19 Severe wind and rolling	63
Figure 3.20 Wind heeling moment	64
Figure 3.21 Ship heel to angle of equilibrium. Angle of equilibrium = $1.27^\circ$	64
Figure 3.22 IMO parameters and for roll angle calculation. Roll angle = $27.28^\circ$	65
Figure 3.23 The wind with gust heeling moment	65
Figure 3.24 The value for GZ curve. The angle of equilibrium with gust is $1.9^\circ$	65
Figure 3.25 GZ curve to verify the angle of equilibrium on wind without gust	66
Figure 3.26 GZ curve for the weather criterion	66
Figure 3.27 Interface for 2008 IS Code weather criterion evaluation	67
Figure 3.28 Results of weather criterion for ASL shape	68
Figure 3.29 Results of weather criterion for KL shape	68
Figure 3.30 Results of weather criterion (IMO modified) for 5415 shape. Result (above) and GZ curve (below)	69
Figure 3.31 Results of weather criterion (Naval Rules) for 5415 shape. Result (above) and GZ curve (below)	70
Figure 3.32 Sample of template with GUI for pure loss of stability Level 1	72
Figure 3.33 Sample of template with GUI for parametric rolling Level 1	72
Figure 3.34 Sample of template with GUI for broaching Level 1	74
Figure 3.35 Result of broaching displayed on GHS screen	74
Figure 3.36 Sample of pop-up result for broaching	74
Figure 3.37 Sample of printed result created within GHS	75
Figure 3.38 <i>MaxVCG</i> curve for pure loss of stability, Vulnerability Level 1	79
Figure 3.39 <i>MaxVCG</i> curve for pure loss of stability, Vulnerability Level 1 (zoom)	79
Figure 3.40 <i>MaxVCG</i> curve for parametric rolling, Vulnerability Level 1	80

Figure 3.41 <i>MaxVCG</i> curve for parametric rolling, Vulnerability Level 1 (zoom)	80
Figure 3.42 <i>MaxVCG</i> curves representing pure loss of stability for ASL shape	84
Figure 3.43 <i>MaxVCG</i> curves representing pure loss of stability for 5415 shape	84
Figure 3.44 <i>MaxVCG</i> curves representing pure loss of stability for PV shape	85
Figure 3.45 <i>MaxVCG</i> curves representing pure loss of stability for 120m_C shape	85
Figure 3.46 <i>MaxVCG</i> curves representing pure loss of stability for KL shape	86
Figure 3.47 <i>MaxVCG</i> curves representing parametric rolling for ASL shape	87
Figure 3.48 <i>MaxVCG</i> curves representing parametric rolling for 5415 shape	87
Figure 3.49 <i>MaxVCG</i> curves representing parametric rolling PV shape	88
Figure 3.50 <i>MaxVCG</i> curves representing parametric rolling for 120m_C shape	88
Figure 3.51 <i>MaxVCG</i> curves representing parametric rolling for KL shape	89
Figure 4.1 Conceptual model of an experimental setup. Extracted from (Barlow, William, and Pope 1999)	91
Figure 4.2 Body plan (left) and perspective view (right) of the ASL shape	93
Figure 4.3 Body plan (left) and perspective view (right) of the 5415 shape	93
Figure 4.4 Flow chart for model preparation	94
Figure 4.5 Model orientation in GHS (top) in Rhinoceros (bottom)	95
Figure 4.6 Flow chart for 3D modelling	96
Figure 4.7 Flow chart for milling process	96
Figure 4.8 Moving weight and transverse distance for inclining test	101
Figure 4.9 Comparison of natural roll period test for the ASL shape	104
Figure 4.10 Comparison of natural roll period test for the 5415 shape	105
Figure 4.11 Location of longitudinal rod on model 5415	106
Figure 4.12 The superstructure above water line for the ASL shape	107
Figure 4.13 The superstructure above water line for the 5415 shape	107
Figure 4.14 Perspective view of the test rig	107
Figure 4.15 Side view of test section with spoiler and dummy test section floor	108
Figure 4.16 View from control room toward test section	108
Figure 4.17 TSI Electronic pressure sensor model 9565-P	108
Figure 4.18 DP-CALC Micro manometer 5825 used to verify the wind velocity in the test section	109
Figure 4.19 A set of tubes used to collect static and dynamic pressure	109
Figure 4.20 Arrangement of loads and accelerometer in the model hull	109
Figure 4.21 Both models fixed with rod before the test	110
Figure 4.22 Rod location to the fore of the model	110
Figure 4.23 Rod location to the aft of the model	111
Figure 4.24 Model ASL shape is ready in wind tunnel test section	112
Figure 4.25 Model 5415 shape is ready in wind tunnel test section	112
Figure 4.26 Self levelling cross-line laser used in this experiment	113
Figure 4.27 The rotating table is turned 15° to simulate the wind direction from starboard 75°	113
Figure 4.28 The rotating table is turned 15° to simulate the wind direction from port 105°	114
Figure 4.29 The ASL shape was fitted with a bilge keel	114
Figure 4.30 General arrangement of low speed wind tunnel, UTM	115

Figure 4.31 ArduFlyer setup	116
Figure 4.32 Velocity profile in the test section after the test rig was ready	117
Figure 4.33 Comparison of boundary layer with the models	117
Figure 4.34 Rod used for the model to heel at roll back angle ( $\phi_1$ )	120
Figure 4.35 Definition used in this experiment	122
Figure 4.36 Graph of wind velocity and angle of stable heel for ASL shape and 5415 shape for the experimental results and GHS calculation	123
Figure 4.37 The <i>GZ</i> curves for the ASL shape and 5415 shape	123
Figure 4.38 Roll back angle ( $\phi_{2*}$ ) vs roll to windward ( $\phi_1$ ) for the ASL shape	124
Figure 4.39 Roll back angle ( $\phi_{2*}$ ) vs roll to windward ( $\phi_1$ ) for the 5415 shape	124
Figure 4.40 Roll back angle ( $\phi_{2*}$ ) vs roll to windward ( $\phi_1$ ) for ASL with bilge keel configuration	125
Figure 4.41 Roll back angle ( $\phi_{2*}$ ) vs roll to windward ( $\phi_1$ ) for the ASL shape with and without bilge keel configuration	125
Figure 4.42 Angle of stable heel for wind from starboard 75° and port 105°	126
Figure 4.43 Explanation of yaw angle impact on angle of stable heel	127
Figure 4.44 Roll back angle ( $\phi_{2*}$ ) vs roll to windward ( $\phi_1$ ) for the ASL shape and 5415 shape with wind from beam wind and port 105°	128
Figure 4.45 Comparison of results with IMO rules and Naval Rules	128
Figure 4.46 Angle of stable heel for the ASL shape	130
Figure 4.47 Drag coefficient vs heel angle obtained by calculation for the ASL shape	130
Figure 4.48 Angle of stable heel for the 5415 shape	131
Figure 4.49 Drag coefficient vs heel angle obtained by calculation for the 5415 shape	131
Figure 5.1 Three main steps in CFD	133
Figure 5.2 Domain for the ASL shape	134
Figure 5.3 Domain for the 5415 shape	134
Figure 5.4 Sketch showing definition of quantities used in defining the free surface pressure boundary condition. Extracted from (Hirt and Nichols 1981)	135
Figure 5.5 Cross-sectional grid (x-z plane) for the ASL shape domain	138
Figure 5.6 Cross-sectional grid (x-z plane) for the 5415 shape domain	138
Figure 5.7 <i>GZ</i> curve for the ASL and 5415 shape in 2D and 3D geometry	140
Figure 5.8 Simulation of drag coefficient results (static condition)	142
Figure 5.9 Drag coefficient of various bodies 3-dimensional (left) and 2-dimensional (right) at Reynolds Number between $10^4$ and $10^6$ . Extracted from (Hoerner 1965)	142
Figure 5.10 $C_D$ for ASL ship at 15 degrees leeward (static condition)	143
Figure 5.11 The flow view when model is upright (Velocity magnitude of x-direction)	143
Figure 5.12 $C_D$ for the ASL shape at 15 degree leeward (dynamic condition)	144
Figure 5.13 Results comparison for roll back angle ( $\phi_{2*}$ ) vs roll to windward ( $\phi_1$ ) for the ASL shape	145
Figure 5.14 Results comparison for roll back angle ( $\phi_{2*}$ ) vs roll to windward ( $\phi_1$ ) for the 5415 shape	146
Figure 5.15 Experimental value of $C_D$ , $C_L$ and $C_M$ from wind tunnel test. Extracted from (Ishida, Taguchi, and Sawada 2006).	148

## List of Tables

Table 2.1 Nominal wind environments, adapted from Yamagata (1959)	13
Table 2.2 IMO Rules for Intact Stability Criteria	16
Table 2.3 Naval Ship Intact Stability Criteria. Extracted from (Deybach 1997)	18
Table 2.4 Naval Intact Stability Criteria – The Weather Criterion. Extracted from (Deybach 1997)	21
Table 2.5 Comparison on the weather criterion for the IMO and the Naval rules	22
Table 2.6 Formula for wind heeling arm of the IMO and Naval Rules Criteria	22
Table 2.7 The approaches for estimating aerodynamic effect	23
Table 2.8 Current references for IMO document on second generation intact stability criteria	25
Table 2.9 Wave case occurrences for pure loss of stability	31
Table 2.10 Wave cases	33
Table 2.11 Wave case occurrences for parametric rolling	35
Table 2.12 Value for wave steepness factor, $s$	36
Table 2.13 Previous experimental work related to ship stability	40
Table 3.1 Main characteristics of the models	56
Table 3.2 Variable used for 5415 shape	67
Table 3.3 List of developed macro using GHS	71
Table 3.4 Sample of macro code developed in GHS for pure loss of stability Level 2 criteria 1	73
Table 3.5 Description of 120m_C model	76
Table 3.6 Results of the 5 ships for IMO and Naval Rules	81
Table 3.7 Result of ASL and 5415 shape on weather criterion	81
Table 3.8 Input parameters for weather criterion results	81
Table 4.1 Main characteristics of the ship and model scale	92
Table 4.2 Specification of Euromod MP65	97
Table 4.3 Photographs of model creation	98
Table 4.4 Procedure to change $VCG$	102
Table 4.5 Natural roll period formula	102
Table 4.6 Results for pre-test of the ASL shape	104
Table 4.7 Results for pre-test of the 5415 shape	105
Table 4.8 Scaling ratio used in this experiment	118
Table 4.9 Wind tunnel test matrix	119
Table 4.10 Roll angle ( $\phi_1$ ) value for the ASL and 5415 shapes	121
Table 5.1 Parameters used for the ASL shape and 5415 shape	136
Table 5.2 Number of cells used for this simulation	137

Table 5.3 Properties for 2D and 3D of the ASL and 5415 shape	140
Table 5.4 Natural roll period results comparison, (in seconds)	141
Table 5.5 $C_D$ for the 5415 shape (dynamic condition)	144
Table 5.6 Weather criterion comparison results for the ASL shape	147
Table 5.7 Weather criterion comparison results for the 5415 shape	147
Table 5.8 Elements which contribute to the weather criterion	149

## **List of Annexes**

- A Current document for SGISC
- B Publications



# Table of Contents

<b>Acknowledgements</b>	<b>i</b>
<b>Abstract</b>	<b>ii</b>
<b>List of Symbols</b>	<b>iii</b>
<b>List of Abbreviations</b>	<b>v</b>
<b>List of Figures</b>	<b>vii</b>
<b>List of Tables</b>	<b>xi</b>
<b>List of Annexes</b>	<b>xiii</b>
<b>Table of Contents</b>	<b>xiv</b>
Chapter 1 – Introduction	1
1.1 Background	1
1.2 Problem Statement	5
1.3 Objectives	6
1.4 Research Scope	6
1.5 Significance of the Study	7
1.6 Organisation on this Thesis	7
Chapter 2 – Rules	9
2.1 Ship Stability	9
2.2 Background of Intact Stability Code (IMO)	12
2.3 Background of the Naval Rules	16
2.4 The Weather Criterion	18
2.5 Comparison the IMO Rules and the Naval Rules for the weather criterion	21
2.6 Development of Second Generation Intact Stability Code	24
2.6.1 Pure Loss of Stability	26
2.6.2 Parametric Rolling	26
2.6.3 Surf-Riding/Broaching	27
2.6.4 Dead Ship Stability	28
2.6.5 Excessive Acceleration	29

2.7	Evaluation of Second Generation Intact Stability	30
2.7.1	Pure Loss of Stability	30
2.7.2	Parametric Rolling	32
2.7.3	Surf-Riding/Broaching	35
2.7.4	Dead Ship Condition	35
2.7.5	Excessive Acceleration	36
2.8	Earlier Experimental Work	36
2.9	Model Selection	40
2.10	Weather Criterion Explanation	41
2.11	Wind Tunnel	44
2.12	Wind Healing Arm	45
2.13	Roll Damping	48
2.14	Current Research Approach	49
Chapter 3 – General Hydro Statics (GHS) and Results		52
3.1	Introduction to GHS	52
3.2	Background Information on the Ships	53
3.3	Ship Description	54
3.3.1	The ASL Shape	54
3.3.2	The 5415 Shape	54
3.3.3	The PV Shape	55
3.3.4	The 120m_CS Shape	55
3.3.5	The KL Shape	56
3.4	Current 2008 Intact Stability Code	58
3.4.1	Righting Lever Curve Properties	59
3.4.2	The Weather Criterion	63
3.5	Macro Code Developed in GHS	71
3.6	Code Verification	75
3.7	Results and Discussion	80
3.7.1	2008 Intact Stability and Naval Rules	80
3.7.2	Pure Loss of Stability Failure Mode	81
3.8	Conclusion	89
Chapter 4 –Experimental Setup and Results		91
4.1	Introduction to the Wind Tunnel Test	91

4.2	Model Selection	92
4.3	Model Preparation for the Wind Tunnel Test	93
4.3.1	Model Construction	94
4.3.2	Model Verification	100
4.3.3	Model Pre-Test	100
4.3.4	Pre-Test Results	103
4.4	Test Rig Design	105
4.5	UTM's Low Speed Wind Tunnel	114
4.6	Instrumentation and Data Collection	115
4.7	Wind Velocity Profile Test	116
4.8	Scaling Criteria	117
4.9	Test procedure	118
4.9.1	Wind Off Test (Natural Roll Period)	120
4.9.2	Wind On Test	120
4.9.3	Roll Angle ( $\phi_1$ ) Prediction	121
4.10	Results and discussion	121
4.10.1	Angle of Stable Heel ( $\phi_0$ ) versus Wind Velocity	122
4.10.2	Roll Back Angle ( $\phi_2^*$ ) versus Roll to Windward ( $\phi_1$ )	123
4.10.3	Ratio $\phi_2^*$ and $\phi_1$ with Bilge Keel	125
4.10.4	Yaw Angle Effect on Stable Heel	126
4.10.5	Effect of Roll to Windward ( $\phi_1$ ) and Roll Back Angle ( $\phi_2^*$ ) With Yaw Angle	127
4.10.6	Comparison of IMO GHS and Experimental Results	128
4.10.7	Comparison of IMO GHS Drag Coefficient and Experimental Results	129
4.11	Conclusion	131
Chapter 5 –2-Dimensional Numerical Simulation and Results		133
5.1	Introduction	133
5.2	Computational Setup	135
5.3	Mesh Management	136
5.4	CFD: The ISIS-CFD Flow Solver	138
5.5	Result and Discussion	139
5.5.1	GZ Curve (2-dimensional)	139
5.5.2	Natural Roll Period	140
5.5.3	Drag Coefficient for Static Ship Simulation	141

5.5.4	Drag Coefficient for Dynamic Ship Simulation	143
5.5.5	Results Comparison of Roll Back Angle	145
5.5.6	The Weather Criterion	146
5.5.7	Scrutiny of the Weather Criterion by IMO Naval, Naval Rules, Experiment and 2 Dimensional Simulation	148
5.6	Conclusion	149
Chapter 6 – Conclusion		150
6.1	Conclusion	150
6.2	Concluding Remarks	150
6.3	Suggestions for Future Works	151
Resume Etendu		153
Executive Summary		162
References		170

# Chapter 1 – Introduction

This section defines the overview of this research project. It explains the importance of the research, the objectives, the scope and significant impacts of this study for the maritime industry. In the final paragraph, the organisation of the chapters in this thesis is explained.

## 1.1 Background

Ship stability is an extremely important subject in the field of Naval Architecture, its fundamentals having wider implications for the design and operation of ships and floating units. Moreover, “stability” is a concept which, in Naval Architecture, has a very broad meaning, embracing ship stability fundamentals including ship dynamics and ultimately ship safety. Safety and stability are two key aspects of the successful design of ships in addition to maintain the balance between the efficiency and performance of the ship. Modern ship designs are outpacing the regulators’ rules and guidelines.

This research does not go into detail on the history of the ship stability theory nor the development of stability rules. The main focus is on the origin and development of the second generation intact stability rules concerning the adaptation of new rules to existing codes. Thus, this paper aims to explore the current and future potential methods for a direct assessment of the weather criterion or dead ship condition.

Humans have floated for thousands of years throughout the oceans without knowing exactly how and why this was possible. Archimedes introduced the basic laws of the hydrostatics of floating bodies in 300 B.C. He was the first person to formulate the basic law of buoyancy. He also laid the foundations of the stability of floating bodies by introducing the concept of the balance of couples of force and moments known as the *Law of the Lever*. In layman’s terms, Archimedes’ principle states that when a body is partially or completely immersed in a fluid, it experiences an apparent loss in weight. The losing weight is equal to the weight of the fluid displaced by the immersed part of the body.

The concepts in naval architecture known as buoyancy and stability were founded on the roots of Archimedes’ principle. Indeed, the development of ship stability as a science occurred very late in the 18th century with two different approaches based on the introduction of the metacentre and the righting moment as stated by Francescutto (Francescutto 2016). These approaches were developed by Bouguer and Euler respectively.

Nowadays, a basic requirement to minimise the risk of the capsizing of ships is known as intact stability. The International Code on Intact Stability, 2008 (2008 IS Code) is based on a *state-of-the-art* concept, available at the time it was developed, taking into account the sound design and engineering principles and experience from operating ships (IMO 2009). It applies to all types of ships or marine vehicles of 24m in length and operating in international waters. It is a guideline for the ship designer, ship operator, and classification society to design, build and commission the ship before it commences its service at sea. A comprehensive background study of intact stability development was written by Kuo & Welaya (Welaya and Kuo 1981). Their article, "A review of intact stability research and criteria", stated that the first righting arm curve was proposed by Reed in 1868, but the application was presented by Denny in 1887. In addition, in 1935, Pierrottet tried to rationally establish the forces which tend to capsize a ship and proposed a limiting angle to which the dynamic level of the ship must be equal or greater than the sum of the effort of the inclining moments. However, Pierrottet's proposal was too restrictive in the design process, and it was not accepted. Kuo and Welaya also mentioned the famous doctoral thesis written by Jaakko Rahola in 1939. Rohola's thesis evoked widespread interest throughout the world at that time, because it was the first comprehensive study. It also proposed a method to evaluate intact stability, which did not require complex calculations.

The intact stability code used for naval ships is known as the Naval Rules. The naval ship intact stability criterion was defined during World War II (WWII). Before WWII, the criteria used were based on metacentric height ( $GM$ ), a range of stability and maximum righting arm. For the damaged stability criterion, it is required that the ship to have two flooded compartments (symmetrical flooding) and sink below the margin line (Frederic 1997). Since the physics for the Intact Stability Code for the International Maritime Organisation (IMO) and the Naval Rules are the same, the rules should not be significantly different, and the basis for both criteria should be understood and well written for the reference of future generations.

In 1975, the First International Conference for ship stability was held at the University of Strathclyde and Tsuchiya presented a new method for treating the stability of fishing vessels (Tsuchiya 1975). He introduced a list of coefficients to define the weather stability criteria. He disregarded the idea of a stability assessment using simple geometrical stability standards such as metacentric height and freeboard, or the shape of the righting arm curve. He proposed some factors which, in his opinion, were crucial. He introduced a certain coefficient which should be calculated and plotted on a diagram as a function of metacentric height and the freeboard for every stability assessment. He concluded that his proposed method should be confirmed by a comparison with actual data on fishing boat activities and empirical stability standards.

In 1993, the first generation intact stability criteria were originally codified at the IMO as a set of recommendations in Res A.749(18) by taking into account the former Res.A.167 (ES.IV) ("Recommendation on intact stability of passenger and cargo ships under 100 meters in length" which contained statistical criteria, heeling due to passenger crowding, and heeling due to high speed turning, 1968) and Res A.562.(14) ("Recommendation on a severe wind and

rolling criterion (Weather Criterion) for the intact stability of passenger and cargo ships of 24 meters in length and over," 1985). These criteria were codified in the 2008 IS Code and became effective as part of both SOLAS and the International Load Line Convention in 2010 in IMO Res MSC.269(85) and MSC.207(85)(Peters et al. 2012).

The revision of the 2008 Intact Stability Criteria (2008 IS Code) started in 2001 with a critical analysis submitted by the Italian delegation to the IMO concerning the need for updating and tuning some coefficients of the weather criterion, given its excessive weight in determining the limiting VCG for ships with large values of the beam to draught ratio. This was considered an opportunity to “shake up” the 2008 IS Code foundations and place them on a more physical basis through the development of new performance-based criteria originally intended to replace the old criteria (Francescutto 2016). The new IS Code will be known as the Second Generation Intact Stability Criteria (SGISC). After much comprehensive discussion and thorough debates in the IMO and several conferences, it was subsequently decided that the following possible stability failures should be individually addressed (Bassler et al. 2009; Francescutto and Umeda 2010; Peters et al. 2011):

- a. Dead ship condition;
- b. Following/stern quartering seas associated with matters related to stability in waves, in particular, reducing righting levers of a ship situated on a wave crest;
- c. Parametric resonance, including consideration of matters related to large acceleration and loads on cargo and stability variation in waves;
- d. Broaching, including consideration of matters related to manoeuvrability and course keeping ability as they affect stability;
- e. Excessive acceleration.

Moreover, the SGISC will be structured into three levels which are: Vulnerability Level 1, Vulnerability Level 2 and Direct Assessment. The 1<sup>st</sup> level vulnerability, through simple calculation, should efficiently identify ships called “unconventional”, for which the particular stability failure mode considered could represent a potential risk. The other two levels should confirm or reject this, thus reducing the number of false positives. It is expected that the 2<sup>nd</sup> level vulnerability can be used, in the case of failure, to develop “operational limitations” as an alternative to design modifications. Specific “Operational Guidelines” should be added as a sort of “fourth level”, in the acknowledgement that not all situations could be dangerous. Direct assessments are intended to employ the most advanced *state-of-the-art* technology available, either by numerical analysis or experimental work for quantitative validation.

The International Conference on Stability of Ship Ocean Vehicles (STAB) and the International Ship Stability Workshop (ISSW) are certainly the venues where the expertise and



contemporary developments in the naval architect field tend to be collected and thoroughly debated. An experimental evaluation of weather criteria was carried out at the National Maritime Research Institute in Japan for the direct assessment of the proposal of dead ship condition. The researchers conducted a wind tunnel test with wind speeds varying from 5m/s to 15 m/s. The results showed some differences compared to their previous experimental work. For example, the wind heeling moment depended on the heel angle and the centre of drift force was higher than the half draught (Ishida, Taguchi, and Sawada 2006). The experimental validation procedures for numerical intact stability assessment with the latest examples were presented by Umeda and his research members in 2014 (Umeda et al. 2014). They equipped the seakeeping and manoeuvring basin of the National Research Institute of Fisheries Engineering in Japan with a wind blower to examine dead ship stability assessment.

A review of available methods for the application of second level vulnerability criteria was presented at STAB 2009 (Bassler et al. 2009). They concluded that the choice of environmental conditions for the vulnerability criteria is at least as important as the criteria themselves. A test application of the second generation IMO intact stability criteria on a large sample of ships was presented during STAB 2012. Additional work remains to be carried out to determine a possible standard for the criteria and environmental conditions before finalising the second generation intact stability criteria (Wandji, Veritas, and Corrigan 2012). During the ISSW 2013, Umeda presented the current status of the development of second generation intact stability criteria and some recent efforts that had been made (Umeda 2013). The discussion covered the five failure modes: pure loss of stability, parametric rolling, broaching, harmonic resonance under dead ship condition and excessive acceleration.

With regard to ship stability, evaluation of the ship stability in beam seas and winds requires a deliberate consideration of the modelling of wind and wave forces. However, much research has been devoted to the hydrodynamics of ship rolling motions and relatively limited work has been dedicated to wind heeling loads on ships. This situation is particularly surprising when considering that the current intact stability criteria are based largely upon the heeling of ships under wind forces. Dealing with the weather condition, the 2008 IS Code addressed this phenomenon in the weather criterion (as contained in IMO Res A.749). While waiting for the SGISC to be enforced, computer code is being used to compute the stability performance that must be developed in pace with the development of the rules. The code must be validated before it is widely used in the ship design process.

Most research on ships has involved experimental work in the towing tank facility. A proper modelling of the typical environmental wave characteristics is fundamental to gain accurate estimations of the ship motion. Understanding the aerodynamics and wind effect also has the same importance as understanding the wave characteristics. However, limited research activities on understanding the aerodynamic effect have created a gap in the naval architecture area. For the current intact stability code, the effect of wind is studied in the weather criteria section. In 2016, during the IMO Subcommittee on Ship Design and Construction (SDC), the weather criterion was improved in the failure mode of dead ship condition for the SGISC. The

Vulnerability Level 1 for dead ship condition is used in the same criterion as stated in the 2008 IS Code. The scenario of dead ship condition is explained in Figure 1.1 (IMO 2016).

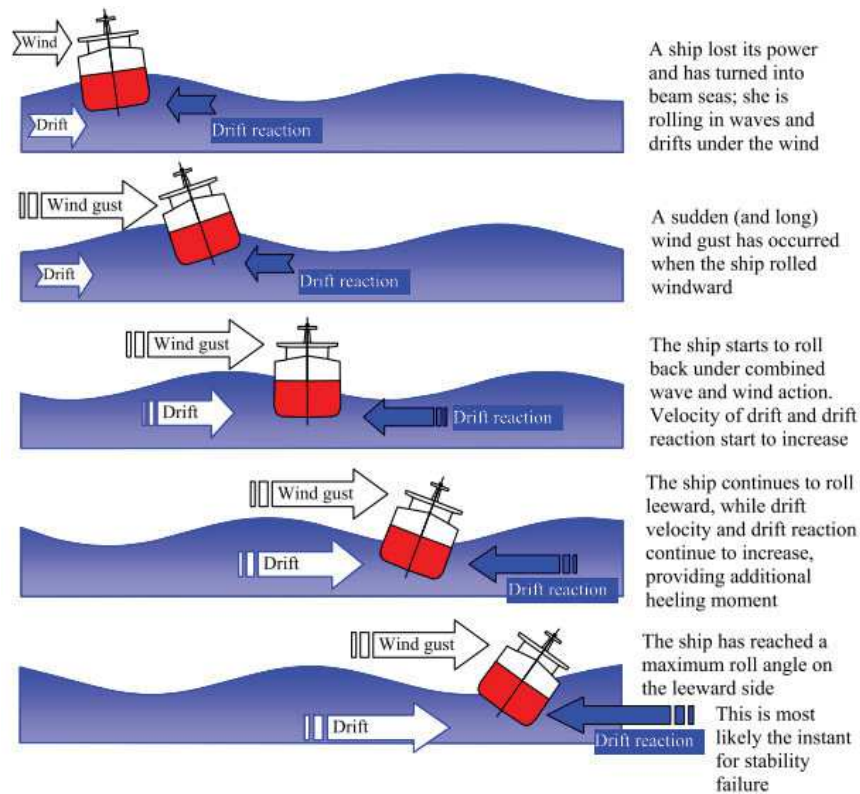


Figure 1.1 Scenario of dead ship condition. Extracted from (IMO 2016)

The draft amendment of the IS Code regarding the vulnerability criteria and the standards (Levels 1 and 2) related to dead ship condition and excessive acceleration are included in SDC 3/INF.10 Annex 1 and 2 (IMO 2015). The Level 1 check for dead ship condition is the same method as that used for the current IS Code 2.3 which is the weather criterion. If it fails, the design should progress to Level 2 check and Direct Assessment. Direct assessment procedures for stability failure are intended to employ the most advanced *state-of-the-art* technology available, either by numerical analysis or experimental work for a quantitative validation as stated in SDC 1/INF.8 Annex 27 (IMO 2013). This research will propose the option for a direct assessment of dead ship condition for the second generation intact stability criteria. To the best of the authors' knowledge, to date, there has been no proposal submitted to the IMO for direct assessment by experimental approach for dead ship condition. Therefore, the contribution of this research will open a new method to explore the possibility of verifying the dead ship condition and weather criterion.

## 1.2 Problem Statement

There are two major concerns in ship stability for the survivability of the ship at sea which are the buoyancy and stability. Insufficient buoyancy may lead to sinking, and insufficient stability may cause capsizing. A set of regulations and guidelines for ship

construction are in place and have been enforced by the authorities. The evolution of ship appearance, loading condition, technological advancement and environmental disturbance have changed the *state-of-the-art* of ship design. The requirement for understanding ship stability, motion, behaviour, and response towards actual sea conditions has now become crucial. This research study proposes some solutions for dealing with the new regulations in the second generation intact stability criteria which will be enforced very soon. A macro code is being developed using the General Hydrostatic (GHS) software for the Level 1 and 2 criteria for parametric rolling, pure loss of stability, broaching and dead ship condition. Dead ship condition is related to the weather criterion in the 2008 IS Code. Experimental work was performed in the wind tunnel and two ship models were tested. The results showed the safety margin pertaining to the weather criterion. Finally, illustrative examples are presented to verify the existing and future regulations that can prevent certain obvious dangerous situations.

### 1.3 Objectives

The objectives of this research are to:

- a. Propose the macro code for computing the Level 1 and 2 for SGISC;
- b. Validate the proposed stability computer code with other stability software;
- c. Identify the effect of roll angle to windward due to wave action ( $\phi_1$ ) in weather criteria;
- d. Identify the roll back angle ( $\phi_2$ ) in weather criteria;
- e. Identify the yaw angle effect of rolling back angle;
- f. Validate the results through stability calculations, experiments and simulations;
- g. Explain the impacts of aerodynamics and hydrostatics on the basic model;
- h. Develop simulation code to compare the results between numerical, experimental and current approaches.

### 1.4 Research Scope

The scopes of this research are:

- a. Code development uses the commercial stability code named General Hydrostatics (GHS),
- b. Only the effects of hydrostatics and aerodynamics are considered during the wind tunnel test,
- c. The damping effect is based on hydrostatics without wave effect,
- d. The analysis in Reynolds-average Navier-Stokes (RANS) solver is 2-dimensional.

## 1.5 Significance of the Study

The limits of wind tunnel experimental results are affecting the development of the weather criterion. The weather criterion is related to the dead ship condition in the second generation intact stability criteria. In SDC 3, the dead ship condition has still not been finalised. This research has used a ship model that has similar hydrostatic properties. Most of the previous studies analysed the moment and force but failed to consider similar hydrostatic properties and thus did not represent the true results of the ship.

## 1.6 Organisation on this Thesis

This research is divided into 6 chapters. Each chapter explains the effort to conduct this research, in detail. As a summary of this effort, the flow of this thesis is shown in Figure 1.2.

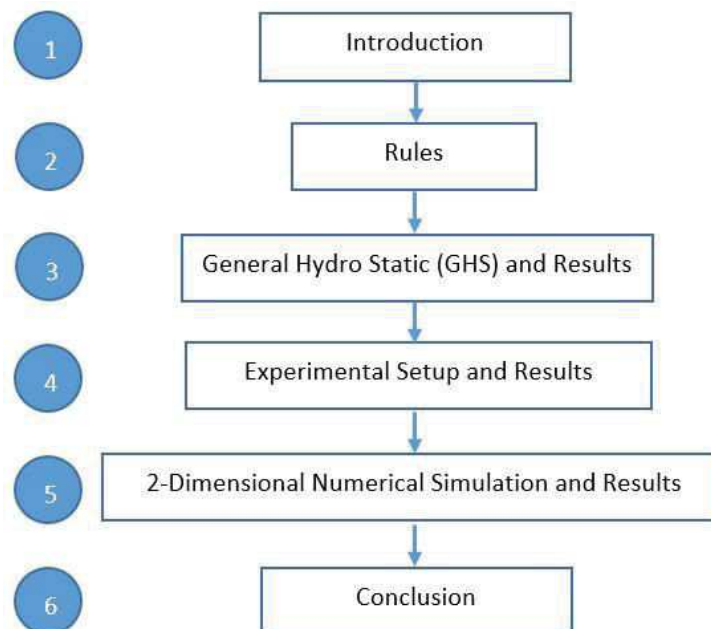


Figure 1.2 Thesis organisation

Chapter 2 presents the existing and proposed intact stability rules. The complete set of the second generation intact stability criteria is given in Annex A but, in this chapter, we highlight the important aspects of these new rules.

In Chapter 3, we verify how these new rules can be implemented in an existing professional hydrostatic solver by means of macros. We used five different ships for the verification. We then concentrate on the weather criterion. This is an existing rule and the IMO computation to verify the ship vulnerability is based solely on hydrostatics although it involves complex hydrodynamic phenomena. The new set of rules includes a Direct Assessment (DA) level. We were interested in developing a DA procedure for this existing criterion.

Firstly, we consider performing a DA by means of experimental trials. Two models were built, equilibrated and tested in the wind tunnel, which included a water tank. Chapter 4 presents the setup and the results. Encouraged by these results, we also wanted to perform a DA by means of Computational Fluid Dynamics (CFD). Because 3-dimensional (3D) is beyond our computing resources, we decided to limit our study to 2-dimensional (2D) CFD.

We show that the method is conservative enough and affordable. The CFD also permitted us to investigate how the drag coefficient of the ship superstructure behaves. We then conclude the study in Chapter 6.

## Chapter 2 – Rules

In this section, a review of studies related to the aspects of importance of this thesis is presented. These studies can be categorised into two areas: the first is the current intact stability criteria related to the 2008 IS Code and the second is the development of the second generation intact stability criteria. Furthermore, a historical review related to intact stability and the weather criterion is provided. A significant topic of this thesis is the experimental work on the weather criterion. The previous experimental works were tabled for comparison with the current research work. Moreover, the variant of the intact stability code for commercial ships which is the 2008 IS Code and for a naval ship which is the Naval Rules are discussed. Some differences between both codes are discussed to understand the principal grounds for each measure.

### 2.1 Ship Stability

Ship stability is an important subject in the naval architect domain. The risk of capsizing has always been of crucial importance to ship designers, ship operators and regulatory bodies. It is a guideline to design, construct and commission the ship before it sets out on its service of a lifetime at sea. Primarily, there are three main objectives to bear in an overview of the critical inspection of ship stability. The first is to provide a better understanding of this difficult problem by analysing and summarising the major research efforts which have been conducted all over the world. The second is to examine and evaluate the background and basis for the existing stability criteria. The third is to draw conclusions which could help those who require the findings of stability studies and to serve as a guideline to future research efforts. The analytical and experimental research studies are classified under the three different categories of conventional approaches, theoretically based studies, experimental studies and correlation with theory (Welaya and Kuo 1981).

Fundamentally, ship stability is divided into two categories which are intact stability and damage stability. Intact stability is the obligatory criteria to be fulfilled before the ship design continues to further stages such as seakeeping, manoeuvring, and endurance. Intact stability means that the ship is in a standard operation and configuration. The hull is not breached in any compartment. In ship design, another requirement to be fulfilled by the ship designer is damage stability.

The damage stability standard has been intensively debated over the past decade by the Subcommittee on Stability and Load Lines and on Fishing Vessel Safety (SLF), based on the

“probabilistic” method of determining damage stability, which is different from the previously used “deterministic” method. Although the methods are different, the objective of both methods is the same as “ships shall be as efficiently subdivided as is possible, having regard to the nature of the service for which they are intended. The degree of the subdivision shall vary with the subdivision length of the ship and with the service, in such manner that the highest degree of subdivision corresponds with the ships of greatest subdivision length, primarily engaged in the carriage of passengers”.

Stability is the ability of the totally submerged or partially submerged body to float upright, meaning when a sudden external force is applied to the ship that resulted in an angle of list, she should be able to come back into an upright position. Longitudinal stability and transverse stability are different. In fact, longitudinal stability is sufficient because the length of the ship is not comparable to the moment caused by an external force in the longitudinal direction. Transverse stability is a major concern in ship design. In this research, most of the analysis examines the transverse stability requirement.

Presently, ship stability in an intact condition is formed by the “design oriented” IMO/SOLAS regulations or class rules. The objective of the design approach is to verify specific design loading conditions and determine limitations regarding the acceptable *VCG* values to guarantee a “sufficient static roll that is restored” according to specific requirements. Fulfilment of this requirement is implicitly assumed to provide a “sufficient level of safety”. Some general indications are given by regulations regarding the risk involved in having too large a static in restore, since this can lead to excessive accelerations (Shigunov et al. 2011). However, such indications do not typically translate into quantitative limitations on *GM*. Some quantitative indications regarding too large metacentric heights can be applied in the preparation of the cargo securing manual, for those vessels for which this is relevant. The main weakness of such an approach is that the criteria used for the determination of acceptable/unacceptable loading conditions are mostly semi-empirical in nature, and do not provide explicit information regarding the specific possibility of dangerous phenomena that a vessel could be prone to in a specific loading condition. Moreover, in several cases, existing regulations do not sufficiently cover certain dangerous phenomena, which are typically associated with large amplitude ship motions under the action of wind and waves. This could lead to an increase in the risk of crew injuries, and loss or damage of cargo in heavy seas, despite fulfilling the current regulation.

To mitigate the existing issues of the 2008 IS Code, a delegation from Italy submitted the critical analysis to the IMO, concerning the need to update and tune some coefficients of the weather criterion, given its excessive weight in determining the limiting *VCG* for ships with large values of the beam to draught ratio. The last stability criteria were indeed identified as a source of difficulties due to their partly or totally empirical character which originated a non-uniform distribution of safety among different ship typologies. At the same time, their structure rendered these criteria quite difficult to modify without a possible significant loss in ship safety level of the ship covering the present world fleet. The first element of the long work undertaken in the improvement of the IMO Intact Stability Code in 2001 was completed in 2008 with the



establishment of an ad-hoc Working Group (WGIS) operating during the Sessions of the SLF and intersessions between them.

This part of the WGIS activity was mostly devoted to restructuring the previous Intact Stability Code (IMO 1993) in several parts and making Part A of the new International Code on Intact Stability, 2008 (IS Code, 2008) mandatory under the provisions of both SOLAS and ILLC Conventions. This action was partly a consequence of the development of a Formal Safety Assessment (FSA) study, made by the German Delegation at the IMO, proving the potential cost effectiveness implied in this change of legal status. The Code was also subjected to some polishing, clarification, and elimination of some ambiguities. In addition, explanatory notes to the 2008 IS Code were issued, mostly consisting of a review of the history of intact stability leading to the present regulatory situation. It is noteworthy, however, that the explanatory notes also contain guidance for an alternative application of “criteria regarding the righting lever curve properties”, in particular, the rule requiring the position of the maximum of *GZ* to be above 25°.

The framework of the SGISC can be seen as a shift of paradigm, from the current situation where ships are regarded as safe when designed and loaded in accordance with the current stability criteria under the assumption that they are operated on the basis of generic good seamanship to a situation where ships would also be designed considering the possibility of developing ship-specific operational guidance as a means for keeping the likelihood of stability failures below an acceptable limit. The present target date for addressing “guidelines for direct stability assessment” and “requirements for development of ship-specific operational guidance” within SGISC has been set to that of SDC 4, which is expected to be held in 2017 (Backalov et al. 2016).

For the weather criterion, an alternative way of assessment, completely or partially based on experiments on scale models in the towing tank/wind tunnel, has been opened, based on both the obsolescence of the existing weather criterion due to the variations in ship forms and loading, and the need to correct some inconsistencies in the original formulation. Notwithstanding the importance of this work, the most important part of the initial scope of the revision is the formulation and implementation of a new generation of intact stability criteria performance, which is still, to a large extent, lying on the carpet. The time past is in any case important for proving the potential cost-effectiveness implied in the new criteria and for the maturation of some important concepts connected with the dangerous phenomena to be covered, the basic structure and dictionary, and the philosophy of application of the new criteria (Francescutto 2016).

As a consequence, a new rule by the SGISC will be implemented as an additional requirement in the intact stability criteria. The historical theory of ship stability for the previous and future criteria must be clearly explained for future expertise in the naval architect field.

## 2.2 Background of Intact Stability Code (IMO)

The basis of ship stability is its geometry and weight distribution. In other words, it is grounded on the righting arm ( $GZ$ ) curve of the ship in still water. Even though it seems a very old concept, it is useful and involves having a few drastic assumptions, and it is still the foundation of most existing regulations. There are four main assumptions behind the approach. The first is that the buoyancy remains constant, the second is that any contribution due to kinetic energy or energy dissipation is ignored, the third is that all types of excitation are of a potential nature and stationary and the fourth is that coupling and other hydrodynamic forces can be ignored (Welaya and Kuo 1981).

A comprehensive background study of intact stability development was written by Kuo & Welaya (Welaya and Kuo 1981). Their paper on "A review of intact stability research and criteria" stated that the first righting arm curve was proposed by Reed in 1868, but the application was presented by Denny in 1887. In addition, in 1935, Pierrottet tried to rationally establish the forces which tend to capsize a ship and proposed a limiting angle at which the dynamic level of the ship must be equal to or greater than the sum of the effort made by the inclining moments. However, Pierrottet's proposal was too restrictive in the design process, and it was not accepted. Kuo and Welaya also mentioned the famous doctoral thesis written by Jaakko Rohala in 1939. Rohala's thesis evoked widespread interest throughout the world at that time because it was the first comprehensive study that proposed a method to evaluate intact stability which did not require complex calculations. The study was based on the results of official enquiries related to 34 cases of capsizing (Rohala 1939). The bibliography about Rohala's life and his work on stability was written by Arjava (Arjava and Risto 2015).

A typical paper on conventional ship stability was read in 1951 by Skinner. In this paper, he considered three cases of endangered small vessels. These are wave heeling moment, adverse wind couple and shipping of water. In his study, he plotted the heeling and righting moments on the same diagram and compared the area under the two curves. From this information, he concluded that the effect of shipping of water, although a contributory factor, is insufficient in itself to cause loss and that cargo shift is unlikely to be a basic cause of the loss of small ships in a fully loaded condition. In all of his calculations, Skinner concentrated on the beam sea, which he regarded as the most critical condition.

In ship stability, the IMO and International Towing Tank Conference (ITTC) are the two main contributors to the marine engineering domain. The IMO is a United Nation specialised agency with responsibility for the safety and security of shipping and the prevention of marine pollution by ships. As a specialised agency in the United Nations (UN), the IMO is the global standard-setting authority for the safety, security and environmental performance of international shipping. The ITTC is a voluntary association of worldwide organisations that have the responsibility for the prediction of the hydrodynamic performance of ships and marine installations based on the results of physical and numerical experiments. For the weather criterion, the symbols used by the IMO are stated in their 2008 code (IMO 2009) and those of the ITTC are stated in the ITTC Symbols and Terminologies List (ITTC 2014). The significant

difference in both standards is the symbol used for angle of heel. ITTC uses a phi ( $\phi$ ) and IMO uses a  $\phi$ . In this thesis, the heel angle is represented by the ITTC standard which is phi ( $\phi$ ).

The IMO Sub-Committee on Subdivision and Stability was formed in 1962, and the first international stability criteria were adopted in 1968 with Resolution A.167 (IMO 1968). These criteria which apply to passenger and cargo ships under 100 metres in length, use the righting arm curve, and are based on a famous doctoral thesis by Rohala (Rohala 1939). This resolution was followed by Resolution A. 562 (IMO 1985) which applies to passenger and cargo ships over 24 meters in length and includes criteria considering the wind and the balance between capsizing and restoring energy. These resolutions were updated by Resolution A.749 (IMO 1993) which combines the requirements of Resolutions A.167, A.206 (ships carrying deck cargo), A.168 (fishing vessels) and A.562 into a single intact stability code. Resolution A.749 uses simplified equations and tables. It does not show its method of calculation from the fundamental principles. Working papers presented at meetings of the Subcommittee on Subdivision, Stability and Load Lines during the late 1970's and early 1980's were used to reconstruct the basis and history of A.749. In 1979, Japan proposed a weather criteria to complement the righting arm criterion of Resolution A.167 which considers the wind with gusts (IMO 1979). It considers that the ship is rolling in waves with an amplitude of  $\phi_1$  (rollback angle), around an equilibrium heel angle ( $\phi_0$ ) due to a steady wind. The ship is subjected to a gust when at its maximum heel to windward. Dynamic stability must be sufficient to prevent the ship from heeling to leeward beyond the flooding angle  $\phi_2$ . Sufficient dynamic stability is achieved when area  $A_2$ , is equal to or greater than area  $A_1$ . The steady wind speed proposed by Japan is  $26 \text{ ms}^{-1}$  for ocean-going ships and  $19 \text{ ms}^{-1}$  for coastal ships. According to Yamagata, the selection of  $26 \text{ ms}^{-1}$  is the average between the maximum winds of a tropical cyclone (called a typhoon by the Japanese) and the steadier winds in the immediate aftermath. It also made allowance for waves that tend to be younger and therefore steeper in short duration winds compared to the more fully developed waves that occur with time. However, for the examination of the actual data presented, especially Table III by Yamagata (1959) (adapted as Table 2.1 here), would suggest a higher value (Yamagata 1959). Gust speed is  $\sqrt{1.5}$  times the steady wind speed (or 1.5 times the steady heeling moment). No justification for the choice of wind speed or gust speed is given in the working paper. Heeling moments are calculated using these wind speeds as in the US Navy criteria, but without the cosine square term. The heeling arm does not vary with the heel angle.

Table 2.1 Nominal wind environments, adapted from Yamagata (1959)

Event	Average trailing wind speed ( $\text{ms}^{-1}$ )	Maximum wind speed at centre ( $\text{ms}^{-1}$ )	Application
Barometric Gradient	10	-	Smooth water
Front	15	-	Inshore
Low	15	32	Offshore
Typhoon	20	50	Ocean going

The Japanese criteria specify roll amplitude based on resonant roll amplitude (in degrees) in regular waves:

$$\phi = \sqrt{\frac{\pi \cdot r \cdot \phi_w}{2N}} \quad (2.1)$$

Where:

- $r$  = effective wave slope factor =  $0.73 + 0.6 (OG/T)$ ,
- $OG$  = vertical distance between G and water line (m),
- $T$  = ship draught (m),
- $s$  = wave steepness = wave height / wave length =  $h / \lambda$ ,
- $\phi_w$  = wave slope =  $180 \times s$  (degrees),
- $N$  = Bertin's roll damping coefficient = 0.02.

Based on this resonant amplitude, Japan proposed the following standard rolling amplitude in irregular wave ( $\phi_1$ ):

$$\phi_1 = 0.7\phi = \sqrt{\frac{138 \cdot r \cdot s}{N}} \quad (2.2)$$

Where:

- $s$  = wave steepness = wave height / wave length =  $h / \lambda$ ,

Wave steepness is calculated using the relation between wave steepness and wave age developed by (Sverdrup and Munk 1947). Wave age is represented by the wave speed / wave speed ratio. For a given wind speed ( $26 \text{ ms}^{-1}$  in this case), wave steepness is given as a function of the wave period,  $T$  (in seconds) by using the deep water wave relationship:

$$\text{Wave speed} = C = \sqrt{\frac{138 \cdot r \cdot s}{N}} = \frac{g}{2\pi} T \quad (2.3)$$

Japan proposed a linear approximation of the resulting curve with:

$$s = 0.151 - 0.0072 T \quad (2.4)$$

Resonant roll amplitude occurs when the wave excitation period is equal to the natural roll period of the ship. The wave steepness is calculated at this roll period. The natural roll period is:

$$T = 2\pi \frac{k_x}{\sqrt{g GM}} \quad (2.5)$$

Where:

- $k_x$  = radius of gyration about the longitudinal axis (m).

The USSR (IMCO 1982) proposed an alternative method to calculate the amplitude of rolling. This method is derived from the “Rules of the Register of Shipping of the USSR,” and it was obtained by approximation from calculations of rolling amplitudes in irregular seas for different types of ships. The calculations are based on the fundamental equations of motion with the coefficients obtained from experimental data. In contrast to the Japanese criteria, this method takes into account the dependence of the roll damping coefficient on the hull form and the effect of appendages. The members of the Subcommittee completed calculations for a number of existing ships using the Japanese weather criteria, USSR criteria and Resolution A.167. The Japanese weather criteria were found to be more constraining than A.167 at low displacement. A combination of these methods proposed by the Subcommittee resulted in the following expression for roll back angle:

$$\phi_1 = \frac{k X_1 X_2}{C} \phi_{1\text{Japan}} \quad (2.6)$$

Where:

- $\phi_{1\text{Japan}}$  = rolling amplitude calculated with the Japanese method,
- $k, X_1$  and  $X_2$  = correction factors described in the USSR method and provided in A. 749 Tables
- $C$  = coefficient from test calculations = 0.76.

Resolution A.749 specifies a combination of the area requirement under the righting arm curve required by A.167, and a dynamic energy balance with a wind requirement or “weather criteria”. The IMO rules regarding intact stability can be divided into two parts which are the righting arm curve and the weather criterion. The requirements of the IMO rules are stated in Table 2.2. The *GZ* curve for weather criterion is shown in Figure 2.1 (Symbol for angle of heel is  $\phi$  in Figure 2.1 is equal to  $(\phi)$  as ITTC symbol).

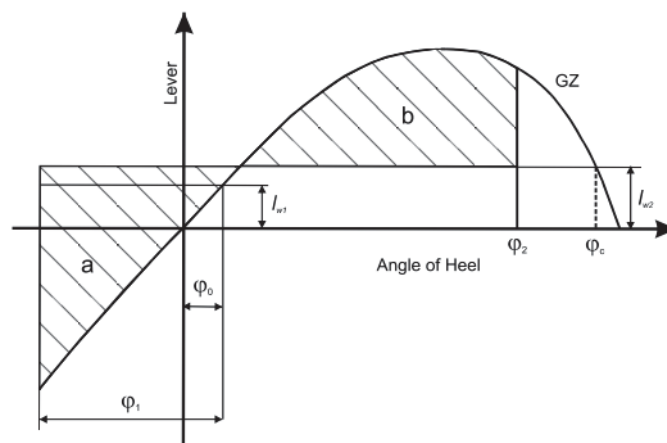


Figure 2.1 *GZ* curve for the weather criterion. Extracted from (IMO 2009)

Table 2.2 IMO Rules for Intact Stability Criteria

Criteria	Limit
<u>1. Righting lever curve properties</u>	
Criteria on righting arm curve ( <i>GZ</i> ): Area under <i>GZ</i> curve with heel angle:	
a. 0 to 30°	> 0.055 m.rad
b. 0 to 40° or flood	> 0.090 m.rad
c. 30° to 40° or flood	> 0.030 m.rad
Righting arm at abs 30 degree	> 0.2 m
Abs angle at maximum righting arm	> 25 degrees
<i>GM</i> Upright	> 0.15 m
<u>2. Severe wind and rolling criterion (Weather criterion) refer Figure 2.1.</u>	
a. Angle of stable heel ( $l_{w1}$ )	< 16 degrees or 80% of angle of the deck immersion
b. With lever (wind + gust) the area $b$ must greater than $a$ .	$b > a$

### 2.3 Background of the Naval Rules

From a naval perspective, naval vessels are not required to obey the IMO regulations considering naval ships to be special ships. To a certain extent, a navy has the same concerns relative to stability failures as all ship owners, architects and operators. The significant differences arise from the fact that a navy is not governed by IMO regulations; that the naval vessel is often costlier than a commercial vessel; and that the naval vessel may not have the luxury of avoiding dangerous weather conditions when performing her missions, while a commercial vessel may be able to choose an alternate route. In addition to these differences, a navy often has access to more research and development funds to investigate these issues than the commercial builder and operator (Reed 2009).

The current naval ship intact stability criteria are based on the static righting arm curve which are largely empirical and do not explicitly consider many other variables which can have a major impact on the dynamic intact stability. However, they are well accepted by the naval architecture community, and within the bounds of conventional hull forms, have proven to be a reliable, generally conservative, and an ordinal measure of intact stability. Defining rational criteria and methodology for assessing ship intact stability poses a difficult and complex problem. The survival of the ship is a dynamic and non-linear phenomenon with many potential capsizing scenarios which can be created to simulate the worst case scenarios in a real sea condition (Brown and Deybach 1998). The IMO Intact Stability Code 2008 for weather criteria considers wind with gusts and a rollback angle which is dependent on the ship's static righting arm and other ship roll characteristics.



The US Navy and other navies have their own rules on the weather criteria. They are relying on the empirical WWII weather criteria until a more sophisticated method is developed and validated. The information on the criteria used by the navies depends on each country. It is a variable based on the loading condition and measurement method. A comparison of intact stability criteria can be seen in Table 2.3.

Before WWII, intact stability criteria were based primarily on  $GM$ , range of stability and maximum righting arm. These criteria were greatly influenced by (Rohala 1939). Rohala's approach was reflected in the intact stability criteria as stated in Table 2.3. The primary source of data for the US Navy stability criteria was the typhoon of December 1944. The 1994 Pacific typhoon season was an extremely active season in the annual cycle of tropical cyclone formation in the Western North Pacific, with a total of 41 tropical cyclones during the course of the season. The US Pacific Fleet was caught in a major tropical typhoon and many ships were lost. An extensive analysis was made of how the ships weathered the typhoon. The results were correlated with the characteristics of the ships to determine the relevant variables and their effect on survival. Three capsized destroyers and ships that only marginally survived provided particularly useful data. Some had heel angles up to 80 degrees. One survived only because the loss of its stack reduced its sail area. In 1946, the results of this analysis were summarised in an internal memo by Section 456 of the Bureau of Ships, and new ocean weather criteria were proposed. From the data gathered during the typhoon, a wind speed of 100 knots was chosen as a nominal value for modelling tropical storms (nominal value measured at 33 feet above the waterline). This wind speed was specified for new designs. The nominal wind speed specified for ships already in service was 90 knots (Brown and Deybach 1998).

Heeling arm was calculated with a cosine square multiplication factor. It was used to model the reduction due to heeling of the projected sail area above the water line and the height of the centroid of the sail area above the centre of lateral resistance. Referring to Figure 2.2, the ratio of the righting arm at the intersection of the wind heeling arm and righting arm curve (point C,  $\theta_0$ ) to the maximum righting arm,  $GZ(\theta_0)/GZ_{MAX}$ , was 0.67 and greater for the destroyers that capsized. Ships that survived had a ratio of 0.51 to 0.54. To provide a margin for a gust, the specified maximum ratio was 0.6. (Symbol for angle of heel, theta ( $\theta$ ) in Figure 2.2 is equal to ( $\phi$ ) as ITTC symbol).

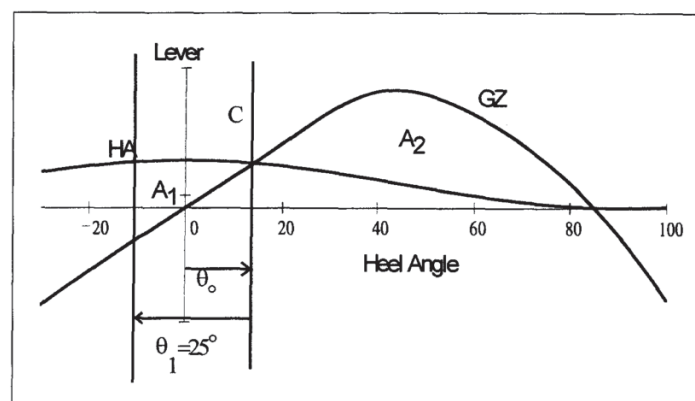


Figure 2.2 US Navy Stability Criteria. Extracted from (Deybach 1997)

Table 2.3 Naval Ship Intact Stability Criteria. Extracted from (Deybach 1997)

Criteria	US	France	Canada	UK
Condition of loading	Minimum operating and full load	Minimum operating	Operational light loading	Light seagoing
<b>Criteria on GZ curve</b>				
Area under curve				
From 0° to 30°	NA	≥ 0.080 m.rad	NA	≥ 0.080 m.rad
From 0° to 40°	NA	≥ 0.133 m.rad	NA	≥ 0.133 m.rad
From 30° to 40°	NA	≥ 0.048 m.rad	NA	≥ 0.048 m.rad
GZ maximum	NA	≥ 0.3m	≥ 0.3m	≥ 0.3m
Heel angle corresponding to GZ maximum	NA	≥ 30°	NA	≥ 30°
Transverse GM with free-surface correction	NA	≥ 0.3m	≥ 0.05m	≥ 0.3m
Capsizing angle	NA	≥ 60°	NA	≥ 60°

The ability of a ship to right itself in a dynamic sea state was evaluated by comparing heeling and restoring energy.  $A_2$ , the area under the righting arm curve between the angle of equilibrium ( $\phi_0$ ) and the extreme intersection between righting arm and wind heeling arm curves was compared with  $A_1$ , the area under the righting arm curve between the roll back angle ( $\phi_1$ ) and the equilibrium heel angle ( $\phi_0$ ) as shown in Figure 2.2. The destroyers that capsized had less than a 15% margin. The surviving ships had an 80% to 110% margin. To provide for gusts and calculation inaccuracies, the specified margin was 40%. The rollback angle to windward was assumed to be 25°. No justification of this angle is found in the memo. In 1948, the tentative criteria were included in a Design Data Sheet (DDS). In 1963, the criteria were refined and documented by (Sarchin and Goldberg 1963). This version of the criteria was adopted by the US Navy in DDS 079-1 (1975), UK Navy in Def Stan 02-109 (UK MOD 2000) and in part by many of the world's navies.

## 2.4 The Weather Criterion

The IMO version of the weather criterion follows closely Yamagata's "Standard of stability adopted in Japan", which was suggested as far back as 1957 while the basic idea had been introduced by Watanabe in 1938 or perhaps even earlier (Spyrou 2011). The ship is assumed to obtain a stationary angle of a stable heel due to side wind loading represented by a lever  $lw_1$  which is not dependent on the heel angle and is the result of a  $26 \text{ ms}^{-1}$  wind velocity. "Around" this angle, the ship is assumed to perform due to a side wave action resonant rolling motion as a result of which on the weather side it reaches momentarily a maximum angle  $\phi_1$ . As at this position the ship is most vulnerable to excitations from the weather side, it is further



assumed that it is acted upon by a gust of wind represented by a lever  $lw_2 = 1.5 lw_1$ . This is translated into a  $\sqrt{1.5}=1.2247$  increase in the wind velocity experienced and assumed to affect the ship for a short period of time, but at least equal to half the natural period under the assumption of resonance.

The requirement for the weather criterion for the IMO rules is stated in the 2008 IS Code Part A – Mandatory Criteria, Chapter 2 – General Criteria, Paragraph 2.3 (IMO 2009). The criterion included in that Code was based on the best *state-of-the-art* concepts, available at the time it was developed, taking into account the sound design and engineering principles and experience gained from operating ships. The interim guidelines for alternative assessment of the weather criterion are stated in MSC.1/Circ.1200 (IMO MSC.1/Circ.1200 2006). It was approved in 2006 and aimed at providing the industry with alternative means (in particular, model experiments) for the assessment of severe wind and the rolling criterion (the weather criterion). The interim guidelines should be applied when the wind heeling lever and/or the angle of roll need to be determined by means of model experiments. To assist in the comprehension of the weather criterion, the IMO provides the explanatory notes to the interim guidelines for an alternative assessment of the weather criterion (IMO MSC.1/Cir.1227 2007). This explanatory note provides an example of the alternative assessment of severe wind and rolling criteria (the weather criterion) based on a series of model tests. To date, these documents are the main reference for the weather criterion provided by the IMO. For naval ships, it contains a slightly different method for evaluating the criterion.

Figure 2.3 and Figure 2.4 show the weather criterion based on IMO and Naval Rules (Spyrou 2011). (Symbol for angle of heel, theta ( $\theta$ ) in Figure 2.3 and Figure 2.4 is equal to ( $\phi$ ) as ITTC symbol).

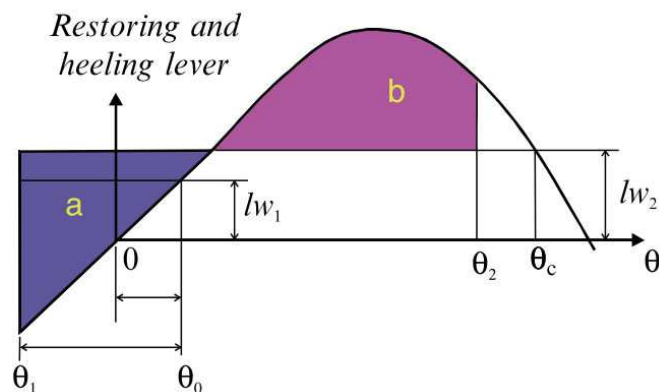


Figure 2.3 The IMO weather criterion. Extracted from (Spyrou 2011)

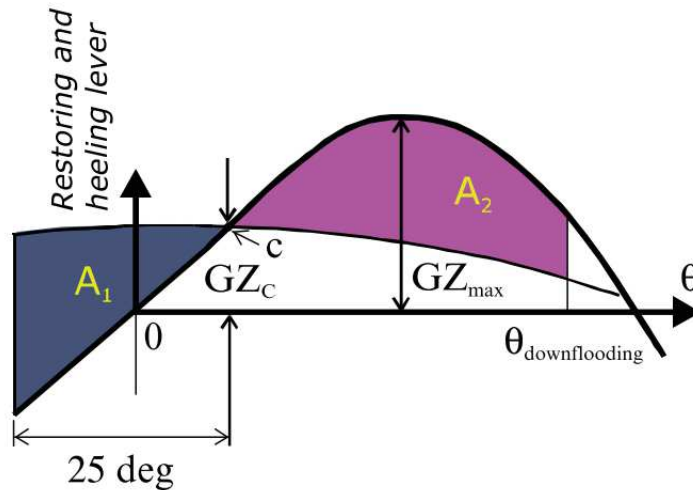


Figure 2.4 The Naval rules weather criterion. Extracted from (Spyrou 2011)

In the IMO rules, the ship is subjected to a steady wind pressure acting perpendicular to the ship's centreline which results in a steady wind heeling level,  $l_{w1}$ . Heel angle caused by  $l_{w1}$  is known as the angle of equilibrium ( $\phi_0$ ). The IMO stated that this angle should not exceed  $16^\circ$  or 80% of the angle of deck edge immersion. Then, the ship is assumed to roll owing to wave action to an angle of roll ( $\phi_1$ ) to windward. The  $\phi_1$  use the parameters stated in the IS Code as follows:

$$\phi_1 = 109 \cdot k \cdot X_1 \cdot X_2 \cdot (r.s)^{0.5} \text{ (degrees)} \quad (2.7)$$

Where:

- $k$  = a factor of the underwater surface with bilge keel or bar keel,
- $X_1$  = a factor based on the ratio of breadth and draught,
- $X_2$  = a factor of block coefficient.

The  $X_1$  and  $X_2$  areas obtained are based on Tables 2.3.4-1 and 2.3.4-2 of the 2008 IS Code (IMO 2009). The  $k$  value is 1 for a rounded-bilged ship having no bilge or bar keels and 0.7 for a ship having sharp bilges. For others, the  $k$  value can be referred to in Tables 2.3.4-3 of the 2008 IS Code. The  $k$  value is a factor based on the total overall area of bilge keels, or area of the lateral projection of the bar keel, or the summation of these areas, length of the ship and breadth. Then, the ship rolls from  $\phi_0$  to  $\phi_1$  (windward) and the ship is subjected to a gust of wind pressure which results in the gust of wind heeling,  $l_{w2}$ . The area under the curve is calculated with respect to  $l_{w2}$ . The requirement states that area B must be bigger than area A. Area A is the rolling energy and area B is the capsizing energy.

In 1962, Sarchin & Goldberg presented the "naval version" of the weather criterion which, whilst more stringent, adheres to the same principle with only a few minor differences (Sarchin and Goldberg 1963). This work is the basis for the stability standards applied by most western Navies nowadays as evidenced by documents such as N.E.S 109 (2000) of the British Navy, DTS 079-1 of the U.S. Navy, NAV-04-A013 of the Italian Navy.

Due to limited published data on the weather criterion for the Naval Rules, only 4 navies have publicly published their intact stability criteria. The Naval Rules for the United States, France, and Canada are stated in Table 2.4 (Deybach 1997).

Table 2.4 Naval Intact Stability Criteria – The Weather Criterion. Extracted from (Deybach 1997)

Criteria	US	France	Canada	UK
Condition of loading	Minimum operating and full load	Minimum operating	Operational light loading	Light seagoing
<b>Weather Criterion</b>				
<i>WHA</i>	$0.0195V^2 .A.z.cos^2\theta/ (1000.\Delta)$			
Ratio between righting arm at equilibrium and maximum righting arm	$\leq 0.6$	$\leq 0.6$	$\leq 0.6$	$\leq 0.6$
Equilibrium heel angle at wind i. 100 knots ii. 90 knots	NA NA	$\leq 30^\circ$ NA	$\leq 30^\circ$ NA	NA $\leq 30^\circ$
Windward roll-back angle	$25^\circ$	$25^\circ$	$25^\circ$	$25^\circ$
Ratio between capsizing and restoring energy	$\geq 1.4$	$\geq 1.4$	$\geq 1.4$	$\geq 1.4$
Maximum angle for $A_2$ area	NA	NA	$\geq 70^\circ$	$\geq 70^\circ$

Where:

- $V$  = velocity (knots),
- $z$  = vertical distance from centre of wind force to half draught (m),
- $A$  = area of projected area ( $m^2$ ),
- $\Delta$  = displacement (tonnes).

For the Naval Rules, the ship is subject to a steady wind speed of 90 knots which is varied with the square of the heel angle. The amplitude resonance rolls due to beam waves are prescribed at 25 degrees. The Naval Rules state that the angle of stable heel should not exceed 20 degrees and the  $GZ$  at that point is less than 60% of the maximum  $GZ$ . The energy requirement of the requirement prescribes that a substantial margin of potential energy should be available at the limit and a substantial margin of the overturning energy as shown in Figure 2.4. This is expressed through the relationship  $A_2 \geq 1.4A_1$ .

## 2.5 Comparison the IMO Rules and the Naval Rules for the weather criterion

The principles of calculating the weather criterion for both the IMO rules and Naval Rules are almost similar. The potential energy of wind and waves should be able to be

countered by overturning energy. The significant differences between both rules are presented in Table 2.5.

Table 2.5 Comparison on the weather criterion for the IMO and the Naval rules

Criteria	IMO Rules	Naval Rules
Wind heeling arm (WHA) i. Velocity ii. Curve	26ms <sup>-1</sup> or 50.54 knots Constant with heel angle	100 knots Cosine square with heel angle
Angle of stable heel	16°	20°
Ratio between capsizing and restoring energy ( $A_2/A_1$ ) based on $lw_2$ (gust)	≥ 1	nil
Ratio between capsizing and restoring energy ( $A_2/A_1$ ) based on $WHA$ 100 knots	nil	≥ 1.4
Roll windward due to beam wave	Vary based on ship characteristic	25°

The calculation for wind heeling arm ( $WHA$ ) is different in the IMO and Naval Rules. For the IMO, the calculation of  $WHA$  or wind heeling levers ( $lw_1$ ) is constant at any heel angle (Part A, Ch 2, Para 2.3.3)(IMO 2009). For the Naval Rules, the  $WHA$  is calculated based on wind velocity. The calculation for obtaining the  $WHA$  is shown in Table 2.6.

Table 2.6 Formula for wind heeling arm of the IMO and Naval Rules Criteria

Criteria	IMO rules	Naval rules
Wind heeling arm, ( $lw_1$ ) ( $lw_2 = 1.5 lw_1$ )	$\frac{P \cdot A \cdot Z}{1000 \cdot g \cdot \Delta}$	$\frac{0.0195 \cdot V^2 \cdot A \cdot Z \cdot \cos^2 \phi}{1000 \cdot \Delta}$

Where:

- $P$  = wind pressure of 504 Pa,
- $A$  = projected lateral area (m<sup>2</sup>),
- $Z$  = vertical distance from the centre of  $A$  to the centre of the underwater lateral area,
- $\Delta$  = displacement (t),
- $g$  = gravitational acceleration of 9.81 (ms<sup>-1</sup>),
- $V$  = wind velocity (knots),
- $\phi$  = heel angle (degrees).

The coefficient 0.0195 is derived from the combination of physical constants and the unit used for wind speed (Luquet et al. 2015). It uses 1 nautical miles = 1852 km where:

$$WHA = \frac{1}{2} \cdot \frac{\rho C_y}{g} \cdot \left(\frac{1852}{3600}\right)^2 = 0.0195 \quad (2.8)$$

Where:

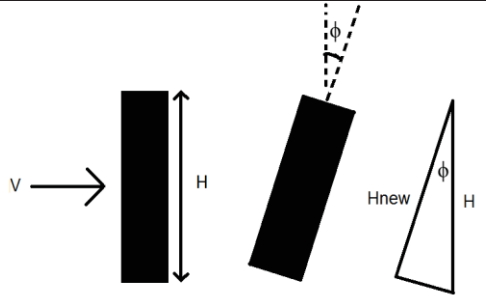
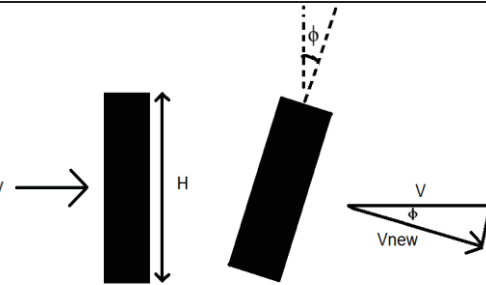
$\rho$  = density = 1.29 kg/m<sup>3</sup>,

$C_y$  = coefficient for y-axis = 1.12,

$g$  = gravitational acceleration of 9.81 (m/s).

To determine the effect of heel angle, there are two approaches to estimate the aerodynamic effect, either by considering that the wind velocity is constant and that the projected area decreases relatively or that the wind velocity decreases relatively and that the projected area is constant (Table 2.7).

Table 2.7 The approaches for estimating aerodynamic effect

<p>Velocity constant Area decreases</p>		<p>Area = Height x length <math>H_{new} = H \cos \phi</math></p> <p>Area<sub>new</sub> = <math>H_{new}</math> x length</p> <p>Velocity = <math>V</math></p>
<p>Velocity decreases Area constant</p>		<p><math>V_{new} = V \cos \phi</math></p> <p>Lateral projected area = <math>H \times L</math> (remain the same as heel angle = 0)</p>

In civil industry, an important problem in modelling winds in urban areas concerns the estimation of drag induced by a group of buildings with different densities. However, in contrast to bulk drag coefficients based on the total drag on an obstacle, the sectional drag coefficient requires knowledge of the detailed vertical profiles of the drag force and mean velocity within the building canopy. These are difficult to obtain experimentally, and information about drag coefficient,  $C_D(z)$  is therefore scarce (Santiago et al. 2008). A wind tunnel test was conducted and obtained the  $C_D$  for a group of buildings. The  $C_D$  obtained from this experiment was around 1.15 (Hagishima et al. 2009).

To the author's best knowledge, there is no statement mentioned in the literature regarding the cosine square used in Naval Rules. For the author, the cosine square originates from the velocity where  $V_{new} = V \cos \phi$ . Since the calculation of the *WHA* has the velocity square, the cosine square has appeared in the *WHA* for Naval Rules.

## 2.6 Development of Second Generation Intact Stability Code

The development of the second generation intact stability criteria (SGISC) started in 2002 with the reestablishment of the intact stability working group by the IMO Subcommittee on Stability and Load Lines and on Fishing Vessels Safety (SLF). However, due to other priorities, the actual work on the second generation of intact stability criteria did not start until the 48<sup>th</sup> session of the SLF, in September 2005. The working group decided that the second generation of intact stability criteria should be performance-based and address three fundamental modes of stability failures (SLF 48/21, paragraph 4.18):

- a. Restoring arm variation problems, such as parametric excitation and pure loss of stability;
- b. Stability under dead ship condition, defined by SOLAS regulation II-1/3-8;
- c. Manoeuvring related problems with waves, such as broaching-to.

A similar formulation was included in the preamble of the 2008 IS Code, as a direction for long-term development. However, the restoring arm variation problem was considered as two modes of parametric roll and pure loss of stability; hence, four stability failure modes were considered (Belenky, Bassler, and Spyrou 2011).

The first steps in the development of the criteria have shown that the development is a formidable task. Among the first proposals for these criteria was that which was contained in SLF 49/5/2 and with supporting information presented in SLF49/INF.3. This proposal suffered from multiple theoretical shortcomings and was rejected by the working group at the 49th session of SLF (July 2006). The development of the SGISC clearly required a new approach.

A significant part of that consideration was in general agreement that the second generation criteria should be based on the physics of the phenomena leading to intact stability failure. Modes of operations and design of new ships take on characteristics that cannot, with confidence, rely solely on the statistics of failures and regression-based techniques. In addition, there was a general agreement on the desirability of relating the new criteria to probability, or some other measures of the likelihood of stability failures, as methods of risk analysis have gained greater acceptance and become standard tools in other industries.

During the discussions of the working group, the notion was expressed that, in general, it is bad practice to submit completely new technologies to the SLF. They should be first published in a technical journal, preferably also presented and discussed at technical conferences. In particular, the international conferences on the stability of ships and ocean vehicles (STAB) and international ship stability workshops (ISSW) are very appropriate venues to discuss these advances.

In the SLF’s 53<sup>rd</sup> meeting, after sufficient experience had been gained with the early discussion in SLF 51<sup>st</sup> and SLF 52<sup>nd</sup> meetings, the Sub-Committees agreed that the second generation intact stability criteria should be initially considered as the recommendation criteria in Part B of the 2008 IS Code and be transferred to Part A at a future date, unless the Committee were to decide to delay this action. The flow chart endorsed by the committee is shown in Figure 2.5 (IMO 2011). This figure provides a simple understanding of the implementation of the second generation intact stability criteria in the flow diagram. The second generation intact stability criteria are an additional requirement on top of the current 2008 intact stability criteria and do not replace the current code. Every design should pass the 2008 IS Code 2.2 for the righting arm curve requirement and the 2008 IS Code 2.3 for the weather criterion. Then, the design should be checked for the failure modes of dead ship condition, pure loss of stability, parametric rolling and surf-riding/broaching. The design should pass each failure mode at any level. It is not necessary to follow the sequence described in Figure 2.5 ((IMO 2011) Annex 3). To the author’s best knowledge (after SDC3 at the IMO London on Jan 2016), the latest document to be referred to is listed in Table 2.8 (as attached in Annex A).

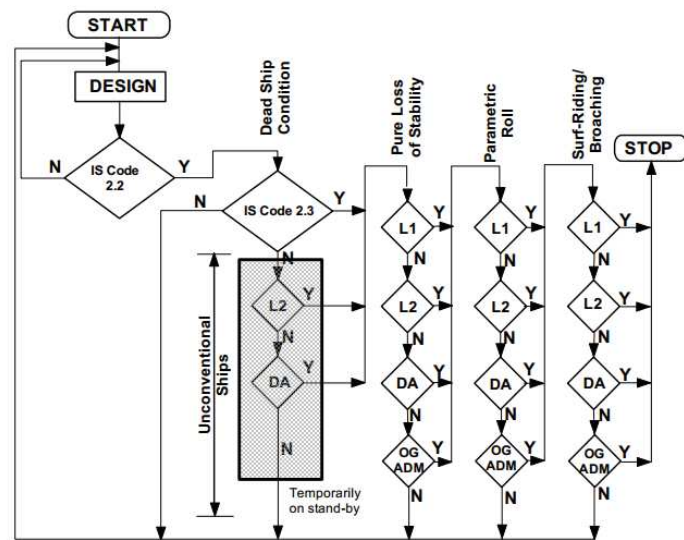


Figure 2.5 Flow chart for the implementation of second generation intact stability criteria. Extracted from (IMO 2011)

Table 2.8 Current references for IMO document on second generation intact stability criteria

Failure mode	Formula	Explanatory notes
Pure loss of stability	SDC 2/WP.4, annex 1	SDC 3/WP.5 annex 3
Parametric rolling	SDC 2/WP.4, annex 2	SDC 3/WP.5 annex 4
Surf-riding/broaching	SDC 2/WP.4, annex 3	SDC 3/WP.5 annex 5
Dead ship condition	SDC 3/WP.5, annex 1	SDC 3/WP.5 annex 6
Excessive acceleration	SDC 3/WP.5 Annex 2	SDC 3/WP.5 annex 7
Plan of action for SGISC	SDC 3/WP.5 annex 8	

Inherently, for the SGISC, the “proposed amendment document” consists of the description of the amendment to be inserted in the 2008 IS Code. This document will explain



briefly each failure mode and describe the formula for Levels 1 and 2. Moreover, it has the “draft explanatory notes” which explain and describe the details of the failure modes. It starts with the physical background, calculation for Level 1 and Level 2 criteria, examples of application, and other related information based on each failure mode. In both documents, each failure mode has its own documents.

### 2.6.1 Pure Loss of Stability

When a ship is travelling through waves, the submerged portion of the hull changes. These changes may become especially significant if the length of the wave is comparable to the length of the ship. Figure 2.6 shows the change of the water plane and GZ curve corresponding to the wave trough and wave crest (Belenky, Bassler, and Spyrou 2011).

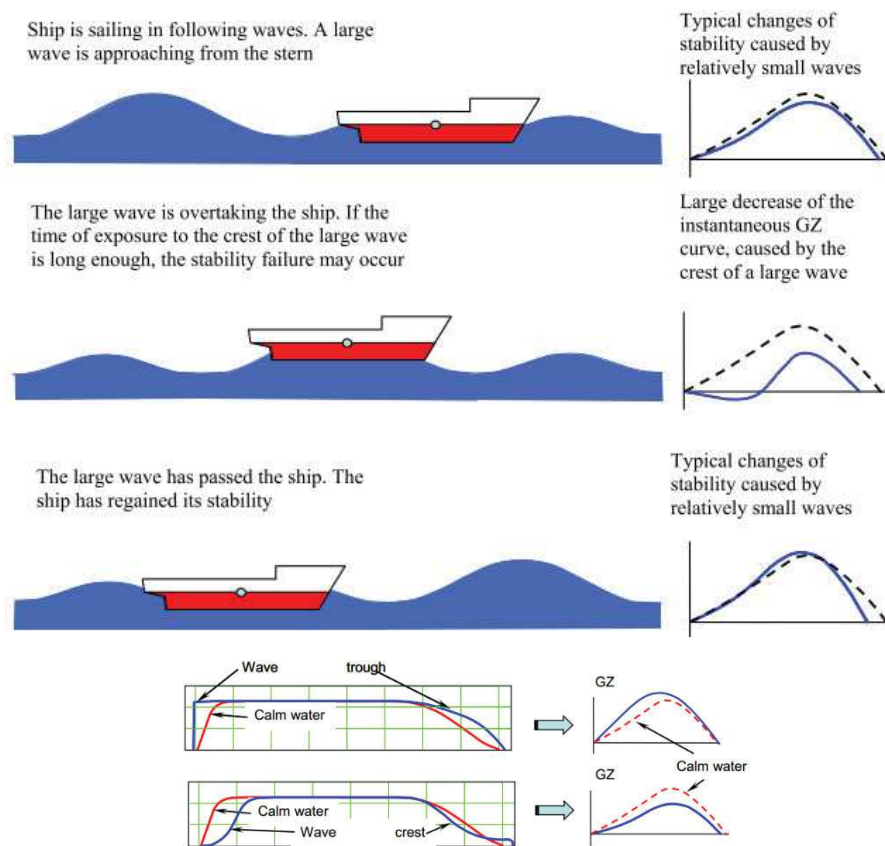


Figure 2.6 Stability corresponding to water plane changes during the water trough and the wave crest. Extracted from (Belenky, Bassler, and Spyrou 2011)

### 2.6.2 Parametric Rolling

Parametric roll (short for parametric roll resonance) is an amplification of roll motions caused by a periodic variation in transverse stability in waves. The phenomenon of parametric rolling is predominantly observed in the head, following bow and stern-quartering seas when the ship's encounter frequency is approximately twice the ship roll natural frequency and the



roll damping of the ship is insufficient to dissipate additional energy (accumulated because of parametric resonance). Figure 2.7 shows the development of parametric roll resonance (IMO 2015).

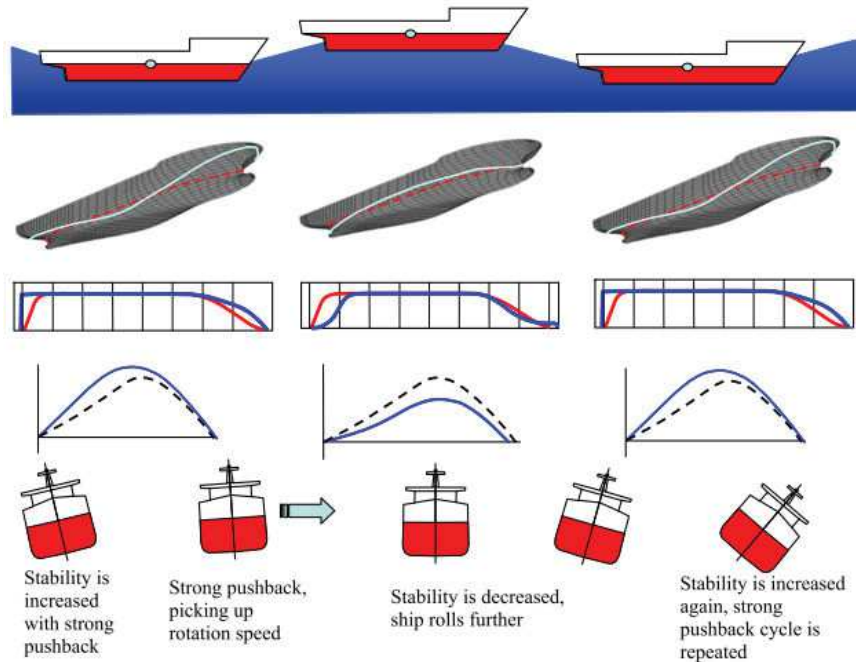


Figure 2.7 Development of parametric resonance. Extracted from (IMO 2015)

### 2.6.3 Surf-Riding/Broaching

Broaching (short for "broaching-to") is a violent uncontrollable turn that occurs despite maximum steering efforts to maintain the course. As with any other sharp turn events, broaching is accompanied by a large heel angle, which has the potential effect of a partial or total stability failure. Broaching is usually preceded by surf-riding which occurs when a wave, approaching from the stern, "captures" a ship and accelerates the ship to the speed of the wave (i.e., the wave celerity) (Peters et al. 2012). Surf-riding is a single wave event in which the wave profile does not vary relative to the ship. Because most ships are directionally unstable in the surf-riding condition, this manoeuvring yaw in-stability leads to an uncontrollable turn – termed "broaching".

Because surf-riding usually precedes broaching, the likelihood of the occurrence of surf-riding can be used to formulate the vulnerability criteria for broaching. In order for surf-riding to occur, several conditions need to be satisfied:

- a. The wavelength should be between one and three times the ship length;
- b. The wave must be sufficiently steep to produce a sufficient wave surfing force;
- c. The ship's speed should be comparable to the wave celerity.

Large ships (i.e. over 200 metres in length) do not surf-ride because the waves of this and greater length tend to travel faster than the ship (i.e. 34 plus knots) and these ships have too much mass (i.e. inertia) to allow them to accelerate to the wave speed before the wave passes.

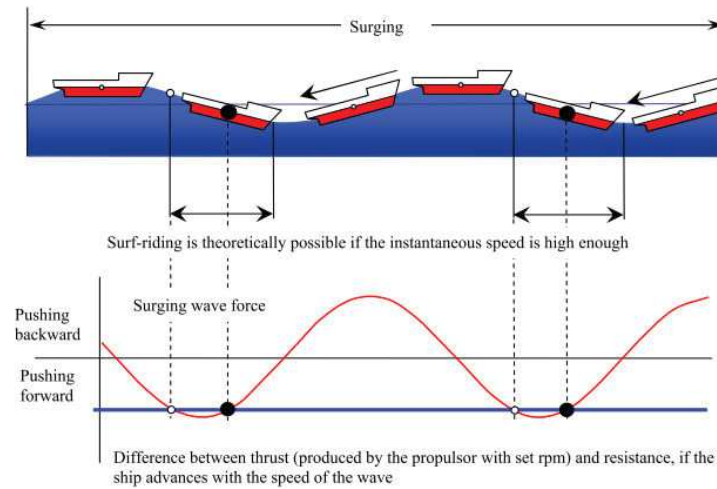


Figure 2.8 Force acting on a ship in following waves. Extracted from (IMO 2016)

#### 2.6.4 Dead Ship Stability

The dead ship condition is the first mode of stability failure addressed with a physics-based severe wind-and-roll criterion, also known as the "weather criterion", which was adopted by the IMO in 1985 (Res. A.562(14)) and is now embodied in Section 2.3 of the 2008 IS Code, Part A. The scenario of the weather criterion is shown in Figure 2.9. This scenario assumes that a ship has lost its power and has turned into beam seas, where it is rolling under the action of waves as well as heeling and drifting under the action of wind. Drift-related heel is a result of the action of two forces: the wind aerodynamic force and the hydrodynamic reaction caused by the transverse motion of the ship.

Next, a sudden and long gust of wind occurs. The worst possible instant for this is when the ship has rolled at the maximum windward angle; in this case, the action of wind is added to the action of waves. The strengthening wind increases the drift velocity, and this leads to an increase in the hydrodynamic drift reaction. The increase in the drift velocity leads to the increase in the hydrodynamic reaction, and therefore the increase in the heeling moment by the aerodynamic and hydrodynamic forces. The gust is assumed to last long enough for the ship to roll completely to the other side; the achieved leeward roll angle is the base of the criterion. If it is too large, some openings may be flooded and the stability of the ship is considered insufficient (Belenky, Bassler, and Spyrou 2011).

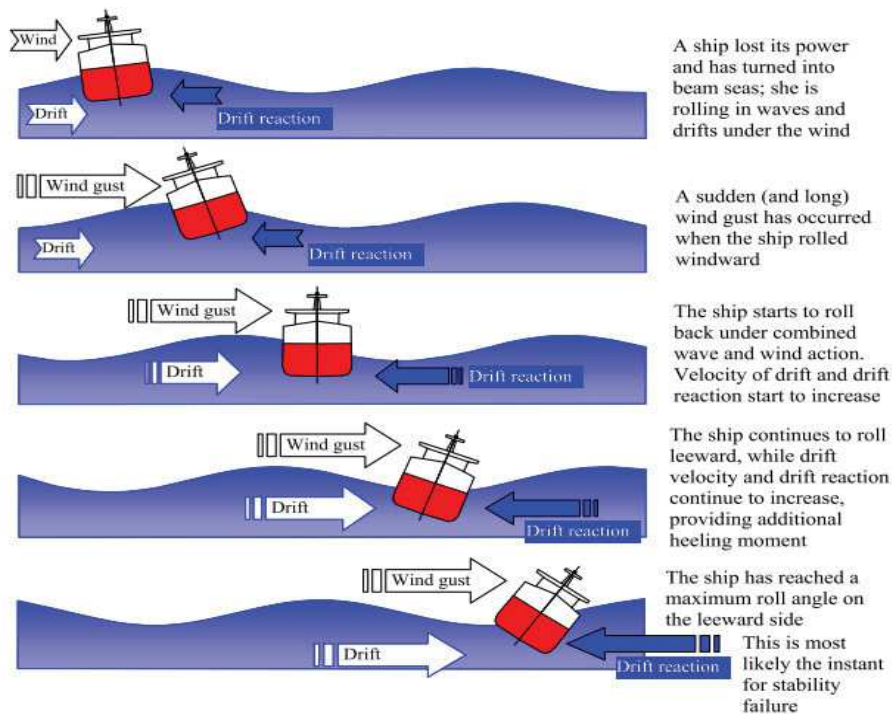


Figure 2.9 Scenario of stability failure in dead ship conditions. Extracted from (Belenky, Bassler, and Spyrou 2011)

### 2.6.5 Excessive Acceleration

When a ship is rolling, the load in higher locations covers longer distances. The period of roll motions is the same for all the cargo locations on board the ship. To cover a long distance during the same period of time, the linear velocity must be larger. As the velocity changes its direction every half period, a larger linear velocity leads to larger linear accelerations. A large linear acceleration means a larger inertial force, as expressed in Figure 2.10. Horizontal accelerations are more dangerous than vertical accelerations, whereby large accelerations are mostly caused by roll motions so they have a predominantly lateral direction. If the GM value is large, the period of roll movement is smaller. Therefore, for the same roll angle, the changes in linear velocity occur faster, causing the accelerations to be larger (IMO, 2015).

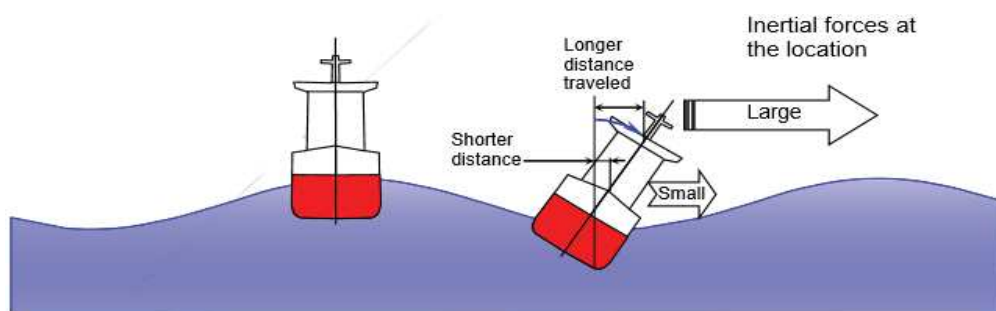


Figure 2.10 Scenario of stability failure related to excessive accelerations. Extracted from (IMO 2015)

## 2.7 Evaluation of Second Generation Intact Stability

A significant part of the consideration is the general agreement that the SGISC should be based on the physics of the phenomena leading to intact stability failure. Design and modes of operation of new ships take on characteristics that cannot, with confidence, rely solely on the statistics of failures and regression-based techniques. In addition, there is a general agreement of the desirability of relating the new criteria to probability, or some measures of the likelihood of stability failures, since methods of risk and analysis have gained greater acceptance and become the standard tools in aviation and land industries (Belenky, Bassler, and Spyrou 2011). The latest formula written for second generation intact stability criteria can be obtained in the IMO Document Library. To the author's best knowledge, the latest update is presented in Table 2.8.

### 2.7.1 Pure Loss of Stability

The provisions given apply to all ships for which the Froude number,  $F_n$ , corresponds to the service speed exceeding 0.24. The calculation includes the minimum value of GM in different wave characteristics. The detail of this criterion is stated in SDC 2/WP.4 Annex 1. The  $F_n$  is calculated using the formula below:

$$F_n = V_S / [\sqrt{(g \cdot L)}] \quad (2.9)$$

#### Level 1 Pure loss of stability

$$GM_{\min} > R_{PLA} \quad (2.10)$$

Where;

$V_S$  = Vessel speed (m/s)

$F_n$  = Froude number,

$g$  = gravitational acceleration = 9.81 m/s<sup>2</sup>.

$L$  = Ship length (m)/

$R_{PLA}$  = 0.05 m,

$GM_{\min}$  = can be obtained either by method A or B.

#### Method A.

$$GM_{\min} = KB + \frac{I_L}{V} - KG, \text{ only if } \frac{V_{D-V}}{A_w(D-d)} \geq 1.0 \quad (2.11)$$

#### Method B.

$GM_{\min}$  may be determined as the minimum value calculated for the ship including free surface correction (m), corresponding to the loading condition under consideration, considering the ship to be balanced in sinkage and trim on a series of waves with the following characteristics:

Wavelength =  $L$ ,

Wave height =  $L \cdot S_w$ ; the  $S_w$  value for pure loss of stability is 0.0334.

The wave crest is to be centred amidships and at  $0.1L$ ,  $0.2L$ ,  $0.3L$  and  $0.5L$  forward and  $0.1L$ ,  $0.2L$ ,  $0.3L$  and  $0.5L$  aft thereof.

Where:

$S_w$  = wave steepness.

### Level 2 Pure loss of stability

For Level 2, a ship is considered not to be vulnerable to the pure loss of stability failure mode if the largest value among the two criteria,  $CR_1$  and  $CR_2$ , when they are underway at the service speed, is less than  $R_{PL0}$ .  $R_{PL0} = 0.06$ . It uses the probabilistic approach where the wave case occurrences are taken into account as follows:

$$CR_1 = \sum_{i=1}^N W_i C1_i = \text{Weighted criterion 1} \quad (2.12)$$

$$CR_2 = \sum_{i=1}^N W_i C2_i = \text{Weighted criterion 2} \quad (2.13)$$

Where;

$W_i$  = a weighting factor of wave case occurrences in Table 2.9,

$N$  = number of wave cases corresponding to non-zero probabilities in wave case occurrences table.

Table 2.9 Wave case occurrences for pure loss of stability

		Number of occurrences: 100 000 / Tz (s) = average zero up-crossing wave period														
$H_s$ (m)	3.5	4.5	5.5	6.5	7.5	8.5	9.5	10.5	11.5	12.5	13.5	14.5	15.5	16.5	17.5	18.5
0.5	1.3	133.7	865.6	1186.0	634.2	186.3	36.9	5.6	0.7	0.1	0.0	0.0	0.0	0.0	0.0	0.0
1.5	0.0	29.3	986.0	4976.0	7738.0	5569.7	2375.7	703.5	160.7	30.5	5.1	0.8	0.1	0.0	0.0	0.0
2.5	0.0	2.2	197.5	2158.8	6230.0	7449.5	4860.4	2066.0	644.5	160.2	33.7	6.3	1.1	0.2	0.0	0.0
3.5	0.0	0.2	34.9	695.5	3226.5	5675.0	5099.1	2838.0	1114.1	337.7	84.3	18.2	3.5	0.6	0.1	0.0
4.5	0.0	0.0	6.0	196.1	1354.3	3288.5	3857.5	2685.5	1275.2	455.1	130.9	31.9	6.9	1.3	0.2	0.0
5.5	0.0	0.0	1.0	51.0	498.4	1602.9	2372.7	2008.3	1126.0	463.6	150.9	41.0	9.7	2.1	0.4	0.1
6.5	0.0	0.0	0.2	12.6	167.0	690.3	1257.9	1268.6	825.9	386.8	140.8	42.2	10.9	2.5	0.5	0.1
7.5	0.0	0.0	0.0	3.0	52.1	270.1	594.4	703.2	524.9	276.7	111.7	36.7	10.2	2.5	0.6	0.1
8.5	0.0	0.0	0.0	0.7	15.4	97.9	255.9	350.6	296.9	174.6	77.6	27.7	8.4	2.2	0.5	0.1
9.5	0.0	0.0	0.0	0.2	4.3	33.2	101.9	159.9	152.2	99.2	48.3	18.7	6.1	1.7	0.4	0.1
10.5	0.0	0.0	0.0	0.0	1.2	10.7	37.9	67.5	71.7	51.5	27.3	11.4	4.0	1.2	0.3	0.0
11.5	0.0	0.0	0.0	0.0	0.3	3.3	13.3	26.6	31.4	24.7	14.2	6.4	2.4	0.7	0.2	0.0

$$C1_i = \begin{cases} 1 & \Phi_v < R_{PL1} \\ 0 & \text{otherwise} \end{cases} \quad (2.14)$$

$$C2_i = \begin{cases} 1 & \phi_s < R_{PL2} \\ 0 & \text{otherwise} \end{cases} \quad (2.15)$$

Where;

$\phi_V$  = angle of vanishing stability,

$\phi_s$  = angle of heel under action of a heeling lever,  $R_{PL3}$ ,

$R_{PL1}$  =  $30^\circ$ ,

$R_{PL2}$  =  $15^\circ$  for passenger ships and  $25^\circ$  for other ships,

$R_{PL3}$  =  $8 (H_i/\lambda) dF_n^2$ .

## 2.7.2 Parametric Rolling

Evaluation of the parametric rolling risk is based on metacentric height ( $GM$ ). The calculation includes the maximum and minimum value of  $GM$  in different wave characteristics (González et al. 2014). The details of this criterion are stated in SDC 2/WP.4 Annex 2.

### Level 1 Parametric rolling

$$\frac{\Delta GM_1}{GM_C} > R_{PR} \quad (2.16)$$

Where;

$R_{PR}$  = 1.87, if the ship has a sharp bilge; otherwise;

=  $0.17 + 0.425 (100A_k/LB)$ , if  $C_m \geq 0.96$ ;

=  $0.17 + (10.625 \times C_m - 9.775) (100A_k/LB)$ , if  $0.94 < C_m < 0.96$ ;

=  $0.17 + 0.2125 (100A_k/LB)$ , if  $C_m \leq 0.94$ ; and  $(100A_k/LB)$  should not exceed 4;

$GM_C$  = metacentric height of the loading condition in calm water including surface correction,

$\Delta GM_1$  = the amplitude of the variation of the metacentric height obtained either by method A or B,

$C_m$  = midship section area coefficient.

### Method A.

$$\Delta GM_1 = \frac{I_H - I_L}{V}, \text{ only if } \frac{V_D - V}{A_w(D-d)} \geq 1.0 \quad (2.17)$$



Method B.

$GM_{min}$  may be determined as the minimum value calculated for the ship including free surface correction (m), corresponding to the loading condition under consideration, considering the ship to be balanced in sinkage and trim on a series of waves with the following characteristics:

Wavelength =  $L$ ;

Wave height =  $L \cdot S_w$ ; the  $S_w$  value for parametric rolling is 0.0167

The wave crest is to be centred amidships and at  $0.1L$ ,  $0.2L$ ,  $0.3L$  and  $0.5L$  forward and  $0.1L$ ,  $0.2L$ ,  $0.3L$  and  $0.5L$  aft thereof.

**Level 2 Parametric rolling**

For level 2, a ship is considered not to be vulnerable to the parametric rolling failure mode if  $R_{PRO}$  ( $R_{PRO} = 0.06$ ) is greater than either  $C1$  or  $C2$ .

$$C1 = \sum_{i=1}^N W_i C1_i = \text{Weighted criterion 1} \quad (2.18)$$

$$C2 = \sum_{i=1}^N W_i C2_i = \text{Weighted criterion 2} \quad (2.19)$$

Where;

$W_i$  = a weighting factor of wave case in Table 2.10,  $N$  = number of wave cases corresponding to non-zero probabilities in wave case occurrences table.

Table 2.10 Wave cases

Wave case number	Weight $W_i$	Wave length $\lambda_i$ (m)	Wave height $H_i$ (m)
1	0.000013	22.574	0.350
2	0.001654	37.316	0.495
3	0.020912	55.743	0.857
4	0.092799	77.857	1.295
5	0.199218	103.655	1.732
6	0.248788	133.139	2.205
7	0.208699	166.309	2.697
8	0.128984	203.164	3.176
9	0.062446	243.705	3.625
10	0.024790	287.931	4.040
11	0.008367	335.843	4.421
12	0.002473	387.440	4.769
13	0.000658	442.723	5.097
14	0.000158	501.691	5.370
15	0.000034	564.345	5.621
16	0.000007	630.684	5.950

The  $C1$  index can be calculated either using below formula:

$$C1_i = \begin{cases} 0 & \text{Fulfill requirement A or B} \\ 1 & \text{otherwise} \end{cases} \quad (2.20)$$

$$\text{Requirement A} = GM(H_i, \lambda_i) > 0 \text{ and } \frac{\Delta GM(H_i, \lambda_i)}{GM(H_i, \lambda_i)} < R_{PR}$$

$$\text{Requirement } B = V_{PRi} > V_s$$

Where;

$$V_{PRi} = \left| \frac{2\lambda_i}{T\phi} \cdot \sqrt{\frac{GM(H_i\lambda_i)}{GM_C}} \cdot \sqrt{g \frac{\lambda_i}{2\pi}} \right|, \text{ the wave characteristics is based on Table 2.10.}$$

$$C2 = \left[ \sum_{i=1}^3 C2_h(Fn_i) + C2_h(0) + \sum_{i=1}^3 C2_f(Fn_i) \right] / 7 \quad (2.21)$$

$$C2_h(Fn) = \sum_{i=1}^N W_i C_i \quad (2.22)$$

$$C2_f(Fn) = \sum_{i=1}^N W_i C_i \quad (2.23)$$

$$C_i = \begin{cases} 1 & \text{maximum roll angle} > 25^\circ \\ 0 & \text{otherwise} \end{cases} \quad (2.24)$$

Where;

$W_i$  = the weighting factor for the respective wave cases specified in Table 2.11. The maximum roll angle in head and following waves is the calculation of stability in waves and should assume the ship to be balanced in sinkage and trim on a series of waves with the following characteristics:

Wavelength,  $\lambda = L$ ;

Wave height,  $h_j = 0.01 * j \cdot L$ , where  $j = 0, 1, \dots, 10$



Table 2.11 Wave case occurrences for parametric rolling

$H_s$ (m)	Number of occurrences: 100 000 / $T_z$ (s) = average zero up-crossing wave period															
	3.5	4.5	5.5	6.5	7.5	8.5	9.5	10.5	11.5	12.5	13.5	14.5	15.5	16.5	17.5	18.5
0.5	1.3	133.7	865.6	1186.0	634.2	186.3	36.9	5.6	0.7	0.1	0.0	0.0	0.0	0.0	0.0	0.0
1.5	0.0	29.3	986.0	4976.0	7738.0	5569.7	2375.7	703.5	160.7	30.5	5.1	0.8	0.1	0.0	0.0	0.0
2.5	0.0	2.2	197.5	2158.8	6230.0	7449.5	4860.4	2066.0	644.5	160.2	33.7	6.3	1.1	0.2	0.0	0.0
3.5	0.0	0.2	34.9	695.5	3226.5	5675.0	5099.1	2838.0	1114.1	337.7	84.3	18.2	3.5	0.6	0.1	0.0
4.5	0.0	0.0	6.0	196.1	1354.3	3288.5	3857.5	2685.5	1275.2	455.1	130.9	31.9	6.9	1.3	0.2	0.0
5.5	0.0	0.0	1.0	51.0	498.4	1602.9	2372.7	2008.3	1126.0	463.6	150.9	41.0	9.7	2.1	0.4	0.1
6.5	0.0	0.0	0.2	12.6	167.0	690.3	1257.9	1268.6	825.9	386.8	140.8	42.2	10.9	2.5	0.5	0.1
7.5	0.0	0.0	0.0	3.0	52.1	270.1	594.4	703.2	524.9	276.7	111.7	36.7	10.2	2.5	0.6	0.1
8.5	0.0	0.0	0.0	0.7	15.4	97.9	255.9	350.6	296.9	174.6	77.6	27.7	8.4	2.2	0.5	0.1
9.5	0.0	0.0	0.0	0.2	4.3	33.2	101.9	159.9	152.2	99.2	48.3	18.7	6.1	1.7	0.4	0.1
10.5	0.0	0.0	0.0	0.0	1.2	10.7	37.9	67.5	71.7	51.5	27.3	11.4	4.0	1.2	0.3	0.1
11.5	0.0	0.0	0.0	0.0	0.3	3.3	13.3	26.6	31.4	24.7	14.2	6.4	2.4	0.7	0.2	0.1
12.5	0.0	0.0	0.0	0.0	0.1	1.0	4.4	9.9	12.8	11.0	6.8	3.3	1.3	0.4	0.1	0.0
13.5	0.0	0.0	0.0	0.0	0.0	0.3	1.4	3.5	5.0	4.6	3.1	1.6	0.7	0.2	0.1	0.0
14.5	0.0	0.0	0.0	0.0	0.0	0.1	0.4	1.2	1.8	1.8	1.3	0.7	0.3	0.1	0.0	0.0
15.5	0.0	0.0	0.0	0.0	0.0	0.0	0.1	0.4	0.6	0.7	0.5	0.3	0.1	0.1	0.0	0.0
16.5	0.0	0.0	0.0	0.0	0.0	0.0	0.0	0.1	0.2	0.2	0.2	0.1	0.1	0.0	0.0	0.0

### 2.7.3 Surf-Riding/Broaching

Evaluation of the parametric rolling risk is based on the ship length, service speed and propulsion capability. Levels 1 and 2 have a huge gap in terms of the formulation. The details of this criterion are stated in SDC 2/WP.4 Annex 3.

#### Level 1 Broaching

A ship is considered not to be vulnerable to the surf-riding/ broaching failure mode if:

$$L > 200 \text{ m or,} \quad (2.25)$$

$$F_n \leq 0.3 \text{ (at speed = } V_S) \quad (2.26)$$

### 2.7.4 Dead Ship Condition

For the dead ship condition failure mode, Level 1 is exactly the same as the current 2008 IS Code for the weather criterion except for the Table for wave steepness factor,  $s$ . It will be replaced with Table 2.12. For Level 2, it will use the weighted average method considering a different combination of the environmental conditions. The details of this criterion are stated in SDC 3/WP.5 Annex 1.

Table 2.12 Value for wave steepness factor,  $s$

Rolling period, $T$ (s)	Wave steepness factor, $s$
$\leq 6$	0.100
7	0.098
8	0.093
12	0.065
14	0.053
16	0.044
18	0.038
20	0.032
22	0.028
24	0.025
26	0.023
28	0.021
$\geq 30$	0.020

### 2.7.5 Excessive Acceleration

For the excessive acceleration failure mode, Level 1 for excessive acceleration considers the location along the length of the ship where passengers or crew may be present. For Level 2, it will use the weighted average method considering a long-term probability index that measures the vulnerability of the ship to a stability failure in the excessive acceleration mode for the loading condition and location under consideration based on the probability of occurrence of short-term environmental conditions. The details of this criterion are stated in SDC 3/WP.5 Annex 2.

#### Level 1 Excessive acceleration

A ship is not considered to be vulnerable to the excessive acceleration stability failure mode if,

$$\phi k_L (g + 4 \pi^2 h / T^2) < R_{EA1} \quad (2.27)$$

where;

$\phi$  = characteristic roll amplitude (rad),

$k_L$  = factor taking into account simultaneous action roll, yaw, and pitch motions,

$h$  = height above roll axis of the location (m),

$T$  = rolling period (s),

$R_{EA1}$  = limit constant either [2.5] [8.9] [8.69 or below] ( $\text{ms}^{-2}$ )

### 2.8 Earlier Experimental Work

The experimental work related to ship stability is commonly expensive because it may involve the cost of model construction, facility rental and extensive special equipment. Some universities, research centres and governmental organisations have conducted several

experiments to verify the stability characteristic. Table 2.13 shows the summary of the experiments conducted in this field of study.

An experiment of a large passenger ship for the weather criterion was conducted in a wind tunnel at the Vienna Model Basin, Italy in 2003 (Bertaglia et al. 2003). This experiment aimed to obtain the experimental forces and moment acting on two ships, built at Ficantieri shipyard. The test involved beam wind direction with various heel angles. Wedges were created to correct the heeled floating position. The measurement was performed with the wind speed of  $13\text{ms}^{-1}$  with Reynolds number of  $2 \times 10^6$  (reference of length)  $2.3 \times 10^5$  (reference of beam). The test configuration is shown in Figure 2.11.

For the SGISC, the Japanese attempted to obtain validation of a new draft of new generation intact stability criteria (Umeda et al. 2011). The models of CEHIPAR 2792 and ro-ro ships were tested in beam wind and waves to validate the numerical simulation. This experiment was conducted at the seakeeping and manoeuvring basin of the National Research Institute of Fisheries Engineering (NRIFE). An optical fibre gyroscope inside the model was used to detect the roll, pitch and yaw angle. A wind blower with 36 axial flow fans and controlled by inverters with a v/f control law was used to simulate a wind effect. The blower used in this experiment is shown in Figure 2.12. To facilitate the development of the direct assessment guidelines as a part of second generation intact stability criteria, an experiment combining the wave and wind effect was conducted (Umeda et al. 2014). The overview of the experimental setup is shown in Figure 2.13.

To explore the effect of the scaling criteria, an experiment on three different scales of CEHIPAR 2792 ship was conducted at El Pardo Model Basin (CEHIPAR) (Bulian, Francescutto, and Fucile 2010). Three tests were performed, which were free roll decays, roll tests in regular beam waves and drift tests. This was the first experiment to address roll damping scale effects. The test arrangement is shown in Figure 2.14.

With regard to SGISC, several experiments were carried out to validate the mathematical models for Level 1 and Level 2 as reported in conference papers (Umeda et al. 2011; Kubo et al. 2012; Umeda et al. 2014).

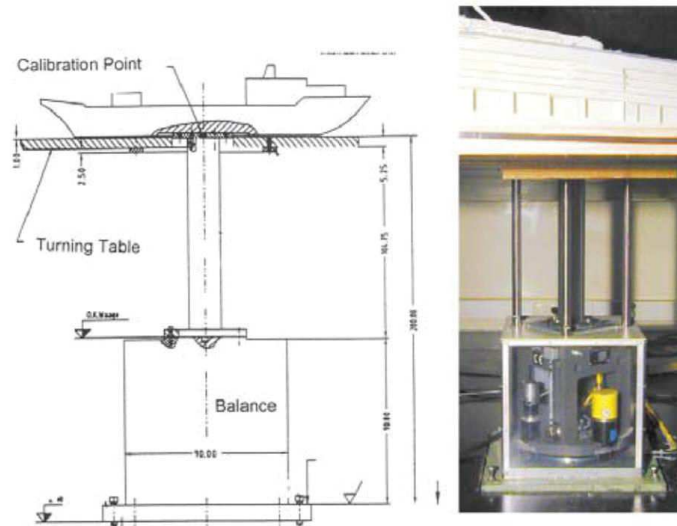


Figure 2.11 Test configuration at Vienna Model Basin. Extracted from (Bertaglia et al. 2003)

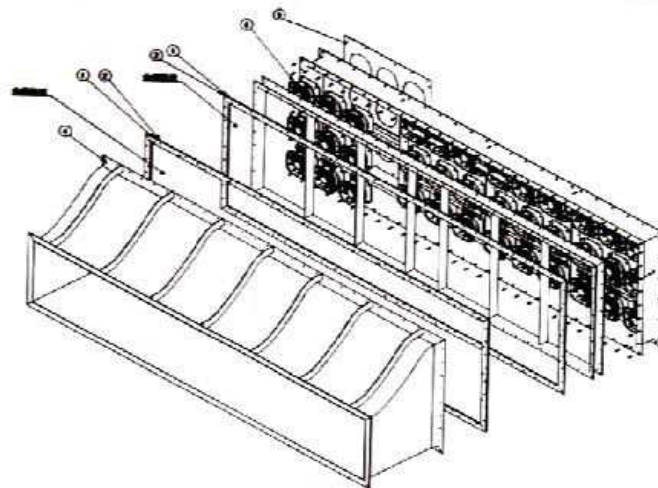


Figure 2.12 Wind blower used for the experiment at NRIFE. Extracted from (Umeda et al. 2014)

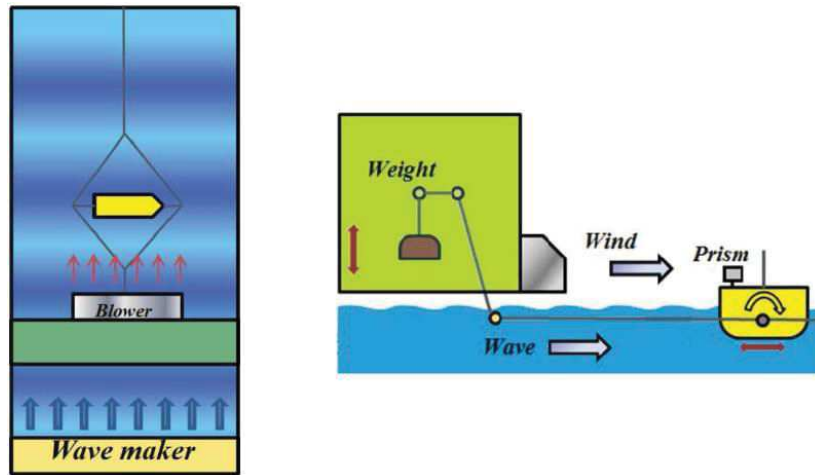


Figure 2.13 An overview of test setup; Top view (Left) Lateral view (Right). Extracted from (Umeda et al. 2014)

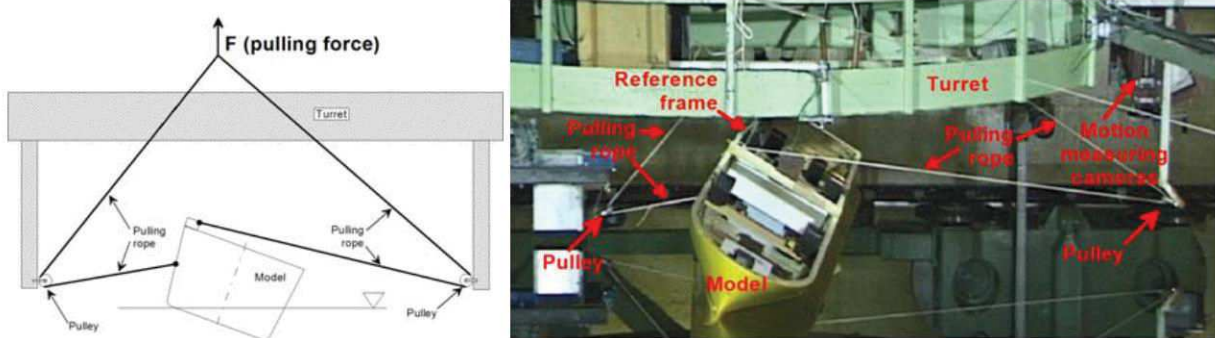


Figure 2.14 Schematic diagram (left) and actual realisation (right) of the experimental arrangement used for roll decay tests. Extracted from (Bulian, Francescutto, and Fucile 2010)

Table 2.13 Previous experimental work related to ship stability

No	Title /Method /Reference	Country
1	Evaluation of the parameters for the weather criterion. Tested in wind tunnel with static heeling angle. Measuring the force acting on the model. (Bertaglia et al. 2003)	Italy
2	Validation procedures for dead ship stability. Wind applied in basin. Measuring wind velocity at 15 points. (Umeda et al. 2014)	Japan
3	Evaluation of the Weather Criterion by Experiments and its Effect to the Design of a RoPax Ferry. Tested in wind tunnel with static heeling angle. Evaluating wind heeling arm. (Ishida, Taguchi, and Sawada 2006)	Japan
4	Remarks on experimental validation procedures for numerical intact stability assessment with latest examples. Comparison between model experiments and numerical simulation for stability under dead ship condition and pure loss of stability in astern waves. (Umeda et al. 2014)	Japan
5	Total stability failure probability of a ship in irregular beam wind and waves: model experiment and numerical simulation. Quantify total stability failure probability due to beam wind and wave condition. (Kubo et al. 2012)	Japan
6	An experimental investigation in the framework of the alternative assessment for the IMO weather criterion. Investigating the weather criterion with free roll decays, roll test in regular beam waves and drift test using three GEOSIM models (1: 33, 1:50 and 1:60). (Bulian, Francescutto, and Fucile 2010)	Italy

## 2.9 Model Selection

In this thesis, there are two models used for the experimental analysis. The selection of the ship model is important because it will attract researchers' attention and it might lead the results to be validated or discussed in other researchers' works.

The first model uses the simple basic shape of a container ship. This model is known as the "ASL shape". The characteristics of the ASL shape are that it is 140 metres in length, has a beam of 20 metres, a design draught of 6 metres and the displacement is at 26,994 metric



tonnes. For the superstructure arrangement, it has two box shapes representing the bridge and container. The model scale is 1/100<sup>th</sup>.

The second model is a research ship model, the well-known DTMB 5415 (Molgaard 2000). Model 5415 was conceived as a preliminary design for a navy surface combatant. The hull geometry includes both a sonar dome and transom stern. There is no full-scale ship that exists. Model 5415 has undergone various tests in deep water, both appended and bare hull, rotating arm test and free model tests. To the author's best knowledge, there is no report on the stability results of weather criteria for Model 5415 published. The experimental assessment of intact and damaged ship motions in the head, beam and quartering sea was reported by (Begovic et al. 2013). The experiment was carried out in the Kelvin Hydrodynamic Laboratory in the University of Strathclyde, Glasgow. During the tests, the motion responses of the model in 6 degrees of freedom (d.o.f) were measured using a QUALISYS motion capture system.

## 2.10 Weather Criterion Explanation

The weather criterion adopted by the IMO as Resolution A.562, is based on a number of simplifying assumptions. Figure 2.15 shows the flow chart to explain the procedure step by step. The ship floats with the design loading condition. Then, the ship attains a stationary angle of stable heel ( $\phi_0$ ) due to the side wind loading represented by  $l_{w1}$ . The  $\phi_0$  must obey Rule 1 which is presented in Figure 2.16. If Rule 1 fail, the design process should be reviewed at the design office. If passed, the design process proceeds with the impact on rolling due to wave action. The ship is assumed to perform a resonant rolling motion due to wave action, as a result of which it reaches a momentary maximum angle ( $\phi_1$ ) toward windward. As of this position, the ship is most vulnerable in terms of weather-side excitations and it is further assumed that the ship is acted upon by a gust of wind represented by a lever  $l_{w2}$  by equation,  $l_{w2} = 1.5 l_{w1}$ . The ship then rolls freely. At this stage, the  $\phi_2$  is obtained. Rule 2 is shown in Figure 2.17. Two requirements must be fulfilled which are the area under  $l_{w2}$  where Area b must be equal or greater than Area a and the  $\phi_2$  must be less than  $50^\circ$  or  $\phi_c$ , whichever is less. The  $\phi_c$  is an angle of second intercept between the wind with the gust heeling lever,  $l_{w2}$  and  $GZ$  curve.

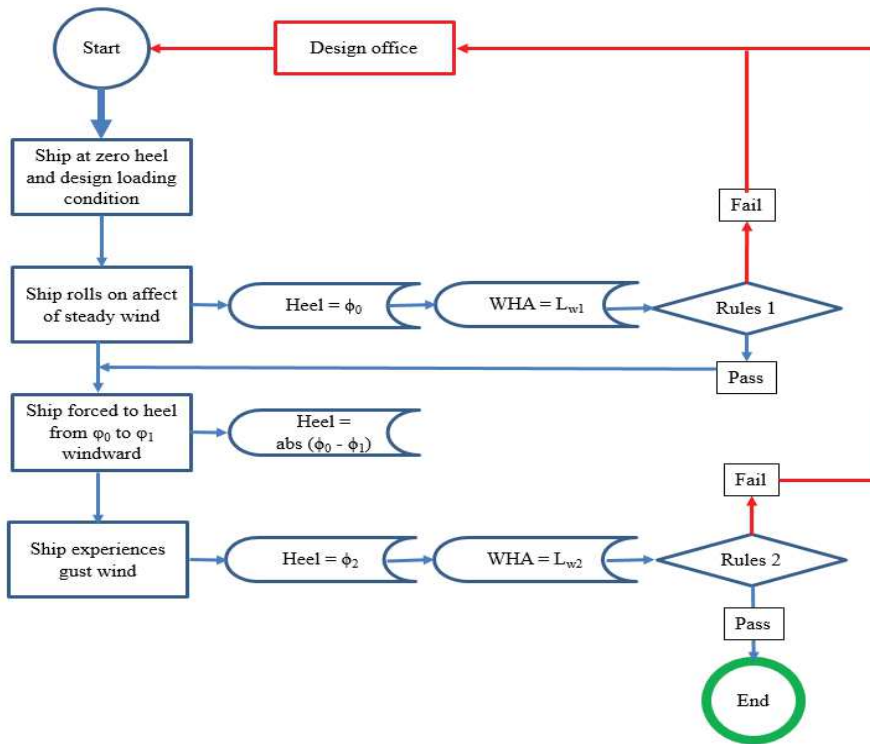


Figure 2.15 Flow chart for the weather criterion

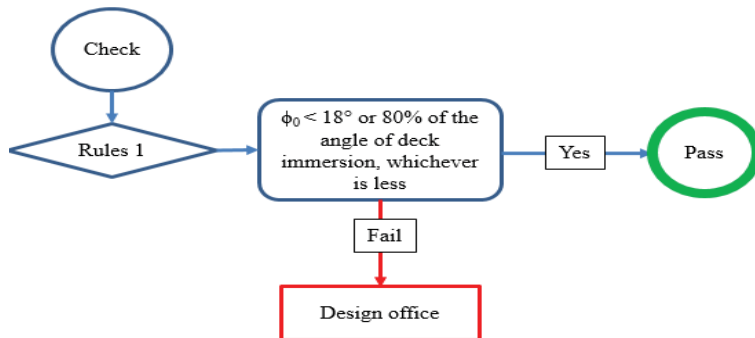


Figure 2.16 Rules 1 for the weather criterion

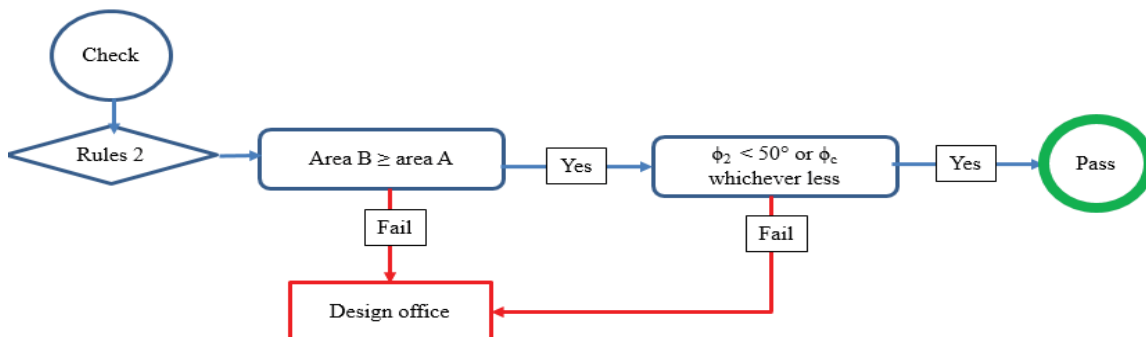


Figure 2.17 Rules 2 for the weather criterion



In the 2008 IS Code, the two most critical parameters required to evaluate the weather criterion are the wind heeling arm,  $l_{w1}$  and the angle of roll to windward due to wave action,  $\phi_1$ . Figure 2.18 and Figure 2.19 show the input values required to calculate  $l_{w1}$  and  $\phi_1$ . The formulae used in the weather criterion are as below:

$$L_{w1} = (P \cdot A \cdot Z) / 1000 \cdot g \cdot \Delta \text{ (metres)} \quad (2.28)$$

$$L_{w2} = 1.5 l_{w1} \text{ (meters)} \quad (2.29)$$

$$\phi_1 = 109 \cdot k \cdot X_1 \cdot X_2 \cdot (r \cdot s)^{0.5} \text{ (degrees)} \quad (2.30)$$

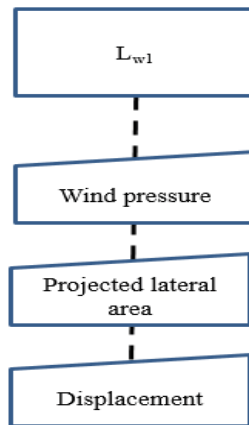


Figure 2.18 Input values for determining wind heeling arm

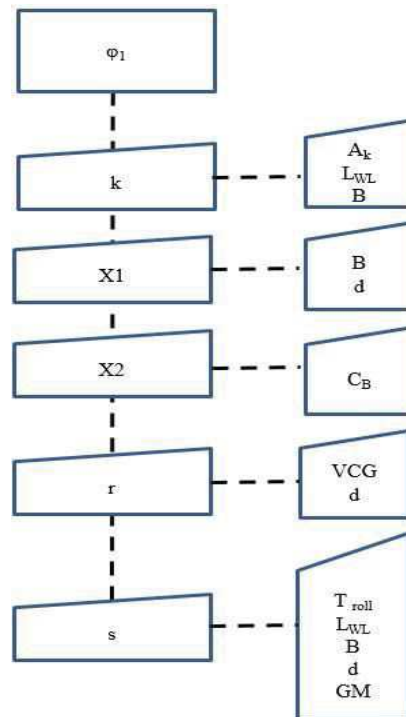


Figure 2.19 Input values for determining  $\phi_1$

## 2.11 Wind Tunnel

The IMO has provided an alternative means for the assessment of severe wind and rolling criteria (the weather criterion). It provides guidelines to determine the wind heeling lever and angle of roll due to wave action. The guidelines provide the industry with alternative means to modelled experiments in the wind tunnel and the towing tank (IMO MSC.1/Circ.1200 2006). In these guidelines, the angle of roll is referred to as  $\phi$ , while in the 2008 IS Code, the angle of the roll is referred to as  $\theta$ . This contradiction sometimes creates a misunderstanding for beginners. The steady wind heeling lever,  $l_{W1}$ , is obtained by the following equation:

$$l_{W1} = \frac{M_w(\phi)}{\Delta} = \frac{M_{wind}(\phi) + M_{water}(\phi)}{\Delta} \quad (2.31)$$

Where;

- $M_w(\phi)$  = total heeling moment when the ship is drifting laterally due to a beam steady wind ( $90^\circ$  heading angle) with an angle of heel,  $\phi$ ;  
 $\Delta$  = displacement (N) of the ship.

Determination of  $l_{W1}$  requires a load cell in the wind tunnel (Figure 2.20) and towing tank (Figure 2.21). The determination of  $\phi_1$  is performed by three methods either by a direct measurement, a three-step procedure or a parameter identification technique. An example of a roll test in beam wave is shown in Figure 2.22. These methods are explained in the guidelines. This model experiment decouples the wind and water effect on the ship model. Therefore, the actual reaction of the ship model toward the wind and water effect is not simulated continuously.

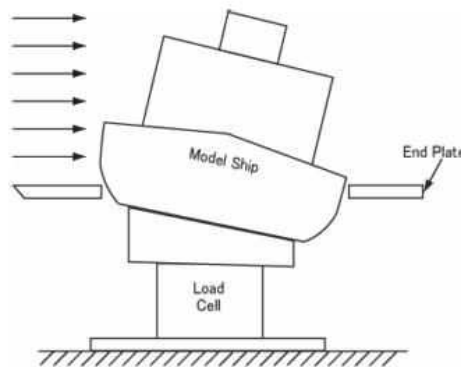


Figure 2.20 Arrangement for test in wind tunnel. Extracted from (IMO MSC.1/Circ.1200 2006)

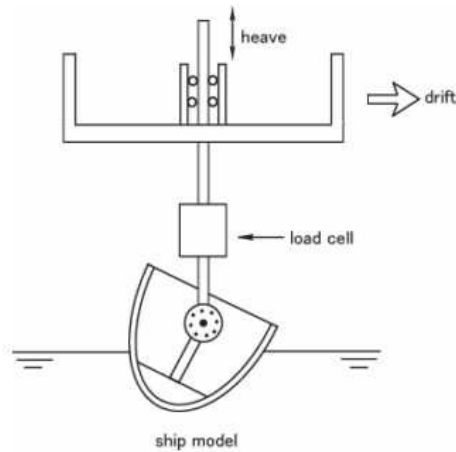


Figure 2.21 Arrangement for drifting test. Extracted from (IMO MSC.1/Circ.1200 2006)

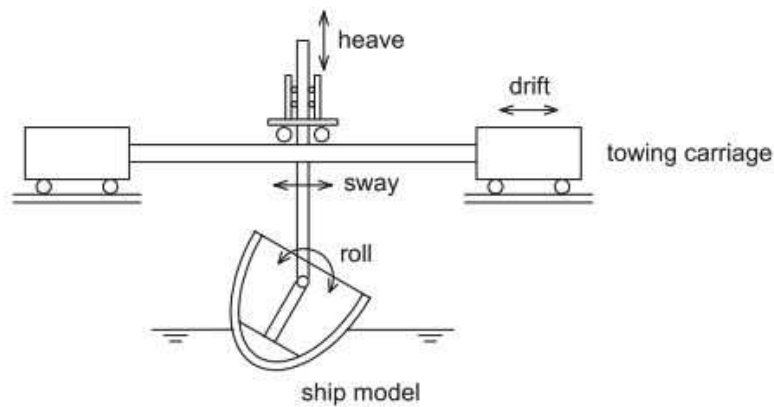


Figure 2.22 Arrangement for roll test in beam waves. Extracted from (IMO MSC.1/Circ.1200 2006)

## 2.12 Wind Healing Arm

Verification of the ship stability for the weather criterion is based on the effect of wind. Strong winds can increase the heeling angle and increase the risk of capsizing. Thus, the selection of wind profile is critical. The IMO uses a wind speed of  $26 \text{ ms}^{-1}$  (50.5 knots) as the nominal wind speed in its weather criterion. The wind with a gust factor of 1.225 ( $\sqrt{1.5}$ ) can give a gust wind speed of  $31.6 \text{ ms}^{-1}$  (61.9 knots).

The IMO applies this criterion to all standard types of ships or marine vehicles of 24m length and above (IMO 2009). The selection of  $26 \text{ ms}^{-1}$  is an average between the maximum winds of a tropical cyclone (called a typhoon by the Japanese) and the more steady winds in the immediate aftermath as cited by Hayes et al. (Hayes et al. 2015). The examination of the actual data presented by Yamagata is shown in Table 2.1.

To the author's best knowledge, there is no actual historical evidence available for the development of the wind speed for weather criteria in the Naval Rules. The defining event for formulating USN intact stability was Typhoon Cobra in 1944. It was described as a Force 12 with an average wind of 50 to 75 knots and gusts as high as 120 knots. Brown and Deybach reported that the USN identified 100 knots as a reasonable wind velocity for ship survival in a tropical storm (Brown and Deybach 1998).

Some of the assumptions in the 2008 IS Code for the wind heeling arm are very common with other stability rules which are simplistic and do not reproduce faithfully the physics of the studied phenomenon (Luquet et al. 2015). Examples of such assumptions include:

- a. Fixed value for aerodynamic drag coefficient regardless of the ship geometry or heel angles (e.g  $C_D = 1.12$ ),
- b. Fixed location (centroid of projected lateral areas) of application of aero and hydrodynamic forces,
- c. Worst case is zero speed with a beam wind,
- d. Constant wind speed. Gusting is accounted for as either an increase in wind lever arm or by defining the requirement for righting arm area ratios (naval stability rules),
- e. No variation in amplitude of wind against altitude (IMO) or simple wind profile (Naval Rules),
- f. Simplified windage area.

The wind heeling moment formula in the French military regulation, IG 6018 is derived from the work of Sarchin and Goldberg. It requires a reference wind speed at 10 metres in height above the waterline), assumes a wind speed profile ( $\sim h^{1/7}$ ) and integral method over the projected surface area exposed to wind. The integration method is simplified by dividing this surface area into horizontal strips, each being subjected to a constant wind speed depending on the average height of the considered strip. The inclining lever arm in metres or  $BLI$ , due to wind (wind heeling moment divided by  $\Delta.g$ ), is then obtained by summing the influence of each strip as follows:

$$B.L.I = \sum \frac{0.0195 \cdot A_i \cdot h_i \cdot V_i^2}{1000 \cdot \Delta} \cos^2 \phi \quad (2.32)$$

Where,

- $V_i$  = wind speed at strip centre (knots);  
 $A_i$  = projected area of each strip ( $m^2$ );  
 $h_i$  = vertical distance between the centre of the strip and the drift centre (assumed to be immersed at  $T/2$ ) (m);  
 $\phi$  =heel angle ( $^\circ$ ), vessel displacement (t).

The coefficient 0.0195 is derived from the combination of physical constant and the units used for wind speed:

$$\frac{1}{2} \frac{\rho C_y}{g} \left( \frac{1.852}{3.6} \right)^2 = 0.0195 \quad (2.33)$$

Where;

- $C_y$  = 1.12,  
 $\rho$  = 1.29  $kg/m^3$ ,  
 $g$  = 9.81  $m^2/s$ .

The formula used in the naval regulations of the Netherlands are similar to the French regulations, except that they use a  $\cos^3$  term and do not take into account the wind speed profile. An advantage of this formulation lies in its ability to model the decay of the heeling moment while maintaining a non-zero value at  $\phi= 90^\circ$ . The choice to keep one quarter of the zero heel value is seen as somewhat arbitrary. The wind heeling arm formula is as follows:

$$B.L.I = \frac{P.A.I}{1000.\Delta} \cdot \frac{1+3 \cos^3 \phi}{4} \quad (2.34)$$

$$P = \frac{C_w \cdot \rho_t \cdot V^2}{2} \quad (2.35)$$

Where;

- $P$  = wind pressure (Pa)  
 $A$  = windage surface area ( $m^2$ ),  
 $I$  = distance between the half-draught and the windage area centre,  
 $C_w$  = 1.2,  
 $\rho_t$  = 0.125  $kg.s^2.m^{-4}$ ,  
 $V$  = wind velocity (m/s).

In the regulations established by the IMO, which therefore apply to commercial vessels, the pressure applied to the windage surface is specified instead of the wind speed. In addition, the heeling moment is considered invariant with the heel angle. The B.L.I is calculated as follows:

$$B.L.I = \frac{P.A.Z}{1000.\Delta.g} \quad (2.36)$$

Where;

- $P$  = pressure applied to windage surface (Pa),  
 $Z$  = distance between the centre of the windage area and the centre of the underwater lateral area (assumed by default located at  $T/2$ ) (m),  
 $A$  = projected lateral area (m<sup>2</sup>).

This formulation is acceptable as it applies mainly to large commercial vessels such as container ships or tankers, which by their shape have a windage surface almost independent of the heel angle. It is possible to compute an equivalent wind speed by comparing the IMO and naval formula at zero heel. When compared with the French regulations, the following relation is obtained:

$$V = \sqrt{\frac{P}{0.0195.g}} \quad (2.37)$$

Where;

- $P$  = 504 Pa (IMO without gust),  
 $C_y$  = 1.12,  
 $V$  = 51 knots (IMO wind) or 63 knots (IMO wind with gust) instead of 100 knots generally used in naval stability rules for combatants.

As a conclusion, there is still a gap between the regulation, experimental and full scale analyses. The weather criterion or dead ship condition failure mode needs enhancement to minimise the capsizing risk. Several models should be tested to verify the proposed SGISC rules which are able to mitigate the issues raised by the Subcommittee of Ship Design and Construction.

### 2.13 Roll Damping

According to the strip theory, motion damping arises because of the oscillating hull that radiates energy in the form of waves away from the ship. For most motions, this constitutes the major mechanism for the dissipation of energy. So, the strip theory estimates of motion damping are generally adequate and a reasonable motion prediction is usually obtained. Unfortunately, rolling motion is an exception to this general rule. The wave making damping  $b_{44w}$  predicted for the potential flow around most hull forms is only a small fraction of the total roll damping which is experienced in reality. Additional important damping contributions are illustrated in Figure 2.23.

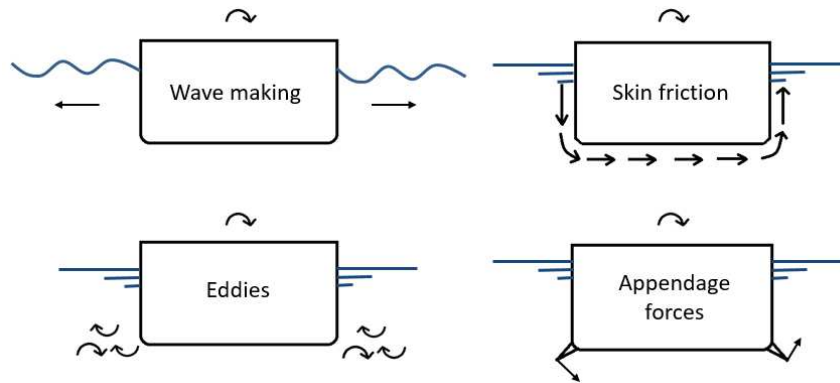


Figure 2.23 Sources of roll damping

Hull forms with relatively sharp corners at the bilges or at the keel will shed eddies as the ships rolls. This absorbs a good deal of energy and is a significant source of additional roll damping. Skin friction forces on the surface of the rolling hull may also be significant and any appendages will generate forces which oppose the rolling motion. Eddy shedding, skin friction and the appendage forces experienced at low forward speed arise because of the influence of viscosity which is neglected in the strip theory (Lloyd 1998).

## 2.14 Current Research Approach

The latest developments of the second generation intact stability criteria (SDC 3) were studied. An evaluation of SGISC was executed using five ships. These ships were designed in a 3D model. Hydrostatic solver software was used to evaluate the stability characteristics. Only criteria of SGISC that related to hydrostatic information were evaluated. The results were then checked against other hydrostatic solver results to verify the code developed in GHS. The development of GHS code is explained in Chapter 3.

In the SGISC domain, several approaches were reported based on the calculation method. Therefore, another approach was determined for this research work. Until the SDC 3, there was no draft or recommendation for the direct assessment of dead ship condition. In contrast, the first level of dead ship condition failure mode is the same as that used in the weather criterion of the 2008 IS Code. Therefore, this research explores the possibility of introducing direct assessment for dead ship condition.

As the first step, an experiment was prepared. Two models were selected to be made and tested in a wind tunnel. The first model was a containership shape and the second model was a naval ship shape. These construction models were tested for displacement, weight, VCG and natural roll period verification. Good agreements were obtained for both models. Then, the experimental work started with the angle of stable heel ( $\phi_0$ ) test. Both results were compared with the angle of stable heel value obtained by GHS based on IMO rules. Generally, the IMO is always conservative. As expected, GHS produced a higher value than the

experimental value. However, this phenomenon does not appear for DTMB. Therefore, a study to understand the results obtained by GHS and experiment was made. The drag coefficient was then explained the physics of the results for example; the physics of the results of the drag coefficient in particular was examined.

The second step studied was the angle of heel to windward due to waves ( $\phi_1$ ). Both the IMO and Naval Rules have a different approach to determining the  $\phi_1$  and the wind velocity. Therefore, several sets of  $\phi_1$  and several sets of wind velocity were used in this experiment. In the results and discussion section, the results presented were obtained by interpolation. The details of the wind tunnel test procedure are explained in Chapter 4.

The next objective in the development of the SGISC is to define the requirements and procedures necessary for direct assessment. This is a formidable task. Not only must the most advanced technologies available be used, but they also need to be available worldwide. Direct assessment will be based on two methods; experimental and fast-time domain simulation (Peters et al. 2012). A conceptual scheme of the assumed underlying simplified physical modelling of the phenomenon is shown in Figure 2.24. The overview of the logic of the short term modelling is as follows (IMO 2016):

- a. Ship characteristic parameters are assumed to be available (displacement, righting lever, roll damping, windage area characteristics, etc.);
- b. The environmental conditions are specified regarding wind and waves;
- c. The wind state is provided as a mean wind speed and a wind gustiness spectrum;
- d. The mean heeling moment due to wind is determined starting from the mean wind speed;
- e. The spectrum of the roll moment due to the wind gust is determined starting from the wind gustiness spectrum;
- f. The sea state is provided concerning a sea elevation spectrum, from which a wave slope spectrum is directly determined;
- g. The spectrum of roll moment due to the waves is determined starting from the wave slope spectrum;
- h. The total spectrum of roll moment is assumed to be given by the sum of the spectrum of roll moment due to wind gustiness and the spectrum of roll moment due to waves;



- i. The dynamics of roll is then assumed to be modelled by means of a nonlinear 1-DOF equation of motion, which considers the ship characteristics (roll restoring, roll natural period and roll damping), the mean heeling moment due to the mean wind, and the irregular roll moment due to the combined effect of gust and waves.

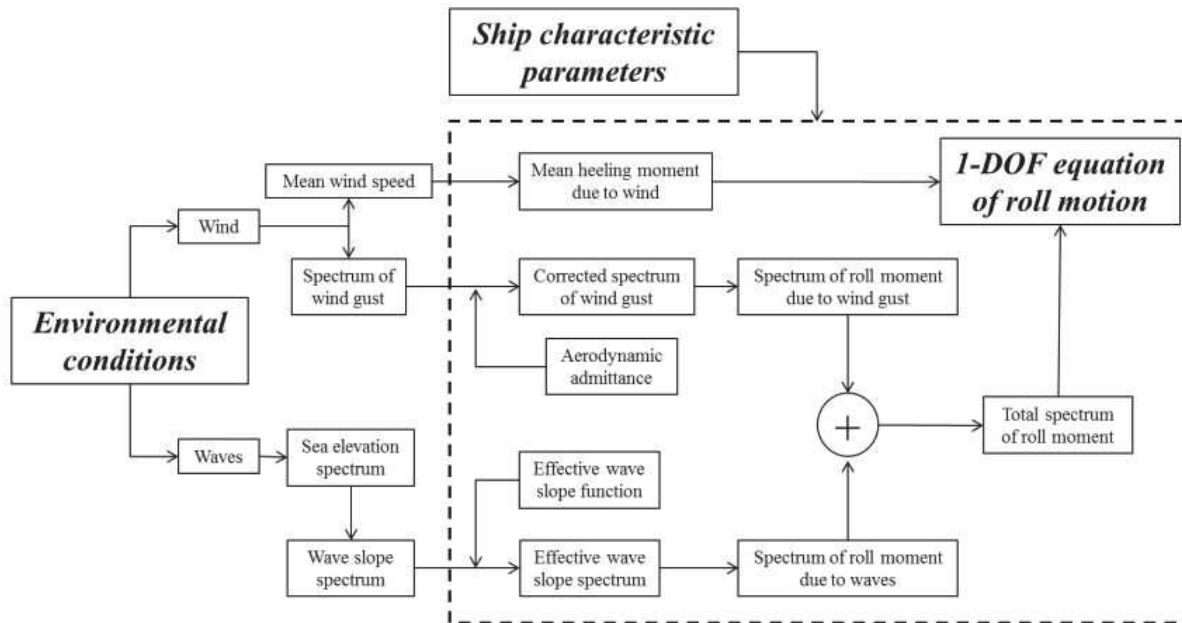


Figure 2.24 Conceptual scheme of the assumed simplified physical modelling for the short-term assessment. Extracted from (IMO 2016)

Therefore, a 2-dimensional RANSE was proposed to validate the GHS® and experimental results. In this research, a CFD code named FINE/Marine® was used. It is a commercial code used in the marine industry and academic domain. The development of the simulation process is presented in Chapter 5. At the end, a conclusion on the overall research is presented in Chapter 6.

## Chapter 3 – General Hydro Statics (GHS) and Results

This section describes the hydrostatic solver used in this research work. It explains the basic command used for the 2008 IS code and continues to the second generation intact stability code which is at the final stage of approval at the Sub-committee on Ship Design and Construction, International Marine Organisation. The code validation using other hydrostatic solvers is also presented.

### 3.1 Introduction to GHS

GHS is an abbreviation of General Hydrostatics. It was created in 1972 for the purpose of serving the naval architecture industry with ship stability calculations. Creative Systems is the originator of GHS. GHS is a PC-based simulator of vessels in fluids and fluids in a vessel such as ships, yachts, docks, drilling platforms, buoys, and tanks. The software is capable of calculating the tank characteristics, longitudinal strength, ground reaction, multi-body and grain ship calculations. GHS can be applied to evaluate the ship based on the 2008 IS Code. In addition, GHS is commonly used for the design and evaluation of all types of ships and floating structures. It addresses flotation, trim, stability and strength by counting the forces involved using mathematical and geometrical models of the vessels (\*.gf format). The primary capabilities of GHS are:

- a. Handling a complex calculation of stability criteria;
- b. True centre of gravity (*CoG*) shifts of tank contents both transversely and longitudinally for better realism and accuracy;
- c. Tank modes for flooding, damage, spilling, water-on-deck and many others;
- d. Heeling about any axis (essential for some shapes - drilling units, for example - and where longitudinal stability is a problem);
- e. Wind heeling moments derived from the geometry at any heel, trim, and axis angle;
- f. Ease of modelling complex structures and interior spaces;

- g. Detailed and flexible graphics depicting the conditions of flotation, flooding and tank loading;
- h. Ground modelling for vessels partly or totally supported by the ground;
- i. Multi-body capability for interactions between vessels.

The process flow in GHS for handling the 2008 IS Code for the righting arm ( $GZ$ ) curve properties is as shown in Figure 3.1.

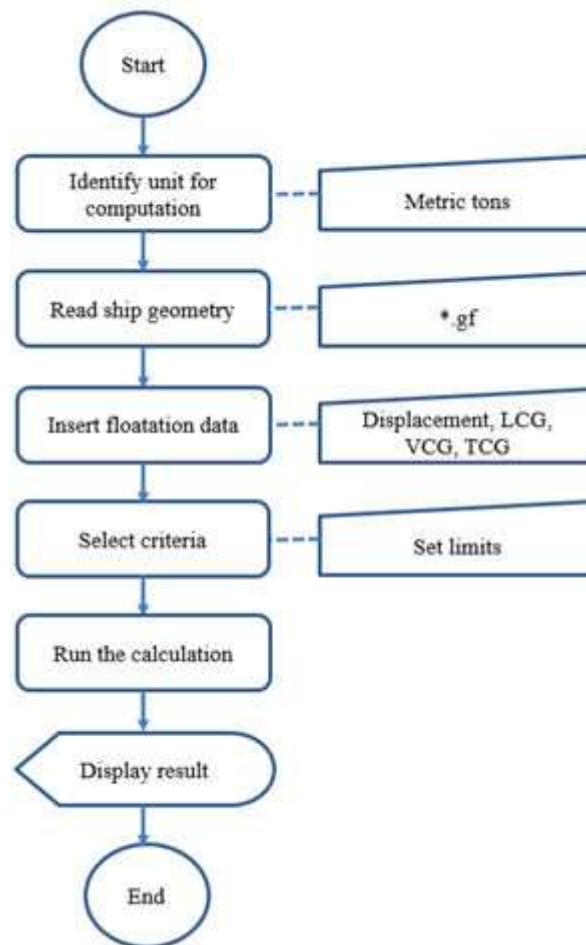


Figure 3.1 Process flow of GHS for the 2008 IS Code

### 3.2 Background Information on the Ships

Five ships were used to investigate the stability performance of the selected ships which involved progressing from a basic shape for easy understanding by theoretical formula to a complex shape which was the frigate shape. All ships were designed in 3D software named

Rhinoceros. The ships were designed to be full scale because GHS is unable to compute hydrostatic data based on scale models. The names of the ships are as listed:

- a. ASL shape;
- b. 5415 shape;
- c. PV shape;
- d. 120m container ship shape;
- e. KL shape.

### 3.3 Ship Description

#### 3.3.1 The ASL Shape

The ASL shape is a basic shape with a simple hull and superstructure for easier understanding of the physical effects. It presents the geometry of a container ship. It has a cylinder hull which allows the model to have a maximum roll angle with a minimum damping effect. On the deck, it has two boxes. The first box represents a bridge and the second box represents a container deck layout. The perspective view is as shown in Figure 3.2. The main characteristics are shown in Table 3.1.

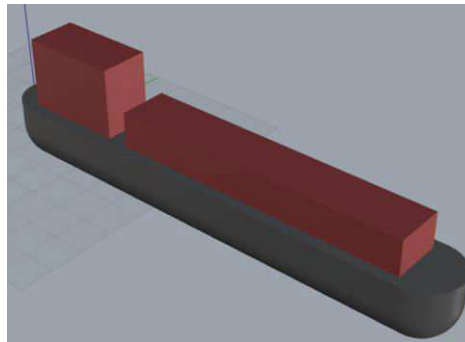


Figure 3.2 The ASL shape

#### 3.3.2 The 5415 Shape

The 5415 shape is a frigate hull. It was conceived as a preliminary design for a navy surface combatant in the US Navy. The hull geometry includes both a sonar dome and transom stern. It has a superstructure that represents the main configuration of a frigate such as the bridge, exhaust stacks, and hangar. This model has been studied for more than ten years as part of an international collaboration between IIHR, INSEAN and DTMB. The perspective view is as shown in Figure 3.3.

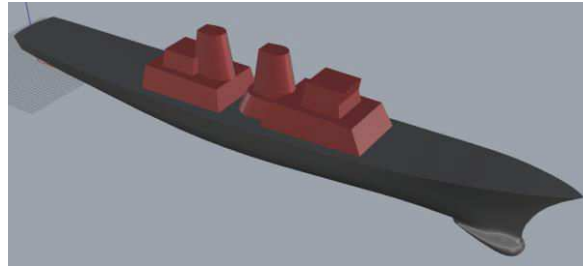


Figure 3.3 The 5415 shape

### 3.3.3 The PV Shape

The PV shape is a conventional patrol vessel hull. It is a common hull without any special appendages such as bulbous bow, sonar array or bow thruster. This hull uses a twin controllable pitch propeller and the geometry is without the superstructure arrangement. The perspective view is as shown in Figure 3.4.

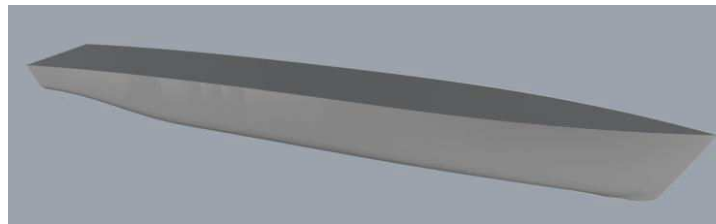


Figure 3.4 The PV shape

### 3.3.4 The 120m\_CS Shape

The 120m\_C shape is a model from the DELFT ship (marine software) database. This hull has a bulbous bow to minimise drag, increase speed and fuel efficiency. This shape is without a superstructure arrangement. The perspective view is as shown in Figure 3.5.

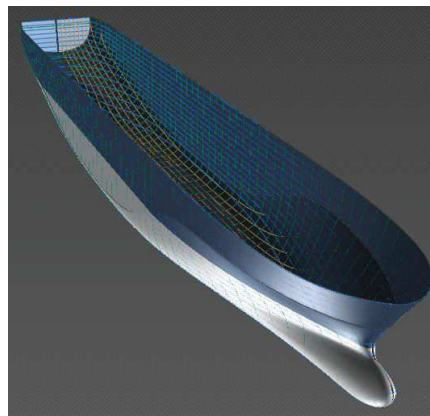


Figure 3.5 The 120m containership shape

### 3.3.5 The KL Shape

The KL shape is a conventional container ship. It is an academic geometry used in ENSTA Bretagne as a sample geometry for stability calculation. It has three boxes on deck. The first box represents a bridge, the second box represents the container layout and the third box represents a bow superstructure. The perspective view is as shown in Figure 3.6.

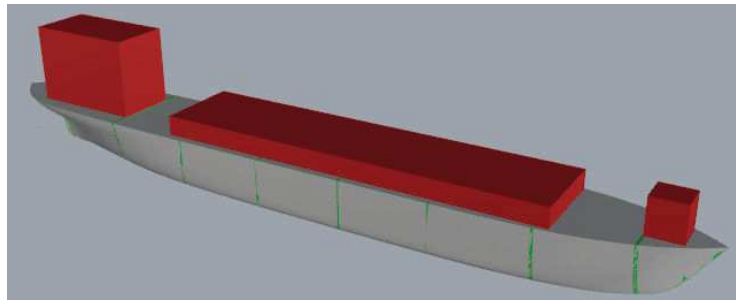


Figure 3.6 The KL shape

Table 3.1 Main characteristics of the models

Model Name	ASL	5415	PV	120m_C	KL
LOA, m	140	153.3	91.1	120.0	253.0
B, m	20.00	20.54	12.00	19.00	33.00
$\Delta$ , tonnes	26,994	8,624	1,653	12,522	30,800
Draught	12.000	6.150	3.400	7.500	5.775
GM, m	0.206	1.952	1.370	6.000	5.827
KM, m	10.206	9.507	7.17	8.532	18.197
VCG, m	10.000	7.555	5.000	2.532	12.37
LCG, m	70.037	71.665	42.853	64.206	135.508
IMO roll angle, °	16.19	17.40	13.14	19.22	27.274
Angle of downflooding, °	30.96	22.71	30.71	38.58	37.64

Generally, the stability of a ship can be expressed by a *GZ* curve at the loading condition. A *GZ* curve is a graph of a model at the design loading condition showing the righting arm heel against the heel angle. In the 2008 IS Code, the criteria of *GZ* curve is stated in Part 2.2, and the *GZ* curve for each model is as shown in Figure 3.7 to Figure 3.11. For Figure 3.7, the *GZ* curve has a weird shape where it has a bended curve from 0 to 10 degrees. This is the result of the ASL hull shape which has a cylinder shape without any bilge keel. This is purposely designed as such in order to evaluate the least stable shape in this research.

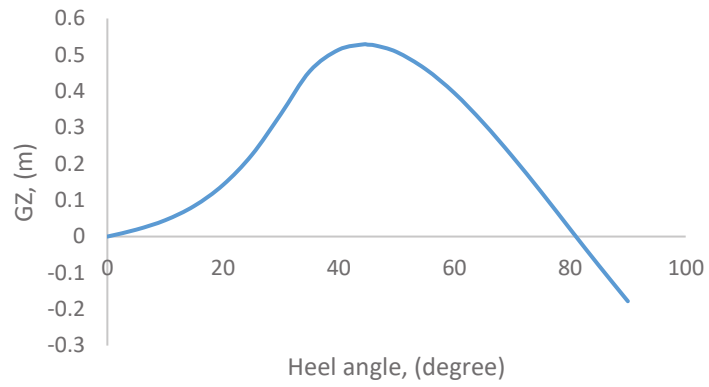


Figure 3.7 *GZ* curve for the ASL shape

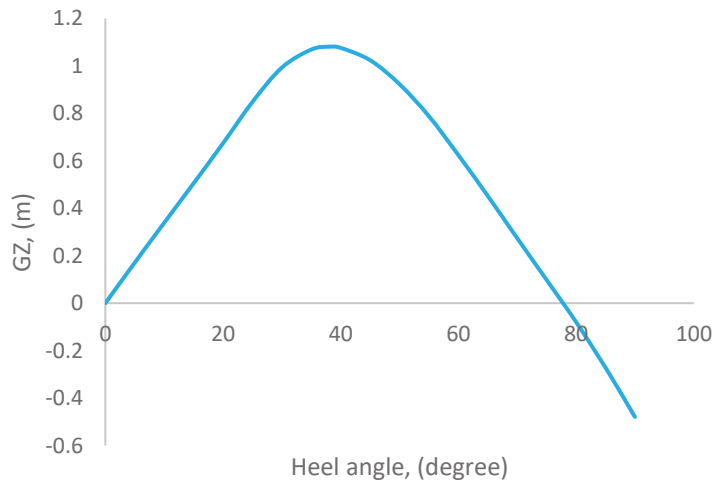


Figure 3.8 *GZ* curve for the 5415 shape

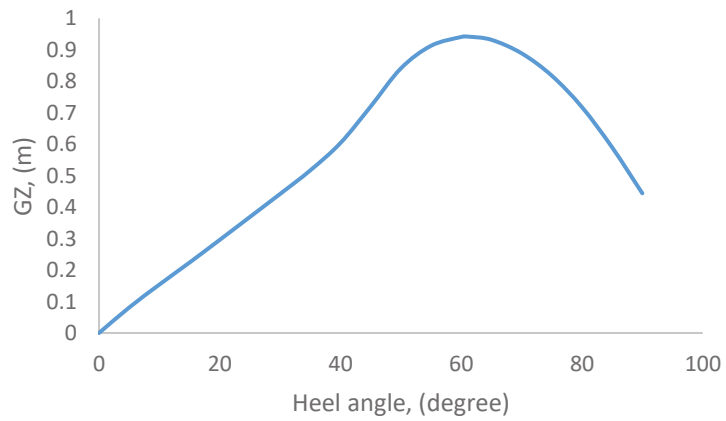


Figure 3.9 *GZ* curve for the PV shape

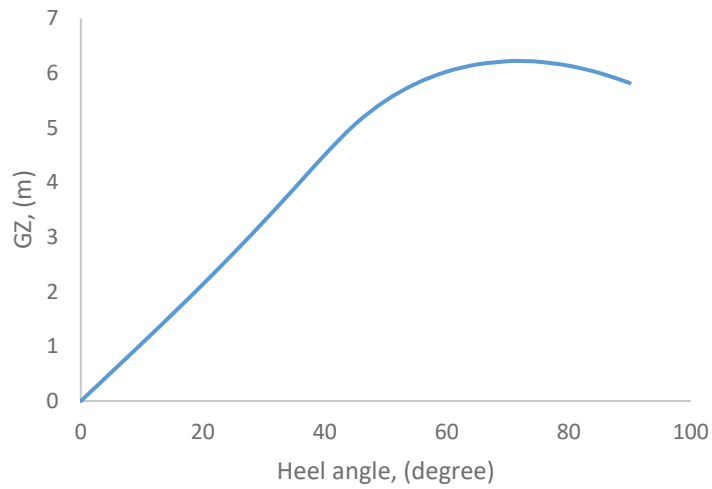


Figure 3.10 *GZ* curve for the 120m containership shape

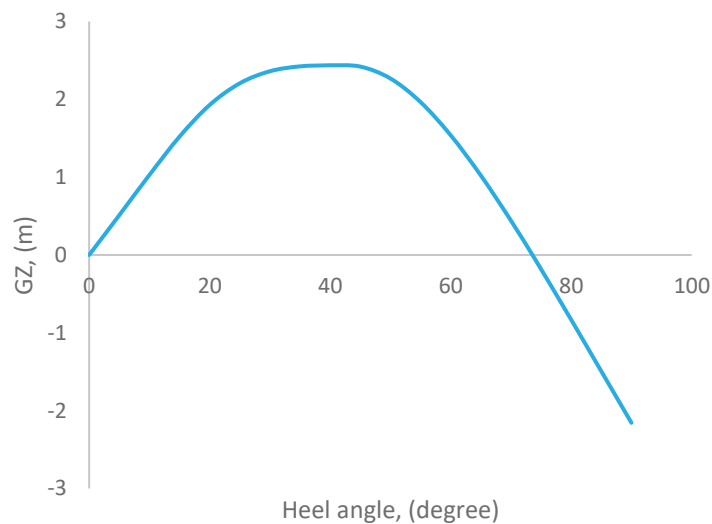


Figure 3.11 *GZ* curve for the KL shape

### 3.4 Current 2008 Intact Stability Code

The 2008 IS Code has two parts. The first part is Part A which is a mandatory criterion and the second is Part B which is recommended for certain types of ships and additional guidelines. In this chapter, the calculation using GHS will be checked based on Part A Chapter 2 – General Criteria. In this chapter, two main criteria must be satisfied which are the criteria regarding the righting lever curve properties (*GZ* curve) and the severe wind and roll criteria (the weather criterion).



### 3.4.1 Righting Lever Curve Properties

This criterion evaluates the righting lever curve obtained by a hydrostatic solver and either it fulfils the requirement which means that it has met the stability limit or not. It addresses the area under the curve and slope of the curve. The limit can be written as follows:

- |    |         |   |                  |
|----|---------|---|------------------|
| a. | Limit 1 | Area from abs 0 to abs 30 degree            | > 0.0550 m.-rad, |
| b. | Limit 2 | Area from abs 0 to abs 40 degree or flood   | > 0.0900 m.-rad, |
| c. | Limit 3 | Area from abs 30 to abs 40 degrees or flood | > 0.0300 m.-rad, |
| d. | Limit 4 | Righting arm at abs 30 degree               | > 0.200 m,       |
| e. | Limit 5 | Absolute angle at maximum righting arm      | > 25.00 degrees, |
| f. | Limit 6 | <i>GM</i> (metacentric height) Upright      | > 0.150 m.       |

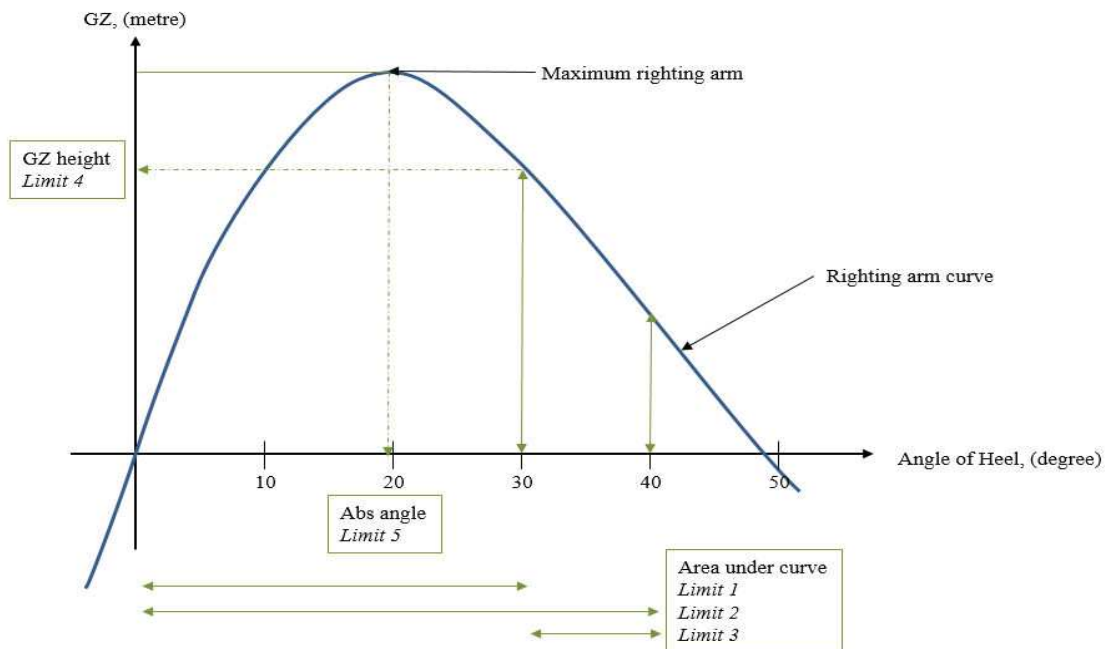


Figure 3.12 Limits in righting arm curve

Limit 1 to 6 could be described in a graphical approach as shown in Figure 3.12. In GHS, the criteria for the 2008 IS Code have been developed and are currently used in the ship design stage. In this thesis, the unit used is the SI-unit and the water density is  $1.025 \text{ kg/m}^3$  (sea water). GHS is adequate to produce the results of ships with the margin value. The margin value provides the designer with an understanding of the stability. All six limits are evaluated and the results including the margin valued are presented. For this example, all limits are passed and shown in green. If the result reveals failure at any limit, that result appears in red. An interface for beginner users to evaluate the weather criterion was developed. The interface is shown in Figure 3.13. This interface provides quick access to evaluate basic ships against the 2008 IS Code righting arm curve properties. The results for the five ships for their righting arm curve properties are shown in Figure 3.14 to Figure 3.18.

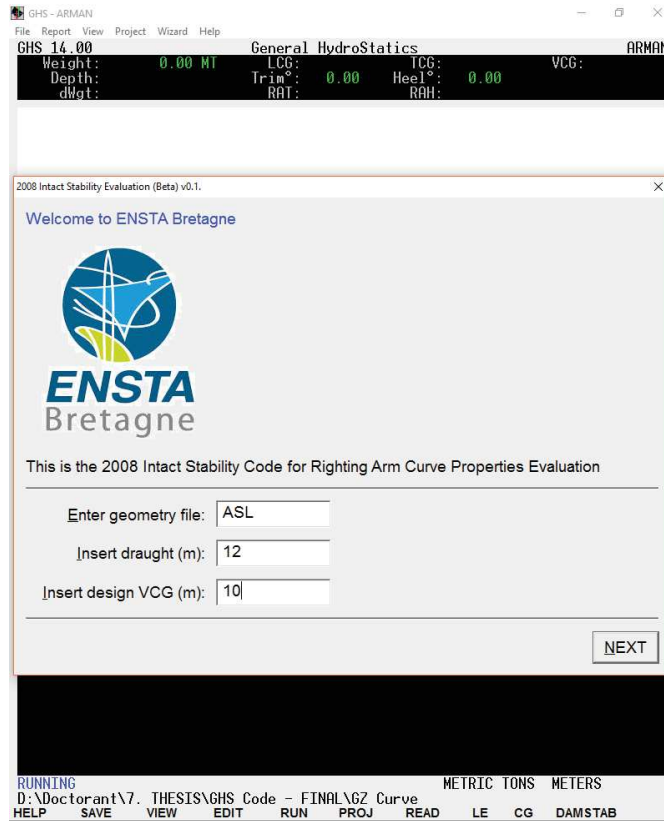


Figure 3.13 Interface for 2008 IS Code righting arm curve evaluation

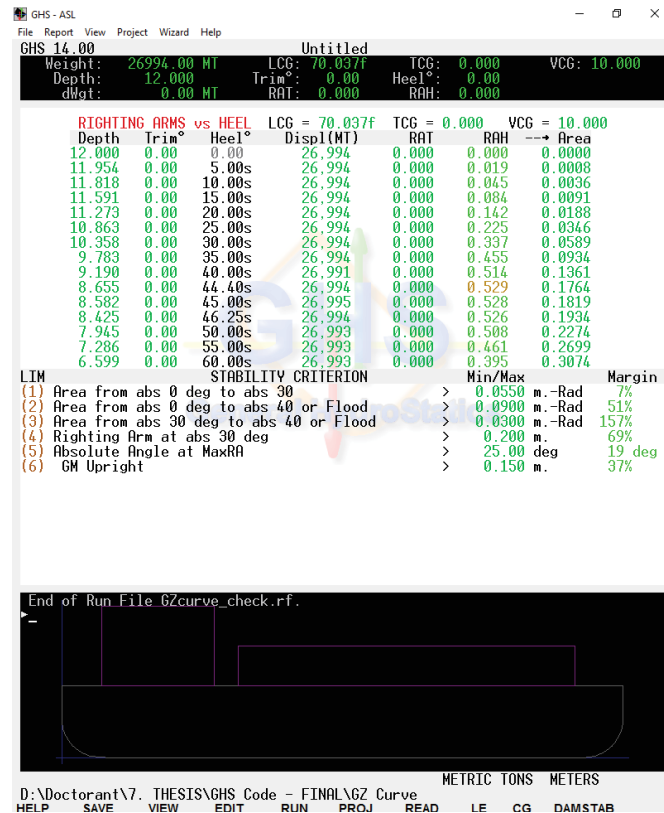


Figure 3.14 Results of righting arm properties for ASL shape

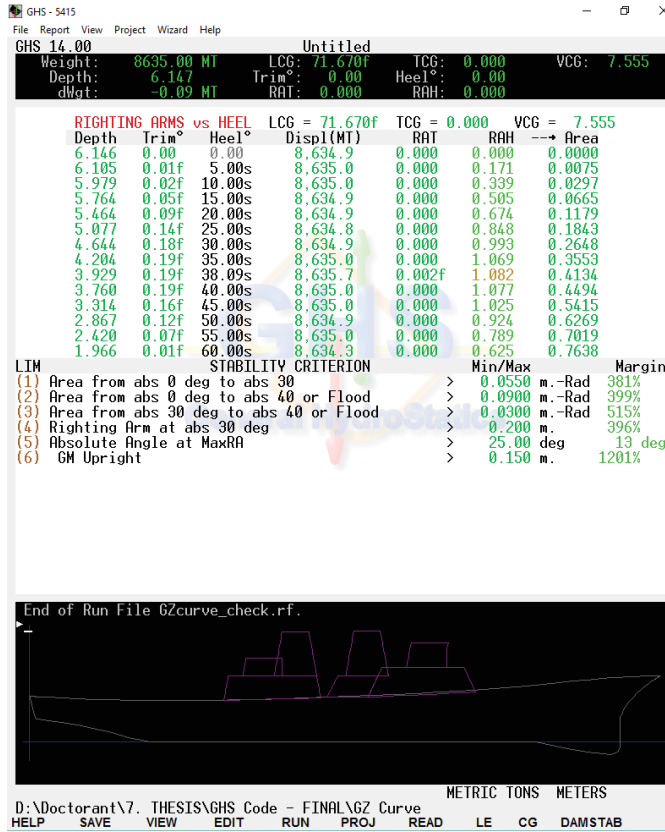


Figure 3.15 Results of righting arm properties for 5415 shape

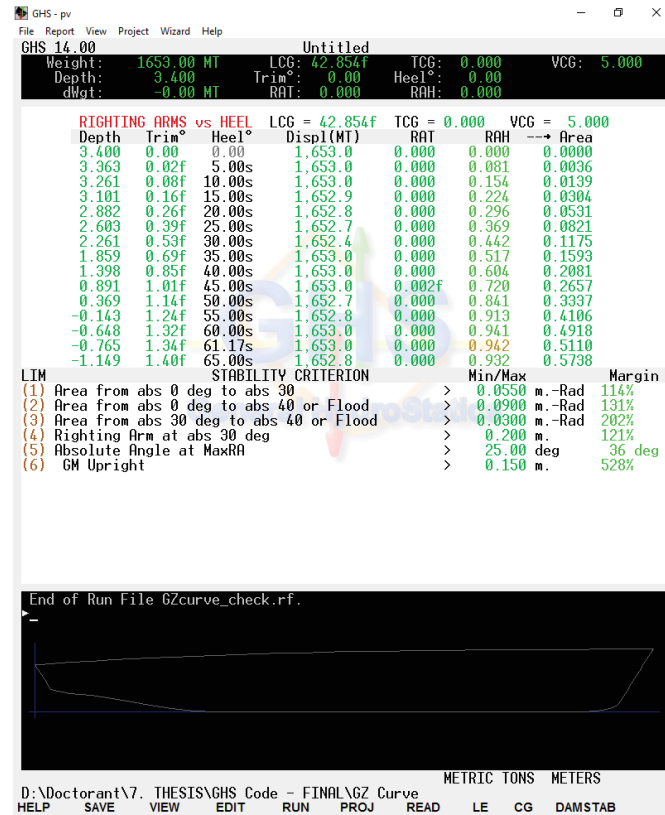


Figure 3.16 Results of righting arm properties for PV shape

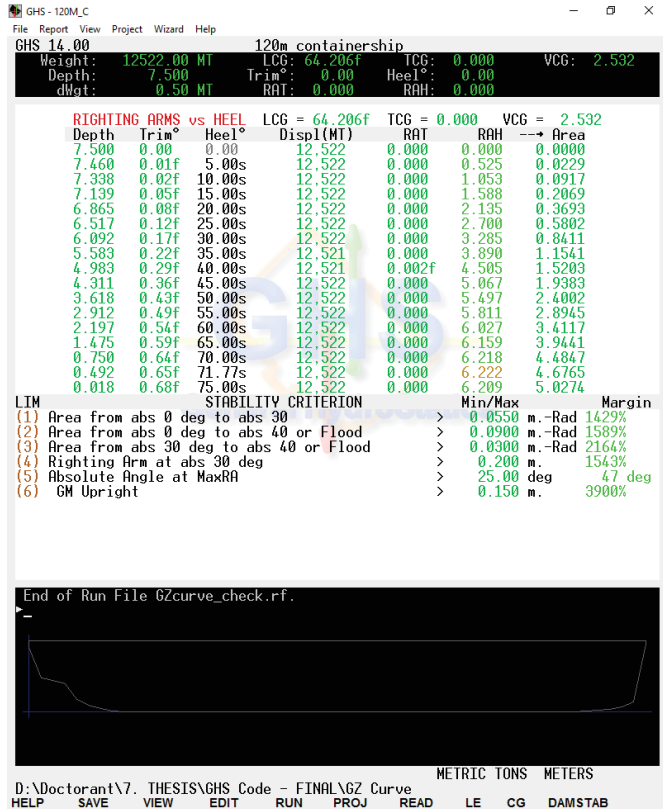


Figure 3.17 Results of righting arm properties for 120m containership shape

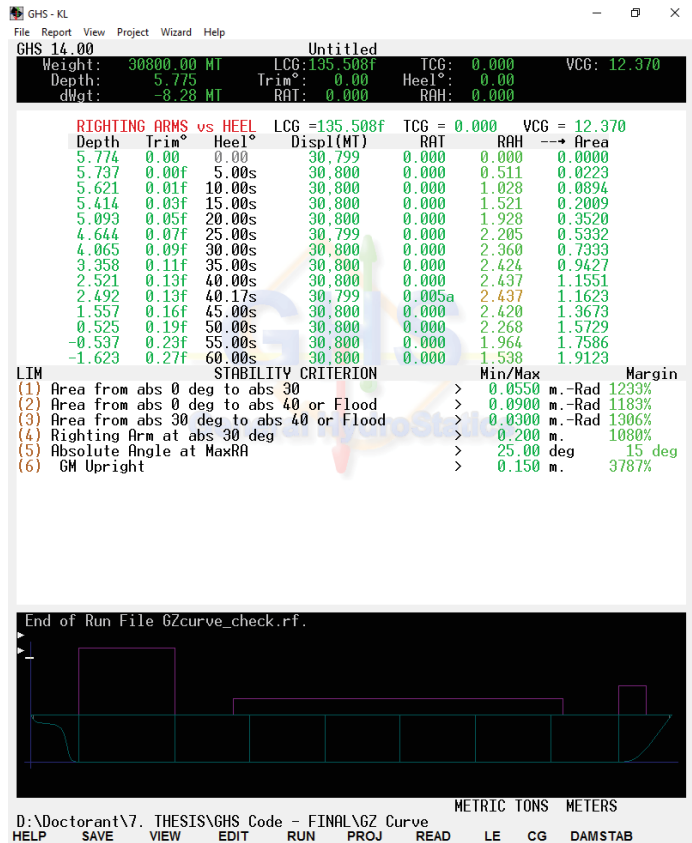


Figure 3.18 Results of righting arm properties for KL shape

### 3.4.2 The Weather Criterion

This criterion evaluates the ability of a ship to withstand the combined effects of beam wind and rolling due to wave action. The beam wind is a steady wind at a velocity of  $26 \text{ ms}^{-1}$ . The rolling angle due to wave is obtained by two methods, either using the formula based on the 2008 IS code or by experimental models. In principle, two limits must be satisfied which are:

- a. Limit 1 – angle of equilibrium  $> 16$  degrees or 80% of the angle of deck edge immersion,
- b. Limit 2 - area  $b \geq$  area  $a$ .

The above limits can be graphically described as in Figure 3.19.

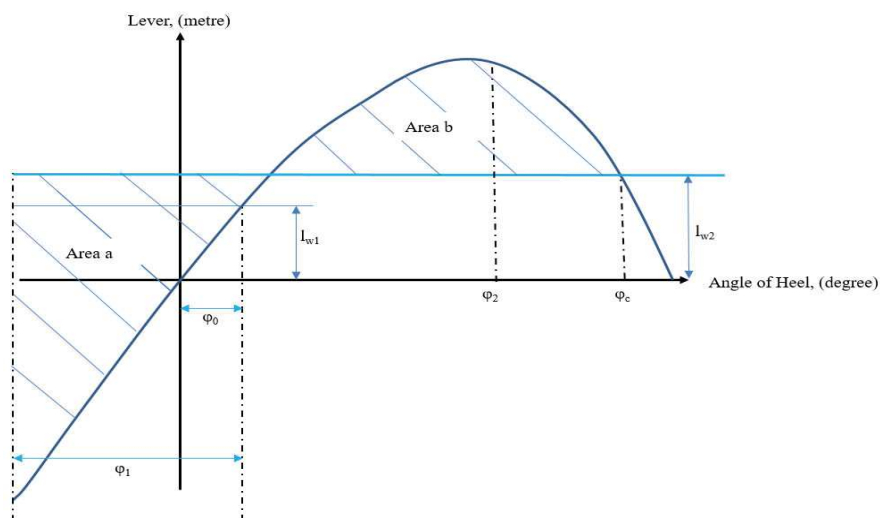


Figure 3.19 Severe wind and rolling

The 2008 IS Code Part 2.3 (IMO 2009) describes the weather criterion. GHS is capable of evaluating the weather criterion. Procedures to evaluate the criterion are described as follows:

- a. Read the geometry in GHS;
- b. Define the design weight,  $LCG$  and critical point;
- c. Solve the draught and  $LCG$ ;
- d. Insert the wind pressure as stated in the IS Code;
- e. Insert command to use an IMO parameter for the roll angle calculation;
- f. Insert the limit;
- g. Receive the report from GHS;
- h. Check the  $\phi_1$  with a  $GZ$  curve in GHS without wind effect. Verify the  $\phi_0$  from GHS with  $GZ$  curve.

Figure 3.20 shows the wind heeling moment, based on pressure as indicated in the weather criterion. Moment is =  $LPA \times SF \times Arm \times Pressure$  where  $LPA$  = lateral plane area,  $SF$  = shape factor,  $Arm$  = lever from the underwater centre to the above-water centre.  $HCP$  = height of the centre of pressure (centroid). GHS computes the total area that is subject to the wind effect. Figure 3.21 shows the angle of equilibrium base of the wind applied. The angle of equilibrium is 1.27°. Figure 3.22 shows the parameters used for the calculation of roll angle based on the IMO weather criterion. The roll angle is 27.28° which is the roll back angle. Figure 3.23 shows the wind with gusts and the ship heeling to 25.99 starboard. This angle is calculated from the rollback angle minus the angle of equilibrium. Figure 3.23 shows the  $GZ$  curve result for the weather criterion. The angle of equilibrium wind and gust heeling moment is 1.9° which also appears in Figure 3.24.

To verify the wind heeling moment, we need to calculate the wind arm. Wind heeling moment =  $RAH \times displacement$ , where  $RAH$  = righting arm heeling. Figure 3.20 shows that the wind heeling moment is 3,807.65. With the displacement of 30,800, the value of  $RAH$  with wind will be 0.124 (Figure 3.21). Referring to Figure 3.25, the  $RAH$  of 0.1236 will have the heel angle of 1.27° (after interpolation). Figure 3.25 shows the  $GZ$  curve without the wind effect. The  $GZ$  curve for the weather criterion is shown in Figure 3.26. The GHS interface for the weather criterion is as follows:

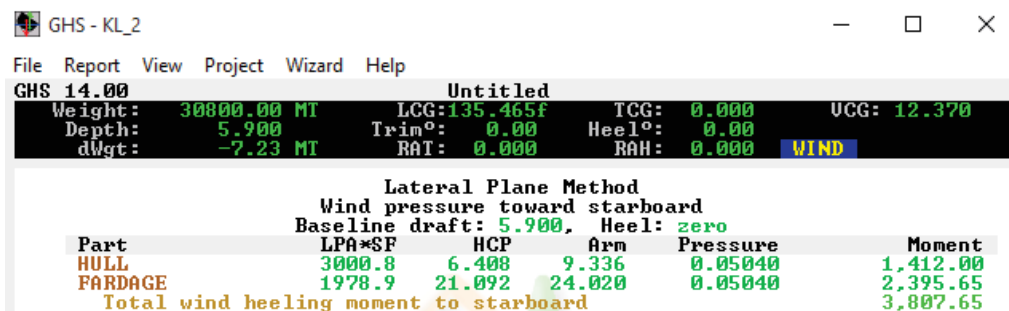


Figure 3.20 Wind heeling moment

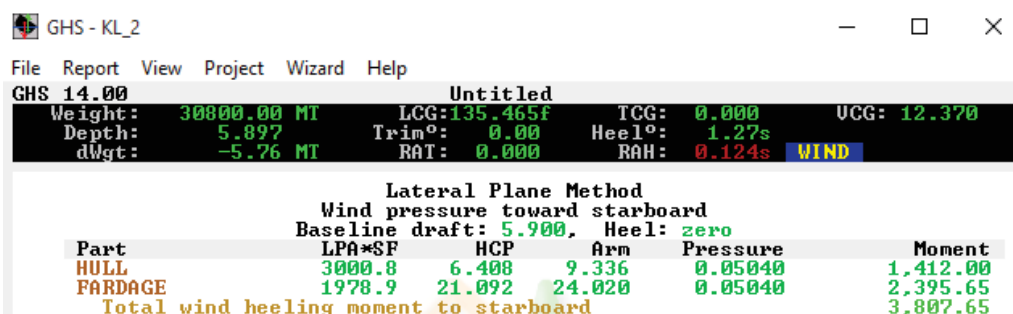


Figure 3.21 Ship heel to angle of equilibrium. Angle of equilibrium = 1.27°

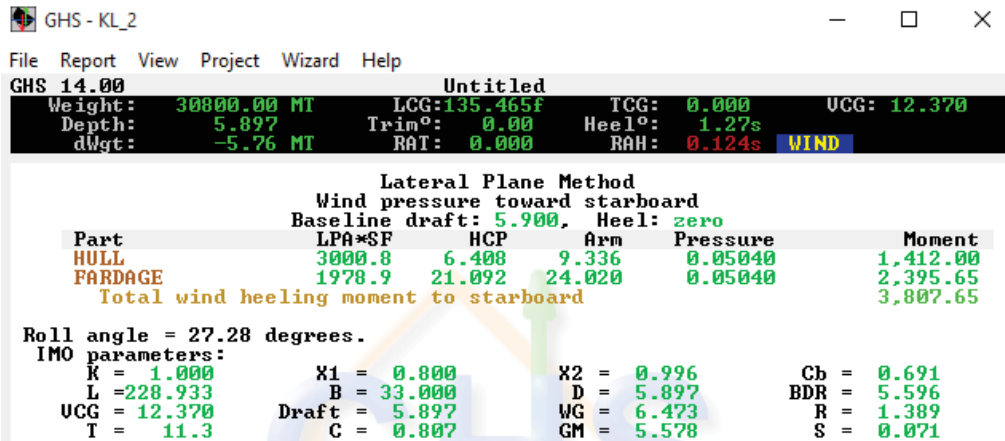


Figure 3.22 IMO parameters and for roll angle calculation. Roll angle = 27.28°

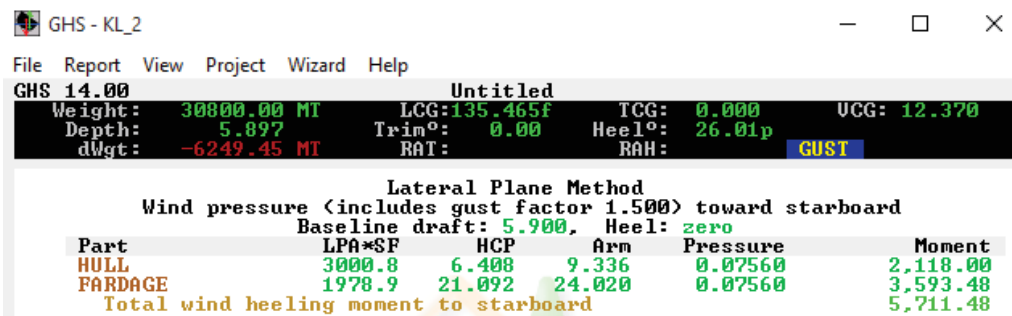


Figure 3.23 The wind with gust heeling moment

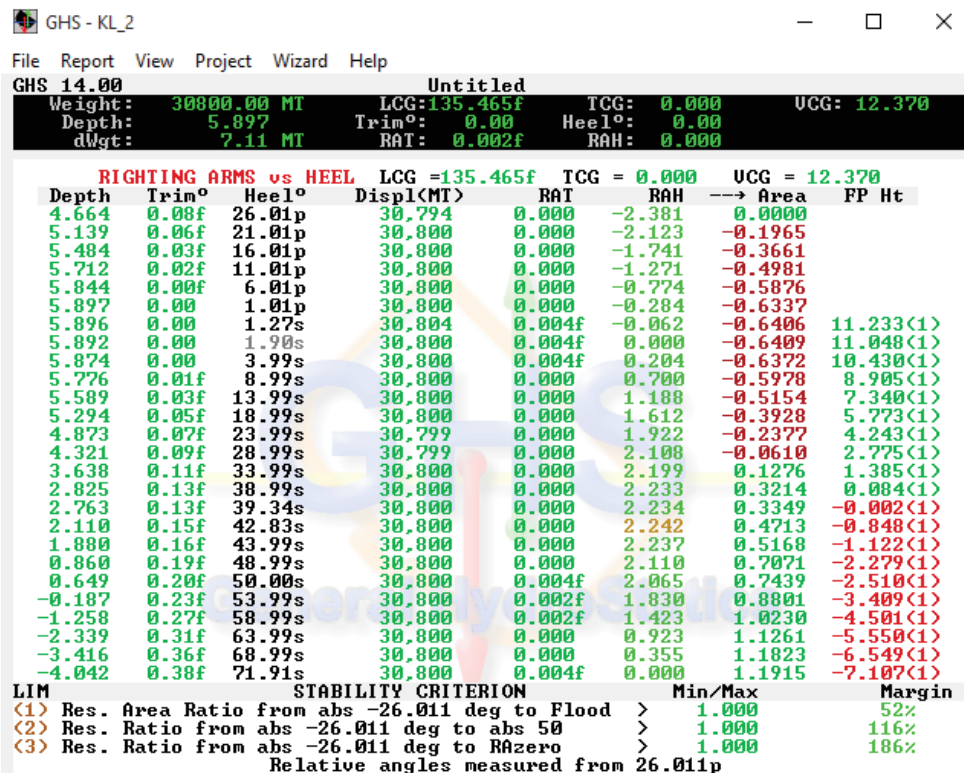


Figure 3.24 The value for GZ curve. The angle of equilibrium with gust is 1.9°



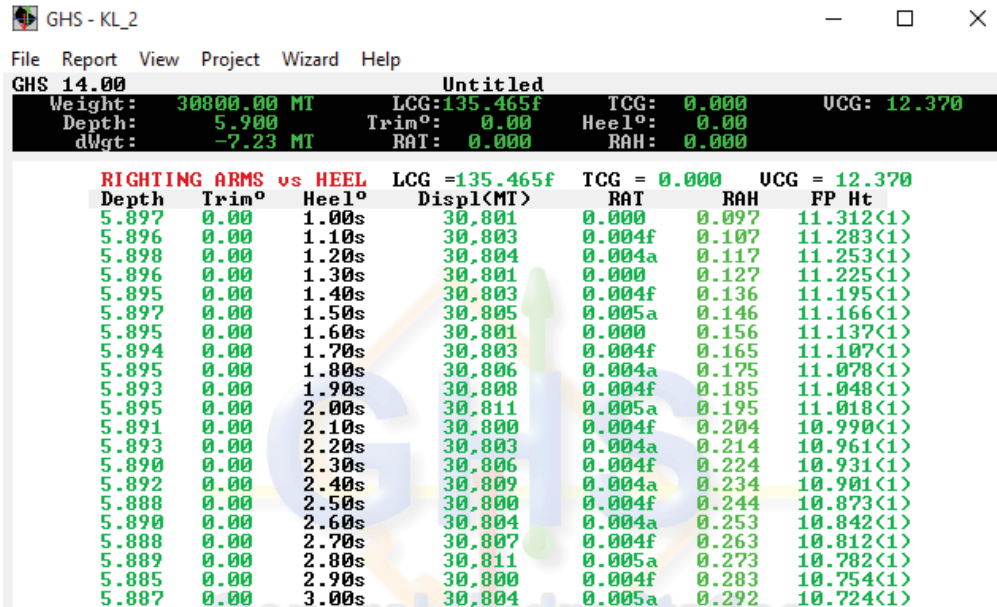


Figure 3.25 GZ curve to verify the angle of equilibrium on wind without gust

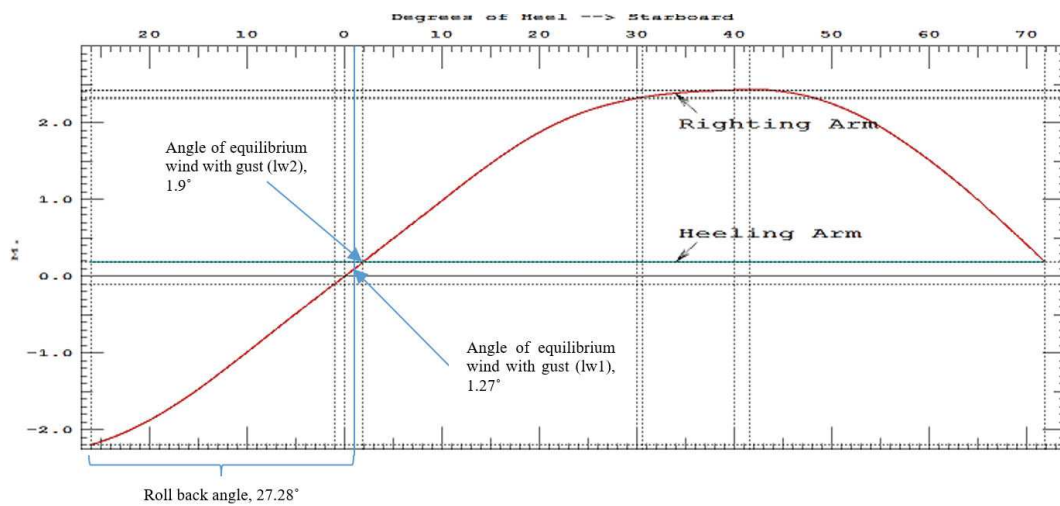


Figure 3.26 GZ curve for the weather criterion

The evaluation of the weather criterion required a ship with superstructure. Therefore, 3 out of the 5 ships, which were the ASL, 5415 and KL shapes, were used. An interface for beginner users to evaluate this criterion was developed. The interface is shown in Figure 3.27. This interface gives a quick access to the evaluation of the basic ship against the 2008 IS Code weather criterion. The results obtained by GHS for ASL and KL shapes are shown in Figure 3.28 to Figure 3.29.

Figure 3.30 shows the results based on the modified IMO weather criterion. It used the wind velocity recommended by the Naval Rules (100 knots) and  $\phi_1$  is  $25^\circ$ . The heeling arm was at 100 knots and no gust effects were considered. The wind heeling arm was constant (without cosine squared). The criterion was capsizing and restoring energy was more than 1. The weather criterion in respect of the Naval Rules was programmed in GHS editor. The Naval Rules use a wind velocity of 100 knots with heel arm with cosine squared. The ratio between



capsizing and restoring energy is more than 1.4. Using the IMO modified criterion, the ratio of area under the curve for 1.0 was obtained at 35.2° was obtained at 40.9°. For a ratio of 1.0, the ship failed the weather criterion for angle of down flooding with less than 73% of the area.

Figure 3.31 shows the results based on the weather criterion of the Naval Rules. It used the wind velocity of the Naval Rules (100 knots) and  $\phi_1$  was 25° regardless of the ship characteristics. The wind level was in relation to cosine squared. As expected, with the cosine square squared for wind heeling arm, both angles of 35.2° and 40.9° obtained more margin compared to a constant wind heeling lever (Figure 3.30). The cosine square provided more area under the curve for the righting moment. The summary of the criteria used to obtain the result for the 5415 shape is shown in Table 3.2.

Table 3.2 Variable used for 5415 shape

	IMO modified	Naval Rules
Wind velocity	100 knots	100 knots
Wind heeling arm	Constant	Cosine squared
Criteria	Area $A_1 =$ Area $A_2$	Area $A_1 =$ Area $A_2$ Area $A_1 =$ 1.4 times Area $A_2$
Result	Figure 3.30	Figure 3.31

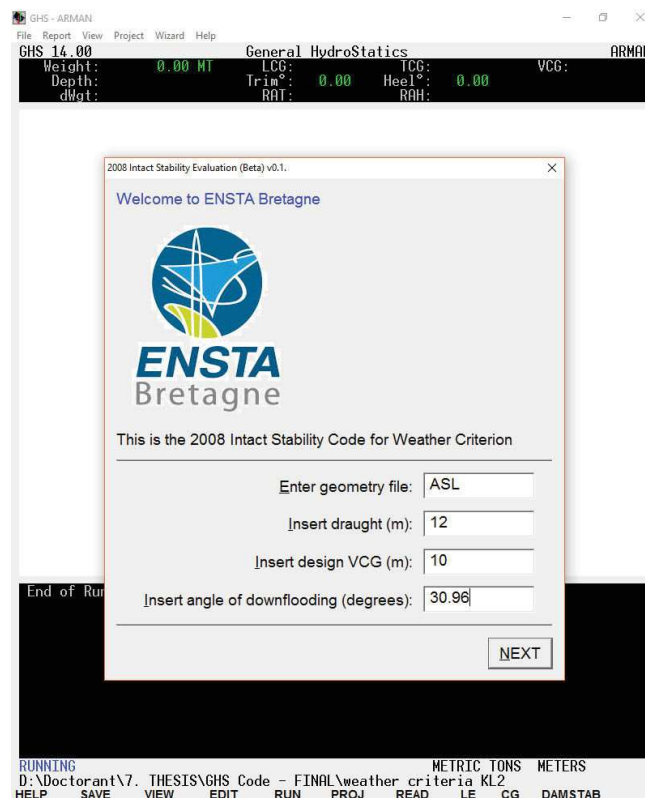


Figure 3.27 Interface for 2008 IS Code weather criterion evaluation

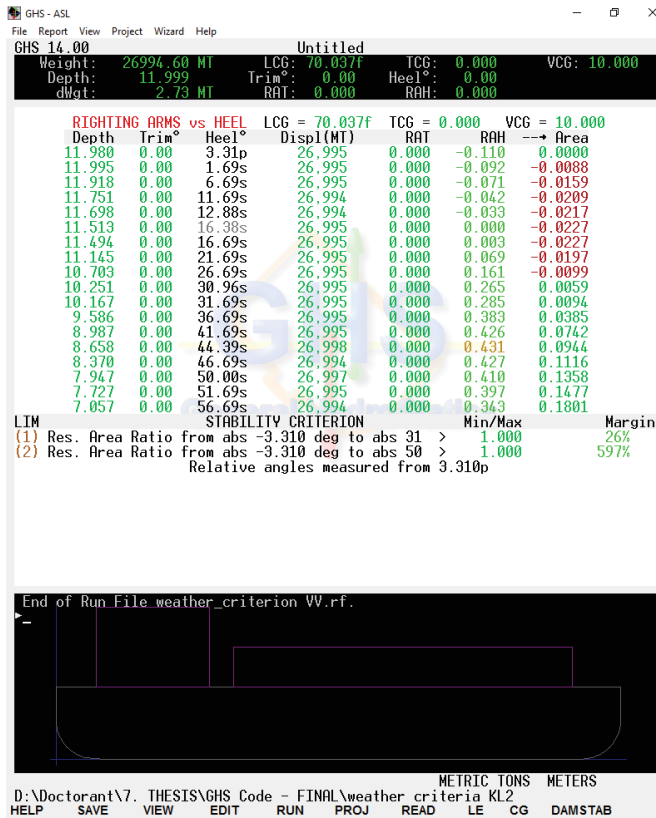


Figure 3.28 Results of weather criterion for ASL shape

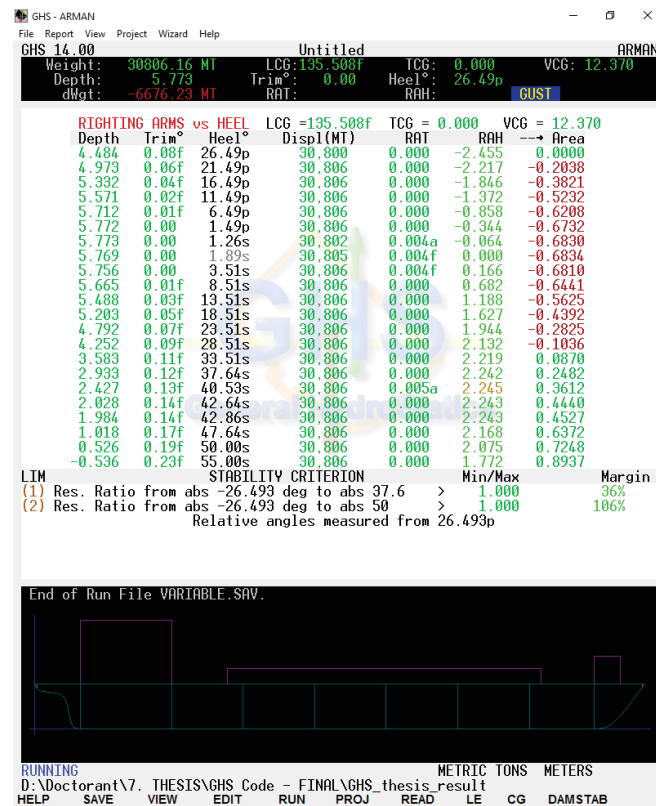


Figure 3.29 Results of weather criterion for KL shape

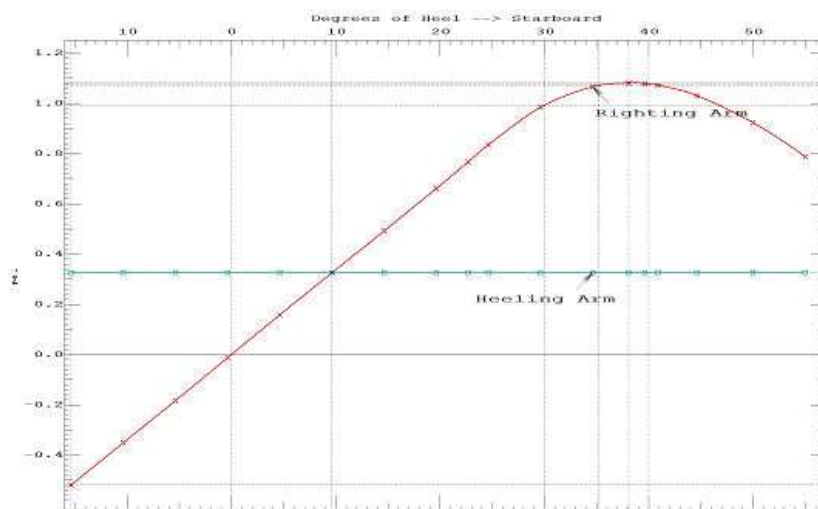
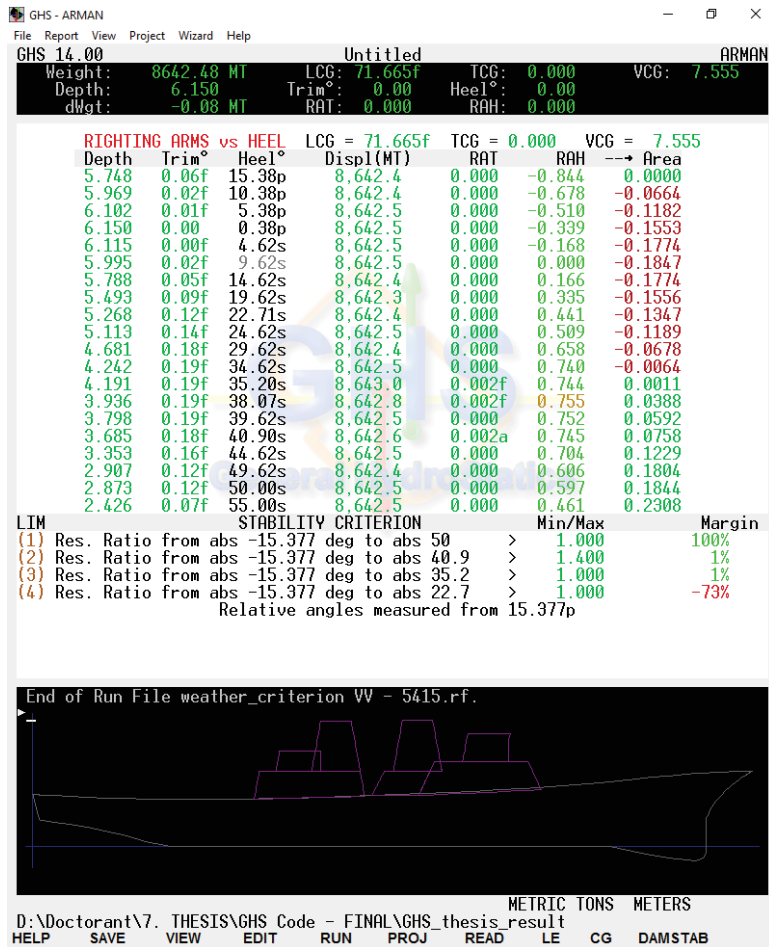


Figure 3.30 Results of weather criterion (IMO modified) for 5415 shape. Result (above) and GZ curve (below)

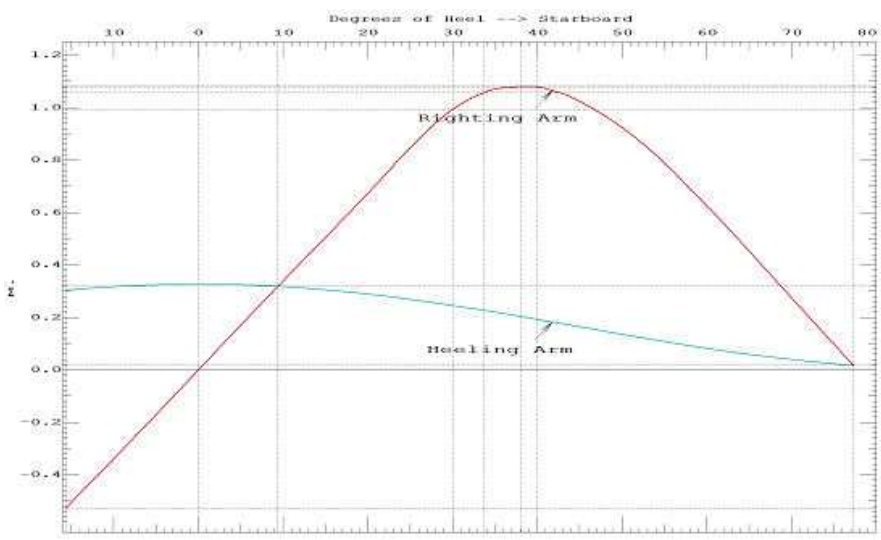
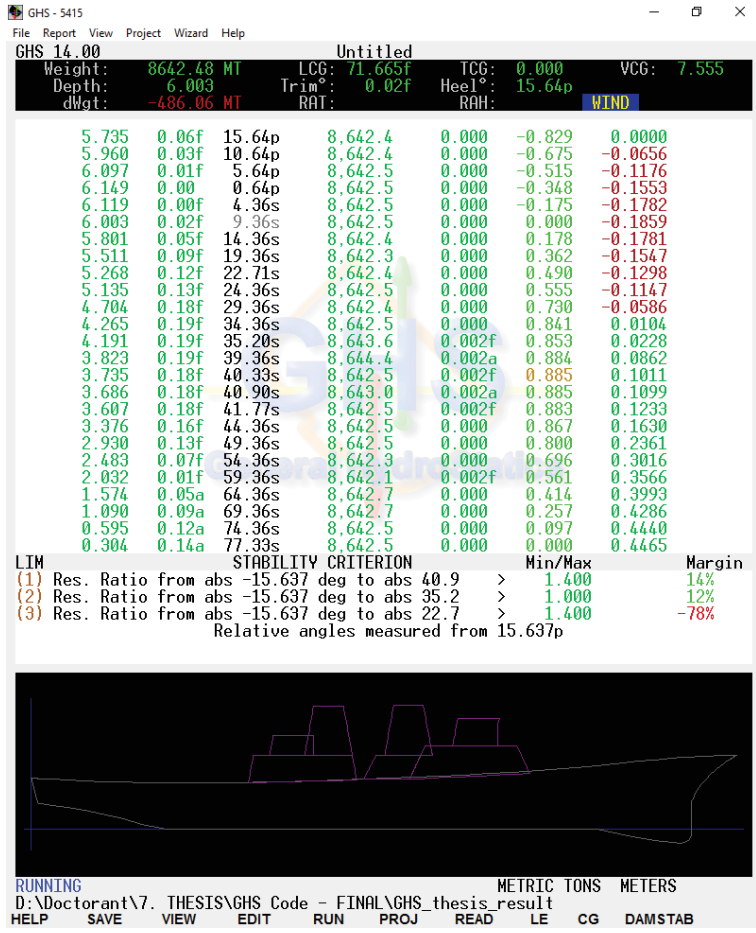


Figure 3.31 Results of weather criterion (Naval Rules) for 5415 shape. Result (above) and GZ curve (below)

### 3.5 Macro Code Developed in GHS

The development of macro code using GHS software introduces an easy application for a beginner user to evaluate their designed ship or vessel against the second generation intact stability criteria. The macro code list developed is given in Table 3.3. GHS enables the user to build and develop macros or source code within GHS. This macro code can be configured to the user's requirements. Some of the variables related to hydrostatics can be used to compute the new code introduced in the SGISC. Therefore, it is possible to evaluate the SGISC within GHS. The sample of macro code developed to evaluate the Vulnerability Level 2 Criteria 1 for pure loss of stability is shown in Table 3.4. For pure loss of stability Vulnerability Level 1, the calculation will involve the *GM* value based on various wave heights consisting of different wave lengths and wave crest positions. In this case, GHS is able to provide the required information.

To assist beginner users with GHS, a macro code could be developed to help them to use GHS and master the macro code. Figure 3.32, Figure 3.33 and Figure 3.34 show the sample of templates with Graphical User Interface (GUI) for pure loss of stability, parametric rolling and broaching. To use these templates, the user only needs to have a model of the ship in a geometry file (\*.gf). Then, basic information about the ship needs to be inserted in the template. Within a few minutes, GHS will present the result in GHS (see Figure 3.35) or in a dialogue box (see Figure 3.36). Generally, the results must be presented to the classification society in a printed version. GHS also offers a function to print out the results as shown in Figure 3.37.

Table 3.3 List of developed macro using GHS

Criteria	Source Code		User-friendly interface	
	DC	MAXVCG	DC	MAXVCG
Pure loss of stability				
Level 1 Method A	√	√	√	√
Level 1 Method B	√	√	√	√
Level 2 C1	√	√	√	√
Level 2 C2	√	√	√	√
Parametric rolling				
Level 1 Method A	√	√	√	√
Level 1 Method B	√	√	√	√
Level 2 C1A	√	√	√	√
Level 2 C1B	√	√	√	√
Level 2 C2	√		√	
Broaching	√	-	√	-
Level 1	√	-	√	-

Where; DC – Design condition, MAXVCG – maximum VCG

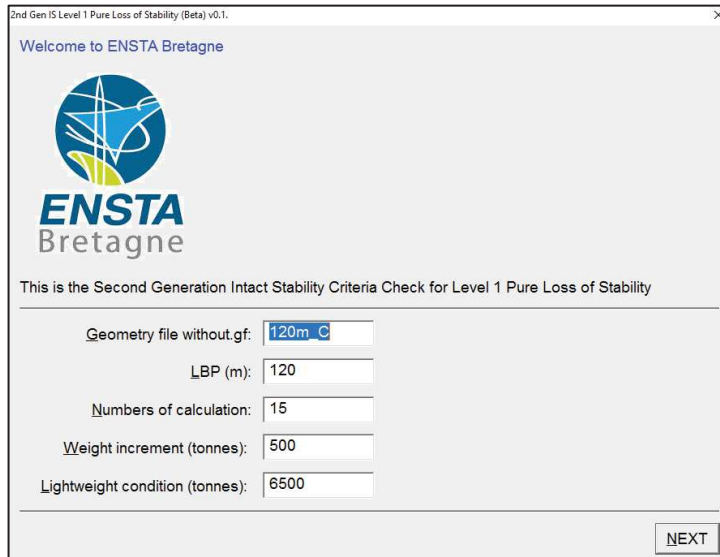


Figure 3.32 Sample of template with GUI for pure loss of stability Level 1



Figure 3.33 Sample of template with GUI for parametric rolling Level 1

Table 3.4 Sample of macro code developed in GHS for pure loss of stability Level 2 criteria 1

<pre> `Determine maxvcg with Second Generation Intact Stability Criteria `For pure loss of stability Level 2 Criteria 1 `Based on SDC2/INF.10  ` This method is to compute the PLOS L2 C1 with single VCG and check if either passed or failed ` Check the final value of PR C1 and compare to the value in IMO Document.  CHDIR "D:\Doctorant\7. THESIS\GHS Code - FINAL\GHS Code_evaluation\PLOS"  clear clear all clear variable `DEFINE VARIABLE v ingf weight1 vcg1 v angle_var `angle of varnishing v startvcg `vcg to start computation v C1C `criteria C1 current v C1T `criteria C1 total  PROJ PL_L2C1 `CREATE TEMPLATE `INPUT "Geometry file without.gf:" ingf `geometry to be analyse `INPUT "Weight (tonnes):" weight1 `INPUT "Design VCG (metres):" VCG1  `DEFINE PARAMETERS set ingf = k1_2 set weight1 = 6500 set vcg1 = 20.5 set C1t = 0  `PERFORMING HYDROSTATIC CALCULATION read {ingf} weight {weight1} solve draft solve lcg tcg set angle_var = START  `DISPLAY RESULT FOR EACH WAVE CHARACTERISTIC \varnishing angle C1 C1totwave length Weightage  vcg {vcg1}  `CREATE MACRO FOR WAVE CREST POSITION macro dwave macro crestp wave (sin) %%91 %1 %2 /noprnt solve if angle_var = START then set angle_var = {rostabh} if {rostabh}&lt; {angle_var} then set angle_var = {rostabh}  \ {angle_var} {C1c} {C1t} %1 %%91 `for verification // .crestp 0 .crestp 36 .crestp 72 .crestp 108 .crestp 144 .crestp 180 .crestp 216 .crestp 252 .crestp 288 .crestp 324 / </pre>	<pre> (continue...)  `CREATE RULES if {angle_var} &lt; 30 then set C1C = %3 else set C1C = 0 set C1T = {C1T} plus {c1C} \ {angle_var} {C1c} {C1t} %1 %2 `for verification  `CREATE MACRO WITH WAVE HEIGHT AND WAVE LENGTH ` wave phase / length / height / weight / case No .DWAVE 22.574 0.7 0.000013 1 .DWAVE 37.316 0.99 0.001654 2 .DWAVE 55.743 1.715 0.020912 3 .DWAVE 77.857 2.589 0.092799 4 .DWAVE 103.655 3.464 0.199218 5 .DWAVE 133.139 4.41 0.248788 6 .DWAVE 166.309 5.393 0.208699 7 .DWAVE 203.164 6.531 0.128984 8 .DWAVE 243.705 7.25 0.062446 9 .DWAVE 287.931 8.08 0.02479 10 .DWAVE 335.843 8.841 0.008367 11 .DWAVE 387.440 9.539 0.002473 12 .DWAVE 442.723 10.194 0.000658 13 .DWAVE 501.691 10.739 0.000158 14 .DWAVE 564.345 11.241 0.000034 15 .DWAVE 630.684 11.9 0.000007 16  \The Index for PR C1 (Opt 6-A) = {C1t}  `RESULT DISPLAY TEMPLATE PASS "YOUR RESULTS ARE" "Your vessel is not vulnerable to Level 2 Criteria 1 PLOS"/color:9 "Congratulation"/color:9 "FINISH" EXIT /  TEMPLATE FAILED "YOUR RESULTS ARE" "Your vessel is vulnerable to Level 2 Criteria 1 PLOS"/color:4 "FINISH" EXIT /  `CREATE RULE IF {C1t}&lt;0.06 THEN .PASS ELSE .FAILED </pre>
--	--



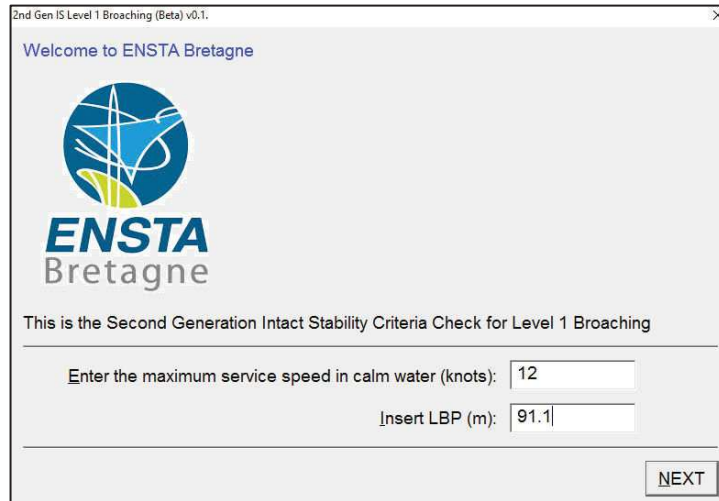


Figure 3.34 Sample of template with GUI for broaching Level 1



Figure 3.35 Result of broaching displayed on GHS screen

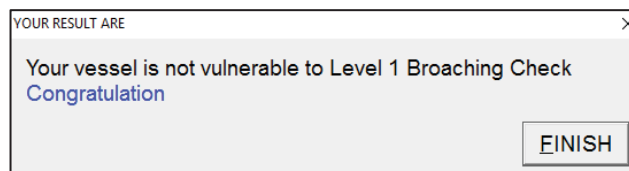


Figure 3.36 Sample of pop-up result for broaching

```
10/10/16 19:57:13          ENSTA Bretagne          Page 1
GHS 14.00                General HydroStatics          BR

Report for Broaching Level 1 Check
LBP is 91.1
Service speed is 12 knots or 6.1728 m/s
The Froude No is 0.20648 and Fn (broaching) = 0.3
Your vessel pass the Froude No Criteria.
Your vessel failed the length criteria.
Your vessel pass. Congratulation.
```

Figure 3.37 Sample of printed result created within GHS

### 3.6 Code Verification

Validation is the determination and evaluation process of the whole computer code or calculation method to ensure compliance with the requirements specified by related rules and regulations. Validation is defined as the evidence which demonstrates that the computer code or calculation method is correct and correlates with the results by utilising different methods. In this case, the comparison is performed using GHS and Calcoque for Level 1 parametric rolling and pure loss of stability calculation.

Calcoque is a three-dimensional hydrostatic computer code developed at the French Naval Academy for academic and research use. It computes equilibrium, intact and damage stability and bending moment. The software can handle the current intact stability rules for civilian ships and the regulations for naval vessels applied by the French Navy (Grinnaert 2017). The hydrostatic solver consists of three main algorithms. The first transforms a classic representation of the ship in sections into a volume mesh. The second algorithm cuts the volume mesh in a plane, generating two volume sub-meshes (one on each side of the plane) and a surface mesh at the intersection. The third searches for the balance position of the ship on calm water and on static waves with three degrees of freedom (sinkage, heel, trim) or two degrees of freedom (fixed heel) (Grinnaert, Billard, and Laurens 2015). These algorithms are partially described in a handbook (Laurens and Grinnaert 2013).

Level 1 criteria are conservative and can be easily implemented in a stability solver. For parametric rolling, the formula used for calculating Level 1 is stated in SDC 2/INF.10 Annex 16. It is the working version of the proposed amendment to Part B of the 2008 IS Code to assess the vulnerability of ships to the parametric rolling stability failure mode (IMO 2014). The description of the model tested in both programmes is shown in Table 3.5.

Table 3.5 Description of 120m\_C model

File name	120m_C
Type	Container Ship
Source	<a href="http://www.delftship.net">www.delftship.net</a>
Length	120.7 meters
Beam	19 meters
Draught	7.5 meters
Block coefficient	0.6682
$A_k$ (total overall projected of the bilge keels)	16.9706 m <sup>2</sup>
$R_{PR}$	0.485

For parametric rolling Level 1, two methods can be used to calculate the  $\Delta GM$ . The first method is based on the maximum and minimum draught and the second method taken into account the static wave with 11 positions of wave crests; where the wave crests are centred at the longitudinal centre of gravity and at  $0.1L$ ,  $0.2L$ ,  $0.3L$ ,  $0.4L$  and  $0.5L$  forward and  $0.1L$ ,  $0.2L$ ,  $0.3L$ ,  $0.4L$  and  $0.5L$  aft thereof.  $L$  is the length of the ship at the waterline (m). The vulnerability of the ship is based on the  $R_{PR}$  index. The ship is not considered to be vulnerable to the parametric rolling stability failure mode if  $\Delta GM/GM \leq R_{PR}$ . The  $R_{PR}$  index is calculated from:

$$\begin{aligned}
 R_{PR} &= 0.17 + 0.425 \left( \frac{100A_k}{LB} \right), \text{ if } C_M > 0.96; \text{ or} \\
 &= 0.17 + (10.625 \times C_M - 9.775) \left( \frac{100A_k}{LB} \right), \text{ if } 0.94 < C_M < 0.96; \text{ or} \\
 &= 0.17 + 0.2125 \left( \frac{100A_k}{LB} \right), \text{ if } C_M < 0.96; \text{ or} \\
 &= 1.87, \text{ if ship has a sharp bilge}
 \end{aligned}$$

Where  $C_m$  is the midship section coefficient of the full loading condition in calm water. The formula of the first method is:

$$\begin{aligned}
 \Delta GM &= \frac{I_H - I_L}{2V}, \text{ only if } \frac{V_D - V}{A_W (D - d)} \geq 1.0 \\
 \delta d_H &= \min \left( D - d, \frac{L \cdot S_W}{2} \right) \\
 \delta d_L &= \min \left( d - 0.25d_{full}, \frac{L \cdot S_W}{2} \right)
 \end{aligned}$$

As an example, a sample ship of a 120m containership is taken into account. The detailed parameters used for the calculation are as follows:

Water density : 1.025 kg/m<sup>3</sup> (sea water)

Weight: 7,000 tonnes

Displacement: 6829.27 m<sup>3</sup>

Displacement = Weight / water density = 7,000/1.025

Draught: 4.649 m at loading condition (computed using GHS)

BM: 6.501 m at loading condition (computed using GHS)

L: 120

To calculate the  $R_{PR}$ , the  $C_M$  value is used. Using GHS command, the  $C_M$  for the ship at the loading condition can be obtained using the function (COMPONENT HULL\HULL /FORM). Then, GHS will show the value of  $C_B = 0.647$  and  $C_P = 0.666$ . The  $C_M = C_B/C_P = 0.647/0.666 = 0.9714$ . Therefore, the formula to compute  $R_{PR}$  is

$$R_{PR} = 0.17 + 0.425 \left( \frac{100A_k}{LB} \right), \text{ if } C_M > 0.96$$

Where  $A_k = 16.9706 \text{ m}^2$ ,  $L = 120.7 \text{ m}$  and  $B = 19 \text{ m}$ .

$$= 0.17 + 0.425 \left( \frac{100 \times 16.9706}{120.7 \times 19} \right)$$

$$= 0.485$$

To evaluate the vulnerability,  $\Delta GM/GM$  must be calculated. The step by step procedure to calculate  $\Delta GM/GM$  is shown below (subscript  $H$  presents high draught and  $L$  presents low draught):

$$\Delta GM = \frac{I_H - I_L}{2V}$$

$$\delta d_H = L \cdot S_w / 2 \text{ (for this ship).}$$

$$S_w = 0.0167, \text{ therefore;}$$

$$\delta d_H = 120.7 \times 0.0167 / 2 = 1.0078$$

$$d_H = d + \delta d_H = 4.649 + 1.0078 = 5.657$$

$$d_L = d - \delta d_L = 4.649 - 1.0078 = 3.641$$

$$I_H = BM_{(dH)} \times \bar{V}_{(dH)}$$

$$BM_{(dH)} = 7.973 \text{ (computed using GHS – change draught, solve weight } lcg \text{ } tcg)$$

$$_{(dH)} = 5,245.51 \text{ tonnes,}$$

$$\bar{V} = _{(dH)} / _{(dH)} = 5,245.51/1.025 = 5,117.57 \text{ m}^3$$

$$I_H = 7.973 \times 5,117.57 = 40,802.39 \text{ m}^4$$

$$I_L = BM_{(dL)} \times \bar{V}_{(dL)}$$

$BM_{(dL)} = 5.543$  (computed using GHS – change draught, solve weight  $l_{cg} t_{cg}$ )

$(dH) = 8,853.75$  tonnes,

$$\nabla = (dH) / (dH) = 8,853.75 / 1.025 = 8,637.80 \text{ m}^3$$

$$I_H = 5.543 \times 8,637.80 = 47,879.33 \text{ m}^4$$

$$\frac{I_H - I_L}{2V} = \frac{40,802.39 - 47,879.33}{2 \times 6829.27} = 0.518133$$

The  $GM$  value is based on  $VCG$ . From rules,

$$\frac{\Delta GM}{GM} = 0.485$$

$$GM = GM \text{ (at } VCG = 0) - KG$$

$$\frac{\Delta GM}{GM \text{ (at } VCG=0) - VCG} = 0.485$$

$$\Delta GM = 0.485 GM \text{ (at } VCG = 0) - 0.485 VCG$$

$$maxVCG = (-\Delta GM + 0.485 GM \text{ (at } VCG = 0)) / 0.485$$

For the loading condition,  $GM$  at  $v_{cg} = 0$  is 9.013 (computed using GHS), and  $\Delta GM = 0.518133$ , therefore  $maxVCG = 7.945$  m. A similar calculation process is required for different displacement values.

Comparison graphs are plotted for Method A, Method B and the current IS Code 2008. The legend for both graphs is; PL – pure loss of stability, PR – parametric rolling, AA – Arman Ariffin results, FG – Francois Grinnaert results, IMO 2.2 – IMO GZ curve limits, A – Method A, B - Method B. Figure 3.38 shows the  $maxVCG$  for pure loss of stability. It is clearly shown that both results obtained by GHS and Calcoque are consistent. When the same graph is zoomed in as shown in Figure 3.39, there are some deviations due to the different methods used which are GHS using the strip method and Calcoque using the volumetric method. Figure 3.40 shows the  $maxVCG$  for parametric rolling. It is also shows that both results obtained by GHS and Calcoque are consistent. When the same graph is zoomed in as shown in Figure 3.41, there are some deviations at the 13,500 mt displacement for Method A. This divergence is the result of the hydrostatic solvers used in this calculation which are the strip and volumetric method.

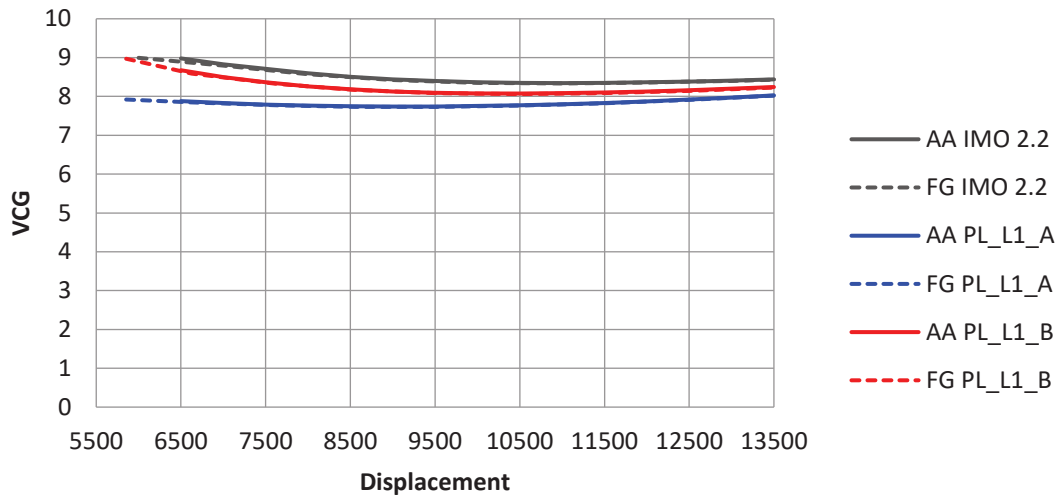


Figure 3.38 *MaxVCG* curve for pure loss of stability, Vulnerability Level 1

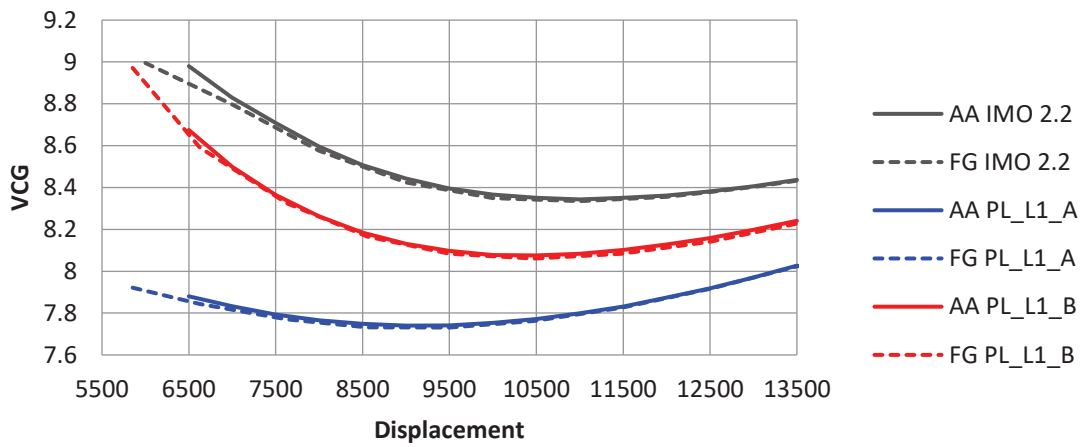


Figure 3.39 *MaxVCG* curve for pure loss of stability, Vulnerability Level 1 (zoom)

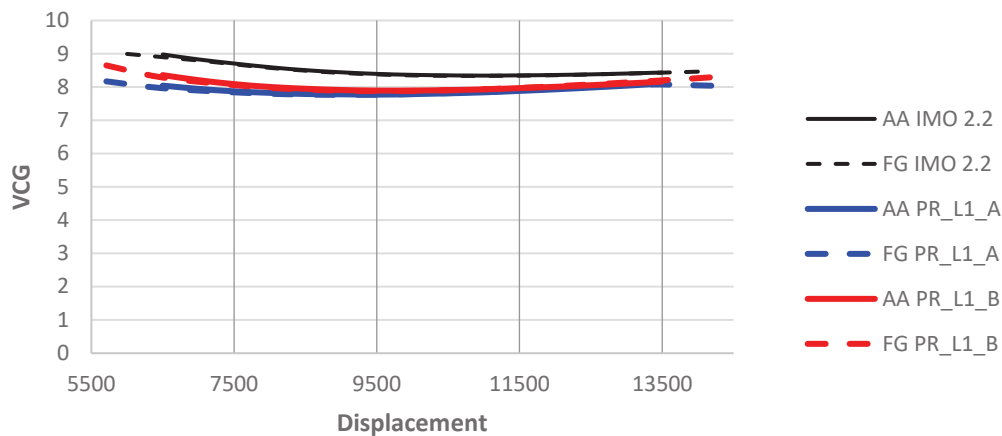


Figure 3.40 *MaxVCG* curve for parametric rolling, Vulnerability Level 1

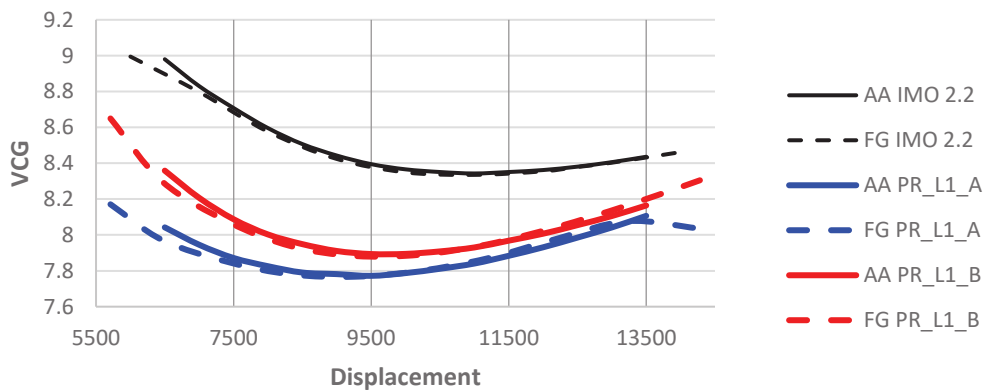


Figure 3.41 *MaxVCG* curve for parametric rolling, Vulnerability Level 1 (zoom)

### 3.7 Results and Discussion

#### 3.7.1 2008 Intact Stability and Naval Rules

The results for 2008 IS Code on GZ curve and weather criterion is presented in Table 3.6. All 5 ships pass the 2008 IS Code for both the GZ curve and weather criterion evaluation. For the weather criterion based on the Naval Rules, the ASL shape passed and the 5415 shape failed. The 5415 shape failed at the downflooding angle as shown in Figure 3.31. The 5415 shape is an academic geometry and no actual ship was constructed using this hull and superstructure. The main reasons for failing this criterion were the huge windage area and low freeboard height. For further comprehension of the 5415 shape, a wind tunnel test was conducted to obtain experimental results. The detailed results of the ASL shape and 5415 shape for the weather criterion are presented in Table 3.7 and the input parameters used are shown in

Table 3.8. Even though the Naval Rules required the factor of cosine squared for the wind heeling arm, there was no need for this factor for the IMO rules as the wind heeling arm remained constant. This is for consistency and ease in the discussion process.

Table 3.6 Results of the 5 ships for IMO and Naval Rules

Ship	2008 IS Code – GZ curve	2008 IS Code – Weather criterion	Naval Rules – Weather Criterion
ASL	Pass	Pass	-
5415	Pass	Pass	Fail (for angle of down flooding)
PV	Pass	Pass	-
120m_C	Pass	Pass	-
KL	Pass	Pass	-

Table 3.7 Result of ASL and 5415 shape on weather criterion

Ship	$\phi_0$	Start angle	$\phi_2$	$\phi_{2a}$ ( $A_2 = A_1$ )	$\phi_{2a}$ ( $A_2 = 1.4 A_1$ )	Roll amplitude ( $\phi_0$ – start angle)	Rules
ASL	12.88	-3.31	24.3	-	-	33.198	IMO
5415	9.62	-15.38	-	35.2	40.9	50.58	Naval Rules

# IMO roll angle for ASL = 16.19° and Naval rules for 5415 shape = 25°

Table 3.8 Input parameters for weather criterion results

Input	Wind velocity	Wind pressure (kg/m <sup>2</sup> )	Gust	$\phi_0$	Criteria
ASL	26 ms <sup>-1</sup> (50.54knots)	0.05194	1.5	At 26 ms <sup>-1</sup>	$A_2 = A_1$ based on gust heeling arm (31.843 ms <sup>-1</sup> )
5415	100 knots (51.44 ms <sup>-1</sup> )	0.20333	No gust	At 100 knots	$A_2 = A_1$ based on heeling arm (100knots)

### 3.7.2 SGISC Evaluation

*MaxVCG* curves associated with pure loss of stability and parametric rolling were computed for five ship models. The characteristics of the models have been described in Chapter 3.3. GHS performed the hydrostatic computation for calm water and static waves. The results were presented at the 12<sup>th</sup> International Conference on the Stability of Ships and Ocean Vehicles, Glasgow (Ariffin, Mansor, and Laurens 2015), Smart Ship Technology in London (Ariffin, Mansor, and Laurens 2016c) and 15<sup>th</sup> International Ship Stability Workshop in Stockholm (Ariffin, Mansor, and Laurens 2016a). All computations were performed with a sea water density of 1.025 kg/m<sup>3</sup>. The limit for the IMO curve was based on the 2008 IS Code



Part 2.2 for righting arm properties. For the SGISC, the computation was performed using the user-developed macro during this research.

The graphs were plotted for  $maxVCG$  versus the displacement for each model and each failure mode. The results are presented, starting with pure loss of stability and continuing with parametric rolling. For pure loss of stability, the calculation was performed for Level 1 Method A and Method B. For parametric rolling, the calculations were carried out for Level 1 (Method A and Method B), and Level 2 Criteria C1. The C1 has two rules. First, the average  $GM$  for each wave case should be more than 0 and the ratio of deviation of  $GM$  with average  $GM$  for each wave case should be less than  $R_{PR}$ . Second, the cruising speed of the vessel should be lower than the vessel speed corresponding to the parametric resonance condition. The calculation for C1 only considered the average  $GM$  for each wave because all five models are a concept design, so there is no real information on bilge keel and vessel service speed. In every graph, there is a vertical dotted line which represents the design loading condition. The designed  $VCG$  is represented by a black dot on the vertical line of the design loading condition.

### 3.7.2.1 Pure loss of stability failure mode

Figure 3.42 shows the results of pure loss of stability for the ASL shape. For all displacements, the results for Method B are above Method A, showing that Method A is more conservative than Method B. For the light ship condition, a significant difference in  $maxVCG$  value is obtained. The  $maxVCG$  curve converges with the increment of the displacement. For the IMO code, the curve is always lower than Level 1 Method B. For the displacement, which is more than the design condition, both methods showed very similar values because of the water plane area for this displacement which was the same. This is explained by the hull above water up to the cargo deck for the ASL shape which is constant because of the "box shape". As expected, Method A is more stringent than Method B and the 2008 IS Code (Ariffin, Mansor, and Laurens 2016b).

Figure 3.43 shows the results of pure loss of stability for the 5415 shape. For all displacements, the results for Method B are higher than Method A, showing that Method A is more conservative than Method B. For the IMO code, the curve is close to Level 1 Method B and both IMO and Level 1 Method B have no impact on the increase in displacement. For level Method A, the  $maxVCG$  curve increased with the increment of the displacement. As expected, Method A is more stringent than Method B and the 2008 IS code.

Figure 3.44 shows the results of pure loss of stability for the PV shape. For all displacements, the results for Method B are above Method A, showing that Method A is more conservative than Method B. For the IMO code, the curve is close to Level 1 Method B and both IMO and Level 1 Method B have no impact on the increase in displacement. For level Method A, the  $maxVCG$  curve increased with the increment of the displacement. As expected, Method A is more stringent than method A and 2008 IS Code. For the 5415 shape and the PV

shape, the results showed a similar trend because the prismatic coefficient ( $C_P$ ) was in the range of a naval ship. A low  $C_P$  represents a hull with fine ends and a high  $C_P$  represents a hull with relatively full ends. The  $C_P$  provides an indication of the distribution of displacement. It is an indication of the fineness of the ends relative to the midsection of the hull. A low  $C_P$  indicates fine ends and a large mid-body. A high  $C_P$  shows more displacement distributed toward the ends.

Figure 3.45 shows the results of pure loss of stability for the 120m\_C shape. For all displacements, the curve for Level 1 Method A is at the bottom, Level 1 Method B is in the middle and IMO at the top. There is a significant difference between the IMO code and Level 1 Method B. As expected, Method A is more stringent than Method B and the 2008 IS Code.

Figure 3.46 shows the results of pure loss of stability for the KL shape. For all displacements, the curve for Level 1 Method A is at the bottom, IMO in the middle and Level 1 Method B at the top. For this shape, Level 1 Method B is more conservative than the IMO code. As expected, Method A is more stringent than Method B and the 2008 IS Code.

The five models as presented can be categorised into three groups which are the academic shape group containing the ASL, the naval shape group containing the 5415 and PV shapes and the container ship shape group containing the 120m\_C and KL shapes. Each group displays a similar trend for the *maxVCG* curve. It is concluded that the characteristics of each underwater hull contribute to the results of the calculation for Level 1 Method A and the method for pure loss of stability.

As a conclusion for pure loss of stability, all five models showed consistency as to the conservativeness of the rules where Level 1 Method A is more conservative than Level 1 Method B, followed by Level 2. For the ASL, 120m\_C and KL shapes, the design *VCG* were passed for all criteria. For the 5145 and PV shapes, the design *VCG* were passed only for the IMO, Level 1 Method B and Level 2, but failed on the criteria Level 1 Method A. This means that the container shape passed the new rules but not the naval shape where the Level 1 Method A is conservative.

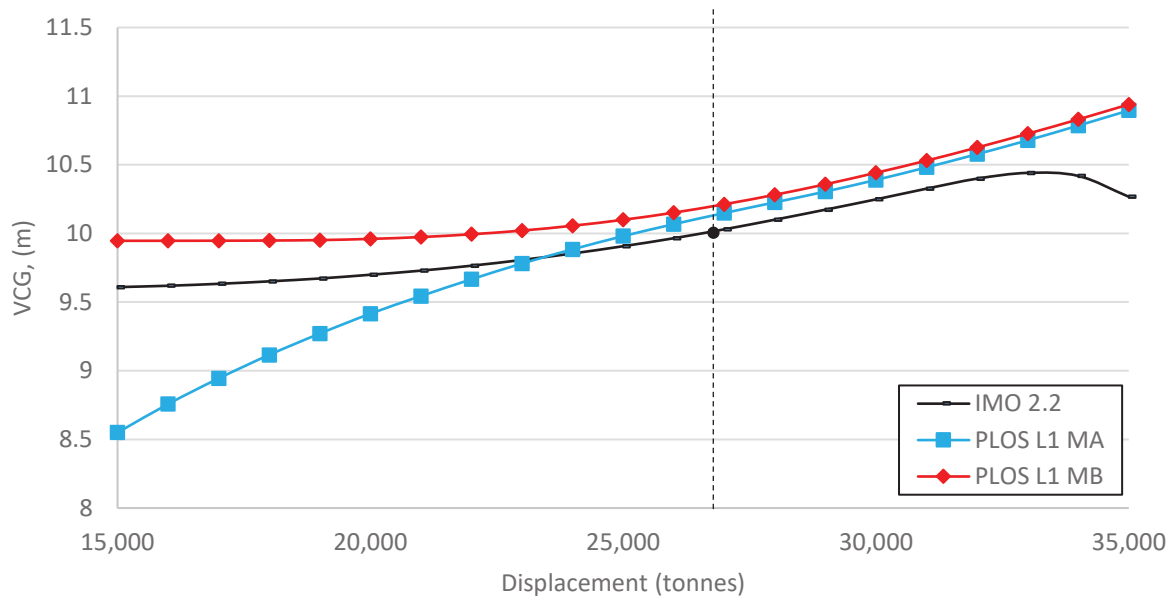


Figure 3.42 *MaxVCG* curves representing pure loss of stability for ASL shape

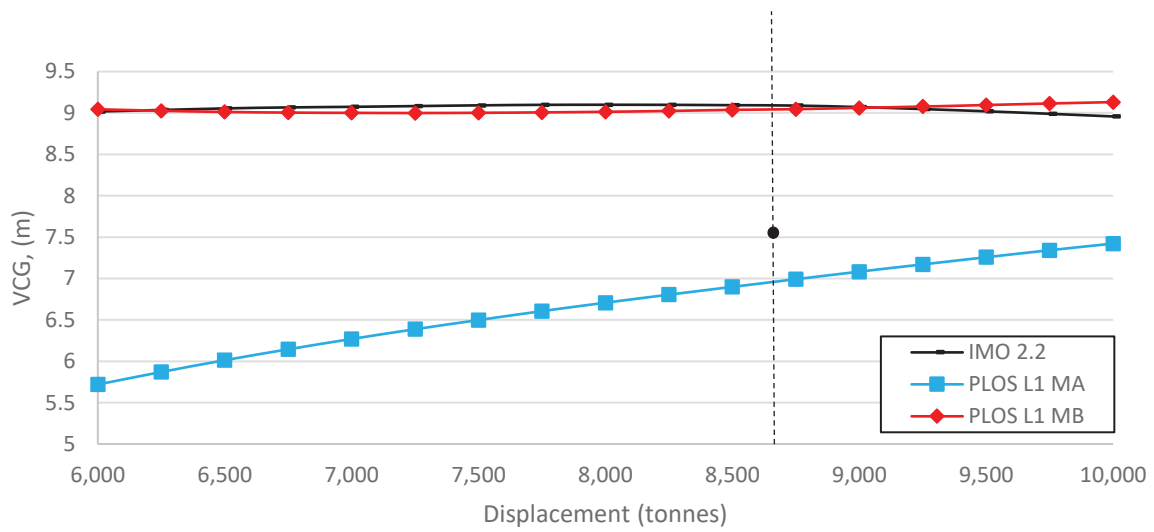


Figure 3.43 *MaxVCG* curves representing pure loss of stability for 5415 shape

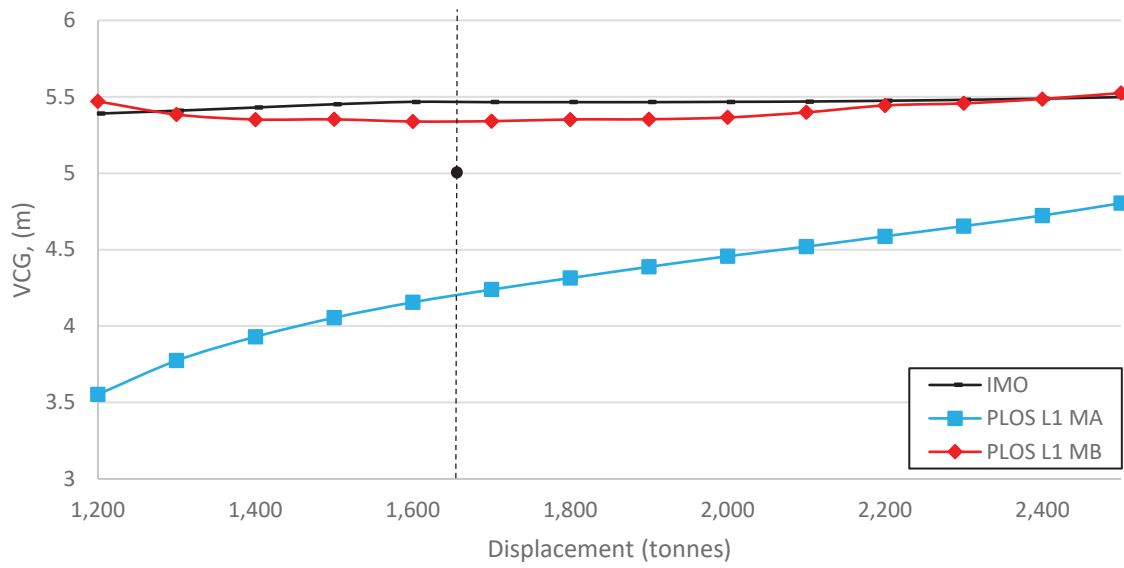


Figure 3.44 *MaxVCG* curves representing pure loss of stability for PV shape

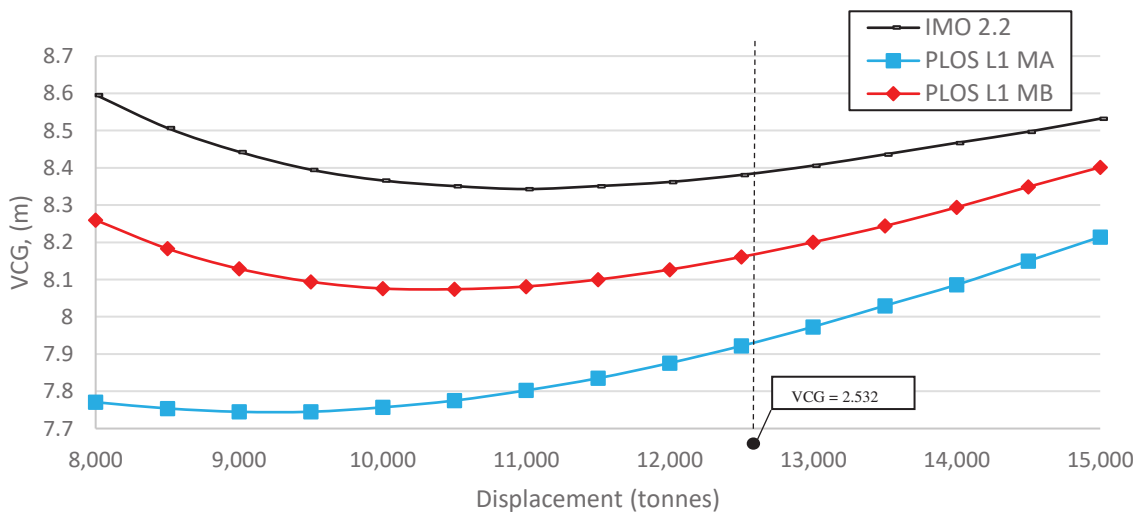


Figure 3.45 *MaxVCG* curves representing pure loss of stability for 120m\_C shape

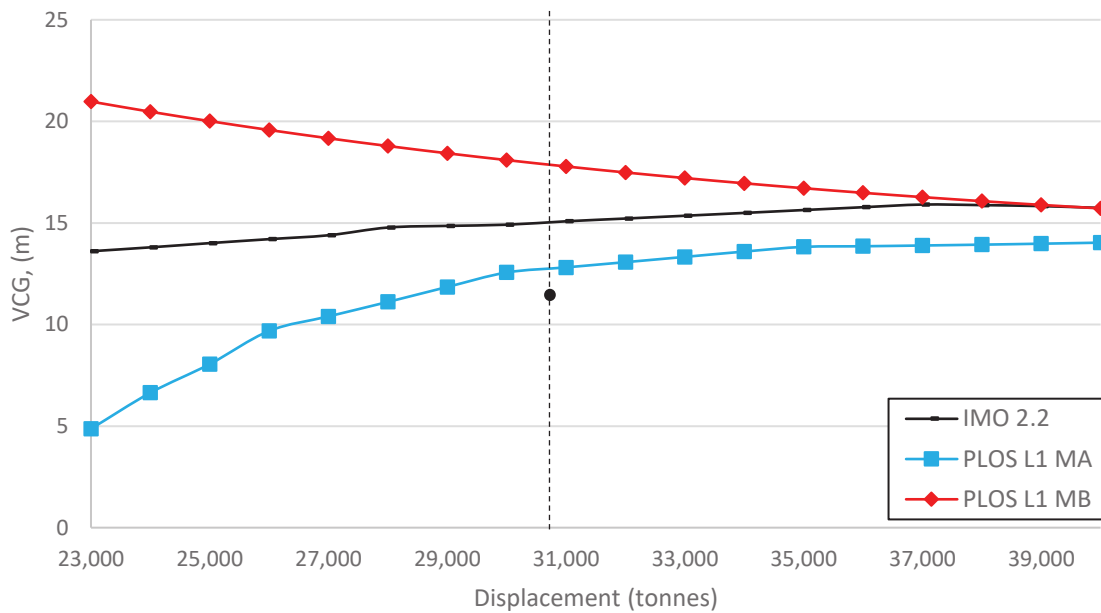


Figure 3.46 *MaxVCG* curves representing pure loss of stability for KL shape

### 3.7.2.2 Parametric rolling failure mode

Figure 3.47 shows the results of parametric rolling for the ASL shape. The curves for Level 1 Method A, Method B and Level 2 are above the IMO code, except for the displacement of less than 20,000 mt. For the displacement of more than 20,000, the results showed no significant difference in *maxVCG* due to the ASL shape which has a cylinder shape underwater and box shape above the water line.

Figure 3.48 shows the results of parametric rolling for the 5415 shape. The bottom curve is Level 1 Method A, followed by Level 1 Method B, then IMO and on top is Level 2. As expected, Level 1 is more conservative than Level 2. Figure 3.49 shows the results of parametric rolling for the PV shape. The curve position of PV shape is similar to the 5415 shape except for the displacement of more than 2,000 mt where the curve of Level 1 Method B and IMO code intercept each other.

Figure 3.50 shows the results of parametric rolling for the 120m\_C shape. The bottom curve is Level 1 Method A, followed by Level 1 Method B, then IMO and on top is Level 2. As expected, Level 1 is more conservative than Level 2. The results also showed that Level 2 is less conservative than the IMO code. Figure 3.51 shows the results of parametric rolling for the KL shape. The results for the KL shape are different compared to the 120m\_C shape. The IMO curve intercepts with the other curves. For a comparison with the new rules, the bottom curve is Level 1 Method A, followed by Level 1 Method B and on top is the Level 2 curve. As expected, Level 1 is more conservative than Level 2.

As a conclusion for parametric rolling, all five models showed consistency as to the conservativeness of the rules where Level 1 Method A is more conservative than Level 1 Method B and followed by Level 2. For the ASL, 120m\_C and KL shapes, the designed VCG passed for all criteria. For the 5145 and PV shapes, the designed VCG passed only for the IMO, Level 1 Method B and Level 2, but failed over the criteria of level Method A. This presumed that the container shape passed the new rules but not the naval shape where Level 1 Method A is conservative.

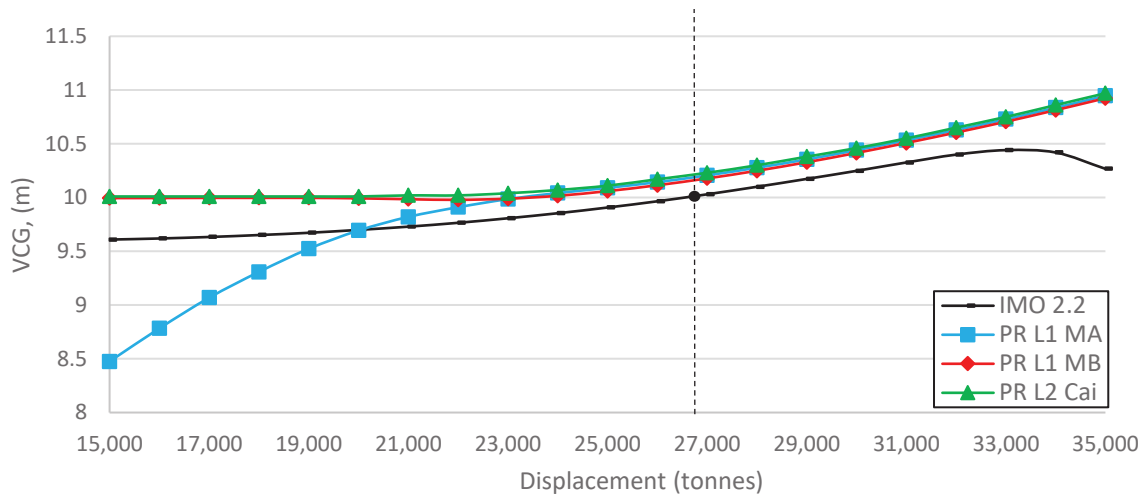


Figure 3.47 *MaxVCG* curves representing parametric rolling for ASL shape

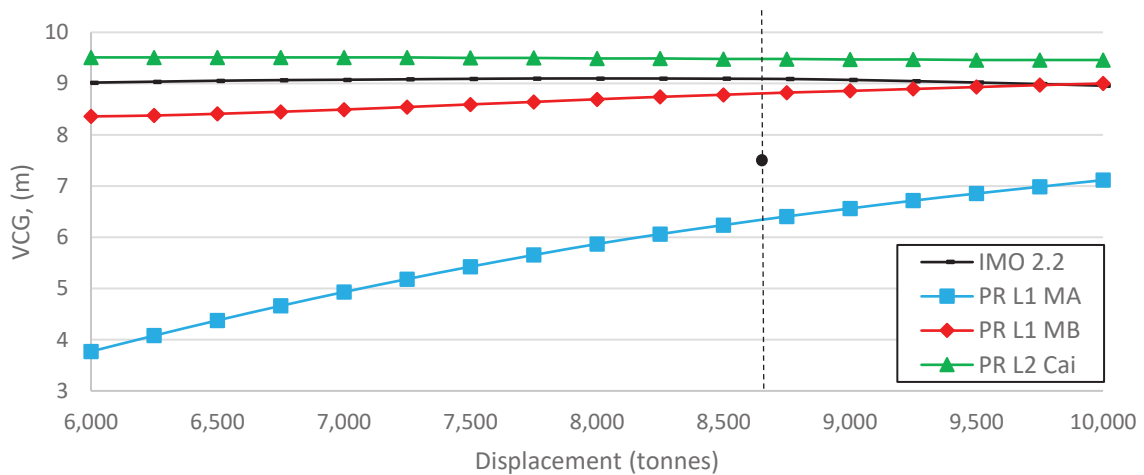


Figure 3.48 *MaxVCG* curves representing parametric rolling for 5145 shape

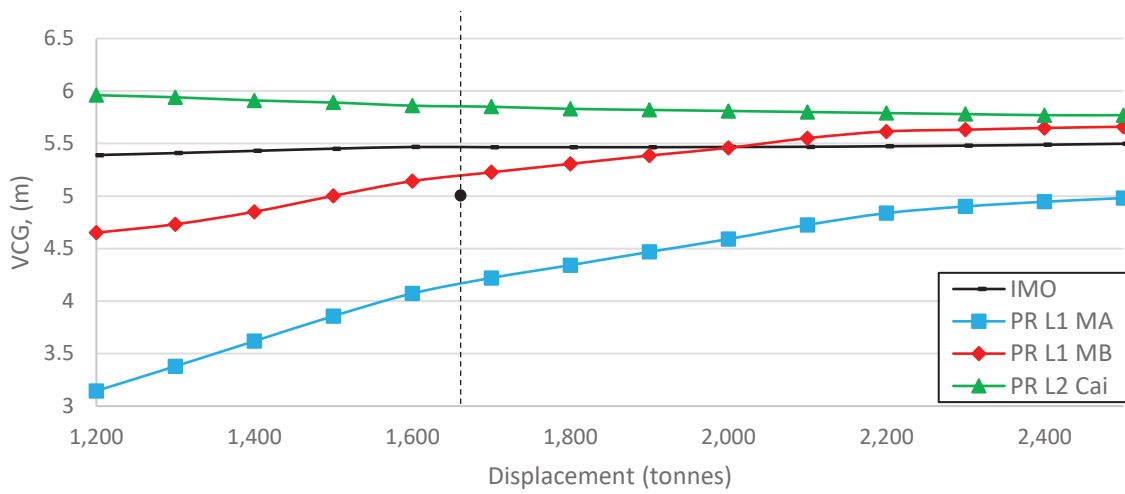


Figure 3.49 *MaxVCG* curves representing parametric rolling PV shape

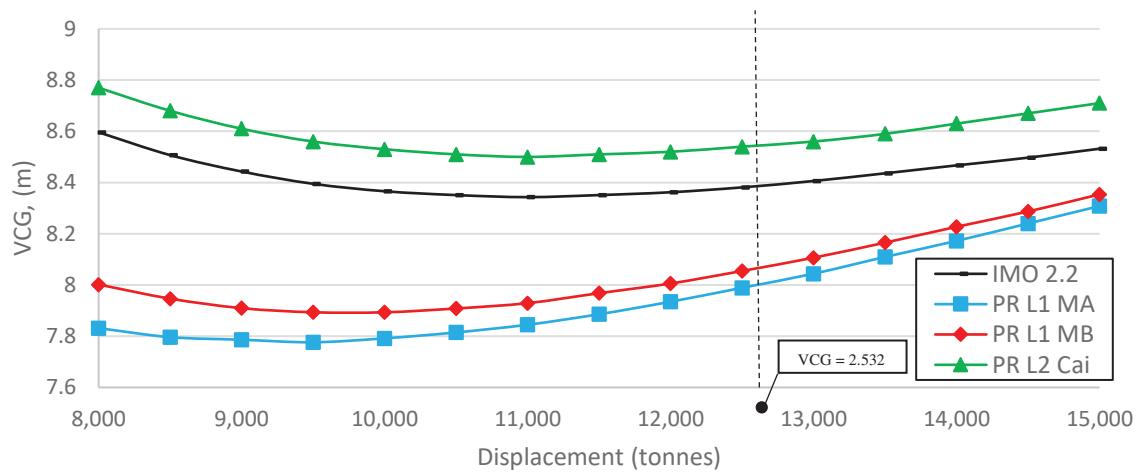


Figure 3.50 *MaxVCG* curves representing parametric rolling for 120m\_C shape

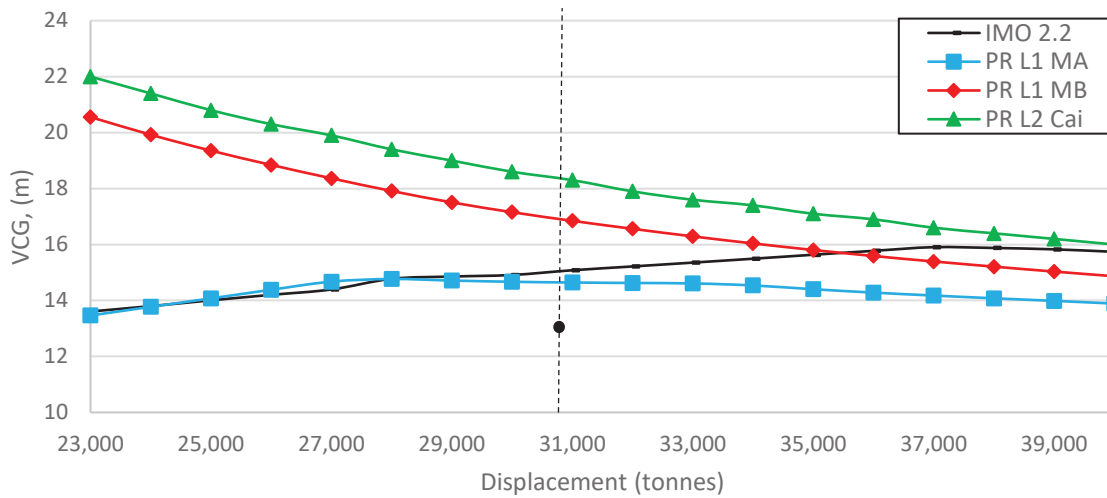


Figure 3.51 *MaxVCG* curves representing parametric rolling for KL shape

### 3.8 Conclusion

GHS is a hydrostatic solver and able to perform Level 1 and some Level 2 for pure loss of stability and parametric rolling failure modes of the second generation intact stability criteria. High-level customisation in GHS macro editor allows the user to customise the script based on new rules. It also provides some degree of understanding for naval architects during the design stage.

All five ships tested in GHS passed the righting arm curve and weather criterion except for the 5415 shape. The 5415 shape, passed the righting arm curve but failed on the weather criterion when using both IMO modified or Naval Rules. To the author’s best knowledge, no proceeding or paper have been published on aerodynamics studies using the 5415 shape with superstructure. To date, most of the results of the 5415 shape present the hydrodynamics, seakeeping, manoeuvrability and propeller performance.

An extensive analysis of the pure loss of stability and parametric rolling was presented by (Grinnaert 2017). He performed the calculation for Level 1 and Level 2 for several models of civilian and naval ships using Calcoque software and discovered that the computation of *maxVCG* curves associated with the Level 1 and Level 2 criteria for different civilian and military vessels reveals that Level 2 can be more conservative than the second Level 1 method for both failure modes. This phenomenon is not expected in the future regulation.

In accordance with the SGISC, for dead ship condition, a ship that fails the weather criterion should be evaluated at Level 2 or by direct assessment. Since the 5415 shape failed the modified IMO and Naval Rules, it is of great interest to check the ship by direct assessment.



To date, no proposal has been presented at an IMO level. Therefore, this is an opportunity to propose a method to evaluate dead ship condition by direct assessment. Direct assessment procedures for stability failure are designed to employ the most advanced state-of-the-art technology available either by numerical analysis or experimental work for quantitative validation as stated in SDC 1/INF.8 Annex 27 (Ariffin, Mansor, and Laurens 2016a).

An accurate prediction of roll motion is of fundamental importance when ship safety is assessed. In the case of an intact ship, the accuracy in the prediction of roll motion is, for a large set of dynamic phenomena, strongly dependent on the accuracy of the prediction of roll damping. However, for conventional ships, roll damping is governed by viscous effects, and this makes accurate roll damping prediction a very difficult task. (Ba et al. 2016). During the Design for Safety Conference in Hamburg, a researcher from China proposed the Green function based on the 3D panel method (Feng et al. 2016). The 3D panel method results agree quite well with the experimental results, while the empirical formula can help improve the prediction accuracy, it is still not accurate. During their presentation, they presented a simulation result which had partial deletions. This method was considered to be invalid and they had to run the simulation again. This shows the level of difficulty faced by the CFD in obtaining good simulation results.

For the dead ship condition, the latest approach for experimental validation procedures was conducted at Osaka University (Umeda et al. 2014). This paper aims to facilitate the guidelines of the direct stability assessment as a part of the second generation stability criteria. The most challenging part of this experiment is to obtain the wind velocity profile generated by wind fans. To the author's best knowledge, none of the experiments concerning the aerodynamic and hydrodynamic effects on one test rig in a wind tunnel test section has been proposed or reported. In the next chapter, an experimental direct assessment of the dead ship condition is presented.

## Chapter 4 –Experimental Setup and Results

This section describes the experimental work conducted in this research. It explains the details of the test rig and lists the step by step procedure during the wind tunnel test. The results obtained during the experiments are presented and discussed in detail.

### 4.1 Introduction to the Wind Tunnel Test

There is extensive literature on the design of wind tunnel experiments that can provide valuable guidance for designing and conducting the experiment. Each experimental work should be based on the nature of the problem. In fact, the basic diagram to develop an experimental work is shown in Figure 4.1. The elements of the input vector are variables such as the angle of yaw, roll back angle and etc. The elements of the controllable vector will be variables such as the model size, tunnel size, model material, model construction process, conduct time of the experiment, model nominal configuration and choice of test rig. Some variables may appear in either the input vector or the controllable factors, depending on their immediate purpose. The elements of the output vector will be responses such as the roll and pitch angle. Elements of the uncontrollable factors of vector will include elements such as turbulence level of the incoming stream, temperature in many facilities, relative humidity, model deformation and surface deterioration over time (Barlow, William, and Pope 1999).

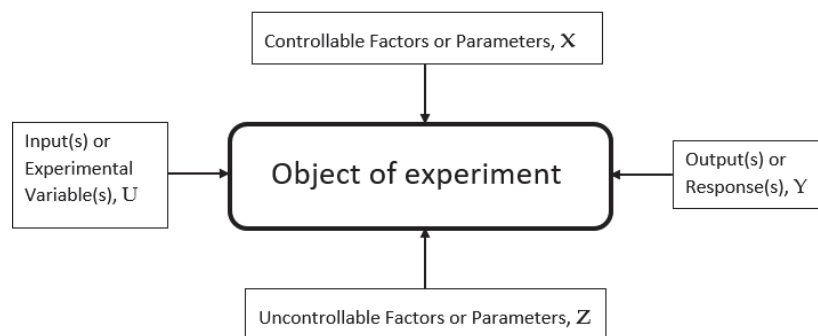


Figure 4.1 Conceptual model of an experimental setup. Extracted from (Barlow, William, and Pope 1999)

Wind force acting on the top side of the superstructures of ships can generate significant loads that must frequently be accounted for in the design process. When the ship is intact, these forces affect the sizing of the propulsion machinery, manoeuvring thrusters and mooring and

berthing arrangements. When a ship is damaged, these forces can determine the very survival of the ship and its crews. So, the immediate problem of sinking is replaced by the only slightly less catastrophic possibility of capsizing (Barlow, William, and Pope 1999).

The IMO have interim guidelines for alternative assessment of the weather criterion (IMO MSC.1/Circ.1200 2006). This document provides an alternative assessment of the weather criterion, aiming at providing the industry with alternative means which is, in particular, a model experiment. The procedure to determine the angle of roll and the wind heeling lever are described in this document. Two separate tests should be conducted which are the wind tunnel test and the drift test in the towing tank. To provide a broader understanding of the above guidelines, IMO provides an explanatory note to the Interim guidelines for an alternative assessment of the weather criterion (IMO MSC.1/Cir.1227 2007). This explanatory note provides the calculation of a RoPax ferry as an example. Despite having two separate experiments for the weather criterion, this research proposes a single experiment to evaluate the weather criterion with methodology and approach.

## 4.2 Model Selection

Two models were used for the experimental work. The first model is an academic container ship geometry referred to as the “ASL shape”. The second model is a research ship model, the well-known DTMB 5415 (Molgaard 2000). The 5415 DTMB model is widely used for research studies in seakeeping (Begovic, Day, and Incecik 2011; Jones and Clarke 2010; Yoon et al. 2015). The main characteristics of the ships and the model scale are shown in Table 4.1. The body plan and perspective view for the “ASL shape” is shown in Figure 4.2 and the 5415 shape in Figure 4.3 (Ariffin, Mansor, and Laurens 2016d).

Table 4.1 Main characteristics of the ship and model scale

Ship Scale	ASL		5415	
	Full	Model	Full	Scale
<i>LOA</i> , (m)	140.00	1.400	153.30	1.533
<i>BOA</i> , (m)	20.00	0.200	20.54	0.205
Draught, (m)	12.00	0.120	6.15	0.061
Displacement, (tonnes)	26,994	0.027	8,642	0.0086
<i>VCG</i> , (m)	10.000	0.100	7.555	0.076
<i>LCG</i> , (m)	70.037	0.700	71.665	0.700
<i>KM</i> , (m)	10.206	0.100	9.507	0.090
<i>GM</i> , (m)	0.206	0.002	1.952	0.019
Windage area (beam and upright), (m <sup>2</sup> )	2,240	0.224	1,441.5	0.144

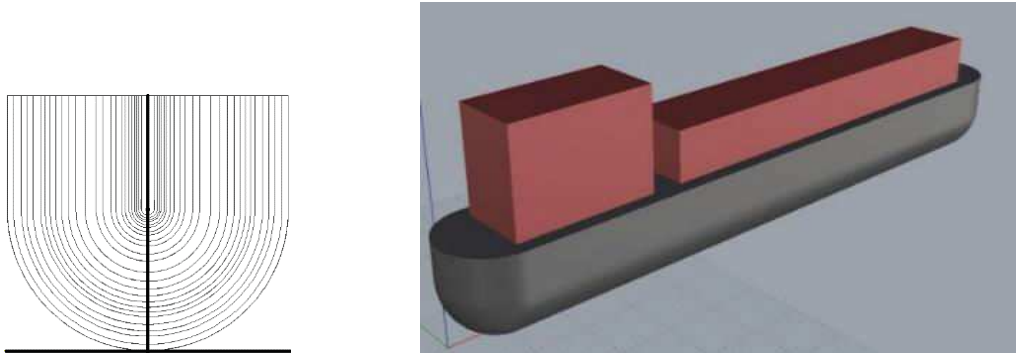


Figure 4.2 Body plan (left) and perspective view (right) of the ASL shape

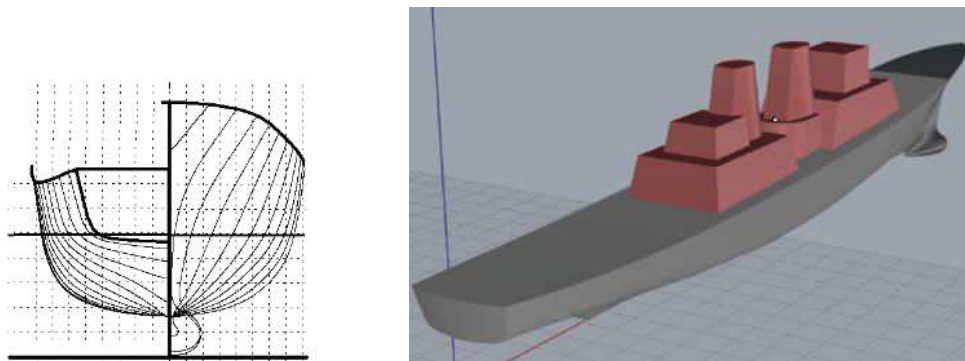


Figure 4.3 Body plan (left) and perspective view (right) of the 5415 shape

### 4.3 Model Preparation for the Wind Tunnel Test

Preparation of the model to be tested in a wind tunnel test requires high precision and robust quality. The dimensional accuracy plays an important role. Due to the high velocity of wind in the test section, the model must be able to stand up to the maximum test velocity. Therefore, a proper model fabrication is required. Figure 4.4 shows the flow chart of the model preparation. The preparation process consists of three main steps which are the model construction, model verification and model pre-test.

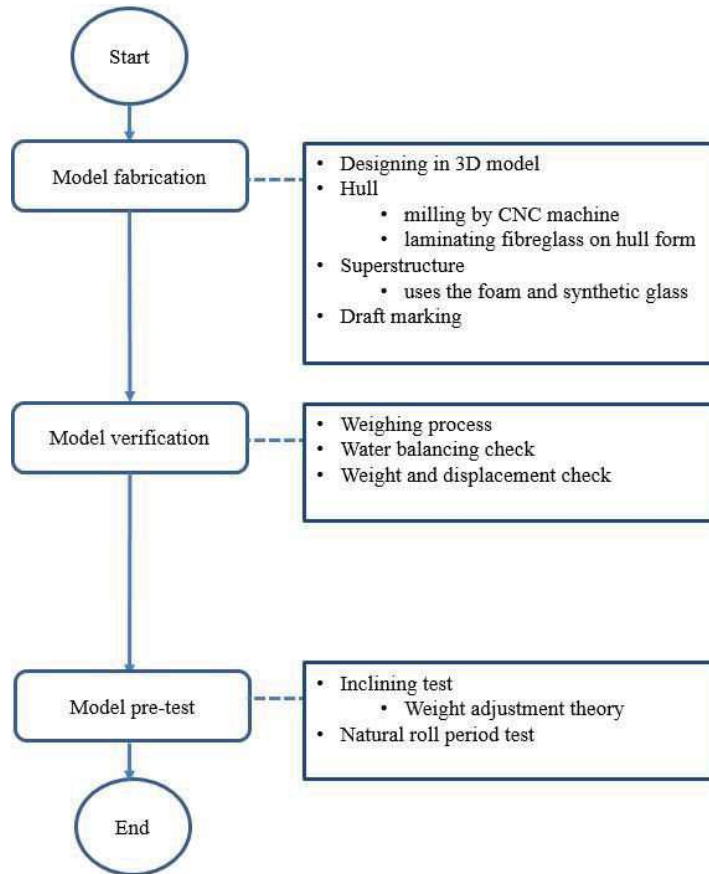


Figure 4.4 Flow chart for model preparation

### 4.3.1 Model Construction

#### 3D modelling

Model creation starts with 3D modelling using software named Rhinoceros 5. Rhinoceros 5 is a 3D modelling tool that can create, edit, analyse, document, render, animate and translate Non-uniform Rational Basis Spline (NURBS) curves, surface and solids, point clouds and polygon mesh. It has no limits as to complexity, degree, or size. The special feature of Rhinoceros is the plug-in named Orca 3D. Orca 3D is a marine designer plug-in for Rhino. The Orca 3D has 2 levels: Level 1 which includes the hull design & fairing and intact hydrostatics & stability and Level 2 which includes the speed/power prediction and weight & cost tracking.

The process starts by modelling the hull curve from the lines plan. Then, a surface is created from the lines plan. On the completion of the hull, the hydrostatic data can be obtained by Rhinoceros. The orientation of axis for the 3D drawing can be customised based on the user requirements. For easy transferring of the model from Rhino to General Hydrostatics (GHS), both software use the same orientation of axis as shown in Figure 4.5.

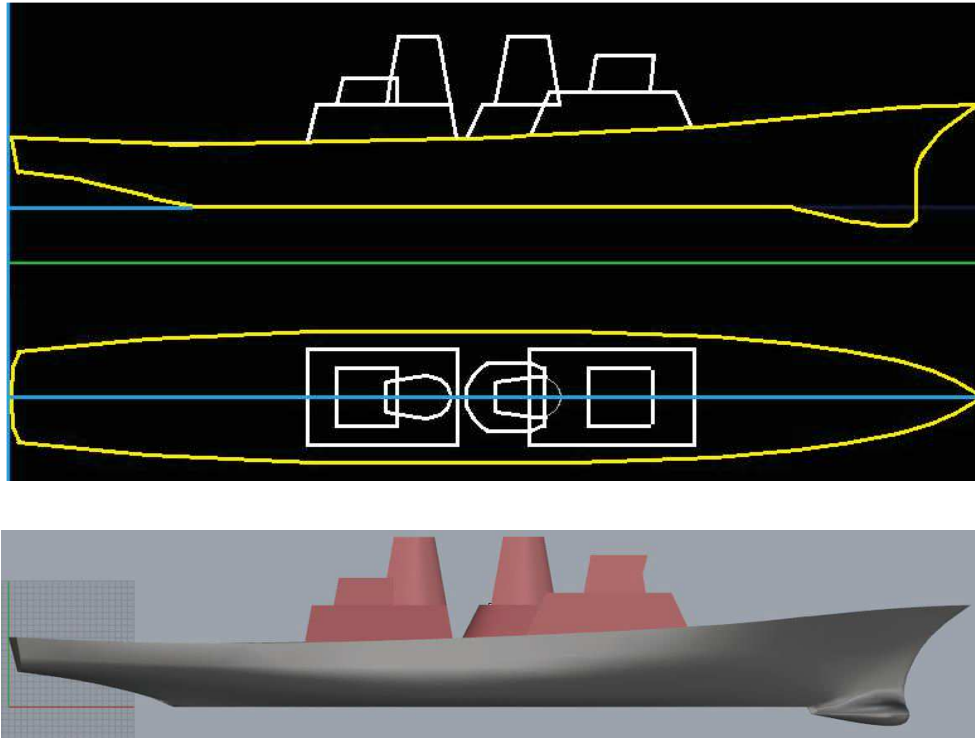


Figure 4.5 Model orientation in GHS (top) in Rhinoceros (bottom)

The flow chart for the 3D modelling is shown in Figure 4.6. The process starts with the selection of models. The objective of the selection is to have various types of vessel for this research. Then, the lines plan is obtained and the design process in Rhinoceros started. After the model is designed in Rhinoceros, it is checked using a plug-in named Orca 3D. This plug-in is capable of deriving the hydrostatic information from the model in Rhinoceros. It is also able to attach the GHS Data such as hull, tank, windage, shapes and critical points. On completion in Rhinoceros, the file is exported to a geometry file (\*.gf). In GHS, the model is verified again for its hydrostatic information. Then, the model is tested with the 2008 IS Code which consists of the righting arm curve and weather criterion.

### **The milling process**

The creation of both models was conducted at ENSTA Bretagne, France. The flow chart for the creation process is shown in Figure 4.7. After the model was designed in Rhinoceros, it was exported to a \*.igs file. This file was opened in CATIA to validate the geometry. After the geometry was validated, it was exported to STRATO Pro. The STRATO Pro is software for the milling process. This software is capable of changing and creating a milling code used in the CNC machine. The machining quality and technique are defined in STRATO Pro.

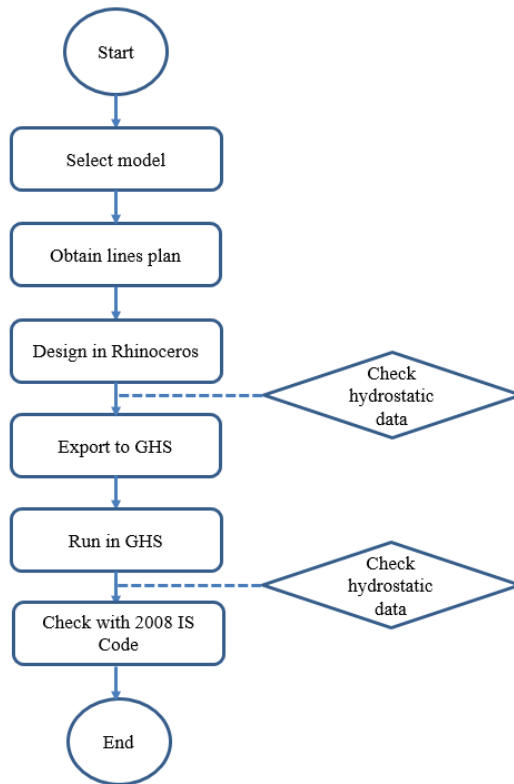


Figure 4.6 Flow chart for 3D modelling

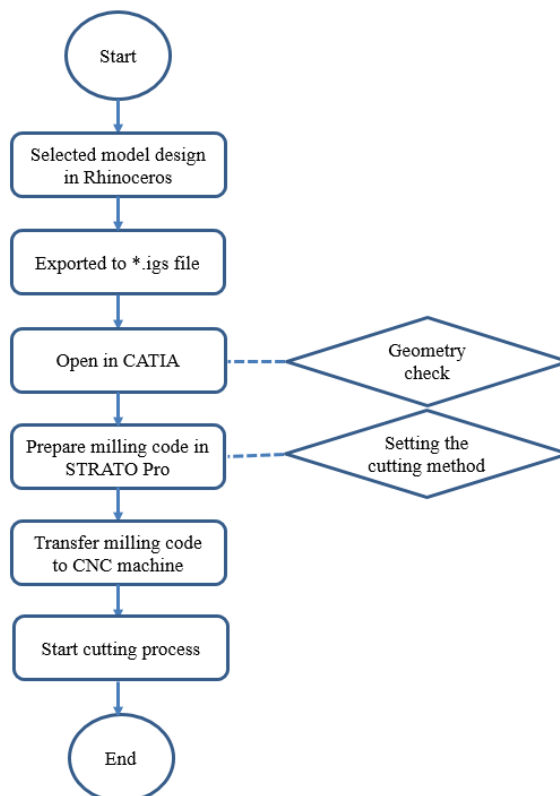


Figure 4.7 Flow chart for milling process

A CNC machine was used in the milling process. The machine is called the Euromod MP65. The specifications of the machine are shown in Table 4.2.

Table 4.2 Specification of Euromod MP65

Model	Euromod MP65
Processing areas X/Y/Z (mm)	800/650/250
Gap (mm)	350
Machine dimension WxDxH (mm)	1,480 x 1,510 x 1,960
Processing speed mm/s	Max 250
Drive motor	Servo motor

The material used for milling is a Thermeo ® Polyurethane. The dimension (W x D x H) is 1.2 x 1 x 0.08 metres with the density of 35 kgm<sup>-3</sup>. Table 4.3 shows photographs of the model creation procedure. It starts with the milling process. The milling process uses a strata method where each hull form is divided into the maximum processing volume of the machine. For the ASL hull, it was divided into four parts and for the 5415 hull, it was divided into six parts. Each model was then assembled using double sided tape in order to allow the laying of fibreglass. Two forms of fibreglass were used in this model creation which were chopped strand mat and woven mat fibreglass. To bond the fibreglass, an epoxy resin with hardener were used at a ratio of (resin: hardener) 2:1. Each hull was laminated with three layers of fibreglass. The three layers of fibreglass were based on the weight estimation computed by GHS with a calculation of the fibreglass strength. The superstructure of ASL was made from synthetic glass and the superstructure of 5415 was made from foam. Foam is a light weight material and it will not affect the centre of gravity location.

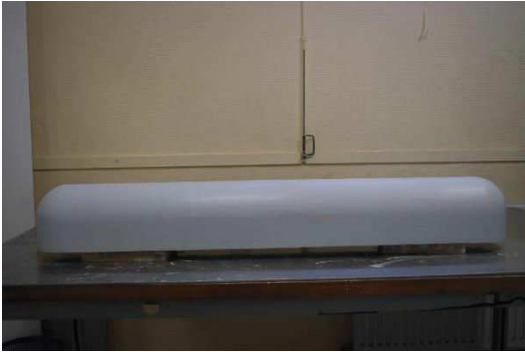
After both hulls were completely covered by fibreglass, the surface preparation process started. A set of sandpapers was used to define the exact curve of the hull. The process started with a coarse sandpaper finishing with fine sand papers. After the surface had been well prepared, the surface imperfections were corrected using an epoxy mastic. This material is commonly used to fill the holes in fibreglass surfaces. It can also be used to create the correct curved surface. After the surface was corrected, the sanding process was repeated. Once completed, the painting started. One layer of primer and two layers of lacquer were used.

After the painting process had been completed, the hull was allowed to dry at ambient temperature. After the hull was completely dry, the draught marking process started. The hull was positioned on the labelling table. A labelling table is a table which has a perfect horizontal surface. A digital height gauge was used to mark the vertical height on the hull. It had a precision of 0.01mm. The digital height gauge had a sharp pointer that scratched a mark on the model hull. Then, the marks were labelled with a permanent marker. We used six positions of draught marks which were forward - port, mid - port, aft - port, forward -stbd, mid -stbd, and aft -stbd. These six positions allowed for the identification of the trim and list angle of the model.



Table 4.3 Photographs of model creation

ASL shape	5415 shape
Milled foam for hull	
	
	
	
Laminated with fibreglass	
	

ASL shape	5415 shape
Premier (undercoat or basecoat) coat	
	
Final coat	
	
Draught marking process	
Model in basin	
	

### 4.3.2 Model Verification

Model verification is an important process to verify that the model has been constructed based on the real design. Any deviation from the dimensions may affect the experimental results. The process started with the weighing process of the hull, superstructure, the lead weights and measuring device. All items had to be weighed before they were fixed to the model. A water balance check was conducted to confirm that the model had perfect angles of list and trim. A water balance was used to measure these angles. At the same time, the draught marks were also measured. Two devices were used for the data recording, the first being the Ardu Flyer device and the second a smartphone (Djebli et al. 2016)

Based on Archimedes' principle the upward buoyant force that is exerted on a body immersed in a fluid is equal to the weight of the fluid that the body displaces and this acts in the upward direction. In order to verify the volume of the displaced water, the model was placed in a basin to measure the draught at the designed weight. The weight of the ASL shape was 26.994 kg and the 5415 shape was 8.635 kg. These values were obtained by GHS.

### 4.3.3 Model Pre-Test

The model pre-test is a procedure to test the model's hydrostatic information. An inclining test and natural roll period test were conducted for both models. The inclining test is a method to place the essence of the gravity location. It is usually conducted inshore in calm weather or in still water, and free of mooring restraints to achieve accuracy. The *GM* situation is defined by moving weights transversely to produce a known overturning moment. Knowing the restoring properties (buoyancy) of the vessel from its dimensions and floating position and measuring the equilibrium angle of the weighted vessel, the *GM* can be computed. In this trial, the weight shifts had to be recognised and the angles of tilt measured. The effects of any mooring can be calculated and deducted. A series of weight movements were used to obtain an average and variance for *GM* (Hanson 1985). The detailed steps of the inclining test are as follows:

- a. Weight measurement for the hull, superstructure, weights and all accessories to be used in the model for the experimental work;
- b. The model was fitted with superstructure and all accessories. All items had to be fixed in their position to avoid any movement;
- c. A known distance was marked on the deck. This distance was used to compute the moment;

- d. 10 plates of 10g lead were located on the starboard side of the deck. The centre of the weight was located exactly at the marked point (Figure 4.8). The weight was adjusted to achieve 0 degree of list;
- e. A lead weight was moved to the port side on the marked point. Then, the change of angle of list was recorded. The test continued until all lead weights were moved to the port side. The angle of list was also recorded.

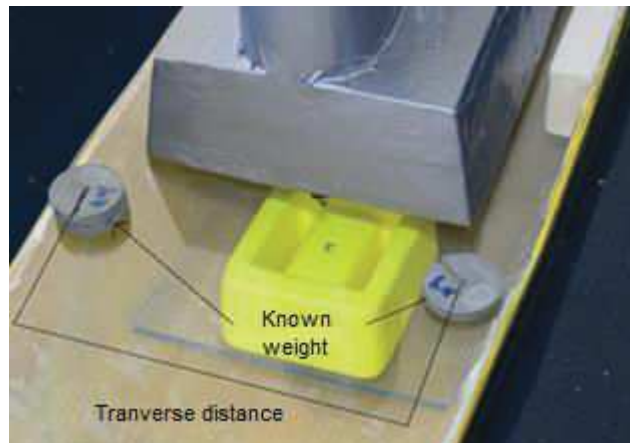


Figure 4.8 Moving weight and transverse distance for inclining test

To change the *VCG* vertically, a mass must be moved within the model. Below is an example of calculation to change the *VCG*. The method to change the *VCG* is shown in Table 4.4.

The natural roll period test is a test to measure a complete oscillation of the ship to ensure the most accurate result. It should be conducted in calm water, with no waves and a minimum of objects nearby that may affect the damping factor. The natural roll period of a ship is the duration it takes for an inclined ship, without any external moments, to perform a whole rolling cycle. This time depends on three main aspects which are the stability of the ship, the mass moment of inertia and the inclining angle. A higher stability of the ship in general leads to a shorter roll period, because the up righting ability increases. On the other hand, a lower stability leads to a longer roll period (IMO SLF 54/INF.9 2011). For this pre-test, a model was inclined to an initial angle (between 5 to 10 degrees) and then released. The result was an oscillation around the static heel of equilibrium, and the ship oscillated in its own natural roll period. The natural roll period can be determined by equations as shown in Table 4.5.

On the completion of the model pre-test, both models were evaluated using a hydrostatic solver. The primary function of evaluating the model was to verify the data used

in the calculation. It should be based on real data and pass the 2008 IS Code. Furthermore, the models were also evaluated with the SGISC for further analysis.

Table 4.4 Procedure to change VCG

Design condition	<ul style="list-style-type: none"> <li>➤ VCG: 10 cm</li> <li>➤ Displacement: 26.994 kg</li> </ul>
First result from inclining test	<ul style="list-style-type: none"> <li>➤ VCG: 12 cm</li> <li>➤ Displacement: 27 kg</li> </ul>
Movement of weight	<ul style="list-style-type: none"> <li>➤ VCG must be reduce by 2cm</li> <li>➤ Moment = Displacement x distance</li> <li>➤ Moment by ship = Moment by moving weight</li> <li>➤ 27kg x 0.02m = 0.54 kg.m</li> </ul>
Solution	<ul style="list-style-type: none"> <li>➤ Moving downward a moment of 0.54kg.m.</li> <li>➤ A weight of 10.8 kg is placed 0.05m lower than previous position.</li> </ul>

Table 4.5 Natural roll period formula

Method	Equation (unit in SI)	Source
2008 IS Code – IMO weather criterion	$T_R = \frac{2 \cdot C \cdot B}{\sqrt{GM}}$	(IMO 2009)
Naval architecture for non-naval architects	$T_R = \frac{0.76 \cdot B}{\sqrt{GM}}$	(Benford 1991)
Stability and Trim for the Ship's Officer	$T_R = \frac{0.8 \cdot B}{\sqrt{GM}}$	(La Dage and Van Gemert 1956)
Ship & Naval Architecture	$T_R = \frac{2 \cdot \pi \cdot K_T}{\sqrt{g \cdot GM}}$ $K_T = \frac{B}{3}$	(R. Munro-Smith 1988)
Weiss formula	$T_R = \frac{2 \cdot \pi \cdot i}{\sqrt{g \cdot GM}}$ $i = \frac{I_{xx}}{\Delta} \approx 0.4 B$	(IMO SLF 54/INF.9 2011)

Where:

$T_R$  = Natural roll period (second);

$B$  = beam (m);

$L$  = ship length (m);

$T$  = draught (m);

$GM$  = metacentric height (m);

$$\Delta = \text{displacement (kg);}$$
$$C = 0.373 + [0.023 (B/T)] - [0.043 (L/100)]$$

#### 4.3.4 Pre-Test Results

The results for the natural roll period test were compared with several methods. Each method was well established and had been widely used in the naval architecture domain. In this research, three main methods were used. The first was the calculation method based on formulae, second was the simulation method using the Fine Marine software and third was the experimental result prior to the wind tunnel test. The details of the pre-test results for the ASL shape are shown in Table 4.6 and Figure 4.9. The details of the pre-test results for the 5415 shape is shown in Table 4.7 and Figure 4.10.

The natural roll period simulation for the ASL and 5415 shapes was slightly different. The 5415 shape was more sensitive due to the time step calculation. For the ASL shape, the time step value used was 0.015s and the 5415 shape used the time step value of 0.005s. Both said time steps and shapes showed the same results as the time step of 0.001s. Indeed, small time steps should be selected for accurate prediction, and fixed time steps should be preferred to adaptive schemes.

Table 4.6 Results for pre-test of the ASL shape

Method	Natural roll period (seconds)
Formula: IMO	3.6198
WEISS formula	3.5373
Benford, 1991	3.3490
Simulation Fine Marine	3.3750
Experimental Prior to wind tunnel test	3.4815

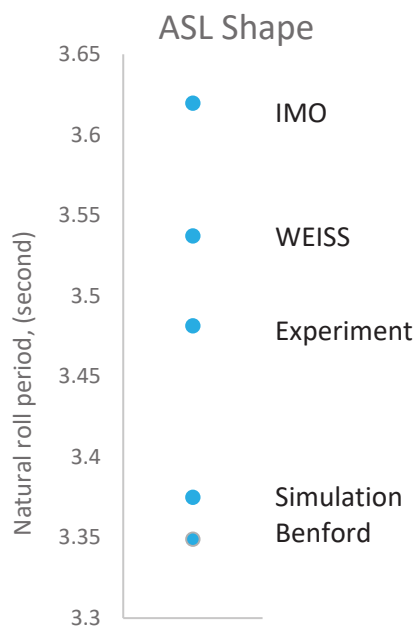


Figure 4.9 Comparison of natural roll period test for the ASL shape



Table 4.7 Results for pre-test of the 5415 shape

Method	Natural roll period (seconds)
Formula: IMO	1.1214
WEISS formula	1.1844
Benford, 1991	1.1213
Simulation Fine Marine	1.1750
Experimental Prior to wind tunnel test	1.1102

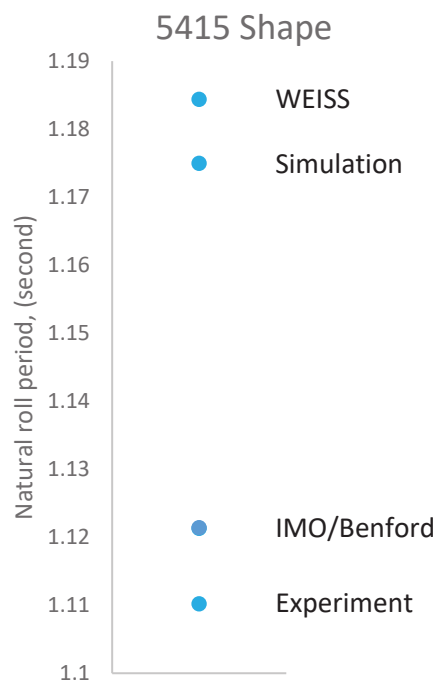


Figure 4.10 Comparison of natural roll period test for the 5415 shape

#### 4.4 Test Rig Design

Dealing with air in the test section is the norm in a wind tunnel experiment. Meanwhile, dealing with water in the test section requires additional precaution because the instrument underneath the test section floor is not designed to be watertight. In this experiment, a water tank of the dimensions (length x width x height) 1600mm x 400mm x 240mm was constructed using 8mm glass. The water tank joints were properly sealed to avoid any water leakage. For safety reasons, a small watertight curtain was located underneath the dummy test section platform to collect any water leakage. To prevent the models from moving transversally, a rod with a diameter of 4mm (see Figure 4.11) held both the ASL shape and 5415 shape. The rod



was located at the centre of buoyancy (*CoB*). For the ASL shape, the *CoB* location was at 6.88 cm from the keel, and for the 5415 shape, the position was at 3.66cm from the keel. The superstructures above the waterline for both models are shown in Figure 4.12 and Figure 4.13. To avoid the wind velocity from accelerating at the water tank, a spoiler was used to create a good velocity profile. The height of the spoiler was at the same level as the water tank to avoid any obstruction. The concept drawing of the test rig is shown in Figure 4.14.

The spoiler used in the test section is shown in Figure 4.15. The spoiler was attached to the test section floor and the dummy test section floor. During the test, the wind velocity was controlled from the control room. The control room faced the test section to allow emergency action to be taken rapidly (Figure 4.16). At the same time, an electronic pressure sensor (Figure 4.17) was used to measure the static pressure and dynamic pressure. Since the wind velocity was the main concern in this test, a secondary instrument, a micro-manometer, was used to measure the wind velocity in the wind tunnel (Figure 4.18). The velocity profile in the test section needed to be verified before the test was conducted. A set of tubes was used to measure the static and dynamic pressure (Figure 4.19). Each tube was placed vertically at a distance of 2.5mm. Only the velocity profile was obtained and verified; the model was balanced before being placed in the water tank. The model was balanced with a set of loads and an accelerometer. The accelerometer contained sensors and a battery (Figure 4.20). All loads and sensors were placed correctly and firmly to avoid any disturbance during the experimental work. The height of the plumb placed in the hull was also considered to make sure the model presented the correct *GM* and natural roll period. The longitudinal rod used on both models was not to penetrate the hull model. It was to avoid any risk of leakage during the experiment. Therefore, the rod was properly glued at both the fore and aft of the model (Figure 4.21). At the water tank, a “double L” plate was used to prevent the longitudinal rod from moving in a transverse direction. With this plate, the model was allowed to float freely and have the correct centre of buoyancy every time it heeled. The plate was located at the fore (Figure 4.22) and aft (Figure 4.23) of the water tank. It was fixed to the dummy floor test section.

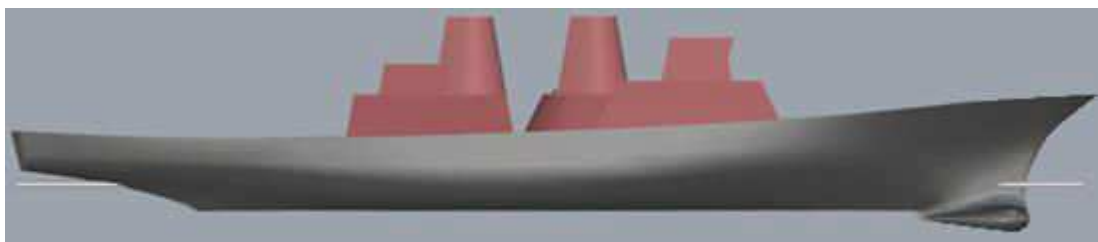


Figure 4.11 Location of longitudinal rod on model 5415

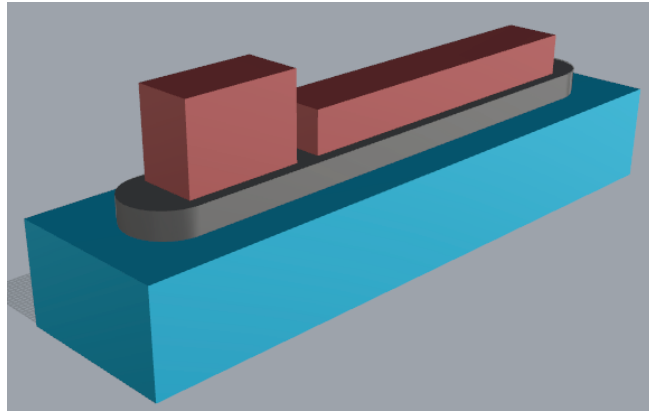


Figure 4.12 The superstructure above water line for the ASL shape

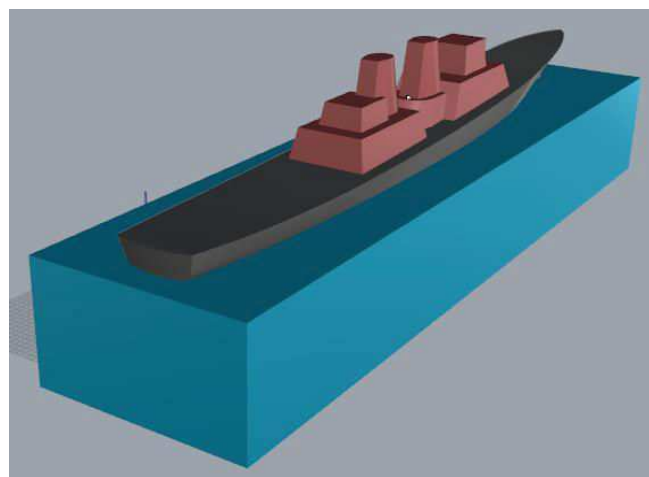


Figure 4.13 The superstructure above water line for the 5415 shape

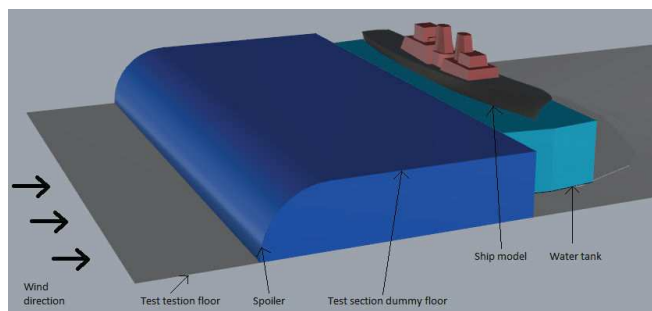


Figure 4.14 Perspective view of the test rig



Figure 4.15 Side view of test section with spoiler and dummy test section floor



Figure 4.16 View from control room toward test section



Figure 4.17 TSI Electronic pressure sensor model 9565-P



Figure 4.18 DP-CALC Micro manometer 5825 used to verify the wind velocity in the test section

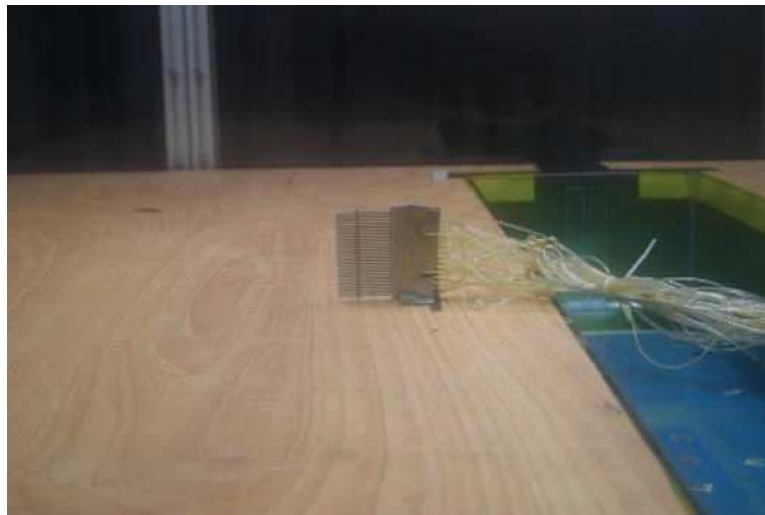


Figure 4.19 A set of tubes used to collect static and dynamic pressure



Figure 4.20 Arrangement of loads and accelerometer in the model hull



Figure 4.21 Both models fixed with rod before the test

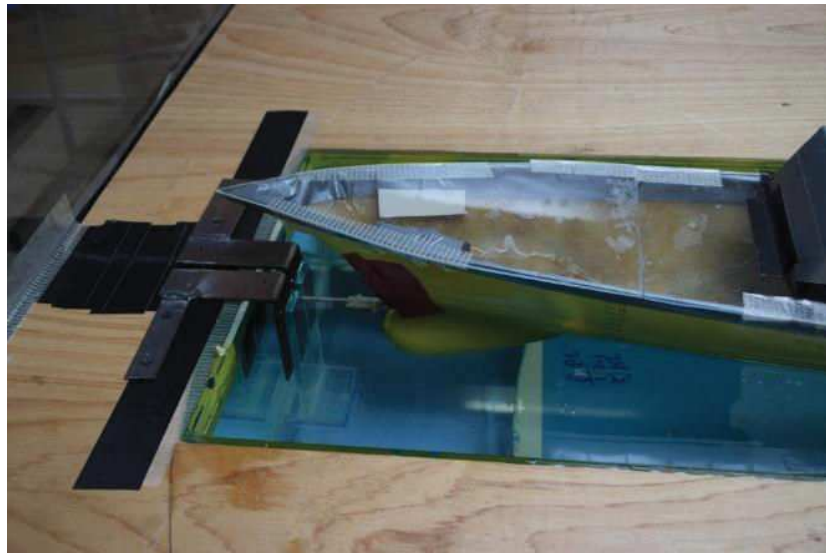


Figure 4.22 Rod location to the fore of the model

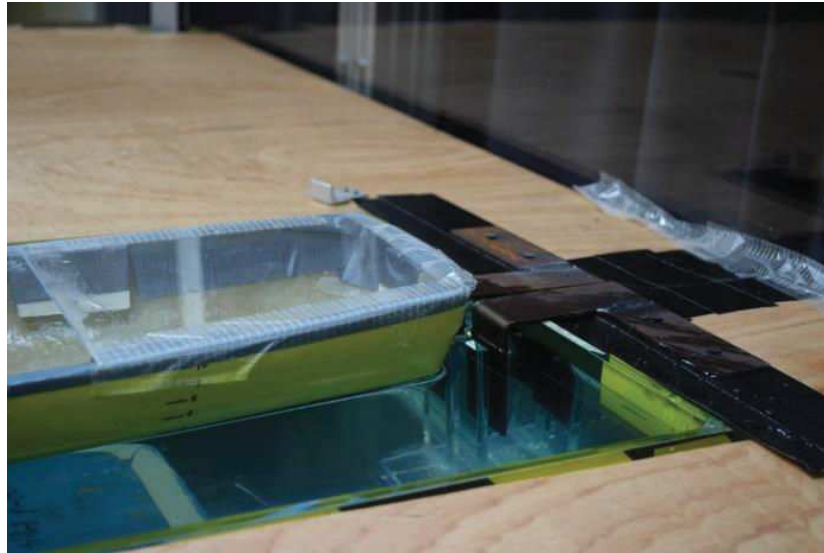


Figure 4.23 Rod location to the aft of the model

The models were placed in the water tank as shown in Figure 4.24 and Figure 4.25. The starboard side of the model faced the windward (wind direction). In order to confirm the model was up right prior to commencing the test, a self-levelling cross line laser was used. This instrument provided a perfect vertical and horizontal line continuously during the test (Figure 4.26). After the completion of the wind direction from the beam of the model, the rotating table was turned to 15 degrees. This was to allow a change in wind direction. Figure 4.27 shows the arrangements with the wind direction from starboard 75 degrees. Figure 4.28 shows the arrangements with the wind direction from port 105 degrees. The last test was conducted on the ASL shape with a bilge keel arrangement. The bilge keel dimensions were 1000 mm x 5 mm. It was placed 2 cm from the keel. Based on the 2008 IS Code Weather Criterion – Table 2.3.4-3 - Values of factor  $k$ , this bilge keel's configuration was  $A_k = 1 \times 0.005$ ,  $L_{WL} = 1.4$  and  $B = 0.2$ , where  $(A_k \times 100)/(L_{WL} \times B) = 1.786$  and contributed to the  $k$  factor of 0.90996. The bilge keel was fixed to the hull of the ASL shape as shown in Figure 4.29.





Figure 4.24 Model ASL shape is ready in wind tunnel test section



Figure 4.25 Model 5415 shape is ready in wind tunnel test section

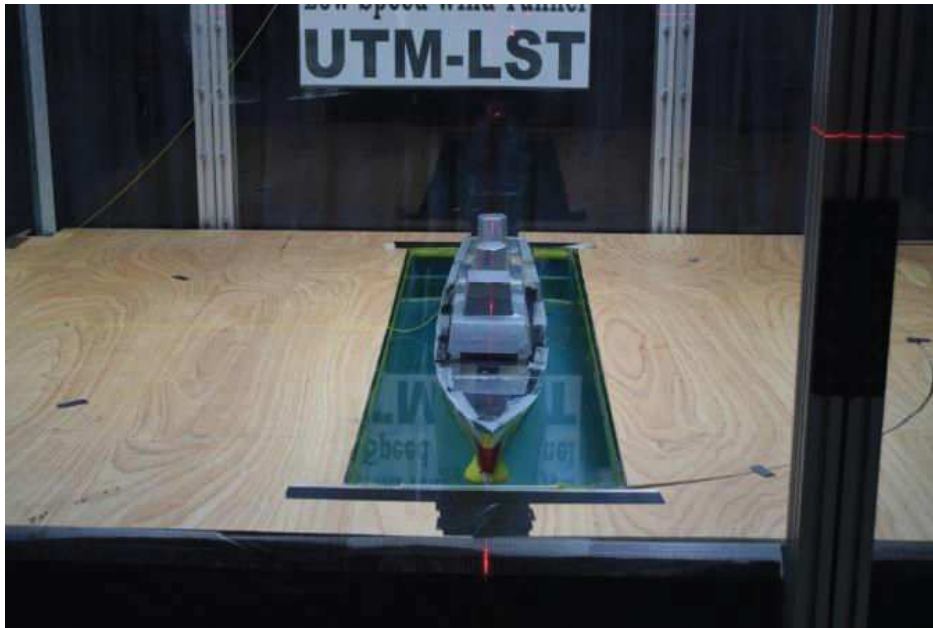


Figure 4.26 Self levelling cross-line laser used in this experiment



Figure 4.27 The rotating table is turned 15° to simulate the wind direction from starboard 75°





Figure 4.28 The rotating table is turned  $15^\circ$  to simulate the wind direction from port  $105^\circ$



Figure 4.29 The ASL shape was fitted with a bilge keel

#### 4.5 UTM's Low Speed Wind Tunnel

The wind tunnel test is the commonly used method in research works as reported in the literature. The wind tunnel method is commonly used for reasons of safety and economy. Model scale tests are cheaper and offer a controlled environment. However, it can be difficult to obtain an accurate simulation of the atmosphere and geometric characteristics of the ship. There are three important components in the wind tunnel which are known as the test section, fan motor and settling chamber. The general arrangement of the wind tunnel is shown in Figure 4.30.

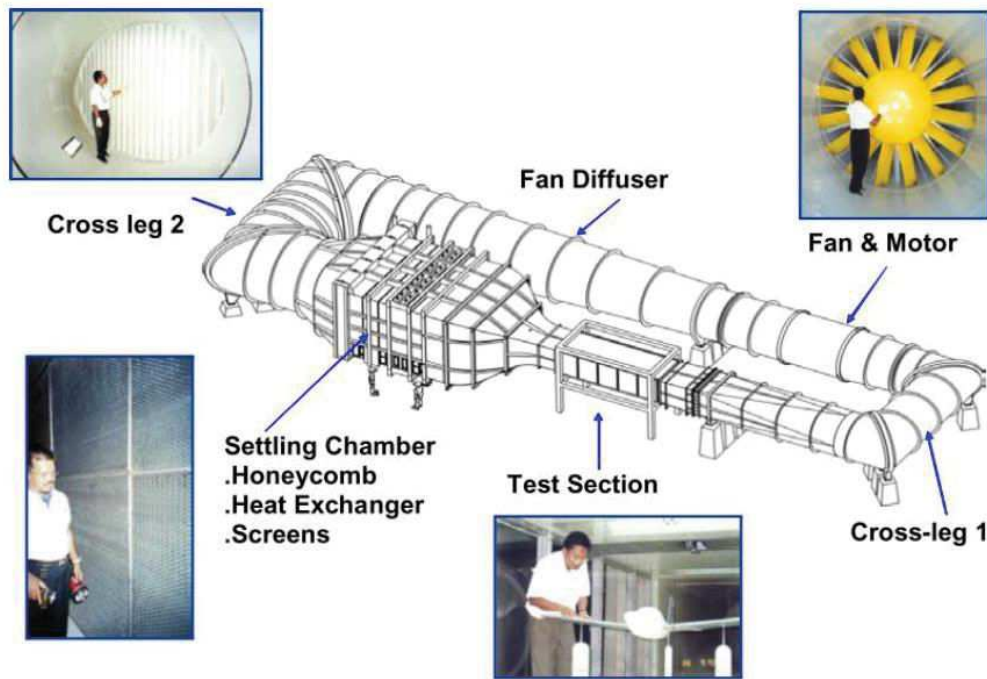


Figure 4.30 General arrangement of low speed wind tunnel, UTM

The main laboratory facility is the *state-of-the-art* low speed wind tunnel with a maximum speed of 288 km/h. The wind tunnel has an excellent flow quality with 2.0 m (W)×1.5 m (H)×5.8 m (L) test section size. It has a flow uniformity of less than 0.15%, a temperature uniformity of less than 0.2°C, a flow angularity uniformity of less than 0.15° and a turbulence level of less than 0.06%. This facility, the first of its kind in Malaysia, became operational in June 2001. The wind tunnel is housed inside the Aeronautical Engineering Laboratory building. The wind tunnel is furnished with a compressed air facility for general purpose applications. The test section is connected to the wind tunnel control room via a metal structure platform (Noor and Mansor 2013).

#### 4.6 Instrumentation and Data Collection

For the velocity profile test, a set of electronic pressure sensors was used. The TSI pressure sensor model 9565-P (USA) was used to measure the pressure from the free stream probe located near the top of the test section (see Figure 4.17). It was calibrated prior to the wind tunnel test to ensure the accuracy of the test results, using standards in accordance with the United States National Institute of Standards and Technology (NIST). The calibration system is registered with ISO-9001:2008 and meets the requirements of ISO 1 0012:2003. The FlowKinetic pressure measurement system was calibrated using the TSI pressure sensor. A total of 30 FlowKinetic tubes were calibrated where each tube was connected to the TSI pressure sensor for the calibration process (see Figure 4.18). Upon completion of the calibration process, the FlowKinetic pressure measurement system was reset to the atmospheric pressure for the data collection process. The system contains independent pressure sensors. They are

high accuracy temperature compensating differential pressure transducers with scan rates of up to 250 kHz. The system was connected to a personal computer via a USB cable.

Measuring the motion of the ship model is the main interest in this experiment. Therefore, an accelerometer ArduFlyer was used. The ArduFlyer is a complete open source autopilot system. Its design comes from 3D robotics and it is fully compatible with various open source codes. For data collection, interface software named Mission Planner was used. This software was created by Micheal Osborne from Australia. In this research, only the attitude of the model was collected (pitch, roll and yaw). The connection setup on the model and at the ground station are shown in Figure 4.31.

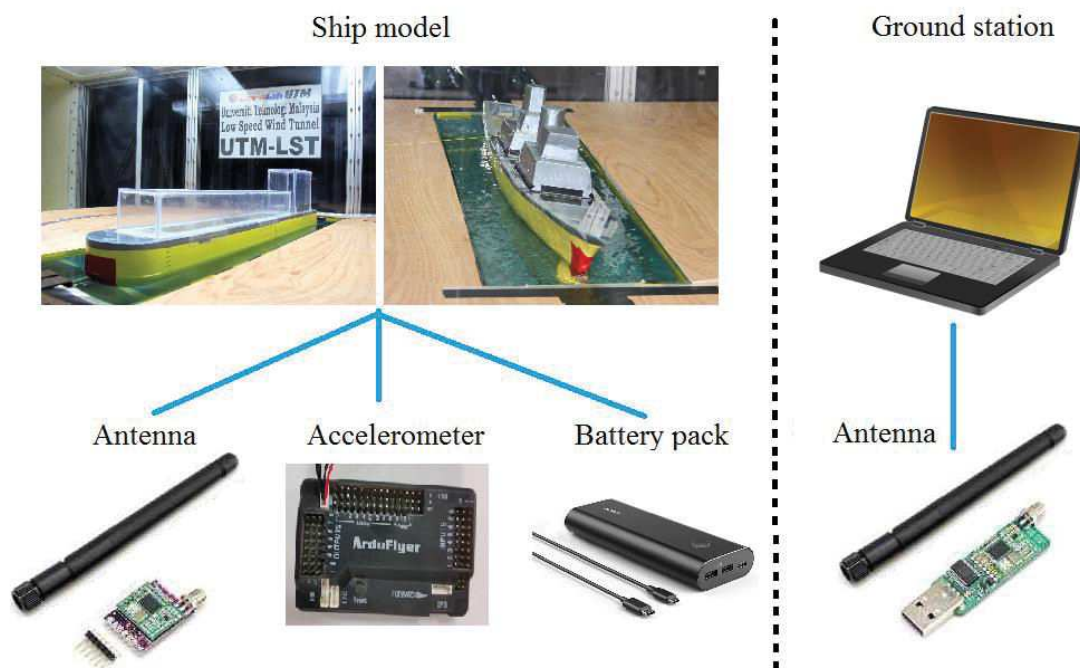


Figure 4.31 ArduFlyer setup

#### 4.7 Wind Velocity Profile Test

After the test rig had been properly installed in the test section, the boundary layer measurement was conducted. The boundary layer in the test section played a main role in this experiment. To investigate the boundary layer thickness, a set of tubes was used (see Figure 4.19). This set of tubes was able to profile the wind velocity at every 2.5 mm from the test section floor. The power law of the velocity profile is given by

$$U = az^m \quad (\text{Eq 4.1})$$

Where;  $m$  and  $a = (U_1/z_1^m)$  are constants for the given conditions of surface roughness and turbulence (Ariffin 2014). The typical value of index  $m$  for rough sea is between 0.11 and 0.15

(Yesilel 2007; Carton 2000). After the velocity profile test, the boundary layer thickness before the experiment was 30mm. The velocity profile in the wind tunnel is shown in Figure 4.32. The height of the boundary layer relative to the models is shown in Figure 4.33. The black dotted curve is the experimental value and red dotted curve is a theoretical value.

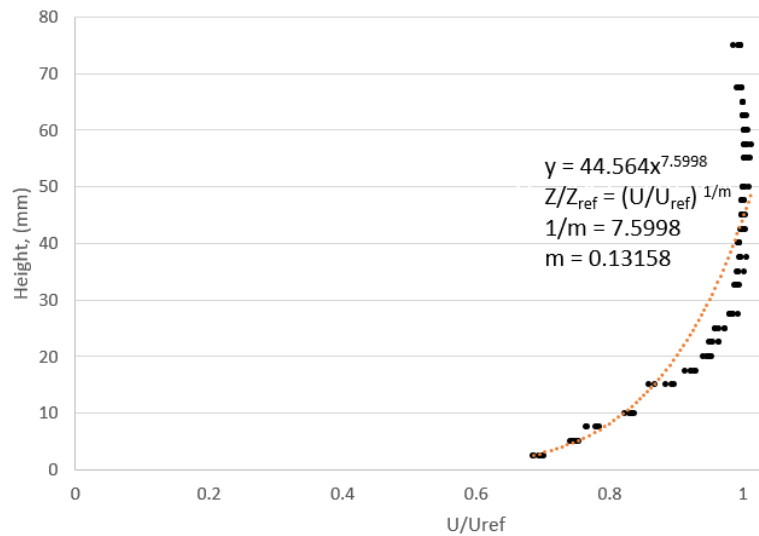


Figure 4.32 Velocity profile in the test section after the test rig was ready

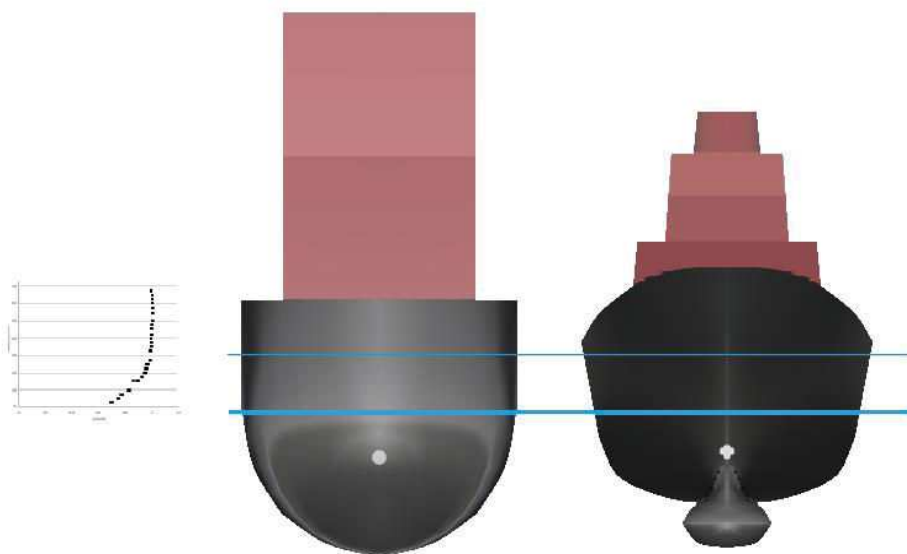


Figure 4.33 Comparison of boundary layer with the models

#### 4.8 Scaling Criteria

The fundamental concept is that the model of the ship and the wind should be at approximately the same scale. In some cases, a limited number of wind tunnels is able to accommodate a full scale model in the test section such as at NASA Langley's 30x60 foot tunnel, Virginia USA, MIRA full scale aerodynamic wind tunnel, London, United Kingdom, and S2A full scale wind tunnel, Paris, France.

A full-scale wind tunnel is expensive in terms of management and maintenance. Therefore, most universities have smaller scale wind tunnels for their research activities. A scaled down model is widely used in the marine industry, either for wind tunnel tests or towing tank tests. The scaling criteria play an important role to ensure that the results obtained by the wind tunnel present a similar behaviour on a full scale (Bertram 2012).

In this research, two models were constructed for the wind tunnel analysis as explained in Section 4.3. The scaling ratio was obtained from the naval architect's theory. Table 4.8 shows the scaling ratio used in this experiment.

Table 4.8 Scaling ratio used in this experiment

Parameter	Unit	Ratio (full-scale: model)	Example
Length	metre	1:100	Ship dimension
Mass	Kilogram	1:1,000,000	Displacement
Wind velocity	m/s	1:10	

#### 4.9 Test procedure

After the boundary layer thickness was verified, the experiment started with the wind off test. Wind off is a test which represents the natural roll of the model. Wind on is a test which simulates the model motion reaction to the wind in the test section. The test matrix is shown in Table 4.9.

Table 4.9 Wind tunnel test matrix

Test No	Model	Wind	Wind velocity (ms <sup>-1</sup> )	Wind direction	Bilge keel	Initial angle (°)
Angle of stable heel test						
1	ASL	on	2.0	90° starboard	No	0
2	ASL	on	2.5	90° starboard	No	0
3	ASL	on	3.0	90° starboard	No	0
4	ASL	on	3.5	90° starboard	No	0
5	ASL	on	4.0	90° starboard	No	0
6	ASL	on	4.5	90° starboard	No	0
7	ASL	on	5.0	90° starboard	No	0
8	ASL	on	5.5	90° starboard	No	0
9	ASL	on	6.0	90° starboard	No	0
10	5415	on	5.0	90° starboard	No	0
11	5415	on	6.0	90° starboard	No	0
12	5415	on	7.0	90° starboard	No	0
13	5415	on	8.0	90° starboard	No	0
14	5415	on	9.0	90° starboard	No	0
15	ASL	on	2.0	75° starboard	No	0
16	ASL	on	2.5	75° starboard	No	0
17	ASL	on	3.0	75° starboard	No	0
18	ASL	on	3.5	75° starboard	No	0
19	ASL	on	4.0	75° starboard	No	0
20	ASL	on	4.5	75° starboard	No	0
21	5415	on	5.0	75° starboard	No	0
22	5415	on	6.0	75° starboard	No	0
23	5415	on	7.0	75° starboard	No	0
24	5415	on	8.0	75° starboard	No	0
25	5415	on	9.0	75° starboard	No	0
26	ASL	on	2.0	105° port	No	0
27	ASL	on	2.5	105° port	No	0
28	ASL	on	3.0	105° port	No	0
29	ASL	on	3.5	105° port	No	0
30	ASL	on	4.0	105° port	No	0
31	ASL	on	4.5	105° port	No	0
32	5415	on	4.0	105° port	No	0
33	5415	on	5.0	105° port	No	0
34	5415	on	6.0	105° port	No	0
35	5415	on	7.0	105° port	No	0
Natural roll period test						
36	5415	off	-	-	No	15°, 10°
37	5415	off	-	-	No	15°, 10°
38	ASL	off	-	-	Yes	15°, 10°
Roll back angle test						
39	ASL	on	2	90° starboard	No	
40	ASL	on	3.2	90° starboard	No	
41	ASL	on	3.8	90° starboard	No	
42	ASL	on	4	90° starboard	No	
43	5415	on	5.1	90° starboard	No	
44	5415	on	6.5	90° starboard	No	
45	5415	on	7	90° starboard	No	
46	ASL	on	2	90° starboard	Yes	



#### 4.9.1 Wind Off Test (Natural Roll Period)

Wind off is a term used in the wind tunnel test. It is a term to differentiate between the natural condition and with wind condition. Meanwhile, in naval architecture, the natural condition for a ship is known as the natural roll period as explained in Section 4.3.3.

#### 4.9.2 Wind On Test

The wind on test is a test where wind is applied at a certain velocity in the test section. In this experiment, the wind on test was divided into two sections. The first section was for the angle of stable heel measurement. The second section was for identifying the roll back angle based on IMO weather criterion and Naval Rules. The Reynold number for this experiment is from  $3.23 \times 10^4$  to  $1.1 \times 10^5$ .

For the angle of stable heel test, a model was placed in the water tank. It was weighed properly to ensure the correct hydrostatic behaviour. The test started with the model upright. Then, the wind slowly increased. At every test velocity, there was a 2-minute period to allow the model to become stable in relation to the particular wind velocity. This duration was required to ensure the uniform flow of wind in the test section. Then, a measurement was taken at a dedicated wind velocity. The wind velocity was increased for further data collection. The test was ended when the water started to be on deck.

For the roll back angle, a model was placed in the water tank. It was weighed properly to ensure the correct hydrostatic behaviour. The test started with the model upright. Then, specific wind velocity was applied. Once the wind flow was stable, a rod was used to apply a force on the model to create a roll back angle (Figure 4.34). The rod was inserted from the top and pointed to the deck in the windward direction. The applied angle was based on the IMO and Naval Rules roll angle. Some tolerance was applied to ensure the consistence of the measured value. In this test, the motion was recorded using the Arduflyer accelerometer.

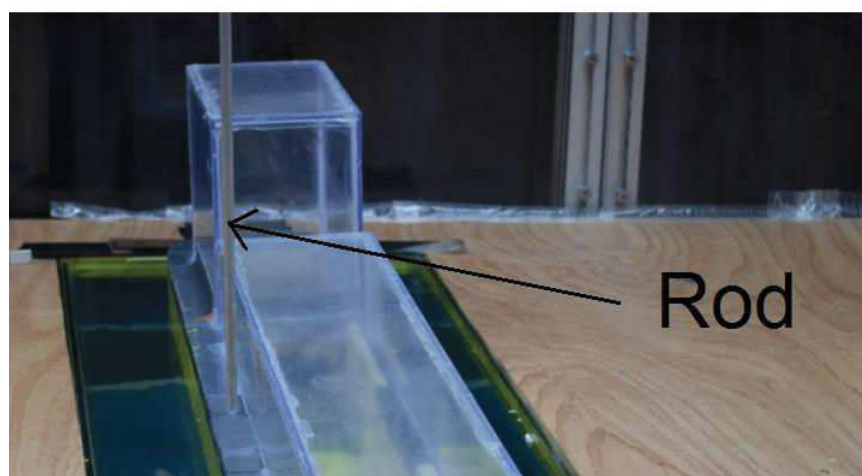


Figure 4.34 Rod used for the model to heel at roll back angle ( $\phi_1$ )

### 4.9.3 Roll Angle ( $\phi_1$ ) Prediction

To perform the wind tunnel test, the roll angle needed to be computed prior to the experiment. In general, there are two methods to compute the roll angle ( $\phi_1$ ). Commercial ship tests normally use the guidelines in the IMO 2008 IS Code and naval vessel tests, use the Naval Rules. The roll angle for the IMO varies based on the ship characteristics and angles for the Naval Rules are listed in Table 2.4. For this experiment, the roll angle values are listed in Table 4.10.

For  $\phi_1$ , the test wind velocity is stated in Table 4.9 No 39-46. For each wind velocity, several values of  $\phi_1$  (angle of roll to windward due to wave action) are used. The maximum value of  $\phi_1$  is the value reached at deck immersion. The data collected on roll back angle and wind velocity allow the interpolation calculation to obtain the exact value of  $\phi_2$ .

Table 4.10 Roll angle ( $\phi_1$ ) value for the ASL and 5415 shapes

Model	IMO Rules	Naval Rules	Roll angle ( $^\circ$ )
ASL	16.19 $^\circ$	25 $^\circ$	0 to 45 $^\circ$
5415	17.40 $^\circ$	25 $^\circ$	0 to 45 $^\circ$
ASL with bilge keel (where $k = 0.90996$ )	14.73 $^\circ$	25 $^\circ$	0 to 45 $^\circ$

### 4.10 Results and discussion

After the boundary layer thickness was verified, the experiment started with the wind off test. Wind off is a test which represents the natural roll of the model. Wind on is a test which simulates the model motion reaction to the wind in the test section. The test matrix is shown in Table 4.9

This experiment was conducted at a low speed wind tunnel at the Universiti Teknologi Malaysia. The presentation of the results is based on the abbreviation and symbology used in the 2008 IS Code (the weather criterion). In this chapter, the  $\phi_{2*}$  is a heel angle from the angle of stable heel to angle of second intercept between wind heeling lever  $l_{W1}$  and  $GZ$  curves as shown in Figure 4.35. It is an expression of an energy balance; the work done by the wind excitation as the ship rolls from the wind-side to the lee-side should not exceed the potential energy at the limiting angle.



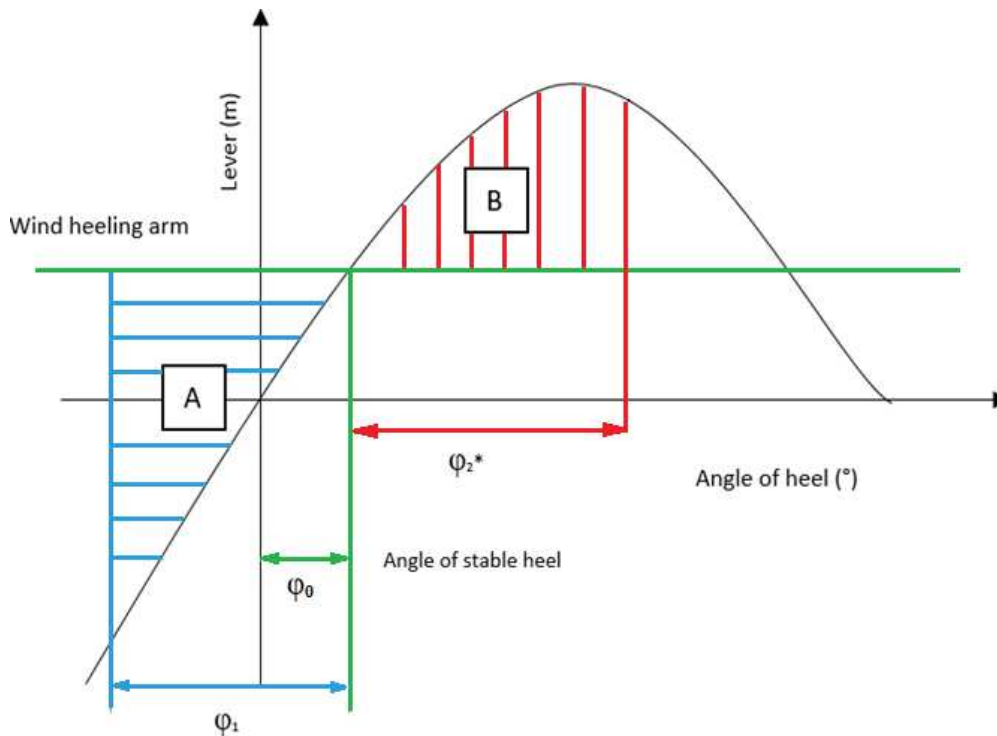


Figure 4.35 Definition used in this experiment

#### 4.10.1 Angle of Stable Heel ( $\phi_0$ ) versus Wind Velocity

Figure 4.36 shows the graph for the angle of stable heel,  $\phi_0$  versus wind velocity for the two models and two methods; IMO and experimental. The 5415 curves follow a parabolic shape since as we can see in Figure 4.37, the GZ curve of 5415 shape follows a linear curve (red curve) up to  $30^\circ$ . Furthermore, the experimental curve is below the IMO curve which indicates that the drag coefficient  $C_D$ , of the ship silhouette is smaller than 1 and the value is assumed in the IMO formula (Figure 4.36). The ASL curves present different shapes and behaviour. At first, they did not show the parabolic shape (blue curve) because as we can see in Figure 4.37, the GZ curve is only linear up to  $5^\circ$ . Furthermore, the experimental curve for this case is above the IMO curve (Figure 4.36). That is explained by the fact that the drag coefficient  $C_D$ , for the box shape of the ASL is more than 1. In fact, this is confirmed by the many references that exist, giving the drag coefficients of basic shapes, see for example (Scott, 2005; Blendermann 1994).

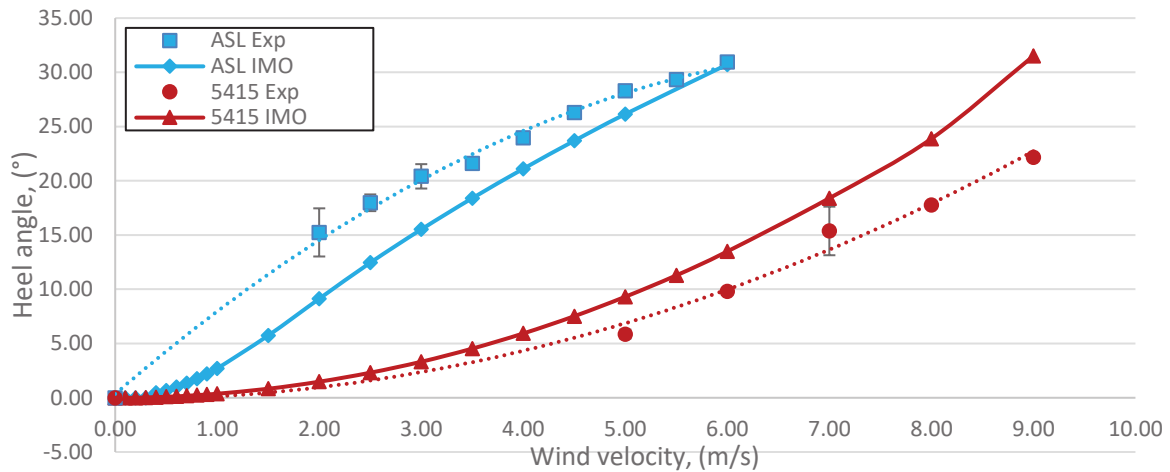


Figure 4.36 Graph of wind velocity and angle of stable heel for ASL shape and 5415 shape for the experimental results and GHS calculation

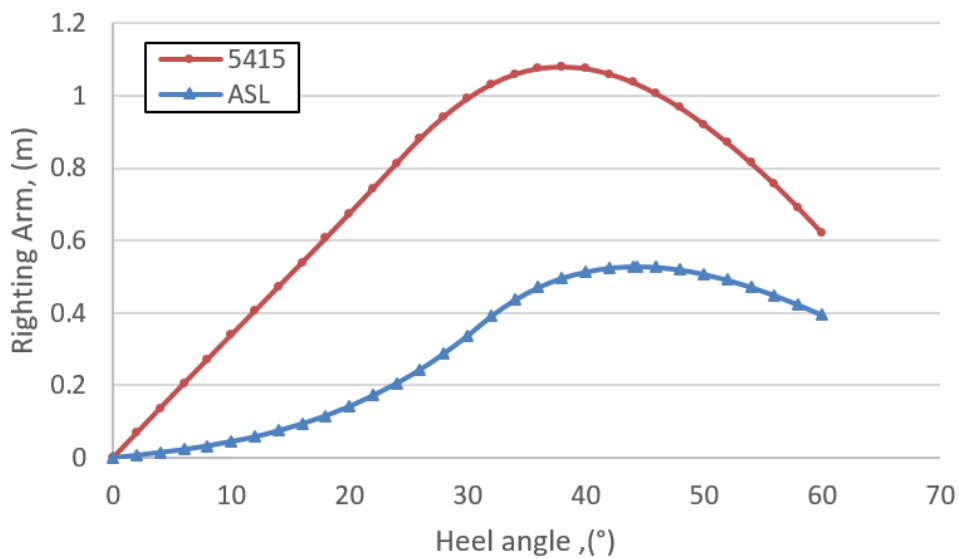


Figure 4.37 The GZ curves for the ASL shape and 5415 shape

#### 4.10.2 Roll Back Angle ( $\phi_2^*$ ) versus Roll to Windward ( $\phi_1$ )

Figure 4.38 shows the roll back angle ( $\phi_2^*$ ) versus roll to windward ( $\phi_1$ ) for the ASL shape for the wind velocity range of 2 m/s to 4 m/s. Figure 4.39 shows the roll back angle ( $\phi_2^*$ ) versus roll to windward ( $\phi_1$ ) for the 5415 shape. In the absence of damping, the results should be like a swing where  $\phi_2^*$  follows  $\phi_1$ . The straight lines in Figure 4.38 and Figure 4.39 represent an equal energy dispersal and absorption (theoretical value) both leeward and windward. The ASL shape shows that the experimental results diverged from the theoretical values and the

5415 shape shows that it converged to the theoretical value. In fact, the ASL shape had a rounded hull and is imposed to null damping. The ASL shape has more damping because of the work done by the wind heeling arm which is taken into account. This phenomenon is not present for the 5415 shape because the  $GZ$  curves for both ASL and 5415 shapes are different. Referring to Figure 4.37, the 5415 shape has a linear  $GZ$  curve from 0 to 30° and the ASL shape has a non-linear curve from 0 angle. Therefore, the area under the wind heeling arm contributed a significant influence to the roll back angle. Figure 4.40 shows the roll back angle ( $\phi_{2*}$ ) versus roll to windward ( $\phi_1$ ) for the ASL with bilge keel configuration for the wind velocity range of 2.3 m/s to 2.4 m/s. The results suggest a far more complex behaviour where the hydrostatic force shape plays an important role.

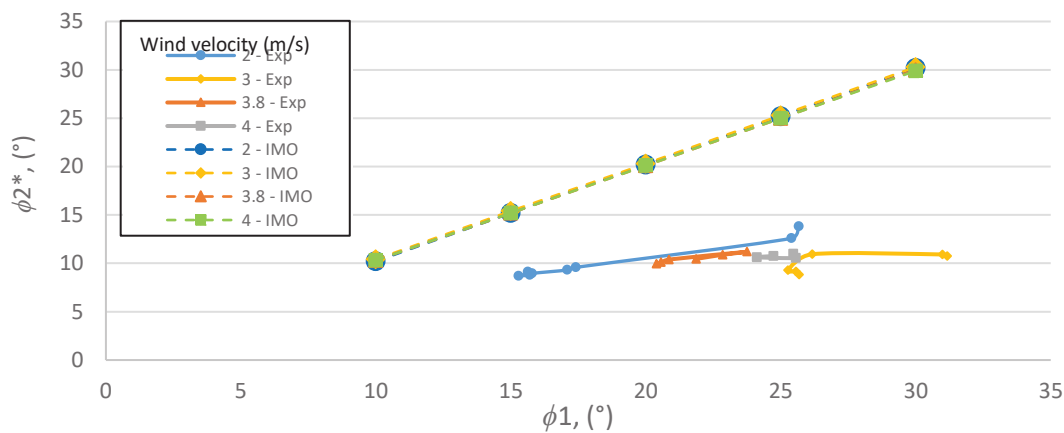


Figure 4.38 Roll back angle ( $\phi_{2*}$ ) vs roll to windward ( $\phi_1$ ) for the ASL shape

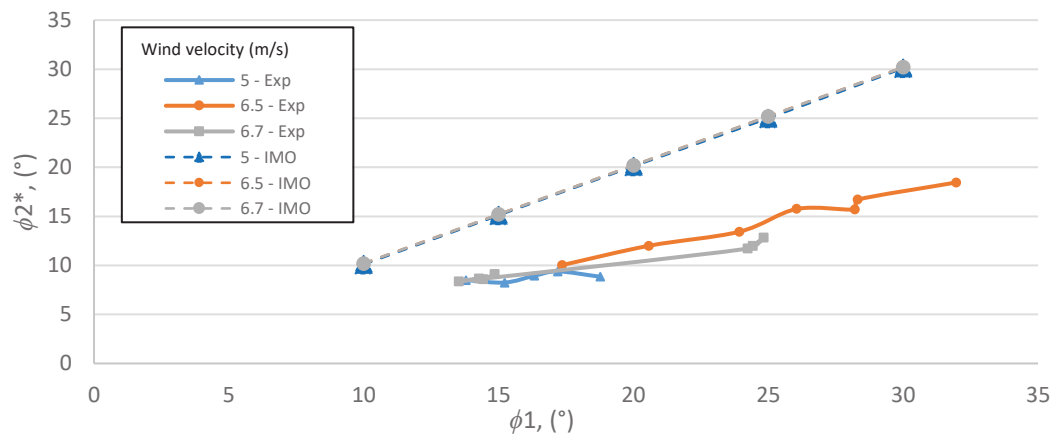


Figure 4.39 Roll back angle ( $\phi_{2*}$ ) vs roll to windward ( $\phi_1$ ) for the 5415 shape

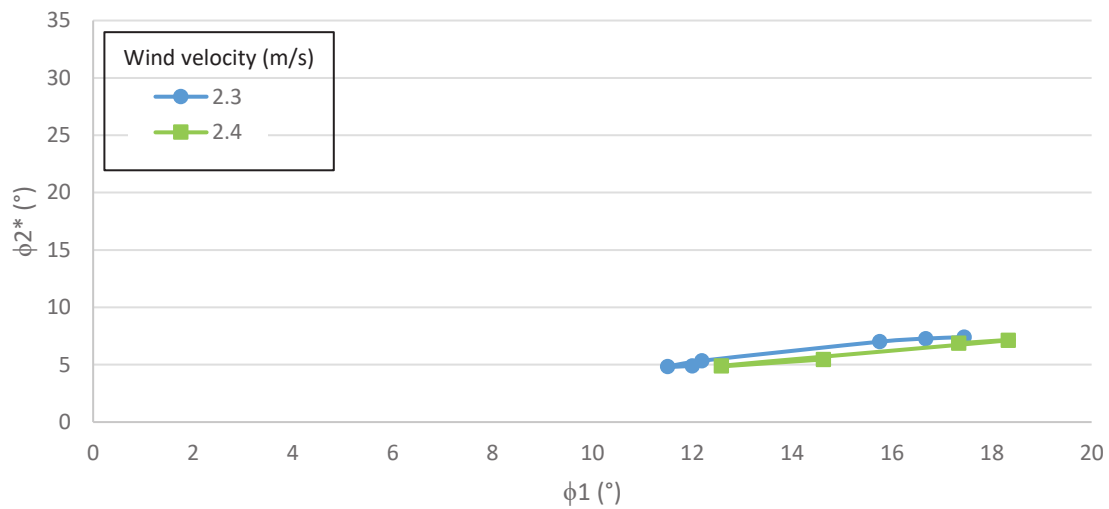


Figure 4.40 Roll back angle ( $\phi_2^*$ ) vs roll to windward ( $\phi_1$ ) for ASL with bilge keel configuration

#### 4.10.3 Ratio $\phi_2^*$ and $\phi_1$ with Bilge Keel

Figure 4.41 shows the ratio ( $\phi_2^*/\phi_1$ ) for the ASL shape and the ASL with a bilge keel. The wind velocity for this test is 2 m/s. For the bare ASL, the average ratio is 0.55, and for the ASL with bilge keel, the average ratio is 0.43. As expected, the configuration with bilge keel contributed to more roll damping than the configuration without bilge keel.

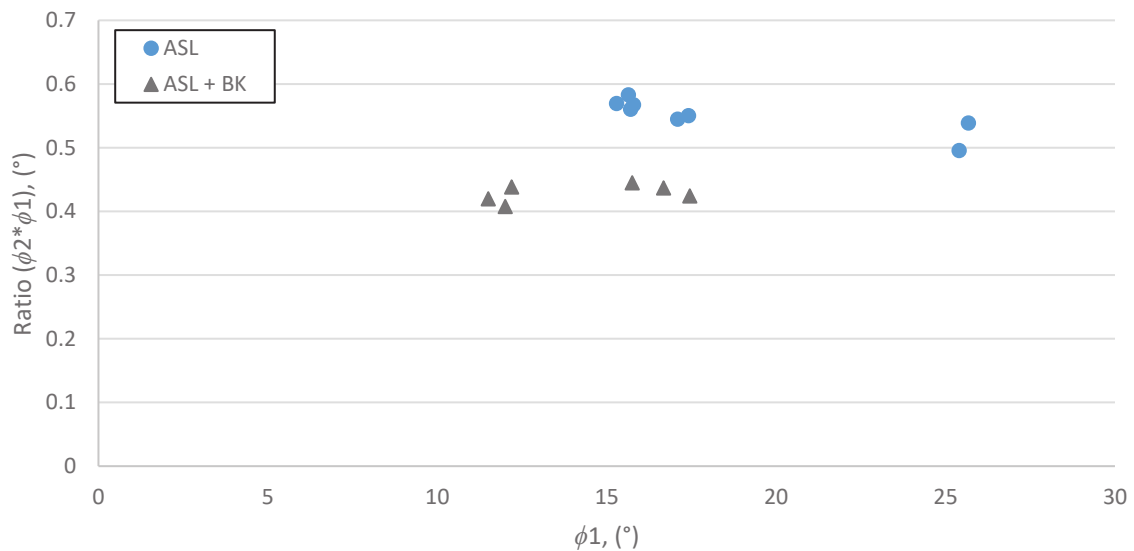


Figure 4.41 Roll back angle ( $\phi_2^*$ ) vs roll to windward ( $\phi_1$ ) for the ASL shape with and without bilge keel configuration

#### 4.10.4 Yaw Angle Effect on Stable Heel

Figure 4.42 shows the angle of stable heel for the ASL and the 5415 both with the wind direction from starboard 75° and port 105°. For the ASL, the values of  $\phi_0$  are smaller for the beam wind than those obtained with the yaw angles. In other words, the assumption of the beam wind in the IMO code is not necessarily conservative. This phenomenon also appeared for the 5415. This phenomenon is explained by the frontal area value facing the windward as shown in Figure 4.43. When the yaw angle changes from beam wind (black box) to head wind (red box), the frontal area facing windward increases until it is perpendicular (blue box) to the hypotenuse line (orange line). Then, the frontal area will decrease until the yaw angle is 90° (head wind).

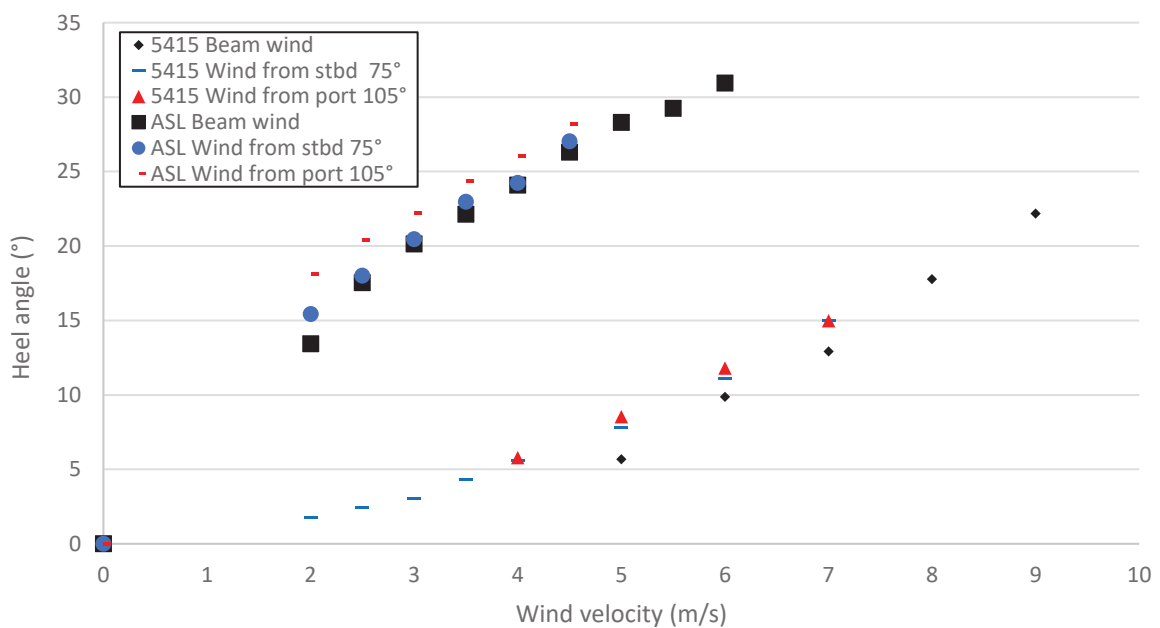
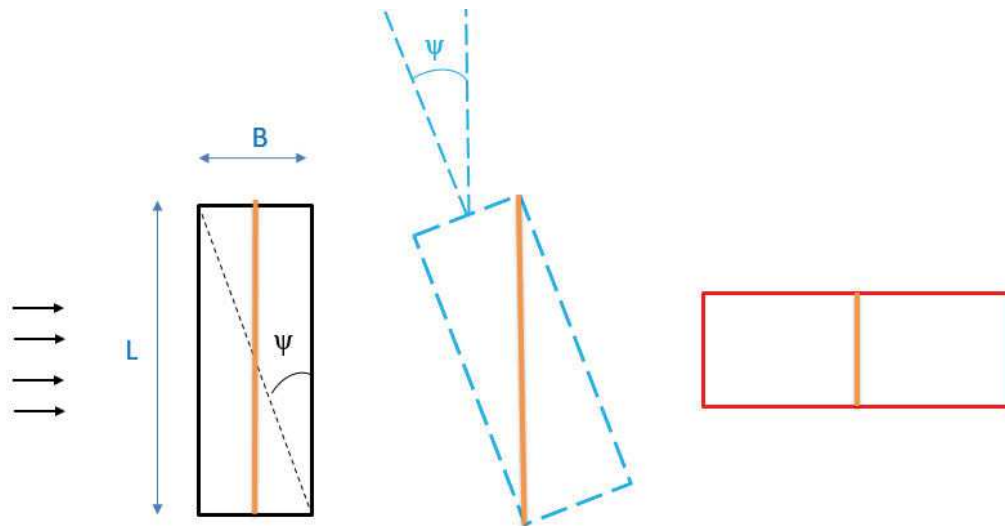


Figure 4.42 Angle of stable heel for wind from starboard 75° and port 105°



<b>Terminology</b>	Beam wind	-	Head wind
<b>Yaw angle</b>	0°	$\psi$	90°
<b>Frontal area facing windward (times height)</b>	L	$= \sqrt{(B^2 + L^2)}$	B
<b>Area value</b>	Nearly maximum	Maximum	Minimum

Figure 4.43 Explanation of yaw angle impact on angle of stable heel

#### 4.10.5 Effect of Roll to Windward ( $\phi_1$ ) and Roll Back Angle ( $\phi_2^*$ ) With Yaw Angle

Figure 4.44 shows the results for  $\phi_1$  and  $\phi_2^*$  for the ASL and the 5415 with beam wind and wind from starboard 75°. For the ASL, the beam wind has a higher  $\phi_2^*$  than wind from starboard 75° and for the 5415, the beam wind has a smaller  $\phi_2^*$  than wind from starboard 75°. The two models have a different response to the yaw angle. The behaviour is a combination of the superstructure geometry, the *GZ* curve and the damping.

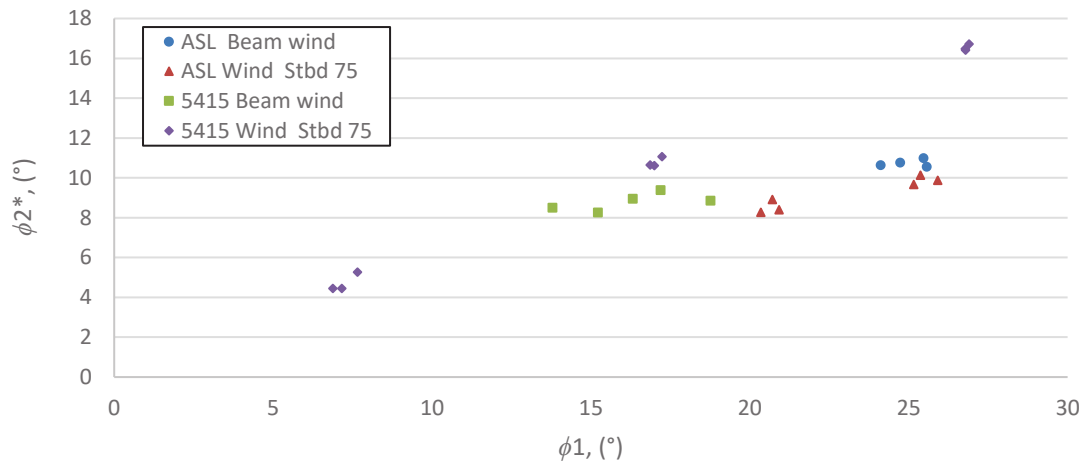


Figure 4.44 Roll back angle ( $\phi_2^*$ ) vs roll to windward ( $\phi_1$ ) for the ASL shape and 5415 shape with wind from beam wind and stbd 75°

#### 4.10.6 Comparison of IMO GHS and Experimental Results

Figure 4.45 shows the comparison of results between IMO GHS and the experimental results. For the ASL, the counter roll back angle ( $\phi_2^*$ ) obtained from experimental results is 24.07°, lower than the IMO's which is 29.638°. Therefore, the IMO result is more conservative. For the 5415, the counter roll back angle ( $\phi_2^*$ ) obtained from experimental results is 16.31°, lower than the Naval Rules which is 33.82° for ratio capsizing and restoring energy 1.0 and 39.45° for ratio capsizing and restoring energy 1.4. Therefore, the IMO and Naval rules are always more conservative. Note that the 5415 shape does not pass the naval criterion, but should this proposed direct assessment procedure be accepted, it would satisfy the rule.

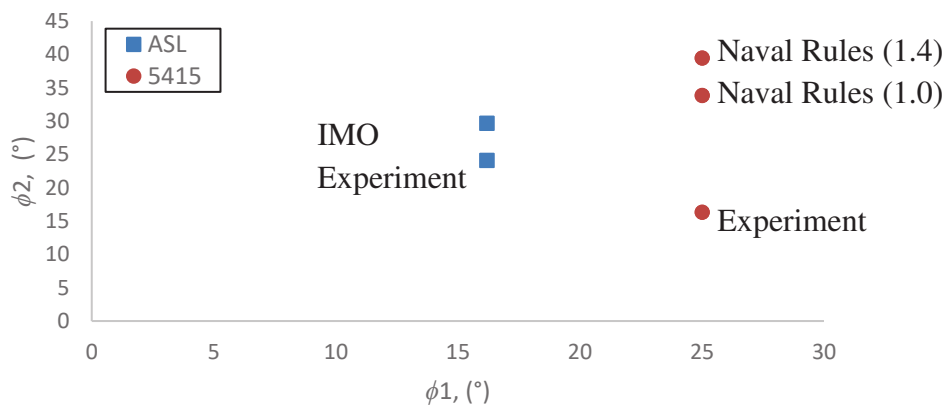


Figure 4.45 Comparison of results with IMO rules and Naval Rules

#### 4.10.7 Comparison of IMO GHS Drag Coefficient and Experimental Results

The wind force is related to the wind drag coefficient,  $C_D$  by means of the Eq 4.2(IMO MSC.1/Circ.1200 2006).

$$F_{wind}(\phi) = \frac{1}{2} \cdot \rho_{air} \cdot U^2 \cdot A_L \cdot C_D \cdot (\phi) \quad (4.2)$$

Where:

- $\rho_{air}$  = air density (1.222 kg/m<sup>3</sup> for full scale prediction);
- $U^2$  = wind velocity (ms<sup>-1</sup>);
- $A_L$  = lateral projected area of the ship exposed to wind in upright position, (m<sup>2</sup>).

Based on IS Code 2008, wind heeling lever,  $l_{w1}$  are constant values at all angles of inclination and shall be calculated as Eq 4.3.

$$L_{w1} = \frac{P \cdot A \cdot Z}{1000 \cdot g \cdot \Delta} \quad (4.3)$$

Where:

- $P$  = wind pressure of 504 Pa. The value of  $P$  used for ships in restricted service may be reduced subject to the approval of the Administration;
- $A$  = projected lateral area of the portion of the ship and deck cargo above the waterline (m<sup>2</sup>);
- $Z$  = vertical distance from the centre of  $A$  to the centre of the underwater lateral area or approximately to a point at one half the mean draught (m);
- $g$  = gravitational acceleration of 9.81 ms<sup>-2</sup>;
- $\Delta$  = displacement (tonnes).

The drag coefficient is calculated using the wind heeling lever equal to the wind force that causes the ship to heel. The  $Z$  value is obtained by GHS (Eq 4.3) where the  $Z$  average value is used (Eq 4.4).

$$\text{Heeling moment} = \sum P (h_i) * A_i * Z_i \quad (4.4)$$

$$Z_{\text{average}} = \frac{\text{Total heeling moment}}{\text{Total Area}} \quad (4.5)$$

Where:

- $\sum$  = the summation of the above water lateral plane elements represented by  $h_i$ ,  $A_i$  and  $l_i$ ;
- $P$  = wind pressure at distance of centroid of the  $i$ -th lateral plane element above water level;
- $A_i$  = lateral area of the  $i$ -th element;
- $l_i$  = vertical lever arm of the  $i$ -th element from its centroid to the centroid of the  $i$ -th underwater lateral plane.



For the ASL shape, the results for the angle of stable heel are shown in Figure 4.46. With this graph, the  $C_D$  is obtained using the formula Eq 4.2 to 4.5. In GHS, the drag coefficient used is 1.2. It can be customised based on user defined value. The  $C_D$  of the experimental value is higher than the  $C_D$  used in GHS. The value decreases from 0 degree until 30 degrees of heel angle. At 30 degrees, the  $C_D$  has almost the same value in the experiment and GHS. The  $C_D$  results for various heel angles are shown in Figure 4.47.

For the 5415 shape, the results for the angle of stable heel are shown in Figure 4.48. With this graph, the  $C_D$  is obtained using the formula Eq 4.1 to 4.4. In GHS, the drag coefficient used is 1.2. It can be customised based on user defined values. The value increases from 0 degree until 15.38 degrees of heel angle. Then, it slightly decreases to the region of 0.9. The  $C_D$  results for various heel angles are shown in Figure 4.49. A study on aerodynamic loads on heeled ships was studied using the simulation method (Luquet et al. 2014). They simulated the aerodynamic loads of a F70 frigate. The drag coefficient they obtained for the F70 frigate was 0.86.

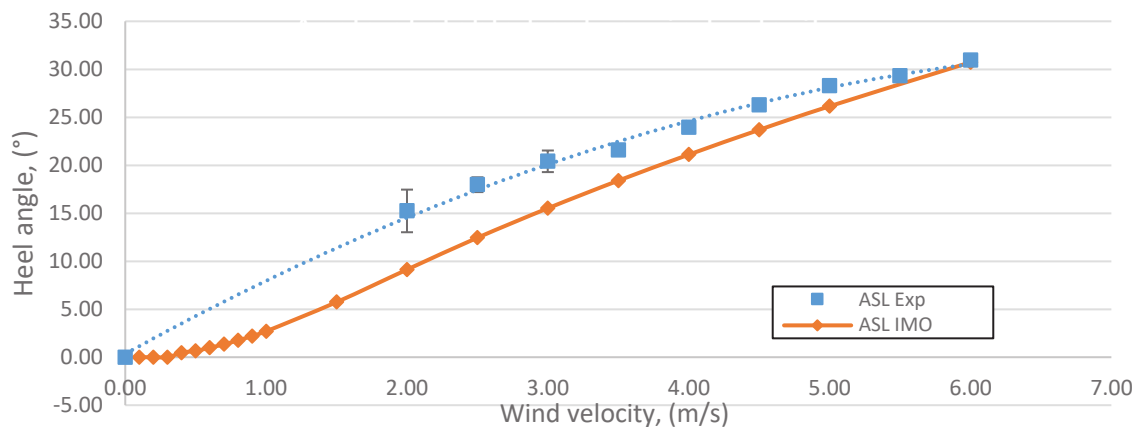


Figure 4.46 Angle of stable heel for the ASL shape

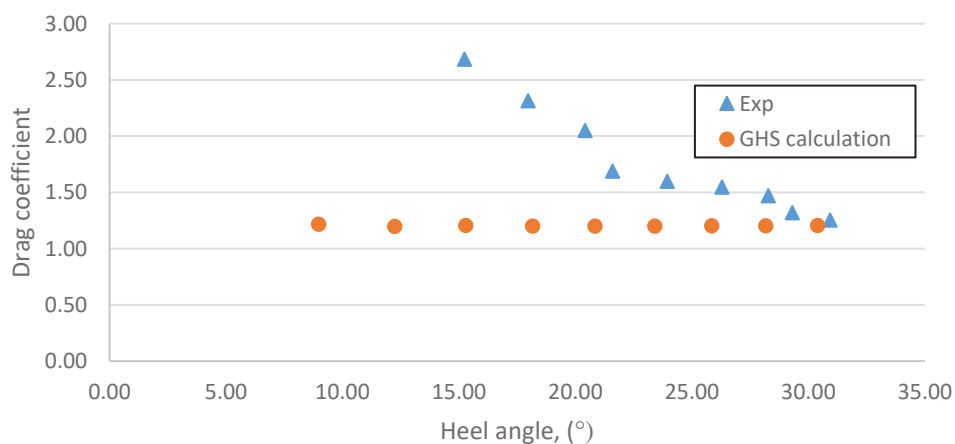


Figure 4.47 Drag coefficient vs heel angle obtained by calculation for the ASL shape

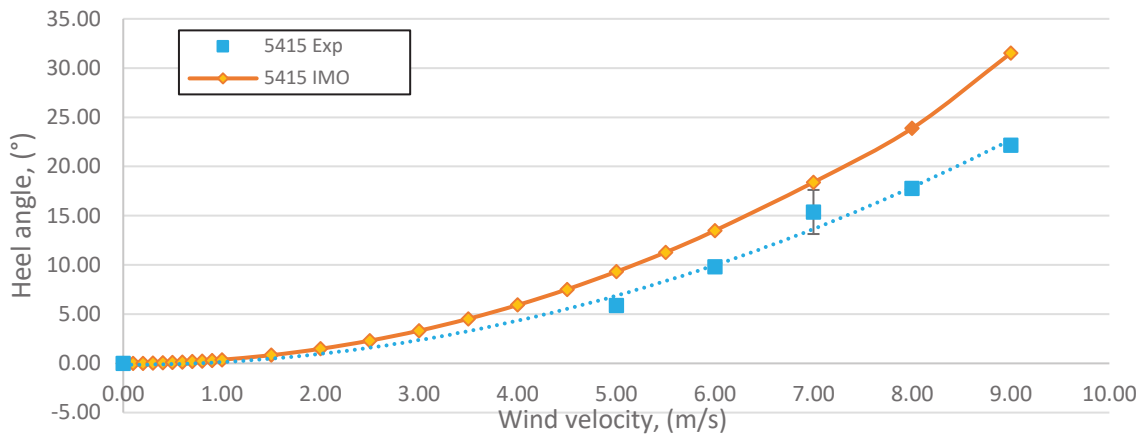


Figure 4.48 Angle of stable heel for the 5415 shape

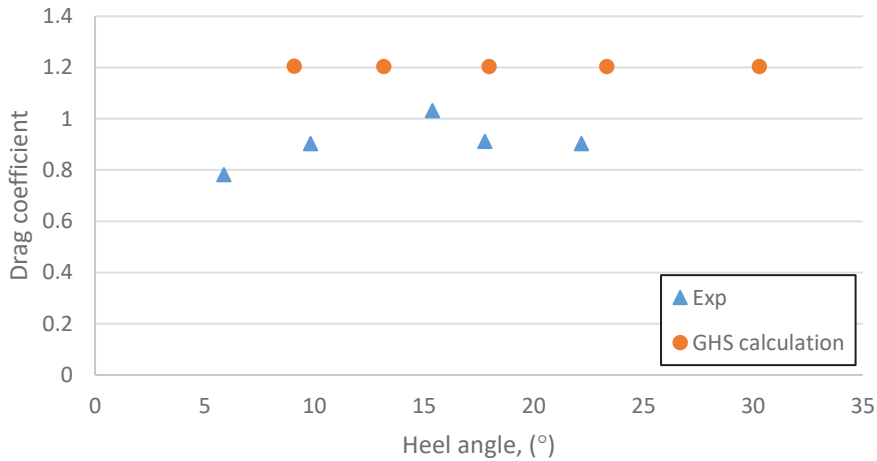


Figure 4.49 Drag coefficient vs heel angle obtained by calculation for the 5415 shape

## 4.11 Conclusion

Experimental work on the evaluation of the weather criterion in the wind tunnel test is possible. The wind tunnel is not designed to be water proof. Therefore, additional safety precautions are required to minimise the risk of water splash that may cause critical damage to equipment or tools underneath the test section. For the first rule concerning the weather criterion, which is an angle of stable heel, the experimental result for the ASL shape shows a higher value than GHS. For the 5415 shape, the experimental result shows a lower value than GHS. This phenomenon is explained by the drag coefficient of the tested shapes. For the second rule in the weather criterion, which is an area under the curve, both shapes show the

experimental results are less conservative than GHS. Therefore, this may allow more margin for ship designers during the design stage.

The angle of stable heel ( $\phi_0$ ) is based on 26 m/s wind velocity for the IMO Rules and 100 knots for the Naval Rules. The reassessment of wind velocity has been discussed and presented by (Bertaglia et al. 2003; Spyrou 2011; Hayes et al. 2015). A standardised set of wind velocities for stability analyses would mean that the use of wind speed would become more transparent. Matching the Reynolds number, is another challenge that could lead to future research. The selection of the angle of heel to windward due to wave action ( $\phi_2$ ) is also the main parameter that affects the weather criterion. The IMO and Naval Rules have different methods to evaluate the angle. In the SGISC, the wave scatter diagram is used to evaluate some of the failure modes for Level 2 with a probabilistic approach. This may significantly improve the selection of ( $\phi_1$ ). For the verification process, a fast time-domain simulation could be used to validate the experimental results and increase the level of confidence in the current weather criterion as provided by the IMO and Naval Rules (Peters et al. 2012).

## Chapter 5 –2-Dimensional Numerical Simulation and Results

This section presents the simulation process used in this research. The unsteady flow around the free rolling hull section is computed using the ISIS-CFD flow solver, developed by the EMN (Equipe Modélisation Numérique) from the Ecole Centrale de Nantes (ECN). ISIS solves the incompressible unsteady Reynolds-averaged Navier-Stokes equations (RANSE). Two models have been simulated with unsteady time configuration, multi-fluid and 2-dimensional simulations. The method of 2-dimensional simulation as a direct assessment approach for dead ship condition is presented. This approach explains the phenomenon obtained by the IMO rules and experimental work as explained in previous chapters.

### 5.1 Introduction

A commercial code named FINE<sup>TM</sup>/Marine is used for this research work. It is a NUMECA developed software Flow Integrated Environment for computations on unstructured hexahedral meshes dedicated to Marine applications. The resolution of Computational Fluid Dynamics (CFD) problems involves three main steps as shown in Figure 5.1.

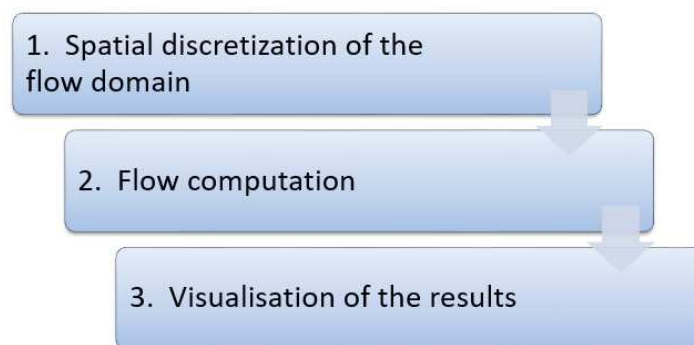


Figure 5.1 Three main steps in CFD

Three software codes were created to perform the simulations. The first software code (developed by NUMECA), HEXPRESS<sup>TM</sup>, is an automated all-hexahedral unstructured grid generation system. The second software code (developed by the CNRS and the Ecole Centrale de Nantes), the flow solver ISIS-CFD, is a 3D unstructured flow solver able to simulate Euler or Navier-Stokes (laminar or turbulent) flows (Deng et al. 1994). The third software code (developed by NUMECA), CFView<sup>TM</sup>, is a highly interactive Computational Field Visualization system (Numecca International 2013).

Two domains were created to simulate the roll behaviour of the two models' shapes. They are multi-fluid two-dimensional analyses with the scale model. These domains are shown in Figure 5.2 and Figure 5.3. The yellow line represents the boundary of water and air ( $y=0$ ). Both models are placed in each domain with the design draught.

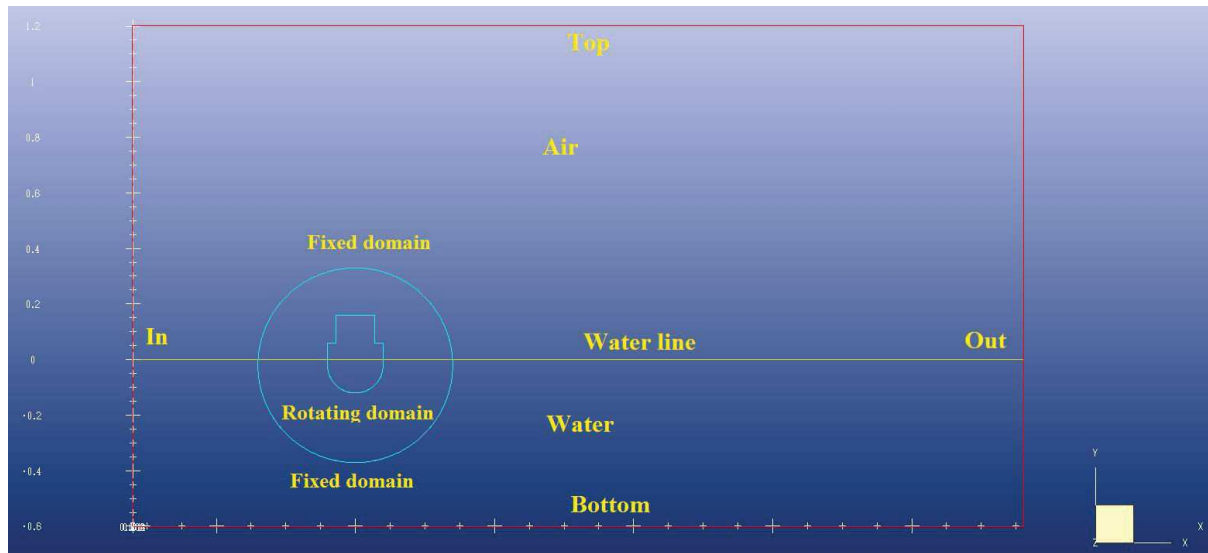


Figure 5.2 Domain for the ASL shape

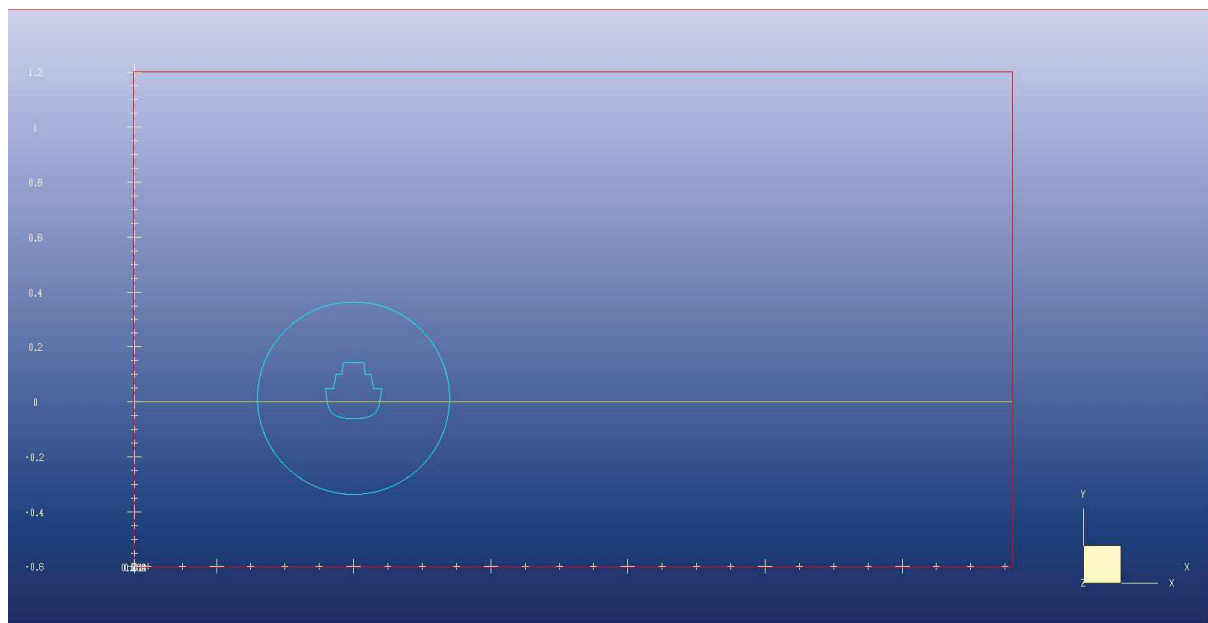


Figure 5.3 Domain for the 5415 shape

The simulation was performed in “unsteady state”. Unsteady state refers to the condition where the flow properties at a particular point in the system change over time. This configuration allows access to additional parameters for unsteady flow simulation. In reality, the flow around a ship is unsteady. The fluid properties used in incompressible fluid, means that the density is constant. “Static ship” means the simulation was executed with zero degrees

of freedom (d.o.f) and all axes were fixed. Both fixed domain and rotating domain are static. “Dynamic ship” means that the simulation was executed with 2 d.o.f. (roll and heave), where the model is allowed to roll around the z-axis. The fixed domain does not move and the rotating domain moves when the ship rolls, because of the wind force. To represent the boundary between water and air, the method of volume of fluid (v.o.f.) is used. This method is more flexible and efficient than other methods for treating complicated free boundary configuration because no remeshing is needed. In cells containing a free surface, the density of the fluid is a weighted average of the air and water densities. This is also the case for viscosity. Moreover, in cells containing a free surface, a different procedure is required because the pressure is assumed specified at the surface. In this case, the surface cell pressure,  $P_{i,j}$ , is computed as in (Eq 6.1) the value obtained from a linear interpolation (or extrapolation) between the desired pressure at the surface  $P_S$  and a pressure  $P_N$ , inside the fluid and  $\eta = d_c/d$  is the ratio of the distance between cell centres to the distance between the free surface and the centre of the neighbouring cell as shown in Figure 5.4 (Hirt and Nichols 1981).

$$P_{i,j} = (1-\eta) P_N + \eta P_S \quad (6.1)$$

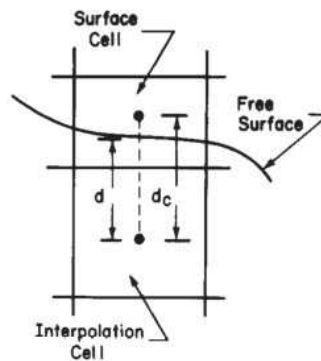


Figure 5.4 Sketch showing definition of quantities used in defining the free surface pressure boundary condition. Extracted from (Hirt and Nichols 1981)

## 5.2 Computational Setup

Numerical computations were performed for three cases (natural roll period, angle of stable heel and roll back angle). All cases used the same domain size. This was a closed domain which consisted of a fixed rectangular domain embedding a rotating circular subdomain containing the 2D ship model. The y-axis represents the water line level. In FINE<sup>TM</sup>/Marine, the parameters used for the computational process are customisable.

For physical configuration, the time configuration was unsteady flow. It is multi-fluid where fluid 1 is water with a dynamic viscosity of 0.00104362 Pa.s and density of 998.4 kg.m<sup>-3</sup>, and fluid 2 is air with a dynamic viscosity of 0.0000185 Pa.s and density of 1.2 kgm<sup>-3</sup>. Boundary conditions in FINE<sup>TM</sup>/Marine were classed as solid, external and mirror. The ship model in the rotating domain was solid with a wall function. The external boundary condition

was divided into four sides which were in, out, top and bottom. "Bottom", "top" and "out" patches used the prescribed pressure with an updated hydrostatic pressure. The "In" patch used the far field function. For the computation with wind effect, the wind profile was set at the "in" patch with the profile direction to the y-axis. The wind profile was set to have the same profile as the wind tunnel boundary layer as discussed in Section 4.7. It is important to simulate the same boundary layer thickness to obtain a good result in simulation. For the body motion, we just specified two dimensional analyses. Two degrees of freedom (d.o.f) were solved; translation in y-axis and rotation around z-axis. The translation in x-axis was fixed because the model was fixed by a longitudinal rod to avoid the model impacting the water tank (see Section 4.4). For the natural roll simulation, the initial angle was set to 0.3 rad (17.1887°) toward the wind source (windward). For an angle of stable heel simulation to determine  $\phi_0$ , the initial angle was set to 0. All parameters were the same for both models except those appearing in Table 5.1.

Table 5.1 Parameters used for the ASL shape and 5415 shape

Parameter	ASL shape	5415 shape
Flow model	k-omega (SST-Menter)	k-omega (SST-Menter)
Control variables		
Max no of non-linear iteration	8	8
Convergence criteria	2	2
Time step law	Uniform	Uniform
Time step value (natural roll)	0.015	0.005
Time step value (wind)	0.005	0.005
Inertial data		
Centre of gravity (Y_CG)	-0.02 m	0.01405 m
Mass	19.20285 kg/m	8.635kg/m
Inertia matrix	0.18 kg.m	0.0635 kg.m

### 5.3 Mesh Management

The mesh was generated using HEXPRESS<sup>TM</sup>. It is an automatic unstructured hexahedral mesh generator software code designed to automatically generate mesh around complex 2D and 3D geometries. Five steps were involved in the mesh generation: **1) Initial mesh**; which automatically creates an initial hexahedral mesh of the bounding box of the computational domain. An initial coarse mesh is generated by a subdivision of the domain with a minimum number of cells. **2) Adapt to geometry**; HEXPRESS<sup>TM</sup> successively modifies the mesh by cell anisotropic subdivision until the cell sizes match some particular geometry criteria. **3) Snap to geometry**; HEXPRESS<sup>TM</sup> projects the mesh on the geometry and recovers lower dimensional geometry features by some very specific corner and curve capturing. The robustness and accuracy of these algorithms are unique to HEXPRESS<sup>TM</sup>. **4) Optimise**; HEXPRESS<sup>TM</sup> optimises the mesh to ensure that all cells are convex and of high quality. The optimisation algorithms are unique to HEXPRESS<sup>TM</sup>. **5) Viscous layers**; HEXPRESS<sup>TM</sup>

inserts additional layers of high aspect ratio cells in the mesh by further isotropic cell subdivisions to generate a mesh suitable for resolving highly sheared flows. The number of cells obtained for the simulations are shown in Table 5.2.

Table 5.2 Number of cells used for this simulation

Shape	ASL shape	5415 shape
Total number of cells	16,488	15,396
Total number of vertices	34,356	32,118

An automatic grid refinement (AGR) procedure is available in FINE<sup>TM</sup>/Marine (Wackers et al. 2012). The advantage of AGR is the ability to predict the onset of all the vertical structures visible in detailed experiments without any significant influence of the turbulence closure. An AGR algorithm was implemented in FINE<sup>TM</sup>/Marine flow solver, which automatically refined the mesh during the computation. The adaptive refinement process consisted of a series of numerical solutions and error estimations, followed by appropriate improvements in the discretisation. All the results presented in this research are with the assistance of the AGR (Numeca International 2013). According to Fine Marine Manual (Numeca International 2013), the procedure for AGR works as follows:

- a. The refinement criterion is calculated, based on the current flow field. The criterion is represented by a scalar or a vector field (for directional refinement).
- b. In the second step, this criterion is transformed into the decision of which cells should be refined or coarsened. This decision may depend on the type or on the orientation of the cells, but it does not depend on the specific way the criterion is calculated and it is the same for all criteria.
- c. Finally, the coarsening and refinement of cells are performed where needed. Part of the refinement is the automatic load balancing; when computing in parallel, parts of the refined grid are moved from one processor to another, to keep the same total number of cells on each processor.

The mesh near the ship model was fine whereas it became much coarser as it approached the outer boundary, except near the free surface. The mesh in the boundary layer around the ship was particularly refined. The meshes used for these simulations are shown in Figure 5.5 for the ASL shape and in Figure 5.6 for the 5415 shape.



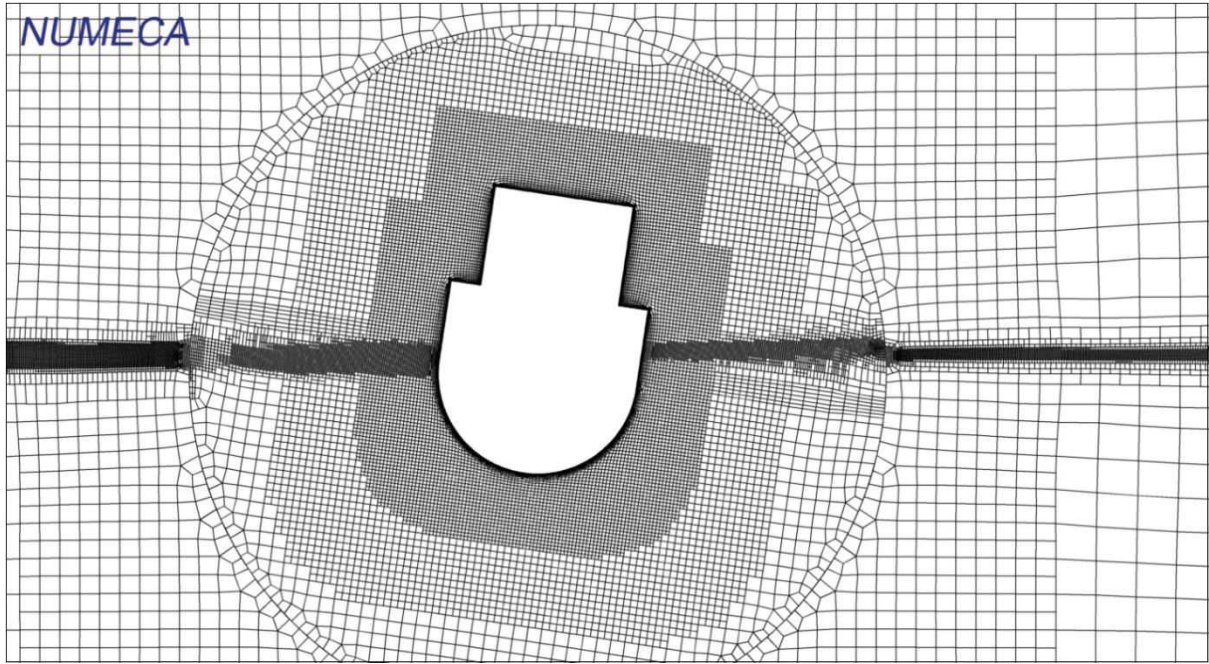


Figure 5.5 Cross-sectional grid (x-z plane) for the ASL shape domain

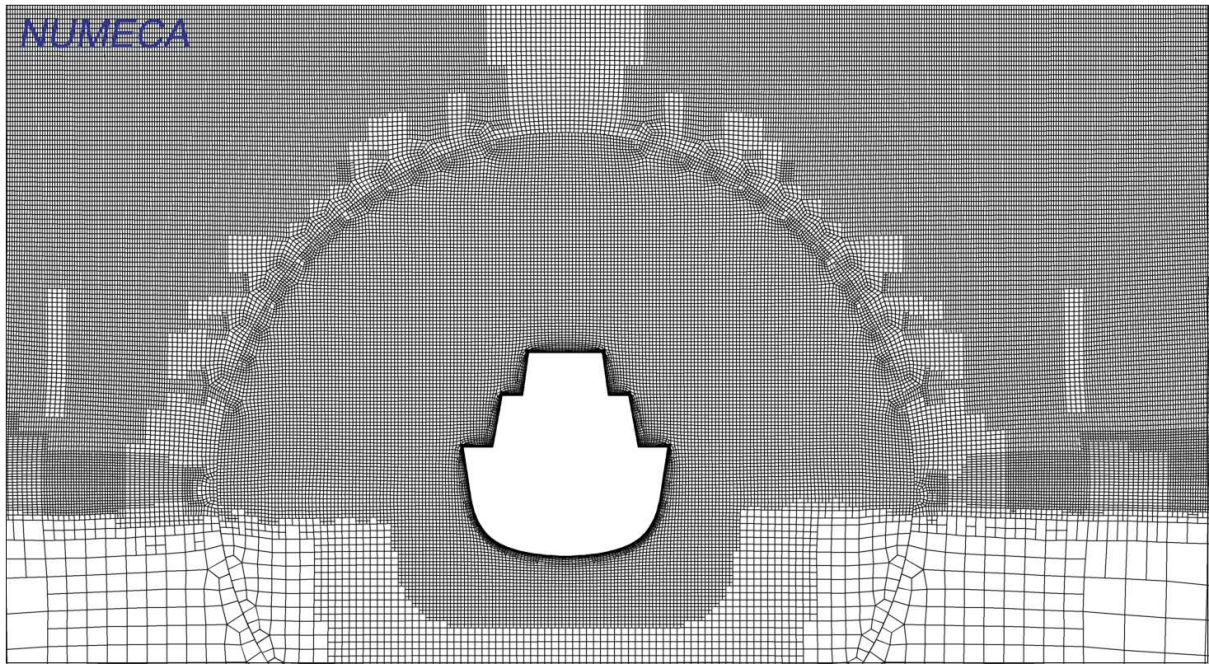


Figure 5.6 Cross-sectional grid (x-z plane) for the 5415 shape domain

#### 5.4 CFD: The ISIS-CFD Flow Solver

The solver ISIS-CFD, available as a part of the FINE<sup>TM</sup>/Marine computing suite, is an incompressible unsteady Reynolds-Averaged Navier-Stokes (URANS) solver mainly devoted to marine hydrodynamics. The discretisation is based on an entirely unstructured face-based finite volume method to build the spatial discretisation of the transport equations. Pressure-

velocity coupling is enforced through a Rhie & Chow SIMPLE type approach: at each time step, the velocity updates come from the momentum equations and the pressure is given by the mass conservation law, transformed into a pressure equation. The method features several sophisticated turbulence models; apart from the classical two-equation  $k-\varepsilon$  and  $k-\omega$  models, there is the isotropic two-equation Explicit Algebraic Stress Model (EASM), as well as the Reynolds Stress Transport Models, which are available with or without rotation corrections (Visonneau et al. 2015). With an increase in the complexity of the simulation tools, the computational effort also tends to escalate.

For this research  $k-\omega$  (SST-Menter) was used as a turbulence model. The  $k-\omega$  (SST-Menter) (SST for shear-stress transport) model, combines several desirable elements of existing two-equation models. The two major features of this model are a zonal blending of model coefficients and a limitation on the growth of the eddy viscosity in rapidly strained flows. The shear stress transport modelling also modifies the eddy viscosity by forcing the turbulent shear stress to be bounded by a constant times the turbulent kinetic energy inside boundary layers (a realisability constraint). This modification improves the prediction of flows with strong adverse pressure gradients and separation. This turbulence model is widely used in marine research (A. D. Wnęk et al. 2010; Jaouen et al. 2011; Luquet et al. 2014; Fureby et al. 2016; Billard et al. 2005).

## **5.5 Result and Discussion**

### **5.5.1 GZ Curve (2-dimensional)**

Between 2-dimensional (2D) and 3-dimensional (3D) simulations the computer power required is very significantly different. To adapt the computer power requirement to our computer resources, only 2D ship simulations were performed. The ship intact stability 2008 code for Part 2.2 and 2.3 was solely dependent on the shape of its  $GZ$  curve. A comparison of the  $GZ$  curves for 2D and 3D is presented in Figure 5.7. The 2D geometry is an extruded shape of the midship cross section. In many cases, 2D simulations are enough to study and to explain flow phenomena. We anticipate that 2D simulations in our case will lead to more conservative results which of course serve our purpose. We note that the 2D and 3D curves of the ASL shape are almost identical and that is because the underwater hull section of the 3D shape is almost constant along the ship. The 2D  $GZ$  curve of the 5415 shape is higher than the 3D  $GZ$  curve. This is the result of the midship section that was used for the hydrostatic computation. The water plane area of the 2D shape was therefore larger. The properties for the ASL shape and the 5415 shape for 2D and 3D are shown in Table 5.3.

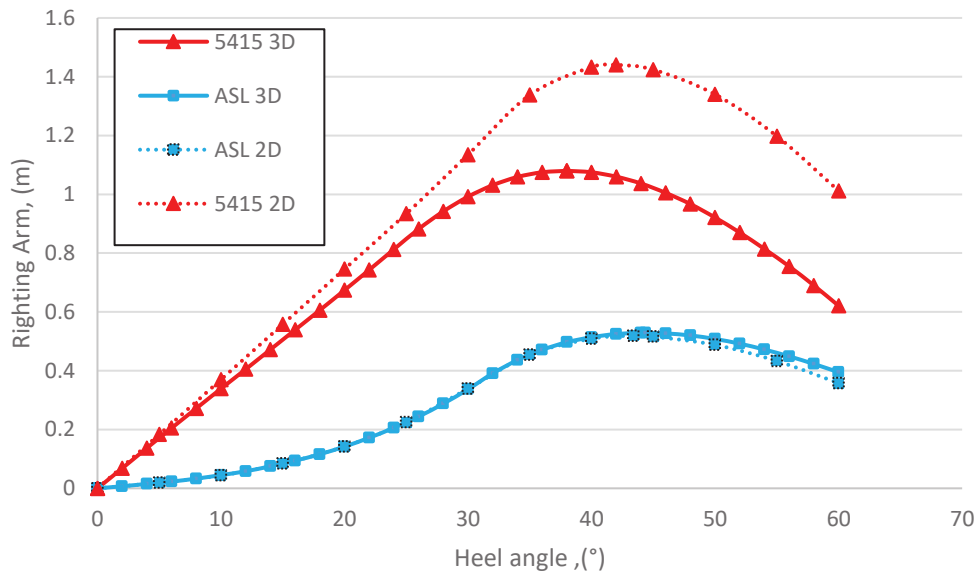


Figure 5.7 GZ curve for the ASL and 5415 shape in 2D and 3D geometry

Table 5.3 Properties for 2D and 3D of the ASL and 5415 shape

Geometry	ASL shape		5415 shape	
	3D	2D	3D	2D
Displacement, (tonnes)	26,994	28,277	8,624	12,261
Moment Inertia				
$I_L$ (m <sup>4</sup> )	$4.171 \times 10^6$	$4.573 \times 10^6$	$2.521 \times 10^6$	$5.326 \times 10^6$
$I_T$ (m <sup>4</sup> )	$8.766 \times 10^4$	$9.332 \times 10^4$	$4.927 \times 10^4$	$7.132 \times 10^4$
Length/breadth	7.00	7.00	7.45	8.64
Length/draught	11.67	11.67	15.57	24.93
Breadth/draught	1.667	1.667	2.090	2.885
Waterplane area (m <sup>2</sup> )	2,712	2,800	2,100	2,719

## 5.5.2 Natural Roll Period

Natural roll period simulations were performed to evaluate the ability of the 2D simulations. Natural roll period is an important parameter to be verified before the simulation process continues to the next stage. The natural roll period result comparison is shown in Table 5.4. The simulation results obtained were reliable and fully satisfactory.



Table 5.4 Natural roll period results comparison, (in seconds)

Ship	ASL shape	5415 shape
Formula:		
IMO	3.620	1.121
WEISS	3.537	1.184
Benford	3.349	1.121
Simulation	3.375	1.175
Experiment	3.482	1.110

### 5.5.3 Drag Coefficient for Static Ship Simulation

We saw that the  $C_D$  is of particular importance in determining  $\phi_0$ . In the experiment, it could not be measured and the IMO  $C_D$  remained constant with a value of 1.2. By integration of the pressure forces in the x-direction, the CFD solver was able to give the drag force and therefore the drag coefficient. Figure 5.8 shows the  $C_D$  for the ASL and 5415 shape for the static ship condition. As expected, the ASL shape obtained higher  $C_D$  than the 5415 shape due to the ship superstructure arrangement. The ASL shape had two cuboid shapes, which represented a bridge and container arrangement while the 5415 shape had a trapezoidal shape representing a frigate bridge, funnel and hangar. Figure 5.9 shows the  $C_D$  for 2D and 3D obtained by experiment (Hoerner 1965). For the same shape, the 3D object produced lower  $C_D$  than the 2D test. This simulation was executed in 2D and the experiment was in 3D. Therefore, it is expected that the  $C_D$  results obtained by simulation (2-dimensional) are higher than  $C_D$  results obtained in the experiment.

We note that for the 5415 shape, the  $C_D$  was as expected higher than the experiment and roughly equal to the IMO. The ASL shape case was less clear. We did not obtain the same strange behaviour that we had in the experiment (see Figure 4.47). The  $C_D$  was higher than the 5415 shape as expected. The results in Figure 5.8 are an average over time. In fact, the  $C_D$  fluctuated over time as shown in Figure 5.10 which presents the  $C_D$  over time for a heel angle leeward  $15^\circ$  of the static condition. The  $C_D$  obtained by simulation at the static angle fluctuated chaotically even though the heel angle was fixed. The  $C_D$  was the result of the pressure integration on the ship surface in the x-direction. The complex flow around the ASL shape is shown in Figure 5.11. Two big vortices appear above the bridge area on the leeward side. The vortices position depended on time. Therefore, the force acting on the superstructure surface was not stable even in the static heel angle simulation. This shows the complexity of the force measurement. For further investigation, a simulation with a dynamic ship was performed and is explained in next section.

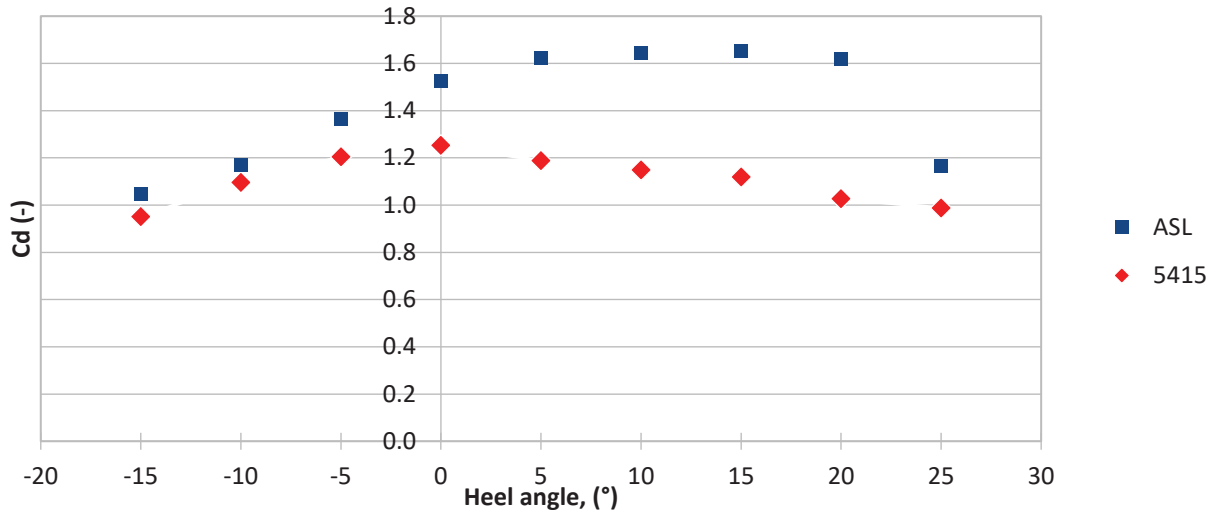


Figure 5.8 Simulation of drag coefficient results (static condition)

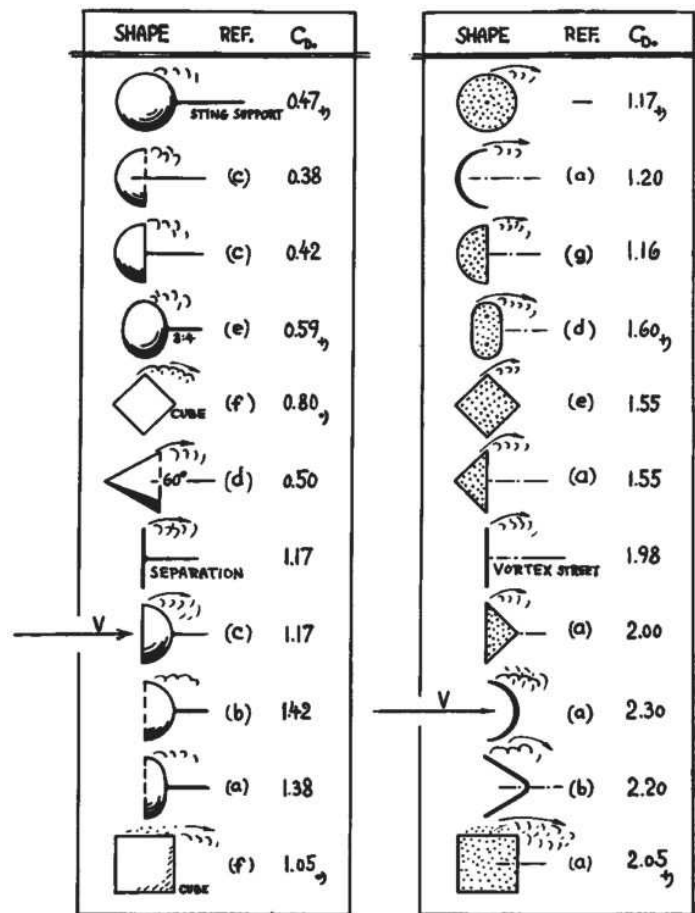


Figure 5.9 Drag coefficient of various bodies 3-dimensional (left) and 2-dimensional (right) at Reynolds number between  $10^4$  and  $10^6$ . Extracted from (Hoerner 1965)

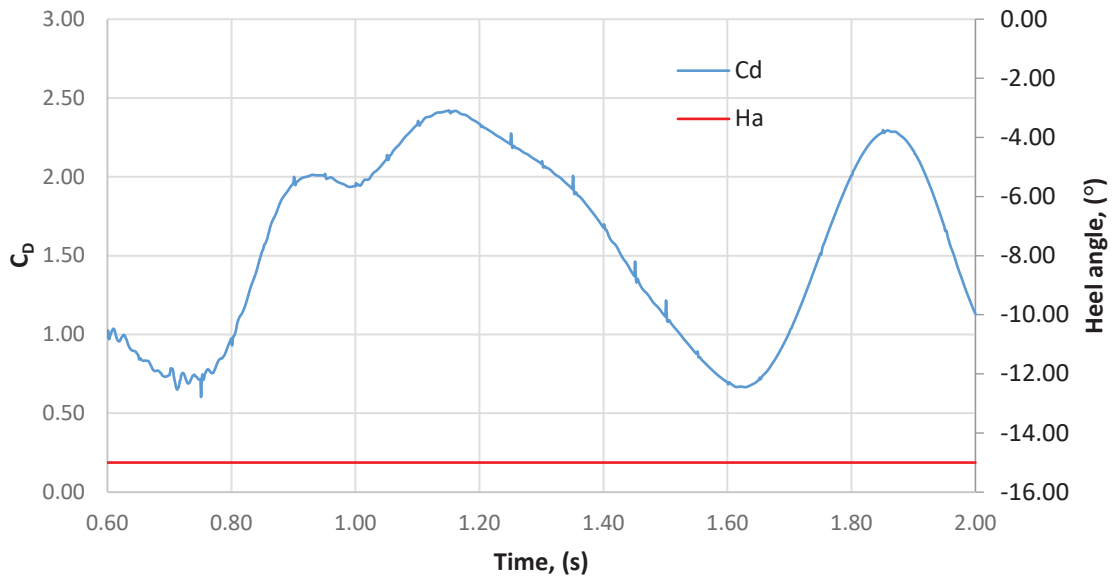


Figure 5.10  $C_D$  for ASL ship at 15 degrees leeward (static condition)

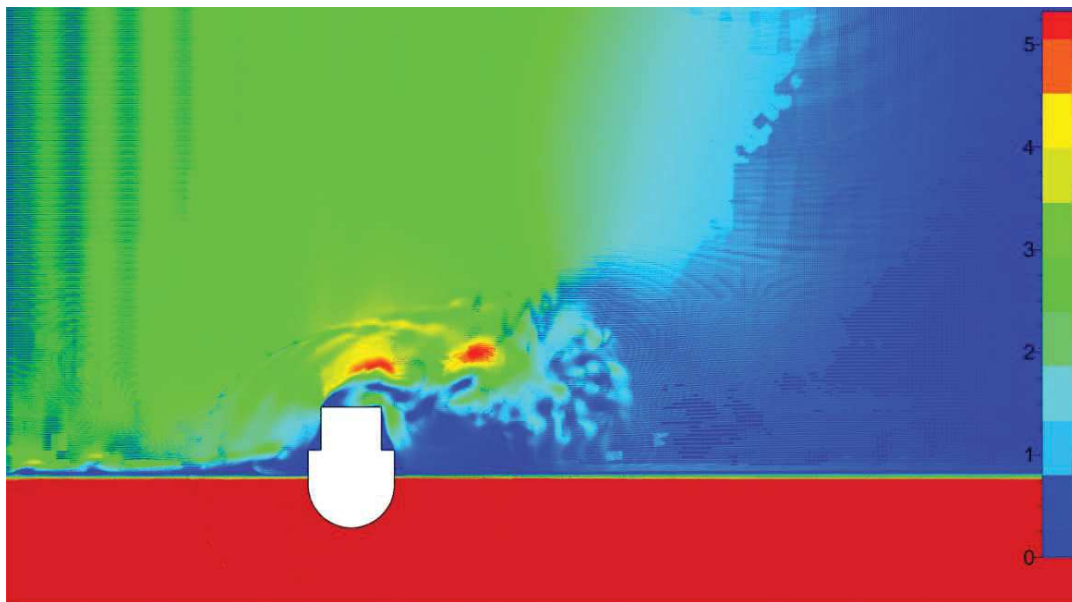


Figure 5.11 The flow view when model is upright (Velocity magnitude of x-direction)

### 5.5.4 Drag Coefficient for Dynamic Ship Simulation

Figure 5.12 shows the  $C_D$  for the ASL shape in a dynamic ship condition with wind velocity of  $2.6 \text{ ms}^{-1}$ . The  $C_D$  curve oscillates chaotically. The oscillation is the result of the dynamic ship simulation where the model was free to roll. The simulation computed the

righting moment of hydrostatic and wind heeling moment to determine the stable position. Therefore, the equilibrium position was relatively impossible to obtain in the dynamic simulation. The same situation was observed during experimental work where the model kept rolling with a small magnitude (approx. 2 degrees) although the wind velocity was fixed. The observed unsteady was therefore also detected by the simulation. To the author's best knowledge, there are no facilities in a wind tunnel to measure and determine force and drag coefficients in dynamic experiments. This is due to the complexity of the physics and reality. Therefore, a  $C_D$  calculation is performed using the angle of stable heel from simulation results. Table 5.5 shows the  $C_D$  of the 5415 shape in a dynamic ship. The  $C_D$  obtained by simulation was far lower than experiments and the IMO. It indicates the complexity and unsteady of the simulation and therefore, that improvement of the simulation code to address the instability of dynamic ships is required. The results presented in Figure 5.12 and in Table 5.5 show that attempting to compute the  $C_D$  in dynamic modes may not be pertinent.

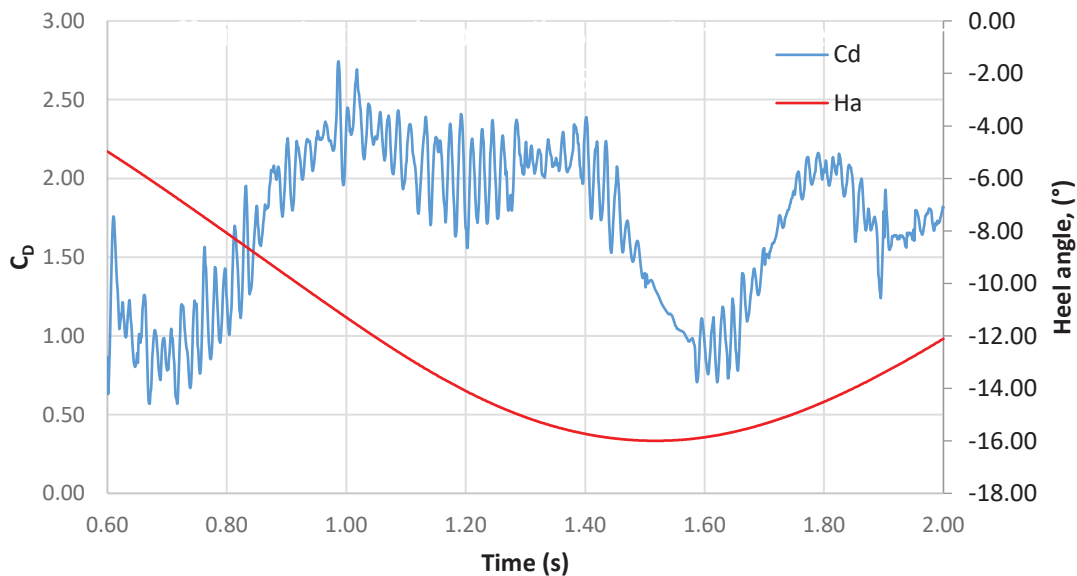


Figure 5.12  $C_D$  for the ASL shape at 15 degree leeward (dynamic condition)

Table 5.5  $C_D$  for the 5415 shape (dynamic condition)

Phi0	1.708	5.291	7.185	°
Wind heeling lever, $l_{W1}$	$6.25246 \times 10^{-4}$	$19.4 \times 10^{-4}$	$26.5 \times 10^{-4}$	m
Wind velocity, $U$	2.600	5.000	6.000	$\text{ms}^{-1}$
Centre of aerodynamics to half draft height, $z$	0.102	0.102	0.102	m
Density, $\rho$	1.200	1.2000	1.2000	$\text{kgm}^{-3}$
Windage area, $A$	0.1461	0.1461	0.1461	$\text{m}^2$
Wind pressure, $P$	4.056	15.0	21.6	Pa
Displacement, $\Delta$	0.0056	0.0056	0.0056	t
$C_D$	0.570	0.477	0.453	-

### 5.5.5 Results Comparison of Roll Back Angle

Figure 5.13 shows the results comparison for the roll back angle ( $\phi_{2*}$ ) versus roll to windward ( $\phi_1$ ) for the ASL shape. As expected, the simulation obtained lower values than the IMO and higher than the experiment. The simulation results are closer to the IMO results. The same behaviour also appeared for the 5415 shape as shown in Figure 5.14. For the ASL shape, the simulation results deviated slightly from the IMO results but for the 5415 shape, the simulation results were closer to the IMO results. Both figures express the ability of the 2-dimensional simulation to be utilised for weather criterion verification. These results show the reliability of 2-dimensional simulation to predict the weather criterion even though there are minor deviations in results obtained by simulations, IMO calculations and experiments. 3-dimensional simulations require high computer power to perform complex calculations. In addition, the computation time also increases tremendously. Therefore, 3-dimensional simulation is unnecessary.

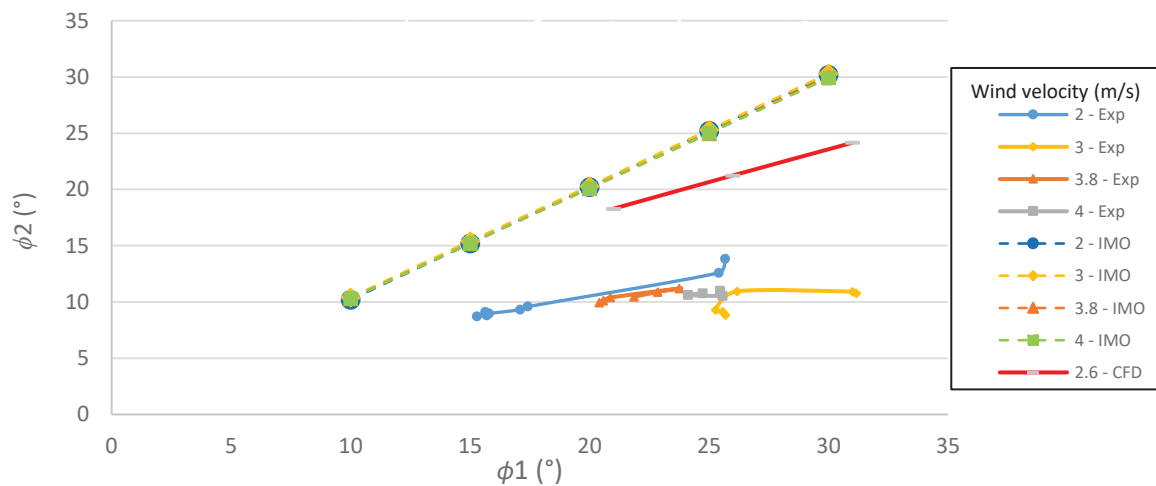


Figure 5.13 Results comparison for roll back angle ( $\phi_{2*}$ ) vs roll to windward ( $\phi_1$ ) for the ASL shape



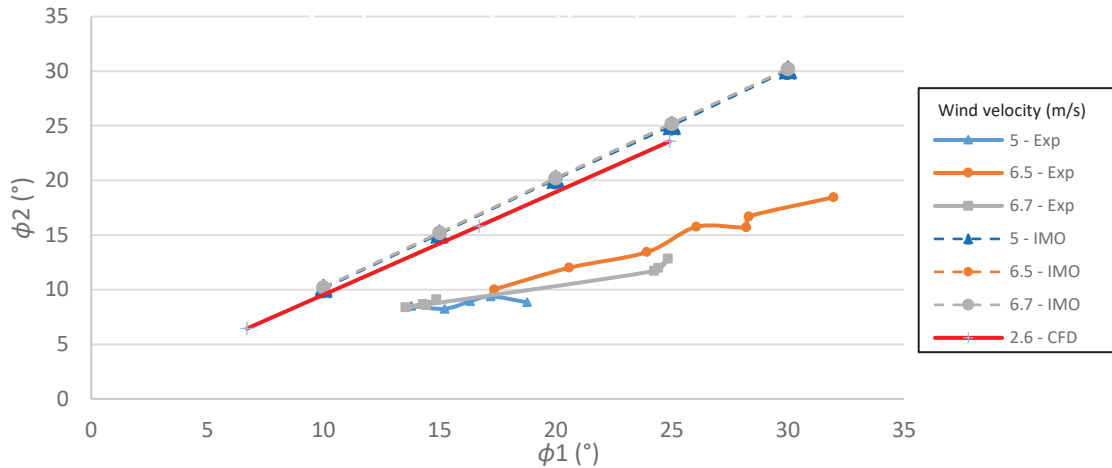


Figure 5.14 Results comparison for roll back angle ( $\phi_2^*$ ) vs roll to windward ( $\phi_1$ ) for the 5415 shape

### 5.5.6 The Weather Criterion

The weather criterion was investigated through three methods; IMO regulations adopting the GHS code, the wind tunnel experiment and simulation in FINE<sup>TM</sup>/Marine. For the ASL shape, the results are presented in Table 5.6. Wind velocity of  $26\text{ms}^{-1}$  was chosen in order to satisfy the IMO IS Code 2008. The angle of stable heel,  $\phi_0$  obtained by simulation ( $26.3^\circ$ ) was the highest, followed by the experiment ( $17.98^\circ$ ) and IMO ( $12.63^\circ$ ). This phenomenon is explained by the impact of drag coefficient. The drag coefficient for the square shape in 2D was 2.05 and 3D was 1.05 as shown in Figure 5.9. The wind drag coefficient contributed a significant influence to the wind force. Therefore, the angle of stable heel for simulation was greater than the experiment because the drag coefficient for 3D (experiment) was lower than the 2D (simulation). In IMO, the drag coefficient was 1.13 (Bertaglia et al. 2003) regardless of the heel angle. The ASL shape was a box shape and contributed a higher drag coefficient than the IMO expectation.

The  $\phi_2$  is a limiting angle to the lee-side. Expressed as an energy balance, the work done by the wind excitation as the ship rolls from the wind-side to the lee-side should not exceed the potential energy at the limiting angle,  $\phi_2$ .  $\phi_1$  was calculated using the IMO formula. As expected, the IMO obtained the highest value of  $\phi_2$ , which was  $29.64^\circ$  followed by simulation\_A ( $27.29^\circ$ ), experiment ( $25.19^\circ$ ) and simulation\_B ( $31.65^\circ$ ). The  $\phi_1$  is an angle calculated from the angle of stable heel (lever of  $l_{W1}$ ) toward windward. Simulation\_A used an  $l_{W1}$  obtained by the experiment and simulation B used an  $l_{W1}$  obtained by simulation.

Concerning roll amplitude, the highest roll amplitude was obtained from IMO, followed by simulation\_A, the experiment and simulation\_B. The IMO was always conservative. The simulation and experiment had good comparative results.

Table 5.6 Weather criterion comparison results for the ASL shape

Result	$\phi_0$	Wind heeling lever	Start angle	$\phi_2$	Roll amplitude ( $\phi_2$ - start angle)
IMO	12.63°	$l_{W1}$	-3.56°	29.64°	33.198°
Experiment	17.98°	$l_{W1}$	1.79°	25.19°	23.4°
Simulation _A	17.98°	$l_{W1}$ (Exp)	1.79°	27.29°	25.5°
Simulation _B	26.3°	$l_{W1}$ (Simulation)	10.11°	31.65°	21.54°

Note:  $\phi_1$  (IMO formula) = 16.19°

For the 5415 shape, the results are presented in Table 5.7. A wind velocity of 100 knots ( $51.44\text{ms}^{-1}$ ) was chosen in order to satisfy most Naval Rules. The  $\phi_0$  value obtained by simulation ( $11.75^\circ$ ) was the highest, followed by the experiment ( $7.29^\circ$ ) and IMO values ( $9.88^\circ$ ). As expected, simulation provided the highest value, followed by Naval Rules and experimental values. This phenomenon is explained by the impact of drag coefficient which also transpired for the ASL shape. The experimental value was lower than the IMO value because the experimental result was based on the 3D condition and Naval Rules value was based on the constant drag coefficient. The simulation value was higher than Naval Rules due to the assumption that  $C_D$  for Naval Rules is lower than 2D simulation. A group of researchers (Ishida, Taguchi, and Sawada 2006) from Japan conducted an experiment to investigate the drag, lift and heeling moment coefficient for a Ro-Pax ferry with several angles. Their results are shown in Figure 5.15. The graph illustrates the deviation of drag coefficient concerning various heel angles despite the Naval Rules, considering identical drag coefficient at all heel angles (Luquet et al. 2015).

For Naval Rules,  $\phi_1$  is fixed at  $25^\circ$  despite any hull shape of a naval ship. The  $\phi_2$  is an angle where  $A_2 \geq 1.4A_1$ . To make a fair comparison,  $\phi_{2a}$  is proposed. The  $\phi_{2a}$  is an angle where  $A_2 = A_1$ . As expected, the Naval Rules obtained the highest value of  $\phi_{2a}$ , which is  $35.2^\circ$ , followed by simulation \_A ( $19.24^\circ$ ) and the experiment ( $15.29^\circ$ ).

In the perspective of roll amplitude, the highest roll amplitude was obtained from Naval Rules, followed by experiment and simulation. The Naval Rules were always conservative. Simulation and experiment had good results in comparison.

Table 5.7 Weather criterion comparison results for the 5415 shape

Result	$\phi_0$	Start angle	$\phi_{2a}$ ( $A_2=A_1$ )	$\phi_2$ ( $A_2=1.4 A_1$ )	Roll amplitude ( $\phi_2$ -start angle)
Naval Rules	9.88°	-15.12°	35.2°	40.8°	50.32°
Experiment	7.29°	-17.71°	15.29°	-	33.00°
Simulation	11.75°	-13.25°	19.24°	-	32.49°

Note:  $\phi_1$  (Naval rules) =  $25^\circ$

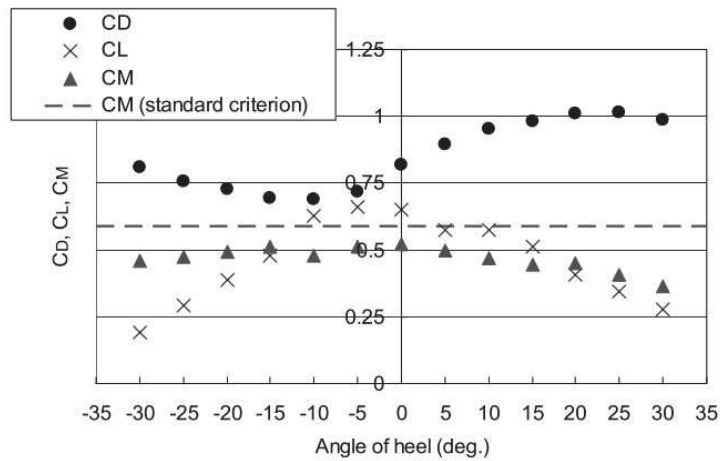


Figure 5.15 Experimental value of  $C_D$ ,  $C_L$  and  $C_M$  from wind tunnel test. Extracted from (Ishida, Taguchi, and Sawada 2006).

### 5.5.7 Scrutiny of the Weather Criterion by IMO Naval, Naval Rules, Experiment and 2 Dimensional Simulation

The weather environment of a ship operates in a random field. In fact, uncertainty covers other operational parameters. The IMO and Naval Rules implement a general assessment for the weather criterion with a significant safety margin. Utilising numerical simulations to predict extreme events is often a popular choice to directly address the problem. However, there are some issues related to the statistical treatment of the results.

Table 5.8 shows the elements that have a significant impact on the results obtained by these three methods. Drag coefficient, damping and aerodynamic fluctuation all add up to a significant impact on the weather criterion. For the dead-ship condition of second generation intact stability criteria, direct assessment will introduce the evaluation process by experiment or simulation validation. IMO delegations have been preparing the proposal for direct assessment of the dead ship condition. Simulation is a very complicated and time-consuming process. It requires computer power, and suitable solvers to compute the mathematical model and high mesh quality. 3-dimensional simulation needs much longer calculation time than 2-dimensional simulation. Validation and verification are other challenging stages before finalising the direct assessment. Therefore, this thesis proposes a certain and simple method to validate the weather criterion through an experimental trial with wind tunnel tests and 2-dimensional simulations. The IMO and Naval Rules require a high safety margin and 2-dimensional simulation has shown itself to be slightly more conservative than experimental results. To the author's best knowledge, the method proposed in this thesis fulfils the current weather criteria evaluation and is able to express the response of scale model ships.

Table 5.8 Elements which contribute to the weather criterion

Elements	IMO and Naval Rules	Experiment	Simulation 2D	Conservativeness
Drag coefficient	-+	=	+	Yes
Damping	-	=	+	Not necessary
Fluctuating aerodynamic force	-	=	=	Not necessary

Notes: + is conservative, - is less conservative and = is close to reality

## 5.6 Conclusion

Our results consistently showed the weather criterion for both the ASL and the 5415 shapes. The IMO is the most conservative result, followed by simulation and then the experimental result. The conservativeness sequence obtained by this research work is the same principle as that used in the development of second generation intact stability criteria.

Therefore, a 2-dimensional simulation approach is reliable in order to obtain the weather criterion result and a possible tool for the direct assessment of the dead ship condition failure mode. Validation remains an important problem for all tools that might be used in a dead ship condition failure mode. It could be interesting to repeat the experimental procedure with 2D shapes, i.e. the extruded mid-ship section along the whole length of the ship.

# Chapter 6 – Conclusion

## 6.1 Conclusion

The objectives of the thesis have been achieved. It was possible to implement the stability criteria of the intact second-generation in the GHS© code of stability, a code commonly used by professionals. Five vessels were considered to verify this implementation. The next step was to introduce a direct verification of the weather criterion. We developed and used an experimental wind tunnel method as well as a simplified CFD calculation method. In both cases, the results show that the maximum roll angle reached by the two vessels in this study is lower than that given by the regulatory calculation. The experimental method is certainly closer to reality and the 2-dimensional CFD remains conservative without being as binding as the regulations.

## 6.2 Concluding Remarks

The response of a ship with intact stability rules and the weather criterion has been examined in several series of hydrostatic computation, Reynolds-averaged Navier–Stokes (RANS) equations and wind tunnel experiments performed at the wind tunnel facility in the Aeronautics Laboratory, Universiti Teknologi Malaysia. This research has been extended to the evaluation of the Second Generation Intact Stability Criteria (SGISC) which are under development at the International Maritime Organisation and will be implemented soon. The results of this research work have contributed to the understanding of ship response in simulations and experimental trials.

The principal conclusions of this research study are:

- a. Level 1 and some Level 2 rules in the Second Generation Intact Stability Criteria can be evaluated using an existing hydrostatic solver with an additional command using macro functions.
- b. The maximum wind heeling moment is not always in the beam wind direction.
- c. The direct assessment (DA) for the dead ship condition for the SGISC could use the existing rules such as the weather criterion for verification.

- d. Levels 1 and 2 are purely based on hydrostatic information and statistical approach. Therefore, Level 3 should come up with the simulation and experimental method to analyse hydrodynamic behaviour. For Operational Guidelines, it should address real situations such as the response of the actual data of ship motion available on board.

One of the main issues of the research work was the determination of the drag coefficient. The IMO assumes that the drag coefficient of the ship structure facing a beam takes the value of 1.2, and this whatever its geometry. It is not possible to directly measure the drag force in the experiment, but it could be deduced from the angle of stable heel since the righting arm is known. We also noted that the stable heel angle is in fact oscillating which made us suspect that the drag coefficient changes over time. The CFD confirmed these instabilities. The average drag coefficient is as expected but the fluctuations are important even if the ship is static, and in the case of the dynamics, the amplitude of the oscillation is of the same order, but the behaviour is much more chaotic. Nevertheless, the 2D CFD method we proposed as a direct assessment of the weather criterion is still valid. One may argue that its results are close to the IMO results but since 3D CFD is out of range, it remains the best CFD solution. Moreover, if the possibility exists, it is advised to perform the experimental approach.

### **6.3 Suggestions for Future Works**

For future research study, drag coefficient analysis could be one of the interesting subjects to be performed. An experimental analysis could also be conducted using these models (ASL and 5415 shapes) in the wind tunnel without the water tank to measure the drag force at the static condition with a variable angle of heel. However, as we saw in Chapter 5, because of the unsteadiness of the flow around the ship superstructures, the drag coefficient is unsteady anyway.

On the other hand, a 2D model of both ASL and 5415 shapes could also be conducted in the wind tunnel with the current experimental approach. The 2D model means the midship areas of these models are extruded along the ship's length. Both results are worth verifying with the current results for more clarification on the dead ship condition failure mode.

In view of CFD, the 3D simulation is still out of range, unless massive computer resources are available. To explore further the 3D simulation, a comparison should be made of the cost of running the experiment and the procurement of a powerful computer. In contrast, the 2D simulation could be performed using different CFD solvers. The results obtained could be compared with the current results for further explanation of the simulation accuracy.

Direct assessments for the other four failure modes are still under development. Experimental trials in a towing tank with a wave generator could be the best option. Furthermore, the most challenging part is to simulate the induced roll on the ship model.

Several methods could be explored such as the use of a dynamic load inside the model, utilisation of magnetic field to control the moving load or externally forcing the ship model at specific times and points.

In general, the 3D CFD is not advisable for seakeeping. Therefore, the direct assessment of the four other failure modes cannot be done using this tool. Unlike the weather criterion, there is no way to have recourse to a simplified 2D setup since it concerns a coupling between pitch and roll. Potential flow codes are a far better option. Frequency domain potential flow codes do not include these features, but it is possible to develop a time domain post-processor that includes ways to assess risks of pure loss of stability or parametric roll. Many developments are performed using this and similar approaches. The International Ship Stability Workshop which is organized every year is probably the best source of documentation for anyone who wishes to follow the progress made in this domain.

## Resume Etendu

La stabilité du navire est la pierre angulaire de l'architecture navale. La pression hydrostatique est à l'origine de la poussée d'Archimède qui permet aux navires de flotter. Pour être stable à l'état initial il ne suffit pas que le centre de gravité ( $G$ ) soit positionné à la verticale du centre de carène ( $B$ ), il faut aussi que le métacentre ( $M$ ) défini pour la première fois par Pierre Bouguer, soit au-dessus du centre de gravité ( $GM > 0$ ). Mais cette stabilité initiale n'est pas suffisante pour résister au vent et à la houle. Créées pour la plupart au dix-neuvième siècle les sociétés de classification comme le Bureau Veritas fondé en 1828 ont commencé à classer les navires en fonction de leur fiabilité et ceci à la demande des compagnies d'assurance. Les premières règles étatiques apparaissent dans la dernière décennie du dix-neuvième siècle et l'Organisation Maritime International (OMI) est fondée en 1948. Son premier rôle est d'assurer la sécurité maritime. Cette tâche se subdivise en un certain nombre de chapitres dont le premier est la stabilité du navire à l'état intact. Le code en vigueur a été adopté en 2008. Il impose une valeur minimum du  $GM$  à l'état initial ainsi que cinq autres contraintes pour la courbe de moment de rappel en fonction de l'angle de gîte. Le code impose également un critère de résistance au vent et à la houle de travers. Ce dernier critère que l'on appelle le critère météorologique, doit assurer la survie du navire sans motorisation et affrontant une mer forte. Parallèlement à ces critères qui concernent les navires civils, les marines militaires imposent également un code généralement plus sévère.

Cette réglementation internationale a certes permis de fortement limiter les accidents liés à une stabilité à l'état intact insuffisante mais on déplore toujours des accidents alors que les navires qui en étaient victimes satisfaisaient à toutes les exigences de la réglementation en vigueur. Peu de victimes humaines ont été recensées suite à ces accidents pourtant médiatiques, spectaculaires et surtout coûteux. Les phénomènes à l'origine de ces accidents ont été identifiés. Il a été recensé cinq phénomènes :

- a. Perte de stabilité en gîte lorsque le navire est par mer d'arrière ou trois-quarts arrière
- b. Roulis paramétrique par mer de face ou mer d'arrière
- c. Le navire part au surf par mer d'arrière



- d. Navire sans motorisation par mer et vent de travers
- e. Accélération excessive du mouvement de roulis

Pour prévenir ces types d'accidents, l'OMI travaille à la mise en place d'un nouveau code de réglementation du navire à l'état intact communément appelé le code de seconde génération et on parle donc des critères de stabilité du navire à l'état intact de seconde génération. L'avant dernier phénomène est normalement pris en compte dans le critère météorologique du code actuel. Le dernier phénomène est encore à l'étude. Quant aux trois autres, il existe maintenant des critères qui peuvent encore être modifiés mais il est question de faire entrer la nouvelle réglementation en vigueur dès 2019. Personne ne semble croire sérieusement que cette échéance sera respectée mais il est certain que le nouveau code sera appliqué dans un très petit nombre d'années. La mise en place de la réglementation probabiliste pour la stabilité du navire après avarie en 2009 a pris ainsi beaucoup de professionnels du domaine au dépourvu et il en sera certainement de même avec celle-ci.

Il a donc été décidé que l'importance de cette future réglementation de la stabilité du navire à l'état intact méritait que l'on s'y intéresse notamment par le biais d'une étude longue comme celle-ci. Dans un premier temps, il a fallu comprendre les termes de cette nouvelle réglementation qui est beaucoup plus compliquée que la précédente. Il a fallu également comprendre en quoi ces nouveaux critères permettront de prévenir les accidents identifiés comme étant liés aux cinq modes de défaillance adressés par les critères de stabilité à l'état intact de seconde génération. Ces cinq modes de défaillance sont tous liés à l'hydrodynamique et non à la seule hydrostatique.

Tel qu'il est énoncé dans la réglementation en vigueur, alors qu'il est fortement lié à des phénomènes hydrodynamiques et aérodynamiques, le critère météorologique ne requiert qu'un calcul hydrostatique pour être vérifié. Par vent de travers le navire démuné de sa motorisation dérive et prend de la gîte. L'angle de gîte est calculé en équilibrant le moment inclinant et le moment de rappel hydrostatique. Le moment inclinant est dû à l'action du vent sur les superstructures et à la force hydrodynamique de réaction exercée sur la carène. Autour de cet angle d'équilibre on vient appliquer un mouvement de roulis réglementaire calculé à partir des données géométriques du navire et de son *GM*. On applique ensuite une rafale brutale de vent au moment où le navire démarre sa demi-période de roulis dans le sens du vent. Le critère s'applique sur l'angle de roulis maximum que le navire va atteindre. Pour calculer cet angle on applique le théorème de l'énergie cinétique qui permet la comparaison directe de l'aire sous la courbe du moment inclinant et de l'aire sous la courbe de rappel hydrostatique. Le principe de ce calcul réglementaire est d'être conservatif et d'être vérifié sans avoir recours à un complexe calcul hydrodynamique ou à des essais sur maquette très difficiles à mettre en œuvre.

Les quatre autres modes de défaillance sont également la combinaison de phénomènes cinématiques et hydrodynamiques très complexes à reproduire par un calcul direct ou par des essais. Comme pour le critère météorologique, les membres de l'OMI ont défini des méthodes de calcul ne faisant intervenir que le calcul hydrostatique. Si l'on prend par exemple la perte de stabilité en gîte lorsque le navire est par mer d'arrière, le calcul réglementaire proposé dans le code de deuxième génération demande de calculer la hauteur métacentrique  $GM$  pour les différentes positions de la vague dont la longueur est la même que celle du navire car c'est le cas le plus défavorable. Pour chacun des modes de défaillance, le nouveau code propose une méthode de calcul simple qui donne des résultats très conservatifs. Conscients de ce fait, les membres de l'OMI se sont accordés pour proposer un deuxième niveau de calcul faisant intervenir des hypothèses plus proches de la réalité ainsi qu'une pondération par des statistiques de vagues. Les deux premiers niveaux ne faisant intervenir que des calculs hydrostatiques de façon à pouvoir être implémentés dans les codes de calculs hydrostatiques existants. Si le navire satisfait aux critères d'un de ces deux niveaux, il est considéré comme non vulnérable au mode de défaillance visé. En plus de ces deux niveaux de vérification, la réglementation proposée prévoit une vérification directe. Les détails de cette vérification directe (Direct Assessment) ne sont pas encore établis mais deux voies principales ont été évoquées, la simulation numérique par résolution des équations de Navier-Stokes et les essais expérimentaux sur maquette en bassin de carène.

Le code de deuxième génération de stabilité du navire à l'état intact se résume par le diagramme de la Figure 1. L'IS code 2.2 signifie « Intact Stability » et correspond aux critères aujourd'hui en vigueur sur la hauteur métacentrique initiale et sur les paramètres de la courbe de moment de rappel en fonction de l'angle de gîte. L'IS code 2.3 correspond au critère météorologique existant. On voit donc que le nouveau code ne viendra pas remplacer le code en vigueur mais s'ajouter à celui-ci. Ce n'est pas ce qui s'est passé avec la SOLAS (Safety Of Life At Sea) quand la réglementation concernant la stabilité du navire après avarie est passée des règles déterministes aux règles probabilistes.

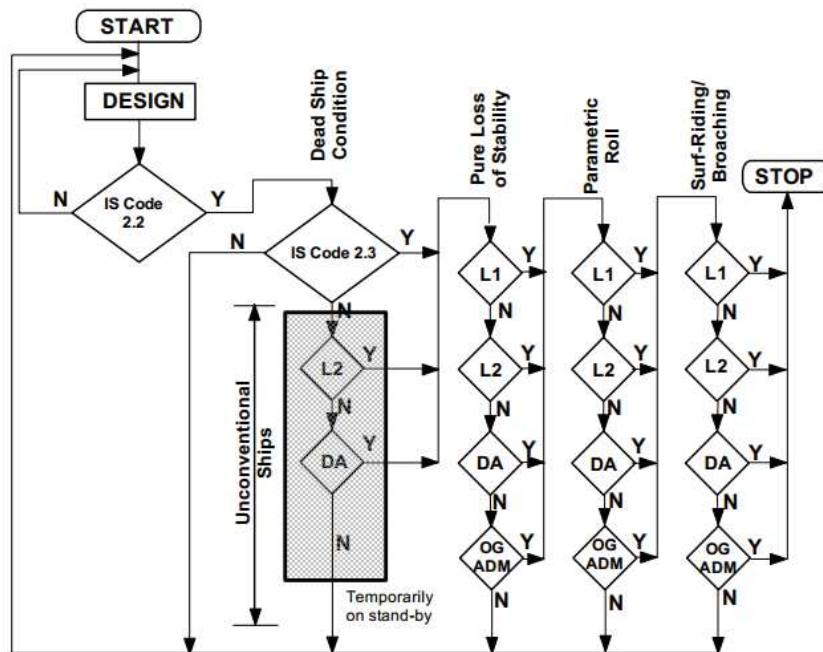


Figure 1. Résumé du code de deuxième génération de la stabilité du navire à l'état intact.

Tout ce qui précède est détaillé dans les deux premiers chapitres du manuscrit.

Dans un premier temps, on s'est attaché à vérifier si l'implémentation des nouvelles règles proposées dans un code industriel existant était possible sans avoir à modifier profondément le code de calcul. Le code industriel dont nous disposons est GHS©. GHS© (General HydroStatics) est développé par Creative Systems, Inc., compagnie basée dans l'état du Washington aux Etats Unis d'Amérique. Le code est basé sur la méthode des tranches ce qui ne l'empêche pas de pouvoir traiter toutes les structures flottantes. L'interface utilisateur est un langage de commande qui permet également d'écrire des macros et donc d'avoir un contrôle presque complet. L'apprentissage des commandes et du langage est assez fastidieux mais une fois la maîtrise acquise, le code permet de tout gérer y compris l'interface utilisateur à travers les commandes de Windows©.

Cinq navires présentés au chapitre 3 ont été utilisés pour tester l'implémentation des niveaux 1 et 2 du roulis paramétrique et de la perte de stabilité. Le critère concernant le départ au surf du navire ne dépend que du nombre de Froude. Comme le critère concernant l'accélération excessive du mouvement de roulis n'existe pas encore, il ne reste en fait que ces deux-là. Les cinq navires sont le DTMB5415, une frégate de l'US Navy, le PV, un patrouilleur, le 120m\_CS, un porte-container, le KL, un cargo, et finalement une forme académique simple que nous avons baptisé l'ASL. Pour chaque carène, les caractéristiques principales sont

présentées ainsi que leurs comportements hydrostatiques. Afin de vérifier l'implémentation des nouvelles règles dans GHS©, nous avons comparé avec succès les courbes de *maxVCG* (c.à.d. la hauteur maximum que peut prendre le centre de gravité tout en passant le critère de stabilité) en fonction du déplacement obtenues avec GHS© à celles obtenues par une implémentation dans un autre code par un autre développeur pour le cas du 120m-CS. Les courbes de *maxVCG* en fonction du déplacement sont ensuite données pour les cinq navires. La réglementation de deuxième génération propose de décliner le niveau 1 (L1) en deux sous-niveau A et B, le niveau B se voulant moins contraignant. C'est en effet ce que l'on constate, le critère de niveau 1 A (L1A) pour le roulis paramétrique comme pour la perte de stabilité est très contraignant. En appliquant le critère de niveau 1 A (L1A), on constate que les navires PV et DTMB5415 avec leurs chargements de conception ne passeraient pas la nouvelle réglementation proposée sachant qu'ils satisfont bien sûr à la réglementation en vigueur. Pour le roulis paramétrique, les courbes de *maxVCG* pour les critères de niveau 1 sont bien plus basses que pour le niveau 2 dont les courbes sont souvent proches de celles obtenues en appliquant les critères en vigueur sur la courbe de rappel hydrostatique (IS code 2.2). On ferme le Chapitre 3 en concluant que les niveaux 1 et 2 de la nouvelle réglementation sont tout à fait implémentables dans un code de stabilité industriel comme GHS©. Les codes développés dans le cadre de ce travail de thèse sont disponibles. Ils ne sont pas optimisés car ce n'était pas le but de notre étude mais les calculs sont somme toute assez rapides.

Maintenant quand on regarde la Figure 1, on voit deux niveaux supplémentaires de vérification : DA et OG-ADM. Le niveau OG-ADM est encore en discussion à l'OMI car il s'agirait de restreindre la navigation du navire dans des zones considérées comme trop dangereuses étant donnée sa vulnérabilité. Le niveau DA par contre signifie « Direct Assessment ». Il s'agit de prouver par des essais ou par des calculs que le navire n'est pas vulnérable au mode de défaillance examiné même s'il ne satisfait pas aux critères de niveaux 1 et 2. La suite du travail de thèse consiste à examiner et à proposer des essais et des calculs qui pourraient s'apparenter au Direct Assessment et pour cela nous avons préféré reprendre le cas du navire sans motorisation par mer et vent de travers.

Pour cette partie, nous avons choisi de retenir les formes DTMB5415 et ASL. Le Chapitre 4 est consacré aux essais en soufflerie. Il a fallu tout d'abord fabriquer les maquettes en respectant la taille de la soufflerie qui est celle de l'UTM à Johor-Bahrú en Malaisie. Les maquettes doivent d'abord respecter les géométries des carènes et des superstructures mais aussi respecter les inerties et les caractéristiques hydrostatiques. Les maquettes ont été fabriquées à l'ENSTA Bretagne puis expédiées à Johor-Bahrú en Malaisie. Il était donc primordial de vérifier les respects de ces caractéristiques avant le départ des maquettes. On a vérifié les hauteurs métacentriques *GM* avec la balance à parallélogramme de l'ENSTA

Bretagne en plaçant les maquettes dans un bassin. Nous avons ensuite mesuré les périodes de roulis naturelles des deux maquettes qui ont été comparées aux différentes formules proposées dans la littérature.

Le dispositif expérimental est délibérément simple pour pouvoir être proposé comme une méthode de vérification directe applicable aux besoins de la construction navale industrielle. On ne cherche pas à obtenir le mouvement de roulis dû aux vagues créées par le vent. Le dispositif expérimental doit permettre de placer la maquette dans un bassin dans lequel elle est libre en roulis. Elle est placée perpendiculairement au souffle. L'échelle des maquettes étant au 100<sup>ème</sup>, la vitesse du vent est le 10<sup>ème</sup> de la vitesse réelle. Dans un premier temps, on compare l'angle de stabilité en gîte  $\phi_0$  obtenu dans la soufflerie en fonction de la vitesse du vent et de celui obtenu par le calcul réglementaire. Pour l'ASL la courbe expérimentale est au-dessus de la courbe obtenue avec les règles de l'OMI dans GHS© alors que c'est l'inverse pour la frégate DTMB5415. Il s'agit des courbes de la Figure 4.36 du mémoire, reprise ici à la Figure 2. La forme parabolique de ces courbes pour le DTMB5415 est bien conforme au fait que la courbe de rappel hydrostatique est linéaire sur la plage d'angles considérée (0 à 30°) et que la force du vent est proportionnelle à la vitesse au carré. En regardant la courbe de stabilité de la forme ASL qui n'est pas linéaire, on comprend l'allure de la courbe de  $\phi_0$  en fonction de la vitesse du vent. L'origine des différences entre les courbes expérimentales et les courbes obtenues avec les calculs OMI est liée à la force hydrodynamique s'appliquant sur les superstructures. Le calcul règlementaire utilisé par GHS© implique que le coefficient de traînée aérodynamique du navire,  $C_D$ , est égal à 1,2 et ceci quelle que soit la forme de ces superstructures. Pour la silhouette de la frégate DTMB5415, on trouve que le  $C_D$  devrait plutôt être pris égal à 0.85 ce qui est le cas pour ce type de navire. Pour la forme ASL qui est un simple parallélogramme rectangle, le  $C_D$  est supérieur à 1,2 et diminue quand le bateau s'incline. Les résultats sont donc conformes aux attentes et on montre que la réglementation n'est pas toujours conservative.

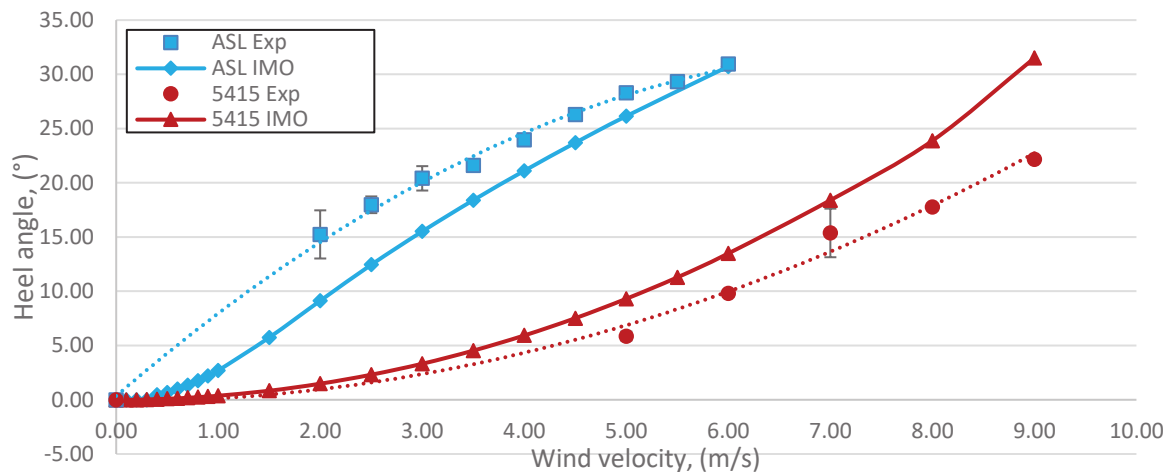


Figure 2 Courbes de l'angle de gîte en fonction de la vitesse de vent latéral pour les formes ASL et 5415. Comparaison des résultats expérimentaux au calcul réglementaire GHS.

Le critère météorologique concerne surtout l'angle maximum de roulis  $\phi_2$  que va prendre le navire lors d'une rafale de vent. Comme l'amplitude de roulis dû aux vagues,  $\phi_1$ , n'est pas représentée explicitement, l'intention est d'utiliser la valeur donnée par le calcul réglementaire. On vérifie la sensibilité du résultat à ce paramètre en examinant le résultat en fonction de sa valeur. Pour les deux navires et ceci pour toutes les valeurs de  $\phi_1$ , le résultat de l'OMI est bien au-dessus des valeurs expérimentales ce qui montre que la réglementation est très conservatrice. On constate également que les quilles antiroulis agissent non seulement sur l'amplitude de roulis  $\phi_1$ , comme permet de le prendre en compte la réglementation, mais aussi sur le ratio  $\phi_2 / \phi_1$  ce qui indique que leur effet est nettement sous-estimé par la réglementation.

Les maquettes étant placées sur un plateau tournant, on s'est également intéressé à faire varier le cap ce qui correspond à faire varier l'angle d'incidence du vent. Les plus hautes valeurs de l'angle de stabilité en gîte  $\phi_0$  ne sont pas obtenues par vent latéral. Encore une fois, le  $C_D$  des superstructures est à l'origine de cet effet. La conséquence sur l'angle maximum de roulis  $\phi_2$  peut s'avérer importante pour les plus grandes vitesses.

Le Chapitre 4 a montré comment la vérification directe (Direct Assessment) peut être effectuée de manière expérimentale. Il faut toutefois disposer d'une soufflerie de grande taille, un moyen d'essai pas forcément à la portée de tous. L'autre approche envisagée est l'approche numérique. Un calcul à surface libre 3D par résolution des équations de Navier-Stokes s'avère aussi très coûteux en temps à moins de disposer d'un très gros ordinateur. La décision a donc été prise de limiter nos investigations à des calculs 2D. Le principe est de montrer un calcul conservatif par rapport à la réalité mais moins conservatif que la réglementation en vigueur.

L'objet du Chapitre 5 est donc de présenter la méthode proposée et d'en comparer les résultats aux essais et à la réglementation en vigueur, afin de vérifier si elle reste conservative. On reprend donc les mêmes deux modèles qu'au Chapitre 4, la frégate DTMB5415 et la forme académique ASL en ne conservant que le maître couple. On recalcule les courbes de stabilité de ces formes 2D. On vérifie également le critère météorologique pour ces formes. Le solveur FINE<sup>TM</sup>/Marine© développé à l'Ecole Centrale de Nantes est ensuite utilisé pour résoudre le problème à surface libre par résolution des équations de Navier-Stokes. Le système consiste d'un seul degré de liberté, le roulis. Pour chacun des deux modèles, on calcule ensuite la période de roulis naturelle, la valeur de l'angle de gîte  $\phi_0$  en fonction de la vitesse du vent et finalement la valeur de l'angle de roulis maximum  $\phi_2$  qui prend le navire après avoir imposé l'amplitude de roulis réglementaire  $\phi_1$ . Les résultats montrent que les angles de roulis maximum  $\phi_2$  obtenus avec cette approche sont supérieurs à la réalité (conservatifs) et inférieurs au calcul OMI (moins restrictifs). On peut donc proposer cette approche comme une vérification directe (Direct Assessment) du critère météorologique.

Pour les essais comme pour les calculs, la valeur de l'angle de gîte d'équilibre  $\phi_0$  est lié à la valeur du coefficient de traînée,  $C_D$ . Maintenant si on part du même angle ( $\phi_0 - \phi_1$ ) on devrait retrouver la même hiérarchie dans les résultats. Ainsi le  $C_D$  numérique de la forme ASL étant bien supérieur à celui de l'OMI, l'angle  $\phi_2$  devrait être également supérieur or ce n'est pas le cas. La première explication qui vient à l'esprit c'est dû à l'amortissement. La forme ASL a justement été choisie pour sa géométrie circulaire qui n'engendre aucun amortissement à part le frottement qui est assez négligeable par rapport aux forces en jeu.

Pour comprendre ou plutôt confirmer ce que nous pensions être à l'origine de ce résultat, les valeurs des coefficients de traînée,  $C_D$ , ont été relevées en fonction de l'angle de gîte avec le bateau statique et avec le bateau libre en roulis. Ce deuxième type de mesures est malheureusement quasi impossible sur maquette mais la simulation en mode dynamique le permet. Le comportement du  $C_D$  en fonction de l'angle de gîte en mode statique est assez monotone, par contre, quand le navire est libre en roulis, son comportement est très chaotique. En s'inclinant avec le vent le  $C_D$  baisse de façon très brutale pouvant même devenir négatif ce qui donne une chance au rappel hydrostatique de réagir tout aussi brutalement et ainsi de suite. On se retrouve avec une alternance de moment dominant dont la fréquence est imprédictible. Au final, la physique du phénomène est beaucoup plus complexe, voire imprévisible, par rapport à la simple application du théorème de l'énergie cinétique suggérée par le calcul réglementaire qui est très conservatif.

En conclusion, les objectifs de la thèse sont atteints. On a bien vérifié qu'il était possible d'implémenter les critères de stabilité du navire à l'état intact de deuxième génération dans le



code de calcul de stabilité GHS©, un code utilisé couramment par les industriels du domaine. Cinq navires ont été considérés pour vérifier cette implémentation. On s'est ensuite intéressé à établir ce que serait une vérification directe du critère météorologique. On propose une méthode expérimentale en soufflerie ainsi qu'une méthode simplifiée de calcul CFD. Dans les deux cas, les résultats montrent que l'angle de roulis maximum atteint par les deux navires étudiés est inférieur à celui donné par le calcul réglementaire. La méthode expérimentale est certainement plus proche de la réalité et le calcul CFD reste conservatif sans être aussi contraignant que la réglementation.



## Executive Summary

The stability of the ship is the cornerstone of naval architecture. Hydrostatic pressure is at the origin of the buoyancy force of Archimedes which allows a ship to float. To be stable in the initial state, it is not enough for the centre of gravity ( $G$ ) to be positioned vertically in the centre of hull ( $B$ ), it is also necessary for the metacentre ( $M$ ) defined for the first time by Pierre Bouguer, to be above the centre of gravity ( $GM > 0$ ). However, this initial stability is not sufficient to withstand wind and swell. Established for the most part in the nineteenth-century, classification societies such as Bureau Veritas, founded in 1828, began to classify ships according to their reliability and this at the request of insurance companies. The first state rules appeared in the last decade of the nineteenth-century and the International Maritime Organisation (IMO) was founded in 1948. The primary role was to ensure maritime safety. This task was subdivided into a number of chapters, the first of which is the stability of the intact vessel. The current code was adopted in 2008. It imposes a minimum  $GM$  value in the initial state and five other constraints for the return moment curve as a function of the heeling angle. The code also imposes a criterion of resistance to wind and cross-waves. This last criterion, called the weather criterion, must ensure the survivability of the ship without propulsion and facing a strong sea. In addition to these criteria for civilian ships, military marines also impose a generally more stringent code.

This international regulation has certainly made it possible to greatly reduce the accidents linked to insufficient intact stability, but accidents are always deplorable, whereas the vessels which were victims of accidents meet all the requirements of the regulations in force. Few human victims have been recorded as a result of these mediatised, spectacular and, above all, costly accidents. The phenomena responsible for these accidents have been identified. Five phenomena have been identified:

- a. Loss of stability in heel when the vessel is in the stern or quartering seas;
- b. Parametric rolling by head or stern wave;
- c. The vessel is broaching by stern wave;
- d. Ship without motorisation by swell and cross wind;
- e. Excessive acceleration of roll motion.

In order to prevent these types of accidents, the IMO is working to establish a new intact ship regulatory code commonly known as the second-generation code, and therefore the vessel's stability second generation intact criteria. The existing phenomenon is normally taken into account in the weather criterion of the current code. The current phenomenon is still under study. As for the other three, there are now criteria that can still be changed, but it is a question of bringing the new regulation into force by 2019. No one seems to believe seriously that this deadline will be met, but it is certain that the new code will be applied soon. The implementation of the probabilistic regulations for the stability of the damaged ship in 2009 thus caught many professionals in the field unprepared, and it will certainly be the same with this one.

It was therefore decided that the importance of this future regulation of the stability of the intact vessel should be taken into account in a long study such as the present one. First, it was necessary to understand the terms of these new regulations which are much more complicated than the previous regulation. It is also necessary to understand how these new criteria will prevent accidents identified as being related to the five failure modes addressed by the second generation intact stability criteria. These five failure modes are all related to hydrodynamics and not solely to hydrostatics.

As stated in the regulations in force, while it is strongly related to hydrodynamic and aerodynamic phenomena, the weather criterion requires only a hydrostatic calculation to be verified. In crosswinds, the vessel will drift and take shelter. The heeling angle is calculated by balancing the heeling moment and the hydrostatic restoring moment. The heeling moment is due to the action of the wind on the superstructure and to the hydrodynamic force of reaction exerted on the hull. Around this equilibrium angle, a regulatory rolling motion calculated from the geometrical data of the ship and its metacentric height ( $GM$ ) is applied. A sudden gust of wind is then applied when the vessel starts its half roll period in the direction of the wind. The criterion applies to the maximum roll angle that the vessel will reach. To calculate this angle, we apply the theory of kinetic energy which allows direct comparison of the area under the curve of the heeling moment and the area under the hydrostatic restoring curve. The principle of this regulatory calculation is to be conservative and to be verified without resorting to complex hydrodynamic computation or tests on models which are very difficult to implement.

The four other modes of failure are also the combination of very complex kinematic and hydrodynamic phenomena to be reproduced by direct calculation or by tests. As for the weather criterion, IMO members have defined calculation methods involving only hydrostatic calculation. For example, if we take the loss of stability in heeling when the vessel is in a stern wave, the regulatory calculation proposed in the second generation code requires the  $GM$  to be

computed for the different positions of the wave which has the same length as the ship because this is the worst case. For each of the failure modes, the new code proposes a simple calculation method which gives very conservative results. Aware of this fact, IMO members agreed to propose a second level of calculation involving hypotheses closer to reality and a weighting by wave statistics. The first two levels only involve hydrostatic calculations so that they can be implemented in existing hydrostatic calculation codes. If the vessel meets the criteria for one of these two levels, it is considered invulnerable to the intended mode of failure. In addition to these two levels of verification, the proposed regulation provides for direct verification. The details of this direct assessment have not yet been established, but two main avenues have been discussed, the numerical simulation by resolution of the Navier-Stokes equations and experimental tests on models.

The second generation stability code for the intact ship can be summarised in the diagram in Figure 1. The IS Code 2.2 means "Intact Stability" and corresponds to the current metacentric height and the parameters of the restoring moment curve as a function of the heeling angle. The IS Code 2.3 corresponds to the existing weather criterion. We can see that the new code will not replace the existing code, but will be added to it. This did not happen with the SOLAS when the regulations concerning the stability of the damaged ship went from the deterministic rules to the probabilistic rules.

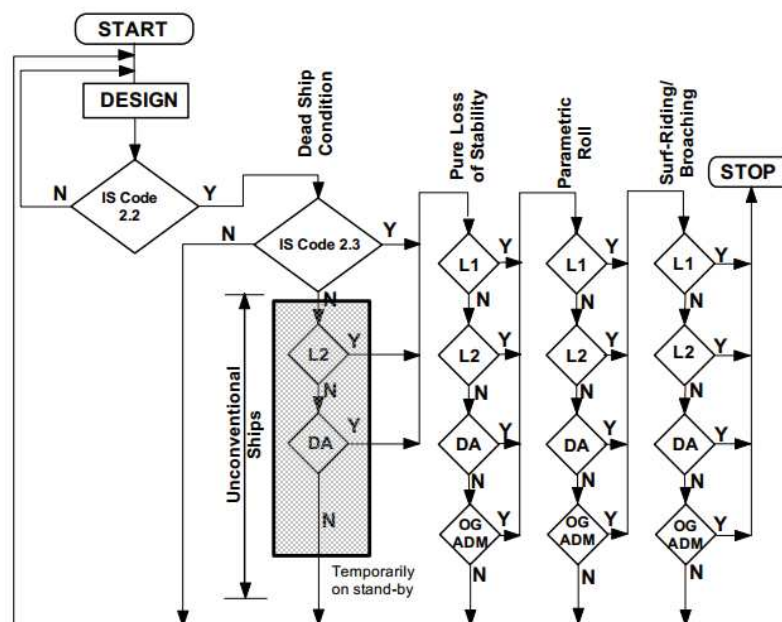


Figure 1: Summary of Second Generation Intact Stability Criteria

All the above is detailed in the first two chapters of the manuscript.

The first step was to check whether the implementation of the new rules proposed in an existing industrial code was possible without having to modify the calculation code profoundly. The industrial code we have is GHS©. The GHS© (General Hydro Statics) was developed by Creative Systems, Inc., a Washington-based company in the United States of America. The code is based on the strip method which does not prevent it from being able to process all the floating structures. The user interface is a command language that also allows you to write macros and thus has almost complete control. The learning of commands and language is rather tedious, but once the mastery is acquired, the code allows everything to be managed including the user interface through the commands of Windows©.

Five vessels presented in Chapter 3 were used to test the implementation of Levels 1 and 2 of parametric roll and loss of stability. The criterion for the surfing of the vessel depends only on the Froude number. Since the criterion concerning the excessive acceleration of the rolling motion does not yet exist, in fact only these two remain. The five ships are the DTMB5415, a US Navy frigate, the PV, a patrol boat, the 120m-CS, a container carrier, the KL, a freighter, and finally a simple academic form that we have ASL shape. For each hull, the main characteristics are presented as well as their hydrostatic behaviour. In order to verify the implementation of the new rules in GHS©, we have successfully compared the curves of *maxVCG* (i.e. the maximum height that the centre of gravity can assume while passing the stability criterion) as a function of the displacement obtained with GHS© and to those obtained by an implementation in another code by another developer for the case of the 120m\_CS. The curves of *maxVCG* as a function of the displacement are then given for the five ships. Second generation regulation proposes to divide Level 1 (L1) into two methods; A and B, Level B being less restrictive. This is indeed what has been observed, the criterion of Level 1 A (L1A) for the parametric roll as for the loss of stability is very constraining. Applying Level 1 A (L1A) criterion, it has been determined that the PV and DTMB5415 vessels with their design loads would not pass the proposed new regulations knowing that they naturally meet the regulations in force. For parametric roll, the curves of *maxVCG* for the Level 1 criteria are much lower than for Level 2 which has curves that are often close to those obtained by applying the criteria in force on the hydrostatic return curve (IS Code 2.2). Chapter 3 comes to a close by concluding that Levels 1 and 2 of the new regulations are fully implementable in an industrial stability code such as GHS©. The codes developed in the framework of this thesis are available. They are not optimised because this was not the purpose of our study but the calculations are quite fast.

Now when looking at Figure 1, we see two additional levels of verification: DA and OG-ADM. The OG-ADM level is still under discussion at the IMO as it would restrict the vessel's navigation to areas considered too risky given its vulnerability. The DA level, on the

other hand, means "Direct Assessment". It is a matter of proving by tests or calculations that the ship is not vulnerable to the mode of failure examined even if it does not meet the criteria of Levels 1 and 2. The next step of the thesis was to examine and to propose tests and calculations which could be similar to the Direct Assessment and to do so, we preferred to take again the case of the ship without propulsion by sea and cross wind.

For this part, we chose to retain the DTMB 5415 and ASL shapes. Chapter 4 is devoted to wind tunnel testing. First of all, the models had to be constructed according to the size of the wind tunnel, which is that of the UTM in Johor-Bahru, Malaysia. The models had to first respect the geometries of the hulls and superstructures and also respect the inertias and the hydrostatic characteristics. The models were constructed at ENSTA Bretagne and then shipped to Johor-Bahru in Malaysia. Therefore, it was essential to verify the respect of these characteristics before shipping the models. The  $GM$  metacentric heights were checked with the ENSTA Bretagne parallelogram scale by placing the models in a basin. We then measured the natural rolling periods of the two models, which were compared with the different formulas proposed in the literature.

The experimental design is deliberately simple to be proposed as a direct assessment method applicable to the needs of industrial shipbuilding. One does not seek to obtain the rolling movement due to the waves created by the wind. The experimental device must allow the model to be placed in a basin in which it is free to roll. It is placed perpendicularly to the breadth. The scale of the models being  $1/100^{\text{th}}$ , the speed of the wind is the  $10^{\text{th}}$  of the real speed. In a first step, the angle of stability in heel  $\phi_0$  obtained in the wind tunnel was compared as a function of the wind speed and that obtained by the regulatory calculation. For the ASL the experimental curve was above the curve obtained with the rules of the IMO in GHS© whereas it was the reverse for the frigate DTMB5415. These are the curves presented in Figure 4.36 of the document, shown here as Figure 2. The parabolic shape of these curves for the DTMB5415 is consistent with the fact that the hydrostatic curve is linear over the range of angles considered (0 to  $30^\circ$ ) and that the force of the wind is proportional to the squared speed. Looking at the stability curve of the ASL form which is not linear, we can understand the curve  $\phi_0$  as a function of the wind speed. The origin of the differences between the experimental curves and the curves obtained with the IMO calculations was related to the hydrodynamic force applied to the superstructures. The regulatory calculation used by GHS© implies that the aerodynamic drag coefficient of the ship,  $C_D$ , is equal to 1.2 and this, whatever the shape of these superstructures. For the silhouette of the frigate DTMB5415, it was found that the  $C_D$  should rather be taken as equal to 0.85 which is the case for this type of ship. For the ASL shape, which is a simple cuboid shape, the  $C_D$  was greater than 1.2 and decreased when the

boat heeled. The results are therefore in line with expectations and it has been shown that the regulations are not always conservative.

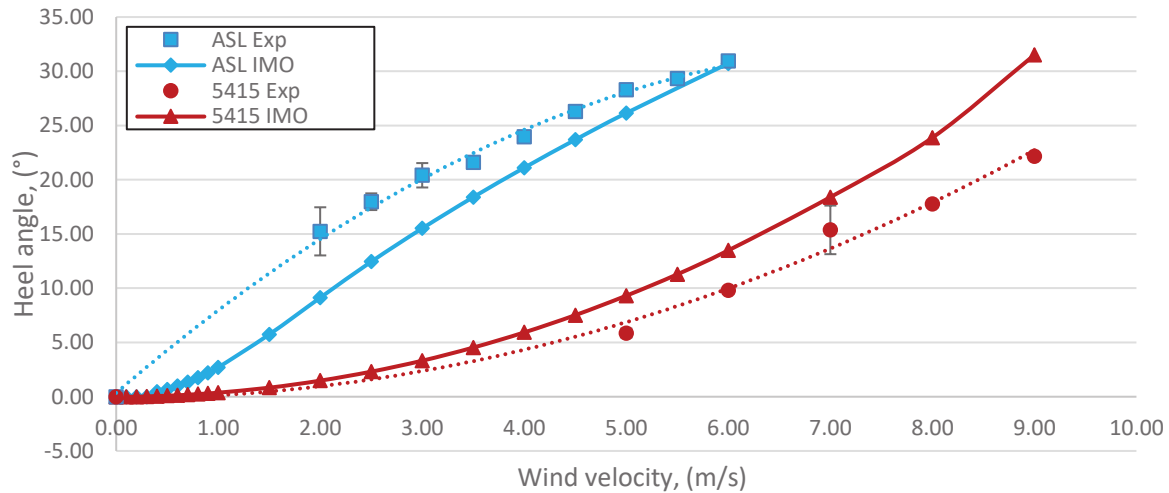


Figure 2 Graph of wind velocity and angle of stable heel for the ASL shape and 5415 shape for the experimental results and GHS calculation

The weather criterion concerns mainly the maximum angle of roll  $\phi_2$  that the ship will take during a gust of wind. Since the roll amplitude due to waves,  $\phi_1$ , was not explicitly represented, the intention was to use the value given by the regulatory calculation. The sensitivity of the result to this parameter was checked by examining the result as a function of its value. For both vessels and for all the values of  $\phi_1$ , the IMO result was well above the experimental values, which shows that the regulation is very conservative. It has also been observed that the bilge keels act not only on the roll amplitude  $\phi_1$ , which the regulations have taken into account, but also on the ratio  $\phi_2 / \phi_1$  which indicates that their effect is clearly underestimated by the regulations.

The models being placed on a turntable, attention was made to varying the heading, which corresponded to the varying the direction of the wind. The highest values of the heel stability angle  $\phi_0$  were not obtained by the lateral wind. Again, the  $C_D$  of the superstructures was the source of this effect. The consequence on the maximum roll angle  $\phi_2$  can be significant for higher speeds.



Chapter 4 showed how direct assessment could be carried out experimentally. However, it is necessary to have a large wind tunnel, a test facility which is not necessarily within everyone's budget. The other approach envisaged is the numerical approach. A 3D free surface computation by solving the Navier-Stokes equations is also very costly in time unless a very powerful calculator is available. The decision was therefore taken to limit our investigations to 2D calculations. The principle was to show a conservative calculation with respect to reality but less conservative than the regulations in force.

The purpose of Chapter 5 is therefore to present the proposed method and to compare the results with the tests and the regulations in force, in order to verify whether it remains conservative. Therefore, took the same two models as in Chapter 4, the frigate DTMB5415 and the academic form ASL while retaining only the master pair. The stability curves of these 2D shapes were recalculated. The weather criterion for these shapes was also verified. The Fine<sup>TM</sup>/Marine solver developed at the Ecole Centrale de Nantes was then used to solve the free surface problem by solving the Navier-Stokes equations. The system consisted of a one degree of freedom, roll. For each of the two models, the natural rolling period, the angle of heel  $\phi_0$  as a function of the wind speed and finally the value of the maximum roll angle  $\phi_2$  which takes the vessel after imposing the regulatory rolling amplitude  $\phi_1$  were simulated. The results show that the maximum roll angles  $\phi_2$  obtained with this approach were superior to reality (conservative) and lower than the IMO calculation (less restrictive). Therefore, this approached could be proposed as a Direct Assessment of the weather criterion.

For the tests as for the calculations, the value of the equilibrium heeling angle  $\phi_0$  is related to the value of the drag coefficient,  $C_D$ . Now if we start from the same angle ( $\phi_0 - \phi_1$ ) we should find the same hierarchy in the results. Thus, since the numerical  $C_D$  of the ASL form is much greater than that of the IMO, the angle  $\phi_2$  should also be greater or it is not the case. The first explanation that comes to mind is due to damping. The ASL shape was chosen for its circular geometry which produces no damping other than friction which is quite negligible compared to the forces involved.

In order to understand or rather confirm what we thought was the cause of this result, the values of drag coefficients,  $C_D$ , were taken as a function of the angle of heel with the static ship and not allow to roll. This second type of measurements is unfortunately almost impossible on models but dynamic simulation allows it. The behaviour of the  $C_D$  as a function of the heeling angle in static ship is rather monotonous, but when the ship is free in roll, its behaviour is very chaotic. By bowing with the wind the  $C_D$  drops in a very critical way which can even become negative, which gives a chance to the hydrostatic recall to react equally critically and so on. We find ourselves with an alternation of the dominant moment which is

of unpredictable frequency. In the end, the physics of the phenomenon is much more complex, even unpredictable, compared to the simple application of the theory of kinetic energy suggested by the regulatory computation which is very conservative. In conclusion, the objectives of the thesis have been achieved. It verified that it was possible to implement the stability criteria of the intact second-generation vessel in the GHS© code of stability, a code commonly used by industrialists in the field. Five vessels were considered to verify this implementation. The next step was to establish what would be a direct verification of the weather criterion. We propose an experimental wind tunnel method and a simplified CFD calculation method. In both cases, the results show that the maximum roll angle reached by the two vessels studied is lower than that given by the regulatory calculation. The experimental method is certainly closer to reality and the calculation CFD remains conservative without being as binding as the regulations.



## References

- A. D. Wnęk, A. Paço, X-Q. Zhou, and C Guedes Soares. 2010. “Numerical and Experimental Analysis of the Wind Forces Acting on LNG Carrier.” In *V European Conference on Computational Fluid Dynamics-ECCOMAS CFD 2010*, 14–17. Lisbon, Portugal.
- Ariffin, Arman. 2014. “Air Flow and Superstructure Interaction on a Model of a Naval Ship.” Universiti Teknologi Malaysia.
- Ariffin, Arman, Shuhaimi Mansor, and Jean-Marc Laurens. 2015. “A Numerical Study for Level 1 Second Generation Intact Stability Criteria.” In *12th International Conference on Stability of Ships and Ocean Vehicles*, 183–93. Glasgow, UK.
- Ariffin, Arman, Shuhaimi Mansor, and Jean-Marc Laurens. 2016a. “Conduction of a Wind Tunnel Experiment to Investigate the Ship Stability Weather Criterion.” In *15th International Ship Stability Workshop*. Stockholm, Sweden.
- Ariffin, Arman, Shuhaimi Mansor, and Jean-Marc Laurens. 2016b. “Implementation of Second Generation Intact Stability Criteria into the Stability Calculation Software.” In *3rd Maritime Technology and Engineering*. Lisbon, Portugal.
- Ariffin, Arman, Shuhaimi Mansor, and Jean-Marc Laurens. 2016c. “Real-Time Evaluation of Second Generation Intact Stability Criteria.” In *Smart Ship Technology Conference*. London, UK.
- Ariffin, Arman, Shuhaimi Mansor, and Jean-Marc Laurens. 2016d. “The Weather Criterion : Experimental Wind Tunnel Results.” In *6th International Maritime Conference on Design for Safety*. Hamburg, Germany.
- Arjava, Jouni, and Jalonen Risto. 2015. *The Rahola Criterion-The Life and Work of Professor Jaakko Rahola*.
- Ba, Igor, Gabriele Bulian, Jakub Cichowicz, Eleftheria Eliopoulou, Dimitris Konovessis, Jean-françois Leguen, Anders Rosén, and Nikolaos Themelis. 2016. “Ship Stability, Dynamics and Safety : Status and Perspectives from a Review of Recent STAB Conferences and ISSW Events.” *Ocean Engineer* 116: 312–49.
- Backalov, Igor, Gabriele Bulian, Anders Rosén, Vladimir Shigunov, and Nikolaos Themelis.

2016. "Improvement of Ship Stability and Safety in Intact Condition through Operational Measures : Challenges and Opportunities." *Ocean Engineering* 120: 353–61.
- Barlow, Jewel B, Jr H. Rae William, and Alan Pope. 1999. *Low-Speed Wind Tunnel*. 3rd ed. John Wiley & Sons, Inc.
- Bassler, Christopher C, Vadim Belenky, Gabriele Bulian, Kostas J Spyrou, and N Umeda. 2009. "A Review of Available Methods for Application to Second Level Vulnerability Criteria." In *10th International Conference on Stability of Ship and Ocean Vehicles*, 111–28. St Petersburg, Russia.
- Begovic, E., G. Mortola, A. Incecik, and a. H. Day. 2013. "Experimental Assessment of Intact and Damaged Ship Motions in Head, Beam and Quartering Seas." *Ocean Engineering* 72. Elsevier: 209–26.
- Begovic, E, A. H. Day, and A. Incecik. 2011. "Experimental Ship Motion and Load Measurements in Head and Beam Seas." In *9th Symposium on High Speed Marine Vehicles*, 1–8. Naples, Italy.
- Belenky, Vadim, Christopher C Bassler, and Konstantinos J Spyrou. 2011. Development of Second Generation Intact Stability Criteria. (No. NSWCCD-50-TR-2011/065) NAVAL SURFACE WARFARE CENTER, CARDEROCK DIVISION, HYDROMECHANICS DEPARTMENT
- Benford, Harry. 1991. *Naval Architecture for Non-Naval Architects*. Society of Naval Architects.
- Bertaglia, Gianfranco, Andrea Serra, Alberto Francescutto, and Gabriele Bulian. 2003. "Experimental Evaluation of the Parameters for the Weather Criterion." In *8th International Conference on Stability of Ships and Ocean Vehicles*, 253–64. Madrid, Spain.
- Bertram, Volker. 2012. *Practical Ship Hydrodynamics*. Butterworth Heinemann.
- Billard, J. Y., C. Sarraf, R. Jaouen, and H. Djeridi. 2005. "Investigation of Thickness Effects on 2D NACA Symmetric Foils." In *Oceans 2005 - Europe*, 2:1298–1303. Brest, France.
- Blendermann, W. 1994. "Parameter identification of wind loads on ships." *Journal of Wind Engineering and Industrial Aerodynamics* 51(3): 339-351
- Brown, A. J., and Lt. F. Deybach. 1998. "Towards A Rational Intact Stability Criteria For Naval Ships." *Naval Engineers Journal* 110 (1): 65–77.
- Bulian, Gabriele, Alberto Francescutto, and Fabio Fucile. 2010. "An Experimental Investigation in the Framework of the Alternative Assessment for the IMO Weather Criteria." In *HYDRALAB III Joint User Meeting*, 1–4. Hannover, Germany.

- Carton, Xavier. 2000. "Hydrodynamical Modeling of Oceanic Vortices." *Surveys in Geophysics* 22 (3).
- Deng, G. B., J. Piquet, P. Queutey, and M. Visonneau. 1994. "A New Fully Coupled Solution of the Navier-Stokes Equations." *International Journal for Numerical Methods in Fluids* 19 (7): 605–39.
- Deybach, Frederic. 1997. "Intact Stability Criteria for Naval Ships." Massachusetts Institute of Technology.
- Djebli, Mohamed Abdelkader, Benameur Hamoudi, Omar Imine, and Lahouari Adjlout. 2016. "The Application of Smartphone in Ship Stability Experiment." *Journal of Marine Science and Application*. 14(4), 406-412
- Feng, Pei-yuan, She-ming FAN, Li-Wei YU, and Ning MA. 2016. "Study on the Correction of Wave Surge Forces to Improve Surf-riding/Broaching Vulnerability Criteria Check Accuracy." In *6th International Maritime Conference on Design for Safety*. Hamburg, Germany.
- Francescutto, Alberto. 2016. "Intact Stability Criteria of Ships – Past , Present and Future." *Ocean Engineering* 120. Elsevier: 312–17.
- Francescutto, Alberto, and Naoya Umeda. 2010. "Current Status of New Generation Intact Stability Criteria." In *International Ship Stability Workshop*.
- Fureby, C, B Anderson, D Clarke, L Erm, S Henbest, M Giacobello, D Jones, et al. 2016. "Experimental and Numerical Study of a Generic Conventional Submarine at 10 ° Yaw." *Ocean Engineering* 116. Elsevier: 1–20.
- González, Marcos Míguez, Vicente Díaz Casás, Luis Pérez Rojas, Fernando Junco Ocampo, and Daniel Pena. 2014. "Application of Second Generation IMO Intact Stability Criteria to Medium – Sized Fishing Vessels." In *The 14th International Ship Stability Workshop*. Kuala Lumpur, Malaysia.
- Grinnaert François, Jean-Yves Billard, and Jean-Marc Laurens. 2015. "Calcoque: A Fully 3D Ship Hydrostatic Solver." In *International Conference on Stability of Ships and Ocean Vehicles*, 203–12.
- Grinnaert, Francois. 2017. "Etude et Implémentation Des Critères de Seconde Génération Dans Un Code de Stabilité." Université de Bretagne Occidentale.
- Hagishima, Aya, Jun Tanimoto, Koji Nagayama, and Sho Meno. 2009. "Aerodynamic Parameters of Regular Arrays of Rectangular Blocks with Various Geometries." *Boundary-Layer Meteorology* 132 (2): 315–37.
- Hanson, E.O. 1985. "An Analytical Treatment of the Accuracy of the Results of the Inclining

- Experiment.” *Naval Engineers Journal* 97 (4): 97–115.
- Hayes, Peter, Warren Smith, Martin Renilson, and Stuart Cannon. 2015. “A Reassessment of Wind Speeds Used for Intact Stability Analysis.” In *International Conference on Stability of Ships and Ocean Vehicles*, 441–50. Glasgow, UK.
- Hirt, C. W., and B. D. Nichols. 1981. “Volume of Fluid (VOF) Method for the Dynamics of Free Boundaries.” *Journal of Computational Physics* 39 (1): 201–25.
- Hoerner, S.F. 1965. *Fluid-Dynamic Drag: Practical Information on Aerodynamic Drag and Hydrodynamic Resistance*. Bakersfield: Hoerner Fluid Dynamics.
- IMCO. 1982. “IMCO - Sub-Committee on Subdivision, Stability and Load Lines - 27th Session.”
- IMO. 1968. “Resolution A.167 ‘Recommendation on Intact Stability for Passenger and Cargo Ships under 100metres in Length.’”
- IMO. 1979. “Intact Stability, Stability of Ships in Ballast Condition, Weather Criteria.”
- IMO. 1985. “Resolution A. 562 "Recommendations on a Severe Wind and Rolling Criterion for the Intact Stability of Passanger and Cargo Ships of 24 Metres in Length and Over.”
- IMO. 1993. “Resolution A.749 ‘Code on Intact Stability for All Types of Ships Covered by IMO Instruments.’”
- IMO. 2009. “International Code of Intact Stability, 2008.” London.
- IMO. 2011. “SLF 53/WP.4 Report of the Working Group (Part 1).”
- IMO. 2013. “SDC 1/INF.8 - Development of Second Generation Intact Stability Criteria.”
- IMO. 2014. “SDC 2/INF.10 Second Generation Intact Stability Criteria.”
- IMO. 2015. “SDC 3/INF.10 Finalization of Second Generation Intact Stability Criteria.”
- IMO. 2016. “SDC 3/WP.5 Finalization of Second Generation Intact Stability Criteria.”
- IMO MSC.1/Cir.1227. 2007. “Explanatory Notes to the Interim Guidelines for Alternative Assessment of the Weather Criterion.”
- IMO MSC.1/Circ.1200. 2006. “Interim Guidelines for Alternative Assessment of the Weather Criterion.”
- IMO SLF 54/INF.9. 2011. “Development of Second Generation Intact Stability Criteria.”
- Ishida, Shigesuke, Harukuni Taguchi, and Hiroshi Sawada. 2006. “Evaluation of the Weather Criterion by Experiments and Its Effect to the Design of a RoPax Ferry.” In *International Conference on Stability of Ships and Ocean Vehicles*, 9–16. Rio de Janeiro, Brazil.
- ITTC. 2014. “ITTC Symbols and Terminology List.” *ITTC Quality Systems Group*.
- Jaouen, F., A.H. Koop, G. Vaz, and P. Crepier. 2011. “RANS Predictions of Roll Viscous Damping of Ship Hull Sections.” In *International Conference on Computational Methods*

- in Marine Engineering*, 1–18. Lisbon, Portugal.
- Jones, D.a., and D.B. Clarke. 2010. “Fluent Code Simulation of Flow around a Naval Hull: The DTMB 5415.” Victoria, Australia.
- Kubo, Takumi, Naoya Umeda, Satoshi Izawa, and Akihiko Matsuda. 2012. “Total Stability Failure Probability of a Ship in Irregular Beam Wind and Waves: Model Experiment and Numerical Simulation.” In *11th International Conference on Stability of Ships and Ocean Vehicles*.
- La Dage, J.H., and L. Van Gemert. 1956. *Stability and Trim for the Ship’s Officer*. Edited by William E. George. 4th ed. Cornell Maritime Press, Inc.
- Laurens, Jean-Marc, and François Grinnaert. 2013. *Stabilité Du Navire: Théorie, Réglementation, Méthodes De Calcul (Cours Et Exercices Corrigés)*. Ellipses, Paris.
- Luquet, Romain, Pierre Vonier, Jean-françois Leguen, and P. Perdon. 2014. “Chargements Aerodynamiques Sur Un Navire Avec Gite.” In *14èmes Journées de L’ Hydrodynamique*, 1–13.
- Luquet, Romain, Pierre Vonier, Andrew Prior, and Jean François Leguen. 2015. “Aerodynamics Loads on a Heeled Ship.” *12th International Conference on the Stability of Ships and Ocean Vehicles*, no. June: 14–19.
- Lloyd, A.R.J.M. 1998. *Seakeeping: Ship Behaviour in Rough Weather*. Hampshire: International Book Distributors Ltd.
- Molgaard, Axel. 2000. “PMM-Test with a Model of a Frigate Class DDG-51.” Lyngby, Denmark.
- Noor, Alias Mohd, and Shuhaimi Mansor. 2013. “Measuring Aerodynamic Characteristics Using High Performance Low Speed Wind Tunnel at Universiti Teknologi Malaysia.” *Journal of Applied Mechanical Engineering* 3 (1): 1–7.
- Numeca International. 2013. “User Manual Fine Marine v3 (Including ISIS-CFD).” Brussels.
- Peters, W, V M Belenky, C M Bassler, K M Spyrou, N M Umeda, G V Bulian, and B V Altmayer. 2012. “The Second Generation Intact Stability Criteria: An Overview of Development.” *Transactions - The Society of Naval Architects and Marine Engineers* 119 (225–264).
- Peters, William S, Vadim Belenky, Christopher C Bassler, and Kostas J Spyrou. 2011. “On Vulnerability Criteria for Parametric Roll and Surf-Riding.” In *International Ship Stability Workshop*, 1–6.
- R. Munro-Smith. 1988. *Ships & Naval Architecture*. London: The Institute of Marine Engineers.

- Reed, Arthur M. 2009. "A Naval Perspective on Ship Stability." In *International Conference on Stability of Ships and Ocean Vehicles*, 21–44.
- Rohala, Jaakko. 1939. "The Judging of the Stability of Ships and the Determination of the Minimum Amount of Stability." Doctoral Thesis, Technical University of Finland.
- Santiago, J. L., O. Coceal, A. Martilli, and S. E. Belcher. 2008. "Variation of the Sectional Drag Coefficient of a Group of Buildings with Packing Density." *Boundary-Layer Meteorology* 128 (3): 445–57.
- Sarchin, T.H, and L.L Goldberg. 1963. "Stability and Buoyancy Criteria for U.S. Naval Surface Ships." *Society of Naval Architects and Marine Engineers*. SNAME Transactions.
- Shigunov, V., Rathje, H., El Moctar, O., and Altmayer, B. and Lloyd, G., 2011. "On the Consideration of Lateral Accelerations in Ship Design Rules." In *International Ship Stability Workshop*, 27–35.
- Spyrou, Kostas J. 2011. "A Basic for Developing a Rational Alternative to the Weather Criterion Problems and Capabilities." In *Contemporary Ideas on Ship Stability and Capsizing in Waves*, 25–46.
- Sverdrup, H. U, and W.H Munk. 1947. "Wind, Sea and Swell: Theory of Relations for Forecasting."
- Tsuchiya, T. 1975. "An Approach for Treating the Stability of Fishing Boats." In *International Conference on Stability of Ships and Ocean Vehicles*.
- UK MOD. 2000. "Ministry of Defence Defence Standard 02-109 ( NES 109 )" 712 (1).
- Umeda, Naoya. 2013. "Current Status of Second Generation Intact Stability Criteria Development and Some Recent Efforts." In 13<sup>th</sup> *International Ship Stability Workshop*.
- Umeda, Naoya, Daichi Kawaida, Yuto Ito, Yohei Tsutsumi, Akihiko Matsuda, and Daisuke Terada. 2014. "Remarks on Experimental Validation Procedures for Numerical Intact Stability Assessment with Latest Examples." In 14<sup>th</sup> *International Ship Stability Workshop*, 77–84.
- Umeda, Naoya, Satoshi Izawa, Hiroyuki Sano, Hisako Kubo, Keisuke Yamane, and Akihiko Matsuda. 2011. "Validation Attempts on Draft New Generation Intact Stability Criteria." In 12<sup>th</sup> *International Ship Stability Workshop*, 19–26.
- Visonneau, Michel, Patrick Queutey, Jeroen Wackers, Ganbo Deng, and Patrick Queutey. 2015. "Omae2015-41372 Assessment of Statistical and Hybrid LES Turbulence Closures," 1–10.
- Wackers, Jeroen, Ganbo Deng, Alban Leroyer, Patrick Queutey, and Michel Visonneau. 2012. "Adaptive Grid Refinement for Hydrodynamic Flows." *Computers and Fluids* 55.

Elsevier Ltd: 85–100.

Wandji, Clève, and Philippe Corrigan. 2012. “Test Application of Second Generation IMO Intact Stability Criteria on a Large Sample of Ships.” In 11<sup>th</sup> *International Conference on Stability of Ships and Ocean Vehicles*, 129-139.

Welaya, Y, and Cheng Kuo. 1981. “A Review of Intact Ship Stability Research and Criteria.” *Ocean Engineering* 8: 65–84.

Yamagata, M. 1959. “Standard of Stability Adopted in Japan.” *Trans INA*, no. 101: 417–43.

Yesilel, H. 2007. “Ship Airwake Analysis by CFD Method.” Istanbul Technical University.

Yoon, Hyunse, Claus D. Simonsen, Lanfranco Benedetti, Joseph Longo, Yasuyuki Toda, and Frederick Stern. 2015. “Benchmark CFD Validation Data for Surface Combatant 5415 in PMM Maneuvers – Part I: Force/moment/motion Measurements.” *Ocean Engineering* 109. Elsevier: 705–34.





## Annex A

Current references for IMO document on second generation intact stability criteria

Failure mode	Formula	Explanatory notes
Pure loss of stability	SDC 2/WP.4, annex 1	SDC 3/WP.5 annex 3
Parametric rolling	SDC 2/WP.4, annex 2	SDC 3/WP.5 annex 4
Surf-riding/broaching	SDC 2/WP.4, annex 3	SDC 3/WP.5 annex 5
Dead ship condition	SDC 3/WP.5, annex 1	SDC 3/WP.5 annex 6
Excessive acceleration	SDC 3/WP.5 Annex 2	SDC 3/WP.5 annex 7
Plan of action for SGISC	SDC 3/WP.5 annex 8	



## ANNEX 1

### DRAFT AMENDMENTS TO PART B OF THE 2008 IS CODE WITH REGARD TO VULNERABILITY CRITERIA OF LEVELS 1 AND 2 FOR THE PURE LOSS OF STABILITY FAILURE MODE

#### PART B

#### Recommendations for ships engaged in certain types of operations, certain types of ships, and additional guidelines

#### Chapter 2

#### Recommended design criteria for certain types of ships

1 A new section "2.10" is added with the following:

#### "2.10 Assessment of ship vulnerability to the pure loss of stability failure mode

##### 2.10.1 Application

2.10.1.1 The provisions given hereunder apply to all ships for which the Froude number,  $F_n$ , corresponding to the service speed exceeds 0.24<sup>1</sup>.

For the purpose of this section,  $F_n$ , is determined using the following formula:

$$F_n = \frac{V_s}{\sqrt{gL}}$$

Where,

- $V_s$  = Service speed, m/s
- $L$  = Length of the ship (m);
- $g$  = acceleration due to gravity, 9.81 m/s<sup>2</sup>

2.10.1.2 For each condition of loading, a ship that:

- .1 meets the standard contained in the criteria contained in 2.10.2 is considered not to be vulnerable to the pure loss of stability failure mode;
- .2 does not meet the standard contained in the criteria contained in 2.10.2 should be subject to more detailed assessment of vulnerability to the pure loss of stability failure mode by applying the criteria contained in 2.10.3.

2.10.1.3 For each condition of loading, a ship that neither meets the criteria contained in 2.10.2 nor meets the criteria contained in 2.10.3 should be subject to either:

- .1 a direct stability assessment for the pure loss of stability failure mode that is performed according to recommended specifications developed by the Organization<sup>2</sup>, from which operational guidance procedures are developed to the satisfaction of the Administration; or

<sup>1</sup> The criteria may not be applicable to a vessel with extended low weather deck due to increased likelihood of water on deck or deck-in-water. See explanatory notes for further guidance."

<sup>2</sup> To be developed.

.2 operational limitations based on outcomes of application of 2.10.3<sup>3</sup>

$GM_{min}$  should be corrected for the free surface effect as recommended in chapter 3. The use of the simplified estimation of  $GM_{min}$  described in 2.10.2.1 without initial trim effect can be applied for ships having non-even keel condition as a conservative estimation.

2.10.1.4 A detailed assessment of vulnerability according to the criteria contained in 2.10.3 or a direct stability assessment as provided in 2.10.1.3.1 may be performed without the requirement to perform a more simplified assessment in 2.10.2 or 2.10.3, respectively.

## 2.10.2 Level 1 Vulnerability Criteria for Pure Loss of Stability

2.10.2.1 A ship is considered not to be vulnerable to the pure loss of stability failure mode if

$$GM_{min} > R_{PLA}$$

Where,  $R_{PLA}$  = 0.05 m;  
 $GM_{min}$  = the minimum value of the metacentric height including free surface correction (m) calculated as either:

- a longitudinal wave passing the ship calculated as provided in 2.10.2.3;
- or
- provided in 2.10.2.2.

2.10.2.2 As provided by 2.10.2.1,  $GM_{min}$  may be determined according to:

$$GM_{min} = KB + \frac{I_L}{V} - KG, \quad \text{only if } \frac{V_D - V}{A_w(D-d)} \geq 1.0,$$

Where,

$KB$  = height of the vertical centre of buoyancy corresponding to the loading condition under consideration (m);

$KG$  = height of the vertical centre of gravity corresponding to the loading condition under consideration (m);

$I_L$  = moment of inertia of the waterplane at the draft  $d_L$  ( $m^4$ );

$V$  = volume of displacement corresponding to the loading condition under consideration ( $m^3$ );

$d_L$  =  $d - \delta d_L$  (m);

$d$  = draft amidships corresponding to the loading condition under consideration (m);

$\delta d_L$  =  $Min(d - 0.25d_{full}, \frac{L \cdot S_w}{2})$  (m);  
 and  $d - 0.25d_{full}$  should not be taken less than zero;

$S_w$  = 0.0334;

$D$  = moulded depth at side to the weather deck (m);

$V_D$  = volume of displacement at waterline equal to  $D$  ( $m^3$ ); and

$A_w$  = waterplane area at the draft equal to  $d$  ( $m^2$ ).

$d_{full}$  = draft corresponding to the fully loaded departure condition (m).

---

<sup>3</sup> Guidance to be developed by the Organization

2.10.2.3 As provided by 2.10.2.1,  $GM_{min}$  may be determined as the minimum value calculated for the ship including free surface correction (m), corresponding to the loading condition under consideration, considering the ship to be balanced in sinkage and trim on a series of waves with the following characteristics:

wavelength  $\lambda = L$ ;

wave height  $h = L \cdot S_W$ , where  $S_W = 0.0334$ ; and

the wave crest is to be centred amidships, and at  $0.1L$ ,  $0.2L$ ,  $0.3L$ ,  $0.4L$  and  $0.5L$  forward and  $0.1L$ ,  $0.2L$ ,  $0.3L$  and  $0.4L$  aft thereof.

### 2.10.3 Level 2 Vulnerability Criteria for Pure Loss of Stability

2.10.3.1 A ship is considered not to be vulnerable to the pure loss of stability failure mode if the largest value among the two criteria,  $CR_1$  and  $CR_2$ , calculated according to paragraphs 2.10.3.3 and 2.10.3.4, respectively, when underway at the service speed, is less than  $R_{PLO}$ ,

Where,  $R_{PLO} = 0.06$ .

2.10.3.2 Each of the two criteria,  $CR_1$  and  $CR_2$ , represents a weighted average of certain stability parameters for a ship considered to be statically positioned in waves of defined height ( $H_i$ ) and length ( $\lambda_i$ ) obtained from Table 2.10.3.2.

Where,

$$CR_1 = \sum_{i=1}^N W_i C1_i = \text{Weighted criterion 1};$$

$$CR_2 = \sum_{i=1}^N W_i C2_i = \text{Weighted criterion 2};$$

$W_i$  = a weighting factor obtained from Table 2.10.3.2 or a similar table of wave data satisfactory to the Administration;

$N$  = number of wave cases corresponding to non-zero probabilities in table 2.10.3.2, for which  $C1_i$  and  $C2_i$  are evaluated;

$C1_i$  = Criterion 1 evaluated according to 2.10.3.3;

$C2_i$  = Criterion 2 evaluated according to 2.10.3.4;

**Table 2.10.3.2**  
**Wave case occurrences**

$H_s$ (m)	Number of occurrences: 100 000 / Tz (s) = average zero up-crossing wave period															
	3.5	4.5	5.5	6.5	7.5	8.5	9.5	10.5	11.5	12.5	13.5	14.5	15.5	16.5	17.5	18.5
0.5	1.3	133.7	865.6	1186.0	634.2	186.3	36.9	5.6	0.7	0.1	0.0	0.0	0.0	0.0	0.0	0.0
1.5	0.0	29.3	986.0	4976.0	7738.0	5569.7	2375.7	703.5	160.7	30.5	5.1	0.8	0.1	0.0	0.0	0.0
2.5	0.0	2.2	197.5	2158.8	6230.0	7449.5	4860.4	2066.0	644.5	160.2	33.7	6.3	1.1	0.2	0.0	0.0
3.5	0.0	0.2	34.9	695.5	3226.5	5675.0	5099.1	2838.0	1114.1	337.7	84.3	18.2	3.5	0.6	0.1	0.0
4.5	0.0	0.0	6.0	196.1	1354.3	3288.5	3857.5	2685.5	1275.2	455.1	130.9	31.9	6.9	1.3	0.2	0.0
5.5	0.0	0.0	1.0	51.0	498.4	1602.9	2372.7	2008.3	1126.0	463.6	150.9	41.0	9.7	2.1	0.4	0.1
6.5	0.0	0.0	0.2	12.6	167.0	690.3	1257.9	1268.6	825.9	386.8	140.8	42.2	10.9	2.5	0.5	0.1
7.5	0.0	0.0	0.0	3.0	52.1	270.1	594.4	703.2	524.9	276.7	111.7	36.7	10.2	2.5	0.6	0.1
8.5	0.0	0.0	0.0	0.7	15.4	97.9	255.9	350.6	296.9	174.6	77.6	27.7	8.4	2.2	0.5	0.1
9.5	0.0	0.0	0.0	0.2	4.3	33.2	101.9	159.9	152.2	99.2	48.3	18.7	6.1	1.7	0.4	0.1
10.5	0.0	0.0	0.0	0.0	1.2	10.7	37.9	67.5	71.7	51.5	27.3	11.4	4.0	1.2	0.3	0.0
11.5	0.0	0.0	0.0	0.0	0.3	3.3	13.3	26.6	31.4	24.7	14.2	6.4	2.4	0.7	0.2	0.0

12.5	0.0	0.0	0.0	0.0	0.1	1.0	4.4	9.9	12.8	11.0	6.8	3.3	1.3	0.4	0.1	0.0
13.5	0.0	0.0	0.0	0.0	0.0	0.3	1.4	3.5	5.0	4.6	3.1	1.6	0.7	0.2	0.1	0.0
14.5	0.0	0.0	0.0	0.0	0.0	0.1	0.4	1.2	1.8	1.8	1.3	0.7	0.3	0.1	0.0	0.0
15.5	0.0	0.0	0.0	0.0	0.0	0.0	0.1	0.4	0.6	0.7	0.5	0.3	0.1	0.1	0.0	0.0
16.5	0.0	0.0	0.0	0.0	0.0	0.0	0.0	0.1	0.2	0.2	0.2	0.1	0.1	0.0	0.0	0.0

2.10.3.2.1 For calculating the restoring moment in waves, the following wavelength and wave height should be used:

$$\text{Length } \lambda = L; \text{ and}$$

$$\text{Height } h = 0.01 \cdot iL, \quad i = 0, 1, \dots, 10.$$

The index for each of the two criteria,  $CI_i$  and  $C2_i$ , should be calculated according to the formulations given in 2.10.3.3 and 2.10.3.4, respectively, for the loading condition under consideration with effect of free surface included and the ship assumed to be balanced in sinkage and trim in a series of waves with the characteristics set out in Table 2.10.3.2.

In these waves to be studied, the wave crest is to be centred amidships, and at  $0.1L$ ,  $0.2L$ ,  $0.3L$ ,  $0.4L$  and  $0.5L$  forward and  $0.1L$ ,  $0.2L$ ,  $0.3L$  and  $0.4L$  aft thereof.

2.10.3.2.2 For each combination of  $H_s$  and  $T_z$ ,  $W_i$  is obtained as the value in Table 2.10.3.2 divided by the amount of observations given in this table, which is associated with a  $H_i$  as calculated in 2.10.3.2.3 below and  $\lambda_i$  is taken as equal to  $L$ . The indexes for each  $H_i$ , should be linearly interpolated from the relationship between  $h$  and the indexes obtained in 2.10.3.2.1 above<sup>4</sup>.

2.10.3.2.3 The 3% largest effective wave height,  $H_i$ , for use in evaluation of the requirements is calculated by filtering ocean waves within ship length. For this purpose, an appropriate wave spectrum shape should be assumed<sup>5</sup>.

### 2.10.3.3 Criterion 1

Criterion 1 is a criterion based on a calculation of the angle of vanishing stability,  $\phi_v$ , as provided in the following formula:

$$CI_i = \begin{cases} 1 & \phi_v < R_{PL1} \\ 0 & \text{otherwise} \end{cases}$$

Where,  $R_{PL1} = 30$  degrees

The angle of vanishing stability,  $\phi_v$ , should be determined as the minimum value calculated as provided in 2.10.3.2.1 for the ship without consideration of the angle of downflooding.

<sup>4</sup> See the explanatory notes.

<sup>5</sup> See the explanatory notes.

#### 2.10.3.4 **Criterion 2**

Criterion 2 is a criterion based on a calculation of the angle of heel,  $\phi_s$ , under action of a heeling lever specified by  $R_{PL3}$  as provided in the following formula:

$$C2_i = \begin{cases} 1 & \phi_s > R_{PL2} \\ 0 & \textit{otherwise} \end{cases}$$

Where,  $R_{PL2}$  = 15 degrees for passenger ships; and  
 = 25 degrees for other ships

$R_{PL3}$  =  $8(H_i/\lambda)dF_n^2$ ;  
 $H_i$  = as provided in 2.10.3.2.3;  
 $\lambda$  = as provided in 2.10.3.2.1;  
 $d$  = as provided in 2.10.2.2; and  
 $F_n$  = as provided in 2.10.1.1.

The calculation should be performed as provided in 2.10.3.2.1.

\*\*\*





## ANNEX 2

### DRAFT AMENDMENTS TO PART B OF THE IS CODE WITH REGARD TO VULNERABILITY CRITERIA OF LEVELS 1 AND 2 FOR THE PARAMETRIC ROLLING FAILURE MODE

#### PART B

Recommendations for ships engaged in certain types of operations, certain types of ships, and additional guidelines

#### Chapter 2

#### Recommended design criteria for certain types of ships

1 A new section "2.11" is added with the following:

#### **"2.11 Assessment of ship vulnerability to the parametric rolling failure mode**

##### **2.11.1 Application**

2.11.1.1 For each condition of loading, a ship that:

- .1 meets the standard contained in the criteria contained in 2.11.2 is considered not to be vulnerable to the parametric rolling failure mode;
- .2 does not meet the standard contained in the criteria contained in 2.11.2 should be subject to more detailed assessment of vulnerability to the parametric rolling failure mode by applying the criteria contained in 2.11.3.

2.11.1.2 For each condition of loading, a ship that meets neither standard contained in the criteria contained in 2.11.2 nor 2.11.3 should be subject to either:

- .1 a direct stability assessment for the parametric rolling failure mode that is performed according to recommended specifications developed by the Organization<sup>6</sup>, from which operational guidance procedures are developed to the satisfaction of the Administration; or
- .2 operational limitations based on outcomes of application of 2.11.3 with guidance to be developed by the Organization.

2.11.1.3 A detailed assessment of vulnerability according to the criteria contained in 2.11.3 or a direct stability assessment as provided in 2.11.1.2.1 may be performed without the requirement to perform a more simplified assessment in 2.11.2 or 2.11.3, respectively.

---

<sup>6</sup> To be developed.

## 2.11.2 Level 1 Vulnerability Criteria for Parametric Rolling

2.11.2.1 A ship is considered not to be vulnerable to the parametric rolling failure mode if:

$$\frac{\Delta GM_1}{GM_C} \leq R_{PR}$$

Where,

$$R_{PR} = 1.87, \text{ if the ship has a sharp bilge}^7; \text{ and, otherwise,}$$

$$= 0.17 + 0.425 \left( \frac{100A_k}{LB} \right), \text{ if } C_m \geq 0.96;$$

$$= 0.17 + (10.625 \times C_m - 9.775) \left( \frac{100A_k}{LB} \right), \text{ if } 0.94 < C_m < 0.96;$$

$$= 0.17 + 0.2125 \left( \frac{100A_k}{LB} \right), \text{ if } C_m \leq 0.94; \text{ and}$$

$$\left( \frac{100A_k}{LB} \right) \text{ should not exceed } 4;$$

$GM_C$  = metacentric height of the loading condition in calm water including free surface correction (m);

$\Delta GM_1$  = the amplitude of the variation of the metacentric height (m) calculated as either:

- a longitudinal wave the ship calculated as provided in 2.11.2.3; or
- provided in 2.11.2.2.

$C_m$  = midship section coefficient of the fully loaded condition in calm water;

$A_k$  = total overall projected area of the bilge keels (no other appendages)<sup>8</sup> (m<sup>2</sup>);

$L$  = Length of the ship (m); and

$B$  = moulded breadth of the ship (m).

2.11.2.2 As provided by 2.11.2.1,  $\Delta GM$  may be determined according to:

$$\Delta GM_1 = \frac{I_H - I_L}{2V}, \text{ only if } \frac{V_D - V}{A_w(D - d)} \geq 1.0,$$

Where,

$D$  = moulded depth at side to the weather deck (m);

$V_D$  = volume of displacement at a waterline equal to  $D$  and at zero trim (m<sup>3</sup>);

$V$  = volume of displacement corresponding to the loading condition under consideration (m<sup>3</sup>);

$A_w$  = waterplane area at the draft equal to  $d$  (m<sup>2</sup>);

$d$  = draft amidships corresponding to the loading condition under consideration (m);

$$\delta d_H = \text{Min} \left( D - d, \frac{L \cdot S_w}{2} \right) \text{ (m);}$$

<sup>7</sup> See the explanatory notes.

<sup>8</sup> See the explanatory notes.

$$\delta d_L = \text{Min}(d - 0.25d_{full}, \frac{L \cdot S_W}{2}) \text{ (m)}^9,$$

and  $d - 0.25d_{full}$  should not be taken less than zero;

$$d_H = d + \delta d_H \text{ (m);}$$

$$d_L = d - \delta d_L \text{ (m);}$$

$$S_W = 0.0167;$$

$$L = \text{length as defined in 2.11.2.1 (m);}$$

$$I_H = \text{moment of inertia of the waterplane at the draft } d_H \text{ and at zero trim (m}^4\text{);}$$

$$I_L = \text{moment of inertia of the waterplane at the draft } d_L \text{ and at zero trim (m}^4\text{);}$$

$$d_{full} = \text{draft corresponding to the fully loaded departure condition (m).}$$

2.11.2.3 As provided by 2.11.2.1,  $\Delta GM_I$  may be determined as one-half the difference between the maximum and minimum values of the metacentric height calculated for the ship, including free surface correction, corresponding to the loading condition under consideration, considering the ship to be balanced in sinkage and trim on a series of waves with the following characteristics:

wavelength  $\lambda = L$ ;

wave height  $h = L \cdot S_W$ , where  $S_W = 0.0167$ ; and

the wave crest is to be centred amidships, and at  $0.1L$ ,  $0.2L$ ,  $0.3L$ ,  $0.4L$  and  $0.5L$  forward and  $0.1L$ ,  $0.2L$ ,  $0.3L$  and  $0.4L$  aft thereof.

### 2.11.3 Level 2 Vulnerability Criteria for Parametric Roll

2.11.3.1 A ship is considered not to be vulnerable to the parametric rolling failure mode if  $R_{PRO}$  is greater than either:

- .1 the value of  $CI$  calculated according to paragraph 2.11.3.2; or
- .2 the value of  $C2$  calculated according to paragraph 2.11.3.3,

Where,

$$R_{PRO} = 0.06$$

2.11.3.2 The value for  $CI$  is calculated as a weighted average from a set of waves specified in 2.11.3.2.3.

$$CI = \sum_{i=1}^N W_i C_i$$

Where,

$W_i$  = the weighting factor for the respective wave specified in 2.11.3.2.3;

$C_i$  = 0, if the requirements of either the variation of  $GM$  in waves contained in 2.11.3.2.1 or the ship speed in waves contained in 2.11.3.2.2 is satisfied; and

= 1, if not;

$N$  = the number of wave cases as specified in 2.11.3.2.3.

<sup>9</sup> See the explanatory notes.

2.11.3.2.1 The requirement for the variation of  $GM$  in waves is satisfied if, for each wave specified in 2.11.3.2.3:

$$GM(H_i, \lambda_i) > 0 \quad \text{and} \quad \frac{\Delta GM(H_i, \lambda_i)}{GM(H_i, \lambda_i)} < R_{PR} \quad ,$$

Where,

- $R_{PR}$  = as defined in 2.11.2.1;
- $\Delta GM(H_i, \lambda_i)$  = one-half the difference between the maximum and minimum values of the metacentric height calculated for the ship (m), corresponding to the loading condition under consideration, considering the ship to be balanced in sinkage and trim on a series of waves characterized by a  $H_i$ , and a  $\lambda_i$ ;
- $GM(H_i, \lambda_i)$  = the average value of the metacentric height calculated for the ship (m), corresponding to the loading condition under consideration<sup>10</sup>, considering the ship to be balanced in sinkage and trim on a series of waves characterized by a  $H_i$ , and a  $\lambda_i$ ;
- $H_i$  = a wave height specified in 2.11.3.2.3 (m); and
- $\lambda_i$  = a wave length specified in 2.11.3.2.3 (m).

2.11.3.2.2 The requirement for the ship speed in waves is satisfied if, for a wave specified in 2.11.3.2.3:

$$V_{PRi} > V_s$$

Where,

- $V_s$  = the service speed (m/s); and
- $V_{PRi}$  = the reference ship speed (m/s) corresponding to parametric resonance conditions, when  $GM(H_i, \lambda_i) > 0$ :
- $$= \left| \frac{2\lambda_i}{T_\phi} \cdot \sqrt{\frac{GM(H_i, \lambda_i)}{GM_C}} - \sqrt{g \frac{\lambda_i}{2\pi}} \right|$$
- $T_\phi$  = the roll natural period in calm water (s);
- $GM_C$  = as defined in 2.11.2.1;
- $GM(H_i, \lambda_i)$  = as defined in 2.11.3.2.1 (m);
- $\lambda_i$  = a wave length specified in 2.11.3.2.3 (m);
- $g$  = gravitational acceleration of 9.81 m/s<sup>2</sup>; and
- $||$  = the absolute value operation

2.11.3.2.3 The specified wave cases for evaluation of the requirements contained in 2.11.3.2.1 and 2.11.3.2.2 are presented in Table 2.11.3.2.3. In Table 2.11.3.2.3,  $W_i$ ,  $H_i$ ,  $\lambda_i$  are as defined in 2.11.3.2 and 2.11.3.2.1.

<sup>10</sup> See the explanatory notes

**Table 2.11.3.2.3**  
**Wave cases**

Wave case number	Weight $W_i$	Wave length $\lambda_i$ (m)	Wave height $H_i$ (m)
1	0.000013	22.574	0.350
2	0.001654	37.316	0.495
3	0.020912	55.743	0.857
4	0.092799	77.857	1.295
5	0.199218	103.655	1.732
6	0.248788	133.139	2.205
7	0.208699	166.309	2.697
8	0.128984	203.164	3.176
9	0.062446	243.705	3.625
10	0.024790	287.931	4.040
11	0.008367	335.843	4.421
12	0.002473	387.440	4.769
13	0.000658	442.723	5.097
14	0.000158	501.691	5.370
15	0.000034	564.345	5.621
16	0.000007	630.684	5.950

2.11.3.2.4 In the calculation of  $\Delta GM(H_i, \lambda_i)$  and  $GM(H_i, \lambda_i)$  in paragraph 2.11.3.2.1, the wave crest should be located at amidship, and at  $0.1 \lambda_i$ ,  $0.2 \lambda_i$ ,  $0.3 \lambda_i$ ,  $0.4 \lambda_i$ , and  $0.5 \lambda_i$  forward and  $0.1 \lambda_i$ ,  $0.2 \lambda_i$ ,  $0.3 \lambda_i$ , and  $0.4 \lambda_i$  aft thereof.

2.11.3.3 The value of  $C2$  is calculated as an average of values of  $C2(F_{ni})$ , each of which is a weighted average from the set of waves specified in 2.11.3.4.2, for each set of Froude numbers and wave directions specified:

$$C2 = \left[ \sum_{i=1}^3 C2_h(F_{ni}) + C2_h(0) + \sum_{i=1}^3 C2_f(F_{ni}) \right] / 7$$

Where,

$C2_h(F_{ni})$  =  $C2_h(F_{ni})$  calculated as specified in 2.11.3.3.1 with the ship proceeding in head waves with a speed equal to  $V_i$ ;

$C2_f(F_{ni})$  =  $C2_f(F_{ni})$  calculated as specified in 2.11.3.3.1 with the ship proceeding in following waves with a speed equal to  $V_i$ ;

$F_{ni}$  =  $V_i / \sqrt{Lg}$  = Froude number corresponding to ship speed,  $V_i$ ;

$V_i$  =  $V_s K_i$ , means the ship speed (m/s)

$V_s$  = ship service speed (m/s);

$g$  = as defined in 2.11.3.2.2;

$K_i$  = as obtained from Table 2.11.3.3<sup>11</sup>; and

$L$  = Length as defined in 2.11.2.1 (m).

<sup>11</sup> See the explanatory notes

**Table 2.11.3.3**  
**Corresponding speed factor,  $K_i$**

$i$	$K_i$
1	1.0
2	0.866
3	0.50

2.11.3.3.1 The value of  $C2(Fn)$  is calculated as a weighted average from the set of waves specified in 2.11.3.4.2 for a given Froude number and wave direction.

$$C2_h(Fn) = \sum_{i=1}^N W_i C_i$$

$$C2_f(Fn) = \sum_{i=1}^N W_i C_i$$

Where,

$W_i$  = the weighting factor for the respective wave cases specified in 2.11.3.4.2;

$C_i$  = 1, if the maximum roll angle evaluated according to 2.11.3.4 exceeds 25 degrees, and

= 0, otherwise;

$N$  = total number of wave cases for which the maximum roll angle is evaluated for a combination of speed and ship heading.

2.11.3.4 The maximum roll angle in head and following waves is evaluated as recommended in 2.11.3.4.1 for each speed,  $V_i$ , defined in 2.11.3.3. For each evaluation, the calculation of stability in waves should assume the ship to be balanced in sinkage and trim on a series of waves with the following characteristics:

wavelength,  $\lambda = L$ ;

wave height,  $h_j = 0.01 \cdot jL$ , where  $j=0,1,\dots,10$ .

For each wave height,  $h_j$ , the maximum roll angle is evaluated.

2.11.3.4.1 The evaluation of roll angle should be carried out using a method in accordance with the guidelines<sup>12</sup>.

2.11.3.4.2  $W_i$  is obtained from Table 2.11.3.4.2 or an equivalent table of wave data satisfactory to the Administration. Each cell of the Table corresponds to an average zero up-crossing wave period,  $T_z$ , and a significant wave height,  $H_s$ . With these two values, a representative wave height,  $Hr_i$ , should be calculated using a procedure<sup>13</sup>. The maximum roll angle, corresponding to the representative wave height,  $Hr_i$ , is obtained by linear interpolation of the maximum roll angles for different wave heights,  $h_j$ , obtained in 2.11.3.4.1. This maximum roll angle should be used for evaluation of  $C_i$  given in 2.11.3.3.1.

<sup>12</sup> See the explanatory notes.

<sup>13</sup> See the explanatory notes.

**Table 2.11.3.4.2**  
**Wave case occurrences**

	Number of occurrences: 100 000 / $T_z$ (s) = average zero up-crossing wave period															
$H_s$ (m)	3.5	4.5	5.5	6.5	7.5	8.5	9.5	10.5	11.5	12.5	13.5	14.5	15.5	16.5	17.5	18.5
0.5	1.3	133.7	865.6	1186.0	634.2	186.3	36.9	5.6	0.7	0.1	0.0	0.0	0.0	0.0	0.0	0.0
1.5	0.0	29.3	986.0	4976.0	7738.0	5569.7	2375.7	703.5	160.7	30.5	5.1	0.8	0.1	0.0	0.0	0.0
2.5	0.0	2.2	197.5	2158.8	6230.0	7449.5	4860.4	2066.0	644.5	160.2	33.7	6.3	1.1	0.2	0.0	0.0
3.5	0.0	0.2	34.9	695.5	3226.5	5675.0	5099.1	2838.0	1114.1	337.7	84.3	18.2	3.5	0.6	0.1	0.0
4.5	0.0	0.0	6.0	196.1	1354.3	3288.5	3857.5	2685.5	1275.2	455.1	130.9	31.9	6.9	1.3	0.2	0.0
5.5	0.0	0.0	1.0	51.0	498.4	1602.9	2372.7	2008.3	1126.0	463.6	150.9	41.0	9.7	2.1	0.4	0.1
6.5	0.0	0.0	0.2	12.6	167.0	690.3	1257.9	1268.6	825.9	386.8	140.8	42.2	10.9	2.5	0.5	0.1
7.5	0.0	0.0	0.0	3.0	52.1	270.1	594.4	703.2	524.9	276.7	111.7	36.7	10.2	2.5	0.6	0.1
8.5	0.0	0.0	0.0	0.7	15.4	97.9	255.9	350.6	296.9	174.6	77.6	27.7	8.4	2.2	0.5	0.1
9.5	0.0	0.0	0.0	0.2	4.3	33.2	101.9	159.9	152.2	99.2	48.3	18.7	6.1	1.7	0.4	0.1
10.5	0.0	0.0	0.0	0.0	1.2	10.7	37.9	67.5	71.7	51.5	27.3	11.4	4.0	1.2	0.3	0.1
11.5	0.0	0.0	0.0	0.0	0.3	3.3	13.3	26.6	31.4	24.7	14.2	6.4	2.4	0.7	0.2	0.1
12.5	0.0	0.0	0.0	0.0	0.1	1.0	4.4	9.9	12.8	11.0	6.8	3.3	1.3	0.4	0.1	0.0
13.5	0.0	0.0	0.0	0.0	0.0	0.3	1.4	3.5	5.0	4.6	3.1	1.6	0.7	0.2	0.1	0.0
14.5	0.0	0.0	0.0	0.0	0.0	0.1	0.4	1.2	1.8	1.8	1.3	0.7	0.3	0.1	0.0	0.0
15.5	0.0	0.0	0.0	0.0	0.0	0.0	0.1	0.4	0.6	0.7	0.5	0.3	0.1	0.1	0.0	0.0
16.5	0.0	0.0	0.0	0.0	0.0	0.0	0.0	0.1	0.2	0.2	0.2	0.1	0.1	0.0	0.0	0.0

\*\*\*





## ANNEX 3

### DRAFT AMENDMENTS TO PART B OF THE IS CODE WITH REGARD TO VULNERABILITY CRITERIA OF LEVELS 1 AND 2 FOR THE SURF-RIDING / BROACHING FAILURE MODE

#### PART B

Recommendations for ships engaged in certain types of operations, certain types of ships, and additional guidelines

#### Chapter 2

#### Recommended design criteria for certain types of ships

1 A new section "2.12" is added with the following:

#### "2.12 Assessment of ship vulnerability to the surf-riding/broaching failure mode

##### 2.12.1 Application

2.12.1.1 For ships that do not meet the standard contained in 2.12.2, the procedures of ship-handling on how to avoid dangerous conditions for surf-riding/broaching recommended in Section 4.2.1 of the "*Revised guidance to the master for avoiding dangerous situations in adverse weather and sea conditions*," MSC.1/Circ.1228, may apply subject to the approval of the Administration<sup>14</sup> as an alternative for 2.12.2

2.12.1.2 For each condition of loading, a ship that:

- .1 meets the standard contained in the criteria contained in 2.12.2 is considered not to be vulnerable to the surf-riding/broaching failure mode;
- .2 does not meet the standard contained in the criteria contained in 2.12.2 should be subject to more detailed assessment of vulnerability to the surf-riding/broaching stability failure mode by applying the criteria contained in 2.12.3.

2.12.1.3 For each condition of loading, a ship that meets neither standard contained in the criteria contained in 2.12.2 nor 2.12.3 should be subject to either:

- .1 a direct stability assessment for the surf-riding/broaching failure mode that is performed according to recommended specifications, from which operational guidance procedures are developed to the satisfaction of the Administration; or
- .2 ship specific operational limitations based on outcomes of application of 2.12.3 in accordance with guidance to be developed by the Organization.

2.12.1.4 A detailed assessment of vulnerability according to the criteria contained in 2.12.3 or a direct stability assessment as provided in 2.12.1.3.1 may be performed without the requirement to perform a more simplified assessment in 2.12.2 or 2.12.3, respectively.

---

<sup>14</sup> See the explanatory notes.

### 2.12.2 Level 1 Vulnerability Criteria for surf-riding/broaching

2.12.2.1 A ship is considered not to be vulnerable to the surf-riding/broaching failure mode if 2.12.2.1.1 or 2.12.2.1.2 is true:

- .1  $L > 200\text{m};$
- .2  $Fn \leq 0.3,$

Where,  $Fn$  = Froude number =  $V_s / \sqrt{L g}$   
 $V_s$  = service speed in calm water (m/s);  
 $L$  = Length of ship in metres; and  
 $g$  = the gravitation acceleration of 9.81 m/s<sup>2</sup>

### 2.12.3 Level 2 Vulnerability Criteria for Surf-riding/Broaching

2.12.3.1 A ship is considered not to be vulnerable to the surf-riding/broaching failure mode if the value of  $C$  calculated according to paragraph 2.12.3.2 is less than  $R_{SR}$ ;

2.12.3.2

$$C = \sum_{HS} \sum_{TZ} \left( W2(H_s, T_z) \frac{\sum_{i=1}^{N_\lambda} \sum_{j=1}^{N_a} W_{ij} C2_{ij}}{\sum_{i=1}^{N_\lambda} \sum_{j=1}^{N_a} W_{ij}} \right)$$

Where,

- $R_{SR}$  = 0.005
- $W2(H_s, T_z)$  = the weighting factor of short-term sea state specified in 2.12.3.3 as a function of the significant wave height,  $H_s$ , and the zero-crossing wave period,  $T_z$ ;
- $W_{ij}$  = a statistical weight of a wave specified in 2.12.3.3 with steepness  $(H/\lambda)_j$  and wavelength to ship length ratio  $(\lambda/L)_i$  calculated with the joint distribution of local wave steepness and lengths, which is, with the specified discretization  $N_\lambda = 80$  and  $N_a = 100$ .
- $C2_{ij}$  = the number specified in 2.12.3.5.

2.12.3.3 The value of  $W2(H_s, T_z)$  is obtained as the value in Table 2.12.3.3.2 divided by the amount of observations given in this table. Other sources of wave statistics can be used on the discretion of the Administration.

**Table 2.12.3.3.2**  
**Wave case occurrences**

Number of occurrences: 100 000 / $T_z$ (s) = average zero up-crossing wave period																
$T_z$ (s) ►	3.5	4.5	5.5	6.5	7.5	8.5	9.5	10.5	11.5	12.5	13.5	14.5	15.5	16.5	17.5	18.5
$H_s$ (m) ▼																
0.5	1.3	133.7	865.6	1186.0	634.2	186.3	36.9	5.6	0.7	0.1	0.0	0.0	0.0	0.0	0.0	0.0
1.5	0.0	29.3	986.0	4976.0	7738.0	5569.7	2375.7	703.5	160.7	30.5	5.1	0.8	0.1	0.0	0.0	0.0
2.5	0.0	2.2	197.5	2158.8	6230.0	7449.5	4860.4	2066.0	644.5	160.2	33.7	6.3	1.1	0.2	0.0	0.0
3.5	0.0	0.2	34.9	695.5	3226.5	5675.0	5099.1	2838.0	1114.1	337.7	84.3	18.2	3.5	0.6	0.1	0.0
4.5	0.0	0.0	6.0	196.1	1354.3	3288.5	3857.5	2685.5	1275.2	455.1	130.9	31.9	6.9	1.3	0.2	0.0
5.5	0.0	0.0	1.0	51.0	498.4	1602.9	2372.7	2008.3	1126.0	463.6	150.9	41.0	9.7	2.1	0.4	0.1

Number of occurrences: 100 000 / $T_z$ (s) = average zero up-crossing wave period																	
$T_z$ (s) ▶	3.5	4.5	5.5	6.5	7.5	8.5	9.5	10.5	11.5	12.5	13.5	14.5	15.5	16.5	17.5	18.5	
$H_s$ (m) ▼	3.5	4.5	5.5	6.5	7.5	8.5	9.5	10.5	11.5	12.5	13.5	14.5	15.5	16.5	17.5	18.5	
6.5	0.0	0.0	0.2	12.6	167.0	690.3	1257.9	1268.6	825.9	386.8	140.8	42.2	10.9	2.5	0.5	0.1	
7.5	0.0	0.0	0.0	3.0	52.1	270.1	594.4	703.2	524.9	276.7	111.7	36.7	10.2	2.5	0.6	0.1	
8.5	0.0	0.0	0.0	0.7	15.4	97.9	255.9	350.6	296.9	174.6	77.6	27.7	8.4	2.2	0.5	0.1	
9.5	0.0	0.0	0.0	0.2	4.3	33.2	101.9	159.9	152.2	99.2	48.3	18.7	6.1	1.7	0.4	0.1	
10.5	0.0	0.0	0.0	0.0	1.2	10.7	37.9	67.5	71.7	51.5	27.3	11.4	4.0	1.2	0.3	0.1	
11.5	0.0	0.0	0.0	0.0	0.3	3.3	13.3	26.6	31.4	24.7	14.2	6.4	2.4	0.7	0.2	0.1	
12.5	0.0	0.0	0.0	0.0	0.1	1.0	4.4	9.9	12.8	11.0	6.8	3.3	1.3	0.4	0.1	0.0	
13.5	0.0	0.0	0.0	0.0	0.0	0.3	1.4	3.5	5.0	4.6	3.1	1.6	0.7	0.2	0.1	0.0	
14.5	0.0	0.0	0.0	0.0	0.0	0.1	0.4	1.2	1.8	1.8	1.3	0.7	0.3	0.1	0.0	0.0	
15.5	0.0	0.0	0.0	0.0	0.0	0.0	0.1	0.4	0.6	0.7	0.5	0.3	0.1	0.1	0.0	0.0	
16.5	0.0	0.0	0.0	0.0	0.0	0.0	0.0	0.1	0.2	0.2	0.2	0.1	0.1	0.0	0.0	0.0	

2.12.3.4 The value of  $W_{ij}$  should be calculated using the following formula<sup>15</sup>:

$$W_{ij} = \frac{4\sqrt{g}}{\pi v} \frac{L^{5/2} T_{01}}{(H_s)^3} s_j^2 r_i^{3/2} \left( \frac{\sqrt{1+v^2}}{1+\sqrt{1+v^2}} \right) \Delta r \Delta s \cdot \exp \left[ -2 \left( \frac{L \cdot r_i \cdot s_j}{H_s} \right)^2 \left\{ 1 + \frac{1}{v^2} \left( 1 - \sqrt{\frac{g T_{01}^2}{2\pi r_i L}} \right)^2 \right\} \right]$$

Where,  $v$  = 0.4256;  
 $L$  = as defined in 2.12.2.1;  
 $T_{01}$  = 1.086  $T_z$   
 $s_j$  =  $(H/\lambda)_j$  = wave steepness varies from 0.03 to 0.15 with the increment  $\Delta s = 0.0012$ ; and  
 $r_i$  =  $(\lambda/L)_i$  = wavelength to ship length ratio varies from 1.0 to 3.0 with the increment  $\Delta r = 0.025$ .

2.12.3.5 The value of  $C2_{ij}$  is calculated for each wave as follows:

$$C2_{ij} = \begin{cases} 1 & \text{if } Fn > Fn_{cr}(r_j, s_i) \\ 0 & \text{if } Fn \leq Fn_{cr}(r_j, s_i) \end{cases}$$

Where,  $Fn_{cr}$  = a critical Froude number corresponding to the threshold of surf-riding (surf-riding occurring under any initial condition) which should be calculated in accordance with 2.12.3.5.1 for the regular wave with steepness  $s_j$  and wavelength to ship length ratio  $r_i$ .

2.12.3.5.1 The critical Froude number,  $Fn_{cr}$ , is calculated using the following formula:

$$Fn_{cr} = u_{cr} / \sqrt{L g},$$

Where,  $u_{cr}$  = the critical ship speed (m/s) determined by solving the equation given in 2.12.3.5.2 with the critical propulsor revolutions,  $n_{cr}$ ;

$L$  = as defined in 2.12.2.1; and  
 $g$  = the gravitation acceleration of 9.81 m/s<sup>2</sup>.

<sup>15</sup> See the explanatory notes.

2.12.3.5.2 The critical ship speed,  $u_{cr}$ , is determined by solving the following equation with the critical propulsor revolutions,  $n_{cr}$ :

$$T_e(u_{cr}; n_{cr}) - R(u_{cr}) = 0$$

Where,  $R(u_{cr})$  = the calm water resistance of the ship at the ship speed of  $u_{cr}$ , see 2.12.3.5.3;  
 $T_e(u_{cr}; n_{cr})$  = the thrust delivered by the ship's propulsor(s) in calm water determined in accordance with 2.12.3.5.4; and  
 $n_{cr}$  = the commanded number of revolutions of propulsor(s) corresponding to the threshold of surf-riding (surf-riding occurs under any initial conditions), see 2.12.3.5.6.

2.12.3.5.3 Calm water resistance,  $R(u)$ , is approximated based on available data with a polynomial fit suitable to represent the characteristics of the resistance for the vessel in question<sup>16</sup>. The fit should be appropriate to ensure the resistance is continuously increasing as a function of speed in the appropriate range.

2.12.3.5.4 For a ship using one propeller as the main propulsor, the propulsor thrust,  $T_e(u; n)$ , in calm water may be approximated using a second power polynomial:

$$T_e(u; n) = (1 - t_p) \rho n^2 D_p^4 \{ \kappa_0 + \kappa_1 J + \kappa_2 J^2 \} \text{ (N)}$$

Where,  $u$  = a speed of the ship (m/s) in calm water;  
 $n$  = the commanded number of revolutions of propulsor (1/s);  
 $t_p$  = approximated thrust deduction<sup>16</sup>;  
 $w_p$  = approximated wake fraction<sup>16</sup>;  
 $D_p$  = propeller diameter (m);  
 $\kappa_0, \kappa_1, \kappa_2$  = approximation coefficients for the approximated propeller thrust coefficient in calm water;  
 $J = \frac{u(1 - w_p)}{nD_p}$  = advance ratio; and  
 $\rho$  = density of salt water (1025 kg/m<sup>3</sup>).

In case of a ship having multiple propellers, the overall thrust can be calculated by summing the effect of the individual propellers calculated as indicated above.

For a ship using propulsor(s) other than propeller(s), the propulsor thrust may be evaluated by a method appropriate to the type of propulsor used to the satisfaction of the Administration.

2.12.3.5.5 The amplitude of wave surging force is calculated as:

$$f = \rho g k \frac{H}{2} \sqrt{F_C^2 + F_S^2} \text{ (N)}$$

Where,  $\rho$  = density of salt water (1025 kg/m<sup>3</sup>);  
 $g$  = the gravitation acceleration of 9.81 m/s<sup>2</sup>;  
 $k_i = \frac{2\pi}{r_i L}$  = wave number (1/m);  
 $H_{ij} = s_j r_i L$  = wave height (m);

<sup>16</sup> See the explanatory notes.

---

$s_j$	=	as defined in 2.12.3.4;
$r_i$	=	as defined in 2.12.3.4;
$F_C$	=	$\sum_{i=1}^N \Delta x_i S(x_i) \sin kx_i \exp(-0.5k \cdot d(x_i))$ (m <sup>3</sup> )
$F_S$	=	$\sum_{i=1}^N \Delta x_i S(x_i) \cos kx_i \exp(-0.5k \cdot d(x_i))$ (m <sup>3</sup> )
		$F_C$ and $F_S$ are parts of the Froude-Krylov component of the wave surging force;
$x_i$	=	longitudinal distance from the midship to a station (m), positive for a bow section;
$d(x_i)$	=	draft at station $i$ in calm water (m);
$S(x_i)$	=	area of submerged portion of the ship at station $i$ in calm water (m <sup>2</sup> ), and
$N$	=	number of stations.

2.12.3.5.6 The critical number of revolutions of the propulsor corresponding to the surf-riding threshold,  $n_{cr}$ , may be calculated using a numerical iteration method, for which a particular form of the equation depends on the approximation of resistance in calm water. Recommended numerical iteration methods for this calculation are contained in the explanatory notes."

\*\*\*



**PART B**  
**Recommendations for ships engaged in certain types of operations, certain types of ships, and additional guidelines**

**Chapter 2**  
**Recommended design criteria for certain types of ships**

*A new section "2.13" is added with the following:*

**"2.13 Assessment of ship vulnerability to the dead ship condition failure mode<sup>1</sup>**

**2.13.1 Application**

2.13.1.1 For each condition of loading, a ship that:

- .1 meets the standard contained in the criteria contained in 2.13.2 is considered not to be vulnerable to the dead ship condition failure mode;
- .2 does not meet the standard contained in the criteria contained in 2.13.2 should be subject to more detailed assessment of vulnerability to the failure mode by applying the criteria contained in 2.13.3.

2.13.1.2 For each condition of loading, a ship that neither meets the criteria contained in 2.13.2 nor meets the criteria contained in 2.13.3 should be subject to a direct stability assessment for the dead ship condition failure mode that is performed according to recommended specifications developed by the Organization<sup>2</sup>.

2.13.1.3 A detailed assessment of vulnerability according to the criteria contained in 2.13.3 or a direct stability assessment as provided in 2.13.1.2 may be performed without the requirement to perform a more simplified assessment in 2.13.2 or 2.13.3, respectively.

**2.13.2 Level 1 Vulnerability Criteria for Dead ship condition**

2.13.2.1 A ship in the specified loading condition is considered not to be vulnerable in dead ship condition when fulfilling the requirements of the severe wind and rolling criterion (weather criterion) in Section 2.3 of Part A, but using the value of wave steepness factor,  $s$ , from Table 2.13.2.1 in lieu of that obtained from Table 2.3.4-4 in Section 2.3 of Part A.<sup>3</sup>

---

<sup>1</sup> Application details are reported in the Explanatory Notes

<sup>2</sup> To be developed.

<sup>3</sup> The definition of  $A_k$  in 2.13.2.1 is that in Section 2.3 of Part A.

Table 2.13.2.1 – Values of wave steepness factor,  $s$

Rolling period, $T$ (s)	Wave steepness factor, $s$
≤ 6	0.100
7	0.098
8	0.093
12	0.065
14	0.053
16	0.044
18	0.038
20	0.032
22	0.028
24	0.025
26	0.023
28	0.021
≥ 30	0.020

Where,

- $T$  = rolling period as determined in 2.3.4 of Section 2.3 of Part A (s);  
 $s$  = wave steepness =  $H / \lambda$  ;  
 $H$  = wave height (m); and  
 $\lambda$  = wave length (m).

### 2.13.3 Level 2 Vulnerability Criteria for Dead ship condition

2.13.3.1 A ship is considered not to be vulnerable to the dead ship condition failure mode if:

$$C \leq R_{DS0}$$

- Where,  $R_{DS0}$  = [0.06][0.04];  
 $C$  = a long-term probability index that measures the vulnerability of the ship to a stability failure in the dead ship condition based on the probability of occurrence of short-term environmental conditions as specified according to 2.13.3.2.

2.13.3.2 The value for  $C$  is calculated as a weighted average from a set of short-term environmental conditions specified in 2.13.3.3.

$$C = \sum_{i=1}^N W_i C_{S,i}$$

Where,

- $W_i$  = the weighting factor for the short-term environmental condition specified in 2.13.3.3;  
 $C_{S,i}$  = the short-term dead ship stability failure index for the short-term environmental condition under consideration calculated as specified in 2.13.3.2.1;  
 $N$  = the number of considered short-term environmental conditions according to 2.13.3.3.



2.13.3.2.1 The short-term dead ship stability failure index,  $C_{S,i}$ , for the short-term environmental condition under consideration is a measure of the probability that the ship will exceed specified heel angles at least once in the exposure time considered, taking into account an effective relative angle between the vessel and the waves. Each index  $C_{S,i}$  is calculated according to the following formula:

$$C_{S,i} = 1, \text{ if either:}$$

- .1 the mean wind heeling lever  $\bar{l}_{wind,tot}$  (according to 2.13.3.2.2) exceeds the righting lever ( $GZ$ ) at each angle of heel to leeward, or
- .2 the stable heel angle under the action of steady wind,  $\phi_S$ , is greater than the angle of failure to leeward,  $\phi_{fail,+}$ ;

$$= 1 - \exp(-\lambda_{EA} \cdot T_{exp}), \text{ otherwise;}$$

Where,

The GZ curve, as well as all relevant derived quantities, are to be calculated with free surface correction taken into account<sup>4</sup>;

Heel angles are to be taken as positive to leeward and negative to windward;

$T_{exp}$  = exposure time, to be taken as equal to 3600 s;

$$\lambda_{EA} = \frac{1}{T_{z,C_S}} \cdot \left[ \exp\left(-\frac{1}{2 \cdot RI_{EA+}^2}\right) + \exp\left(-\frac{1}{2 \cdot RI_{EA-}^2}\right) \right] (1/s);$$

$$RI_{EA+} = \frac{\sigma_{C_S}}{\Delta\phi_{res,EA+}};$$

$$RI_{EA-} = \frac{\sigma_{C_S}}{\Delta\phi_{res,EA-}};$$

$T_{z,C_S}$  = reference average zero up-crossing period of the effective relative roll motion under the action of wind and waves determined according to 2.13.3.2.3 (s);

$\sigma_{C_S}$  = standard deviation of the effective relative roll motion under the action of wind and waves determined according to 2.13.3.2.3 (rad);

$\Delta\phi_{res,EA+}$  = range of residual stability to the leeward equivalent area limit angle, to be calculated as

$$\phi_{EA+} - \phi_S, \text{ (rad);}$$

$\Delta\phi_{res,EA-}$  = range of residual stability to the windward equivalent area limit angle, to be calculated as

$$\phi_S - \phi_{EA-} \text{ (rad);}$$

<sup>4</sup> In accordance with Part B, 3.1

$\phi_{EA-}$  = equivalent area virtual limit angle to leeward, to be calculated as

$$\phi_{EA+} = \phi_S + \left( \frac{2 \cdot A_{res,+}}{GM_{res}} \right)^{1/2} \text{ (rad);}$$

$\phi_{EA+}$  = equivalent area virtual limit angle to windward, to be calculated as

$$\phi_{EA-} = \phi_S - \left( \frac{2 \cdot A_{res,-}}{GM_{res}} \right)^{1/2} \text{ (rad);}$$

$\phi_S$  = stable heel angle under the action of steady wind calculated as the first intersection between the righting lever curve ( $GZ$  curve) and the mean wind heeling lever,  $\bar{l}_{wind,tot}$ , determined according to 2.13.3.2.2 (rad);

$A_{res,+}$  = area under the residual righting lever curve (i.e.  $GZ - \bar{l}_{wind,tot}$ ) from  $\phi_S$  to  $\phi_{fail,+}$  (m·rad);

$A_{res,-}$  = area under the residual righting lever curve (i.e.  $GZ - \bar{l}_{wind,tot}$ ) from  $\phi_{fail,-}$  to  $\phi_S$  (m·rad);

$GM_{res}$  = residual metacentric height, to be taken as the slope of the residual righting lever curve (i.e.  $GZ - \bar{l}_{wind,tot}$ ) at  $\phi_S$  (m);

$\phi_{fail,+}$  = angle of failure to leeward, to be taken as  $\min\{\phi_{VW,+}, \phi_{crit,+}\}$  (rad);

$\phi_{fail,-}$  = angle of failure to windward, to be taken as  $\max\{\phi_{VW,-}, \phi_{crit,-}\}$  (rad);

$\phi_{VW,+}$  = angle of second intercept to leeward between the mean wind heeling lever  $\bar{l}_{wind,tot}$  and  $GZ$  curve;

$\phi_{VW,-}$  = angle of second intercept to windward between the mean wind heeling lever  $\bar{l}_{wind,tot}$  and  $GZ$  curve;

$\phi_{crit,+}$  = critical angle to leeward, to be taken as  $\min\{\phi_{f,+}, 50 \text{ deg}\}$  (rad);

$\phi_{crit,-}$  = critical angle to windward, to be taken as  $\max\{\phi_{f,-}, -50 \text{ deg}\}$  (rad);

$\phi_{f,+}, \phi_{f,-}$  = angles of downflooding to leeward and windward, respectively, in accordance with the definition in Part A, 2.3.1.4 (rad);

2.13.3.2.2 The mean wind heeling lever  $\bar{l}_{wind,tot}$  is a constant value at all angles of heel and is calculated according to the following formula:

$$\bar{l}_{wind,tot} = \frac{\bar{M}_{wind,tot}}{W} \text{ (m)}$$

Where,

$\bar{M}_{wind,tot}$  = mean wind heeling moment, to be calculated as

$$\frac{1}{2} \rho_{air} \cdot U_w^2 \cdot C_m \cdot A_L \cdot Z \quad (\text{N} \cdot \text{m});$$

- $W$  = ship displacement force (N)  
 $\rho_{air}$  = air density to be taken as equal to 1.222 kg/m<sup>3</sup>;  
 $U_w$  = mean wind speed, to be calculated as

$$\left( \frac{H_s}{0.06717} \right)^{2/3} \quad (\text{m/s})$$

Different expressions can be used when considering alternative environmental conditions, to the satisfaction of the Administration, in accordance with 2.13.3.3.3;

- $C_m$  = wind heeling moment coefficient, to be taken as equal to 1.22 or as determined by other methods, to the satisfaction of the Administration;  
 $A_L$  = projected lateral area of the portion of the ship and deck cargo above the waterline (m<sup>2</sup>);  
 $Z$  = vertical distance from the centre of  $A_L$  to the centre of the underwater lateral area or approximately to a point at one-half the mean draft,  $d$  (m); and  
 $H_s$  = significant wave height for the short-term environmental condition under consideration, according to 2.13.3.3 (m).

2.13.3.2.3 For the short-term environmental condition under consideration, the reference average zero up-crossing period of the effective relative roll motion,  $T_{z,C_s}$ , and the corresponding standard deviation,  $\sigma_{C_s}$ , to be used in the calculation of the short-term dead ship stability failure index,  $C_{S,i}$ , are determined using the spectrum of the effective relative roll motion under to the action of wind and waves, in accordance with the following formulae:

$$\sigma_{C_s} = (m_0)^{1/2}$$

$$T_{z,C_s} = 2\pi \cdot (m_0 / m_2)^{1/2}$$

Where,

- $m_0$  = area under the spectrum  $S(\omega)$  (rad<sup>2</sup>);  
 $m_2$  = area under the function of  $\omega^2 \cdot S(\omega)$  (rad<sup>4</sup>/s<sup>2</sup>);  
 $\omega$  = generic circular frequency (rad/s);  
 $S(\omega)$  = spectrum of the effective relative roll angle, to be calculated as follows:

$$H_{rel}^2(\omega) \cdot S_{\alpha\alpha,c}(\omega) + H^2(\omega) \cdot \frac{S_{\partial M_{wind,tot}}(\omega)}{(W \cdot GM)^2} \quad (\text{rad}^2/(\text{rad/s}))$$

$$H_{rel}^2(\omega) = \frac{\omega^4 + (2 \cdot \mu_e \cdot \omega)^2}{(\omega_{0,e}^2(\phi_s) - \omega^2)^2 + (2 \cdot \mu_e \cdot \omega)^2}$$

$$H^2(\omega) = \frac{\omega_0^4}{(\omega_{0,e}^2(\phi_s) - \omega^2)^2 + (2 \cdot \mu_e \cdot \omega)^2}$$

$S_{\alpha\alpha,c}(\omega)$  = spectrum of the effective wave slope, to be calculated as

$$r^2(\omega) \cdot S_{\alpha\alpha}(\omega) \quad (\text{rad}^2/(\text{rad/s}))$$

$S_{\alpha\alpha}(\omega)$  = spectrum of the wave slope, to be calculated as

$$\frac{\omega^4}{g^2} \cdot S_{zz}(\omega) \quad (\text{rad}^2/(\text{rad/s}))$$

$g$  = gravitational acceleration of 9.81m/s<sup>2</sup>;

$S_{zz}(\omega)$  = sea elevation spectrum. The standard expression for  $S_{zz}(\omega)$  is as follows:

$$\frac{4 \cdot \pi^3 \cdot H_s^2}{T_z^4} \cdot \omega^{-5} \cdot \exp\left(-\frac{16 \cdot \pi^3}{T_z^4} \cdot \omega^{-4}\right) \quad (\text{m}^2/(\text{rad/s}))$$

Different expressions can be used when considering alternative environmental conditions, to the satisfaction of the Administration, in accordance with 2.13.3.3.3;

$S_{\delta M_{wind,tot}}(\omega)$  = spectrum of moment due to the action of the gust, to be calculated as

$$\left[\rho_{air} \cdot U_w \cdot C_m \cdot A_L \cdot Z\right]^2 \cdot \chi^2(\omega) \cdot S_v(\omega) \quad ((\text{N} \cdot \text{m})^2/(\text{rad/s}))$$

$\chi(\omega)$  = standard aerodynamic admittance function, to be taken as a constant equal to 1.0 . [Alternative formulations can be accepted to the satisfaction of the Administration.];

$S_v(\omega)$  = spectrum of the gust. The standard expression for  $S_v(\omega)$  is as follows:

$$4 \cdot K \cdot \frac{U_w^2}{\omega} \cdot \frac{X_D^2}{(1 + X_D^2)^{\frac{4}{3}}} \quad ((\text{m/s})^2/(\text{rad/s}))$$

with  $K = 0.003$  and  $X_D = 600 \cdot \omega / (\pi \cdot U_w)$ . Different expressions can be used when considering alternative environmental conditions, to the satisfaction of the Administration, in accordance with 2.13.3.3.3;

$W$  = ship displacement force (N);

$GM$  = metacentric height corrected for free surface effects<sup>5</sup> (m);  
 $\mu_e$  = equivalent linear roll damping coefficient calculated according to the stochastic linearization method. This coefficient depends on linear and nonlinear roll damping coefficients and on the specific roll velocity standard deviation in the considered short-term environmental conditions<sup>6</sup>;

$\omega_{0,e}(\phi_S)$  = modified roll natural frequency close to the heel angle  $\phi_S$ , to be calculated as

$$\omega_0 \cdot \left( \frac{GM_{res}(\phi_S)}{GM} \right)^{1/2} \quad (\text{rad/s});$$

$\omega_0$  = upright roll natural frequency (rad/s);  
 $r(\omega)$  = effective wave slope function determined according to 2.13.3.2.4  
 $H_s$  = significant wave height for the short-term environmental condition under consideration, according to 2.13.3.3 (m);  
 $T_Z$  = zero up-crossing wave period for the short-term environmental condition under consideration, according to 2.13.3.3 (s);

and other variables as defined in 2.13.3.2.1 and 2.13.3.2.2.

2.13.3.2.4 The effective wave slope function,  $r(\omega)$ , should be specified using a reliable method, based on computations or derived from experimental data, to the satisfaction of the Administration. In absence of sufficient information the standard methodology<sup>7</sup> for the estimation of the effective wave slope function should be used, which is based on the following assumptions and approximations:

- .1 The underwater part of each transverse section of the ship is substituted by an "equivalent underwater section" having, in general, the same breadth at waterline and the same underwaterplane area of the original section. However:
  - .1 Sections having zero breadth at waterline, such as those in the region of the bulbous bow, are neglected;
  - .2 The draught of the "equivalent underwater section" is limited to the ship sectional draught;
- .2 The effective wave slope coefficient for each wave frequency is determined by using the "equivalent underwater sections" considering only the undisturbed linear wave pressure;
- .3 For each section, a formula is applied, which is exact for rectangles.

The standard methodology is applied [with the ship having zero trim and results are used also for trim different from zero] [considering the actual trim of the ship]. The standard methodology for the estimation of the effective wave slope is applicable only to standard

---

<sup>5</sup> In accordance with Part B, 3.1

<sup>6</sup> The detailed calculation procedure is reported in the Explanatory Notes.

<sup>7</sup> The detailed calculation procedure is reported in the Explanatory Notes.

monohull vessels. For a ship which, to the opinion of the Administration, does not fall in this category, alternative prediction methods should be applied.

2.13.2.5 The upright roll natural frequency should be estimated as follows:

$$\omega_0 = \frac{2\pi}{T_\phi}$$

where  $T_\phi$  is the ship natural roll period defined in 2.11.3.2.2.

2.13.3.3 Short-term environmental conditions used for the assessment of the short-term dead ship stability failure index  $C_{S,i}$  according to 2.13.3.2.1, and weighting factor  $W_i$  used for the determination of the long-term probability index  $C$  according to 2.13.3.2, are specified in Section 3.3 of the Explanatory Notes.

2.13.3.3.3 Alternative environmental conditions can be used, to the satisfaction of the Administration, for ships in restricted service or subject to operational limitations<sup>8</sup>.

\*\*\*

---

<sup>8</sup> In accordance with the guidelines developed by the Organization [to be developed].

## ANNEX 2

### DRAFT AMENDMENTS TO PART B OF THE IS CODE WITH REGARD TO VULNERABILITY CRITERIA OF LEVELS 1 AND 2 FOR THE EXCESSIVE ACCELERATION FAILURE MODE

#### PART B

#### Recommendations for ships engaged in certain types of operations, certain types of ships, and additional guidelines

#### Chapter 2

#### Recommended design criteria for certain types of ships

2 A new section "2.14" is added with the following:

#### "2.14 Assessment of ship vulnerability to the excessive acceleration failure mode

##### 2.14.1 Application

2.14.1.1 The provisions given hereunder apply to each ship in each condition of loading provided that

- .1 the distance from the waterline to the highest location along the length of the ship where passengers or crew may be present exceeds [70%] of the breadth of the ship; and
- .2 the metacentric height exceeds [8%] of the breadth of the ship.

2.14.1.2 A ship is considered not to be vulnerable to the excessive acceleration stability failure mode, if, for each condition of loading and location along the length of the ship where passengers or crew may be present, it either:

- .1 meets the standard contained in the criteria given in 2.14.2;
- .2 meets the standard of the more detailed assessment of vulnerability to the failure mode in the criteria given in 2.14.3; or
- .3 meets the standard of the direct stability assessment for the excessive acceleration failure mode that is performed according to recommended specifications developed by the Organization.

2.14.1.3 For each condition of loading, a ship that neither meets the criteria given in 2.14.2 or 2.14.3 nor meets the standard of the direct stability assessment, should be subject to either:

- .1 operational guidance procedures, developed to the satisfaction of the Administration from the direct stability assessment for the excessive acceleration failure mode; or
- .2 operational limitations based on outcomes of the application of the criteria given in 2.14.3 or on direct stability assessment for the excessive acceleration failure mode.

## 2.14.2 Level 1 Vulnerability Criteria for Excessive Acceleration

2.14.2.1 A ship is not considered to be vulnerable to the excessive acceleration stability failure mode if, for each condition of loading and location along the length of the ship where passengers or crew may be present,

$$\phi k_L (g + 4 \pi^2 h / T^2) < R_{EA1}$$

- Where,  $R_{EA1}$  = [5.3] [8.9] [8.69 or below] m/s<sup>2</sup>
- $\phi$  = characteristic roll amplitude (rad) =  $4.43 r s / \delta_\phi^{0.5}$ ;
- $k_L$  = factor taking into account simultaneous action of roll, yaw and pitch motions,  
=  $1.125 - 0.625 x / L$ , if  $x < 0.2 L$ ,  
= 1.0, if  $0.2 L < x < 0.65 L$ ,  
=  $0.527 + 0.727 x / L$ , if  $x > 0.65 L$ ;
- $x$  = longitudinal distance of the location where passengers or crew may be present from the aft end of  $L$ ;
- $g$  = gravitational acceleration of 9.81 m/s<sup>2</sup>;
- $h$  = height above the roll axis of the location where passengers or crew may be present (m);
- $T$  = rolling period (s) as determined in Explanatory Notes, Section [X.X.X];
- $r$  = non-dimensional effective wave slope =  $\frac{K_1 + K_2 + (OG)(F)}{\frac{B^2}{12C_B d} - \frac{C_B d}{2} - OG}$ ;
- $K_1$  =  $g \beta T^2 (\tau + \tau \tilde{T} - 1 / \tilde{T}) / (4 \pi^2)$ ;
- $K_2$  =  $g \tau T^2 (\beta - \cos \tilde{B}) / (4 \pi^2)$ ;
- $OG$  =  $KG - d$ ;
- $F$  =  $\beta (\tau - 1 / \tilde{T})$ ;
- $\beta$  =  $\sin(\tilde{B}) / \tilde{B}$ ;
- $\tau$  =  $\exp(-\tilde{T}) / \tilde{T}$ ;
- $\tilde{B}$  =  $2 \pi^2 B / (g T^2)$ ;
- $\tilde{T}$  =  $4 \pi^2 C_B d / (g T^2)$ ;
- $s$  = non-dimensional wave steepness as specified in Explanatory Notes, Table [X.X.X];
- $\delta_\phi$  = non-dimensional logarithmic decrement of roll decay, defined according to Explanatory Notes, Section [X.X.X];

For the purpose of determining  $h$ , the roll axis may be assumed to be located at the midpoint between the waterline and the vertical centre of gravity.

## 2.14.3 Level 2 Vulnerability Criteria for Excessive Acceleration

2.14.3.1 A ship is considered not to be vulnerable to the excessive acceleration stability failure mode if, for each condition of loading and location along the length of the ship where passengers or crew may be present,  $R_{EA2}$  is greater than  $C$ ,

- Where,  $R_{EA2}$  =  $[1.1 \cdot 10^{-4}] [0.001] [0.0281 \text{ or above}] [0.043 \text{ or above}]$ ;
- $C$  = a long-term probability index that measures the vulnerability of the ship to a stability failure in the excessive acceleration mode for the loading condition and location under consideration based on the probability of occurrence of short-term environmental conditions as calculated according to chapter 2.14.3.2.



2.14.3.2 The value for  $C$  is calculated as a weighted average from a set of wave conditions specified in 2.14.3.3:

$$C = \sum_{i=1}^N W_i C_i$$

Where,

- $W_i$  = the weighting factor for the short-term environmental wave condition specified in Explanatory Notes, Section [X.X.X];
- $C_i$  = the short-term excessive acceleration stability failure index for the loading condition and location under consideration and for the short-term environmental condition under consideration calculated as specified in 2.14.3.2.1;
- $N$  = the number of wave conditions specified in Explanatory Notes, Section [X.X.X].

2.14.3.2.1 The short-term excessive acceleration condition stability failure index,  $C_i$ , for the loading condition and location under consideration and for the short-term environmental condition under consideration is a measure of the probability that the ship will exceed a specified lateral acceleration at least once in the exposure time considered, calculated according to the following formula:

$$C_i = \exp[-R_2^2 / (2 \sigma_{LAI}^2)];$$

Where,

- $R_2$  = [9.81] m/s<sup>2</sup>;
- $\sigma_{LAI}$  = standard deviation of the lateral acceleration at zero speed and in a beam seaway determined according to 2.14.3.2.2 (m/s<sup>2</sup>);

2.14.3.2.2 The standard deviation of the lateral acceleration at zero speed and in a beam seaway,  $\sigma_{LAI}$ , is determined using the spectrum of roll motions due to the action of waves. The square of this standard deviation is calculated according to the following formula<sup>9</sup>:

$$\sigma_{LAI}^2 = \frac{3}{4} \sum_{j=1}^N (a_y(\omega_j))^2 S_{ZZ}(\omega_j) \Delta\omega$$

- Where,  $\Delta\omega$  = the interval of wave frequency (rad/s) =  $(\omega_2 - \omega_1) / N$  (rad/s);
- $\omega_2$  = the upper limit of the wave frequency spectrum in the evaluation range =  $\min((25 / T), 2.0)$  (rad/s);
- $\omega_1$  = the lower limit of the wave frequency spectrum in the evaluation range =  $\max((0.5 / T), 0.2)$  (rad/s);
- $N$  = the number of intervals of wave frequency in the frequency spectrum evaluation range, not to be taken less than 100;
- $\omega_j$  = wave frequency at the mid-point of the frequency interval considered =  $\omega_1 + ((2j - 1) / 2) \Delta\omega$  (rad/s);
- $S_{ZZ}(\omega_j)$  = wave frequency spectrum, defined in the Explanatory Notes, Section [X.X.X];
- $a_y(\omega_j)$  = lateral acceleration =  $k_L (g \sin \varphi_a(\omega_j) + h \cdot \omega_j^2 \varphi_a(\omega_j))$  (1/s<sup>2</sup>);
- $k_L$  = as defined in 2.14.2.1;
- $g$  = gravitational acceleration of 9.81 m/s<sup>2</sup>;
- $h$  = as defined in 2.14.2.1;

<sup>9</sup> Integration of an equivalent formulation over the range,  $\omega_1$  to  $\omega_2$ , may be substituted.

- $\varphi_a(\omega_j)$  = roll amplitude in regular beam waves of unit amplitude and circular frequency  $\omega_j$  at zero speed, =  $(\varphi_r(\omega_j)^2 + \varphi_i(\omega_j)^2)^{0.5}$  (rad/m);
- $\varphi_r(\omega_j)$  =  $\frac{a(\Delta gGM - I_{xx}\omega_j^2) + b\mu_e\omega_j}{(\Delta gGM - I_{xx}\omega_j^2)^2 + (\mu_e\omega_j)^2}$  (rad);
- $\varphi_i(\omega_j)$  =  $\frac{b(\Delta gGM - I_{xx}\omega_j^2) - a\mu_e\omega_j}{(\Delta gGM - I_{xx}\omega_j^2)^2 + (\mu_e\omega_j)^2}$  (rad);
- $a, b$  = cosine and sine components, respectively, of the Froude-Krylov roll moment in regular beam waves of a unit amplitude, calculated directly or using an appropriate approximation, according to Explanatory Notes, Section [X.X.X];
- $GM$  = metacentric height not corrected for free surface effect (m);
- $B$  = equivalent linear roll damping coefficient (t m s) calculated according to Explanatory Notes, Section [X.X.X];
- $\Delta$  = displacement (t);
- $I_{xx}$  = roll moment of inertia =  $\Delta GM T^2 / (4\pi^2)$  (t m s<sup>2</sup>)

2.14.3.3 Wave conditions are defined according to Explanatory Notes, Section [X.X.X].

2.14.3.4 The value of the weighting factor for the short-term environmental wave condition,  $W_i$ , to be used in the formula in paragraph 2.14.3.2 for a wave condition ( $H_s, T_z$ ) is obtained from the Explanatory Notes, Table [X.X.X] except if the Administration directs the use of other wave statistics for restricted service or operational limitations.

\*\*\*

## ANNEX 3

### DRAFT EXPLANATORY NOTES ON THE VULNERABILITY OF SHIPS TO THE PURE LOSS OF STABILITY FAILURE MODE

[This is the explanatory notes to the "PROPOSED AMENDMENTS TO PART B OF THE 2008 IS CODE TO ASSESS THE VULNERABILITY OF SHIPS TO THE PURE LOSS OF STABILITY FAILURE MODE" as SDC 2/WP.4, annex 1.]

#### Chapter 2 – THE VULNERABILITY OF SHIPS TO THE PURE LOSS OF STABILITY FAILURE MODE

##### 1. Physical background of pure loss of stability

##### 1.1 Variation of stability in waves

1.1.1 When a ship is sailing through waves, the submerged part of the hull changes. These changes may become especially significant if the length of the wave is comparable to the length of the ship. As a first example, one may observe the changes that occur when the trough of a wave is located amidships (see Figure 1). For most ships, the upper part of the bow section is usually wide, due to bow flare. Bow flare provides protection from spray and green water shipping, and also allows additional cargo to be stored on deck. As a result, the bow flare makes the waterplane larger, if the upper part of the bow section becomes partially submerged. The upper part of the aft section of the hull is typically even larger. Apart from cargo stowage considerations, this section must also provide room for steering machinery. Therefore, the after part of the waterplane also increases, once the upper part of the aft section becomes submerged. Unlike the bow and aft sections, the midship section of most ships is almost nearly wall-sided. This means that very little change occurs in the waterplane width with variations in draft. When the wave trough is amidships, the draft at the midship section is low, but as the hull is wall-sided in this region, there is little waterplane change. As a result, when the wave trough is located around the midship section, the overall waterplane area is increased (see Figure 1b).

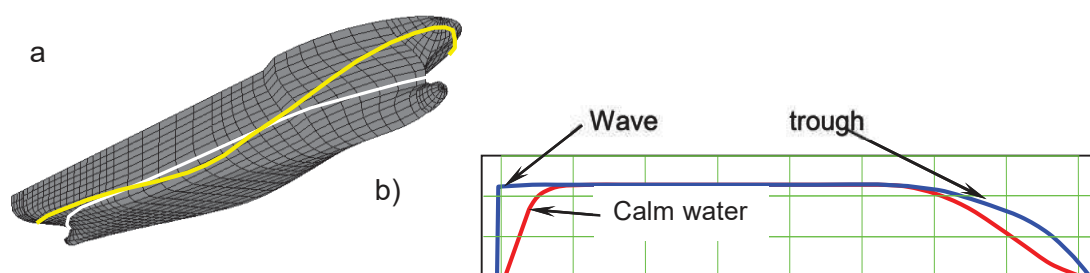


**Figure 1:** Changes in Hull Geometry when a Wave Trough is Amidships (a) 3D View (b) Waterplane

1.1.2 When the wave crest is located near amidships, the situation changes dramatically (Figure 2). The underwater part of the bow section is usually quite narrow, especially around the waterline. Even for a bulbous bow, it is still narrower than for the section with bow flare. The reason for this is the consideration of resistance. The faster the ship is, the narrower its underwater bow section must be. If the wave crest is amidships and the wave has a length similar to a ship length, the wave trough is located around the bow section. This makes the

draft at the bow quite shallow. As a result, the waterplane becomes very narrow in this region. The underwater part of the aft section is also very narrow. The main design consideration is to provide the propulsor with enough inflow to efficiently power the ship. Consideration of energy efficiency impels a designer towards a buttock flow stern design. When the wave crest is located amidships, another wave trough is located near the aft section. The draft at the stern becomes shallow, which makes the waterplane very narrow in the aft part. This also is exaggerated with increased ship speed, as more power must be handled by the propeller. As mentioned previously, the midship section is typically more wall-sided, so it does not significantly affect the waterplane. Figure 2b shows the effect of the wave crest amidships, where the overall waterplane is reduced in area.

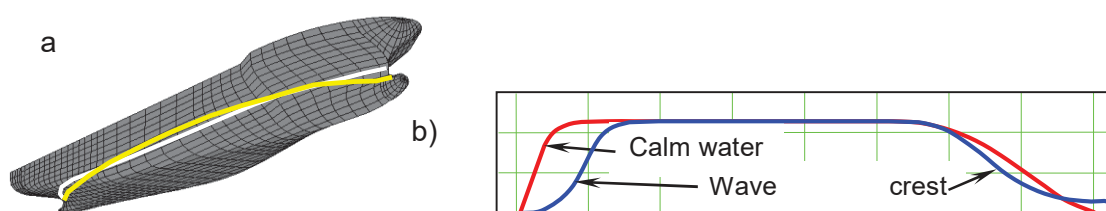


**Figure 2:** Changes in hull geometry when a wave crest is amidships (a) 3D view (b) waterplane

1.1.3 As it is well known from ship hydrostatics, the waterplane area has a significant effect on ship stability. If the waterplane area is reduced, then so is the GZ curve (see Figure 3).

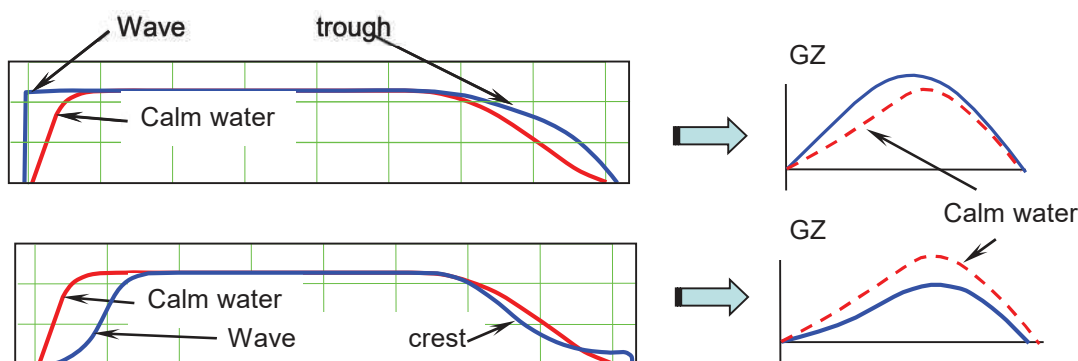


**Figure 3** Stability corresponding to waterplane changes on the wave trough (Top) and the wave crest (Bottom)

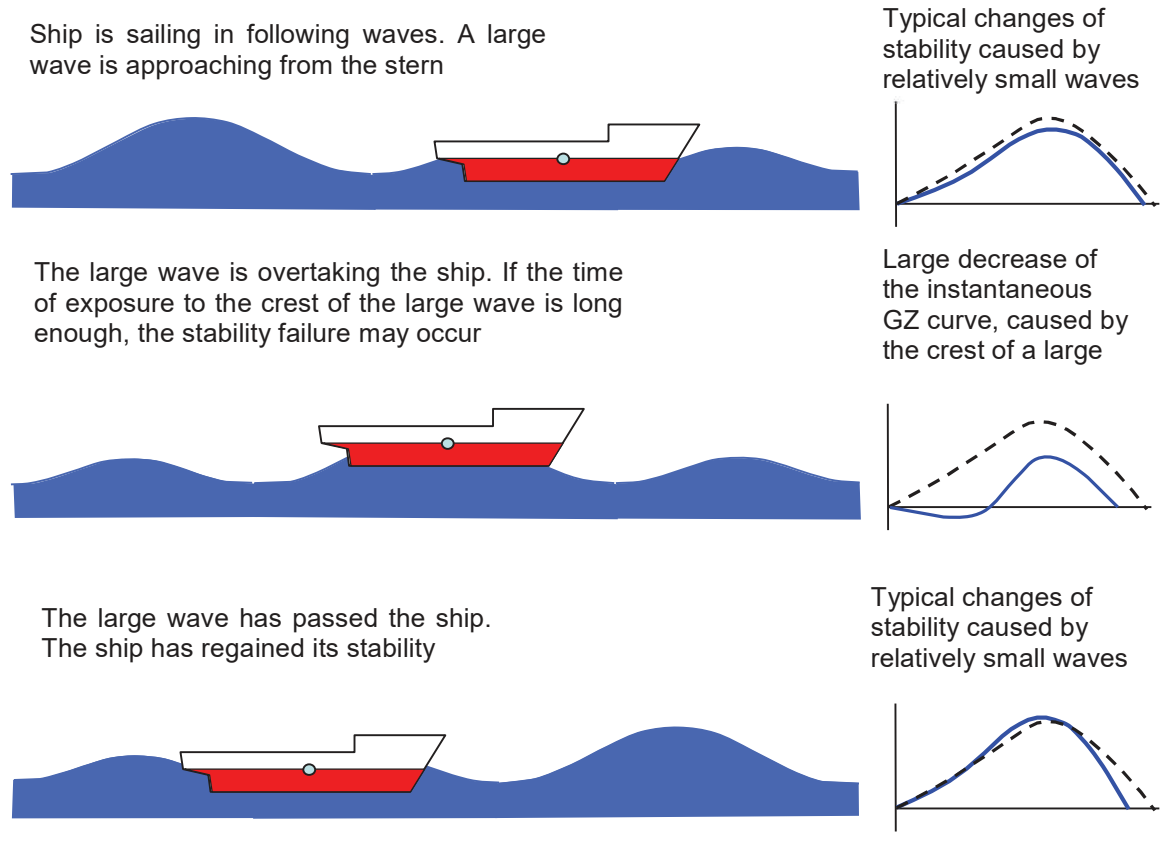
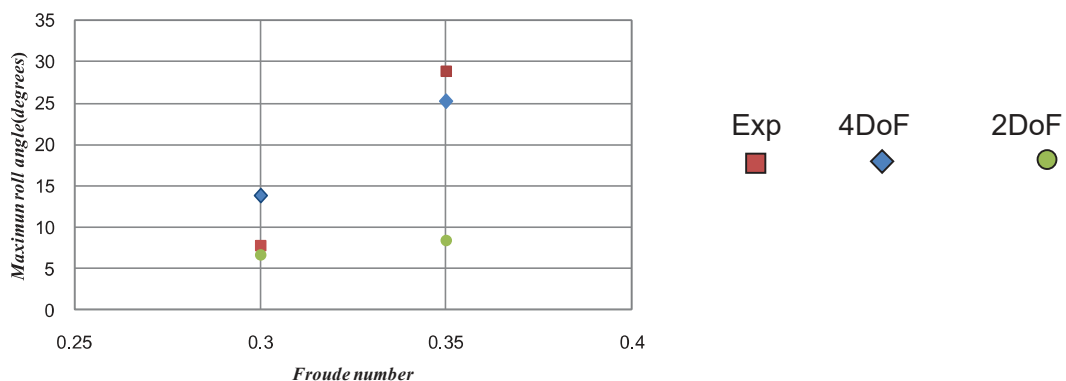


Figure 4 Possible Scenario for the Development of Pure Loss of Stability

## 1.2 Scenario of pure loss of stability

1.2.1 Change of stability in waves, as examined in subsection 1.1, is the physical basis for the stability failure mode known as pure loss of stability. The dynamics of pure loss of stability are different from parametric roll, but are also closely related to the severity and duration of waterplane changes. A possible scenario for the development of a stability failure caused by pure loss of stability is shown in Figure 4.



**Figure 5:** Forward speed effect on pure loss of stability in irregular stern-quartering waves for a containership model in a model basin. Here 2 DoF and 4 DoF mean surge-roll and surge-sway-yaw-roll coupled simulation models, respectively.

1.2.2 A large wave is approaching from the stern, while the ship is sailing with relatively high speed in following seas. If the celerity (speed) of the large wave is just slightly above the ship speed, the time duration for the large wave to pass the ship may be long. Once the crest of the large wave is near the midship section of the ship, its stability may be significantly decreased. Because the wave celerity is just slightly more than ship speed, the condition of decreased stability may exist long enough for the ship to develop a large heel angle, or even capsize. Once the large wave has passed the ship, its stability is regained and the ship will eventually return to the upright position, if she did not already heel too far.

1.2.3 Even if the restoring moment is significantly reduced due to a relative wave profile, this does not simply result in a total or partial stability failure. This is because the external heel moment is required for the stability failures. If no external heel moment exists, the upright condition can be kept except for cases that the metacentric height in waves is negative. As the external moments to be relevant, wave exciting roll moment due to oblique wave heading and heel moment induced by a centrifugal force due to ship manoeuvring motions are candidates. Several existing model experiments using freely running ship models in stern-quartering waves indicate that coupling with manoeuvring motion is essential to explaining the forward speed effect on the stability failures of pure loss of stability. An example is shown in Figure 5. If we take account of only surge-roll coupled motion, the pure loss of stability does not drastically depend on the forward speed. If we take account of also coupling with manoeuvring motions, however, the drastic forward speed effect on pure loss of stability can be explained. Thus, the heel moment induced by the centrifugal force due to ship manoeuvring motions should be included.

1.2.4 Based on the above, the level 2 criteria require that the stable heel angle is sufficiently small under the reduced restoring moment due to a wave and the heeling level due to centrifugal force as a function of the Froude number. In addition, for the case the metacentric height in a wave is negative, the level 2 criteria requires that the loll angle is sufficiently small under the reduced restoring moment due to wave but without heeling lever.

1.2.5 The level 1 criterion is a simplified version of the level 2 criteria. While the level 2 criteria judges the vulnerability with the righting arm curve in waves, the level 1 criterion focuses on the metacentric height in waves. Since small metacentric height does not always result in small value of the maximum righting arm, the level 2 criteria should generally be more conservative than the level 1.

1.2.6 The standards for the level 2 criteria, as well as the applicable speed range, were determined with the reports of major large heel incidents of RoRo ships.

## **2. Supplementing information on Calculation for Checking Vulnerability with Level 1 Criteria**

2.1 The value of  $S_w$  in 2.10.2.1 of the Code Part B can be corrected if operational waterplane area is limited. In this case a wave scattering table should be provided for the specified waterplane area and its quality should be equivalent to the IACS Recommendation No. 34 for the Northern Atlantic. The calculation procedures described in Appendix 1 [of the explanatory notes for parametric roll failure modes] should be applied to this wave scattering table.

2.2 In the calculation of 2.10.2.2 of the Code Part B, a sinusoidal wave should be used without hydrodynamic disturbance due to the ship. The water pressure due to the wave may include the effect of wave particle velocity assuming that water depth is larger than the wavelength. This is because the water wave can be deformed due to the sea bottom effect if water depth is smaller than the wave length.

### 3 Supplementing information on Calculation for Checking Vulnerability with Level 2 Criteria

3.1 In the calculation of 2.10.3.2 of the Code Part B, a sinusoidal wave should be used without hydrodynamic disturbance due to the ship. The water pressure due to the wave should include the effect of wave particle velocity assuming that water depth is larger than the wavelength.

3.2 If operational waterplane area is limited, Table 2.10.3.2 of the Code Part B can be replaced with a wave scattering table for the specified waterplane area, which is equivalent in quality to the IACS Recommendation No. 34 for the Northern Atlantic.

3.3 For determining the indexes for each  $H_i$  in 2.10.3.2, it is necessary to obtain the relationship between  $h$  and the indexes should be obtained by calculation. Here if the index has a peak at the certain wave steepness  $h_p$ , the peak value of the index should be used when the wave steepness is larger than  $h_p$ , as shown in Figure 6.

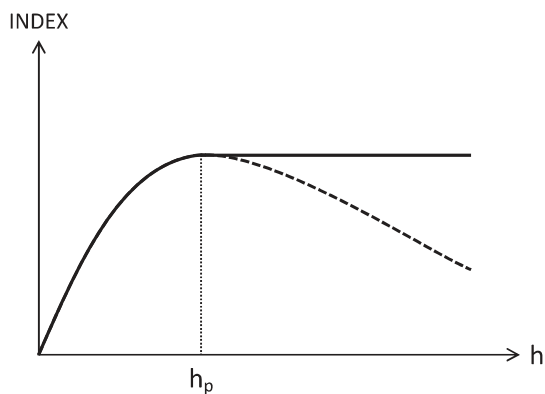


**Figure 6:** relationship between the index and  $h$

3.4 The calculation formula for wave height in 2.10.3. 2 is as follows:

$$H_{3\%}^{eff}(L) = 5.9725\sqrt{m_0} \quad (1)$$

$$m_0 = \int_{0.01\omega_L}^{\omega_L} \left\{ \frac{\left( \frac{\omega^2 L}{g} \sin\left( \frac{\omega^2 L}{2g} \right) \right)^2}{\pi^2 - \left( \frac{\omega^2 L}{2g} \right)^2} \right\} A \omega^{-5} \exp(-B\omega^{-4}) d\omega \quad (2)$$

$$+ \int_{\omega_L}^{3\omega_L} \left\{ \frac{\left( \frac{\omega^2 L}{g} \sin\left( \frac{\omega^2 L}{2g} \right) \right)^2}{\pi^2 - \left( \frac{\omega^2 L}{2g} \right)^2} \right\} A \omega^{-5} \exp(-B\omega^{-4}) d\omega$$

where

$$A = 173H_s^2 T_{01}^{-4} \quad (3)$$

$$B = 691T_{01}^{-4} \quad (4)$$

$$T_{01} = 1.086T_z \quad (5)$$

$$g = 9.81(m/s^2) \quad (6)$$

$$\omega_L = \sqrt{\frac{2g\pi}{L}} \quad (7)$$

$H_s^{eff}$  (m): the effective significant wave height,  $L$ (m): length of the ship,  $H_s$  (m) : the significant wave height, and  $T_z$ (s): the zero-crossing mean wave period.

If  $H_{3\%}^{eff} > 0.1L$ ,  $H_{3\%}^{eff}$  should be set as  $H_{3\%}^{eff} = 0.1L$ .

#### 4 Examples of Checking Vulnerability

As an example, we use the following data of a containership at the full load condition:

$L_{PP}$	262.0 m	ship length between perpendiculars
$L_f$	262.0m	ship length defined in 2008 IS Code
$B$	40.0 m	moulded ship breadth
$D$	24.45 m	moulded ship depth
$d$	11.5 m	moulded mean ship draught
$\tau$	0 m	Initial trim
$LCG$	125.52 m	longitudinal centre of gravity from aft perpendicular
$C_b$	0.559	block coefficient
$GM$	1.965 m	metacentric height with free surface correction
$VCG$	18.4 m	vertical centre of gravity above baseline
$KB$	6.54 m	vertical centre of buoyancy above baseline
$V_s$	12.165 m/s	ship service speed

##### Level 1

Firstly, we calculate the Froude number,  $Fn$ .

$$F_n = V_s / \sqrt{gL} = 12.165 / \sqrt{9.81 \times 262} = 0.240$$

Thus the criteria for pure loss of stability should be applied to the ship.

Secondly, the lower draught is calculated:

$$\delta d_L = \text{Min}\{d - 0.25d_{full}, LS_w/2\} = \text{Min}\{0.75 \times 11.5, 262 \times 0.0334/2\} = \text{Min}\{8.625, 4.3754\} = 4.3754\text{m}$$



$$d_L = d - \delta d_L = 11.5 - 4.3754 = 7.125 \text{ m}$$

so that, according to the hydrostatic data as shown in Figure 7, the relevant  $I_L$  is 665,500m<sup>4</sup>.

Thirdly,  $GM_{min}$  is calculated as follows:

$$GM_{min} = KB + (I_L V) - VCG = KB + (I_L / (C_b \times L_{PP} \times B \times d)) - VCG$$

$$= 6.54 + (665500 / (0.559 \times 262 \times 40 \times 11.5)) - 18.4 = -1.982 \text{ m}$$

Therefore,  $GM_{min} (= -1.982) < R_{LA} (= 0.05)$  so that the ship is judged as vulnerable to pure loss of stability.

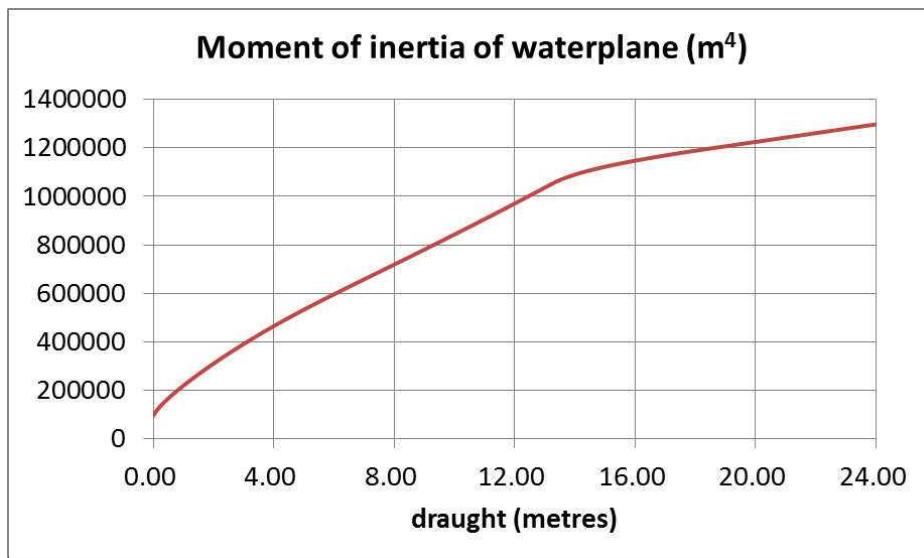


**Figure 7** The relationship between the moment of inertia of waterplane for the sample ship

## Level 2

Firstly, we calculate GZ curves for the ship with the wave steepness ranging from 0 to 0.1. Examples are shown in Figure 8.

Secondly, we apply Criteria 1 and 2 to the ship. The results are as follows:

$CR_1 = 0.000$  where the critical wave steepness for the angle of vanishing stability of 30 degrees is 0.07291.

$CR_2 = 0.003821$  where the critical wave steepness for the angle of heel of 25 degrees is 0.03941.

Thus:

$$\text{Max}\{CR_1, CR_2\} = 0.003821.$$

Since this is smaller than 0.06, the ship is not judged as vulnerable to pure loss of stability.

Figure 8 indicates the possibility of negative GM for the ship exists as the level 1 criterion suggests with some margin. The level 2 criterion explains that, if the ship meets a certain wave crest, significant heel could occur under the riding on crest situation where the ship is

slowly overtaken by a wave crest. However, the level 2 criterion also indicates that the ship rarely meets such waves even in the North Atlantic. This is a physical explanation based on the vulnerability criteria for the pure loss of stability failure of the ship.

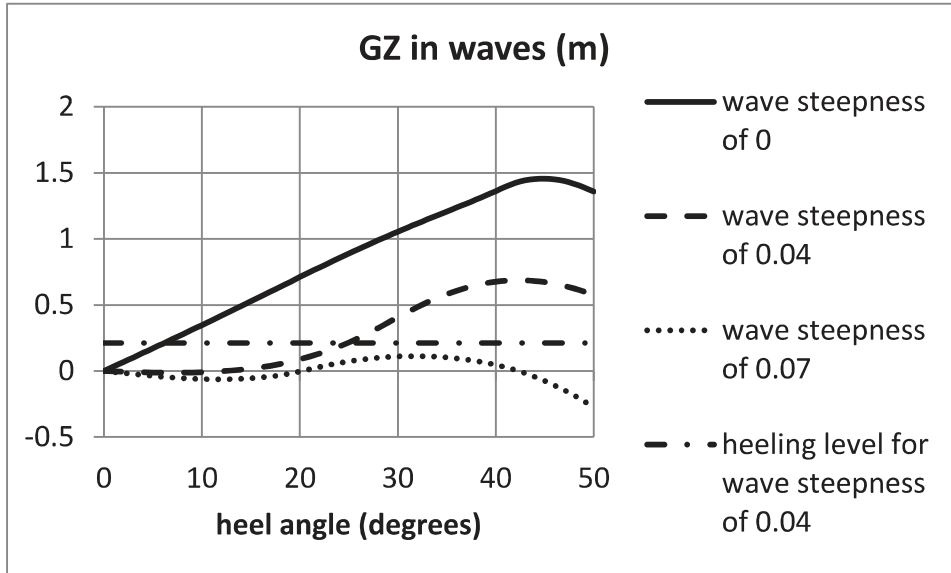


Figure 8: GZ curves for the ship in waves at wave crest amidship.

\*\*\*

## ANNEX 4

### DRAFT EXPLANATORY NOTES ON THE VULNERABILITY OF SHIPS TO THE PARAMETRIC ROLL STABILITY FAILURE MODE

[This is the explanatory notes to the "PROPOSED AMENDMENTS TO PART B OF THE 2008 IS CODE TO ASSESS THE VULNERABILITY OF SHIPS TO THE PARAMETRIC ROLL STABILITY FAILURE MODE" as SDC 2/WP.4, annex 2.]

#### Chapter 3 – THE VULNERABILITY OF SHIPS TO THE PARAMETRIC ROLL STABILITY FAILURE MODE

##### **1 Physical background of parametric roll**

##### **1.1 Development of parametric roll**

- 1.1.1 Parametric roll (short of parametric roll resonance) is an amplification of roll motions caused by periodic variation of transverse stability in waves. The phenomenon of parametric roll is predominantly observed in head, following, bow and stern-quartering seas when ship's encounter frequency is approximately twice of ship roll natural frequency and roll damping of the ship is insufficient to dissipate additional energy (accumulated because of parametric resonance).
- 1.1.2 See Figure 1. If the ship is rolled while on the wave trough, increased stability provides stronger pushback, or restoring moment. As the ship returns to the upright position, its roll rate is greater, since there was an additional pushback from the increased stability. If at that time, the ship has the wave crest at midship, the stability is decreased and the ship will roll further to the opposite side because of the greater speed of rolling and less resistance to heeling. Then, if the wave trough reaches the midship section when the ship reaches its maximum amplitude roll, stability increases again and the cycle starts again. Note that there was one half of the roll cycle associated with the passing of an entire wave. So, there are two waves that pass during each roll period. That means the roll period is about twice that of the wave period, see Figure 2.

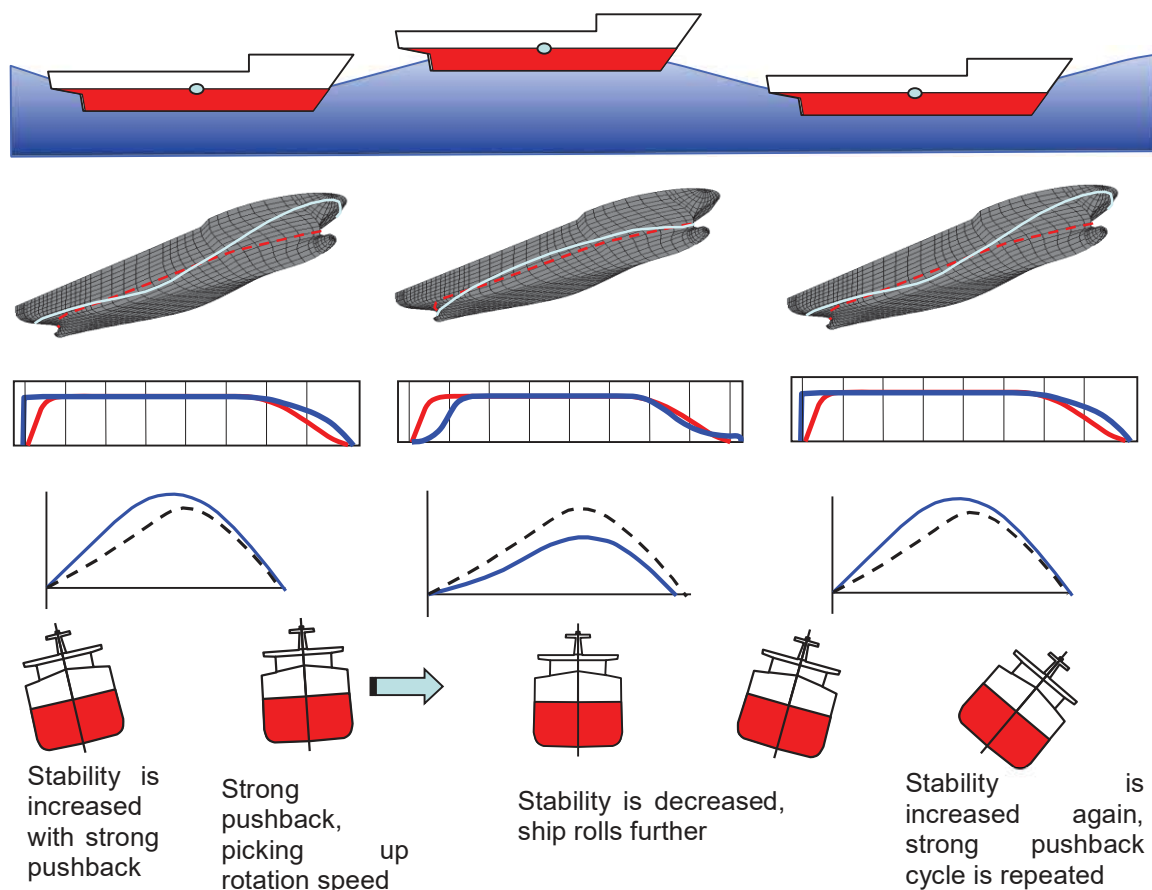


**Figure 1. Development of parametric roll resonance**

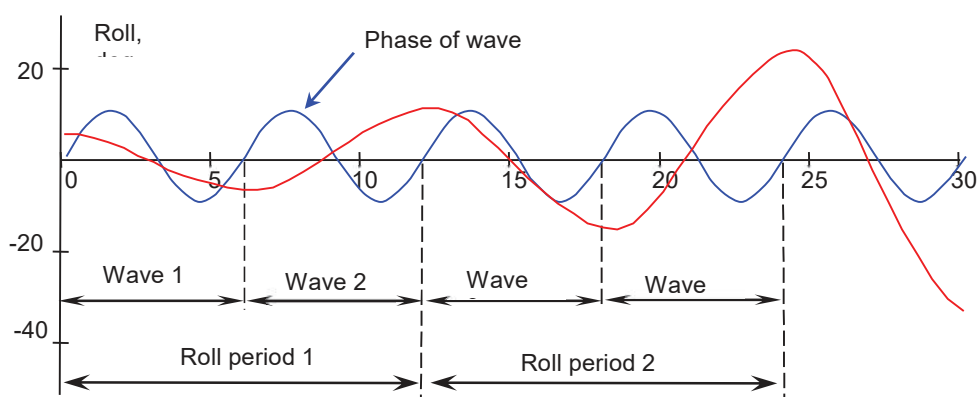


**Figure 2. Time histories plots of parametric roll resonance**

## 1.2 Frequency characteristics of parametric roll

- 1.2.1 Parametric roll is a resonance phenomenon and similar to roll resonance in beam waves (see Figure 3a), parametric roll has a limited frequency range (Figure 3b). The principal difference between the two phenomena is that the span of the frequency range for parametric roll depends on the magnitude of stability change, while the frequency range for roll resonance depends on wave height (Figure 3c). Also, if the beam waves are far from the resonance frequency, the ship only rolls

with very small amplitude. Parametric roll does not exist (the amplitude is equal to zero) outside of the frequency range.

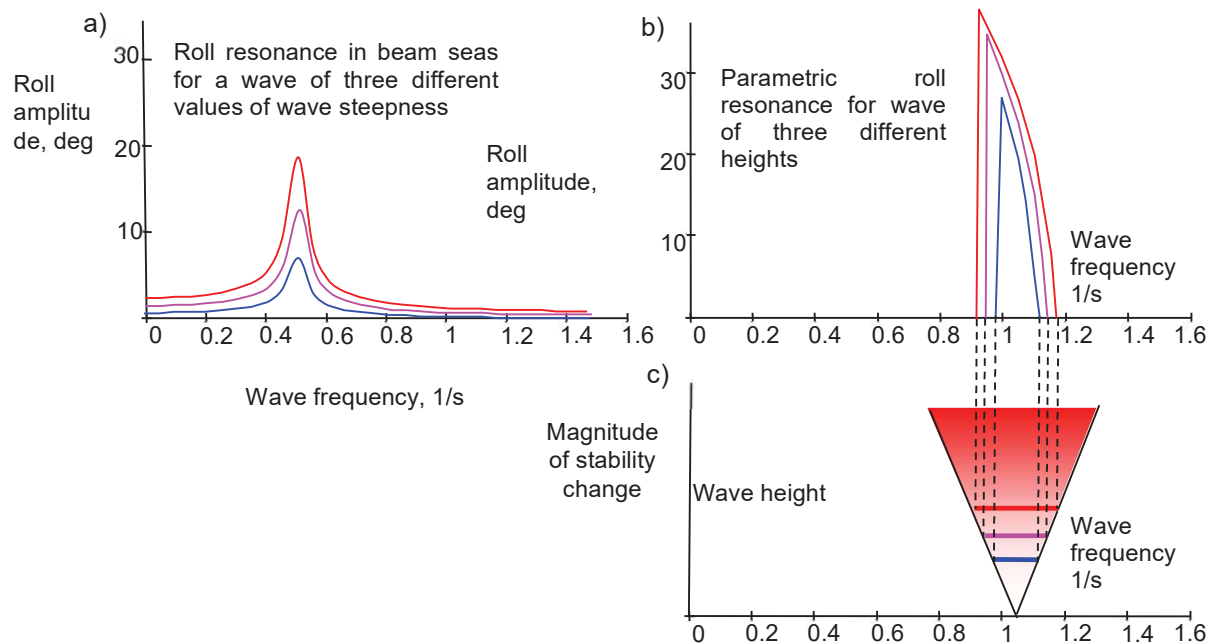


**Figure 3 (a) Roll resonance in beam seas (b) parametric roll resonance (c) frequency range of parametric roll resonance.**

### 1.3 Influence of roll damping

1.3.1 When a ship rolls in calm water after being disturbed, the roll amplitudes decrease successively due to roll damping, see Figure 4. A rolling ship generates waves and eddies, and experiences viscous drag. All of these processes contribute to roll damping. Roll damping may play a critical role in the development of parametric roll resonance. If the "loss" of energy per cycle caused by damping is more than the energy "gain" caused by the changing stability in longitudinal seas, the roll angles will not increase and the parametric resonance will not develop. Once the energy "gain" per cycle is more than the energy "loss" due to damping, the amplitude of the parametric roll starts to grow.

1.3.2 There is then a roll damping threshold for parametric roll resonance. If the roll damping moment is higher than the threshold, then parametric roll resonance is not possible. If the roll damping moment is below the threshold, then the parametric roll resonance can take place. During the parametric roll resonance the combination of harder push-backs due to the increased stability on the wave trough and larger achieved roll angles due to the decreased stability on the wave crest, which occur about twice during the roll period, makes the roll angle grow significantly. The only other condition that has to be met is that the energy loss due to roll damping is not large enough to completely consume the increase of energy caused by parametric roll resonance – the roll damping is below the threshold value.

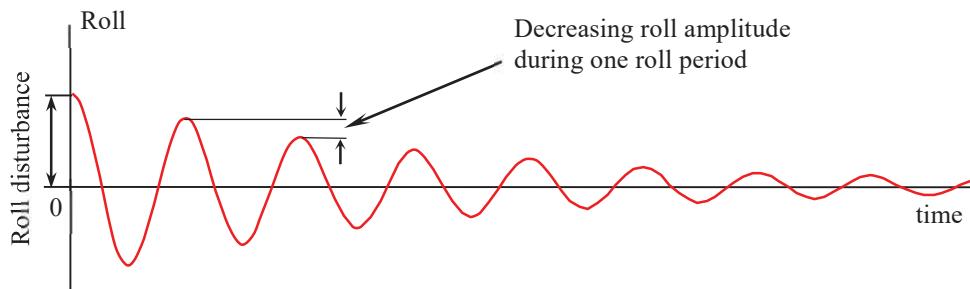


**Figure 4** Successively decreasing roll amplitudes due to roll damping in calm water

#### 1.4 Influence of Speed and Wave Direction

- 1.4.1 The frequency of encounter with waves changes when a ship is in motion. When a ship is sailing in following or stern-quartering seas, the direction of waves and the ship heading are similar (Figure 5a). As a result, the relative speed is small and a ship encounters fewer waves during the same time period (compared to a zero speed case). The encounter period is increased (and the encounter frequency is decreased) in following or stern-quartering waves.
- 1.4.2 When a ship is sailing in head or bow-quartering seas, the direction of waves and the ship heading are opposite (Figure 5b). As a result, the relative speed is large and a ship encounters more waves during the same time (compared with the zero speed case). The encounter period is decreased (and the encounter frequency is increased) in head or bow-quartering waves.
- 1.4.3 The inception of parametric roll depends on the frequency of encounter being in the frequency range where the parametric roll is possible (Figure 3c). Therefore, the development of parametric roll depends on speed and heading.

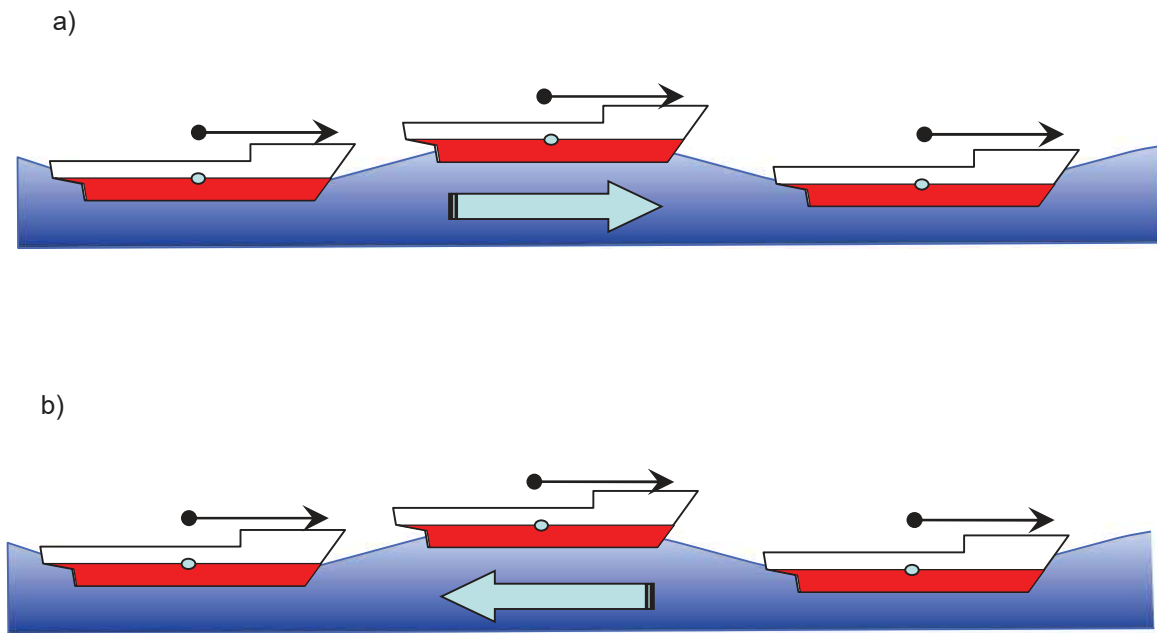


**Figure 5 Influence of speed and wave direction on parametric resonance (a) Following and stern-quartering seas: the encounter period is longer than the wave period (b) Head and bow-quartering seas: the encounter period is shorter than the wave period**

## 2 Supplementing information on Calculation for Checking Vulnerability with Level 1 Criteria

- 2.1 In the calculation of the bilge keel area to be used in 2.11.2.1 of the Code Part B of the fin stabilizers may be regarded as a kind of bilge keel, if they are non-retractable and calculated as a part of total bilge keel area. [On the other hand, the centre skeg should not be included. This is because existing model experiments indicate that the increase of the roll damping due to the centre skeg is almost zero for the case of small rise of floor. This may be because the pressure created by the skeg on the bottom works as a negative roll damping.]
- 2.2 The "sharp bilge" in 2.11.2.1 of the Code Part B means that bilge radius is smaller than 1% of the ship's breadth and the angle between piece-wise lines representing the bilge is smaller than 120°.
- 2.3 The value of  $S_w$  in 2.11.2.2 of the Code Part B can be corrected if operational water area is limited. In this case a wave scattering table shall be provided for the specified water area and its quality shall be equivalent to the IACS Recommendation No. 34 for the Northern Atlantic, shown as Table 2.11.3.4.2. The calculation procedures described in Appendix 1 shall be applied to this wave scattering table for the specified water area.
- 2.4 In the calculation of 2.11.2.3 of the Code Part B, a sinusoidal wave shall be used without hydrodynamic disturbance due to the ship. The water pressure due to the

wave may include the effect of wave particle velocity assuming that water depth is larger than the wavelength.

### **3 Supplementing information on Calculation for Checking Vulnerability with Level 2 Criteria**

- 3.1 In the calculation of 2.11.3.2.1 of the Code Part B, a sinusoidal wave shall be used without hydrodynamic disturbance due to the ship. The water pressure due to the wave may include the effect of wave particle velocity assuming that water depth is larger than the wavelength.
- 3.2 The table 2.11.3.2.3 of the Code Part B can be corrected if operational water area is limited. In this case a wave scattering table shall be provided for the specified water area and its quality shall be equivalent to the IACS Recommendation No. 34 for the Northern Atlantic. The calculation procedures described in Appendix 1 shall be applied to this wave scattering table for the specified water area for the specified water area.
- 3.3 Roll amplitude in 2.11.3.4.1 of the Code Part B as a steady state solution  $\phi = A \cos(\hat{\omega}t - \varepsilon)$  can be calculated by numerical simulation in the time domain with the guidelines according to Appendix 3. Alternatively, the averaging method specified in Appendix 5 can be used.
- 3.4 The roll damping coefficients to be used in Appendices 3 and 5 of this document should be estimated with scaled model tests using the following the procedures in MSC.1/Circ.1200 or alternative test procedures approved by the Administration. In the absence of roll decay model test data, the roll damping coefficients in 3.3 of this document may be estimated using either a simplified Ikeda's method or type-specific empirical data (with bilge keels geometry effect included), if appropriate. The forward speed effect may be taken into account for the lift component using Ikeda's or an equivalent method. The simplified Ikeda's formula is given in Appendix 4. [Alternatively, numerical simulations can be used for the estimation of roll damping, based on the solution of viscous hydrodynamic equations. In this case, validation of simulations should be performed for selected loading conditions to the satisfaction of Administration. Validation should be performed in comparison with model tests performed according to the procedures in MSC.1/Circ.1200 or alternative test procedures approved by the Administration.]
- 3.5 The type-specific empirical data (with bilge keels geometry effect included) can be used with the approval of the Administration. In case of the use of passive or active roll damping devices, the effect of these devices can be taken into account with the satisfaction of the Administration.
- 3.6 If operational water area is limited, the table 2.11.3.4.2 of the Code Part B can be replaced with a wave scattering table for the specified water area, which is equivalent in quality to the IACS Recommendation No. 34 for the Northern Atlantic.
- 3.7 For determining the roll amplitude [or the maximum roll angle] for each  $H_i$  in 2.11.3.4.2 of the Code Part B, it is necessary to obtain the relationship between  $h$  and the roll amplitude shall be obtained by calculation. Here if the roll amplitude has a peak at the certain wave steepness  $h_p$ , the peak value of the roll amplitude should be used when the wave steepness is larger than  $h_p$ .



3.8 The calculation formula for wave height in 2.11.3.4.2 of the Code Part B is as follows:

$$H_{ri} = 4.0043\sqrt{m_0} \quad (1)$$

$$m_0 = \int_{0.01\omega_L}^{\omega_L} \left\{ \frac{\frac{\omega^2 L}{g} \sin\left(\frac{\omega^2 L}{2g}\right)}{\pi^2 - \left(\frac{\omega^2 L}{2g}\right)^2} \right\}^2 A \omega^{-5} \exp(-B\omega^{-4}) d\omega \quad (2)$$

$$+ \int_{\omega_L}^{3\omega_L} \left\{ \frac{\frac{\omega^2 L}{g} \sin\left(\frac{\omega^2 L}{2g}\right)}{\pi^2 - \left(\frac{\omega^2 L}{2g}\right)^2} \right\}^2 A \omega^{-5} \exp(-B\omega^{-4}) d\omega$$

$$\text{where } A = 173 H_{si}^2 T_{01}^{-4} \quad (3)$$

$$B = 691 T_{01}^{-4} \quad (4)$$

$$T_{01} = 1.086 T_{zi} \quad (5)$$

$$g = 9.81 (m/s^2) \quad (6)$$

$$\omega_L = \sqrt{\frac{2g\pi}{L}} \quad (7)$$

$L$ (m): the length of the ship at waterline,  
 $H_{si}$  (m) : the significant wave height, and  $T_{zi}$  (s) , : the zero-crossing mean wave period.

If  $H_{ri} > 0.1L$ ,  $H_{ri}$  should be set as  $H_{ri} = 0.1L$ .

3.9 The natural period in calm water for 2.11.3.2.2 of the Code Part B and for the section 3.3 is calculated as follows:

$$T_\phi = 2C \cdot B / GM^{0.5} \quad (8)$$

where

$$C = 0.373 + 0.023(B/d) - 0.043(L_{wl}/100) \quad (9)$$

$B$  is the moulded breadth of the ship in metres,  $d$  is the mean moulded draught of the ship in metres,  $L_{wl}$  is the length of the ship at waterline in metres, and  $GM$  is the initial metacentric height corrected for the free surface effects in metres

For [containerships] [ships carrying containers], the following formula can be used alternatively for the natural roll period:

$$T_\phi = 2\pi \sqrt{I_{xx} / (mgGM)} \quad (10)$$

where

$$I_{xx} = 1.1m_1(B/3)^2 + 1.1m_1H_{SH}^2 + 1.1\sum\{m_i(y_i^2 + (z_i - z_T)^2) + (b_i^2 + h_i^2)m_i/12\} \quad (11)$$

$m$  is the mass of ship in kilograms,  $H_{SH}$  is the distance from the centre of mass of ship to the centre of mass of the ship without containers on deck in metres,  $m_i$  is the mass of each container loaded on deck in kilograms,  $y_i$  and  $z_i$  in metres, are the transverse and vertical coordinates of the container centre of mass, respectively,  $b_i$  and  $h_i$  in metres, are the breadth and height of the container, respectively,  $z_T$  is the vertical height of the ship centre of gravity in metres, and  $m_1$  is the mass of the ship without containers on deck in kilograms.

[For all ships, the following formula can be alternatively used for  $I_{xx}$ :

$$I_{xx} = mK^2 \quad (12)$$

where

$$\left(\frac{K}{B}\right)^2 = 0.125 \left[ C_u \cdot C_b + 1.10C_u(1-C_b) \left( \frac{H_s}{d} - 2.20 \right) + \left( \frac{H_s}{B} \right)^2 \right] \quad (13)$$

$$C_u = \frac{A_u}{L_u B} \quad (14)$$

$$H_s = D + \left( \frac{A'}{L_{pp}} \right) \quad (15)$$

$C_u$  : upper deck area coefficient

$A_u$  : projected area of upper deck

$L_u$  : overall length of upper deck

$C_b$  : block coefficient

$B$  : moulded breadth

$d$  : mean draught

$H_s$  : effective depth

$D$  : moulded depth

$L_{pp}$  : length between perpendiculars

$A' = A + A_c$

$A'$  : lateral projected area of forecastle and deck house ( $A$ ) and on deck cargoes ( $A_c$ ) ]

#### 4. Relationship between Level 1 and 2 Criteria

- 4.1 The vulnerability level 1 criterion and the first check of level 2 criteria were developed by simplifying the level 2 criteria. The equation (E.1) in appendix 5 used in the second check of the level 2 criteria is the formula for determining the amplitude of parametric roll that the roll frequency is half the wave encounter frequency based on the uncoupled roll equation with nonlinear restoring, nonlinear

roll damping and metacentric height restoring variation. If the roll damping and restoring are linearized, the following approximation should be made:

$$\alpha_E \approx \alpha, \gamma = 0, GM \approx GM_E, \omega_{\phi E} \approx \omega_{\phi}, l_3 = l_5 = 0 \quad (16)$$

Here the suffix E indicates the equivalently linearized value. Furthermore, if the worst case within the linear approximation is assumed, the following relation can be obtained:

$$\hat{\omega} = \omega_{\phi E} \quad (17)$$

In addition, if we assume the mean of metacentric height variation due to waves is small, the following approximation can be used:

$$GM_{mean} = 0 \quad (18).$$

When we substitute the equations (16-18) into the equation (E.1) in Appendix 5, the following formula is obtained:

$$\frac{8\pi^2 \alpha_E}{(2\pi^2 - A^2)\omega_{\phi E}} = \frac{GM_{amp}}{GM_E} \quad (19)$$

Therefore, the occurrence condition for parametric roll with the amplitude for the roll angle used for the equivalent linearization or larger is as follows:

$$\frac{GM_{amp}}{GM_E} > \frac{8\pi^2 \alpha_E}{(2\pi^2 - A^2)\omega_{\phi E}} \approx \frac{4\alpha_E}{\omega_{\phi E}} \quad (20)$$

The right-hand side of this equation indicates the normalized equivalent roll damping coefficient multiplied by 4. In these vulnerability criteria, empirical formulae for the equivalent roll damping as the function of bilge keel area and the midship coefficient, which was developed with the calculation using Ikeda's simplified estimation method. This outcome is used for the vulnerability level 1 criterion and the first check of the level 2 criteria. Therefore, these requirements are simplification of the second check of the level 2 criteria

- 4.2 The difference between the level 1 criterion and the first check of the level 2 criteria are as follows. While the level 2 uses 16 different and typical waves for calculating the metacentric height variation, the level 1 uses the wave having the worst wavelength, i.e. the wavelength to ship length ratio of 1. Thus the level 1 criterion is expected to be more conservative than the first check of the level 2 criteria.
- 4.3 While both the level 1 criterion and the first check of the level 2 criteria judge danger of parametric roll with its occurrence condition, the level 2 criterion judges with the magnitude of parametric roll. This means that, if parametric roll occurs with small amplitude, the second check of level 2 criteria could conclude that the ship is not

vulnerable to stability failure due to parametric roll. Thus, the second check of level 2 criteria is less conservative in principle.

4.4 The standards for the level 1 and 2 criteria were determined with the reports of major large heel incident of a containership.

## 5. Examples of Checking Vulnerability

[As an example, we use the following data of a containership at the full load condition:

$L_{PP}$	262.0 m	ship length between perpendiculars
$L_f$	262.0m	ship length defined in 2008 IS Code
$B$	40.0 m	moulded ship breadth
$D$	24.45 m	moulded ship depth
$d$	11.5 m	moulded mean ship draught
$\tau$	0 m	trim
$LCG$	125.52 m	longitudinal centre of gravity from aft perpendicular
$C_b$	0.559	block coefficient
$C_m$	0.950	midship section coefficient
$GM$	1.965 m	metacentric height with free surface correction
$T_\phi$	25.1 s	ship natural roll period
$VCG$	18.4 m	vertical centre of gravity above baseline
$l_{BK}/L_{pp}$	0.292	bilge keel length normalized with ship length between perpendiculars
$b_{BK}/B$	0.0100	bilge keel width normalized with moulded ship breadth
$V_s$	12.165 m/s	ship service speed

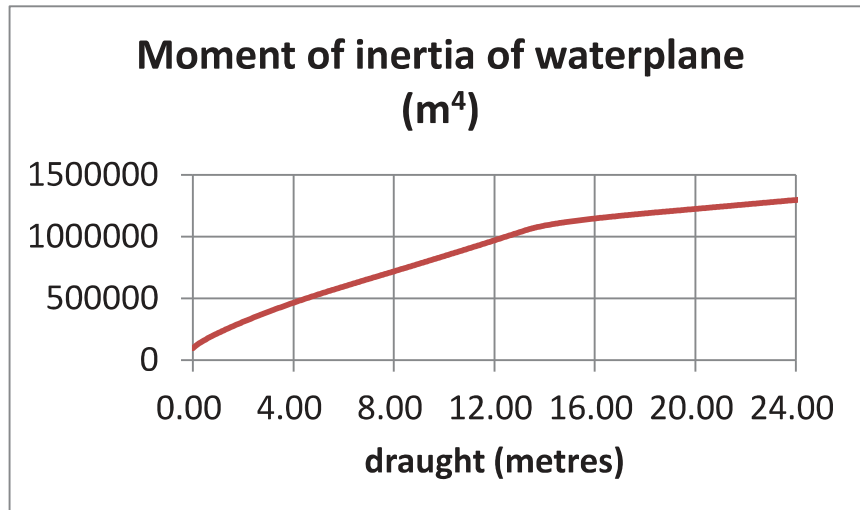


**Figure 1** The relationship between the moment of inertia of waterplane for the subject ship

Level 1

Firstly, we calculate the bilge keel area ratio,  $100A_K/(L_{pp}B)$ .

$$100A_K/(L_{pp}B) = 100 \times (I_{BK}/L_{PP}) \times (b_{BK}/B) \times 2 = 100 \times 0.292 \times 0.01 \times 2 = 0.584$$

Secondly, considering  $C_m = 0.95$  at the full load condition, the standard,  $R_{PR}$ , is calculated:

$$R_{PR} = 0.17 + (10.625 \times C_m - 9.775) \times (100A_K/(L_{pp}B))$$

$$= 0.17 + (10.625 \times 0.95 - 9.775) \times 0.584 = 0.3561$$

Thirdly, the lower draught is calculated:

$$\delta d_L = \text{Min}\{d - 0.25d_{full}, LS_w/2\} = \text{Min}\{0.75 \times 11.5, 262 \times 0.0167/2\}$$

$$= \text{Min}\{8.625, 2.188\} = 2.188 \text{ m}$$

$$d_L = d - \delta d_L = 11.5 - 2.188 = 9.312 \text{ m}$$

so that, according to the hydrostatic data, the relevant  $I_L$  is 799,900m<sup>4</sup>.

Fourthly, the higher draught is calculated:

$$\delta d_H = \text{Min}\{D - d, LS_w/2\} = \text{Min}\{24.45 - 11.5, 262 \times 0.0167/2\} = \text{Min}\{12.95, 2.188\} = 2.188 \text{ m}$$

$$d_H = d + \delta d_H = 11.5 + 2.188 = 13.69 \text{ m}$$

so that, according to the hydrostatic data shown in Figure 1, the relevant  $I_H$  is 1,076,500m<sup>4</sup>.

Fifthly,  $\Delta GM/GM$  is calculated as follows:

$$\Delta GM/GM = (I_H - I_L)/(2V)/GM = (I_H - I_L)/(2 \times C_b \times L_{pp} \times B \times d)/GM$$

$$= (1076500 - 799900)/(2 \times 262 \times 40 \times 11.5 \times 0.559)/1.965 = 1.045$$

Therefore,  $\Delta GM/GM(=1.045) > R_{PR}(=0.3561)$  so that the ship is judged as vulnerable to parametric roll.

**Table 1** Dangerous wave cases identified the first check for the ship

wave			
steepness	$GM_{amp}/GM_{mean}$	$GM_{mean}[m]$	$V_{pr}[m/s]$
0.016217	0.502808	2.011166	2.707489
0.015633	0.625547	2.143438	0.902751
0.014875	0.643971	2.274462	1.385557
0.014031	0.611431	2.304384	3.642522
0.013164	0.570199	2.280052	5.927151
0.012309	0.518479	2.2342	8.323531
0.011513	0.464894	2.180213	10.86715

#### First Check of Level 2

Firstly, using the  $R_{PR}(=0.3561)$  and  $V_S=12.165$  m/s, the dangerous wave cases among 16 are identified as shown in Table 1.

Then, the weighted average is calculated as follows:

$$C1=0.4368$$

Since  $C1 > 0.06$ , the ship is judged as vulnerable to parametric roll.

#### Second Check of Level 2

Firstly, the values of C2 with the critical wave steepness for parametric roll of 25 degrees are calculated for various heading and speed in Table 2.

**Table 2** C2 values for the ship under various heading and speed

Fn/heading	Critical wave steepness	C2(Fn)
0.240/ head	0.05944	0.0000
0.208/ head	0.04952	0.0000
0.120/ head	0.01994	0.0474
0.0/ head & follow	0.009094	0.4624
0.120/ follow	>0.1	0.0000
0.208/ follow	>0.1	0.0000
0.240/ follow	>0.1	0.0000

Then, averaging the above, the final value of C2 is obtained as follows:

$$C2=0.07283$$

Since  $C2 > 0.06$ , the ship is judged as vulnerable to parametric roll.

Level 1 and Table 1 indicate that parametric roll could occur for the ship under the wave steepness of about 0.015 or larger. However, these do not provide any information about the magnitude. Table 2 shows that the parametric roll amplitude could be more than 25 degrees, which could induce cargo damage and so on, only when the ship is zero or very low forward velocity. It also indicates the ship could often meet such sea states in the North Atlantic. This is why the level 2 criterion judges the ship vulnerable to parametric roll danger. At the same time, Table 2 also suggests that ship can be safely operated if the ship service speed is kept under specified sea states.]





## ANNEX 5

### DRAFT EXPLANATORY NOTES ON THE VULNERABILITY OF SHIPS TO THE SURF-RIDING/BROACHING STABILITY FAILURE MODE

[This is the draft explanatory notes to the "PROPOSED AMENDMENTS TO PART B OF THE 2008 IS CODE TO ASSESS THE VULNERABILITY OF SHIPS TO THE SURF-RIDING/BROACHING STABILITY FAILURE MODE" as SDC 2/WP.4, annex 3.]

#### Chapter 4 – THE VULNERABILITY OF SHIPS TO THE SURF-RIDING/BROACHING STABILITY FAILURE MODE

##### 1. Physical background of surf-riding and broaching-to

###### 1.1 General description of surf-riding/broaching failure mode

1.1.1 Broaching (a shortening of "broaching-to") is a violent uncontrollable turn that occurs despite maximum steering efforts to maintain course. As with any other sharp turn event, broaching is accompanied with a large heel angle, which has the potential effect of a partial or total stability failure. Broaching is usually preceded by surf-riding which occurs when a wave, approaching from the stern, "captures" a ship and accelerates the ship to the speed of the wave (i.e. the wave celerity). Surf-riding is a single wave event in which the wave profile does not vary relative to the ship. Because most ships are directionally unstable in the surf-riding condition, this maneuvering yaw instability leads to an uncontrollable turn – termed "broaching."

1.1.2 Because surf-riding usually precedes broaching, the likelihood of surf-riding occurrence can be used to formulate vulnerability criteria for broaching. In order for surf-riding to occur, several conditions need to be satisfied:

- .1 the wave length should be between one and three times the ship length;
- .2 the wave must be sufficiently steep to produce sufficient wave surfing force;  
and
- .3 the ship speed should be comparable to the wave celerity.

[Large ships (i.e. over 200 metres in length) do not surf-ride because waves of this and greater length tend to travel faster than the ship (i.e. 34 plus knots) and these ships have too much mass (i.e. inertia) to allow them to accelerate to the wave speed before the wave passes.]

1.1.3 When a ship proceeds in following waves, three main forces act in the axial direction. Thrust is the force produced by the ship's propulsor to propel the ship forward. Resistance (or drag) is the force that opposes the forward ship motion. The surging wave force is the force imparted by a wave to either push the ship forward or back depending on whether the ship is on the face or back of a wave, respectively. These forces are represented in Figure 1.

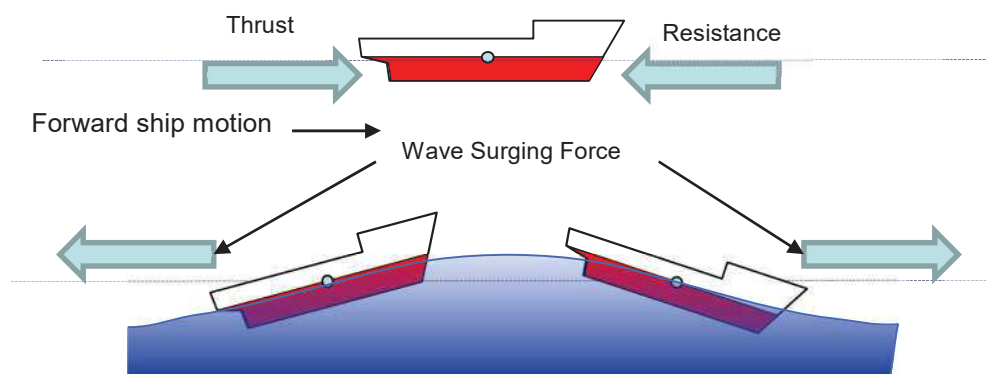


Figure 1. Forces Acting on a Ship in Following Waves

1.1.4 When a surging wave force is present, three conditions are possible:

- .1 *Surging motion.* This condition occurs when the wave surge force is insufficient to overcome the difference between the thrust of the ship's propulsor and the resistance of the ship at the wave celerity. In this case, the ship oscillates from increasing speed when on the front side of the wave to decreasing speed when on the back side of the wave.

The other two conditions involve the two ship speed thresholds that can cause surf-riding and that are directly related to the thrust the ship's propulsor delivers to maintain a given speed.

- .2 Surf-riding under certain initial condition (*first threshold of surf-riding*). This condition occurs is the ship speed for which the forward surge force of the wave at a particular point on the wave can exceed the difference between the thrust of the ship's propulsor and the resistance of the ship at the wave celerity. In this case, surf-riding could occur if the ship is accelerated with some external force under the self-propelled condition.
- .3 Surf-riding under any initial condition (*second threshold of surf-riding*). This is the situation for which the ship kinetic energy is too large for the ship to be overtaken by a wave. Thus the oscillatory surge motion cannot stably exist so that surf-riding occurs regardless the initial ship position and forward speed.

1.1.5 To explain these three conditions more fully and since surf-riding occurs when the ship speed is equal to the wave celerity, locating the position of reference on the wave crest allows a convenient way to understand surf-riding. In this view, when the ship surf-rides, it appears to remain stationary because the reference position moves with the wave.

1.1.6 In the case of surging motion, the thrust delivered by the ship's propulsor is not sufficient to propel the ship to a speed equal to the wave celerity in calm water, which is

depicted in Figure 2a. Figure 2b shows the difference between the thrust and resistance in calm water for the ship located at different positions on a wave; this difference is negative when the resistance is greater than the thrust. Because there is no position on the wave in which the thrust – resistance difference is fully compensated by wave force, the only motion occurring is surging forward and backward depending on the ship's position on the wave.

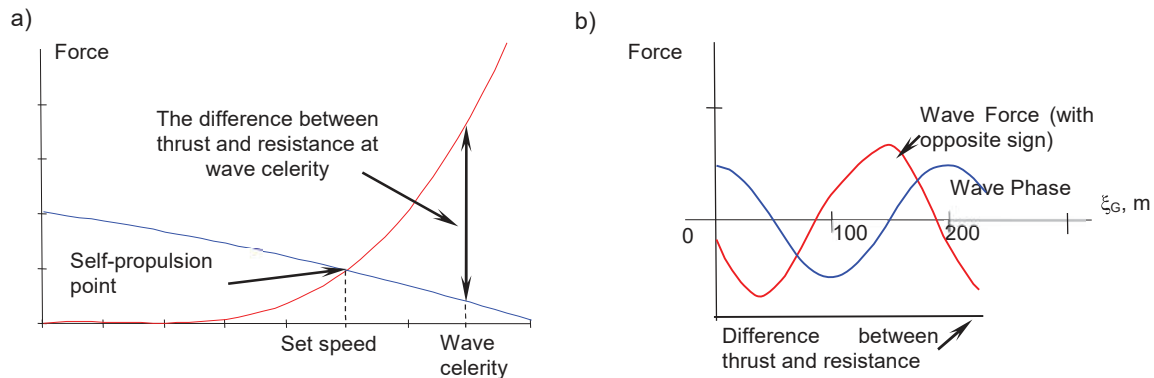


**Figure 2(a) Resistance and Propulsion Showing Self-Propulsion Point and Thrust-Resistance Difference (b) Wave Forces and Balance between Thrust and Resistance Shown for Different Ship Positions on a Wave**

1.1.7 The mechanics of surging can be illustrated using the curves of thrust and resistance as shown in Figure 3. When the ship is on the back side of the wave, the surging force pushes the ship backwards which causes the instantaneous speed to decrease and the resistance to become less than the thrust. This difference is directed forward, against the surging force. When the ship is on the face of the wave, the surging force pushes the ship forward causing the instantaneous speed to increase and the resistance to exceed the thrust. As the wave passes the ship, these two conditions recur.

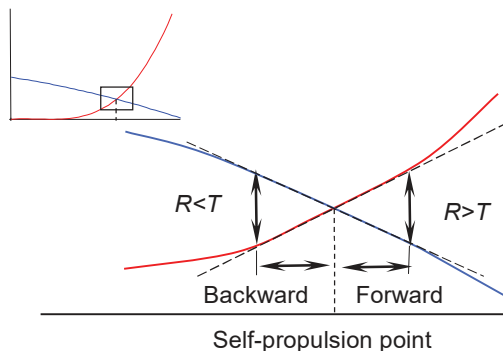


**Figure 3. Small surging motions around self-propulsion point**

## 1.2 Description of surf-riding equilibrium: the first threshold

1.2.1 The value of the wave force depends on the location of the ship on the wave as well as the wave height and wavelength. The face of the wave pushes a ship forward – hence, the forward wave or surge force; while the back slope does the opposite. Indeed, there are neutral points near the wave crest and wave trough. If the wave has appropriate length and height, the surge force is sufficient to offset the negative difference between the thrust and resistance. This creates two points of equilibrium as shown in Figure 4. This figure superimposes the surge force with the difference between thrust and resistance (the

horizontal line below the abscissa) and shows the intersections with the wave force curve to mark the two points of equilibrium on the wave. The stable equilibrium marks the first threshold of surf-riding.

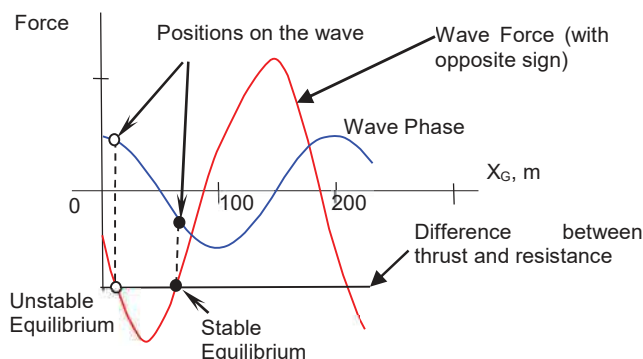


**Figure 4. Wave forces and Balance between Thrust and Resistance for different positions of a Ship on a Wave showing the first threshold of surf-riding.**

### 1.3 The stability of surf-riding equilibrium

1.3.1 Figure 4 provides an example of the two points of equilibrium referred to as stable and unstable. If a ship is considered to be surf-riding in which midship is located about 70 m forward of the wave crest (marked as stable equilibrium near wave trough in Figures 4 and 5), the ship speed will be equal to the wave celerity. If the ship is disturbed from this location forward and toward the wave trough, the surge force decreases. Therefore, the difference between thrust and resistance will cause a decrease in the instantaneous ship speed and the wave will start to overtake the ship. As the ship moves back on the wave face toward the wave crest, the wave surge force increases and pushes the ship back to the stable equilibrium.

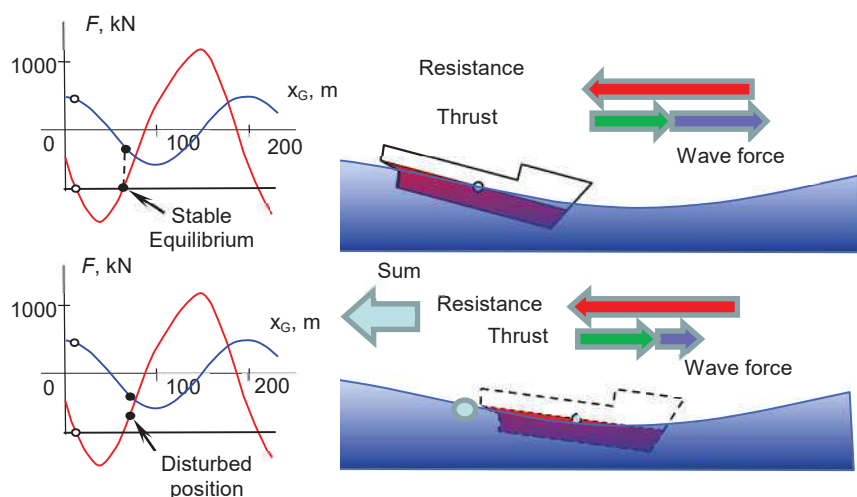


**Figure 5. Disturbance Forward from the Stable Equilibrium**

1.3.2 Conversely to the case shown by Figure 5, Figure 6 considers the ship to be disturbed from the equilibrium backwards -- towards the wave crest. In this case, the wave force becomes larger than the difference between thrust and resistance. Thus, the ship speed will increase and move on the wave forward to the surf-riding equilibrium (trough).

Therefore, in either case (i.e. a disturbance forward or backward), the ship will tend to move toward the equilibrium near the wave trough, which makes this equilibrium stable.

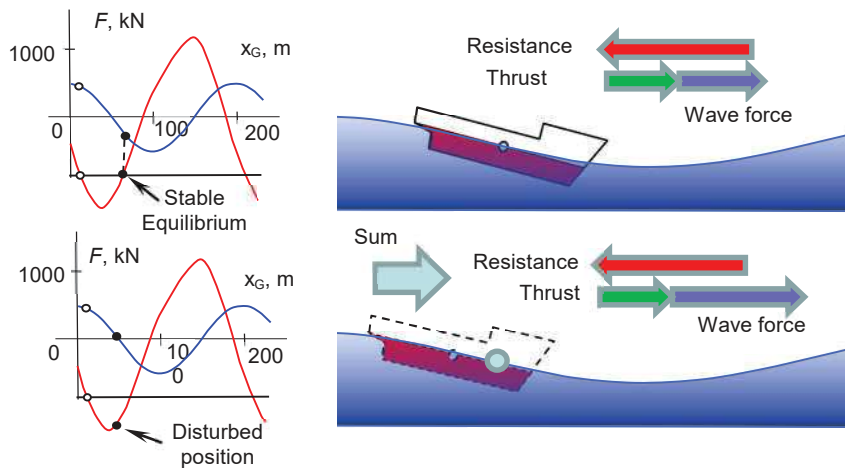


**Figure 6. Disturbance backwards from the Stable Equilibrium**

1.3.3 If a ship is now considered to be surf-riding with the midship located about 30 m forward of the wave crest (marked as unstable equilibria near wave crest in Figure 4), the ship speed will be equal to the wave celerity. If the ship is disturbed from this location forward (towards the wave trough as shown in Figure 7), the wave force increases and will cause the ship speed to increase and move the ship further forward on the wave until it arrives at the stable equilibrium near the wave trough.

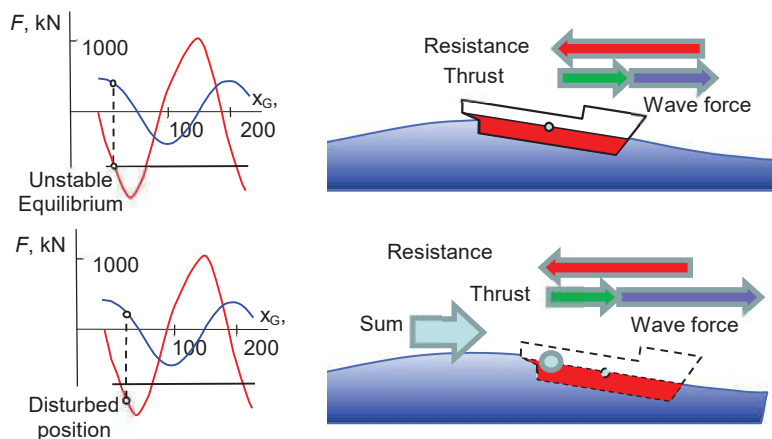


**Figure 7. Disturbance Forward from the Unstable Equilibrium**

1.3.4 Conversely, if the ship is disturbed from this location backward, towards the wave crest as shown in Figure 8, the wave force decreases and the instantaneous speed also starts to decrease. In this case, difference between thrust and resistance will cause a decrease in the instantaneous ship speed which causes the wave to start to overtake the ship. There are several scenarios that consider what may happen next, but in no case does the ship return back to this equilibrium, which makes the equilibrium near the wave crest unstable.

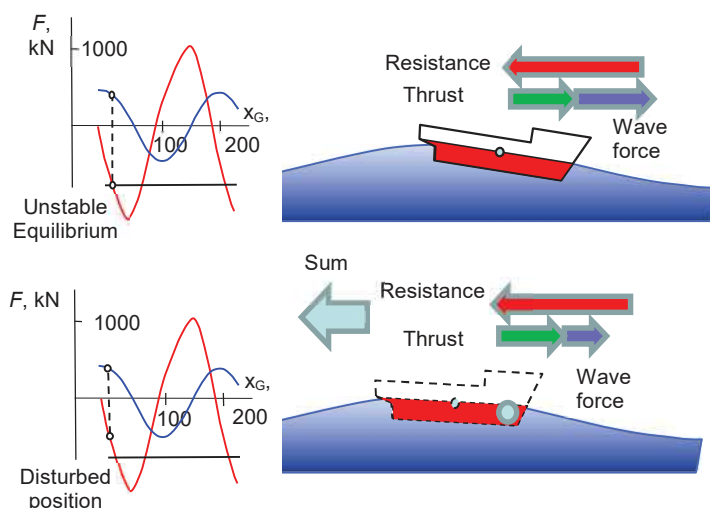


**Figure 8. Disturbance Backward from the Unstable Equilibrium**

1.3.5 If there is no surf-riding equilibrium, surf-riding is not possible and the ship will simply surge. That means that all the combinations of instantaneous speed and position on the wave lead to the same outcome. However, once points of equilibrium appear at certain positions on the wave, not all the combinations of the wave position and instantaneous speed lead to the same response. If a ship is "placed" exactly at the location of the stable equilibrium near wave trough and accelerated to the wave celerity, it will surf-ride. Any small disturbance from this position will return the ship back to equilibrium. If a ship is placed at the unstable equilibrium near the wave crest, accelerated to the wave celerity and then disturbed towards the wave trough, it will end up at the stable surf-riding equilibrium as well. Thus, there is a set of combinations of wave positions and instantaneous speeds that will lead to surf-riding. One can say that these combinations form a "domain of attraction to surf-riding equilibrium." Outside of this domain, two options are possible: surging or surf-riding. So, in principle, once outside of the attraction domain, the ship either continues to surge or is attracted to surf-riding equilibrium on some other wave.

## 1.4 Loss of oscillatory surging motion

1.4.1 When the energy/work balance of the wave surging force and the difference between thrust and resistance is considered, the latter disperses the kinetic energy obtained from wave. When these two works are balanced, the ship's response is surging. However, if a wave provides the ship with more kinetic energy than the difference between thrust and resistance can disperse, this excessive kinetic energy eventually leads to acceleration and to attraction to the surf-riding equilibrium. The surf-riding becomes a new energy balance between the works of wave surging force and the difference between thrust and resistance. The ship surf-rides because of the excessive kinetic energy imparted to the ship.

1.4.2 The face of the wave provides more chances for surf-riding because the wave surging force is directed forward. If the ship is on the back side of the wave, the wave surging force is directed backward but a surging energy balance still may occur because both surging and surf-riding may co-exist for the same speed setting and wave parameters. If the initial kinetic energy level can be dispersed by the difference between thrust and resistance, surging will occur; if not, surf-riding will occur. If the wave parameters are such that the wave adds too much kinetic energy (steep waves) to ship motions that it cannot be dispersed by the difference between thrust and resistance, then surging motions are no longer possible. Even when the ship starts with low initial kinetic energy level on the back slope of the wave with the ship's propulsor delivering a set thrust, each sequential wave will add a bit of kinetic energy that cannot be dispersed; then inevitably surf-riding will occur as the ship moves towards stable equilibrium. This is referred to as the "surf-riding under any initial condition" of surf-riding which is the basis used for the surf-riding vulnerability criteria. The "surf-riding under certain initial condition" is not used for the current criteria.

1.4.3 For a particular wave, the thrust at the surf-riding under any initial condition identifies the critical setting of the ship's propulsor in the vulnerability criterion for which surf-riding becomes inevitable. For approximately consider energy balance during ship runs for one wavelength, the Melnikov analysis or the systematic phase plane analysis can be used to identify the surf-riding under any initial condition. The level 2 vulnerability criteria directly use the Melnikov analysis with many possible combinations of wave height and wavelength at sea and the level 1 vulnerability criteria are empirical estimates based on many calculated results of such analysis under the wave steepness of 1/10, which is known as the practical limit of stable water waves.

## 2. Level 1 Vulnerability Criteria for Surf-riding/Broaching

The criterion and the standard for the Froude number in the level 1 criterion were adopted as a part of MSC.1/Circ.707 in 1995 and then superseded as MSC.1/Circ.1228. This guidance concludes that surf-riding may occur when the ship speed is higher than:

$$V_s \geq \frac{1.8\sqrt{L}}{\cos(180^\circ - \alpha)}$$

where,  $V_s$  = the speed of the ship in knots  
 $\alpha$  = the angle of wave encounter in degrees

Assuming following seas  $\alpha = 180^\circ$  and transforming the formulae to be based on the Froude number yields:

$$F_n \geq \frac{1.8 \cdot 0.5144}{\sqrt{g}} = 0.296 \approx 0.3$$

This is regarded as the lower limit of threshold for surf-riding under any initial condition for conventional ships in worst waves. It is compared with examples of such thresholds calculated for some sample ships with the Melnikov analysis as shown in Figure 9. This result also indicates that the worst wavelength for surf-riding is comparable to the ship length. This means that longer ships require longer waves for surf-riding but the lengths of steep ocean waves have certain limits so that small possibility for surf-riding exists for very long ships. Thus the level 1 vulnerability criteria also requires that the threshold of ship length, i.e. 200 metres.



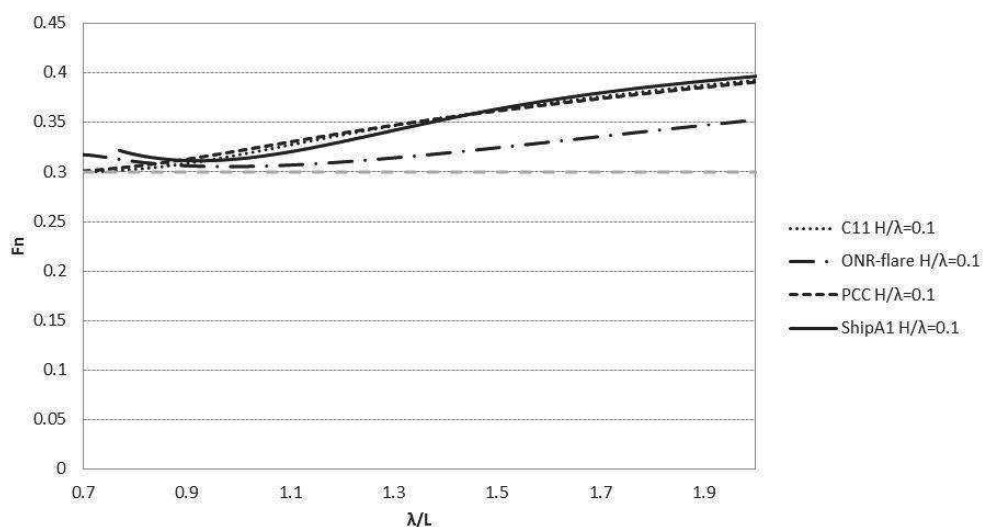


**Figure 9. Thresholds of surf-riding under any initial condition for some sample ships in the wave steepness ( $H/\lambda$ ) of 1/10 with different wavelength to ship length ratio ( $\lambda/L$ ) compared with the nominal Froude numbers ( $F_n$ ) of 0.3.**

### 3. Level 2 Vulnerability Criteria for Surf-riding/Broaching

#### 3.1 Alternative to the assessment of the Level 2 vulnerability criteria

[As contained in 2.12.1.1, for a ship that does not meet the standard contained in 2.12.2, the procedures of ship-handling on how to avoid dangerous conditions for surf-riding/broaching recommended in Section 4.2.1 of the "Revised guidance to the master for avoiding dangerous situations in adverse weather and sea conditions," MSC.1/Circ.1228, may apply subject to the agreement of the approval authority as an alternative for 2.12.2. More specifically, the speed and/or course of the ship should be changed if:

1. the average wavelength is longer than  $0.8 L$ , and
2. the significant wave height is larger than  $0.04 L$ , and
3. the angle of encounter is in the range  $135^\circ < \alpha < 225^\circ$ , and
4. the ship speed is higher than  $(1.8L)/\cos(180 - \alpha)$  (knots).

Here  $L$  means the ship length as defined in the Code,  $\alpha$  means the angle of encounter ( $\alpha = 0^\circ$  in head sea,  $\alpha = 90^\circ$  for sea from starboard).]

#### 3.2 On the assessment of the weighting factor, $W_{ij}$ , in 2.12.3.4 in the Level 2 vulnerability criteria

3.2.1 The calculation formula of,  $W_{ij}$ , in 2.12.3.4 of the vulnerability criteria for surf-riding/broaching is the joint probability density function of local wave steepness and local wavelength under the stationary wave state with a Pierson-Moskowitz type wave spectrum.

3.2.2 The envelope of an irregular wave time history is described with the slowly varying amplitude and phase. Then the joint probability density of the envelope amplitude, phase and their time derivatives can be calculated as the Gaussian process. If the wave spectrum is reasonably narrow, the envelope amplitude can be regarded as one-half the local wave height and the time derivative of the envelope phase can be related to the local wave period because of the wave dispersion relation. Thus, the joint probability density function of the



local wave height and the local wave period can be obtained by transforming the envelope amplitude, phase, and their time derivatives.

### 3.3 On the assessment of resistance, thrust, and the critical number of revolutions in the Level 2 vulnerability criteria

3.3.1 The critical number of revolutions of the propulsor corresponding to the surf-riding threshold,  $n_{cr}$ , (rps) in 2.12.3.5.6 of the vulnerability criteria, can be calculated by solving the following equation by using a numerical iteration method. In the case that the resistance in calm water is approximated with the 5th power polynomial, the critical number of revolutions,  $n_{cr}$ , corresponding to the second surf-riding threshold is calculated by numerical solution of the following equation:

$$2\pi \frac{T_e(c_i, n_{cr}) - R(c_i)}{f_{ij}} + 8a_0 n_{cr} + 8a_1 - 4\pi a_2 + \frac{64}{3} a_3 - 12\pi a_4 + \frac{1024}{15} a_5 = 0$$

where,

$$T_e(c_i, n_{cr}) = \tau_0 n_{cr}^2 + \tau_1 c_i n_{cr} + \tau_2 c_i^2 = \text{thrust, see 3.3.2}$$

$$R(c_i) = \text{resistance, see 3.4.2}$$

$$a_0 = -\frac{\tau_1}{\sqrt{f_{ij}} \cdot k_i \cdot (M + M_x)}$$

$$a_1 = \frac{r_1 + 2r_2 c_i + 3r_3 c_i^2 + 4r_4 c_i^3 + 5r_5 c_i^4 - 2\tau_2 c_i}{\sqrt{f_{ij}} \cdot k_i \cdot (M + M_x)}$$

$$a_2 = \frac{r_2 + 3r_3 c_i + 6r_4 c_i^2 + 10r_5 c_i^3 - \tau_2}{k_i \cdot (M + M_x)}$$

$$a_3 = \frac{r_3 + 4r_4 c_w + 10r_5 c_w^2}{\sqrt{k_i^3 (M + M_x)^3}} \cdot \sqrt{f_{ij}}$$

$$a_4 = \frac{r_4 + 5r_5 c_i}{k_i^2 (M + M_x)^2} f_{ij}$$

$$a_5 = \frac{r_5}{\sqrt{k_i^5 (M + M_x)^5}} \sqrt{f_{ij}^3}$$

$r_1, r_2, r_3, r_4, r_5$  = approximation coefficients for the calm water resistance (see 3.4). If a third order polynomial approximation is used  $r_4 = 0$  and  $r_5 = 0$ .

$M$  = mass of the ship (kg)

$M_x$  = added mass of the ship in surge (kg). In absence of ship-specific data,  $M_x$  may be assumed to be  $0.1 M$ .

$$c_i =$$

$$\sqrt{\frac{g}{k_i}} = \text{wave celerity}$$

$$k_i = 2\pi/\lambda_i = \text{wave number}$$

$$f_{ij} = \rho g k_i \frac{H_{ij}}{2} \sqrt{Fc_i^2 + Fs_i^2}$$

$$Fc_i = \sum_{m=1}^N \Delta x_m S(x_m) \sin kx_m \exp(-0.5k_i \cdot d(x_m))$$

$$Fs_i = \sum_{m=1}^N \Delta x_m S(x_m) \cos kx_m \exp(-0.5k_i \cdot d(x_m))$$

$x_m$  = longitudinal distance from the center of ship mass to a  $m$ -th station (m), positive for a bow section

$d(x_m)$  = draft at  $m$ -th station in calm water (m);

$S(m_i)$  = area of submerged portion of the ship at  $m$ -th station in calm water (m<sup>2</sup>),

$N$  = number of stations.

Notes: The coefficients  $a_1$ ,  $a_2$ ,  $a_3$ ,  $a_4$ , and  $a_5$  do not have indexes of the wave cases in order to keep the formulae simple; however, they do depend on both the wave length and the wave height.

The complete amplitude for the wave case with the wave length,  $\lambda_i$ , and wave height,  $H_{ij}$ , is calculated by formulae from paragraph 2.12.3.5.5

3.3.2 For a ship using one propeller as a main propulsor, the thrust approximation coefficients  $\tau$  are calculated as:

$$\tau_0 = \kappa_0 (1 - t_p) \rho D_p^4$$

$$\tau_1 = \kappa_1 (1 - t_p) (1 - w_p) \rho D_p^3$$

$$\tau_2 = \kappa_2 (1 - t_p) (1 - w_p)^2 \rho D_p^2$$

Where,

$t_p$  = approximate thrust deduction;

$w_p$  = approximate wake fraction;

$D_p$  = propeller diameter (m);

$\rho$  = density of salt water, (1,025 kg/m<sup>3</sup>)

$\kappa_0, \kappa_1, \kappa_2$  = approximation coefficients for the propeller thrust coefficient in calm water (see 3.5);

$$K_T(J) = \kappa_0 + \kappa_1 J + \kappa_2 J^2$$

$$J = \frac{u}{nD_p}$$

$u$  = speed of the ship (m/s) in calm water; and

$n$  = commanded number of revolutions

3.3.3 This formula is based on the Melnikov analysis, by which a boundary between periodic and non-periodic ship surge motions can be identified. Here the periodic motion indicates the case a ship is overtaken by waves, and the non-periodic motion indicates surf-riding, under which a ship runs with a wave.

3.3.4 Alternatively, also other numerical iteration methods can be used with the agreement of the approval authority.

#### 4. On resistance curve fitting

4.1 Calm water resistance,  $R(u)$ , can be estimated either by using geometrically scaled model tests and standard scaling law or using a numerical method approved by the Administration. [The ship's resistance should be estimated to a ship speed up to 20% over the maximum service speed.] The Administration may establish specific requirements on the approximation of the ship's resistance.

4.2 The calm water resistance curve,  $R(u)$ , is constructed based on the available resistance data using a polynomial approximation which may, but need not, include terms up to the 5th power:

$$R(u) \approx \sum_{i=0}^5 r_i u^i = r_0 + r_1 u + r_2 u^2 + r_3 u^3 + r_4 u^4 + r_5 u^5$$

Where,

$u$  = speed of the ship (m/s) in calm water;

$r_0, r_1, r_2, r_3, r_4, r_5$  = approximation coefficients for the calm water resistance

[4.3 The speed range of the resistance test should cover up to the celerity of waves whose length is 1.5 times the ship length. If it is not practical, the resistance curve may be fitted with the three sample points, i.e. MCR 85%, MCR 100% and MCR 110%. Here the following quadratic fitting should be used.

$$R(u) \approx \sum_{i=0}^2 r_i u^i = r_0 + r_1 u + r_2 u^2$$

4.4 Alternatively, data from the ship trial can be used in place of model test data but the correction of loading condition should be executed by a method that the Administration approves.]

4.5 The polynomial fit should be appropriate to ensure the resistance is continuously increasing as a function of speed in the appropriate range. The polynomial fit to approximate resistance curve requires caution. Available data points may not extend to the phase velocity (celerity) of the fastest wave under consideration. If this is the case, the following condition

should be verified for all values of ship speeds,  $u$ , up to the phase velocity of the fastest wave in consideration,  $u_{max}$ :

$$r_0 + r_1 + 2r_2u + 3r_3u^2 + 4r_4u^3 + 5r_5u^4 > 0$$

Where,

$$u_{max} = \sqrt{\frac{3gL}{2\pi}}$$

## 5 On thrust curve fitting for open propellers

5.1 The propeller thrust should be estimated using geometrically scaled model tests and standard scaling law or using a numerical method that is agreeable to the approval authority. The propeller advance ratio range should cover the whole positive range of propeller thrust coefficient. For one propeller, the propeller thrust can be approximated by using a second order polynomial approximation:

$$K_T(J) \approx \sum_{i=0}^2 \kappa_i J^i = \kappa_0 + \kappa_1 J + \kappa_2 J^2$$

where,  $J$  = propeller advance ratio;  
 $\kappa_0, \kappa_1, \kappa_2$  = approximation coefficients for the curve

5.2 In case of a ship having multiple propellers with the same propeller diameter and number of revolutions, the overall thrust can be calculated by summing the effect of individual propellers.

## 6. On thrust curve fitting for propellers

6.1 For ships using propulsor(s) other than open propeller(s) or are using unconventional propulsion arrangement, the propulsor thrust may be evaluated with a method appropriate to the propulsor used and to with the agreement of the approval authority. Recommended procedures are listed in the following paragraphs.

6.2 Podded propulsion: With podded propulsion the underwater body of the unit affects the propeller thrust considerably, and therefore the  $K_T$  curve of the whole pod unit in open water should be used. Otherwise, the same method described in 3.5 can be used.

## 7. On propulsion factors

7.1 Thrust deduction,  $t_p$ , should be evaluated using geometrically scaled model tests and standard scaling law. In absence of ship-specific model test data, the following approximations can be made:

[For single screw ships,  $t_p = 0.1$

For twin screw ships,  $t_p = 0.325 \cdot C_B - 0.1185 \frac{D_p}{\sqrt{Bd}}$

Where,

$C_B$	=	block coefficient
$B$	=	breadth
$d$	=	draught]

Alternative methods can be used with the agreement of the approval authority.

7.2 Wake fraction,  $w_p$ , should be evaluated using geometrically scaled model tests and standard scaling law. [In absence of ship-specific model test data, a conservative assumption of the wake fraction  $w_p$  as 0.1 can be made. ] Alternative methods can be used with the agreement of the approval authority.

## 8. Examples of Checking Vulnerability

As an example, we use the following data of a fishing vessel:

$L_{PP}$	34.5 m
$B$	7.6m
$d$	2.65 m
$trim$	0.30m
$LCB$	1.31 m aft
$C_b$	0.597
$Service Fn$	0.40
$D_p$	2.60 m
$t_p$	0.142
$w_p$	0.156
$M_x/M$	0.0667
$r_0$	0
$r_1$	--435.63
$r_2$	763.62
$r_3$	--271.98
$r_4$	41.611
$r_5$	-1.7335
$\kappa_0$	0.2244
$\kappa_1$	-0.2283
$\kappa_2$	-0.1373

The local breadth  $B$  (m), local draught  $d$  (m) and sectional area  $A$  (m<sup>2</sup>) are provided below as a function of the longitudinal section position (m) measured from the LCG as follows:

X=	-21.65	A=	0.00E+00	B=	0	d=	0
X=	-20.55	A=	1.85E+00	B=	7.1555	d=	0.448703
X=	-19.45	A=	2.61E+00	B=	7.4162	d=	0.539137
X=	-18.35	A=	3.28E+00	B=	7.57	d=	0.629572
X=	-17.25	A=	3.88E+00	B=	7.57	d=	0.715006
X=	-15.53	A=	5.40E+00	B=	7.5857	d=	1.275049
X=	-13.8	A=	7.82E+00	B=	7.58	d=	3.255005
X=	-12.075	A=	1.04E+01	B=	7.5851	d=	3.175004
X=	-10.35	A=	1.28E+01	B=	7.58	d=	3.105004
X=	-6.9	A=	1.61E+01	B=	7.57	d=	2.955002
X=	-3.45	A=	1.76E+01	B=	7.59	d=	2.800001
X=	0	A=	1.71E+01	B=	7.59	d=	2.65
X=	3.45	A=	1.58E+01	B=	7.6	d=	2.499999
X=	6.9	A=	1.38E+01	B=	7.4916	d=	2.354998
X=	10.35	A=	1.04E+01	B=	6.4367	d=	2.199996
X=	12.075	A=	8.00E+00	B=	5.3209	d=	2.134996
X=	13.8	A=	5.24E+00	B=	3.672	d=	2.044995
X=	15.525	A=	2.86E+00	B=	1.9245	d=	1.959995
X=	17.25	A=	1.17E+00	B=	0.91	d=	1.794994

The fitting qualities of resistance and thrust coefficient are shown in Figures 10-11, respectively.

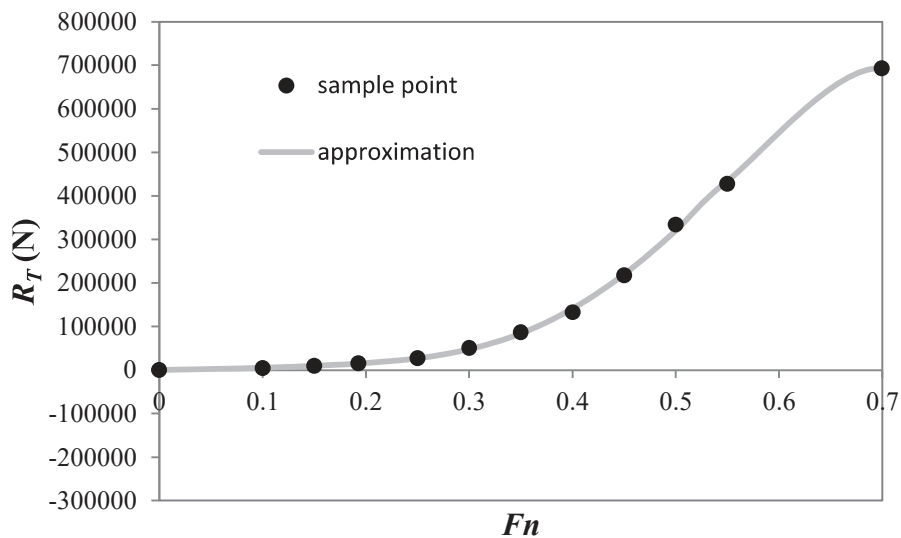


Figure 10 Ship Resistance curve and its approximation using the 5<sup>th</sup> power polynomial.

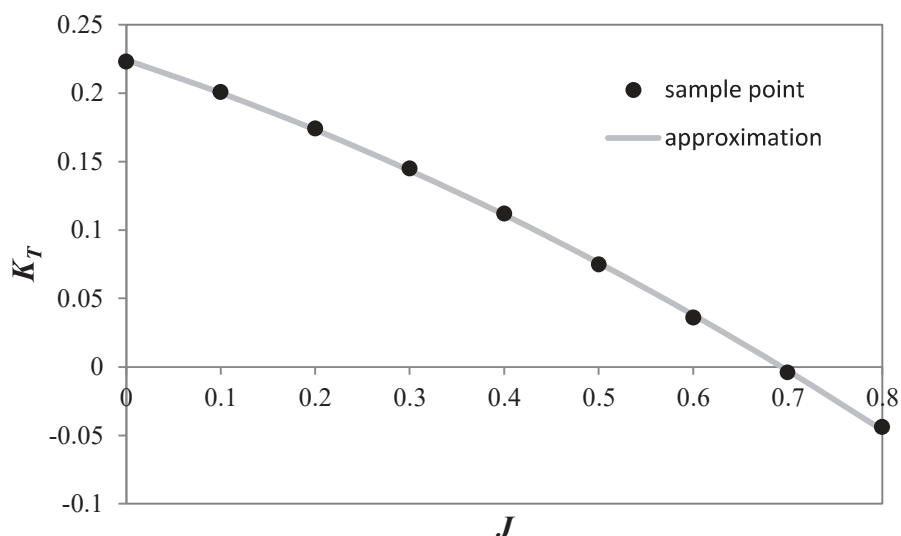


Figure 11 Propeller thrust coefficient curve and its approximation using the 2nd power polynomial.

This ship is judged as vulnerable in the level 1 check because its service Froude number is larger than 0.3 and the ship length is smaller than 200 m.

Thus it is necessary to check the vulnerability with the level 2. First, we have to calculate the critical Froude number for surf-riding under any initial condition using the Melnikov analysis. Examples of the calculated critical Froude numbers for typical local waves are as shown below.

	Critical Froude number with linear wave celerity
$\lambda/L=1.250,$ $H/\lambda=0.0504$	0.3296
$\lambda/L=1.500,$ $H/\lambda=0.0396$	0.3563
$\lambda/L=1.500,$ $H/\lambda=0.0504$	0.3428
$\lambda/L=1.500,$ $H/\lambda=0.0600$	0.3325
$\lambda/L=1.750,$ $H/\lambda=0.0504$	0.3577

Second, the probability index C values are calculated as a function of the calm-water Froude number,  $F_n$  as follows: [

Fn	C with nonlinear wave celerity
0.30	<1.0E-05
0.35	1.89E-02
0.40	5.58E-02
0.45	8.66E-02
0.50	9.19E-02

Fn	C with linear wave celerity
0.30	7.88E-04
0.35	2.31E-02
0.40	5.91E-02
0.45	8.77E-02
0.50	9.19E-02

This means that this subject ship is judged as vulnerable for broaching stability failure in the level 2 check because the C value at designed Froude number of 0.4 is larger than the standard of 0.005.

\*\*\*



## ANNEX 6

### DRAFT EXPLANATORY NOTES ON THE VULNERABILITY OF SHIPS TO THE DEAD SHIP STABILITY FAILURE MODE

[This is the explanatory notes to the "PROPOSED AMENDMENTS TO PART B OF THE 2008 IS CODE TO ASSESS THE VULNERABILITY OF SHIPS TO THE DEAD SHIP STABILITY FAILURE MODE" as SDC 1/INF.8, annex 16. ]

#### Chapter 5 – THE VULNERABILITY OF SHIPS TO THE DEAD SHIP STABILITY FAILURE MODE

##### 1. Physical background of stability failure in dead ship condition

- 1.1. Dead ship condition was the first mode of stability failure addressed with physics-based severe wind-and-roll criterion, also known as the "weather criterion," which was adopted by IMO in 1985 (Res. A.562(14)) and is now embodied in section 2.3 of the 2008 IS Code, Part A. The scenario of the weather criterion is shown in Figure 1. This scenario assumes that a ship has lost its power and has turned into beam seas, where it is rolling under the action of waves as well as heeling and drifting under the action of wind. Drift-related heel is a result of action of a pair of forces: wind aerodynamic force and hydrodynamic reaction caused by transverse motion of the ship.
- 1.2. Next, a sudden and long gust of wind occurs. The worst possible instant for this is when the ship is rolled at the maximum windward angle; in this case, action of wind is added to the action of waves. The strengthening wind increases drift velocity and this leads to an increase of the hydrodynamic drift reaction. The increase of the drift velocity leads to the increase of the hydrodynamic reaction and, therefore, to the increase of the heeling moment by the pair of aerodynamic and hydrodynamic forces. The gust is assumed to last long enough so the ship can roll to the other side completely; the achieved leeward roll angle is the base of the criterion. If it is too large, or some openings may be flooded, the stability of the ship is considered insufficient.

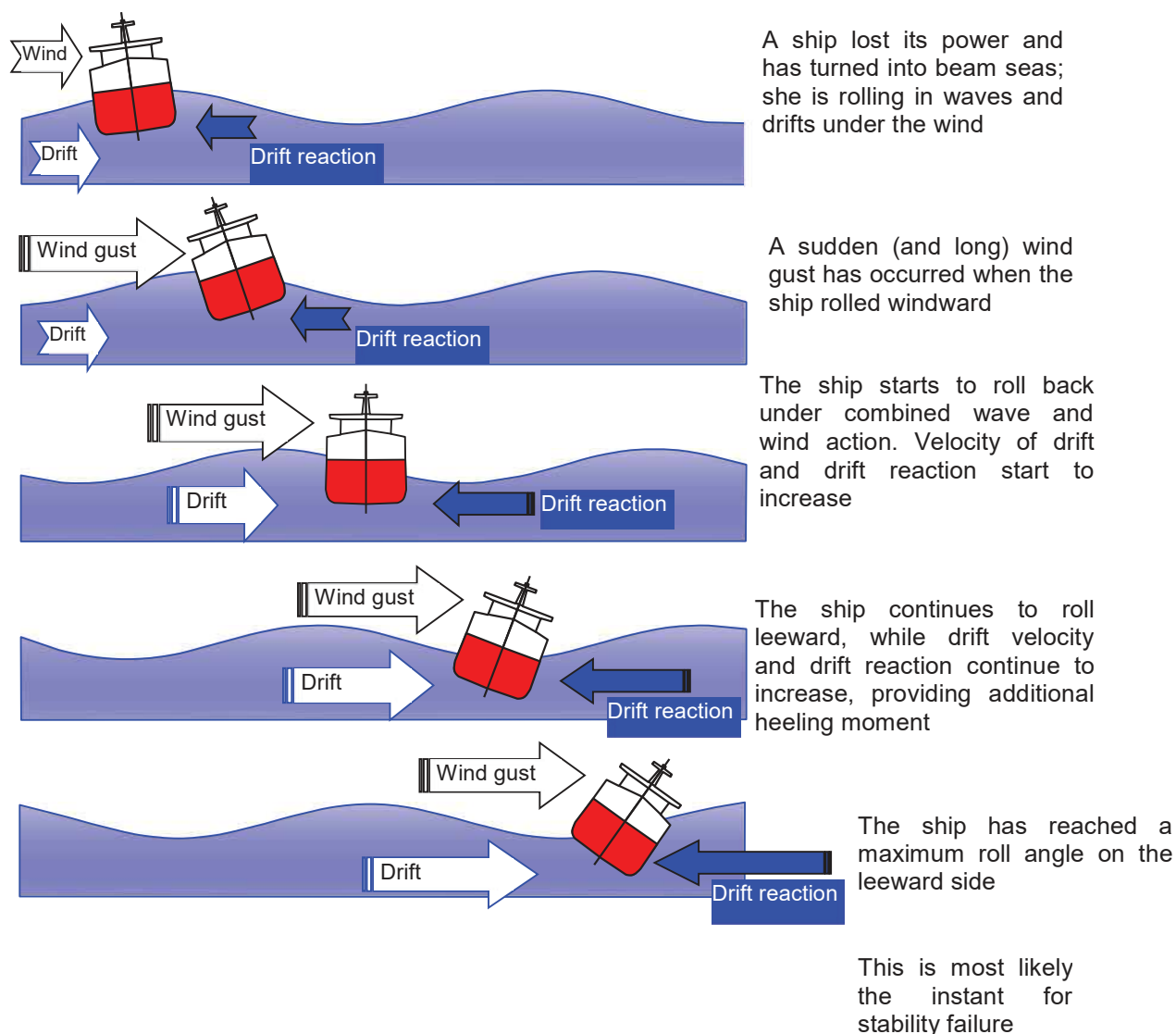


**Figure 1.** Scenario of Stability Failure in Dead Ship Conditions

## 2 LEVEL 1 VULNERABILITY ASSESSMENT

2.1 For the purpose of level 1 vulnerability assessment for dead ship stability failure, the "Severe wind and rolling criterion (weather criterion)" in Part A – 2.3 of the 2008 IS Code should be used, but substituting the steepness factor  $s$  in Table 2.3.4-4 in Part A – 2.3, with the steepness factor  $s$  specified in Table 4.5.1 in MSC.1/Circ.1200. See Figure 2.1.

Table 4.5.1: Wave steepness as a function of the full scale natural roll period

Table 2.3.4-4 – Values of factor  $s$

$T$	$s$
$\leq 6$	0.100
7	0.098
8	0.093
12	0.065
14	0.053
16	0.044
18	0.038
$\geq 20$	0.035

2008 IS Code – Part A

→

To be substituted by

Ship roll period $T_R$ [s]	Wave steepness $s = H/\lambda$
<6	0.100
6	0.100
7	0.098
8	0.093
12	0.065
14	0.053
16	0.044
18	0.038
20	0.032
22	0.028
24	0.025
26	0.023
28	0.021
30	0.020
>30	0.020

MSC.1/Circ.1200 – Chapter 4

Figure 2.1: Substitution of table for the wave steepness factor  $s$  when applying the Weather Criterion methodology in the level 1 vulnerability assessment for dead ship failure mode.

[The area of fin stabilizers, if not retractable, can be included in the bilge keel area  $A_k$  according to 2.3.4 of Part A of the 2008 IS Code.]

### 3 LEVEL 2 VULNERABILITY ASSESSMENT

#### 3.1 Objectives and assumptions

3.1.1 The objective of the level 2 vulnerability assessment methodology is to provide a simplified conservative probabilistic measure of vulnerability of the ship, in the considered loading condition, to the dead ship stability failure mode.

3.1.2 Such measure, indicated as  $C$ , is a long-term probability index ranging from 0.0 to 1.0 which is obtained as a weighted average of short-term indices  $C_S$ , ranging from 0.0 to 1.0. The short-term dead ship failure index  $C_S$  depends on the ship characteristics, on the short-term environmental conditions and on the assumed short-term exposure time.

3.1.3 The short term failure index  $C_S$  is obtained by means of a simplified calculation methodology which takes into account the roll dynamics in the considered short-term environmental conditions.

3.1.4 The long term dead ship failure index  $C$  is obtained by means of weighted average considering the probability of occurrence of different short-term environmental conditions.

3.1.5 Several assumptions are required to provide a suitable tool for level 2 vulnerability assessment. Some of such assumptions are described in the relevant sections of this explanatory notes. However, the fundamental set of underlying assumptions is as follows:

- .1 The ship is assumed to be in dead ship condition in irregular waves and gusty wind for a specified exposure time;
- .2 Wind and waves are assumed to blow / propagate in the same direction and water depth is assumed to be infinite;
- .3 The ship is assumed to remain beam to wind and waves;
- .4 The wind state is characterized by a mean wind speed and a gustiness spectrum;

- .5 The sea state is characterized by a wave elevation spectrum and waves are assumed to be long crested;
- .6 The roll motion of the vessel is modelled as a one-degree of freedom (1-DOF) system;

3.1.6 For the purpose of this assessment, the ship is conventionally assumed to be exposed to each short-term environmental condition for an exposure time of 3600 s (1 hour).

3.1.7 Herein, heeling angles to the leeward side are implicitly assumed to be positive, whereas heeling angles to the windward side are assumed to be negative.

3.1.8 For ships which are not port / starboard symmetric, the short-term dead-ship failure index  $C_S$  is to be determined as the average between the index calculated for wind and waves coming from each of the two sides.

## 3.2 Overview of the methodology

3.2.1 A conceptual scheme of the assumed underlying simplified physical modelling of the phenomenon is shown in Figure 3.1. The overview of the logic of the short-term modelling is as follows:

- .1 Ship characteristic parameters are assumed to be available (displacement, righting lever, roll damping, windage area characteristics, ...)
- .2 The environmental conditions are specified in terms of wind and waves;
- .3 The wind state is provided as a mean wind speed and a wind gustiness spectrum;
- .4 The mean heeling moment due to wind is determined starting from the mean wind speed;
- .5 The spectrum of the roll moment due to the wind gust is determined starting from the wind gustiness spectrum;
- .6 The sea state is provided in terms of a sea elevation spectrum, from which a wave slope spectrum is directly determined;
- .7 The spectrum of roll moment due to the waves is determined starting from the wave slope spectrum;
- .8 The total spectrum of roll moment is assumed to be given by the sum of the spectrum of roll moment due to wind gustiness and the spectrum of roll moment due to waves;
- .9 The dynamics of roll is then assumed to be modelled by means of a nonlinear 1-DOF equation of motion, which takes into account the ship characteristics (roll restoring, roll natural period, roll damping), the mean heeling moment due to the mean wind, and the irregular roll moment due to the combined effect of gust and waves.

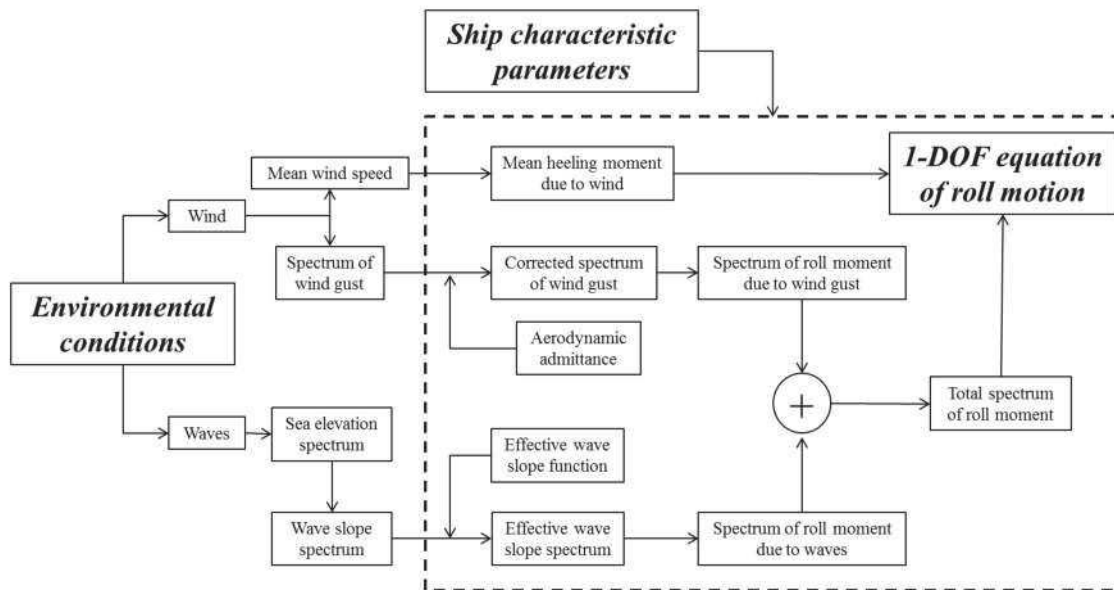


Figure 3.1: Conceptual scheme of the assumed simplified physical modelling for the short-term assessment.

3.2.2 Section 3.3 provides information on:

- .1 The short term characterization of the wind state and of the sea state;
- .2 The short term relation between wind and waves;
- .3 The long-term characterization of the environment;
- .4 The possible application of alternative environmental conditions, to the satisfaction of the Administration.

3.2.3 Once the roll motion equation is set up, it needs to be solved in order to provide the necessary information for the estimation of the short-term failure index  $C_s$ . To this end, a simplified approximate methodology is used in order to obtain an estimation of the short-term roll motion resulting from the 1-DOF modelling. From these information, the short-term failure index  $C_s$  can be determined using simple analytical expressions and the assumed short-term exposure time. Such simplified method is described in Section 3.4.

3.2.4 Herein, energy spectra are so-called single-side spectra, i.e. they are defined in the range of non-negative frequencies.

### 3.4 Environmental conditions

#### 3.3.1 Standard environmental conditions

3.3.1.1 A set of standard environmental conditions is assumed. The characterization of the standard environmental conditions refers to both the short and the long-term. The short-term characterization is given in terms of mean wind speed, spectrum of wind gust and spectrum of sea elevation. The long-term characterization is given in terms of a wave scatter diagram. A deterministic relation is assumed between the mean wind speed and the significant wave height.

3.3.1.2 Waves are characterized, in the short-term, by a significant wave height  $H_S$  (m) and a zero crossing period  $T_Z$  (s), which uniquely define the assumed spectrum of the wave elevation. The spectrum of wave elevation,  $S_{zz}$  ( $m^2/(rad/s)$ ), is of the Bretschneider/Two-parameters Pierson-Moskowitz type. The sea elevation spectrum is a function of the wave circular frequency  $\omega$  (rad/s) and it is assumed to have the following expression:

$$S_{zz}(\omega) = \frac{H_S^2}{4 \cdot \pi} \cdot \left( \frac{2 \cdot \pi}{T_Z} \right)^4 \cdot \omega^{-5} \cdot \exp \left( -\frac{1}{\pi} \cdot \left( \frac{2 \cdot \pi}{T_Z} \right)^4 \cdot \omega^{-4} \right) \quad 3.3.1.2-1$$

3.3.1.3 It is assumed that, in the short-term, the mean wind speed  $U_W$  (m/s) is determined solely from the significant wave height  $H_S$  (m) according to the following expression:

$$U_W = \left( \frac{H_S}{0.06717} \right)^{\frac{1}{1.5}} \quad 3.3.1.3-1$$

3.3.1.4 The wind is assumed to fluctuate around the mean wind velocity. The total wind speed is given by the sum of the mean wind speed  $U_W$  (m/s) and the gust fluctuation speed  $v$  (m/s). The spectrum of the gust,  $S_v$  ( $(m/s)^2/(rad/s)$ ), is of the Davenport type, and it depends on the mean wind speed  $U_W$  (m/s). The gustiness spectrum is a function of the wind fluctuation circular frequency  $\omega$  (rad/s) and it is assumed to have the following expression:

$$\left\{ \begin{array}{l} S_v(\omega) = 4 \cdot K \cdot \frac{U_w^2}{\omega} \cdot \frac{X_D^2}{(1 + X_D^2)^{\frac{4}{3}}} \\ \text{with} \\ K = 0.003 \\ X_D = 600 \cdot \frac{\omega}{\pi \cdot U_w} \end{array} \right. \quad 3.3.1.4-1$$

3.3.1.5 The long-term characterization of the standard environmental conditions is given by means of a wave scatter diagram. The wave scatter diagram reports the probability of occurrence of different sea state conditions of significant wave height  $H_S$  and zero crossing period  $T_Z$ . Such probability of occurrence is defined as  $W_i(H_S, T_Z)$ , where the subscript "i" indicates the generic  $i$ -th scenario. Since the wind state (mean wind speed  $U_w$ , according to 3.3.1.3, and gustiness spectrum  $S_v$ , according to 3.3.1.4) is assumed to be determined deterministically from the significant wave height, the specification of the wave scatter diagram is sufficient. The standard wave scatter diagram is given in Table 3.1 and the corresponding standard values of  $W_i(H_S, T_Z)$  is to be obtained from the values reported in Table 3.1 after dividing by 100000.

**Table 3.1: Standard wave scatter diagram.**

Number of occurrences: 100 000 / $T_z$ (s) = average zero up-crossing wave period / $H_s$ (m) = significant wave height																
$T_z$ (s) ►	3.5	4.5	5.5	6.5	7.5	8.5	9.5	10.5	11.5	12.5	13.5	14.5	15.5	16.5	17.5	18.5
$H_s$ (m) ▼																
0.5	1.3	133.7	865.6	1186.0	634.2	186.3	36.9	5.6	0.7	0.1	0.0	0.0	0.0	0.0	0.0	0.0
1.5	0.0	29.3	986.0	4976.0	7738.0	5569.7	2375.7	703.5	160.7	30.5	5.1	0.8	0.1	0.0	0.0	0.0
2.5	0.0	2.2	197.5	2158.8	6230.0	7449.5	4860.4	2066.0	644.5	160.2	33.7	6.3	1.1	0.2	0.0	0.0
3.5	0.0	0.2	34.9	695.5	3226.5	5675.0	5099.1	2838.0	1114.1	337.7	84.3	18.2	3.5	0.6	0.1	0.0
4.5	0.0	0.0	6.0	196.1	1354.3	3288.5	3857.5	2685.5	1275.2	455.1	130.9	31.9	6.9	1.3	0.2	0.0
5.5	0.0	0.0	1.0	51.0	498.4	1602.9	2372.7	2008.3	1126.0	463.6	150.9	41.0	9.7	2.1	0.4	0.1
6.5	0.0	0.0	0.2	12.6	167.0	690.3	1257.9	1268.6	825.9	386.8	140.8	42.2	10.9	2.5	0.5	0.1
7.5	0.0	0.0	0.0	3.0	52.1	270.1	594.4	703.2	524.9	276.7	111.7	36.7	10.2	2.5	0.6	0.1
8.5	0.0	0.0	0.0	0.7	15.4	97.9	255.9	350.6	296.9	174.6	77.6	27.7	8.4	2.2	0.5	0.1
9.5	0.0	0.0	0.0	0.2	4.3	33.2	101.9	159.9	152.2	99.2	48.3	18.7	6.1	1.7	0.4	0.1
10.5	0.0	0.0	0.0	0.0	1.2	10.7	37.9	67.5	71.7	51.5	27.3	11.4	4.0	1.2	0.3	0.1
11.5	0.0	0.0	0.0	0.0	0.3	3.3	13.3	26.6	31.4	24.7	14.2	6.4	2.4	0.7	0.2	0.1
12.5	0.0	0.0	0.0	0.0	0.1	1.0	4.4	9.9	12.8	11.0	6.8	3.3	1.3	0.4	0.1	0.0
13.5	0.0	0.0	0.0	0.0	0.0	0.3	1.4	3.5	5.0	4.6	3.1	1.6	0.7	0.2	0.1	0.0
14.5	0.0	0.0	0.0	0.0	0.0	0.1	0.4	1.2	1.8	1.8	1.3	0.7	0.3	0.1	0.0	0.0
15.5	0.0	0.0	0.0	0.0	0.0	0.0	0.1	0.4	0.6	0.7	0.5	0.3	0.1	0.1	0.0	0.0
16.5	0.0	0.0	0.0	0.0	0.0	0.0	0.0	0.1	0.2	0.2	0.2	0.1	0.1	0.0	0.0	0.0

### 3.3.2 *Alternative environmental conditions*

3.3.2.1 Alternative environmental conditions can be used, to the satisfaction of the Administration, for ships in restricted service or subject to operational limitations.

3.3.2.2 Such alternative environmental conditions should specify the short-term characteristics of wind state and sea state, together with the probability of occurrence of each short-term environmental condition.

3.3.2.3 The short-term sea state characteristics should be given in terms of a sea elevation spectrum. The short-term wind state should be given in terms of a mean wind speed and a gustiness spectrum.

3.3.2.4 The long-term characterization of the environmental condition should be given in terms of probability of occurrence of each short-term condition. The probability of occurrence of each short-term environmental condition corresponds to the weighting factor  $W_i$ . The set of short-term environmental conditions and corresponding weighting factors should be such that the weighting factors, i.e. the probabilities of occurrence, sum up to one.

## 3.4 **Determination of short-term roll motion characteristics and calculation of the short-term dead-ship stability failure index $C_s$**

### 3.4.1 *Short-term roll motion characteristics*

3.4.1.1 In the determination of the short-term rolling motion characteristics, the ship is assumed to be heeled under the action of mean wind and to be rolling due to the action of beam waves and gusty wind.

3.4.1.2 The mean heeling angle is assumed to be approximated by the angle of heel due to the effect of mean wind. The rolling motion of the vessel is assumed to occur around this



angle, and the relative motion with respect to this angle is assumed to be described by the following linear equation:

$$\ddot{x} + 2 \cdot \mu_e(\sigma_{\dot{x}}) \cdot \dot{x} + \omega_{0,e}^2(\phi_s) \cdot x = \omega_0^2 \cdot m(t)$$

$$\mu_e(\sigma_{\dot{x}}) = \mu + \sqrt{\frac{2}{\pi}} \cdot \beta \cdot \sigma_{\dot{x}} + \frac{3}{2} \cdot \delta \cdot \sigma_{\dot{x}}^2 \quad 3.4.1.2-1$$

$$m(t) = \frac{M(t)}{W \cdot \overline{GM}}$$

where:

- .1  $x = \phi - \phi_s$  (rad) is the roll angle with respect to the static heeling angle  $\phi_s$  due to the action of mean wind;
- .2  $\sigma_{\dot{x}}$  (rad/s) is the standard deviation of the roll velocity;
- .3  $\mu_e(\sigma_{\dot{x}})$  (1/s) is the equivalent linear roll damping coefficient depending on  $\sigma_{\dot{x}}$ ;
- .4  $\mu$  (1/s) is the linear roll damping coefficient (see section 3.5);
- .5  $\beta$  (1/rad) is the quadratic roll damping coefficient (see section 3.5);
- .6  $\delta$  (s/rad<sup>2</sup>) is the cubic roll damping coefficient (see section 3.5);
- .7  $\omega_0$  (rad/s) is the upright roll natural frequency;
- .8  $\omega_{0,e}(\phi_s)$  (rad/s) is an equivalent roll natural frequency which takes into account the nonlinearities of the righting lever close to  $\phi_s$ ;
- .9  $M(t)$  (N·m) is the time dependent roll moment due to the action of waves and gustiness;
- .10  $\overline{W}$  (N) is the ship displacement force;
- .11  $\overline{GM}$  (m) is the upright metacentric height;

3.4.1.3 In order to obtain the short-term failure index  $C_s$ , the following procedure is applied:

- .1 Calculation of steady wind heeling moment considering the effect of drift force and determination of static heeling angle  $\phi_s$  and vanishing stability angles  $\phi_{VW,+}$  (leeward side) and  $\phi_{VW,-}$  (windward side) under the action of steady wind considering the ship righting moment. See 3.4.1.4;
- .2 Calculation of the derivative of righting lever  $\overline{GZ}$  at  $\phi_s$  ("local metacentric height"  $\overline{GM}_{res}$ ) and correction of the natural roll frequency accordingly. See 3.4.1.5;
- .3 Calculation of the spectrum of the total roll moment due to the action of waves and gustiness. See 3.4.1.6;
- .4 Solution of the linearized roll motion equation in frequency domain using the standard spectral method accounting for nonlinear damping with the aim of obtaining the roll motion spectrum. See 3.4.1.7;
- .5 Determination of roll standard deviation and of roll zero crossing frequency using the determined roll spectrum. See 3.4.1.7;



- .6 Calculation of critical angles for dead ship stability failure index calculation using the "equivalent area" approach. See 3.4.2.6;
- .7 Calculation of the final dead ship stability failure index for the specified exposure time. See 3.4.2.7.

3.4.1.4 Calculation of steady heeling moment due to the action of steady wind and drift and associated relevant angles

3.4.1.4.1 The heeling moment  $\overline{M}_{wind,tot}$  ( $N \cdot m$ ) due to the action of the mean wind, and the corresponding moment lever  $\bar{l}_{wind,tot}$  ( $m$ ) are considered independent of the heel angle and are to be calculated as:

$$\overline{M}_{wind,tot} = \frac{1}{2} \rho_{air} \cdot U_w^2 \cdot C_m \cdot A_L \cdot Z$$

$$\bar{l}_{wind,tot} = \frac{\overline{M}_{wind,tot}}{W}$$

3.4.1.4.1-1

where:

- .1  $\rho_{air} = 1.222 kg / m^3$  is the air density;
- .2  $U_w$  ( $m/s$ ) is the mean wind speed;
- .3  $C_m$  is the heeling moment coefficient. In absence of sufficient information, this coefficient can approximately be taken as  $C_m = 1.22$ . Other values can be used, to the satisfaction of the Administration;
- .4  $A_L$  ( $m^2$ ) is the lateral windage area;
- .5  $Z$  ( $m$ ) is the vertical distance from the centre of  $A_L$  to the centre of the underwater lateral area or approximately to a point at one half the mean draught  $T$ ;
- .6  $\Delta$  ( $N$ ) is the ship displacement force;

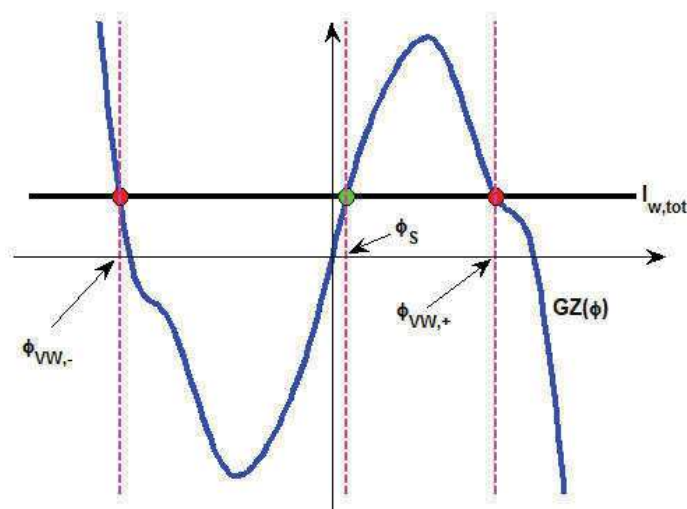


**Figure 3.2: Schematic representation for the stable/unstable equilibrium angles  $\phi_s$ ,  $\phi_{VW,+}$  and  $\phi_{VW,-}$  under the action of mean wind.**

3.4.1.4.2 The static heel angle  $\phi_s$  (rad) is the stable heeling angle under the action of the heeling moment  $\overline{M}_{wind,tot}$  ( $N \cdot m$ ) and corresponding heeling lever  $\bar{l}_{wind,tot}$  defined in 3.4.1.2.1. See Figure 3.2.

3.4.1.4.2 When a static heel angle  $\phi_s$  cannot be found, no further calculations are necessary, since the ship is assumed to be lost in the considered short-term condition, and the short-term dead ship stability failure index  $C_S$  (see 3.4.2) is to be taken equal to 1.0 .

3.4.1.4.3 The angles  $\phi_{VW,+}$  (rad) and  $\phi_{VW,-}$  (rad) are the angles of vanishing stability, to the leeward ( $\phi_{VW,+}$ ) and windward ( $\phi_{VW,-}$ ) side respectively, under the action of the heeling moment  $\overline{M}_{wind,tot}$  ( $N \cdot m$ ) and corresponding heeling lever  $\bar{l}_{wind,tot}$  defined in 3.4.1.4.1. See Figure 3.2.

3.4.1.5 Calculation of derivative of  $\overline{GZ}$  at  $\phi_s$  ("local metacentric height"  $\overline{GM}_{res}$ ) and correction of the natural roll frequency

3.4.1.5.1 The residual metacentric height  $\overline{GM}_{res}$  (m) is the derivative of the residual righting lever curve at  $\phi_s$  (see Figure 3.3). Since the heeling moment due to the steady wind is assumed to be constant, it follows that:

$$\overline{GM}_{res}(\phi_s) = \left. \frac{d(\overline{GZ} - \bar{l}_{wind,tot})}{d\phi} \right|_{\phi=\phi_s} = \left. \frac{d\overline{GZ}}{d\phi} \right|_{\phi=\phi_s} \quad 3.4.1.5.1-1$$

$\bar{l}_{wind,tot}$  not depending on the heeling angle

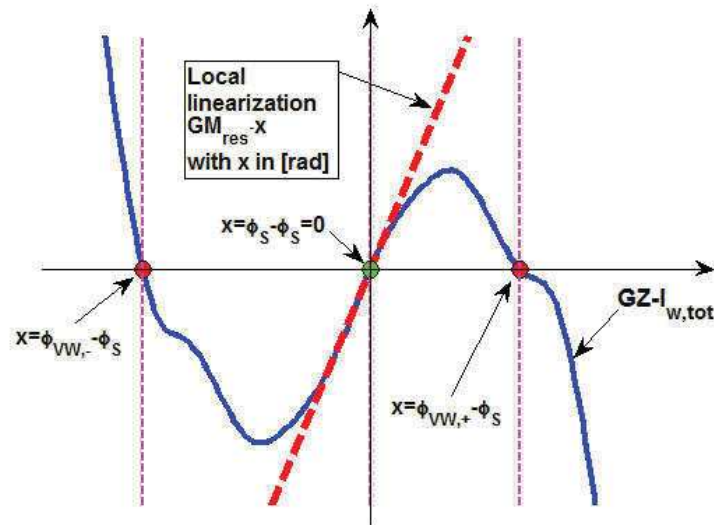


Figure 3.3: Graphical representation of the linearization of the residual righting lever close to the static equilibrium angle under the action of mean wind.

3.4.1.5.2 The modified roll natural frequency  $\omega_{0,e}$  (rad/s) close to the equilibrium angle  $\phi_S$  is determined as:

$$\omega_{0,e}(\phi_S) = \omega_0 \cdot \sqrt{\frac{GM_{res}(\phi_S)}{GM}} \quad 3.4.1.5.2-1$$

### 3.4.1.6 Calculation of spectrum of total roll moment due to the action of waves and gustiness

3.4.1.6.1 The spectrum  $S_{\alpha\alpha}$  (rad<sup>2</sup>/(rad/s)) of the wave slope is to be calculated as:

$$S_{\alpha\alpha}(\omega) = \frac{\omega^4}{g^2} \cdot S_{ZZ}(\omega) \quad 3.4.1.6.1-1$$

where:

- .1  $\omega$  (rad/s) is the circular wave frequency;
- .2  $g = 9.81 \text{ m/s}^2$  is the gravitational acceleration.

3.4.1.6.2 The spectrum  $S_{\alpha\alpha,c}$  (rad<sup>2</sup>/(rad/s)) of the effective wave slope is to be calculated as:

$$S_{\alpha\alpha,c}(\omega) = r^2(\omega) \cdot S_{\alpha\alpha}(\omega) \quad 3.4.1.6.2-1$$

where  $r(\omega)$  (-) is the effective wave slope function as a function of the wave circular frequency (see Section 3.6).

3.4.1.6.3 The spectrum  $S_{M_{waves}}$  ((N·m)<sup>2</sup>/(rad/s)) of the moment due to the action of the waves, as a function of the wave circular frequency  $\omega$  (rad/s), is to be calculated as:

$$S_{M_{waves}}(\omega) = (W \cdot \overline{GM}_{res}(\phi_S))^2 \cdot S_{\alpha\alpha,c}(\omega) = (r(\omega) \cdot W \cdot \overline{GM}_{res}(\phi_S))^2 \cdot S_{\alpha\alpha}(\omega) \quad 3.4.1.6.3-1$$

3.4.1.6.4 The spectrum  $S_{\delta M_{wind,tot}}(\omega)$  ( $(N \cdot m)^2 / (rad / s)$ ) of the moment due to the action of the gust, as a function of the wave circular frequency  $\omega$  ( $rad/s$ ), is to be calculated as:

$$S_{\delta M_{wind,tot}}(\omega) = [\rho_{air} \cdot U_w \cdot C_m \cdot A_L \cdot Z]^2 \cdot \chi^2(\omega) \cdot S_v(\omega) \quad 3.4.1.6.4-1$$

where the function  $\chi(\omega)$  (-) is the aerodynamic admittance function to be calculated in accordance with 3.4.1.6.5.

3.4.1.6.5 The standard aerodynamic admittance function is to be calculated as:

$$\chi(\omega) = 1 \quad 3.4.1.6.5-1$$

[Alternative formulation can be accepted to the satisfaction of the Administration.]

3.4.1.6.6 The spectrum  $S_M(\omega)$  ( $(N \cdot m)^2 / (rad / s)$ ) of the total moment due to the action of waves and gust, as a function of the wave circular frequency  $\omega$  ( $rad/s$ ), is to be calculated as:

$$S_M(\omega) = S_{M_{waves}}(\omega) + S_{\delta M_{wind,tot}}(\omega) \quad 3.4.1.6.6-1$$

### 3.4.1.7 Determination of the spectrum of the roll oscillation and of derived quantities

3.4.1.7.1 The standard deviation  $\sigma_{\dot{x}}$  ( $rad/s$ ) of the roll velocity is obtained by numerically solving the following equation with respect to the single unknown  $\sigma_{\dot{x}}$ :

$$F(\sigma_{\dot{x}}) = 0$$

with

$$F(\sigma_{\dot{x}}) = \sigma_{\dot{x}}^2 - \int_0^{\infty} \frac{\omega^2 \cdot \omega_0^4}{(\omega_{0,e}^2(\phi_S) - \omega^2)^2 + (2 \cdot \mu_e(\sigma_{\dot{x}}) \cdot \omega)^2} \cdot \frac{S_M(\omega)}{(W \cdot \overline{GM})^2} d\omega \quad 3.4.1.7.1-1$$

$$\mu_e(\sigma_{\dot{x}}) = \mu + \sqrt{\frac{2}{\pi}} \cdot \beta \cdot \sigma_{\dot{x}} + \frac{3}{2} \cdot \delta \cdot \sigma_{\dot{x}}^2$$

3.4.1.7.2 Using the standard deviation  $\sigma_{\dot{x}}$  ( $rad/s$ ) determined according to 3.4.1.7.1, the spectrum  $S_x(\omega)$  ( $(rad)^2 / (rad / s)$ ) of the roll motion with respect to  $\phi_S$  is determined as:

$$S_x(\omega) = H^2(\omega) \cdot S_m(\omega)$$

with

$$H^2(\omega) = \frac{\omega_0^4}{(\omega_{0,e}^2(\phi_s) - \omega^2)^2 + (2 \cdot \mu_e \cdot \omega)^2}; S_m(\omega) = \frac{S_M(\omega)}{(W \cdot GM)^2} \quad 3.4.1.7.2-1$$

$$\mu_e = \mu + \sqrt{\frac{2}{\pi}} \cdot \beta \cdot \sigma_{\dot{x}} + \frac{3}{2} \cdot \delta \cdot \sigma_{\dot{x}}^2$$

3.4.1.7.3 Using the spectrum  $S_x(\omega)$  ( $(rad)^2 / (rad/s)$ ) of the roll motion with respect to  $\phi_s$  as determined in 3.4.1.7.2, the following derived quantities can be calculated:

$$\left\{ \begin{array}{l} \text{Roll standard deviation (rad): } \sigma_\phi = \sqrt{m_0} \\ \text{Roll zero crossing frequency (rad/s): } \omega_{z,\phi} = \sqrt{\frac{m_2}{m_0}} \\ \text{Roll zero crossing period (s): } T_{z,\phi} = \frac{2\pi}{\omega_{z,\phi}} \end{array} \right. \quad 3.4.1.7.3-1$$

where

$$m_0 = \int_0^\infty S_x(\omega) d\omega \quad ; \quad m_2 = \int_0^\infty \omega^2 \cdot S_x(\omega) d\omega$$

### 3.4.2 Determination of the short-term dead ship stability failure index $C_S$

3.4.2.1 The calculation of the short-term dead ship stability failure index  $C_S$  is based on an exposure time  $T_{exp}$  equal to 3600 s (1 hour).

3.4.2.2 The short-term dead ship stability failure index  $C_S$  represents a measure of the probability that the ship exceeds specified failure angles to windward or leeward at least once in the considered exposure time. The short-term dead ship stability failure index  $C_S$  ranges from 0.0 to 1.0.

3.4.2.3 When, according to 3.4.1, a static heel angle  $\phi_s$  cannot be found, no further calculations are necessary, since the ship is assumed to be lost in the considered short-term condition, and the short-term dead ship stability failure index  $C_S$  is to be taken equal to 1.0 .

3.4.2.4 The physical failure angle to leeward,  $\phi_{fail,+}$  ( $>0$ ), is defined as:

$$\phi_{fail,+} = \min \{ \phi_{VW,+}, \phi_{crit,+} \} \quad 3.4.2.4-1$$

where  $\phi_{crit,+}$  is a critical angle to leeward (i.e. positive), defined as the minimum between the angle of down-flooding to leeward ( $>0$ ) and 50 deg. When  $\phi_{fail,+}$  is less or equal to the static heel angle  $\phi_s$ , no further calculations are necessary, since the ship is assumed to be lost in the

considered short-term condition, and the short-term dead ship stability failure index  $C_S$  is to be taken equal to 1.0 .

3.4.2.5 The physical failure angle to windward,  $\phi_{fail,-}$ , is defined as:

$$\phi_{fail,-} = \max \{ \phi_{\mathit{W,-}}, \phi_{crit,-} \} \quad 3.4.2.5-1$$

where  $\phi_{crit,-}$  is a critical angle to windward (typically, but not necessarily, negative), defined as the maximum between the angle of down-flooding to leeward (assumed to be negative) and -50 deg.

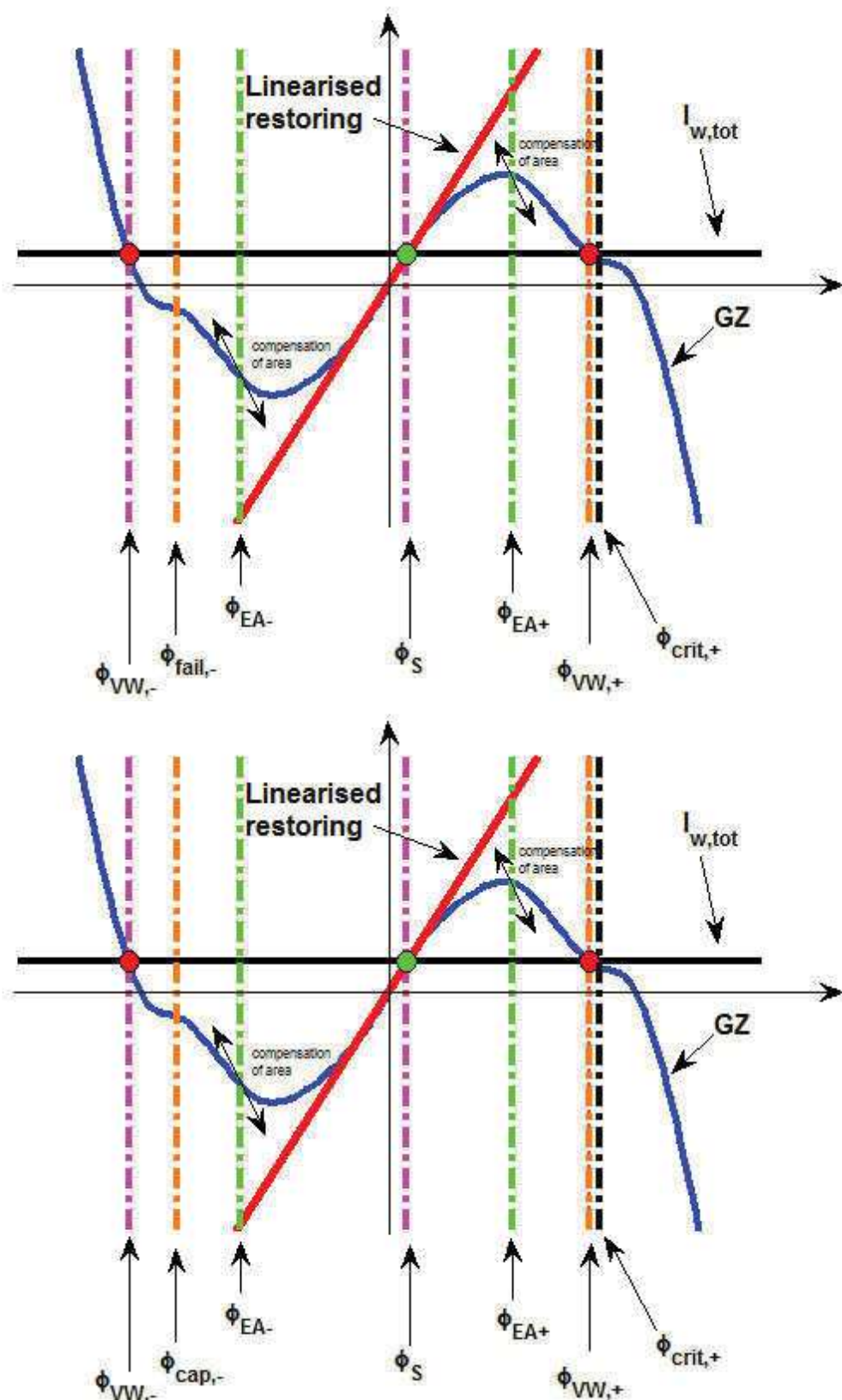


Figure 3.4: Graphical example representation of the relevant angles for the calculation of the dead ship stability failure index using the "equivalent area" approach.

3.4.2.6 In order to take into account the actual shape of the righting lever, two virtual limit angles to leeward and windward are defined, in such a way that the area under the actual

residual righting lever and under the linearized residual righting lever are the same (see Figure 3.4). Such "equivalent area" virtual limit angles are to be calculated as follows:

$$\left\{ \begin{array}{l} \text{windward: } \phi_{EA-} = \phi_S - \sqrt{\frac{-2}{GM_{res}(\phi_S)} \cdot \int_{\phi_{fail,-}}^{\phi_S} \overline{GZ}_{res}(\xi) d\xi} \\ \text{leeward: } \phi_{EA+} = \phi_S + \sqrt{\frac{2}{GM_{res}(\phi_S)} \cdot \int_{\phi_S}^{\phi_{fail,+}} \overline{GZ}_{res}(\xi) d\xi} \\ \overline{GZ}_{res}(\phi) = \overline{GZ}(\phi) - \bar{l}_{wind,tot} \end{array} \right. \quad 3.4.2.6-1$$

3.4.2.7 The short-term dead ship stability failure index, for the considered short-term environmental condition, is finally to be calculated as:

$$\left\{ \begin{array}{l} C_S = 1 - \exp(-\lambda_{EA} \cdot T_{exp}) \\ \lambda_{EA} = \frac{1}{T_{z,C_S}} \cdot \left[ \exp\left(-\frac{1}{2 \cdot RI_{EA+}^2}\right) + \exp\left(-\frac{1}{2 \cdot RI_{EA-}^2}\right) \right] \\ RI_{EA+} = \frac{\sigma_{C_S}}{\Delta\phi_{res,EA+}}; \quad \Delta\phi_{res,EA+} = \phi_{EA+} - \phi_S \\ RI_{EA-} = \frac{\sigma_{C_S}}{\Delta\phi_{res,EA-}}; \quad \Delta\phi_{res,EA-} = \phi_S - \phi_{EA-} \end{array} \right. \quad 3.4.2.7-1$$

where the exposure time  $T_{exp}$  is to be taken equal to 3600 s as specified in 3.4.2.1 and the quantities  $\sigma_{C_S}$  (rad) and  $T_{z,C_S}$  (s) are to be determined as follows:

$$\begin{aligned} \sigma_{C_S} &= \sqrt{m_0} \\ T_{z,C_S} &= 2 \cdot \pi \cdot \sqrt{\frac{m_0}{m_2}} \end{aligned}$$

where

$$m_0 = \int_0^{\infty} S(\omega) d\omega; \quad m_2 = \int_0^{\infty} \omega^2 \cdot S(\omega) d\omega \quad 3.4.2.7-2$$

$$S(\omega) = H_{rel}^2(\omega) \cdot S_{\alpha\alpha,c}(\omega) + H^2(\omega) \cdot \frac{S_{\delta M_{wind,tot}}(\omega)}{(W \cdot GM)^2}$$

$$H_{rel}^2(\omega) = \frac{\omega^4 + (2 \cdot \mu_e \cdot \omega)^2}{(\omega_{0,e}^2(\phi_S) - \omega^2)^2 + (2 \cdot \mu_e \cdot \omega)^2}$$

$$H^2(\omega) = \frac{\omega_0^4}{(\omega_{0,e}^2(\phi_S) - \omega^2)^2 + (2 \cdot \mu_e \cdot \omega)^2}$$



with  $S_{\alpha,c}(\omega)$  determined according to 3.4.1.6.2,  $S_{\delta M_{wind,tot}}(\omega)$  determined according to 3.4.1.6.4,  $\omega_{0,e}(\phi_s)$  determined according to 3.4.1.5.2 and  $\mu_e$  determined according to 3.4.1.7.1.

### 3.5 Estimation of roll damping

3.5.1 In order to perform a prediction of roll motion characteristics according to 3.4.1, roll damping coefficients are to be specified for the considered ship, in the considered loading condition.

3.5.2 [In absence of sufficient information, the standard methodology reported in 3.5.3 should be used. The standard methodology specified by the Organization is based on the so-called "simplified Ikeda's method". However, methods which, to the satisfaction of the Administration, are deemed to be at least equivalently reliable can be used as well.]  
[The roll damping coefficients can be estimated with scaled model tests using the following the procedures in MSC.1/Circ.1200 or alternative test procedures approved by the Administration. In the absence of roll decay model test data, the roll damping coefficients may be estimated using either a simplified Ikeda's method or type-specific empirical data (with bilge keels geometry effect included), if appropriate. The forward speed effect may be taken into account for the lift component using Ikeda's or an equivalent method. The simplified Ikeda's formula is given in Appendix 4 of the Chapter 3 of the explanatory notes. [Alternatively, numerical simulations can be used for the estimation of roll damping, based on the solution of viscous hydrodynamic equations. In this case, validation of simulations should be performed for selected loading conditions to the satisfaction of Administration. Validation should be performed in comparison with model tests performed according to the procedures in MSC.1/Circ.1200 or alternative test procedures approved by the Administration.]]

#### 3.5.3 *Standard methodology for the estimation of roll damping*

3.5.3.1 The standard methodology for the estimation of roll damping is based on two steps:

- .1 At first, the equivalent linear roll damping coefficient is determined as a function of the roll amplitude, assuming the ship to roll with a sinusoidal motion at the roll natural frequency. See 3.5.3.2;
- .2 As a second step, the roll damping coefficients to be used in 3.4.1 are determined from the previously calculated data. See 3.5.3.3.

3.5.3.2 The standard methodology for the calculation of roll damping as a function of the rolling amplitude under sinusoidal periodic motion is that specified in Appendix 4 of the "explanatory notes on the vulnerability of ships to the parametric roll stability failure mode" assuming that the ship is at zero speed. Such methodology allows determining the equivalent linear roll damping coefficient  $B_{44}$  ( $N \cdot m / (rad / s)$ ) as a function of the rolling amplitude  $\phi_a$ , i.e.  $B_{44}(\phi_a)$ .

3.5.3.3 Given the equivalent linear roll damping coefficient,  $B_{44}(\phi_a)$ , calculated as in 3.5.3.2 as a function of the rolling amplitude  $\phi_a$  (rad), the roll damping coefficients  $\mu$  (1/s),  $\beta$  (1/rad),  $\delta$  (s/rad<sup>2</sup>), as specified in 3.4.1.2, should be calculated, in general, by the following least square fitting:

$$\frac{B_{44}(\phi_a) \cdot \omega_0^2}{2 \cdot W \cdot \overline{GM}} \rightarrow \mu + \frac{4}{3 \cdot \pi} \cdot \beta \cdot \omega_0 \cdot \phi_a + \frac{3}{8} \cdot \delta \cdot \omega_0^2 \cdot \phi_a^2 \quad 3.5.3.3-1$$

where  $\omega_0$  (rad/s) is the upright roll natural frequency,  $W(N)$  is the ship displacement force and  $\overline{GM}$  (m) is the upright metacentric height. However, depending on the shape of  $B_{44}(\phi_a)$ , one or more roll damping coefficients can be set a-priori to zero, provided that the final fitting is sufficiently accurate, to the satisfaction of the Administration.

3.5.3.4 When determining the roll damping coefficients through the least square fitting procedure as specified in 3.5.3.3, care should be exercised in order to perform the fitting in a range of rolling amplitudes which is as large as possible, but without extending outside the limits of validity of the method used for the determination of  $B_{44}(\phi_a)$ . Moreover, attention should be paid to avoid, as much as possible, that the roll damping model is used outside the fitting range. In particular, extrapolations should be avoided when the fitting 3.5.3.3-1 is carried out without a-priori setting to zero the cubic damping coefficient  $\delta$ .

### 3.6 Estimation of effective wave slope

3.6.1 In order to perform a prediction of roll motion characteristics according to 3.4.1, the effective wave slope function needs to be specified for the considered ship, in the considered loading condition.

3.6.2 In absence of sufficient information, the standard methodology reported in 3.6.3 should be used. However, methods which, to the satisfaction of the Administration, are deemed to be at least equivalently reliable can be used as well. Such alternative prediction methods can be based on computations or experimental tests, to the satisfaction of the Administration.

#### 3.6.3 *Standard methodology for the estimation of the effective wave slope function*

3.6.3.1 The standard methodology for the estimation of the effective wave slope is applicable only to standard monohull vessels. For a ship which, to the opinion of the Administration, does not fall in this category, alternative prediction methods should be applied according to 3.6.2.

3.6.3.2 The standard methodology for the estimation of the wave slope function is based on the following assumptions and approximations:

- .1 The underwater part of each transverse section of the ship is substituted by an "equivalent underwater section" having, in general, the same breadth at

waterline and the same underwaterplane area of the original section. However:

- .1 Sections having zero breadth at waterline, such as those in the region of the bulbous bow, are neglected;
- .2 The draught of the "equivalent underwater section" is limited to the ship sectional draught;
- .2 The effective wave slope coefficient for each wave frequency is determined by using the "equivalent underwater sections" considering only the undisturbed linear wave pressure;
- .3 For each section, a formula is applied, which is exact for rectangles.

[The standard methodology is applied with the ship having zero trim and results are used also for trim different from zero.]

3.6.3.3 For each longitudinal position  $x$  along the vessel, the draught  $T_{eq}(x)$  (m), the breadth  $B_{eq}(x)$  (m) and the underwater sectional area  $A_{eq}(x)$  (m<sup>2</sup>) of the "equivalent vessel" are to be calculated as follows:

$$\left\{ \begin{array}{l} \text{if } A(x) > 0 \text{ and } B(x) > 0: \\ \text{otherwise:} \end{array} \right. \left\{ \begin{array}{l} \text{if } \frac{A(x)}{B(x)} \leq T(x) \text{ then} \\ \text{if } \frac{A(x)}{B(x)} > T(x) \text{ then} \\ \begin{cases} A_{eq}(x) = 0 \\ B_{eq}(x) = 0 \\ T_{eq}(x) = 0 \end{cases} \end{array} \right. \left\{ \begin{array}{l} \begin{cases} A_{eq}(x) = A(x) \\ B_{eq}(x) = B(x) \\ T_{eq}(x) = \frac{A(x)}{B(x)} \end{cases} \\ \begin{cases} T_{eq}(x) = T(x) \\ B_{eq}(x) = B(x) \\ A_{eq}(x) = B_{eq}(x) \cdot T_{eq}(x) \end{cases} \end{array} \right. \quad 3.6.3.3-1$$

where  $A(x)$  (m<sup>2</sup>),  $B(x)$  (m) and  $T(x)$  (m) are, respectively, the underwater sectional area, the sectional breadth at waterline and the sectional draught of the ship.

3.6.3.4 The underwater volume  $\nabla_{eq}$  (m<sup>3</sup>), the transverse metacentric radius  $BM_{T,eq}$  (m), the vertical position of the centre of buoyancy  $KB_{eq}$  (m) and the vertical position of centre of gravity  $KG_{eq}$  (m) of the "equivalent vessel" are to be calculated as follows:

$$\left\{ \begin{array}{l} \nabla_{eq} = \int_L A_{eq}(x) dx \\ BM_{T,eq} = \frac{1}{\nabla_{eq}} \cdot \int_L \frac{1}{12} \cdot B_{eq}^3(x) dx \\ KB_{eq} = T + \frac{1}{\nabla_{eq}} \cdot \int_L \frac{-T_{eq}(x)}{2} \cdot A_{eq}(x) dx \\ KG_{eq} = KB_{eq} + BM_{T,eq} - \overline{GM} \end{array} \right. \quad 3.6.3.4-1$$

where  $\overline{GM}$  (m) is the upright metacentric height and  $T$  (m) is the draught amidships (at the keel point). The vertical positions  $KB_{eq}$  and  $KG_{eq}$  are defined with respect to the keel line of the ship.

3.6.3.5 The effective wave slope coefficient  $r(\omega)$  as a function of the wave circular frequency  $\omega$  (rad/s) is to be calculated as follows:

$$r(\omega) = \left| \frac{\int C(x) dx}{\nabla_{eq} \cdot GM} \right|$$

where

$$C(x) = \begin{cases} 0 & \text{if } A_{eq}(x) = 0 \text{ and } B_{eq}(x) = 0 \\ A_{eq}(x) \cdot [K_1(x) + K_2(x) + F_1(x) \cdot OG_{eq}] & \text{otherwise} \end{cases}$$

and

$$k_w = \omega^2 / g \quad ; \quad OG_{eq} = KG_{eq} - T$$

$$K_1(x) = \frac{\sin\left(k_w \cdot \frac{B_{eq}(x)}{2}\right) \cdot (1 + k_w \cdot T_{eq}(x)) \cdot e^{-k_w \cdot T_{eq}(x)} - 1}{\left(\frac{k_w \cdot B_{eq}(x)}{2}\right) \cdot k_w^2 \cdot T_{eq}}$$

$$K_2(x) = -\frac{e^{-k_w \cdot T_{eq}(x)}}{k_w^2 \cdot T_{eq}(x)} \cdot \left[ \cos\left(k_w \cdot \frac{B_{eq}(x)}{2}\right) - \frac{\sin\left(k_w \cdot \frac{B_{eq}(x)}{2}\right)}{\left(\frac{k_w \cdot B_{eq}(x)}{2}\right)} \right]$$

$$F_1(x) = -\frac{1 - e^{-k_w \cdot T_{eq}(x)}}{k_w \cdot T_{eq}(x)} \cdot \frac{\sin\left(k_w \cdot \frac{B_{eq}(x)}{2}\right)}{\left(\frac{k_w \cdot B_{eq}(x)}{2}\right)}$$

3.6.3.5-1

#### 4 EXAMPLE OF APPLICATION OF THE LEVEL 2 CRITERION

[As an example, we use the following data of a containership at the full load condition:

$L_f$ (m)	262.0	ship length
$L_{pp}$ (m)	262.0	ship length between perpendiculars
$B$ (m)	40.0	moulded ship breadth
$d$ (m)	11.5	moulded mean ship draught
$\tau$	0.0	trim
$OG$ (m)	7.467	$VCG-d$
$GM$ (m)	1.400	metacentric height with free surface correction
$T$ (s)	24.679	ship natural roll period
$A_L$ (m <sup>2</sup> )	7093.1	lateral windage area
$Z$ (m)	19.708	Vertical distance from the centre of $A_L$ to a point at one-half the mean draught
$C_m$	1.17	wind heeling moment coefficient
$C_b$	0.559	block coefficient

$C_M$	0.950	midship section coefficient
$l_{BK}/L_{pp}$	0.292	bilge keel length normalized with ship length between perpendiculars
$b_{BK}/B$	0.0100	bilge keel width normalized with moulded ship breadth
$\phi_f$	50.0	down flooding angle

The GZ curve of the ship is provided in Figure 4.1

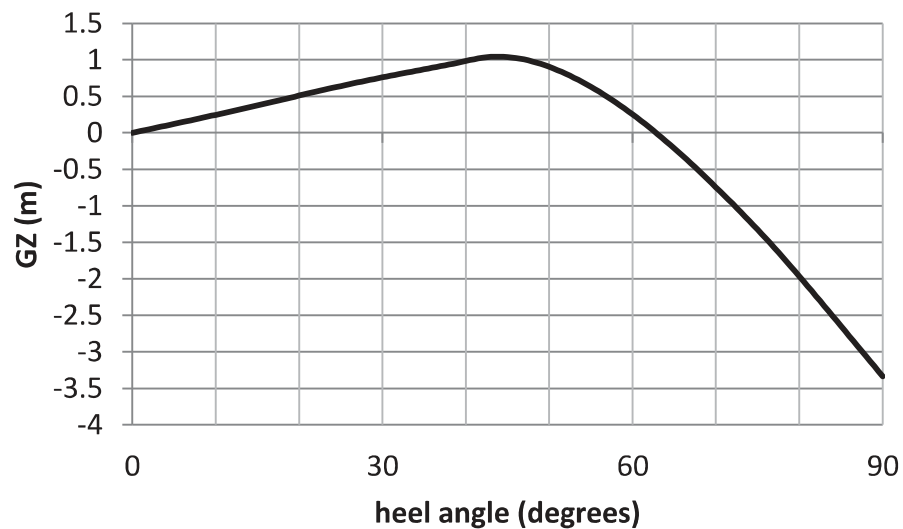


**Figure 4.1** GZ curve of the sample ship

The linear and quadratic roll damping coefficients estimated by Ikeda's simplified method are as follows:

$$\mu = 0.3206E-02, \beta = 0.4741E+00$$

The effective wave slope function estimated by the standard method is as shown in Figure 4.2.

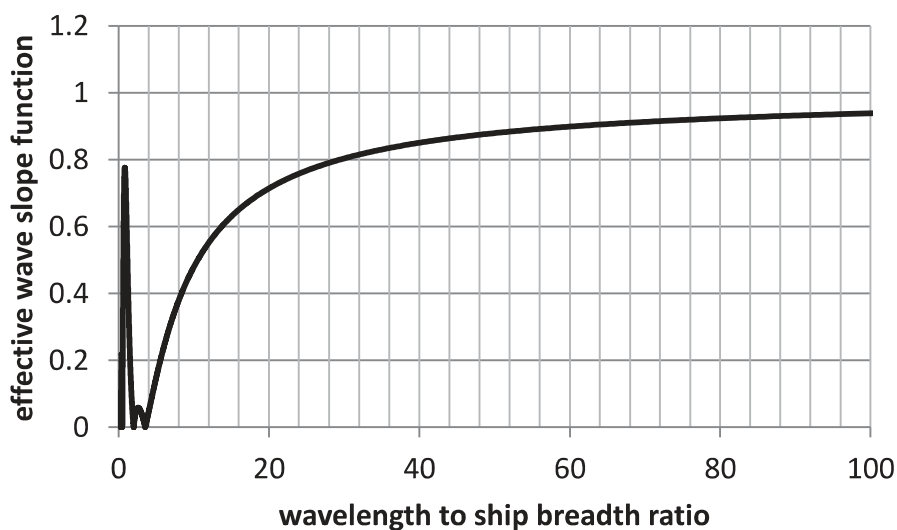


Figure 4.2 Effective wave slope function estimated by the standard method

As a result, the value of  $W_i C_{si}$  can be obtained as the function of the significant wave height and mean zero crossing wave period in Table 4.1

Table 4.1 the value of  $W_i C_{si}$  as the function of the significant wave height and mean zero crossing wave period

H(m)\T(s)	3.5	4.5	5.5	6.5	7.5	8.5	9.5	10.5	11.5	12.5	13.5	14.5	15.5	16.5	17.5	18.5
0.5	0.00E+00	0.00E+00	0.00E+00	0.00E+00	0.00E+00	0.00E+00	0.00E+00	0.00E+00	0.00E+00	0.00E+00	0.00E+00	0.00E+00	0.00E+00	0.00E+00	0.00E+00	0.00E+00
1.5	0.00E+00	0.00E+00	0.00E+00	0.00E+00	0.00E+00	0.00E+00	0.00E+00	0.00E+00	0.00E+00	0.00E+00	0.00E+00	0.00E+00	0.00E+00	0.00E+00	0.00E+00	0.00E+00
2.5	0.00E+00	0.00E+00	0.00E+00	0.00E+00	0.00E+00	0.00E+00	0.00E+00	0.00E+00	0.00E+00	0.00E+00	0.00E+00	0.00E+00	0.00E+00	0.00E+00	0.00E+00	0.00E+00
3.5	0.00E+00	0.00E+00	0.00E+00	0.00E+00	0.00E+00	0.00E+00	0.00E+00	0.00E+00	0.00E+00	0.00E+00	0.00E+00	0.00E+00	0.00E+00	0.00E+00	0.00E+00	0.00E+00
4.5	0.00E+00	0.00E+00	0.00E+00	0.00E+00	0.00E+00	0.00E+00	0.00E+00	0.00E+00	0.00E+00	0.00E+00	0.00E+00	0.00E+00	0.00E+00	0.00E+00	0.00E+00	0.00E+00
5.5	0.00E+00	0.00E+00	1.11E-21	0.00E+00	0.00E+00	0.00E+00	0.00E+00	0.00E+00	0.00E+00	0.00E+00	0.00E+00	0.00E+00	0.00E+00	0.00E+00	0.00E+00	0.00E+00
6.5	0.00E+00	0.00E+00	1.04E-16	0.00E+00	0.00E+00	0.00E+00	0.00E+00	0.00E+00	0.00E+00	0.00E+00	0.00E+00	0.00E+00	0.00E+00	0.00E+00	0.00E+00	0.00E+00
7.5	0.00E+00	0.00E+00	0.00E+00	6.30E-18	0.00E+00	0.00E+00	0.00E+00	0.00E+00	0.00E+00	0.00E+00	0.00E+00	0.00E+00	0.00E+00	0.00E+00	0.00E+00	0.00E+00
8.5	0.00E+00	0.00E+00	0.00E+00	8.45E-15	5.64E-19	0.00E+00	0.00E+00	0.00E+00	0.00E+00	0.00E+00	0.00E+00	0.00E+00	0.00E+00	0.00E+00	0.00E+00	0.00E+00
9.5	0.00E+00	0.00E+00	0.00E+00	1.07E-12	1.15E-15	3.32E-19	0.00E+00	0.00E+00	0.00E+00	0.00E+00	0.00E+00	0.00E+00	0.00E+00	0.00E+00	0.00E+00	0.00E+00
10.5	0.00E+00	0.00E+00	0.00E+00	0.00E+00	1.74E-13	4.36E-16	1.35E-18	0.00E+00	0.00E+00	5.72E-20	5.46E-19	1.57E-18	1.57E-18	3.70E-19	4.40E-20	4.22E-21
11.5	0.00E+00	0.00E+00	0.00E+00	0.00E+00	4.37E-12	5.96E-14	7.42E-16	3.32E-17	1.58E-17	5.17E-17	2.16E-16	3.94E-16	3.94E-16	6.87E-17	1.01E-17	1.74E-18
12.5	0.00E+00	0.00E+00	0.00E+00	0.00E+00	4.44E-11	1.69E-12	5.93E-14	5.14E-15	2.46E-15	5.21E-15	1.36E-14	1.90E-14	1.90E-14	3.10E-15	4.39E-16	0.00E+00
13.5	0.00E+00	0.00E+00	0.00E+00	0.00E+00	0.00E+00	1.94E-11	1.50E-12	2.32E-13	1.31E-13	2.23E-13	4.33E-13	4.78E-13	4.78E-13	6.54E-14	1.92E-14	0.00E+00
14.5	0.00E+00	0.00E+00	0.00E+00	0.00E+00	0.00E+00	1.12E-10	1.33E-11	3.54E-12	2.19E-12	3.21E-12	5.02E-12	4.71E-12	4.71E-12	6.48E-13	0.00E+00	0.00E+00
15.5	0.00E+00	0.00E+00	0.00E+00	0.00E+00	0.00E+00	0.00E+00	6.57E-11	3.39E-11	2.54E-11	4.08E-11	5.11E-11	4.32E-11	4.32E-11	1.11E-11	0.00E+00	0.00E+00
16.5	0.00E+00	0.00E+00	0.00E+00	0.00E+00	0.00E+00	0.00E+00	0.00E+00	1.05E-10	1.08E-10	1.31E-10	1.95E-10	1.22E-10	1.22E-10	0.00E+00	0.00E+00	0.00E+00

Summing up all values in Table 4.1, the long-term probability index is obtained as follows:

$$C = 0.1286E-08$$

Since this is smaller than the standard, this ship is not judged as vulnerable to stability failure under dead ship condition.]

\*\*\*





## ANNEX 7

### DRAFT EXPLANATORY NOTES ON THE VULNERABILITY OF SHIPS TO THE EXCESSIVE ACCELERATION STABILITY FAILURE MODE

#### Chapter [6] – THE VULNERABILITY OF SHIPS TO THE EXCESSIVE ACCELERATION STABILITY FAILURE MODE

##### 1. Physical background of stability failure related to excessive accelerations

###### 1.1. Accelerations caused by ship motions

1.1.1. When a ship is rolling, the objects in higher locations travel longer distances. A period of roll motions is the same for all the location on board the ship. To cover longer distance during the same time, the linear velocity must be larger. As the velocity changes its direction every half a period, larger linear velocity leads to larger linear accelerations. Large linear acceleration means larger inertial force, see Figure 1.

1.1.2. Inertial forces acting in a horizontal plane are more dangerous for a human than vertical inertial forces. The vertical inertia forces cause brief overloading, while horizontal inertial forces cause humans to lose balance, fall or even being thrown against walls, bulkheads or and other structures. Large accelerations are mostly caused by roll motions so they have predominantly lateral direction.

1.1.3. If the GM value is large, the period of roll motion is smaller. Thus, for the same roll amplitude the changes of linear velocity occur faster, so accelerations are larger.

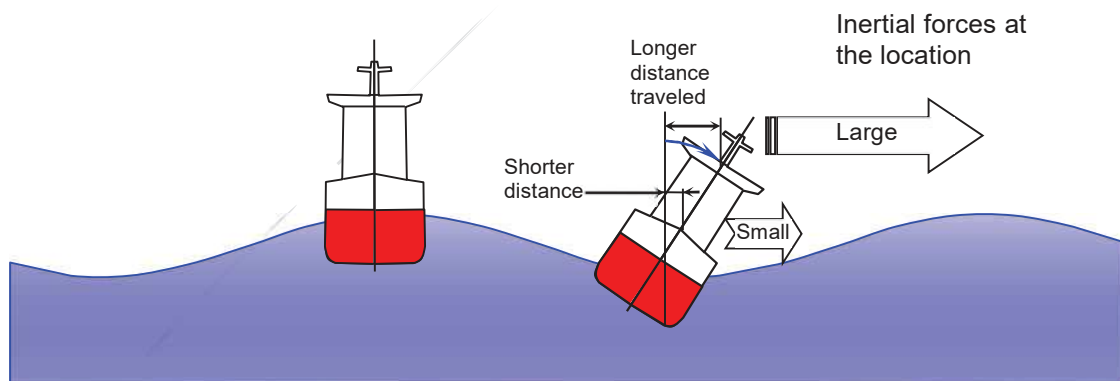


Figure 1. Scenario of stability failure related to excessive accelerations

###### 1.2. Synchronous resonance in ship motions

1.2.1. A large angle of roll may be caused by different physical mechanisms. Some of them are already included as a part of vulnerability assessment of the second generation of IMO stability criteria: pure loss of stability, parametric roll and broaching. Among these phenomena, parametric roll is known to cause excessive accelerations. However, synchronous resonance is not covered by other vulnerability criteria.

1.2.2. Synchronous resonance is a phenomenon of amplification of motion response when the natural frequency of the ship motion is close to the frequency of the wave excitation.

1.2.3. The frequency of wave excitation depends on wave frequency, ship heading relative to waves and ship speed. When a ship sails against the waves (between head and beam wave encounter angles) the frequency of encounter is higher than the frequency of waves. This effect is the strongest in head waves, weakens in bow quartering seas and completely disappears in beam seas. When a ship sails in the same direction as the waves, the frequency of encounter decreases. This effect is the strongest in following seas, weakens in stern quartering seas and completely disappears in beam seas. Higher speed increases this effect.

1.2.4. The motion amplification effect of the synchronous resonance is the strongest when the encounter frequency is close to natural roll frequency, see Figure 2. Increase of the amplitude of excitation (angle of wave slope) leads to increase of resonance effect at all frequencies, however, the strongest increase is around the natural roll frequency, Figure 2a.

1.2.5. Increase of roll damping leads to decrease of motion amplitude; the effect is noticeable around natural frequency, Figure 2b. Thus increase of roll damping helps to mitigate the effects of the synchronous resonance.

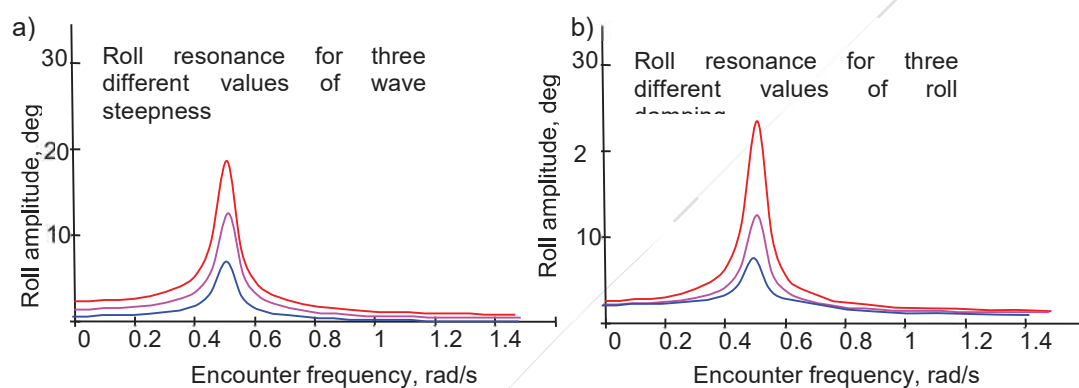


Figure 2. Synchronous roll resonance: influence of wave slope (a) and roll damping (b)

1.2.6. Physical reason of motion amplification near natural frequency (i.e. synchronous resonance) is as follows. The work of excitation is spent on overcoming damping and making the ship to roll with excitation frequency, instead of natural frequency. If the excitation and natural frequency are the same, all the work of the excitation is spent on overcoming damping, so more energy remains in roll motions.

## 2. Level 1 Vulnerability Criterion for Excessive Accelerations

### 2.1. Background Information to Level 1 Criterion

2.1.1. The equation for the variance of roll motion from the Explanatory Notes to Level 2 criterion for excessive accelerations is:

$$\sigma_{\varphi}^2 = \frac{0.75}{m^2 g^2 GM^2} \int_0^{\infty} \frac{(M/\zeta_a)^2 \omega_r^4 S_{\zeta}(\omega) d\omega}{(\omega_r^2 - \omega^2)^2 + \omega_r^2 \omega^2 (\delta_{\varphi} / \pi)^2}$$

where  $\sigma_{\varphi}$  is the standard deviation of roll angle,  $\omega_r$  is the natural roll frequency of the ship,  $g$  is the gravity acceleration,  $S_{\zeta}$  is seaway spectrum and  $\delta_{\varphi}$  is logarithmic decrement of roll decay. After the introduction of the effective wave slope,

$$r = \frac{M}{\zeta_a} \frac{g}{\omega^2 mgGM},$$

the expression for the variance of roll motion becomes:

$$\sigma_\phi^2 = \frac{0.75\omega_r^4}{g^2} \int_0^\infty \frac{r^2 \omega^4 S_\zeta(\omega) d\omega}{(\omega_r^2 - \omega^2)^2 + \omega_r^2 \omega^2 (\delta_\phi / \pi)^2}$$

2.1.2. In the integral on the right-hand-side, the numerator remains finite in the integration region, whereas the denominator approaches zero if the excitation frequency is close to the natural roll frequency and roll damping is low. Thus the dominating contribution to this integral comes from the region of frequencies close to the natural roll frequency. Therefore,  $\omega$  can be replaced with  $\omega_r$  in the numerator; calculating the resulting integral approximately leads to

$$\int_0^\infty \frac{r^2 \omega^4 S_\zeta d\omega}{(\omega_r^2 - \omega^2)^2 + \omega_r^2 \omega^2 (\delta_\phi / \pi)^2} \approx \pi^2 r^2 (\omega_r) \omega_r S_\zeta(\omega_r) / (2\delta_\phi)$$

and the variance of the roll angle becomes

$$\sigma_\phi^2 = 0.0384 r^2 (\omega_r) \omega_\phi^5 S_\zeta(\omega_r) / \delta_\phi$$

2.1.3. Similar approximations lead for the standard deviation of lateral acceleration to the expression

$$\sigma_a = \sigma_\phi (g + \omega_r^2 h)$$

where  $h$  is the height of the considered location above the roll axis. The roll axis can be assumed at the mid height between the waterline and the ship centre of gravity.

2.1.4. Assuming the ITTC spectrum for the wind sea,

$$S_\zeta = 0.313 (h_s \omega_p^2)^2 \exp(-1.25 \omega_p^4 / \omega^4) / \omega^5$$

where  $h_s$  is the significant wave height and  $\omega_p$  is the modal frequency, and applying a spectrum with the modal frequency equal to the natural roll frequency  $\omega_p = \omega_r$  leads to

$$\sigma_\phi = 4.43 rs / \delta_\phi^{0.5}$$

where  $s = 2\pi h_s / (gT_r^2)$  is the seaway steepness, corresponding to the natural roll period of the ship.

## 2.2. Example Application of Level 1 Vulnerability Criteria for Excessive Accelerations

2.2.1. A container ship is considered in this example application. Ship data are given in Table 1; the considered location is the navigational deck.

Table 1. Principal particulars of the ship

Length between perpendiculars $L$	349.5 m
Breadth moulded $B$	51.2 m
Height of the navigational deck above keel	60.0 m
Longitudinal distance from the aft perpendicular to the bridge $x$	218.5 m
Bilge keel area $A_{BK}$	62.0 m <sup>2</sup>
Draft midships $d$	14.0 m
Trim, positive to bow	-0.1 m
Length of waterline $L_{WL}$	348.7 m
Initial $GM$ without free-surface correction	3.422 m
Centre of gravity height above keel $KG$	21.9 m
Block coefficient $C_B$	0.697
Midship section coefficient $C_m$	0.98

### 2.2.2. Calculate

- Factor  $k_L$ , taking into account longitudinal position:

$$x = 218.5 \text{ m}$$

$$k_L = 1.0$$

- Natural roll period  $T_r$ :

$$C = 0.373 + 0.023(B/T) - 0.043(L_{WL}/100) = 0.307$$

$$T_r = 2C \cdot B/GM^{0.5} = 17.0 \text{ s}$$

- Effective wave slope coefficient  $r$ :

$$\tilde{B} = 2\pi^2 B / (gT_r^2) = 0.357, \quad \tilde{T} = 4\pi^2 C_B T / (gT_r^2) = 0.136$$

$$\beta = \sin(\tilde{B}) / \tilde{B} = 0.979, \quad \tau = \exp(-\tilde{T}) / \tilde{T} = 6.418$$

$$K_1 = g\beta T_r^2 (\tau + \tau\tilde{T} - 1 / \tilde{T}) / (4\pi^2) = -4.373, \quad K_2 = g\tau T_r^2 (\beta - \cos\tilde{B}) / (4\pi^2) = 19.251$$

$$F = \beta(\tau - 1 / \tilde{T}) = -0.915, \quad OG = KG - T = 7.858$$

$$r = \frac{K_1 + K_2 + OG \cdot F}{\frac{B^2}{12C_B T} - \frac{C_B T}{2} - OG} = 0.801$$

- Wave steepness  $s$  according to the steepness table for  $T_r = 17.0 \text{ s}$ :

$$s = 0.041$$

- Logarithmic decrement of roll decay  $\delta_\varphi$ :

$$C_m > 0.96$$

$$\delta_\varphi = 0.267 + 0.668 \cdot 100A_{BK} / (L \cdot B) = 0.498$$

- Roll amplitude  $\varphi$ :

$$\varphi = 4.43rs / \delta_\varphi^{0.5} = 0.204 \text{ rad}$$

- Lateral acceleration:

$$h = 60.0 \text{ m} - (KG + T) / 2 = 42.041 \text{ m}$$

$$\varphi k_L (g + 4\pi^2 H / T_r^2) = 3.17 \text{ m/s}^2$$

$$3.17 \text{ m/s}^2 < R_1 = 8.9 \text{ m/s}^2$$

Thus, this loading condition is not vulnerable to excessive lateral accelerations.

### 3. Level 2 Vulnerability Criterion for Excessive Accelerations

#### 3.1. Background Information to Level 2 Criterion

3.1.1. Simplified 1 degree-of-freedom motion model is adopted for the amplitude of roll,

$$I_{xx}\ddot{\theta} + B_{\theta}\dot{\theta} + C_{\theta}\theta = M_{FK}$$

where  $\theta, \dot{\theta}, \ddot{\theta}$  are the roll angle, roll velocity and roll acceleration, rad, rad/s, rad/s<sup>2</sup>, respectively,  $I_{xx}$  is the roll moment of inertia, including the added roll moment of inertia;  $B_{\theta}$  is the linear roll damping coefficient,  $C_{\theta} = mgGM$  is the restoring force coefficient and  $M_{FK}$  is the Froude-Krylov exciting moment.

3.1.2. The roll angle can be described as

$$\theta = \theta_a e^{i\omega_e t}$$

where  $\theta_a$  is the amplitude of roll, rad, and  $\omega_e$  is the encounter frequency, rad/s. Neglecting diffraction effects, the amplitude of the exciting moment can be written as

$$M_{FK} = (a + bi) \cdot e^{i\omega_e t}$$

Parameters  $a$  and  $b$  are the real and imaginary parts of the exciting roll moment, calculated using Froude-Krylov assumption and neglecting the diffraction moment by direct integration of pressure including hydrostatic pressure and pressure due to particle velocity (Smith effect) in beam waves over the mean wetted hull surface of the ship.

3.1.3. Accident investigations<sup>10,11</sup> indicate that forward speed was very low (2 to 4 knots) at the time of accidents. The reasons are, first, increased resistance due to wind, waves and large drift angles and, second, reduced propulsion efficiency in waves. It appears therefore not too conservative to neglect the effect of forward speed on both the encounter frequency and roll damping. Therefore,  $F_n = 0$  and  $\omega_e = \omega$ .

3.1.4. Then roll amplitude  $\vartheta_a(\omega)$  in regular beam waves can be calculated as follows:

$$\vartheta_a(\omega) = (\vartheta_r^2 + \vartheta_i^2)^{0.5}$$

where

$$\vartheta_r = \frac{a(C_{\theta} - I_{xx}\omega_e^2) + bB_{\theta}\omega_e}{(C_{\theta} - I_{xx}\omega_e^2)^2 + (B_{\theta}\omega_e)^2}, \quad \vartheta_i = \frac{b(C_{\theta} - I_{xx}\omega_e^2) - aB_{\theta}\omega_e}{(C_{\theta} - I_{xx}\omega_e^2)^2 + (B_{\theta}\omega_e)^2}$$

$C_{\theta} = mgGM$  is the restoring coefficient, Nm,  $B_{\theta}$  is the equivalent linear roll damping coefficient, Nms,  $I_{xx} = gmGMT_r^2 / (4\pi^2)$  is the roll moment of inertia, kg·m<sup>2</sup>,  $m$  is the ship mass, kg, and  $T_r$  is the natural roll period, s.

<sup>10</sup> Federal Bureau of Maritime Casualty Investigation (2009) Fatal accident on board the CMV Chicago Express during Typhoon "Hagupit" on 24 September 2008 off the coast of Hong Kong

<sup>11</sup> Federal Bureau of Maritime Casualty Investigation (2011) Tödlicher Personenunfall an Bord des CMS CCNI GUAYAS während des Taifuns "Koppu" am 15. September 2009 im Seegebiet vor Hongkong, Untersuchungsbericht 391/09

3.1.5. Taking into account vertical accelerations and yaw motion, as well as the longitudinal position of the considered location, the lateral acceleration,  $a_y(\omega)$ ,  $m/s^2$ , is defined as a function of wave frequency as follows:

$$a_y(\omega) = k_L(g \sin \vartheta_a + h \omega^2 \vartheta_a)$$

where  $k_L$  is the nondimensional factor taking into account vertical accelerations and yaw motion and depending on the longitudinal position of the considered location,  $H$  is the height of the bridge deck above the roll axis,  $m$ , and  $\vartheta_a(\omega)$ ,  $rad$ , is roll amplitude in regular beam waves of frequencies  $\omega$ ,  $rad/s$ .

3.1.6. The root-mean-square value of lateral acceleration is calculated as

$$\sigma = \sqrt{m_0}$$

where

$$m_0 = \int_0^\infty \int_0^{2\pi} |a_y(\omega)|^2 D(\beta - \pi/2) S_\zeta(\omega) d\omega d\beta$$

$D(\beta - \pi/2)$  is the nondimensional seaway energy spreading function,  $\beta$  is the wave direction and  $S_\zeta(\omega)$  is the frequency spectrum of the seaway,  $m^2s/rad$ . The seaway energy spreading function is calculated as

$$D(\beta - \pi/2) = \frac{2}{\pi} \cos^2(\beta - \pi/2) \text{ if } |\beta - \pi/2| < \pi/2 \text{ and } D(\beta - \pi/2) = 0 \text{ otherwise}$$

3.1.7. To simplify the calculation, the nondimensional response-amplitude operators of lateral acceleration are calculated in beam long-crested waves; the influence of short-crestedness is accounted for using a reduction factor 0.75. Introducing integration limits for wave frequency as  $\omega_1 = [\max(0.5/T_r, 0.2)]$   $rad/s$  and  $\omega_2 = [\min(25/T_r, 2.0)]$   $rad/s$ ,  $\sigma^2$  is calculated as

$$\sigma^2 = \int_0^\infty \int_0^{2\pi} |a_y(\omega)|^2 D(\beta - \pi/2) S_\zeta(\omega) d\omega d\beta \approx 0.75 \int_{\omega_1}^{\omega_2} |a_y(\omega)|^2 S_\zeta(\omega) d\omega$$

3.1.8. For the computation of the roll response in each seaway, equivalent linear roll damping coefficient  $B_\vartheta$  is required. For the definition of the equivalent linear roll damping in irregular waves, an equivalent stochastic linearization method can be used; in this case, the equivalent linear roll damping coefficient in each irregular seaway corresponds to the roll amplitude of

$$\vartheta_a = 0.3 T_r \sigma_{\dot{\vartheta}}$$

in a roll decay test, where  $\sigma_{\dot{\vartheta}}$  is the square root of the variance of roll angular velocity in the considered seaway. Because the equivalent linear damping depends on roll motions, iterative procedure will have to be used for each seaway. Alternatively, the equivalent linear roll damping coefficient can be defined at the 15 degree roll amplitude.

3.1.9. The equivalent linear roll damping coefficient as function of the roll amplitude can be defined with the procedure described in Section 6.

3.1.10. The parameters  $a$  and  $b$  can be calculated with the following formulae:

$$a = \rho g \iint_{S_H} e^{k_0 z} \cos(k_0 y) n_4 dS, \quad b = -\rho g \iint_{S_H} e^{k_0 z} \sin(k_0 y) n_4 dS$$

where  $g$  is the gravity acceleration,  $\rho$  is the density of sea water,  $k_0 = \omega^2 / g$  is the wave number,  $x$ ,  $y$  and  $z$  are the coordinates of mean wetted hull surface of ship,  $S_H$  is the mean wetted hull surface of ship, and  $n_4$  is the normal vector of roll. For laterally symmetric ship hulls, the above formulae can be simplified as follows:

$$a = 0, \quad b = mgGMr(\omega^2 / g)$$

where  $r$  is the effective wave slope coefficient. This coefficient should be obtained by the formula specified in Section 3.6 of the Explanatory Notes of vulnerability criteria for dead ship stability.

3.1.11. For each seaway, the exceedance index is calculated as

$$C_i = \exp\{-R_2^2 / (2\sigma_i^2)\}$$

where  $\sigma_i^2$  is the variance of lateral acceleration in the considered seaway, and the long-term exceedance index in a given seaway climate is calculated as

$$C = \sum_i w_i C_i / \sum_i w_i$$

where  $w_i$  are the frequencies of occurrence of each seaway.

### 3.2 Example Application of Level 2 Vulnerability Criteria for Excessive Accelerations

(to be developed)

## 4. Natural Roll Period

4.1. For the definition of the natural roll period  $T$ , three different methods defined in 4.1.1-4.1.3 are presently available:

4.1.1. The first method, using the hull principal particulars only, is used in the current IMO Weather Criterion, as provided in 2.3.4 of Part A.

4.1.2. The second method, using container mass distribution, was recently proposed only for container ships:

$$T = 2\pi \sqrt{I_{xx} / (mgGM)}$$

where

$$I_{xx} = 1.1m_1(B/3)^2 + 1.1m_1l^2 + 1.1 \sum \left\{ m_i \left[ y_i^2 + (z_i - z_T)^2 \right] + (b_i^2 + h_i^2) m_i / 12 \right\}$$



$m$  (t) is the mass of ship,  $l$  (m) is the distance from the centre of mass of ship to the local centre of mass of the ship without containers on deck,  $m_i$  (t) is the mass of each container loaded on deck,  $y_i$  (m) and  $z_i$  (m) are the transverse and vertical coordinates of the container centre of mass, respectively,  $b_i$  (m) and  $h_i$  (m) are the breadth and height of the container, respectively,  $z_T$  (m) is the vertical height of the ship centre of gravity and  $m_1$  (t) is the mass of the ship without containers on deck.

4.1.3. For passenger and cargo ships, the following formula, which was originally used in a domestic weather criterion since 1950's, can be also alternatively used for the natural roll period:

$$I_{xx} = mK^2$$

where 
$$\left(\frac{K}{B}\right)^2 = 0.125 \left[ C_u \cdot C_b + 1.10C_u (1 - C_b) \left( \frac{H_s}{d} - 2.20 \right) + \left( \frac{H_s}{B} \right)^2 \right]$$

$$C_u = \frac{A_u}{L_u B}$$

$$H_s = D + \left( \frac{A'}{L_{pp}} \right)$$

$C_u$  = upper deck area coefficient

$A_u$  = projected area of upper deck

$L_u$  = overall length of upper deck

$C_b$  = block coefficient

$B$  = moulded breadth

$d$  = mean draught

$H_s$  = effective depth  $H_s = D + \left( \frac{A'}{L_{pp}} \right)$

$D$  = moulded depth

$L_{pp}$  = length between perpendiculars

$A' = A + A_c$

$A'$  = lateral projected area of forecastle and deck house ( $A$ ) and on deck cargoes ( $A_c$ )

4.2. Alternatively, natural roll period can be defined for any ship using Direct Assessment methods for Excessive Accelerations failure mode, or from model tests carried out according to MSC.1/Circ.1200 or alternative test procedures approved by the Administration.

## 5. Roll Damping

5.1. In Level 1 vulnerability assessment [for the excessive acceleration stability failure mode], the non-dimensional logarithmic decrement of roll decay  $\bar{\delta}_\phi$  is calculated as  $\bar{\delta}_\phi = 0.5 \cdot \pi \cdot R_{PR}$ , where

$$R_{PR} = \begin{cases} 1.87, & \text{if the ship has a sharp bilge}^{12}; \text{ otherwise,} \\ 0.17 + 0.425 (100 A_k / (L B)), & \text{if } C_m \geq 0.96, \\ 0.17 + (10.625 \cdot C_m - 9.775) (100 A_k / (L B)), & \text{if } 0.94 < C_m < 0.96, \\ 0.17 + 0.2125 (100 A_k / (L B)), & \text{if } C_m \leq 0.94, \text{ and} \\ & (100 A_k / (L B)) \text{ should not exceed 4;} \end{cases}$$

$L$  = length of the ship, m;  
 $B$  = moulded breadth of the ship (m);

<sup>12</sup> See the Explanatory Notes.



- $d$  = mean moulded draft of the ship for the actual loading condition (m);
- $C_B$  = block coefficient for the actual loading condition;
- $KG$  = vertical center of gravity (m), uncorrected for free surface effect;
- $A_k$  = total projected area of bilge keels (m<sup>2</sup>) as defined in 2.11.2.1 and bar keel area (m<sup>2</sup>) as defined in chapter 2.3 of Part A; and
- $C_m$  = midship section coefficient for the actual loading condition as defined in 2.11.2.1.

5.2. In Level 2 vulnerability assessment [for the excessive acceleration stability failure mode], equivalent linear roll damping coefficient  $\mu_e$  (t m s) is calculated according to the stochastic linearization method as a function of the linear and nonlinear roll damping coefficients and standard deviation of roll velocity in the considered environmental conditions<sup>4</sup>.

## 6. Wave Data

6.1. Wave conditions, specified by a significant wave height,  $H_s$ , and an average zero upcrossing wave period,  $T_z$ , are obtained from wave statistics which describe the probability of a wave condition ( $H_s$ ,  $T_z$ ) as the number of occurrences for a given total number of observations.

6.2. The value of the weighting factor for the short-term environmental wave condition,  $W_i$ , for a wave condition ( $H_s$ ,  $T_z$ ) is obtained as the value in the table of wave condition occurrences (Table 2) divided by the number of occurrences given in the table.

**Table 2. Wave condition occurrences**

Number of observations: 100 000 / $T_z$ (s) = average zero up-crossing wave period / $H_s$ (m) = significant wave height																
$T_z$ (s) ►	3.5	4.5	5.5	6.5	7.5	8.5	9.5	10.5	11.5	12.5	13.5	14.5	15.5	16.5	17.5	18.5
$H_s$ (m) ▼																
0.5	1.3	133.7	865.6	1186.0	634.2	186.3	36.9	5.6	0.7	0.1	0.0	0.0	0.0	0.0	0.0	0.0
1.5	0.0	29.3	986.0	4976.0	7738.0	5569.7	2375.7	703.5	160.7	30.5	5.1	0.8	0.1	0.0	0.0	0.0
2.5	0.0	2.2	197.5	2158.8	6230.0	7449.5	4860.4	2066.0	644.5	160.2	33.7	6.3	1.1	0.2	0.0	0.0
3.5	0.0	0.2	34.9	695.5	3226.5	5675.0	5099.1	2838.0	1114.1	337.7	84.3	18.2	3.5	0.6	0.1	0.0
4.5	0.0	0.0	6.0	196.1	1354.3	3288.5	3857.5	2685.5	1275.2	455.1	130.9	31.9	6.9	1.3	0.2	0.0
5.5	0.0	0.0	1.0	51.0	498.4	1602.9	2372.7	2008.3	1126.0	463.6	150.9	41.0	9.7	2.1	0.4	0.1
6.5	0.0	0.0	0.2	12.6	167.0	690.3	1257.9	1268.6	825.9	386.8	140.8	42.2	10.9	2.5	0.5	0.1
7.5	0.0	0.0	0.0	3.0	52.1	270.1	594.4	703.2	524.9	276.7	111.7	36.7	10.2	2.5	0.6	0.1
8.5	0.0	0.0	0.0	0.7	15.4	97.9	255.9	350.6	296.9	174.6	77.6	27.7	8.4	2.2	0.5	0.1
9.5	0.0	0.0	0.0	0.2	4.3	33.2	101.9	159.9	152.2	99.2	48.3	18.7	6.1	1.7	0.4	0.1
10.5	0.0	0.0	0.0	0.0	1.2	10.7	37.9	67.5	71.7	51.5	27.3	11.4	4.0	1.2	0.3	0.1
11.5	0.0	0.0	0.0	0.0	0.3	3.3	13.3	26.6	31.4	24.7	14.2	6.4	2.4	0.7	0.2	0.1
12.5	0.0	0.0	0.0	0.0	0.1	1.0	4.4	9.9	12.8	11.0	6.8	3.3	1.3	0.4	0.1	0.0
13.5	0.0	0.0	0.0	0.0	0.0	0.3	1.4	3.5	5.0	4.6	3.1	1.6	0.7	0.2	0.1	0.0
14.5	0.0	0.0	0.0	0.0	0.0	0.1	0.4	1.2	1.8	1.8	1.3	0.7	0.3	0.1	0.0	0.0
15.5	0.0	0.0	0.0	0.0	0.0	0.0	0.1	0.4	0.6	0.7	0.5	0.3	0.1	0.1	0.0	0.0
16.5	0.0	0.0	0.0	0.0	0.0	0.0	0.0	0.1	0.2	0.2	0.2	0.1	0.1	0.0	0.0	0.0

## 7. Background Information to Definition of Standards in Level 1 and Level 2 Criteria

7.1. For the definition of standards of lateral acceleration, loading condition of the vessel *Chicago Express* at the time of accident was used. This loading condition is summarized in Table 3.

Table 3. Principal particulars of ships in accidents

Draft midships $d$ , m	8.1
Trim, positive to bow, m	-2.0
Initial metacentric height without free-surface correction $GM$ , m	8.54
Natural roll period $\tau_r$ , s	10.54
Natural decrement of roll decay $\delta_\phi$ , -	0.506
Wave steepness $s$ , -	0.075

7.2. Standard for Level 2 assessment was defined by calculation of the attained index  $C$ , which is shown as colour plot in Fig. 3 depending on draught (horizontal coordinate) and uncorrected GM (vertical coordinate); the accident condition is shown as a red dot. The attained value of the index  $C$  for the accident condition  $1.094 \cdot 10^{-4}$ , which is suggested as standard for Level 2 assessment.

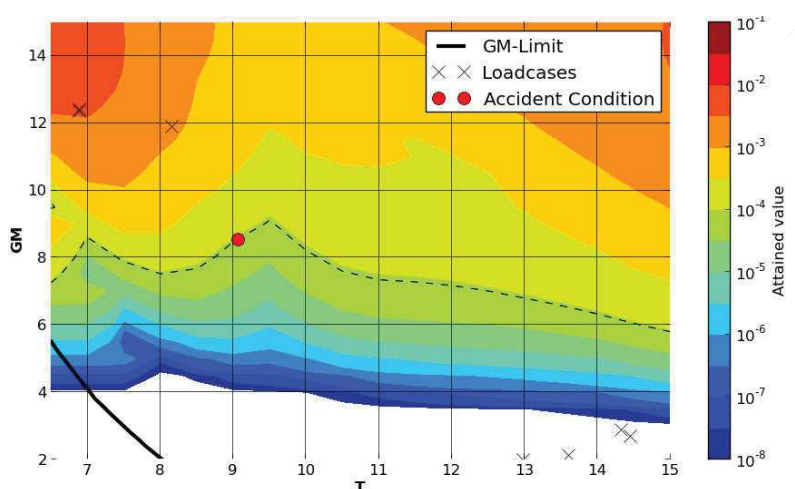


Fig. 3. Attained value of index  $C$  for container ship *Chicago Express*; red dot corresponds to the loading condition during accident, Table 5.1

7.3. To ensure consistency between Level 1 and Level 2 assessment, Level 2 assessment was applied to several ships, and the attained value of the Level 1 criterion,  $\phi k_L (g + 4 \pi^2 h / T^2)$ , was calculated for all conditions of loading for which  $C=1.094 \cdot 10^{-4}$ ; Table 4 shows minimum attained value of  $\phi k_L (g + 4 \pi^2 h / T^2)$  over all loading conditions for each ship. To ensure consistency between Level 1 and Level 2 assessment, the standard for Level 1,  $R_{EAI}$ , should be set to 5.29.

Table 4. Required threshold for  $\phi k_L (g + 4 \pi^2 h / T^2)$  in Level 1 assessment to ensure consistency between Level 1 and Level 2

Ship	Threshold for L1
Container Ship, <i>Chicago Express</i>	6.43
Container Ship, 1700 TEU	5.29
Container Ship, 8400 TEU	7.54
Container Ship, 14000 TEU	7.26
RoPax	6.30
Minimum over all	5.29

7.4 The Correspondence Group conducted sample calculations for 83 ships. The standard values were developed based on these results of sample calculations and those

results for the containership which suffered an accident.

\*\*\*



**ANNEX 8**

**REVISED PLAN OF ACTION FOR MATTERS RELATED TO INTACT STABILITY**

**Finalization of the second generation intact stability criteria**

Further steps with regard to the second generation intact stability criteria (SGISC)

No	Agenda Item/Task	Objective	Deadline
1	Update standards for each mode of stability failure	Based on sample ship calculation results, address inconsistencies between levels 1 and 2 vulnerability criteria	SDC 4
2	Finalize Explanatory Notes for vulnerability criteria	Refine the background for the stability failure phenomena, specific recommendations for the calculations needed for each criteria assessment, and worked examples for each level vulnerability criteria	SDC 4
3	Draft guidelines for direct stability assessment, operational limitations and operational guidance		SDC 4
4	Finalize the guidelines for direct stability assessment, development of ship specific operational limitations and operational guidance		SDC 5
5	Update standards for each mode of stability failure	Based on sample ship calculation results, address inconsistencies between levels 1 and 2 vulnerability criteria and direct stability assessment	SDC 5
6	Prepare a draft MSC circular for approval.	The draft of the second generation intact stability criteria is to be annexed to the MSC circular. The MSC circular is to encourage Member States to apply the interim draft second generation intact stability criteria and submit the experience gained to the Sub-Committee on Ship Design and Construction (SDC).	SDC 5
7	Collect experience of application of interim Second Generation Intact Stability Criteria including application to more diverse population of ships, including small cargo ships, and analyse this experience and complete the second generation intact stability amendments to the 2008 IS Code.	Explore possibilities to simplify and improve criteria and standards.	SDC 6

\*\*\*



## Annex B

List of publications:

### INTERNATIONAL CONFERENCES with REVIEW COMMITTEE and PROCEEDINGS

- [1] Ariffin A., Mansor S., and Laurens JM. (2015), *A Numerical Study for Level 1 Second Generation Intact Stability Criteria*, Proceedings of the 12<sup>th</sup> International Conference on the Stability of Ships and Ocean Vehicles, 15-19 June, Glasgow.
- [2] Ariffin A., Mansor S., and Laurens JM. (2016), *Real-Time Evaluation of Second Generation Intact Stability*, Proceedings of the Smart Ship Technology Conference, 26-27 Jan, London.
- [3] Ariffin A., Mansor S., and Laurens JM. (2016), *Conduction of a wind tunnel experiment to investigate the ship stability weather criterion*, Proceedings of the 15<sup>th</sup> International Ship Stability Workshop, 13-15 June, Stockholm, Sweden.
- [4] Ariffin A., Laurens JM., and Mansor S. (2016), *Implementation of Second Generation Intact Stability Criteria into the Stability Calculation Software*, Proceedings of the 3<sup>rd</sup> International Conference on Maritime Technology and Engineering, 4-6 July, Lisbon, Portugal.
- [5] Ariffin A., Mansor S., and Laurens JM. (2016), *The weather criterion: Experimental wind tunnel results*, Proceedings of the 6<sup>th</sup> International Maritime Conference on Design for Safety, 28-30 Nov, Hamburg, Germany.





# A Numerical Study for Level 1 Second Generation Intact Stability Criteria

Arman Ariffin, *ENSTA Bretagne, LBMS EA 4325, Brest, France*

[arman.ariffin@ensta-bretagne.org](mailto:arman.ariffin@ensta-bretagne.org)

Shuhaimi Mansor, *Faculty of Mechanical Engineering, Universiti Teknologi Malaysia, Malaysia*

[shuhaimi@mail.fkm.utm.my](mailto:shuhaimi@mail.fkm.utm.my)

Jean-Marc Laurens, *ENSTA Bretagne, LBMS EA 4325, Brest, France*

[jean-marc.laurens@ensta-bretagne.fr](mailto:jean-marc.laurens@ensta-bretagne.fr)

## ABSTRACT

During the last International Ship Stability Workshop held in Brest last September, several questions were raised concerning the existing IMO intact stability rules and the new proposed regulations. The lower level (level 1) criteria are conservative but should be easily implemented in stability codes. In this particular study it was investigated if and how an existing and extensively used commercial computer code, in the present case GHS©, could handle level 1 criteria. For simple and realistic cases it was found that a relatively small angle of trim can cause the capsizing of the vessel. These clearly unsafe examples indicate that the existing rules are insufficient. The new intact stability rules aim to deal with failure modes generally associated with extreme weather conditions such as parametric rolling, broaching or pure loss of stability in astern waves but they may also prevent capsizing due to environmental loading. Some of the difficulties encountered with the computation are presented to assess the extent of the necessary development. Finally an illustrative example is presented to verify whether the existing and future regulations can prevent certain obviously dangerous situations.

**Keywords:** *second generation intact stability, weather criterion, GZ curve*

## 1. INTRODUCTION

Intact stability is a basic requirement to minimise the risk of the capsizing of vessels. It is a guideline for the ship designer, ship operator and classification society to design, build and commission the ship before it starts its service life at sea. A comprehensive background study of intact stability development was written by Kuo & Welaya (Welaya & Kuo, 1981). Their paper "A review of intact stability research and criteria", stated that the first righting arm curve was proposed

by Reedin 1868, but the application was presented by Denny in 1887. In addition, in 1935, Pierrottet tried to rationally establish the forces which tend to capsize a ship and proposed a limiting angle at which the dynamic level of the ship must be equal to or greater than the sum of work done by the inclining moments. However, Pierrottet's proposal was too restrictive in the design process and it was not accepted.

Kuo and Welaya also mentioned the famous doctoral thesis written by Jaakko Rahola in 1939. Rahola's thesis evoked

widespread interest throughout the world at that time because it was the first comprehensive study and proposed method to evaluate the intact stability which did not require complex calculations.

The First International Conference for ship stability which was held at the University of Strathclyde in 1975, Tsuchiya presented a new method for treating the stability of fishing vessels (Tsuchiya, 1975). He introduced a list of coefficient to define the weather stability criteria. He disregarded the idea of a stability assessment using simple geometrical stability standards such as metacentric height and freeboard, or the shape of the righting arm curve. He proposed a number of factors which, in his opinion, are crucial. He introduced a certain coefficient which should be calculated and plotted on a diagram as a function of metacentric height and the freeboard for every stability assessment. He concluded that his proposed method should be confirmed by a comparison with actual data on fishing boat activities and empirical stability standards.

The first generation intact stability criteria was originally codified at IMO in 1993 as a set of recommendations in Res A.749(18) by taking into account the former Res.A.167 (ES.IV) ("Recommendation on intact stability of passenger and cargo ships under 100 meters in length" which contained statistical criteria, heeling due to passenger crowding, and heeling due to high speed turning, 1968) and Res A.562.(14) ("Recommendation on a severe wind and rolling criterion (Weather Criterion) for the intact stability of passenger and cargo ships of 24 meters in length and over," 1985). These criteria were codified in the 2008 IS Code and became effective as part of both SOLAS and the International Load Line Convention in 2010 in IMO Res MSC.269(85) and MSC.207(85) (Peters et al., 2012).

The actual work to review IS Code 2008 was highlighted during the 48th session of the SLF in Sept. 2005 (IMO, 2005). The work group decided to address three modes of stability failure:

- a. Restoring arm variation.
- b. Stability under dead ship condition.
- c. Manoeuvring-related problems in waves.

There are two conferences that address the development of second generation intact stability criteria. These are the International Conference on Stability of Ship Ocean Vehicles (STAB) and the International Ship Stability Workshop (ISSW). An experimental evaluation of weather criteria was carried out at the National Maritime Research Institute, in Japan. They conducted a wind tunnel test with wind speeds varying from 5m/s to 15 m/s. The results showed some differences compared to the current estimation. For example the wind heeling moment depended on the heel angle and the centre of drift force was higher than half draft (Ishida, Taguchi, & Sawada, 2006). The experimental validation procedures for numerical intact stability assessment with the latest examples was presented by Umeda and his research members in 2014 (Umeda et al., 2014). They equipped the seakeeping and manoeuvring basin of the National Research Institute of Fisheries Engineering in Japan with a wind blower to examine dead ship stability assessment.

A review of available methods for application to second level vulnerability criteria was presented at STAB 2009 (Bassler, Belenky, Bulian, Spyrou, & Umeda, 2009). They concluded that the choice of environmental conditions for vulnerability criteria is at least as important as the criteria themselves. A test application of second generation IMO intact stability criteria on a large sample of ships was presented during STAB 2012. Additional work remains to be carried out to determine a possible standard for the criteria and environment conditions before finalising the second generation intact stability criteria (Wandji & Corrigan, 2012).

During the ISSW 2013, Umeda presented the current status of the development of second generation intact stability criteria and some recent efforts (Umeda, 2013). The discussion

covered the five failures modes: pure loss of stability, parametric rolling, broaching, harmonic resonance under dead ship condition and excessive acceleration.

**2. BACKGROUND OF IS CODE 2008**

The Intact Stability Code 2008 is the document in force. The code is based on the best "state-of-the-art" concept (IMO, 2008). It was developed based on the contribution of design and engineering principles and experience gained from operating ships. In conjunction with the rapid development of modern naval architecture technology, the IS Code will not remain unchanged. It must be re-evaluated and revised as necessary with the contribution of the IMO Committees all around the globe (IMO, 2008).

The IS Code 2008 is divided into 2 parts. Part A consists of the mandatory criteria and Part B contains the recommendation for certain types of ships and additional guidelines. As stated in Part A, the IS Code applies to marine vehicles of 24 metres in length and more. Paragraph 2.2 of Part A lists the criteria regarding the righting arm curve properties and Paragraph 2.3 describes the severe wind and rolling criteria (weather criterion).

The IS Code 2008 Part A 2.2 sets four requirements for righting arm (GZ) curve properties (Grinnaert and Laurens 2013):

- a. Area under the righting lever curve,
  - i. not less than 0.055 meter-radian up to a 30° heel angle.
  - ii. not less than 0.09 meter-radians up to a 40° heel angle, or downflooding angle.
  - iii. not less than 0.03 meter-radians from a 30° to 40° heel angle or between 30° to the downflooding angle.
- b. The righting lever GZ shall be at least 0.2m for a heel angle greater than 30°.
- c. The maximum righting lever shall occur at a heel angle not less than 25°.

- d. The initial GM shall not be less than 0.15 meters.

The additional requirement for passenger ships is stated in Part A, Paragraph 3.1. It states that:

- a. The angle of heel due to passenger crowding shall not be more than 10°.
- b. A minimum weight of 75kg for each passenger and the distribution of luggage shall be approved by the Administration.
- c. The centre of gravity for a passenger standing upright is 1 m and for a seated passenger 0.3 m above the seat.

The IS Code 2008 Part A 2.3 concerns the weather criterion. The ship must be able to withstand the combined effects of beam wind and rolling at the same time. The conditions are:

- a. the ship is subjected to a steady wind pressure acting perpendicular to the ship's centreline which results in a steady wind heeling lever ( $lw_1$ ).
- b. from the resultant angle of equilibrium ( $\phi_0$ ), the ship is assumed to present an angle of roll ( $\phi_1$ ) to windward due to wave action. The angle of heel under action of steady wind ( $\phi_0$ ) should not exceed 16° or 80% of the angle of deck edge immersion, whichever is less.
- c. the ship is then subjected to a gust wind pressure which results in a gust wind heeling lever ( $lw_2$ ); and under these circumstances, area b shall be equal to or greater than area a, as indicated in Figure 1:

The heeling lever shall be calculated using formula:

$$lw_1 = \frac{P \cdot A \cdot Z}{1000 \cdot g \cdot \Delta} \tag{1}$$

$$l_{w2} = 1.5 l_{w1} \quad (2)$$

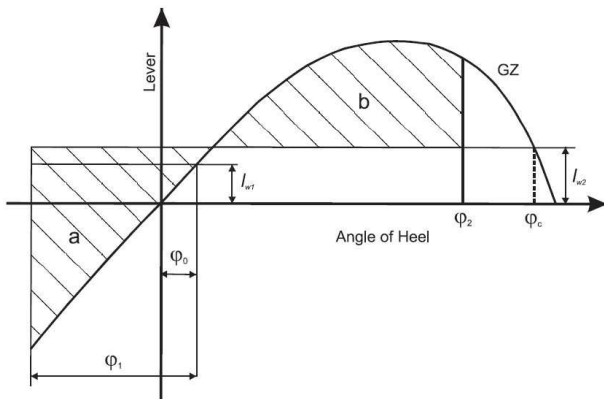


Figure 1 Severe wind and rolling

where  $l_{w1}$  = steady wind heeling angle,  $l_{w2}$  = gust wind heeling lever,  $P$  = wind pressure of 504 Pa,  $A$  = projected lateral area ( $m^2$ ),  $Z$  = vertical distance from the centre of  $A$  to the centre of the underwater lateral area or approximately to a point at one half of the mean draught (m),  $\Delta$  = displacement (t) and  $g$  = gravitational acceleration of  $9.81 \text{ m/s}^2$ .

Part 3.1 of the IS Code 2008 only concerns passenger ships. Passenger ships have to also pass the criteria of Part 2.2 and 2.3. The heeling angle on account of turning should not exceed  $10^\circ$ , when calculated using the following formula:

$$M_R = 0.200 * \frac{v_0^2}{L_{WL}} * \Delta * (KG - \frac{d}{2}) \quad (2)$$

where:  $M_R$  = heeling moment (kNm),  $v_0$  = service speed (m/s),  $L_{WL}$  = length of ship at waterline (m),  $\Delta$  = displacement (tons),  $d$  = mean draught (m),  $KG$  = height of centre of gravity above baseline (m).

The centrifugal force  $F_c$  is equal to  $\Delta V_0^2/2R$  where  $R$  is the radius of gyration. The smaller  $R$ , the higher  $F_c$ . But the formula proposed in the code is  $R = 5L_{wl}$  which is the maximum value  $R$  can take according to manoeuvring code (Veritas, 2011). The formula is therefore not conservative.

### 3. DEVELOPMENT OF A SECOND GENERATION IS CODE

The Sub-Committee on Stability and Load Lines and on Fishing Vessels Safety 48th Session IMO (2005) emphasized the requirement of revising the current IS Code. The importance of the work on the comprehensive review of the current IS Code 2008 would significantly affect the design and ultimately enhance the safety of ships (Mata-Álvarez-Santullano & Souto-Iglesias, 2014).

Intact Stability is a crucial criterion that concerns most of naval architects in the design stage. The current Intact Stability (IS) Code 2008 is in force. Except for the weather criterion the IS Code 2008 only concerns the hydrostatics of the ship. It does not cover the seakeeping behaviour of the ship and first and foremost, it always considers a ship with negligible trim angle. In head seas, the ship can take some significant angle of trim which may affect the righting arm. Van Santen, 2009 also presents an example of a vessel capsizing because of the small angle of trim. For the enhancement and improvement of intact stability criteria, the International Maritime Organisation (IMO) introduced the new generation intact stability criteria in 2008 (Francescutto, 2007).

Figure 2 presents the procedure to apply to the second generation intact stability rule. Once the basic criteria described in Section 2 have been satisfied, each failure mode is verified to satisfaction at the most conservative level.

The development of the second generation intact stability criteria focuses on five dynamical stability failure modes. Performing such a complete calculation of time-depending dynamical phenomena would require well-trained engineers as well as advanced tools (IMO, 2013a). The aim of level 1 is to devise a simple computational method, but the criteria are very conservative. Level 2 criteria are more realistic since wave shape is taken into



account but the computation remains static. Level 3 involves seakeeping simulations.

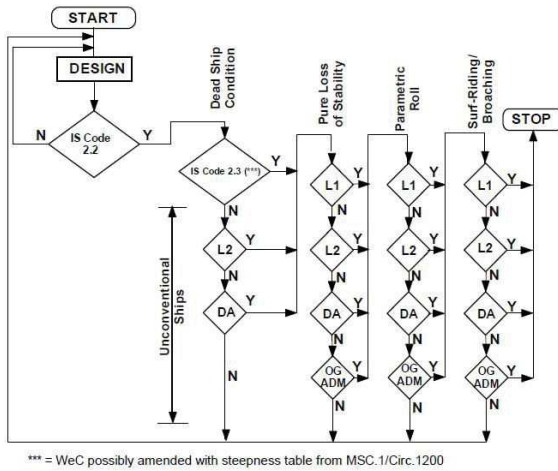


Figure 2 Structure of Second Generation Intact Stability Criteria IMO (2008)

The formula used in this paper is based on SDC1/INF.8 (IMO, 2013b). 1. Parametric rolling stability failure criteria mode as stated in SDC/1 INF.8 Annex 1 (submitted by correspondence group). 2. Pure loss of stability failure mode as stated in SDC/1 INF.8 Annex 2 (submitted by correspondence group). 3. Dead ship stability failure mode as stated in SDC/1 INF.8 Annex 16 (submitted by Italy and Japan). 4. Broaching stability failure mode as stated in SDC/1 INF.8 Annex 15 (submitted by United States and Japan).

### 3.1 Dead Ship Condition for Level 1

Based on SDC/1 INF.8 Annex 16, for level 1 vulnerability criteria for the dead ship stability failure mode, a ship is considered not to be vulnerable to the dead ship stability failure mode if:

$$b \geq a \tag{3}$$

where a and b should be calculated according to the "Severe wind and rolling criterion (weather criterion)" in Part A – 2.3 of the Code12, and substituting the steepness factor s in Table 2.3.4-4 in Part A – 2.3, by the steepness factor s specified in Table 4.5.1 in MSC.1/Circ.1200.

### 3.2 Pure Loss of Stability for Level 1

Based on SDC/1 INF.8 Annex 2, for level 1 vulnerability criteria for the pure loss of stability failure mode, a ship is considered not to be vulnerable to the pure loss of stability failure mode if:

$$GM_{min} > R_{PLA} \tag{4}$$

where  $R_{PLA} = [\min(1,83 d (Fn)^2, 0.05)]m$  and  $GM_{min}$  = the minimum value of the metacentric height [on level trim and without taking free surface effects into consideration] as a longitudinal wave passes the ship calculated as provided in 2.10.2.2 (ref SDC/1 INF.8 Annex 2 ),or

$$GM_{min} = KB + I_L/V - KG \tag{5}$$

$$\text{only if } [(V_D - V)/A_w (D-d)] \geq 1.0 \tag{6}$$

d = draft corresponding to the loading condition under consideration;  $I_L$  = moment of inertia of the waterplane at the draft  $d_L$ ;

$$d_L = d - \delta d_L \tag{7}$$

KB = height of the vertical centre of buoyancy corresponding to the loading condition under consideration; KG = height of the vertical centre of gravity corresponding to the loading condition under consideration; V = volume of displacement corresponding to the loading condition under consideration;

$$[\delta d_L = \min(d - 0.25d_{full}, (L.S_w/2) )] \tag{8}$$

$S_w = 0.0334$ , D = Depth,  $V_D =$  volume of displacement at waterline equal to D,  $A_w =$  waterplane area of the draft equal to d.

### 3.3 Parametric Rolling for Level 1

Based on SDC/1 INF.8 Annex 1 for level 1 vulnerability criteria for the parametric rolling failure mode, a ship is considered not to be vulnerable to the parametric roll failure mode if:

$$\Delta GM/ GM > R_{PR} \tag{9}$$

$$\Delta GM = (I_H - I_L)/2V \tag{10}$$

where  $\Delta GM$  = amplitude of the variation of the metacentric height when a longitudinal wave passes the ship,  $GM$  = metacentric height,  $R_{PR} = 0.5$ ,  $I_H$  = moment inertia of the waterplane at the draft  $d_H$ ,  $I_L$  = moment inertia of the waterplane at the draft  $d_L$ , and  $V$  = volume of displacement corresponding to the loading condition under consideration.

### 3.4 Surf-riding/Broaching for Level 1

Based on SDC/1 INF.8 Annex 15 for level 1 vulnerability criterion for the surf-riding (Spyrou, Themelis, & Kontolefas, 2013)/broaching stability failure mode, a ship is considered not to be vulnerable to the broaching stability failure mode if:

$$F_n < 0.3 \text{ or } L_{BP} > 200\text{m} \tag{11}$$

where  $F_n = V_{max} / (L_{BP} \cdot g)^{0.5}$ ,  $V_{max}$  = maximum service speed in calm water (m/s),  $L_{BP}$  = the length between perpendicular (m), and  $g$  = gravitational acceleration (m/s).

## 4. PROPOSAL FOR EXPERIMENTAL WORK ON WEATHER CRITERIA

The highest level criterion for the second generation intact stability code is the direct stability assessment using a time-domain numerical simulation. The tools should be validated by experimental results. The guideline of direct stability assessment was produced at the initiative of the United States and Japan as in SDC1/INF.8 in Annex 27(IMO, 2013b).

Recent experiments carried out by Umeda and his research members (Umeda et al., 2014) presented during the ISSW 2014 provide examples of comparisons between model experiments and numerical simulations for stability under dead ship condition and for pure

loss of stability in astern waves. The experiment using a model 1/70 CEHIPAR2792 vessel was conducted in a seakeeping and manoeuvring basin. A wind blower consisting of axial flow fans and controlled by inverters with a v/f control law was used to provide the wind input. The experimental setup is shown in Figure 3 and 4. They concluded that for the dead ship condition, an adequate selection of representative wind velocities generated by wind fans is crucial and for the pure loss of stability, an accurate Fourier transform and the reverse transformation of incident irregular waves are important.

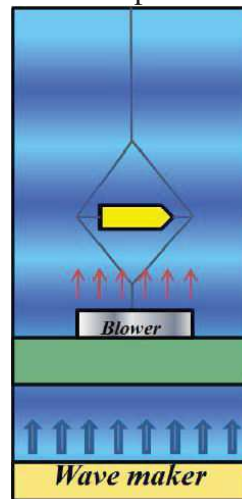


Figure 3 Overview of experimental setup (Umeda et al., 2014).

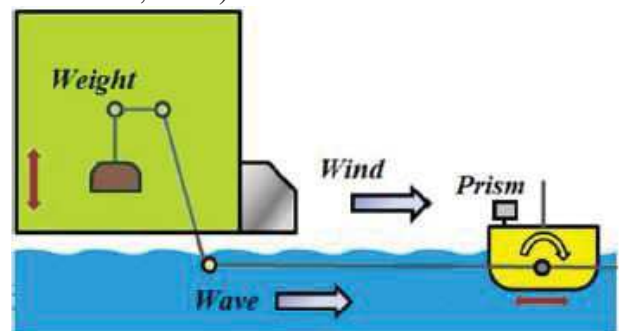


Figure 4 Lateral view of experimental setup (Umeda et al., 2014).

An experimental study will be carried out at the Low-Speed Wind Tunnel of the Aeronautics Laboratory at the Universiti Teknologi Malaysia in 2016. The aim of the study is to validate the weather criterion in the IS Code 2008 using the wind tunnel results. For the dead ship condition, the study will consist of two layered vulnerability criteria and

a direct assessment of each failure mode and a ship is requested to comply with at least one of them. This is because the use of expensive numerical simulations for a direct assessment should be minimised in order to realise a feasible application of the new scheme. It is also essential that the numerical simulations used for the direct assessment should be validated by physical model experiments (Kubo, Umeda, Izawa, & Matsuda, 2012).

**4.1 Wind Tunnel Specifications**

This wind tunnel has a test section of 2 m (width) x 1.5 m (height) x 5.8 m (length). The maximum test velocity is 80m/s (160 knots or 288 km/h). The wind tunnel has a flow uniformity of less than 0.15%, a temperature uniformity of less than 0.2°C, a flow angularity uniformity of less than 0.15° and a turbulence level of less than 0.06% (Mansor, 2008).

The wind tunnel is equipped with a six component balance for load measurements. The balance is a pyramid type with the virtual balance moment at the centre of the test section. The balance has the capacity to measure the aerodynamic forces and moments in 3-D. The aerodynamic loads can be tested as a function of the various wind directions by rotating the model using the turntable. The accuracy of the balance is within 0.04% based on 1 standard deviation. The maximum load range is ±1200N for axial and side loads. It also has the capacity to measure surface pressure using electronic pressure scanners. The balance load range for the wind tunnel is presented in Table 1.

**5. STABILITY EVALUATION**

A naval ship is used for the stability calculation. The ship is a patrol vessel (Ariffin, 2014) with a cruising speed of 12 knots, and a maximum speed of 22 knots. Its overall length is 91.1 metres, the design draft is 3.4 metres and the maximum draft is 3.6 metres for a displacement of 1800 tons. Finally the vessel’s block coefficient,  $C_b$ , is 0.448 and the prismatic coefficient,  $C_p$ , is 0.695.

The body plan of the ship is shown in Figure 4.

Load Component and Accuracy	Type of balance		
	External	Semi-span	Internal
Axial force, $F_x$ (N)	± 1200	± 900	± 182
Side force, $F_y$ (N)	± 1200	± 900	± 356
Normal force, $F_z$ (N)	± 1200	± 4500	± 445
Roll moment, $M_x$ (Nm)	± 450	± 1362	± 7
Pitch moment, $M_y$ (Nm)	± 450	± 250	± 62
Yaw moment, $M_z$ (Nm)	± 450	± 450	± 50
Primary accuracy, % (based on ± 1 standard deviation)	0.04	0.04	<0.10

Table 1 Balance load range (Noor & Mansor, 2013)

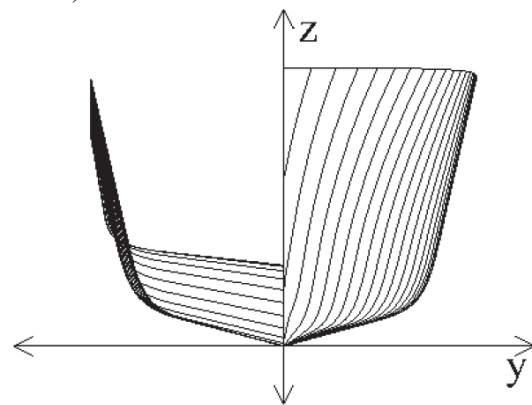


Figure 4 Body plan of the vessel

The level calculations in the present paper are based on a formula in SDC 1/INF.8. Only criteria for level 1 were verified. The results were obtained using the GHS software for the level 1 verification of pure loss of stability and parametric rolling. The VCG for the vessel was varied from 3.0 to 7.0 meters for analysis purposes. Direct calculation was used for the dead ship condition and the surf-riding/broaching.

**5.1 Dead Ship Condition for Level 1**

Based on SDC/1 INF.8 Annex 16, proposed by Italy and Japan, the steepness factor,  $s$  in Part A – 2.3 Table 2.3.4-4 was changed to the steepness factor  $s$  in Table 4.5.1 in MSC.1/Circ.1200. In GHS, the steepness factor is defined by  $s = 0.0992364 + 0.0058416T - 0.0011127T^2 + 0.0000331T^3$  with  $0.035 \leq s \leq 0.1$ . Table 4.5.1 in MSC.1/Circ.1200 is the extension of Table 2.3.4.4. The graft of steepness factor,  $s$  vs roll period,  $T$  in Table 4.5.1 can be computed with the 5<sup>th</sup> order polynomial  $s = 0.016 + 0.0385T - 0.0058T^2 + 0.0003T^3 - 0.000009T^4 + 0.00000009T^5$  with  $0.02 \leq s \leq 0.1$ .

The vessel passed the level 1 dead ship condition using the proposed amended criteria.

**5.2 Pure Loss of Stability for Level 1**

As in SDC/1 INF.8 Annex 2, the  $GM_{min}$  is calculated based on a range of VCG from 3 to 7m. The result shows that the change of VCG will affect the  $GM_{min}$  significantly. With the increment of VCG, the max VCG to pass the IS Code 2008 is 5.46 m and the max. VCG to pass the level 1 pure loss of stability is 6.6 m. The result is shown in Figure 5.

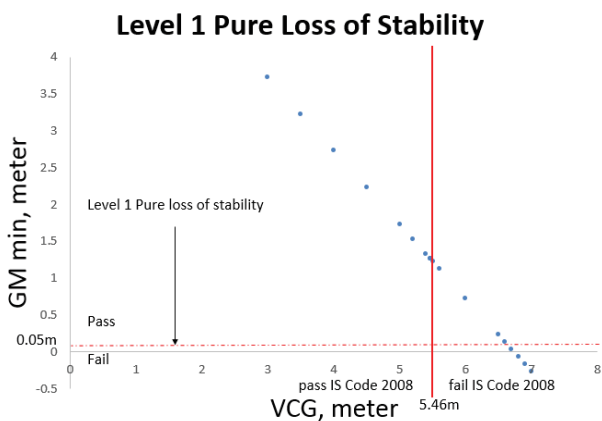


Figure 5 Result of Level 1 Pure loss of stability

It appears that the level 1 pure loss of stability criterion is less restrictive than the existing IS Code 2008 for conventional ships.

**5.3 Parametric Rolling for Level 1**

The  $\Delta GM/GM$  is calculated based on a range of VCG from 3 to 7 m in SDC/1 INF.8 Annex 1. The result shows that the change of VCG affects the  $\Delta GM/GM$  significantly. With the increment of VCG, the max. VCG to pass the IS Code 2008 is 5.46 m and the max. VCG to pass the level 1 pure loss of stability is 5.56 m. The results are shown in Figure 6.

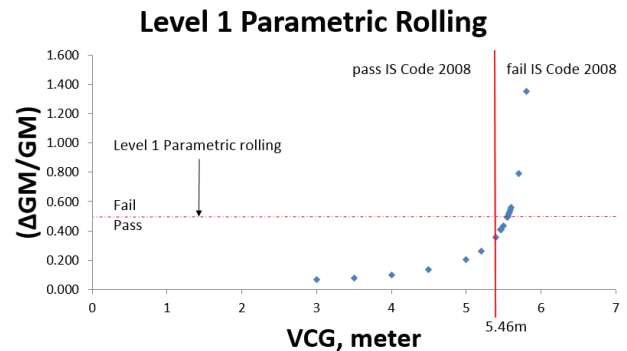


Figure 6 Result of Level 1 Parametric rolling

In this case, the level 1 parametric rolling criterion is less restrictive than the IS Code 2008.

**5.4 Surf-riding/Broaching for Level 1**

In SDC/1 INF.8 Annex 12, proposed by United States and Japan, the criterion is based on ship dimension and maximum speed. The vessel is tested with various speeds. The results show that the maximum speed (22 knots) is vulnerable to broaching and the cruising speed (12 knots) is not vulnerable to broaching. The results are shown in Figure 7. The maximum speed at which the ship is not vulnerable to broaching is 17.4 knots.



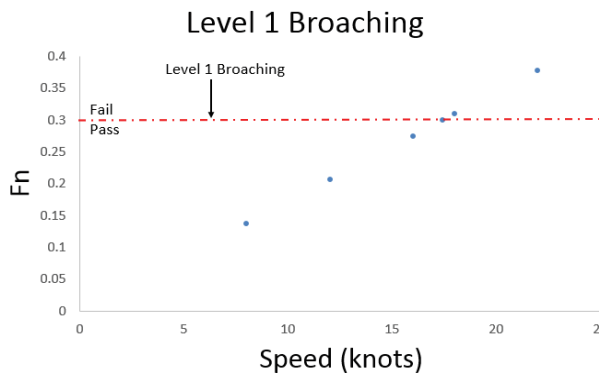


Figure 7 Result of Level 1 Broaching

## 6. DISCUSSION

The patrol boat whose body plan is presented in Figure 4, passes the level 1 criteria for the dead ship condition, the pure loss of stability and the parametric rolling. But it failed to meet the criteria for broaching at maximum speed.

The GHS© code can currently handle the level 1 verification for pure loss of stability, and parametric rolling. The level 1 verification for broaching does not require GHS© output. The level 1 verification for dead ship condition requires a change of the wave steepness value,  $s$  whereas the current code has a range of  $0.035 \leq s \leq 0.1$  but the proposed change for level 1 broaching required a range of  $0.02 \leq s \leq 0.1$ .

## 7. CONCLUSIONS

This paper presents the results for a naval ship for a level 1 verification based on a proposed change of second generation intact stability criteria as outlined in the current state of development by the International Maritime Organisation (IMO).

The vessel which already complied with the existing IS Code 2008, easily passes the level 1 criteria for pure loss of stability and parametric rolling but does not meet the broaching criterion at maximum speed.

The dead ship condition is based on weather criteria and there is no proposed change to the current regulations except for the

wave steepness value. The wind tunnel experimental facility will be used to investigate the possibility of proposing some new or amended rules for the weather criterion.

## 8. ACKNOWLEDGEMENT

The authors would like to acknowledge the support of the Government of Malaysia, the Government of the French Republic and the Direction des Constructions Navales (DCNS).

## 9. REFERENCES

- Ariffin, A. (2014). *Air Flow and Superstructure Interaction on a Model of a Naval Ship*. Master Thesis, Universiti Teknologi Malaysia.
- Bassler, C. C., Belenky, V., Bulian, G., Spyrou, K. J., & Umeda, N. (2009). A Review of Available Methods for Application to Second Level Vulnerability Criteria. In *International Conference on Stability of Ships and Ocean Vehicles* (pp. 111–128).
- Francescutto, A. (2007). The Intact Ship Stability Code: Present Status and Future. In *Proceedings of the 2nd International Conference on Marine Research and Transportation, Naples, Italy, Session A* (pp. 199–208).
- IMO. (2005). *SLF 48/21 Report to the Maritime Safety Committee*.
- IMO. (2009). *International Code of Intact Stability 2008*, London.
- IMO. (2013a). *SDC 1/5/1 - Development of second generation intact stability criteria. Remarks on the development of the second generation intact stability criteria submitted by Germany*.
- IMO. (2013b). *SDC 1/INF.8 - Development of Second Generation Intact Stability Criteria*.

- Ishida, S., Taguchi, H., & Sawada, H. (2006). Evaluation of the Weather Criterion by Experiments and its Effect to the Design of a RoPax Ferry. *International Conference on Stability of Ships and Ocean Vehicles*, 9–16.
- Kubo, T., Umeda, N., Izawa, S., & Matsuda, A. (2012). Total Stability Failure Probability of a Ship in Irregular Beam Wind and Waves: Model Experiment and Numerical Simulation. In *11th International Conference on Stability of Ships and Ocean Vehicles*.
- Laurens, J.-M., & François, G. (2013). *Stabilité Du Navire: Théorie, Réglementation, Méthodes De Calcul (Cours Et Exercices Corrigés)*. Ellipses, Paris.
- Mansor, S. (2008). *Low Speed Wind Tunnel Univeristi Teknologi Malaysia*.
- Mata-Álvarez-Santullano, F., & Souto-Iglesias, A. (2014). Stability, safety and operability of small fishing vessels. *Ocean Engineering*, 79, 81–91.  
doi:10.1016/j.oceaneng.2014.01.011
- Noor, A. M., & Mansor, S. (2013). Measuring Aerodynamic Characteristics Using High Performance Low Speed Wind Tunnel at Universiti Teknologi Malaysia. *Journal of Applied Mechanical Engineering*, 03(01), 1–7. doi:10.4172/2168-9873.1000132
- Peters, W. M., Belenky, V. M., Bassler, C. M., Spyrou, K. M., Umeda, N. M., Bulian, G. V., & Altmayer, B. V. (2012). The Second Generation Intact Stability Criteria : An Overview of Development. *Transactions - The Society of Naval Architects and Marine Engineers*, 119(225-264).
- Spyrou, K. J., Themelis, N., & Kontolefas, I. (2013). What is Surf-Riding in Irregular Seas? In *International Conference on Marine Safety and Environment*.
- Tsuchiya, T. (1975). An Approach for Treating the Stability of Fishing Boats. In *International Conference on Stability of Ships and Ocean Vehicles*.
- Umeda, N. (2013). Current Status of Second Generation Intact Stability Criteria Development and Some Recent Efforts. In *International Ship Stability Workshop*.
- Umeda, N., Daichi Kawaida, Ito, Y., Tsutsumi, Y., Matsuda, A., & Daisuke Terada. (2014). Remarks on Experimental Validation Procedures for Numerical Intact Stability Assessment with Latest Examples. In *International Ship Stability Workshop* (pp. 77–84).
- Van Santen, J. (2009). The Use of Energy Build Up to Identify the Most Critical Heeling Axis Direction for Stability Calculation for Floaring Offshore Structures. In *10th International Conference on Stability of Ship and Ocean Vehicles* (pp. 65–76).
- Veritas, B. (2011). *Rules for the Classification of Steel Ship*.
- Wandji, C., & Corrigan, P. (2012). Test Application of Second Generation IMO Intact Stability Criteria on a Large Sample Ships. In *International Conference on Stability of Ships and Ocean Vehicles* (pp. 129–139).
- Welaya, Y., & Kuo, C. (1981). A Review of Intact Ship Stability Research and Criteria. *Ocean Engineering*, 8, 65–84.

## REAL-TIME EVALUATION OF SECOND GENERATION INTACT STABILITY

### CRITERIA

A Ariffin, and J.M. Laurens, LBMS, École Nationale Supérieure de Techniques Avancées (ENSTA) Bretagne, France  
S. Mansor, Faculty of Mechanical Engineering, Universiti Teknologi Malaysia, Malaysia

### SUMMARY

The performance of a vessel cannot solely be determined as a function of its size, speed and autonomy. The seakeeping behaviour of the vessel in extreme weather conditions is very difficult to predict and the IMO is in the process of introducing new intact stability regulations to deal with failure modes generally associated with extreme weather conditions such as parametric rolling, broaching or pure loss of stability in astern waves. Traditionally, the on-board crew only operates the vessel from one location to another whilst any other repairs, maintenance or decisions will be carried out by a support crew onshore. The rapid increase of computer power and communication technology allows the on-board crew to perform an advanced computation based on the real-time behaviour of the sailing vessel. At the International Maritime Organisation (IMO), the development of second generation intact stability criteria is thoroughly discussed before being implemented and enforced in the maritime industry. The lower level (level 1) criteria are conservative but can be easily implemented in stability codes. In this particular study it is examined how an existing and extensively used commercial computer code, in the present case GHS<sup>©</sup>, can handle level 1 criteria. The possibility of interfacing with and integrating into on-board systems for the evaluation of second generation intact stability criteria based on real-time data collected from on-board systems is explored. The proposal is to interface the stability code with the existing Integrated Platform Management System (IPMS) and Weather Meteorological System (WMS). This paper describes the procedure and presents an illustrative example.

### NOMENCLATURE

A	Projected lateral area (m <sup>2</sup> )
B	Beaufort Number
d	Mean draught (m)
g	Gravitational acceleration (ms <sup>-2</sup> )
GM	Metacentric height (m)
GZ	Righting arm (m)
H <sub>i</sub>	Wave height (m)
KG	Height of centre of gravity above baseline (m).
L <sub>WL</sub>	Length of ship at waterline (m)
l <sub>w1</sub>	Steady wind heeling lever (m)
l <sub>w2</sub>	Gust wind heeling lever (m)
M <sub>R</sub>	Heeling moment (kNm)
n <sub>cr</sub>	Critical propulsion revolution (rpm)
P	Pressure (504 Nm <sup>-2</sup> )
u <sub>cr</sub>	Critical ship speed (m/s)
Z	Vertical distance between A to half draft (m)
Δ	Displacement (tonne)
λ <sub>i</sub>	Wave length (m)
v <sub>0</sub>	Service speed (m/s)

### 1. INTRODUCTION

The performance of a vessel cannot be solely determined as a function of its size, speed and autonomy. The seakeeping behaviour of the vessel in extreme weather conditions is very difficult to predict and the IMO is in the process of introducing new intact stability regulations to deal with failure modes generally associated with extreme weather conditions such as parametric rolling, broaching or pure loss of stability in astern waves. The matter of safety-by-design, both in intact and damaged

condition, has been the main agenda, especially the rule-making process. Nevertheless, it is impossible to ensure safety by design measures only. Design rules implicitly assume a certain level of knowledge, skills, experience and prudence of ship masters and crew. These human factors, which are commonly referred to as “good/prudent seamanship”, therefore represent a crucial aspect in determining the level of ship safety. The skills of existing engineers/navigationers are however challenged by the rapid development of unconventional ships and shipping solutions. In some dangerous, or potentially dangerous, operational situations, it can therefore be a great challenge for ship officers to take the most appropriate decisions to reduce the risk level. Such situations can be effectively addressed by operational measures aimed at providing a decision support for the crew [1].

Intact stability is a basic requirement to minimise the risk of the capsizing of vessels. It is a guideline for the ship designer, ship operator and classification society to design, build and commission the ship before it starts its service life at sea. A comprehensive background study of intact stability development was written by Kuo & Welaya [2]. Their paper "A review of intact stability research and criteria", stated that the first righting arm curve was proposed by Reed in 1868, but the application was presented by Denny in 1887. In addition, in 1935, Pierrrottet tried to rationally establish the forces which tend to capsize a ship and proposed a limiting angle at which the dynamic level of the ship must be equal to or greater than the sum of the inclining moments. However,

Pierrottet's proposal was too restrictive in the design process and it was not accepted.

Rohala's thesis evoked widespread interest throughout the world at that time because it was the first comprehensive study and proposed method to evaluate intact stability which did not require complex calculations [3].

At the First International Conference for ship stability which was held at the University of Strathclyde in 1975, Tsuchiya presented a new method for treating the stability of fishing vessels [4]. He introduced a list of coefficients to define the weather stability criteria. He disregarded the idea of a stability assessment using simple geometrical stability standards such as metacentric height and freeboard, or the shape of the righting arm curve. He proposed a number of factors which, in his opinion, are crucial. He introduced a certain coefficient which should be calculated and plotted on a diagram as a function of the metacentric height and freeboard for every stability assessment. He concluded that his proposed method should be confirmed by a comparison with actual data on fishing boat activities and empirical stability standards.

The first generation intact stability criteria were originally codified at IMO in 1993 as a set of recommendations in Res A.749(18) by taking into account the former Res.A.167 (ES.IV) ("Recommendation on intact stability of passenger and cargo ships under 100 meters in length" which contained statistical criteria, heeling due to passenger crowding, and heeling due to high speed turning, 1968) and Res A.562.(14) ("Recommendation on a severe wind and rolling criterion (Weather Criterion) for the intact stability of passenger and cargo ships of 24 meters in length and over," 1985). These criteria were codified in the 2008 IS Code and became effective as part of both SOLAS and the International Load Line Convention in 2010 in IMO Res MSC.269(85) and MSC.207(85) [5].

The actual work to review the IS Code 2008 was highlighted during the 48th session of the SLF in Sept. 2005 [6]. The work group decided to address three modes of stability failure:

- a. Restoring arm variation.
- b. Stability under dead ship condition.
- c. Manoeuvring-related problems in waves.

There are two main conferences that address the development of second generation intact stability criteria. These are the International Conference on Stability of Ship Ocean Vehicles (STAB) and the International Ship Stability Workshop (ISSW). An experimental evaluation of weather criteria was carried out at the National Maritime Research Institute, in Japan. They conducted a wind tunnel test with wind speeds varying from 5m/s to 15 m/s. The results showed some differences compared to the current estimation. For example the wind heeling

moment depended on the heel angle and the centre of drift force was higher than half draft [7]. The experimental validation procedures for numerical intact stability assessment with the latest examples were presented by Umeda and his research members in 2014 [8]. They equipped the seakeeping and manoeuvring basin of the National Research Institute of Fisheries Engineering in Japan with a wind blower to examine dead ship stability assessment.

A review of available methods for application to second level vulnerability criteria was presented at STAB 2009 [9]. They concluded that the choice of environmental conditions for vulnerability criteria is at least as important as the criteria themselves. A test application of second generation IMO intact stability criteria on a large sample of ships was presented during STAB 2012. Additional work remains to be carried out to determine a possible standard for the criteria and environment conditions before finalising the second generation intact stability criteria [10].

During the ISSW 2013, Umeda presented the current status of the development of second generation intact stability criteria and some recent efforts [11]. The discussion covered the five failure modes: pure loss of stability, parametric rolling, broaching, harmonic resonance under dead ship condition and excessive acceleration.

Nowadays, several research studies are performed to identify the actual wave height and wave length involving data collection and radar utilisation. A real time measurement of the directional ocean spectra was developed by the wave and surface current monitoring system (WaMoS II). The advantage of this system is the continuous availability to record wave data in rough sea, under harsh weather condition with limited visibility and at night. The system uses the unfiltered output from a marine X-Band radar to determine wave and surface current parameters in near real-time. The measurements are based on the backscatter of radar energy from the ocean surface (sea clutter). The backscatter, which is visible on the marine radar, shows the wave patterns. WaMoS II measures and displays all the essential wave field parameters such as significant wave height ( $H_s$ ), peak wave period ( $T_p$ ) and peak wave direction ( $\theta_p$ ), as well as surface current speed ( $U$ ) and current direction ( $\theta_u$ ). It operates automatically and unattended from moored platforms, moving vessels and coastal sites.

A Joint Industry Project named "On board Wave and Motion Estimator (OWME), developed a system capable of predicting vessel motion on board in real time up to two minutes in advance. The wave profiles are derived by means of nautical radar, using the Wave Monitoring System WaMoS II. The OWME modules for wave propagation and vessel motion prediction were successfully verified against scale model tests both in long crested and short crested waves in MARIN's



Seakeeping and Manoeuvring Test [12]. Figure 1 shows the design and data flow of the OWME system and set-up used for its validation.

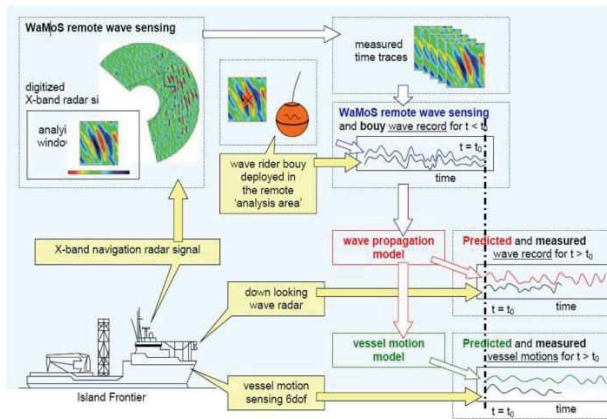


Figure 1: OWME system overview [12]

WaMoS II was also used in the experiment in DELFT, the Netherlands [13]. A comparison of WaMoS II data with buoy data to show the capabilities of nautical microwave radars for sea state measurements was published by Borge et al [14]. Another method of measuring the wave height using X-band radar was conducted in China. According to the X-band radar-image sequences collected from the East Sea in China, the wave heights are retrieved based on a mathematical model. The retrieved wave heights are validated by comparing the radar-derived significant wave heights with the significant wave heights acquired from in-situ buoy sensors [15].

Neural network is an algorithm that imitates the mechanism of neurons in the brain. It can learn a function given by input-output pairs and return approximate outputs for inputs that were not given. Such algorithms are already used in naval architecture for approximation, control and classification. Experimental data were obtained in monochromatic head seas with a hull of a modern container vessel and a nonlinear numerical model using six degrees of freedom with terms defined up to third degree derivatives. This numerical model was shown to provide a good prediction of parametric rolling [16].

The metacentric height (GM) is a measurement of the initial static stability and is used to determine the requirement in most of the rules and regulations. Nowadays, there is a method and system available to compute the actual GM on a sailing ship. It could be used to assess the ship's ability to resist damage, identify the critical situation, and develop all circumstances related to stability [17].

## 2. BACKGROUND OF IS CODE 2008

The Intact Stability Code 2008 is the document in force. The code is based on the best "state-of-the-art" concept

[18]. It was developed based on the contribution of design and engineering principles and experience gained from operating ships. In conjunction with the rapid development of modern naval architecture technology, the IS Code will not remain unchanged. It must be re-evaluated and revised as necessary with the contribution of the IMO Committees all around the globe.

The IS Code 2008 is divided into 2 parts. Part A consists of the mandatory criteria and Part B contains the recommendation for certain types of ships and additional guidelines. As stated in Part A, the IS Code applies to marine vehicles of 24 metres in length and more. Paragraph 2.2 of Part A lists the criteria regarding the righting arm curve properties and Paragraph 2.3 describes the severe wind and rolling criteria (weather criterion).

The IS Code 2008 Part A 2.2 sets four requirements for righting arm (GZ) curve properties [19]:

- a. Area under the righting lever curve,
  - i. not less than 0.055 meter-radian up to a 30° heel angle.
  - ii. not less than 0.09 meter-radians up to a 40° heel angle, or downflooding angle.
  - iii. not less than 0.03 meter-radians from a 30° to 40° heel angle or between 30° to the downflooding angle.
- b. The righting lever GZ shall be at least 0.2m for a heel angle greater than 30°.
- c. The maximum righting lever shall occur at a heel angle not less than 25°.
- d. The initial GM shall not be less than 0.15 meters.

The additional requirement for passenger ships is stated in Part A, Paragraph 3.1. It states that:

- a. The angle of heel due to passenger crowding shall not be more than 10°.
- b. A minimum weight of 75kg for each passenger and the distribution of luggage shall be approved by the Administration.
- c. The centre of gravity for a passenger standing upright is 1 m and for a seated passenger 0.3 m above the seat.

The IS Code 2008 Part A 2.3 concerns the weather criterion. The ship must be able to withstand the combined effects of beam wind and rolling at the same time. The conditions are:

- a. the ship is subjected to a steady wind pressure acting perpendicular to the ship's centreline which results in a steady wind heeling lever ( $l_{w1}$ ).
- b. from the resultant angle of equilibrium ( $\phi_0$ ), the ship is assumed to present an angle of roll ( $\phi_1$ ) to windward due to wave action. The angle of heel under action of steady wind ( $\phi_0$ ) should not exceed

16° or 80% of the angle of deck edge immersion, whichever is less.

c. the ship is then subjected to a gust wind pressure which results in a gust wind heeling lever ( $I_{w2}$ ); and under these circumstances, area b shall be equal to or greater than area a, as indicated in Figure 2:

The heeling lever shall be calculated using formula:

$$I_{w1} = (P \cdot A \cdot Z) / (1000 \cdot g \cdot \Delta) \quad (1)$$

$$I_{w2} = 1.5 I_{w1} \quad (2)$$

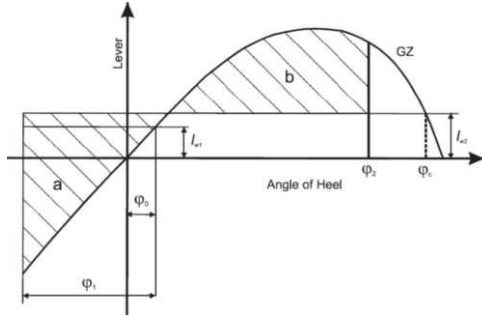


Figure 2: Severe wind and rolling

Part 3.1 of the IS Code 2008 only concerns passenger ships. Passenger ships also have to pass the criteria of Part 2.2 and 2.3. The heeling angle on account of turning should not exceed 10°, when calculated using the following formula:

$$M_R = 0.200 \cdot v_0^2 / L_{WL} \cdot \Delta \cdot (KG - d/2) \quad (3)$$

The centrifugal force  $F_c$  is equal to  $\Delta V_0^2 / R$  where  $R$  is the radius of gyration. The smaller  $R$ , the higher  $F_c$ . But the formula proposed in the code is  $R = 5L_{wl}$  which is the maximum value  $R$  can take according to manoeuvring code [20]. The formula is therefore not conservative.

### 3. DEVELOPMENT OF A SECOND GENERATION IS CODE

The Sub-Committee on Stability and Load Lines and on Fishing Vessels Safety 48th Session IMO (2005) emphasized the requirement of revising the current IS Code. The importance of the work on the comprehensive review of the current IS Code 2008 would significantly affect the design and ultimately enhance the safety of ships [21].

Intact Stability is a crucial criterion that concerns most of naval architects in the design stage. The current Intact Stability (IS) Code 2008 is in force. Except for the weather criterion, the IS Code 2008 only applies to the hydrostatics of the ship. It does not cover the seakeeping behaviour of the ship and first and foremost, it always considers a ship with a negligible trim angle. In head seas, the ship can present a significant angle of trim which may affect the righting arm. Van Santen also presents an example of a vessel capsizing because of the small angle of trim [22]. For the enhancement and improvement of intact stability criteria, the International

Maritime Organisation (IMO) introduced the new generation intact stability criteria in 2008 [23].

Figure 3 presents the procedure to apply to the second generation intact stability rule. Once the basic criteria described in Section 2 have been satisfied, each failure mode is verified to satisfaction at the most conservative level.

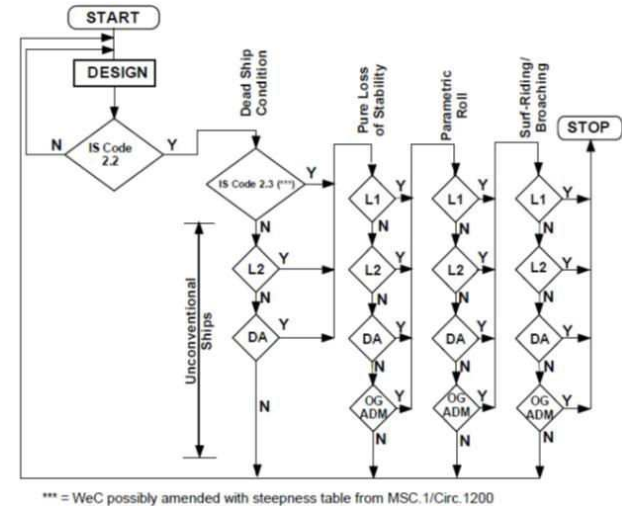


Figure 3: Structure of Second Generation Intact Stability Criteria IMO (2008)

The development of the second generation intact stability criteria focuses on five dynamical stability failure modes. Performing such a complete calculation of time-dependent dynamical phenomena would require well-trained engineers as well as advanced tools [24]. The aim of level 1 is to devise a simple computational method, but the criteria are very conservative. Level 2 criteria are more realistic since wave shape is taken into account but the computation remains static. Level 3 involves seakeeping simulations. The formula used in this paper is based on SDC2/INF.1 [25].

#### 3.1 Dead Ship Condition

If a ship loses her propulsive power, the ship could suffer beam wind and waves as the worst-case harmonic resonance for a longer duration. Or the ship master would select this situation to avoid pure loss of stability, parametric rolling or broaching with possible operational guidance. Thus the ship designer has to at least guarantee the stability safety of ships under dead ship condition [11].

#### 3.2 Pure Loss of Stability

The roll restoring moment of a ship in longitudinal waves can be reduced when a wave crest is situated in the ship centre and the wave length is comparable to the ship's length. In case of astern waves, the ship can start to roll as a result of the restoring reduction with low wave encounter and natural roll frequencies and then the roll induces additional hydrodynamics roll moments due to the unsymmetrical underwater hull shape. The above mechanism is known as "pure loss of stability" [11].

### 3.3 Parametric Rolling

Parametric rolling is an unstable phenomenon, which can quickly generate large roll angles that are coupled with significant pitch motions. The rolling occurs in phase with pitch, and on containerships introduces high load into the containers and affects her stability performance.

### 3.4 Broaching

Broaching is a phenomenon that a ship cannot keep a constant course even with the maximum steering effort. It often occurs when a ship is surf-riding in following waves and the centrifugal force due to accelerated ship forward velocity and large yaw angular velocity could result in capsizing [11].

## 4. CODE VALIDATION

In this paper, a comparison of two different hydrostatic codes was conducted using GHS [26] and Calcoque [27]. A model of a 120 meter long containership was evaluated. The lines plan is presented in Figure 4. The lines plan is available in an open source database on the DELFTship website.

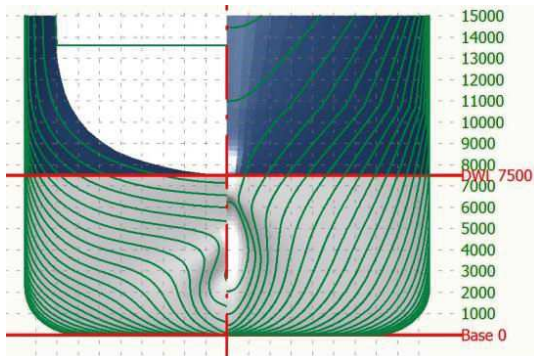


Figure 4: Lines plan of 120 meter long containership

The result comparison is shown in Figure 5 for parametric rolling level 1 and in Figure 6 for pure loss of stability level 1. Figure 5 shows the result for pure loss of stability level 1 for the IS Code 2008, level 1 Method A and level Method B. Figure 6 shows the result for parametric rolling for the IS Code 2008, level 1 Method A and level Method B.

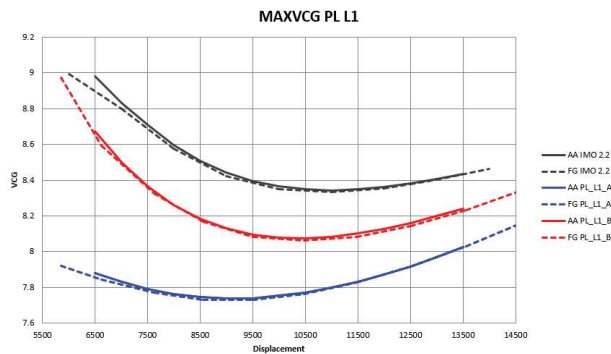


Figure 5: MaxVCG curve for pure loss of stability level 1 check

Both results show the consistency of all results even when the hydrostatic solver used a different method for this comparison. GHS uses a 2D method and Calcoque uses a 3D method. The stability code should be validated before being widely used in industry. The accuracy and consistency of the code will be able to provide sufficient guidelines to ship crew for a decision making process. It is therefore concluded that both hydrostatic solvers are relevant.

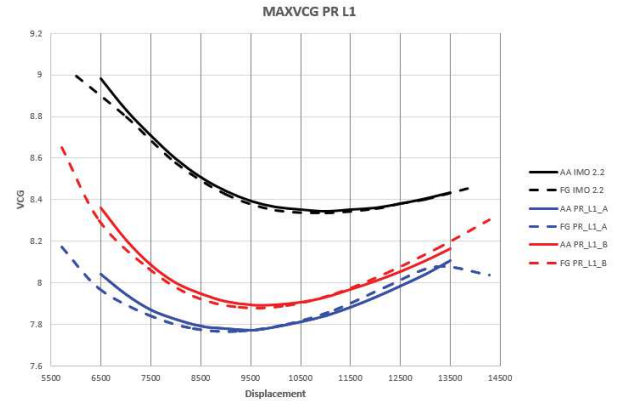


Figure 6: MaxVCG curve for parametric rolling level 1 check

## 5. SYSTEM INTEGRATION

System integration on board is the main role of smart ships. Nowadays, warships and commercial ships are equipped with comprehensive platform automation capabilities that allow to achieve unprecedented levels of ship survivability and operational effectiveness and contribute to crewing reductions.

### 5.1 Integrated Platform Management System

The Integrated Platform Management System (IPMS) is a distributed architecture real-time digital control system. This open architecture system comprises multifunction control consoles and Remote Terminal Units (RTU). RTU are used for process level data acquisition and control. The consoles provide the Human Machine Interfaces (HMI) for operators at various shipboard locations. System-wide connectivity is provided by a redundant databus. Open system architecture allows for the use of a variety of data networks in accordance with customer requirements. It also permits interfacing the IPMS to other systems through fieldbus, serial links, and other interfaces. The typical IPMS configuration is shown in Figure 7.



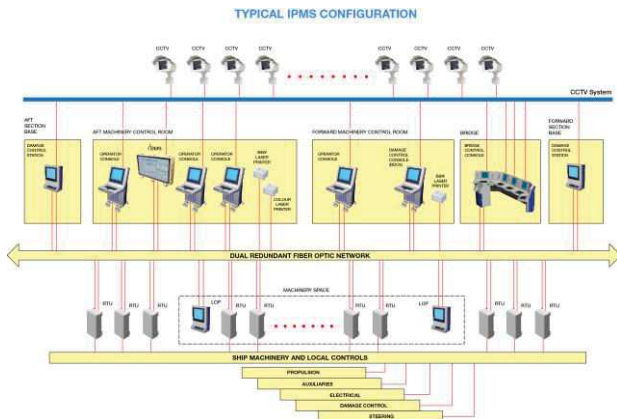


Figure 7: Typical IPMS Configuration [28]

The IPMS contains 5 main subsystems: propulsion, electrical, auxiliary, damage control and steering. The IPMS also continuously records the changes in sensor data and the control commands together with the date and time stamps for each value. Sensor information and other system data can be selected by the operator to be either stored or displayed together with any relevant alarm and warning limit thresholds.

The steering subsystem consists of the data that show the behaviour of the ship based on real time response. Generally the available data are roll angle ( $^{\circ}$ ), roll angle rates ( $^{\circ}/\text{sec}$ ), pitch angle ( $^{\circ}$ ), pitch angle rate ( $^{\circ}/\text{sec}$ ) and heave (metres). The reference of terms used is presented in Figure 8.

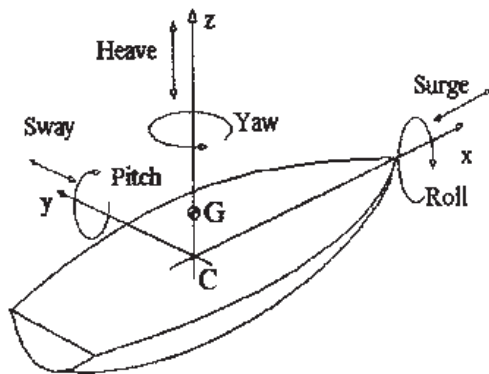


Figure 8: Terminology for ship dynamics

When the ship is moving through the water under propulsion power, various motions can be observed. There are six kinds of motions. These are rolling, surging, pitching, swaying, yawing and heaving. Rolling, pitching and yawing represent the rotary motion of the ship. Surging, swaying and heaving represent the linear motion through the axis.

## 5.2 Weather Meteorological System (WMS)

The Weather Meteorological System (WMS) provides information on weather conditions. It is capable of collecting and recording related information for future analysis. There are various types of systems on the

market that can be easily installed onboard a ship. Generally, this system can provide any combination of a range of sensors such as: multi-point wind speed and direction, atmospheric pressure, temperature and relative humidity, dew point, water temperature and salinity and wave height and sea state. There are some service providers who offer data on visibility and cloud cover.

In maritime literature, the Douglas scale and Beaufort scales are commonly used [29]. The Douglas sea scale was devised in the 1920s by Captain H.P Douglas. He was Vice Admiral Sir Percy Douglas and hydrographer of the Royal Navy. The Douglas Sea Scale is a scale which measures the height of the waves and also measures the swell of the sea. It is very simple to follow and is expressed in one of 10 degrees.

The Beaufort scale was devised in 1805 by Francis Beaufort (later Rear Admiral Sir Francis Beaufort), an Irish Royal Navy officer. Beaufort's scale of wind force was revised in 1874 to reflect changes in the rig of warships, and expanded two decades later to include particulars of the sail required by fishing smacks [30]. A scale of equivalent wind speeds was introduced in 1903, its basis being the formula:

$$V = 1.87 \times \sqrt{B^3} \quad (4)$$

where:

B = Beaufort number

V = wind speed in miles/hour at 30 feet ( $\approx 10$  metres) above the surface of the sea.

## 6. PROPOSED SYSTEM ARCHITECTURE

The integrated system could be used to determine the ship stability performance based on second generation intact stability criteria. The system is able to identify data trend and predict the possibility of the ship entering a risk area.

Based on the latest Ship Design and Construction committee meeting, SDC2 [31] at IMO, the data required for the SGISC analysis is presented in Figure 9.

The proposed integration system diagram is shown in Figure 10. Two main sources of input data will be from the IPMS and the WMS. A data recording system collects the data and categorises it into various divisions. Then, the data will be sent to stability software for analysis. Stability software will indicate whether either current information/situation is risk-based on the SGISC. This information will appear on the bridge and then be recorded for future analysis.

As an example, for parametric rolling level 1, the data required are design GM, current GM and  $R_{PR}$ .  $R_{PR}$  is the maximum attained value for parametric rolling.  $R_{PR}$  is calculated based on ship geometry and this value is fixed based on ship geometry and bilge keel dimension. The



GM design is also fixed. The current GM is changed based on the loading condition. Therefore, the stability software will be able to indicate the risk of parametric rolling level 1 based on the SGISC. It will be able to indicate the value and the margin available. The sample of process flow for parametric rolling level 2B is shown in Figure 11. The parametric rolling level 2B considers the rolling angle of the ship. It is considered vulnerable if the rolling angle is greater than 25°.

Failure mode	Criteria	Input information
<b>Parametric rolling</b>		
Level 1	Design GM Current GM	Loading condition $\lambda_i, H_i$
Level 2	Ship speed, Roll angle	Wave direction
<b>Pure loss of stability</b>		
Level 1	$GM_{min}$	Loading condition $\lambda_i, H_i$
Level 2	$\phi_v$ , or $\phi_s$ , or $\phi_{roll}$ , or GZ max	GZ curve
<b>Broaching</b>		
Level 1	Ship speed	Cruising speed
	Ship length	Ship geometry
Level 2		Loading condition $\lambda_i, H_i$ $u_{cr}, n_{cr}$ other propulsor data

Figure 9: Information required for SGISC

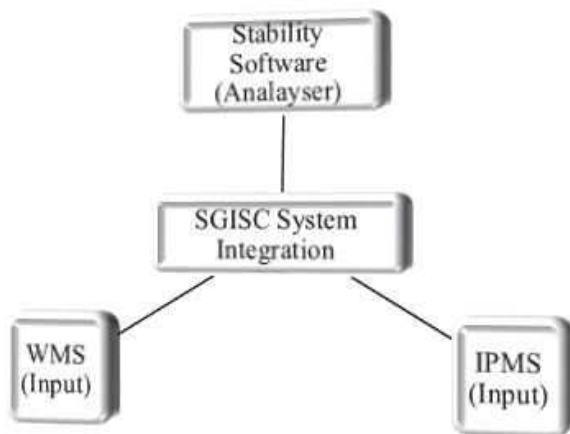


Figure 10: Proposed integration system diagram

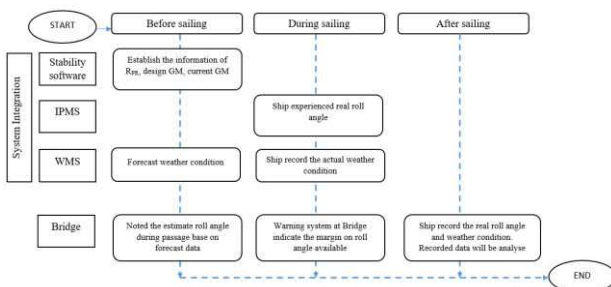


Figure 11: Sample of process flow for parametric rolling level 2B

The WMS also has the capability to record the wind speed. Therefore, it will be able to map the wind speed and correlate it with sea state conditions according to naval practice. Then, we will be able to predict the yearly weather forecast in that area. The use of the Douglas scale and Beaufort scale could contribute to the analysis process because most of the weather condition records are based on sea state conditions.

## 7. DISCUSSION

Based on the SGISC, it is designed to evaluate the stability performance during the design phase. Checks of each failure mode must be performed and should pass at any level either Level 1, 2 or if a direct assessment before the considered design passes the IS Code.

When a ship enters her service life, the precaution stated in SGISC should be taken into account for developing the stability code in future. Therefore, the records of weather condition such as wave characteristics and ship behaviour and dynamic response are important.

The marine X-band radar is capable of recording the wave length and wave height. With the additional data from actual sailing ship, it would therefore be able to map the wave profile and probability of occurrence.

The summary of evaluation process for parametric rolling is shown in Figure 12. Figure 13 shows the evaluation process for parametric rolling criteria. In this failure mode, there are 4 possibilities of conducting the real-time evaluation for Level 1 method B, Level 2Ai, Level 2Aii and Level 2B. These real-time evaluations can provide advice or assistance to the bridge team for the decision making process.

For PRL1A, it is the basic calculation where the amplitude of the variant of the metacentric height is calculated based on the moment of inertia at high and low draft as stated in SDC.2 INF.10 Annex 16 Para 2.11.2.2. This calculation could use stability software. Therefore, this result is not a real-time evaluation.

For PRL1B and PRL2Ai, the calculation involved the wave profile with a statistical approach. With the information from the WMS on the actual wave height and wave length, the result for PRL1B and PRL2Ai will be a real-time evaluation because of the real-time wave profile given by the WMS.

For PRL2Aii, the stability software calculates the reference ship speed corresponding to the parametric resonance,  $V_{PRI}$ . Then, the  $V_{PRI}$  will be sent to the bridge as a guide for the navigator. Based on the rules, the ship must be cruising at not more than  $V_{PRI}$ . The navigation system on the bridge will be able to indicate the margin and alarm when the ship is approaching the  $V_{PRI}$ . With the information from the WMS on the actual wave height and wave length, the result for PRL2Aii will be a real-

time evaluation because of the real-time wave profile provided by the WMS.

Level	Explanation
PRL1A	Compute the GM variant based on ship geometry
PRL1B	Compute the GM variant based on wave length = ship length and wave height = ship length x 0.0167
PRL2Ai	Compute the GM variant based on 16 wave cases
PRL2Aii	Compute the reference ship speed corresponding to the parametric resonance, $V_{PR}$ based on 16 wave cases
PRL2B	Compute the roll angle based on 16 wave cases or table of wave data

Figure 12: Summary of SGISC for parametric rolling

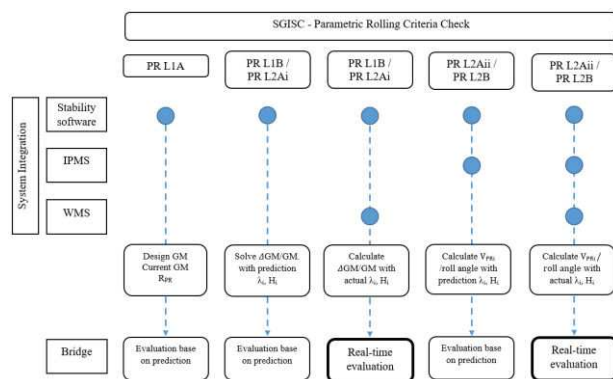


Figure 13: Evaluation of parametric rolling criteria

For PRL2B, the stability software calculates the roll angle. With the information from the WMS on the actual wave height and wave length, the result for PRL2B will be a real-time evaluation because the WMS provides the real-time wave profile. The steering subsystem of the IPMS provides the actual roll angle. This is the real-time roll angle and it could be compared with the calculated roll angle.

The real-time evaluation for parametric rolling is useful for the navigator to understand the limit of the ship based on real-time evaluation. It can help them to make the right decision in severe weather conditions and any sudden change of in loading condition en route.

For PR L2B, the information from the IPMS for the actual roll angle and from the WMS on the wave profile is very useful for the shipowner to understand ship behaviour. Based on the SGISC, the calculation is based on the design stage and quite often the calculation value is different compared to actual value. Therefore, the correlation between the calculated value and the actual value can be examined. This is very valuable data for the reference for the future ship design process.

## 8. CONCLUSION

This paper presents the comparison result for parametric rolling using the GHS and Calcoque. Both results show the consistency of all results even where the hydrostatic solver used for this comparison used a different method.

Since the marine X-band radar is capable of recording the wave length and wave height, it can map the wave profile and probability of occurrence together with the additional data from the actual sailing ship.

The calculated data prior to the sailing of the ship and the real-time data are important to analyse. The relationship between both data should be more understandable and it will facilitate the prediction of the behaviour of the ship at sea.

## 9. ACKNOWLEDGEMENT

The authors would like to acknowledge the support of the Government of Malaysia, the Government of the French Republic and the Direction des Constructions Navales (DCNS).

## 10. REFERENCES

- [1] I. Backalov, G. Bulian, A. Rosen, V. Shigunov, and N. Themelis, "Ship Stability & Safety in Intact Condition through Operational Measures," *Int. Conf. Stab. Sh. Ocean Veh.*, no. June, pp. 14–19, 2015.
- [2] Y. Welaya and C. Kuo, "A Review of Intact Ship Stability Research and Criteria," *Ocean Eng.*, vol. 8, pp. 65–84, 1981.
- [3] J. Rohala, "The Judging of the Stability of Ships and the Determination of the Minimum Amount of Stability," 1939.
- [4] T. Tsuchiya, "An Approach for Treating the Stability of Fishing Boats," in *International Conference on Stability of Ships and Ocean Vehicles*, 1975.
- [5] W. M. Peters, V. M. Belenky, C. M. Bassler, K. M. Spyrou, N. M. Umeda, G. V Bulian, and B. V Altmayer, "The Second Generation Intact Stability Criteria : An Overview of Development," *Trans. - Soc. Nav. Archit. Mar. Eng.*, vol. 119, no. 225–264, 2012.
- [6] IMO, "SLF 48/21 Report to the Maritime Safety Committee," 2005.
- [7] S. Ishida, H. Taguchi, and H. Sawada, "Evaluation of the Weather Criterion by Experiments and its Effect to the Design of a RoPax Ferry," *Int. Conf. Stab. Ships Ocean Veh.*, pp. 9–16, 2006.
- [8] N. Umeda, Daichi Kawaida, Y. Ito, Y. Tsutsumi, A. Matsuda, and Daisuke Terada, "Remarks on Experimental Validation Procedures for Numerical Intact Stability Assessment with Latest Examples," in *International Ship Stability*

- Workshop, 2014, pp. 77–84.
- [9] C. C. Bassler, V. Belenky, G. Bulian, A. Francescutto, K. J. Spyrou, and N. Umeda, *Review of Available Methods for Application to Second Level Vulnerability Criteria Christopher*, vol. 97. Dordrecht: Springer Netherlands, 2011.
- [10] C. Wandji, B. Veritas, and P. Corrigan, “Test Application of Second Generation IMO Intact Stability Criteria on a Large Sample of Ships,” *Int. Conf. Stab. Ships Ocean Veh.*, pp. 145–155, 2012.
- [11] N. Umeda, “Current Status of Second Generation Intact Stability Criteria Development and Some Recent Efforts,” in *International Ship Stability Workshop*, 2013.
- [12] D. Jens, N. Peter, H. Kartin, B. Henk can den, and R. Konstanze, “The On board Wave and Motion Estimator OWME,” *Int. Soc. Offshore Polar Eng.*, 2010.
- [13] J. Vogelzang, K. Boogaard, K. Reichert, and K. Hessner, “Wave height measurements with navigation radar,” *Int. Arch. Photogramm. Remote Sens.*, vol. 33, no. B7, pp. 1652–1659, 2000.
- [14] J. C. N. Borge, K. Reichert, and J. Dittmer, “Use of nautical radar as a wave monitoring instrument,” *Coast. Eng.*, vol. 37, pp. 331–342, 1999.
- [15] F. Wang, G. Yuan, and Z. Lu, “Investigation of Real-Time Wave Height Measurement Using X-Band Navigation Radar,” *Wireless Communications, Networking and Mobile Computing, 2007. WiCom 2007*. pp. 980–983, 2007.
- [16] J. Bellec and M. a S. Neves, “An investigation on parametric rolling prediction using neural networks,” no. 1, pp. 1–7.
- [17] SEPAC, “GM Meter.” [Online]. Available: <http://www.gm-meter.com/index.html>.
- [18] IMO, “International Code of Intact Stability, 2008,” London, 2009.
- [19] J.-M. Laurens and G. François, *Stabilité Du Navire: Théorie, Réglementation, Méthodes De Calcul (Cours Et Exercices Corrigés)*. Ellipses, Paris, 2013.
- [20] B. Veritas, “Rules for the Classification of Steel Ship,” 2011.
- [21] F. Mata-Álvarez-Santullano and A. Souto-Iglesias, “Stability, safety and operability of small fishing vessels,” *Ocean Eng.*, vol. 79, pp. 81–91, Mar. 2014.
- [22] J. Van Santen, “The Use of Energy Build Up to Identify the Most Critical Heeling Axis Direction for Stability Calculation for Floaring Offshore Structures,” in *10th International Conference on Stability of Ship and Ocean Vehicles*, 2009, pp. 65–76.
- [23] A. Francescutto, “The Intact Ship Stability Code: Present Status and Future,” in *Proceedings of the 2nd International Conference on Marine Research and Transportation, Naples, Italy, Session A*, 2007, pp. 199–208.
- [24] IMO, “SDC 1/5/1 - Development of second generation intact stability criteria. Remarks on the development of the second generation intact stability criteria submitted by Germany,” 2013.
- [25] IMO, “SDC 2/INF.10 Second Generation Intact Stability Criteria,” 2014.
- [26] A. Ariffin, S. Mansor, and J.-M. Laurens, “A Numerical Study for Level 1 Second Generation Intact Stability Criteria,” in *International Conference on Stability of Ships and Ocean Vehicles*, 2015, pp. 183–193.
- [27] G. François, J.-Y. Billard, and J.-M. Laurens, “Calcoque: A fully 3D Ship Hydrostatic Solver,” in *International Conference on Stability of Ships and Ocean Vehicles*, 2015, pp. 203–212.
- [28] L3 MAPPs, “Integrated Platform Management System,” 2015. [Online]. Available: <http://www.mapps.l-3com.com/integrated-platform-Management-System.html>.
- [29] WMO, “MMOP Frequently Asked questions (FAQ).pdf,” *FAQ*, 2015. .
- [30] National Meteorological Library and Archive, “Fact sheet 6 - The Beaufort Scale,” 2010.
- [31] IMO - 2014, “SDC 2/INF.10,” pp. 1–6, 2014.

## 11. AUTHORS BIOGRAPHY

Brief biographies are required for all authors e.g.:

**Arman Ariffin** holds the current position of marine engineer at the Royal Malaysian Navy and is pursuing his doctoral study at ENSTA Bretagne, France. He is responsible for the designing of naval ship specifications for new projects. His previous experience includes several positions onboard naval vessels as a chief engineer and he has conducted research in the field of aero-marine technology.

**Jean-Marc Laurens** holds the current position of educator researcher at ENSTA Bretagne. He is responsible for the naval and offshore engineering branch. His previous experience includes being the CFD branch head at the French Towing Tank in Val de Reuil.

**Shuhaimi Mansor** holds the current position of Proton Professor at Proton Berhad. He is responsible for promoting and link R&D activity and collaboration between University and Industry, establishment of UTM-PROTON research activity & human capital development and strategic planning and implementation for advance innovation technology. His previous experience includes working with British Aerospace Plc, UK and Aiolos Eng. Corp, Canada.



# Conduction of a wind tunnel experiment to investigate the ship stability weather criterion

Arman Ariffin, *ENSTA Bretagne, LBMS EA 4325, Brest, France*

[arman.ariffin@ensta-bretagne.org](mailto:arman.ariffin@ensta-bretagne.org)

Shuhaimi Mansor, *Faculty of Mechanical Engineering, Universiti Teknologi Malaysia, Malaysia*

[shuhaimi@mail.fkm.utm.my](mailto:shuhaimi@mail.fkm.utm.my)

Jean-Marc Laurens, *ENSTA Bretagne, LBMS EA 4325, Brest, France*

[jean-marc.laurens@ensta-bretagne.fr](mailto:jean-marc.laurens@ensta-bretagne.fr)

## ABSTRACT

A wind tunnel experiment has been set up to examine several assumptions regarding the weather criterion of the intact stability code. The experimental trials are conducted in the Low-Speed Wind Tunnel of the Aeronautics Laboratory at the Universiti Teknologi Malaysia. Two models are tested. The first model is an academic model that allows comparisons to be made with analytical models. The second model is the DTMB 5415 to present a military realistic case. The models are properly weighted to present the correct hydrostatic characteristics. A water tank is installed in the wind tunnel test section; the models are free to roll around the longitudinal axis passing through the buoyancy centre owing to a frictionless rod. The experimental results are then compared with the results of the stability code using the IMO weather criterion and the military criteria. Finally, in the experimental trials, many configurations are tested to assess the effects of various geometrical parameters.

**Keywords:** *Second generation intact stability criteria, wind tunnel, roll angle*

## 1. INTRODUCTION

Intact stability is a basic requirement to minimise the capsize risk for vessels. It is a guideline for the ship designer, the ship operator and the classification society to design, build and commission the ship before it starts its service life at sea. A comprehensive background study of intact stability development was written by Kuo & Welaya (Welaya & Kuo, 1981). Their paper "A review of intact stability research and criteria", stated that the first righting arm curve was proposed by Reed in 1868, but that the application was presented by Denny in 1887. In addition, in 1935, Pierrottet tried to rationally establish the forces which tend to capsize a ship and proposed a limiting angle at which the dynamic level of the ship must be equal to or greater than the sum of energy exerted by the inclining moments. However, Pierrottet's proposal was too restrictive for the design process and it was not accepted.

Kuo and Welaya also mentioned the famous doctoral thesis written by Jaakko Rahola in 1939. Rohola's thesis evoked widespread interest throughout the world at that time because it was the first comprehensive study and proposed method to evaluate intact stability which did not require complex calculations (Rohala, 1939).

The Sub-Committee on Stability and Load Lines and on Fishing Vessels Safety 48th Session (IMO, 2005) emphasized the requirement of revising the current IS Code. The importance of the comprehensive review of the current IS Code 2008 would significantly affect the design and ultimately enhance the safety of ships (Mata-Álvarez-Santullano & Souto-Iglesias, 2014).

Intact Stability is a crucial criterion that concerns most naval architects at the design stage. The current Intact Stability (IS) Code 2008 is in force. Except for the weather criterion, the IS Code 2008 only applies to the hydrostatics of the ship. It



does not cover the seakeeping behaviour of the ship and first and foremost, it always considers a ship with a negligible trim angle. In head seas, the ship can present a significant angle of trim which may affect the righting arm. Van Santen also presented an example of a vessel capsizing due to of the small angle of trim (Van Santen, 2009).

For the enhancement and improvement of intact stability criteria, the International Maritime Organisation (IMO) introduced the new generation intact stability criteria in 2008 (Francescutto, 2007). Figure 1 presents the procedure to apply to the second generation intact stability rule. Once the basic criteria have been satisfied, each failure mode is verified to satisfaction at the most conservative level.

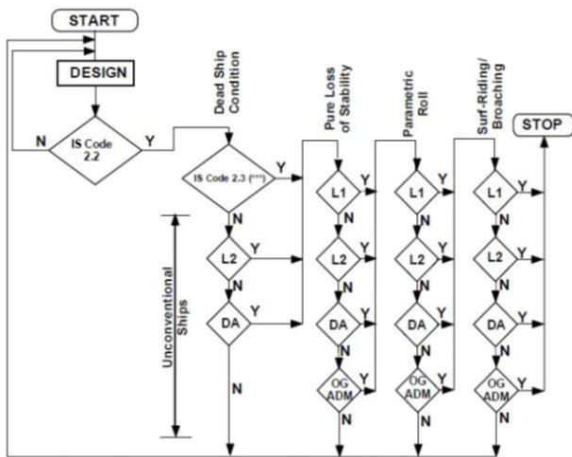


**Figure 1: Structure of Second Generation Intact Stability Criteria**

## 2. DEVELOPMENT OF SECOND GENERATION INTACT STABILITY CRITERIA

The last Sub-committee on Ship Design and Construction meeting at IMO recalled that SDC 2 had agreed, in principle, to the draft amendments of the 2008 IS Code regarding vulnerability criteria and the standards (levels 1 and 2) related to parametric roll, pure loss of stability and surf-riding /broaching (SDC 2/WP.4, annexes 1 to 3). For this purpose, SDC 2 had invited member governments and international organisations to bring the criteria to the attention of ship designers, shipyard operators, ship owners and other interested parties, and to observe and test the application of the finalised vulnerability criteria, in order to gain experience with regard to their use.

The draft amendment of the IS Code regarding vulnerability criteria and the standards (levels 1 and 2) related to dead ship condition and excessive acceleration are contained in SDC 3/INF.10 Annex 1 and 2. The level 1 check for dead ship condition is basically the same method used for current IS Code 2.3 which is weather criteria. If it failed, the design should process to level 2 check and the direct assessment. Direct assessment procedures for stability failure are intended to employ the most advanced state-of-the art technology available either by numerical analysis or experimental work for quantitative validation as stated in SDC 1/INF.8 Annex 27 (IMO, 2013).

## 3. THE WEATHER CRITERION

The IS Code 2008 Part A 2.3 contains the weather criterion. The ship must be able to withstand the combined effects of beam wind and rolling. The conditions are:

- the ship is subjected to a steady wind pressure acting perpendicular to the ship's centreline which results in a steadywind heeling lever ( $lw_1$ ).*
- from the resultant angle of equilibrium ( $\phi_0$ ), the ship is assumed to present an angle of roll ( $\phi_1$ ) to windward due to wave action. The angle of heel under action of steady wind ( $\phi_0$ ) should not exceed  $16^\circ$  or  $80\%$  of the angle of deck edge immersion, whichever is less.*
- the ship is then subjected to a gust wind pressure which results in a gust wind heeling lever ( $lw_2$ ); and under these circumstances, area b shall be equal to or greater than area a, as indicated in Figure 2.*

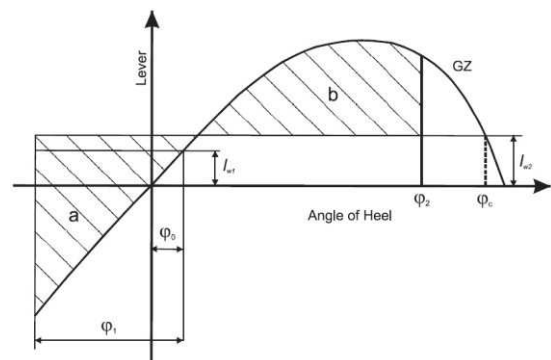


**Figure 2: Severe wind and rolling**

The heeling lever shall be calculated using formula:

$$l_{w1} = \frac{P \cdot A \cdot Z}{1000 \cdot g \cdot \Delta} \quad (1)$$

$$l_{w2} = 1.5 l_{w1} \quad (2)$$

where  $l_{w1}$  = steady wind heeling angle,  $l_{w2}$  = gust wind heeling lever,  $P$  = wind pressure of 504 Pa,  $A$  = projected lateral area ( $m^2$ ),  $Z$  = vertical distance from the centre of  $A$  to the centre of the underwater lateral area or approximately to a point at one half of the mean draught (m),  $\Delta$  = displacement (t) and  $g$  = gravitational acceleration). In Figure 1, a Direct Assessment (DA) can be used to verify the weather criterion for unconventional ships. The DA can be experimental. The present study shows how such an experimental DA can be conducted for two models, a civilian ship and a military ship.

In the weather criterion, two main rules are commonly used. For commercial ship, it uses the IMO weather criterion and for naval ship, it uses the Naval Rules. The IMO Weather criterion is shown in Figure 2 and the weather criterion for naval ship is shown in Figure 3. The significant different between IMO and Naval Rules are presented in the Table 1.

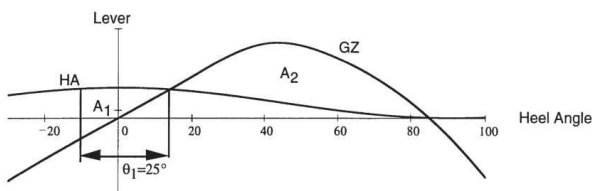


Figure 3: Weather Criteria for Naval Ships

Table 1 Comparison IMO and naval rules for weather criterion

Criterion	IMO	Naval Rules
Wind velocity	26 m/s	100 knots
Roll back angle	various*	25°
WHA	constant	$\cos^2\theta$
Ratio $A2/A1$	$\geq 1$	$\geq 1.4$
Gust	Yes	No

\* roll back angle ( $\phi_1$ ) calculated based on IS Code 2008

# WHA – wind heeling arm,  $A2$  - restoring energy,  $A1$  – capsizing energy

#### 4. SHIP MODEL

Two models were used for the experimental work. The first model is an academic container ship geometry referred as “ASL shape” in the rest of the paper. The second model is a research ship model, the well know DTMB 5415 (Molgaard, 2000). The

5415 DTMB model is widely used for the research study in seakeeping (Begovic, Day, & Incecik, 2011; Jones & Clarke, 2010; Yoon et al., 2015). The basic geometry is presented in Table 2. The body plan and perspective view for “ASL shape” is shown in Figure 4. The body plan and perspective view for “5415 shape” is shown in Figure 5.

Table 2 Basic ship model geometry

Ship model	ASL shape	5415 shape
LOA, (m)	140	153.3
BOA, (m)	20	20.54
Draft, (m)	12	6.15
Displacement, (tonnes)	26,994	8,635
VCG, (m)	10	7.555
LCG, (m)	70.037	70.137
KM, (m)	10.206	9.493
GM, (m)	0.206	1.938

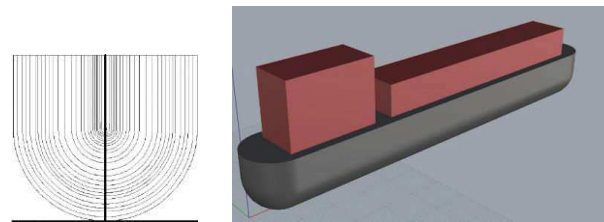


Figure 4: Body plan (left) and perspective view (right) of the ASL shape

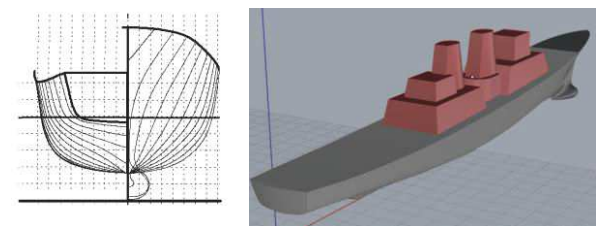


Figure 5: Body plan (left) and perspective view (right) of the 5415 shape

#### 5. EXPERIMENTAL INVESTIGATION

A wind tunnel test was conducted at the low speed wind tunnel facility at Universiti Teknologi Malaysia. This wind tunnel has a test section of 2m (width) x 1.5m (height) x 5.8m (length). The maximum test velocity is 80m/s (160 knots). The wind tunnel has a flow uniformity of less than 0.15%, a temperature uniformity of less than 0.2°C, a flow angularity uniformity of less than 0.15° and a turbulence level of less than 0.06% (Ariffin, Mansor, & Laurens, 2015).

**Ship model**

Two ship models were tested as described in Paragraph 4. Both models were constructed at ENSTA Bretagne, France using the Computer Numerical Control (CNC) machine. The material used was polystyrene. Both models were designed in 3D drawing and imported to CNC machine program for fabrication process. The hulls were divided into six parts for the cutting process. Then, all parts were glued and laminated with a fiberglass. The superstructure used the synthetic glass. The completed ship models are shown in Figure 6.



(a)



(b)

**Figure 6: Complete build ship models (a) ASL shape (b) 5415 DTMB shape**

**Inclining test**

To determine the correct centre of gravity, inclining tests were performed. The inclining test is a procedure which involves moving a series of known weights, normally in transverse direction, and measuring the resulting change in the equilibrium heel angle of the ship. By using this information and applying basic naval architecture principles, the ships' vertical centre of gravity is determined from the GM. We also verified that the natural roll period is as expected. Two devices were used for the data recording, first is the Ardu Flyer device and smartphone (Djebli, Hamoudi, Imine, & Adjlout, 2016).

**Wind tunnel setup**

The models were allowed to heave and roll freely. It was not allowed to yaw because the model must be hold at the longitudinal axis to avoid the model bump to water tank side. The models were fixed with a rod both at bow and stern (Figure 7). It is passing through the point of longitudinal centre of buoyancy. Both rods at bow and stern were aligned using laser light to confirm the shafts positioned at same axis. The arrangement of rod used in this experiment is frictionless therefore, minimum interaction between the rod and rod stand can be obtained.

To allow the model to float in the wind tunnel, a water tank fabricated with glass of 8mm thickness was installed. Since the wind tunnel is not water tight, to avoid any leak of water during the experiment, a dummy pool was placed underneath the platform. The dummy pool is capable to cope the total volume of water if the glass water tank gets damaged. The arrangement in the test section is shown in Figure 8.

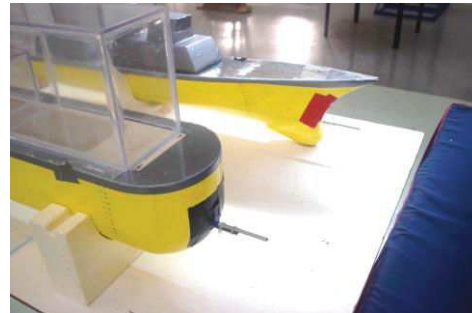


**Figure 7: Rods fixed at ship models**



**Figure 8: Arrangement in the test section.**

The experiment started with the model placed in the water tank with the correct draft (Figure 9). A laser light is used to ensure the vessel is upright. The test started with measurement of the stable heel. The wind tunnel velocity was increased



slowly while the heel angle was recorded using the Ardu Flyer device. The Ardu Flyer is a complete open source autopilot system designed for 3D robotics. This experiment involved three models configuration as stated below:

- a. ASL shape.
- b. 5415 shape.
- c. ASL with bilge keel shape.

A roll back angle ( $\phi_2^*$ ) measure was performed for all the models. The definitions of ( $\phi_1$ ) and ( $\phi_2^*$ ) are shown in Figure 10. The test steps are as follow:

- a. Model placed in water tank.
- b. Wind applied and the wind velocity and heel angle recorded.
- c. Roll back angle ( $\phi_1$ ) applied at the model.
- d. Then model is suddenly released.
- e. The maximum counter roll back angle ( $\phi_2^*$ ) recorded.



(a)



(b)

**Figure 9: Ship models ready to be tested in wind tunnel test section (a) ASL shape (b) 5415 DTMB shape**

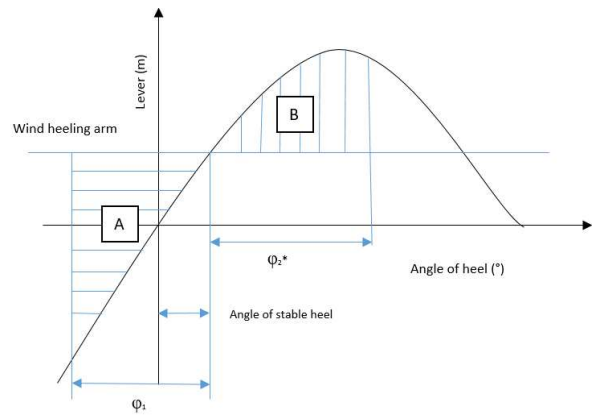


**Figure 10: Definitions used in this experiment**

**Scaling criteria**

The models used in the experiment were scale down to 1:100. It is the same scale used by (Begovic et al., 2011) for the ship motion experiment using DTMB 5415 model. For the GZ curve, the model and full scale ship has a same curve shape but values for the model are divided by  $10^2$ . For weight calculation, values used for the model are divided by  $10^6$ . For the wind velocity, the value used for the model is divided by 10.

**Boundary layer**

When the air flow over the ocean surface from any direction, a natural boundary layer is formed. This means that the wind velocity at the surface is zero and increase with higher altitude. The boundary layer thickness in the test section for this experiment is about 35mm and the velocity profile is shown in Figure 11.

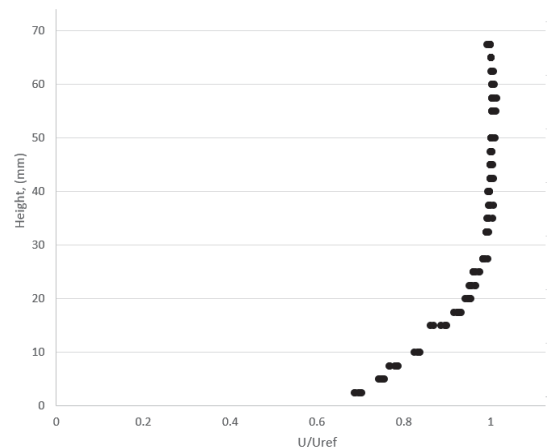


**Figure 11: The velocity profile curve**

To compute the weather criterion, the General Hydro Static software (GHS) was used. The GHS uses a strip method and it is widely used in the

marine industry (Ariffin, Laurens, & Mansor, 2016). In GHS, there are 2 methods to specify the wind either by wind velocity or wind pressure. Specifying a wind velocity,  $V_{wind}$ , in GHS gives a standard velocity profile with  $V_{wind}$  at 10 metres from the ground (Yalla, 2001). When specifying a velocity pressure, a constant value is given. The calculation in this paper for GHS results were obtained using the wind pressure input.

## 6. RESULTS

### Angle of stable heel ( $\phi_0$ ) vs wind velocity

Figure 12 shows the graph for angle of stable heel,  $\phi_0$  versus wind velocity for the two models and two methods; IMO and experimental. The 5415 curves are following a parabolic shape since as we can see in Figure 13, the GZ curve of 5415 shape follows a linear curve up to 30 degrees. Furthermore, the experimental curve is below the IMO curve which indicates that the drag coefficient  $C_D$ , of the ship silhouette is smaller than 1, the value assumed in the IMO formula (Figure 12). The ASL curves present different shapes and behaviour. At first, they do not present the parabolic shape because as we can see in Figure 13, the GZ curve is only linear up to 5 degrees. Furthermore, the experimental curve for this case is above the IMO curve (Figure 12). That is explained by the fact that the drag coefficient  $C_D$ , for the box shape of the ASL is bigger than 1. This can be confirmed by the many references that exist giving the drag coefficients of basic shapes, see for example (Scott, 2005).

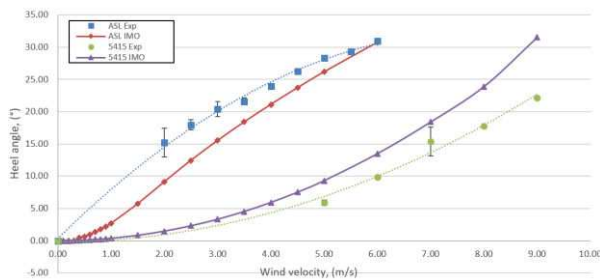


**Figure 12: Graph of wind velocity and angle of stable heel for ASL shape and 5415 shape on the experimental results and GHS calculation**

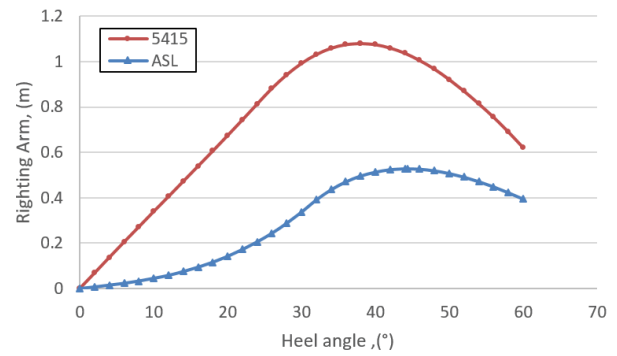


**Figure 13: The GZ curves for ASL shape and 5415 shape**

### Roll back angle ( $\phi_2^*$ ) versus roll to windward ( $\phi_1$ )

Figure 14 shows the roll back angle ( $\phi_2^*$ ) versus roll to windward ( $\phi_1$ ) for ASL shape for wind velocity range of 2 m/s to 4 m/s. Figure 15 shows the roll back angle ( $\phi_2^*$ ) versus roll to windward ( $\phi_1$ ) for 5415 shape. In the absence of damping the results should be like a swing where  $\phi_2^*$  follows  $\phi_1$ . The results suggest a far more complex behaviour where the hydrostatic force shape is playing an important role.

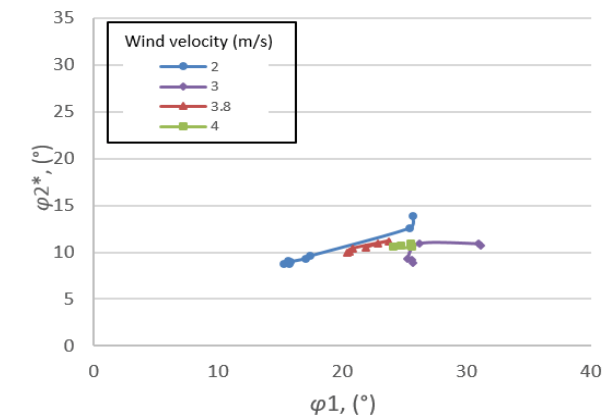


**Figure 14: Roll back angle ( $\phi_2^*$ ) vs roll to windward ( $\phi_1$ ) for ASL shape**

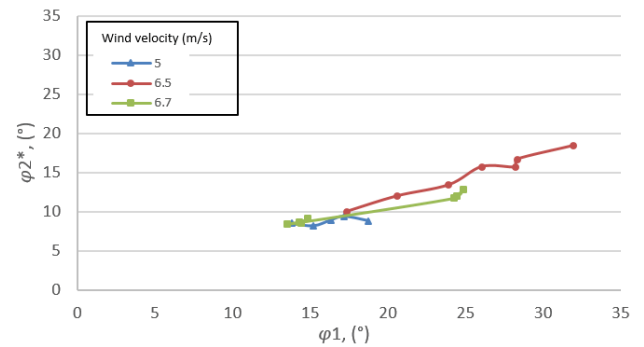


**Figure 15: Roll back angle ( $\phi_2^*$ ) vs roll to windward ( $\phi_1$ ) for 5415 shape.**

**Ratio  $\phi_2^*$  and  $\phi_1$  with bilge keel**

Figure 16 shows the ratio ( $\phi_2^*/\phi_1$ ) for the ASL shape and the ASL with a bilge keel. Both models were tested at wind velocity 2m/s. For the bare ASL, the average ratio is 0.55 and for the ASL with bilge keel, the average ratio is 0.43. As expected, the configuration with bilge keel contributes to more roll damping than configuration without bilge keel.

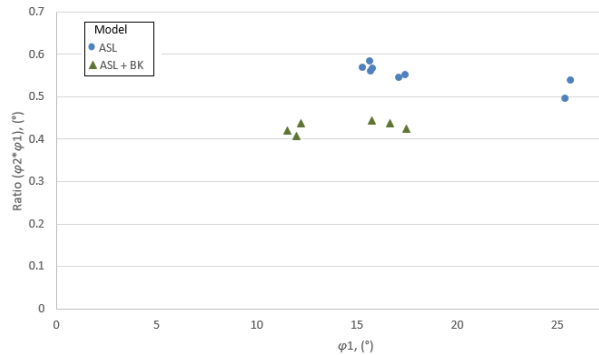


**Figure 16: Roll back angle ( $\phi_2^*$ ) vs roll to windward ( $\phi_1$ ) for ASL shape, 5415 shape and ASL with bilge keel configuration**

**Yaw angle effect on stable heel**

Figure 17 shows the angle of stable heel for the ASL and the 5415 both with the wind direction from star board 75° and port 105°. For the ASL, the values of  $\phi_0$  are smaller for the beam wind than those obtained with the yaw angles. In other words the assumption of the beam wind in the IMO code is not necessarily conservative. This phenomenon also appears for the 5415.

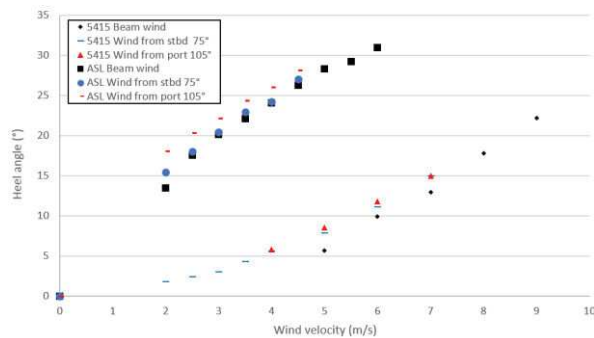


**Figure 17: Angle of stable heel for wind from starboard 75° and port 105°**

**Effect of roll to windward ( $\phi_1$ ) and roll back angle ( $\phi_2^*$ ) with yaw angle**

Figure 18 shows the result for  $\phi_1$  and  $\phi_2^*$  for the ASL and the 5415 with beam wind and wind from starboard 75°. For the ASL, the beam wind

has higher  $\phi_2^*$  than wind from starboard 75° and for the 5415, the beam wind has smaller  $\phi_2^*$  than wind from starboard 75°. The two models have a different response to the yaw angle. The behaviour is a combination of the superstructure geometry, the GZ curve and the damping.

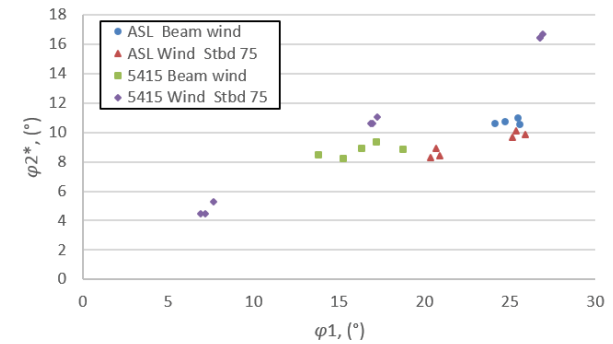


**Figure 18: Roll back angle ( $\phi_2^*$ ) vs roll to windward ( $\phi_1$ ) for 5415 shape with wind from port 105**

**Comparison IMO GHS and experimental result**

Figure 19 shows the comparison results between IMO and experimental results. For the ASL, the counter roll back angle ( $\phi_2^*$ ) obtained from experimental results is 24.07°, lower than IMO which is 29.638°. Therefore, IMO result is more conservative. For the 5415, the counter roll back angle ( $\phi_2^*$ ) obtains from experimental results is 16.31°, lower than Naval Rules which is 33.82° for ratio capsizing and restoring energy 1.0 and 39.45° for ratio capsizing and restoring energy 1.4. Therefore, the IMO and Naval rules are always more conservative.

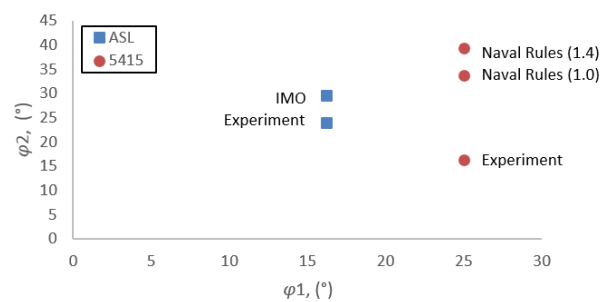


**Figure 19: Comparison result for IMO rules and Naval Rules**

**7. CONCLUSION**

In this paper the authors presented an experimental Direct Assessment (DA) of the weather criterion for two different models; a civilian ship with a simple geometry and a military ship, the well-known DTMB 5415. To conduct the

experiments, the low speed wind tunnel of UTM was used. Both models were placed in a water tank in the wind tunnel. Both models were free to roll so the heel angle could be measured and compared with the IMO and Navy Rules.

Although the assumptions taken by the rules are not always conservative, the final results always show that the experimental values are lower than the values given by the rules.

## 8. ACKNOWLEDGEMENT

The authors would like to acknowledge the support of the Government of Malaysia, the Government of the French Republic and the Direction des Constructions Navales (DCNS).

## 9. REFERENCES

- Ariffin, A., Laurens, J. M., & Mansor, S. (2016). Real-time Evaluation of Second Generation Intact Stability Criteria. In *Smart Ship Technology* (pp. 26–27).
- Ariffin, A., Mansor, S., & Laurens, J.-M. (2015). A Numerical Study for Level 1 Second Generation Intact Stability Criteria. In *International Conference on Stability of Ships and Ocean Vehicles* (pp. 183–193).
- Begovic, E., Day, a. H., & Incecik, a. (2011). Experimental Ship Motion and Load Measurements in Head and Beam Seas. *Proceeding of The 9th Symposium on High Speed Marine Vehicles*, 1–8.
- Djebli, M. A., Hamoudi, B., Imine, O., & Adjlout, L. (2016). The application of smartphone in ship stability experiment The Application of Smartphone in Ship Stability Experiment, (January). <http://doi.org/10.1007/s11804-015-1331-9>
- Francescutto, A. (2007). The Intact Ship Stability Code: Present Status and Future. In *Proceedings of the 2nd International Conference on Marine Research and Transportation, Naples, Italy, Session A* (pp. 199–208).
- IMO. (2005). *SLF 48/21 Report to the Maritime Safety Committee*.
- IMO. (2013). *SDC 1/INF.8 - Development of Second Generation Intact Stability Criteria*.
- Jones, D. a., & Clarke, D. B. (2010). *Fluent Code Simulation of Flow around a Naval Hull: the DTMB 5415*.
- Mata-Álvarez-Santullano, F., & Souto-Iglesias, A. (2014). Stability, safety and operability of small fishing vessels. *Ocean Engineering*, 79, 81–91. <http://doi.org/10.1016/j.oceaneng.2014.01.011>
- Molgaard, A. (2000). *PMM-test with a model of a frigate class DDG-51*.
- Rohala, J. (1939). *The Judging of the Stability of Ships and the Determination of the Minimum Amount of Stability*.
- Scott, J. A. (2005). Drag of Cylinders & Cones. Retrieved from <http://www.aerospaceweb.org/question/aerodynamics/q0231.shtml>
- Van Santen, J. (2009). The Use of Energy Build Up to Identify the Most Critical Heeling Axis Direction for Stability Calculation for Flooding Offshore Structures. In *10th International Conference on Stability of Ship and Ocean Vehicles* (pp. 65–76).
- Welaya, Y., & Kuo, C. (1981). A Review of Intact Ship Stability Research and Criteria. *Ocean Engineering*, 8, 65–84.
- Yalla, S. K. (2001). *Liquid Dampers for Mitigation of Structural Response: Theoretical Development and Experimental Validation*.
- Yoon, H., Simonsen, C. D., Benedetti, L., Longo, J., Toda, Y., & Stern, F. (2015). Benchmark CFD validation data for surface combatant 5415 in PMM maneuvers – Part I: Force/moment/motion measurements. *Ocean Engineering*, 1–30. <http://doi.org/10.1016/j.oceaneng.2015.04.087>



# Implementation of Second Generation Intact Stability Criteria into the Stability Calculation Software

A.Ariffin & J.M. Laurens  
 ENSTA Bretagne, LBMS EA 4325, Brest, France  
 S. Mansor  
 Faculty of Mechanical Engineering, Universiti Teknologi Malaysia, Malaysia

**ABSTRACT:** The Sub-Committee of Ship Design and Construction of International Maritime Organisation (IMO) has undertaken the development of “Second Generation Intact Stability Criteria (SGISC). The intention of the SGISC is to provide a new set of rules covering those phenomena which is not properly covered by present Intact Stability Code 2008. SGISC is additional rules that complement present rules. Five failure modes will be address in SGISC are excessive roll in dead ship condition, pure loss of stability, broaching in-volving loss of maneuverability in following quartering seas, parametric roll, and excessive acceleration. Moreover, these criteria are structured in three levels namely, first level, second level and direct assessment. Specific operational guidelines is added as a sort of “fourth level”, in the acknowledge that not all dangerous situation can be avoided only by design prescriptions. In this particular study, it was investigated if and how an existing and extensively used commercial code, in the present case, General HydroStatics (GHS ®), could handle level 1 and level 2 criteria. Open source ship models were tested to evaluate the vulnerability of the ship to the SGISC. Finally an illustrative example is presented to verify whether the existing and future regulations can prevent certain obviously dangerous situations on naval ship operating in extreme weather.

## 1 INTRODUCTION

Intact stability is a basic requirement to minimise the risk of the capsizing of vessels. It is a guideline for the ship designer, ship operator and classification society to design, build and commission the ship before it starts its service life at sea. A comprehensive background study of intact stability development was written by Kuo & Welaya (Welaya & Kuo, 1981). Their paper "A review of intact stability research and criteria", stated that the first righting arm curve was proposed by Reed in 1868, but that the application was presented by Denny in 1887. In addition, in 1935, Pierrottet tried to rationally establish the forces which tend to capsize a ship and proposed a limiting angle at which the dynamic level of the ship must be equal to or greater than the sum of energy exerted work done by the inclining moments. However, Pierrottet's proposal was too restrictive in the design process and it was not accepted.

Kuo and Welaya also mentioned the famous doctoral thesis written by Jaakko Rahola in 1939. Rohola's thesis evoked widespread interest throughout the world at that time because it was the first comprehensive study and proposed method to evaluate intact stability

which did not require complex calculations (Rohala, 1939).

The Sub-Committee on Stability and Load Lines and on Fishing Vessels Safety 48th Session IMO (2005) emphasized the requirement of revising the current IS

Code. The importance of the work on the comprehensive review of the current IS Code 2008 would significantly affect the design and ultimately enhance the safety of ships (Mata-Álvarez-Santullano & Souto-Iglesias, 2014).

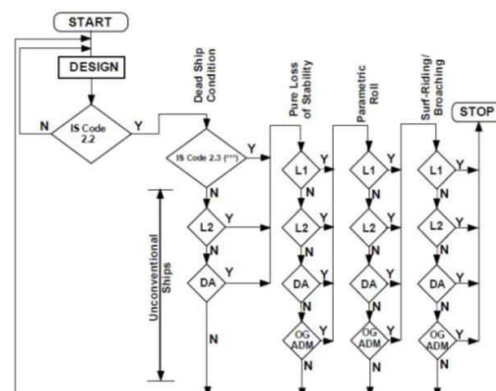


Figure 1: Structure of Second Generation Intact Stability Criteria

Intact Stability is a crucial criterion that concerns most of naval architects in the design stage. The current Intact Stability (IS) Code

2008 is in force. Except for the weather criterion, the IS Code 2008 only applies to the hydrostatics of the ship. It does not cover the seakeeping behaviour of the ship and first and foremost, it always considers a ship with a negligible trim angle. In head seas, the ship can present a significant angle of trim which may affect the righting arm. Van Santen also presents an example of a vessel capsizing due to of the small angle of trim (Van Santen, 2009).

For the enhancement and improvement of intact stability criteria, the International Maritime Organisation (IMO) introduced the new generation intact stability criteria in 2008 (Francescutto, 2007). Figure 1 presents the procedure to apply to the second generation intact stability rule. Once the basic criteria described in Section 2 have been satisfied, each failure mode is verified to satisfaction at the most conservative level.

## 2 PHYSICAL BACKGROUND

### 2.1 Pure loss of stability

When a ship is sailing through waves, the submerged part of the hull changes. These changes may become especially significant if the length of the wave is comparable to the length of the ship. Figure 2 shows the water plane change and GZ curve corresponding to wave trough and wave crest (Belenky, Bassler, & Sprou, 2011).

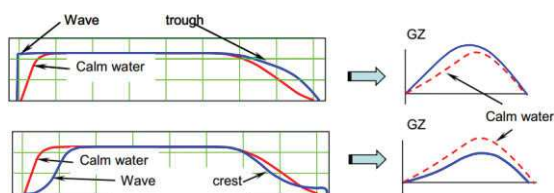


Figure 2. Stability corresponding to water plane changes on the wave trough (Top) and the wave crest (Bottom)

### 2.2 Parametric rolling

Parametric roll (short of parametric roll resonance) is an amplification of roll motions caused by periodic variation of transverse stability in waves. The phenomenon of parametric roll is predominantly observed in head, following, bow and stern-quartering seas

when the ship's encounter frequency is approximately twice the ship roll natural frequency and the roll damping of the ship is insufficient to dissipate additional energy (accumulated because of parametric resonance). Figure 3 shows the development parametric roll resonance (IMO, 2015).

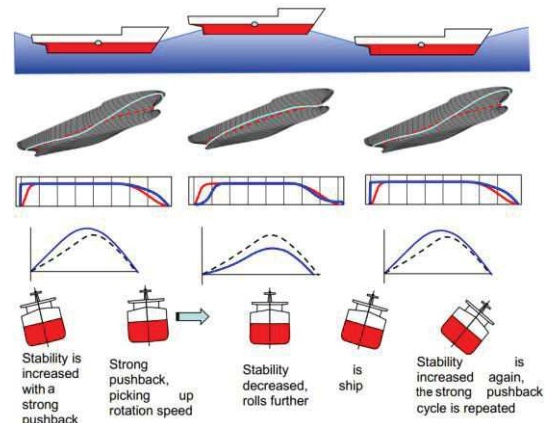


Figure 3. Development of parametric roll resonance

### 2.3 Surf-riding/broaching

Broaching (a shortening of "broaching-to") is a violent uncontrollable turn that occurs despite maximum steering efforts to maintain the course. As with any other sharp turn event, broaching is accompanied by a large heel angle, which has the potential effect of a partial or total stability failure. Broaching is usually preceded by surf-riding which occurs when a wave, approaching from the stern, "captures" a ship and accelerates the ship to the speed of the wave (i.e., the wave celerity). Surf-riding is a single wave event in which the wave profile does not vary relative to the ship. Because most ships are directionally unstable in the surf-riding condition, this maneuvering yaw instability leads to an uncontrollable turn – termed "broaching."

Because surf-riding usually precedes broaching, the likelihood of the occurrence of surf-riding can be used to formulate vulnerability criteria for broaching. In order for surf-riding to occur, several conditions need to be satisfied:

- a. the wave length should be between one and three times the ship length;
- b. the wave must be sufficiently steep to produce a sufficient wave surfing force;
- c. the ship speed should be comparable to the wave celerity.

Large ships (i.e. over 200 meters in length) do not surf-ride because waves of this and greater length tend to travel faster than the ship (i.e. 34 plus knots) and these ships have too much mass (i.e. inertia) to allow them to accelerate to the wave speed before the wave passes. Figure 4 shows the force acting on a ship in following waves (IMO, 2015).

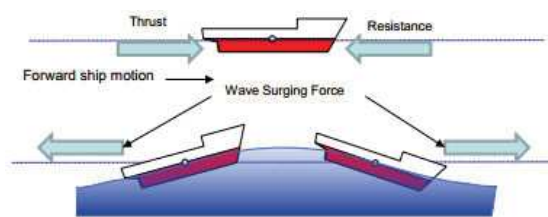


Figure 4. Force acting on a ship in following waves.

#### 2.4 Dead ship stability

The dead ship condition was the first mode of stability failure addressed with physics-based severe wind-and-roll criterion, also known as the "weather criterion," which was adopted by IMO in 1985 (Res. A.562(14)) and is now embodied in section 2.3 of the 2008 IS Code, Part A. The scenario of the weather criterion is shown in Figure 5. This scenario assumes that a ship has lost its power and has turned into beam seas, where it is rolling under the action of waves as well as heeling and drifting under the action of wind. Drift-related heel is a result of the action of a pair of forces: the wind aerodynamic force and hydrodynamic reaction caused by the transverse motion of the ship.

Figure 5. Scenario of stability failure in dead ship conditions

Next, a sudden and long gust of wind occurs. The worst possible instant for this is when the ship has rolled at the maximum windward angle; in this case, the action of wind is added to the action of waves. The strengthening wind increases the drift velocity and this leads to an

increase of the hydrodynamic drift reaction. The increase of the drift velocity leads to the increase of the hydrodynamic reaction and, therefore, to the increase of the heeling moment by the aerodynamic and hydrodynamic forces. The gust is assumed to last long enough for the ship to roll completely to the other side; the achieved leeward roll angle is the base of the criterion. If it is too large, some openings may be flooded and the stability of the ship is considered insufficient (Belenky et al., 2011).

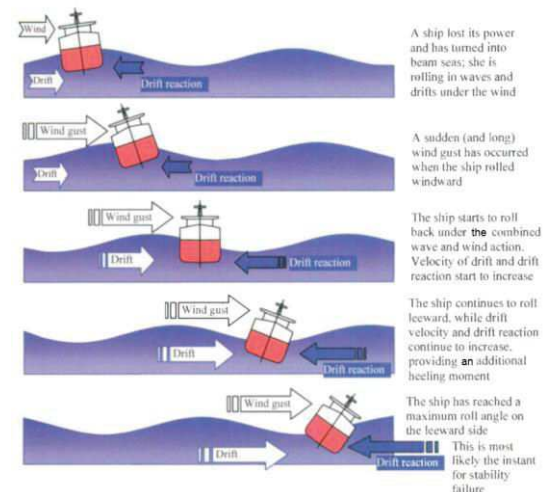


Figure 5. Scenario of stability failure in dead ship conditions

#### 2.5 Excessive acceleration

When a ship is rolling, the cargo in higher locations cover longer distances. The period of roll motions is the same for all the locations onboard the ship. To cover a longer distance during the same period of time, the linear velocity must be larger. As the velocity changes its direction every half period, a larger linear velocity leads to larger linear accelerations. A large linear acceleration means a larger inertial force, as shown in Figure 6. Horizontal accelerations are more dangerous than vertical accelerations. Large accelerations are mostly caused by roll motions so they have a predominantly lateral direction. If the GM value is large, the period of roll motion is smaller. Thus, for the same roll angle, the changes in linear velocity occur faster, causing the accelerations to be larger (IMO, 2015).

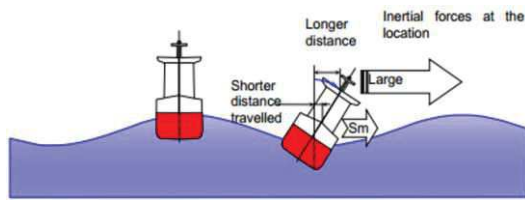


Figure 6. Scenario of stability failure related to excessive accelerations

### 3 DEVELOPMENT OF A SECOND GENERATION IS CODE

The last Sub-committee on Ship Design and Construction meeting at IMO recalled that SDC 2 had agreed, in principle, to the draft amendments of the 2008 IS Code regarding vulnerability criteria and the standards (levels 1 and 2) related to parametric roll, pure loss of stability and surf-riding / broaching (SDC 2/WP.4, annexes 1 to 3). For this purpose, SDC 2 had invited member governments and international organisations to bring the criteria to the attention of ship designers, shipyard, shipoperators owners and other interested parties, and to observe and test the application of the finalized vulnerability criteria, in order to gain experience with regard to their use.

The draft amendment of the IS Code regarding vulnerability criteria and the standards (levels 1 and 2) related to dead ship condition and excessive acceleration were stated in SDC 3 WP.10 Annex 1 and 2.

### 4 STABILITY CALCULATION

The stability calculation in this paper utilised the stability code by Creative System, Inc. namely General Hydrostatic (GHS©). The macro was written by the author based on the latest draft amendment for second generation intact stability criteria.

In this paper, three models were used for the stability calculation. The first model is a basic shape namely “ASL” as a fundamental container ship geometry. The second model is a containership. It is an open source geometry taken from the DELFT Ship website (Ariffin, Laurens, & Mansor, 2016). The third is a

research ship model namely model 5415 DTMB. The 5415 DTMB model are widely used for the research study in sea keeping (Begovic, Day, & Incecik, 2011; Jones & Clarke, 2010; Yoon et al., 2015). The basic ship geometry is presented in Table 1. The body plan for container ship is shown in Figure 7 and for model 5415 shown in Figure 8.

Table 1. Basic ships geometry

Model	ASL	Container Ship	5415
LOA, (m)	140.0	120.7	153.3
BOA, (m)	20	19.00	20.54
Draft, (m)	12	7.5	6.15
Displacement, (tones)	26,994	12,521	8,635
VCG, (m)	10	7	7.555
LCG, (m)	70.037	64.206	70.137
KM, (m)	10.206	8.532	9.493
GM, (m)	0.206	1.532	1.938
R <sub>PR</sub>	0.352	0.485	0.816

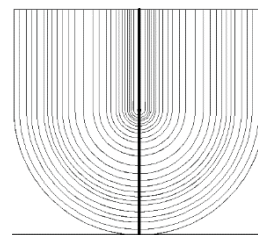


Figure 7. Body plan of the ASL shape

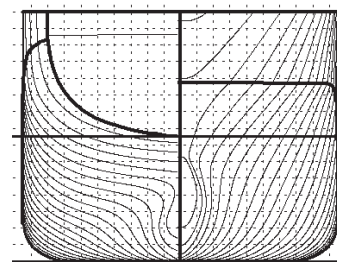


Figure 8. Body plan of the container ship 120m



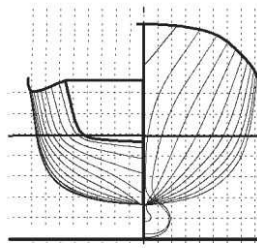


Figure 9. Body plan of the 5415 DTMB

#### 4.1 Pure loss of stability Level 1

The calculation for pure loss of stability level 1 is based on the draft amendment as stated in SDC 2/INF.10 Annex 18. For level 1, the ship is not vulnerable if the GM min is greater than the  $R_{PLA}$ . Based on SDC 2WP.4 Annex 1, the  $R_{PLA}$  is 0.05m. There are 2 methods to compute the  $GM_{min}$ . The first method uses the formula hereunder

$$GM_{min} = KB + I_L/V - KG \quad (1)$$

$$\text{only if } [(V_D - V)/A_W (D-d)] \geq 1.0 \quad (2)$$

$d$  = draft corresponding to the loading condition under consideration;  $I_L$  = moment of inertia of the water plane at the draft  $d_L$ ;

$$d_L = d - \delta d_L \quad (3)$$

$$[\delta d_L = \min(d - 0.25d_{full}, (L \cdot S_w/2))] \quad (4)$$

$KB$  = the height of the vertical centre of buoyancy corresponding to the loading condition under consideration;  $KG$  = the height of the vertical centre of gravity corresponding to the loading condition under consideration;  $V$  = the volume of displacement corresponding to the loading condition under consideration,  $S_w = 0.0334$ ,  $D$  = Depth,  $V_D$  = the volume of displacement at waterline equal to  $D$ ,  $A_W$  = the water plane area of the draft equal to  $d$ .

The second method uses the  $GM_{min}$  calculated for the ship with a free surface correction, corresponding to the loading condition under consideration, considering the ship to be balanced in sinkage and trim on waves with the characteristics hereunder

$$\text{Wavelength, } \lambda = L; \quad (5)$$

$$\text{Wave height, } h = L \cdot S_w, \text{ where } S_w = 0.0334; \quad (6)$$

the wave crest centered at the longitudinal center of gravity and at  $0.1L$ ,  $0.2L$ ,  $0.3L$ ,  $0.4L$ , and  $0.5L$  forward and  $0.1L$ ,  $0.2L$ ,  $0.3L$ , and  $0.4L$  aft.

The result for level 1 pure loss of stability and parametric rolling failure modes are shown in Figure 10 for the ASL model. It appears that the level 1 pure loss of stability and parametric rolling are less restrictive than the existing IS Code 2008 except for the pure loss of stability level 1 method A at the displacement less than 23,000 tones.

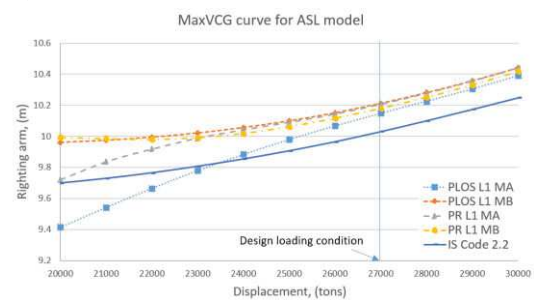


Figure 10. Result for the ASL model

The result for level 1 pure loss of stability and parametric rolling failure modes is shown in Figure 11 for the 120m container ship. It appears that the level 1 pure loss of stability and parametric rolling are more restrictive than the existing IS Code 2008.

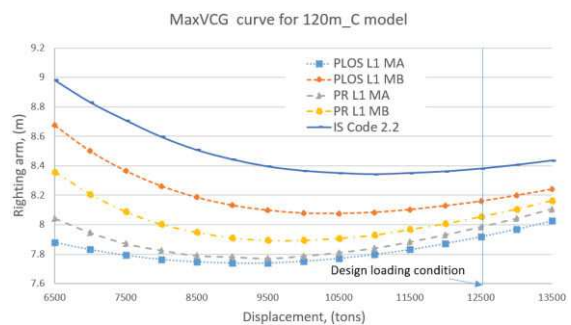


Figure 11. Result for the 120m container ship model

The result for level 1 pure loss of stability and parametric rolling failure modes is shown in Figure 12 for the 5415 model. It appears that the level 1 pure loss of stability and parametric rolling become more restrictive with the existing IS Code 2008 with the increment of displacement. In the design loading condition, the parametric rolling level 1 method B is less restrictive and the pure loss of stability level 1 method A and B and the parametric rolling level

1 method A are more restrictive than the existing IS Code 2008.

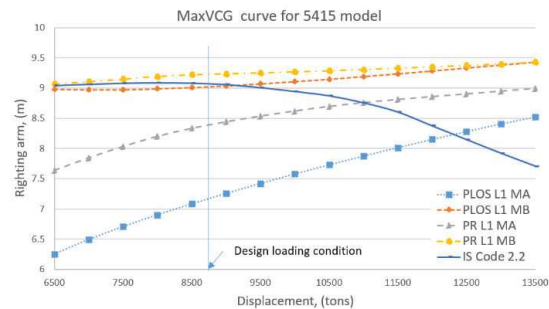


Figure 12. Result for the 5415 model

#### 4.2 Pure loss of stability Level 2

For level 2, a ship is not considered to be vulnerable to the pure loss of stability failure mode if the largest value among the two criteria,  $CR1$  and  $CR2$ , when traveling at the service speed, is less than  $R_{PLO}$ . Based on SDC 2WP.4 Annex 1, the  $R_{PLO}$  is 0.06. The  $CR1$  and  $CR2$  are calculated according to the formula hereunder

$$CR1 = \sum_{i=1}^N Wi C1i \quad (7)$$

$$CR2 = \sum_{i=1}^N Wi C2i \quad (8)$$

$Wi$  = weighting factor

$N$  = number of wave cases

$C1i$  = Criteria 1

$C2i$  = Criteria 2

Criterion 1 is a criterion based on the calculation of the angle of vanishing stability,  $\phi_v$ , as provided in the following formula

$$C1i = \begin{cases} 1 & \phi_v < R_{PL1} \\ 0 & \text{otherwise} \end{cases}$$

Where  $R_{PL1}$  = 30 degree

Criterion 2 is a criterion based on the calculation of the angle of heel,  $\phi_s$ , actioned of a heeling lever specified by  $R_{PL3}$  as provided in the following formula:

$$C1i = \begin{cases} 1 & \phi_s < R_{PL2} \\ 0 & \text{otherwise} \end{cases}$$

Where  $R_{PL1}$  = 15 degree for passenger ships; and = 25 degree for other ships

$$R_{PL3} = 8(Hi/\lambda)dFn^2$$

To simplify the calculation method, the GZ curve is calculated based on a 10 wave steepness from 0.01 to 0.1 with an 0.01 increment and the wave crest is to be centered amidship, and at 0.1L, 0.2L, 0.3L, 0.4L and 0.5L forward and 0.1L, 0.2L, 0.3L and 0.4L aft. Figure 13 shows the GZ curve in waves for the model 5415. The position of the wave crest is at aft perpendicular of the model. The increment of the wave steepness provide the impact to the GZ curve because of the change of the water plane area on different wave characteristics. Figure 14 shows the GZ curve in waves with the wave steepness 0.1 and the position of the wave crest is changed from the aft perpendicular to the forward perpendicular. The change of the water plane area with respect to the wave characteristics contributes to the significant change of the GZ curve. For the model 5415, for the wave steepness 0.1, all curves pass the pure loss of stability level 2 criteria 1.

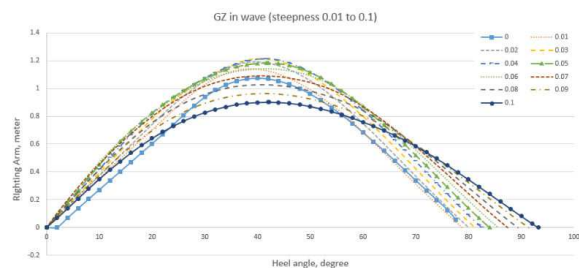


Figure 13 GZ curve for model 5415 with a wave steepness from 0.01 to 0.1 and the wave crest at aft perpendicular.

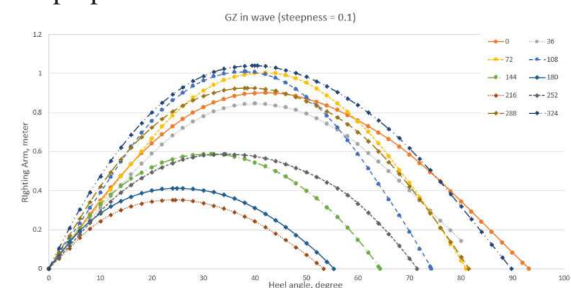


Figure 14 GZ curve for model 5415 with a wave steepness 0.1 where the wave crest position changes from 0.1L to 1L with increment 0.1L.

Table 2. Result for the angle of varnishing stability

Model	ASL	Container ship	5415
Smallest			
$\phi_v$ , (°)	77.967	53.284	15.88
Wave steepness	0.08	0.07	0.1
Wave phase	216	144	216
Largest			
$\phi_v$ , (°)	88.806	172	91.336
Wave steepness	0.1	0.1	0.09
Wave phase	0	234	0

The result of vulnerability for pure loss of stability level 2 criteria 1 for three models is shown in Table 2. The GZ curve for the lowest angle of varnishing stability  $\phi_v$  is shown in Figure 15. The lowest angle of varnishing stability for these three models is greater than 30 degrees. Therefore, all models pass the level 2 criteria for the pure loss of stability failure mode.

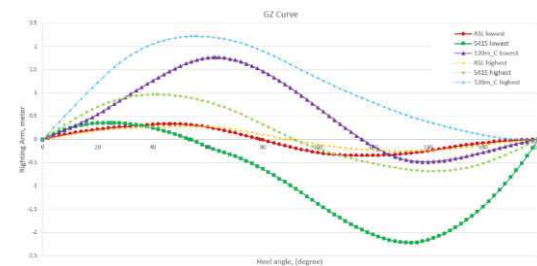


Figure 15 GZ curve for 3 models with the smallest and the largest angle of varnishing stability

## 5 CONCLUSION

This paper presents the result for three model ships for a level 1 pure loss of stability, level 1 parametric rolling and level 2 pure loss of stability failure modes based on draft amendments of the second generation intact stability criteria as outlined in the current state of development by the International Maritime Organisation (IMO).

All three models evaluated in this paper passed the pure loss of stability and parametric rolling levels 1 and 2.

The level 2 criteria require time and effort to evaluate the vulnerability to pure loss of stability and parametric rolling because of the calculation which involves the wave characteristics with a different wave steepness and the 11 numbers of the wave crest position.

## 6 ACKNOWLEDGEMENT

The authors would like to acknowledge the support of the Government of Malaysia, the Government of the French Republic and the Direction des Constructions Navales (DCNS).

## 7 REFERENCES

- Ariffin, A., Laurens, J. M., & Mansor, S. (2016). Real-time Evaluation of Second Generation Intact Stability Criteria. In *Smart Ship Technology* (pp. 26–27).
- Begovic, E., Day, a. H., & Incecik, a. (2011). Experimental Ship Motion and Load Measurements in Head and Beam Seas. *Proceeding of The 9th Symposium on High Speed Marine Vehicles*, 1–8.
- Belenky, V., Bassler, C. C., & Spyrou, K. J. (2011). Development of Second Generation Intact Stability. *Naval Surface Warfare Center, Carderock Division*.
- Francescutto, A. (2007). The Intact Ship Stability Code: Present Status and Future. In *Proceedings of the 2nd International Conference on Marine Research and Transportation, Naples, Italy, Session A* (pp. 199–208).
- IMO. (2015). *SDC 3/INF.10 Finalization of Second Generation Intact Stability Criteria*.
- Jones, D. a., & Clarke, D. B. (2010). *Fluent Code Simulation of Flow around a Naval Hull: the DTMB 5415*.
- Mata-Álvarez-Santullano, F., & Souto-Iglesias, A. (2014). Stability, safety and operability of small fishing vessels. *Ocean Engineering*, 79, 81–91. doi:10.1016/j.oceaneng.2014.01.011
- Rohala, J. (1939). *The Judging of the Stability of Ships and the Determination of the Minimum Amount of Stability*.

Van Santen, J. (2009). The Use of Energy Build Up to Identify the Most Critical Heeling Axis Direction for Stability Calculation for Floaring Offshore Structures. In *10th International Conference on Stability of Ship and Ocean Vehicles* (pp. 65–76).

Welaya, Y., & Kuo, C. (1981). A Review of Intact Ship Stability Research and Criteria. *Ocean Engineering*, 8, 65–84.

Yoon, H., Simonsen, C. D., Benedetti, L., Longo, J., Toda, Y., & Stern, F. (2015). Benchmark CFD validation data for surface combatant 5415 in PMM maneuvers – Part I: Force/moment/motion measurements. *Ocean Engineering*, 1–30.  
doi:10.1016/j.oceaneng.2015.04.087

## The weather criterion: Experimental wind tunnel results

Arman Ariffin<sup>1</sup>, Shuhaimi Mansor<sup>2</sup>, Jean-Marc Laurens<sup>1</sup>

<sup>1</sup>ENSTA Bretagne, IRDL, Brest, France

<sup>2</sup>Faculty of Mechanical Engineering, Universiti Teknologi Malaysia, Malaysia

### ABSTRACT

**The intact stability code, 2008 IS Code, includes a weather criterion. The vessel is subject to a lateral strong wind and a roll motion. The wind force on the sail, the roll amplitude and the bilge keel effect are computed according to a set of empirical formulae given in the 2008 IS Code. The maximum resulting list angle is then computed using the righting arm curve only, neglecting any damping. To verify how conservative, the regulation is, experimental trials have been conducted in the Low Speed Wind Tunnel of the Universiti Teknologi Malaysia for two models: a simple academic shape and the DTMB 5415. The experimental setup is described in the paper. Results have been obtained for several wind velocities, initial heel angles, yaw angles and with and without the bilge keel. The maximum angles of list obtained are compared with results given by the code as implemented within the stability code GHS©. As expected, the code is sometimes barely conservative and sometimes, very conservative.**

### INTRODUCTION

The International Code of Intact Stability 2008 (2008 IS Code) is based on the best “state-of-the-art” concepts available at the time the Code was developed. Since the design technology for modern ships is rapidly evolving, 2008 IS Code should be revised continuously and reevaluated as necessary. Generally, 2008 IS Code consists of two main criteria. First is the criteria regarding righting lever curve properties as stated in (IMO, 2009) Ch 2 Paragraph 2.2 and second is the severe wind and rolling criterion (also known as weather criterion) as stated in (IMO, 2009) Ch 2 Paragraph 2.3.

In 1939, Rohala (Rohala, 1939) wrote a doctoral thesis which evoked widespread interest throughout the world at that time because it was the first comprehensive study and proposed method to evaluate the intact stability which did not require complex calculation (Ariffin, Mansor, & Laurens, 2015). The weather criterion adopted as Resolution A.562 by IMO’s Assembly in 1985 was a leap beyond the “statistical approach” of the earlier Rohala-type general intact ship stability criteria.

In the MSC 81<sup>st</sup>, the guidelines for alternative assessment of the weather criterion were approved by IMO. This guideline are aiming to provide the industry with alternative means (in particular, model experiments) for the assessment of severe wind and rolling criterion (weather criterion) (IMO MSC.1/Circ.1200, 2006). It consists of the guidelines for experimental determination of the wind heeling lever and angle of roll to windward due to wave action. Wind test and drift test were explained in these guidelines.

In the MSC 82<sup>nd</sup> session, IMO approved the explanatory notes to the interim guidelines for an alternative assessment of the weather criterion (IMO MSC.1/Cir.1227, 2007). This explanatory notes provide an example of the alternative assessment of severe wind and rolling criterion (weather criterion) based on a series of model tests following the Interim Guidelines for the alternative assessment of the weather criterion for better understanding of the alternative procedures.

When evaluating the stability of a ship in beam seas and winds, consideration must be given to the modelling of wind and wave forces. While much research has been devoted to the hydrodynamics of ship rolling motions, relatively little work has been devoted to wind heeling loads on ships. This situation is particularly surprising when considering that



current intact stability criteria are based largely upon the heeling of ships under wind forces (McTaggart, 1992).

Naval Engineering Division conducted a wind tunnel test for naval ship 378-WHEC US Navy ship. The test was measuring 4 heeling position (upright) 25°, 50° and 75° and 4 wind velocities (6, 12, 18 and 24 m/s). This experiment concluded that wind heeling moment is about 16% less than calculated value (Paul, 1994).

An experimental wind tunnel to obtain the experiment results of wind forces and moment acting on ship models at various angle, with beam wind was conducted in 2003 (Bertaglia, Serra, Francescutto, & Bulian, 2003). The models used were scale down to 1/125<sup>th</sup> and wedges have been applied to the model to simulate the correct heeled position. The measurement has been performed with an undistributed wind velocity of 13m/s with Reynolds number of  $2 \times 10^6$  (length reference) and  $2.3 \times 10^5$  (breadth reference). This paper concluded that the real centre of underwater forces was assumed at half draught; and seems to be a safe assumption, but further test could be made in order to verify this assumption.

The draft amendment of the IS Code regarding vulnerability criteria and the standards (levels 1 and 2) related to dead ship condition and excessive acceleration are contained in SDC 3/INF.10 Annex 1 and 2. The level 1 check for dead ship condition is basically the same method used for current IS Code 2.3 which is weather criteria. If it failed, the design should process to level 2 check and the direct assessment. Direct assessment procedures for stability failure are intended to employ the most advanced state-of-the-art technology available either by numerical analysis or experimental work for quantitative validation as stated in SDC 1/INF.8 Annex 27 (IMO, 2013).

#### THE WEATHER CRITERION

The IS Code 2008 Part A 2.3 contains the weather criterion. The ship must be able to withstand the combined effects of beam wind and rolling. The conditions are:

- a. the ship is subjected to a steady wind pressure acting perpendicular to the ship's centre line which results in a steady wind heeling lever ( $lw_1$ ).
- b. from the resultant angle of equilibrium ( $\phi_0$ ), the ship is assumed to present an angle of roll ( $\phi_1$ ) to windward due to wave action. The angle of heel under action of steady wind ( $\phi_0$ ) should not exceed 16° or 80% of

the angle of deck edge immersion, whichever is less.

- c. the ship is then subjected to a gust wind pressure which results in a gust wind heeling lever ( $lw_2$ ); and under these circumstances, area b shall be equal to or greater than area a, as indicated in Fig. 1.

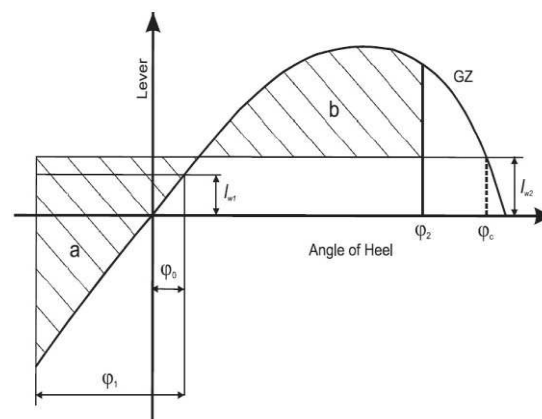


Fig. 1 Severe wind and rolling

The heeling lever shall be calculated using formula:

$$l_{w1} = (P \cdot A \cdot Z) / (1000 \cdot g \cdot \Delta) \quad (1)$$

$$l_{w2} = 1.5 l_{w1} \quad (2)$$

where  $l_{w1}$  = steady wind heeling angle,  $l_{w2}$  = gust wind heeling lever,  $P$  = wind pressure of 504 Pa,  $A$  = projected lateral area ( $m^2$ ),  $Z$  = vertical distance from the centre of  $A$  to the centre of the underwater lateral area or approximately to a point at one half of the mean draught (m),  $\Delta$  = displacement (t) and  $g$  = gravitational acceleration). Direct Assessment (DA) can be used to verify the weather criterion for unconventional ships. The DA can be experimental. The present study shows how such an experimental DA can be conducted for two models, a civilian ship and a military ship.

In the weather criterion, two main rules are commonly used. For commercial ship, it uses the IMO weather criterion and for naval ship, it uses the Naval Rules. The IMO Weather criterion is shown in Fig. 1 and the weather criterion for naval ship is shown in Fig. 2. The significant different between IMO an Naval Rules are presented in the Table 1.

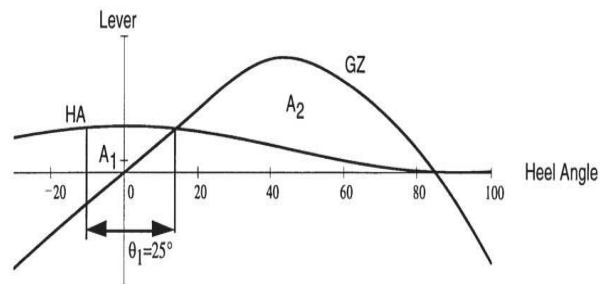


Fig. 2 Weather criterion for naval ship

Table 1: Comparison IMO and naval rules for weather criterion

Criterion	IMO	Naval Rules
Wind velocity	26 m/s	100 knots
Roll back angle	various*	25°
WHA	constant	$\cos 2\theta$
Ratio $A_2/A_1$	$\geq 1$	$\geq 1.4$
Gust	Yes	No

\* roll back angle ( $\phi_1$ ) calculated based on IS Code 2008

# WHA – wind heeling arm,  $A_2$  - restoring energy,  $A_1$  – capsizing energy

#### GHS CODE

In this paper, a software code, General Hydro Static (GHS®) is used. This code is for designing and to evaluate all types of ships and floating structures. It addresses flotation, trim, stability and strength by calculating the force involved using mathematical/geometrical model of the vessels. In GHS, the weather criterion can be evaluated with the presetting of the wind condition. There are two methods to set up the wind in GHS. The first one specifies the wind speed and the second is using the wind pressure. The main difference between both function is that using the wind pressure function, the wind speed is constant at all height. It means that there is no boundary layer for this setting. For wind speed (knots) function, the specified wind speed in knots is given at 10 meters above water plane, assuming a standard boundary layer above the sea level. This is a standard coming from maritime weather forecast (B. Chelton & H.Freilich, 2006).

Since this paper presents a comparison result with experimental work, the function of wind pressure was used. It is because of the boundary layer in the wind tunnel used in this experiment is about 30mm. This boundary layer can be neglected because the value is relatively small compare to the model size in wind tunnel test section.

#### SHIP MODEL

Two models were used for the experimental work. The first model is an academic container ship geometry referred as “ASL shape” in the rest of the paper. The second model is a research ship model, the well know DTMB 5415 (Molgaard, 2000). The 5415 DTMB model is widely used for the research study in seakeeping (Begovic, Day, & Incecik, 2011; Jones & Clarke, 2010; Yoon et al., 2015).

The main particulars of ASL shape are given in Table 2 and for the 5415 DTMB shape in Table 3. The body plan and perspective view for “ASL shape” is shown in Fig. 3. The body plan and perspective view for “5415 shape” is shown in Fig. 4.

Table 2 Main particulars of ASL shape

Ship model	Ship	Model
LOA, (m)	140	1.400
BOA, (m)	20	0.200
Draft, (m)	12	0.120
Displacement, (tonnes)	26,994	0.027
VCG, (m)	10	0.10
LCG, (m)	70.037	0.70
KM, (m)	10.206	0.10
GM, (m)	0.206	0.002

Table 3 Main particulars of 5415 shape

Ship model	Ship	Model
LOA, (m)	153.3	1.533
BOA, (m)	20.54	0.205
Draft, (m)	6.15	0.061
Displacement, (tonnes)	8,635	0.0086
VCG, (m)	7.555	0.076
LCG, (m)	70.137	0.70
KM, (m)	9.493	0.09
GM, (m)	1.938	0.014

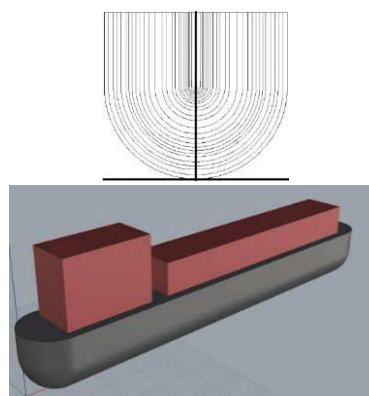


Fig. 3 Body plan (left) and perspective view (right) of the ASL shape

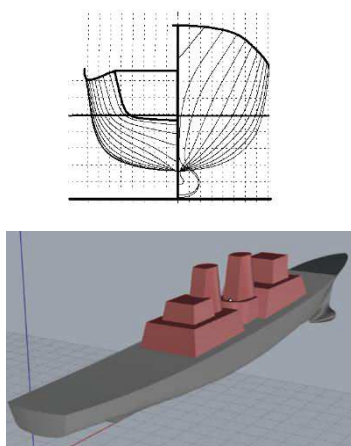


Fig. 4 Body plan (left) and perspective view (right) of the 5415 shape

Both models were constructed at ENSTA Bretagne, France using the Computer Numerical Control (CNC) machine. The material used was polystyrene. Both models were designed in 3D drawing and imported to CNC machine program for fabrication process. The hulls were divided into six parts for the cutting process. Then, all parts were glued and laminated with a fiberglass. The superstructure used the synthetic glass. The completed ship models are shown in Fig. 5.

#### MODEL VERIFICATION

To determine the correct centre of gravity, inclining tests were performed. The inclining test is a procedure which involves moving a series of known weights, normally in transverse direction (Fig. 6), and measuring the resulting change in the equilibrium heel angle of the ship. By using this information and applying basic naval architecture principles, the ships' vertical centre of gravity is determined from the GM. We also verified that the natural roll period is as expected. Two devices were used for the data recording, first is the Ardu Flyer device and smartphone (Djebli, Hamoudi, Imine, & Adjlout, 2016).



(a)



(b)

Fig. 5 Complete build ship models (a) ASL shape (b) 5415 DTMB shape

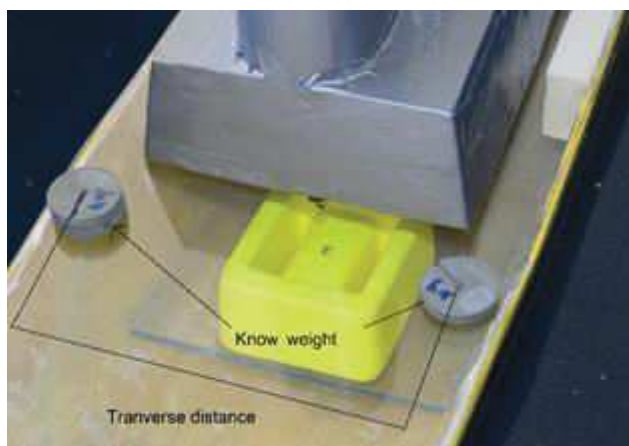


Fig. 6 Moving weight and transverse distance for inclining test

#### EXPERIMENTAL SETUP

A wind tunnel test was conducted at the low speed wind tunnel facility at Univerisiti Teknologi Malaysia. This wind tunnel has a test section of 2m (width) x 1.5m (height) x 5.8m (length). The maximum test velocity is 80m/s (160 knots). The wind tunnel has a flow uniformity of less than 0.15%, a temperature uniformity of less than 0.2°C, a flow angularity uniformity of less than 0.15° and a turbulence level of less than 0.06% (Ariffin et al., 2015).

#### Wind tunnel setup

The models were allowed to heave and roll freely. It was not allowed to yaw because the model must be hold at the longitudinal axis to avoid the model bump to water tank side. The models were fixed with a rod both at bow and stern (Fig. 7). It is passing through the point of longitudinal centre of buoyancy. Both rods at bow and stern were aligned using laser light to confirm the shafts positioned at same axis. The arrangement of rod used in this experiment is frictionless therefore, minimum interaction between the rod and rod stand can be obtained.

To allow the model to float in the wind tunnel, a water tank fabricated with glass of 8mm thickness was installed. The water tank size is 1600mm x



400mm x 240mm (length x width x depth). Since the wind tunnel is not water tight, to avoid any leak of water during the experiment, a dummy pool was placed underneath the platform. The dummy pool is capable to cope the total volume of water if the glass water tank gets damaged. The arrangement in the test section is shown in Fig. 8.



Fig. 7 Rods fixed at ship models



Fig. 8 Arrangement in the test section

The experiment started with the model placed in the water tank with the correct draft (Fig. 9). A laser light is used to ensure the vessel is upright. The test started with measurement of the stable heel. The wind tunnel velocity was increased slowly while the heel angle was recorded using the Ardu Flyer device. The Ardu Flyer is a complete open source autopilot system designed for 3D robotics. This experiment involved three models configuration as stated below:

- a. ASL shape.
- b. 5415 shape.
- c. ASL with bilge keel shape.

A roll back angle ( $\varphi_2^*$ ) measure was performed for all the models. The definitions of ( $\varphi_1$ ) and ( $\varphi_2^*$ ) are shown in Fig. 11. The test steps are as follow:

- a. Model placed in water tank.
- b. Wind applied and the wind velocity and heel angle recorded.
- c. Roll back angle ( $\varphi_1$ ) applied at the model. (using rod in Fig. 10)
- d. Then model is suddenly released.
- e. The maximum counter roll back angle ( $\varphi_2^*$ ) recorded. The is ( $\varphi_2^*$ ) is measure from the

angle of stable heel. With referring to the value used in IS Code 2008, the ( $\varphi_2^*$ ) can be calculate as ( $\varphi_2$ ) - ( $\varphi_0$ ).



(a)



(b)

Fig. 9 Ship models ready to be tested in wind tunnel test section (a) ASL shape (b) 5415 shape

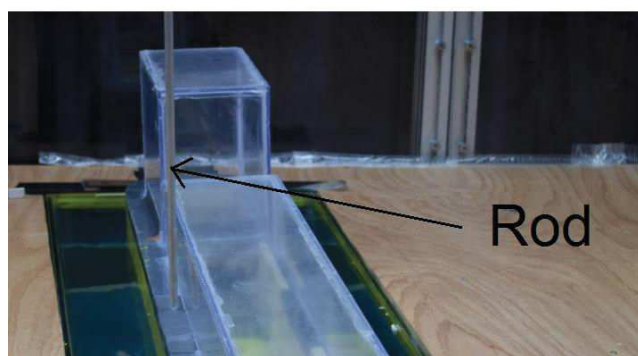


Fig. 10 Rod used to force the model to heel at roll back angle ( $\varphi_1$ )

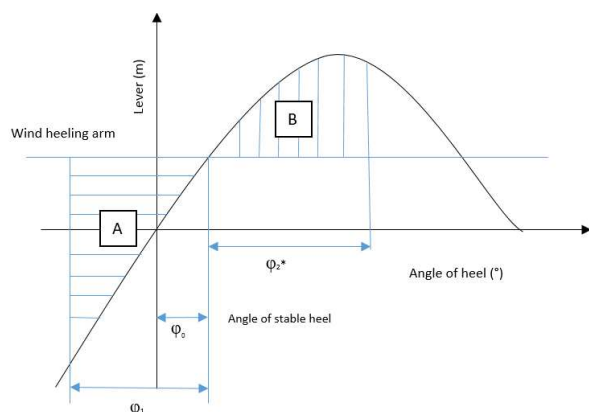


Fig. 11 Definition used in this experiment

### Scaling criteria

The models used in the experiment were scaled down to 1:100. It is the same scale used by (Begovic et al., 2011) for the ship motion experiment using DTMB 5415 model. For the GZ curve, the model and full scale ship has a same curve shape but values for the model are divided by  $10^2$ . For weight calculation, values used for the model are divided by  $10^6$ . For the wind velocity, the value used for the model is divided by 10.

### Boundary layer

When the air flow over the ocean surface from any direction, a natural boundary layer is formed. This means that the wind velocity at the surface is zero and increase with higher altitude. The boundary layer thickness in the test section for this experiment is about 35mm and the velocity profile is shown in Fig. 12. The comparison of boundary layer thickness and the ship models is shown in Fig. 13. The two lines in this figure shows the water line and boundary layer thickness.

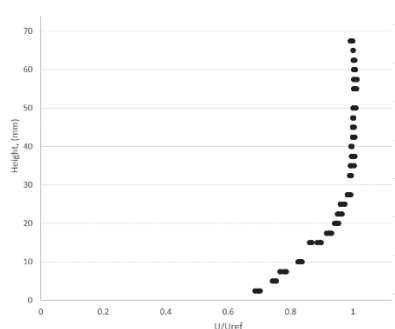


Fig. 12 The velocity profile curve

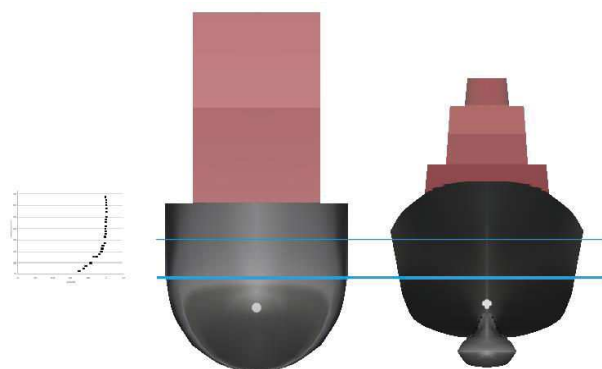


Fig. 13 Comparison of velocity profile and ship models

## RESULT AND DISCUSSION

### Angle of stable heel ( $\phi_0$ ) vs wind velocity

Fig. 14 shows the graph for angle of stable heel,  $\phi_0$  versus wind velocity for the two models and two methods; IMO and experimental. The 5415 curves are following a parabolic shape since as we can see in Fig. 15, the GZ curve of 5415 shape follows a linear curve up to 30 degrees. Furthermore, the experimental curve is below the IMO curve which indicates that the drag coefficient  $C_D$ , of the ship silhouette is smaller than 1, the value assumed in the IMO formula (Fig. 14). The ASL curves present different shapes and behaviour. At first, they do not present the parabolic shape because as we can see in Fig. 15, the GZ curve is only linear up to 5°. Furthermore, the experimental curve for this case is above the IMO curve (Fig. 14). That is explained by the fact that the drag coefficient  $C_D$ , for the box shape of the ASL is bigger than 1. This can be confirmed by the many references that exist giving the drag coefficients of basic shapes, see for example (Sadraey, 2009).

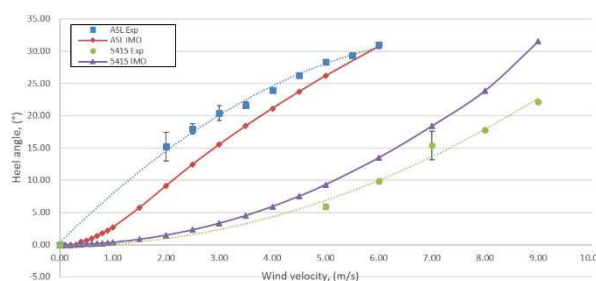


Fig. 14 Graph of wind velocity and angle of stable heel for ASL shape and 5415 shape on the experimental results and GHS calculation

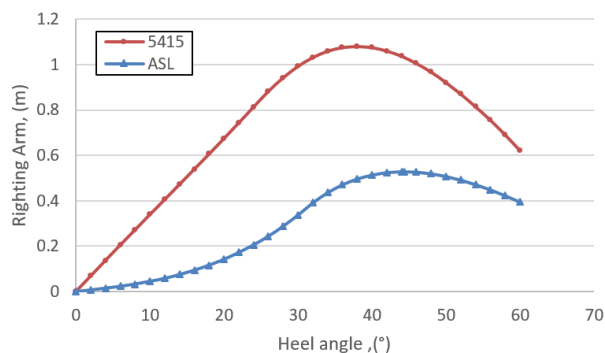


Fig. 15 The GZ curves for ASL shape and 5415 shape

Roll back angle ( $\varphi_2^*$ ) versus roll to windward ( $\varphi_1$ )

Fig. 16 shows the roll back angle ( $\varphi_2^*$ ) versus roll to windward ( $\varphi_1$ ) for ASL shape for wind velocity range of 2 m/s to 4 m/s. Fig. 17 shows the roll back angle ( $\varphi_2^*$ ) versus roll to windward ( $\varphi_1$ ) for 5415 shape. In the absence of damping the results should be like a swing where  $\varphi_2^*$  follows  $\varphi_1$ . The results suggest a far more complex behaviour where the hydrostatic force shape is playing an important role.

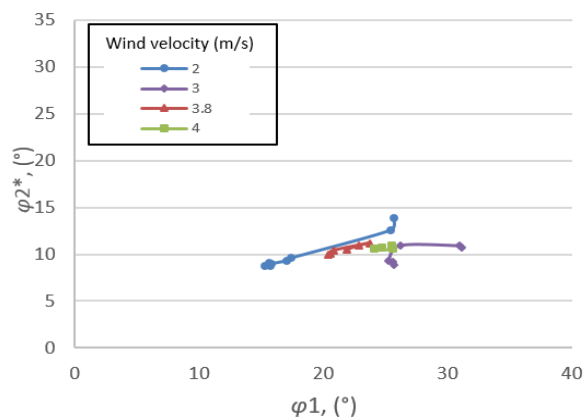


Fig. 16 Roll back angle ( $\varphi_2^*$ ) vs roll to windward ( $\varphi_1$ ) for ASL shape

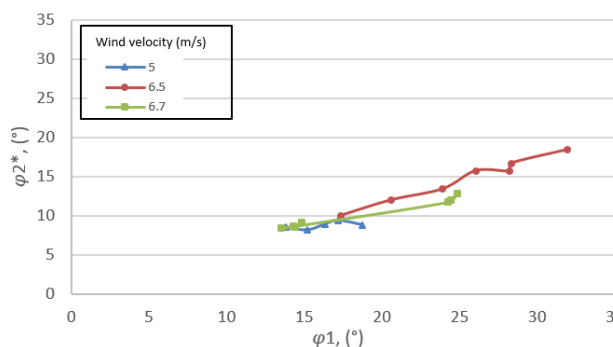


Fig. 17: Roll back angle ( $\varphi_2^*$ ) vs roll to windward ( $\varphi_1$ ) for 5415 shape

Ratio  $\varphi_2^*$  and  $\varphi_1$  with bilge keel

Fig. 18 shows the ratio ( $\varphi_2^*/\varphi_1$ ) for the ASL shape and the ASL with a bilge keel. Both models were tested at wind velocity 2m/s. For the bare ASL, the average ratio is 0.55 and for the ASL with bilge keel, the average ratio is 0.43. As expected, the configuration with bilge keel contributes to more roll damping than configuration without bilge keel.

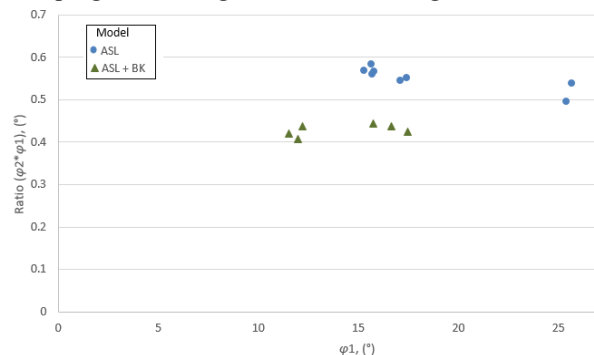


Fig. 18 Roll back angle ( $\varphi_2^*$ ) vs roll to windward ( $\varphi_1$ ) for ASL shape, 5415 shape and ASL with bilge keel configuration

Yaw angle effect on stable heel

Fig. 19 shows the angle of stable heel for the ASL and the 5415 both with the wind direction from star board 75° and port 105°. For the ASL, the values of  $\varphi_0$  are smaller for the beam wind than those obtained with the yaw angles. In other words the assumption of the beam wind in the IMO code is not necessarily conservative. This phenomenon also appears for the 5415.

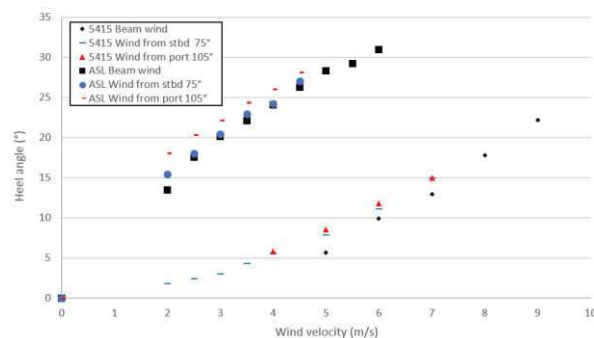


Fig. 19 Angle of stable heel for wind from starboard 75° and port 105°

Effect of roll to windward ( $\varphi_1$ ) and roll back angle ( $\varphi_2^*$ ) with yaw angle

Fig. 20 shows the result for  $\varphi_1$  and  $\varphi_2^*$  for the ASL and the 5415 with beam wind and wind from starboard 75°. For the ASL, the beam wind has higher  $\varphi_2^*$  than wind from starboard 75° and for the 5415, the beam wind has smaller  $\varphi_2^*$  than wind from starboard 75°. The two models have a different

response to the yaw angle. The behaviour is a combination of the superstructure geometry, the GZ curve and the damping.

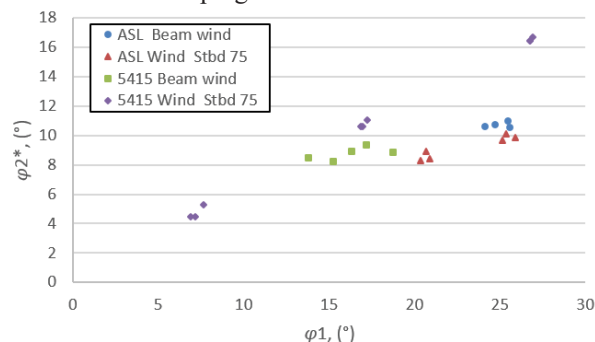


Fig. 20 Roll back angle ( $\varphi_2^*$ ) vs roll to windward ( $\varphi_1$ ) for 5415 shape with wind from port 105°

Comparison IMO GHS and experimental result

Fig. 21 shows the comparison results between IMO and experimental results. For the ASL, the counter roll back angle ( $\varphi_2^*$ ) obtained from experimental results is 24.07°, lower than IMO which is 29.638°. Therefore, IMO result is more conservative. For the 5415, the counter roll back angle ( $\varphi_2^*$ ) obtains from experimental results is 16.31°, lower than Naval Rules which is 33.82° for ratio capsizing and restoring energy 1.0 and 39.45° for ratio capsizing and restoring energy 1.4. Therefore, the IMO and Naval rules are always more conservative.

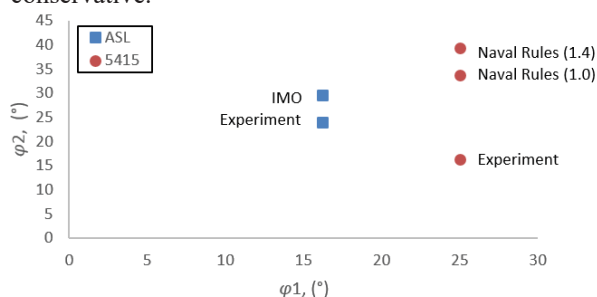


Fig. 21 Comparison result for IMO rules and Naval Rules

## CONCLUSIONS

In this paper the authors presented an experimental Direct Assessments (DA) of the weather criterion for two different models; a civilian ship with a simple geometry and a military ship, the well-known DTMB 5415. To conduct the experiments, the low speed wind tunnel of UTM was used. Both models were placed in a water tank in the wind tunnel. Both models were free to roll so the heel angle could be measured and compared with the IMO and Navy Rules.

Although the assumptions taken by the rules are not always conservative, the final results always show that the experimental values are lower than the values given by the rules.

## ACKNOWLEDGEMENTS

The authors would like to acknowledge the support of the Government of Malaysia, the Government of the French Republic and the Direction des Constructions Navales (DCNS).

## REFERENCES

- Ariffin, A., Mansor, S., & Laurens, J.-M. (2015). A Numerical Study for Level 1 Second Generation Intact Stability Criteria. In *International Conference on Stability of Ships and Ocean Vehicles* (pp. 183–193). Glasgow, UK.
- B. Chelton, D., & H.Freilich, M. (2006). Comments on “Scatterometer-Based Assessment of 10-m Wind Analyses from the Operational ECMWF and NCEP Numerical Weather Prediction Models.” *Monthly Weather Review*, 134(2), 737–742.
- Begovic, E., Day, a. H., & Incecik, A. (2011). Experimental Ship Motion and Load Measurements in Head and Beam Seas. In *Proceeding of The 9th Symposium on High Speed Marine Vehicles* (pp. 1–8). Naples, Italy.
- Bertaglia, G., Serra, A., Francescutto, A., & Bulian, G. (2003). Experimental Evaluation of the Parameters for the Weather Criterion. In *International Conference on Stability of Ships and Ocean Vehicles* (pp. 253–264). Madrid, Spain.
- Djebli, M. A., Hamoudi, B., Imine, O., & Adjlout, L. (2016). The application of smartphone in ship stability experiment The Application of Smartphone in Ship Stability Experiment. *Journal of Marine Science and Application*.
- IMO. (2009). *International Code of Intact Stability, 2008*. London.
- IMO. (2013). *SDC 1/INF.8 - Development of Second Generation Intact Stability Criteria*.
- IMO MSC.1/Cir.1227. (2007). *Explanatory Notes to the Interim Guidelines for Alternative Assessment of the Weather Criterion*.
- IMO MSC.1/Circ.1200. (2006). *Interim Guidelines for Alternative Assessment of the Weather Criterion*.
- Jones, D. a., & Clarke, D. B. (2010). *Fluent Code Simulation of Flow around a Naval Hull: the DTMB 5415*. Victoria, Australia.
- McTaggart, K. a. (1992). Wind effects on intact ship stability in beam seas. *Journal of Wind Engineering and Industrial Aerodynamics*, 44(1-3), 2487–2498.

- Molgaard, A. (2000). *PMM-test with a model of a frigate class DDG-51*. Lyngby, Denmark.
- Paul, H. (1994). 378-WHEC Wind Tunnel Tests by Paul Hirsimaki Naval Engineering Division (G-ENE-5B). *CG Engineers Digest*, 27–37.
- Rohala, J. (1939). *The Judging of the Stability of Ships and the Determination of the Minimum Amount of Stability*. Doctoral Thesis, Technical University of Finland.
- Sadraey, M. (2009). *Aircraft Performance Analysis*. VDM Verlag Dr Muller.
- Yoon, H., Simonsen, C. D., Benedetti, L., Longo, J., Toda, Y., & Stern, F. (2015). Benchmark CFD validation data for surface combatant 5415 in PMM maneuvers – Part I: Force/moment/motion measurements. *Ocean Engineering*, 109, 705–734.





# Etude des Critères de Seconde Génération de la Stabilité du Navire à l'Etat Intact

Le Sous-comité de la conception et de la construction navale de l'Organisation maritime internationale (OMI) a entrepris l'élaboration de critères de stabilité intacts de deuxième génération (SGISC). Le SGISC est une règle supplémentaire qui complète les règles actuelles. En outre, ces critères sont structurés en trois niveaux, à savoir le premier niveau, le deuxième niveau et l'évaluation directe. Les procédures d'évaluation directe pour chaque échec de stabilité sont développées avec la technologie de pointe la plus avancée disponible soit par analyse numérique, soit par travail expérimental pour une analyse quantitative. Dans cette thèse, on présente une implémentation des niveaux 1 et 2 du SGISC dans le solveur hydrostatique, une approche expérimentale pour le navire en détresse dans une tempête et des simulations RANS du même critère. En conclusion, il est possible de mettre en œuvre les critères de stabilité du navire intact de deuxième génération dans le code de stabilité GHS ©, un code couramment utilisé par les industriels dans le domaine. Cinq navires ont été considérés pour vérifier cette mise en œuvre. Une méthode expérimentale utilisant une grande soufflerie et une méthode de calcul CFD simplifiée ont été appliquées sur deux modèles. Dans les deux cas, les résultats montrent que l'angle de roulis maximal atteint par les deux navires étudiés est inférieur à celui donné par le calcul réglementaire. La méthode expérimentale est certainement plus proche de la réalité et le calcul CFD reste conservateur sans être aussi contraignant que la réglementation. En conclusion les méthodes expérimentale et numérique développées et utilisées dans ce travail de thèse peuvent être proposées pour l'évaluation directe du critère.

*Mots clés: critères de stabilité intact de deuxième génération, navire en détresse, évaluation directe, RANSE, Soufflerie*

---

## An Analysis on Second Generation Intact Stability Criteria

The Sub-Committee of Ship Design and Construction of International Maritime Organisation (IMO) has undertaken the development of Second Generation Intact Stability Criteria (SGISC). The SGISC is an additional rule that complement present rules. Five failure modes will be address in SGISC are excessive roll in dead ship condition, pure loss of stability, broaching, parametric roll, and excessive acceleration. Moreover, these criteria are structured in three levels namely, first level, second level and direct assessment. Direct assessment procedures for every stability failure are developed with the most advanced state-of-the art technology available either by numerical analysis or experimental work for quantitative analysis. In this thesis, implementations of Level 1 and Level 2 of the SGISC in the hydrostatic solver, experimental approached for dead ship condition and RANS simulation are presented. In conclusion, it was possible to implement the stability criteria of the intact second-generation vessel in the GHS © code of stability, a code commonly used by industrialists in the field. Five vessels were considered to verify this implementation. An experimental wind tunnel method and a simplified CFD calculation method were used on two different models. In both cases, the results show that the maximum roll angle reached by the two vessels studied is lower than the one given by the regulatory calculation. The experimental method is certainly closer to reality and the calculation CFD remains conservative without being as binding as the regulation. Therefore, the two approaches, numerical and experimental can be proposed to be used for Direct Assessment of the criterion.

*Keyword: second generation intact stability criteria, dead ship condition, direct assessment, RANSE, wind tunnel*



